

**The Cardioprotective Role of the N-3 PUFA Metabolite 19,20-Epoxydocosapentaenoic Acid
(19,20-EDP) in the Setting of Ischemia Reperfusion Injury**

by

Ahmed Mohamed Darwesh Essa

A thesis submitted in partial fulfillment of the requirements for the degree of

Doctor of Philosophy
in
Pharmaceutical Sciences

Faculty of Pharmacy and Pharmaceutical Sciences
University of Alberta

© Ahmed Mohamed Darwesh Essa, 2022

ABSTRACT

Ischemic heart disease (IHD) is a leading cause of cardiovascular morbidity and mortality worldwide. Myocardial ischemia occurs when a coronary artery is occluded and consequently blood supply to the heart is restricted depleting it of oxygen and nutrients. Although early myocardial reperfusion, or restoration of blood flow to the ischemic heart, is the standard therapeutic intervention to rescue viable myocardial tissue, reperfusion itself can paradoxically accelerate the death of injured cardiomyocytes, aggravating the damage and increasing the incidence of developing heart failure (HF). This phenomenon is termed as ischemia-reperfusion (IR) injury. Although the use of the currently available therapies, with early reperfusion, has contributed to the reduction in acute mortality rates after ischemic attacks, the risk of development of HF secondary to IR injury is still significantly high. Therefore, development of new therapeutic strategies to mitigate the consequences of IR injury becomes imperative.

In the heart, mitochondria are the main source of energy that fuel the contractile apparatus. Accumulating literature demonstrates that impaired mitochondrial function has a significant role in the pathogenesis of myocardial IR injury. Moreover, it has been shown that the reactive oxygen species (ROS) burst from damaged mitochondria triggers the activation of the NLRP3 inflammasome which spread the inflammatory surge to the rest of the myocardium exacerbating cardiac injury secondary to IR injury.

Long-chain omega-3 polyunsaturated fatty acids (n-3 PUFA) are essential constituents of the body, which have been attributed to numerous benefits including protection against cardiovascular disease. Docosahexaenoic acid (DHA), a major dietary n-3 PUFA, can be metabolized by cytochromes P450 (CYP) to generate six regioisomeric epoxy lipids termed epoxydocosapentaenoic acids (4,5-, 7,8-, 10,11-, 13,14-, 16,17-, 19,20-EDP). There is growing

evidence indicating that 19,20-EDP mediate many of the salutary effects of the parent compound DHA. However, EDPs are rapidly converted to the corresponding less biologically active vicinal diol by the enzyme soluble epoxide hydrolase (sEH). Accordingly, we hypothesized in this thesis that enhancing the cardiac levels of 19,20-EDP ameliorates IR injury via mitigating mitochondrial damage and limiting NLRP3 inflammasome activation.

First, we investigated the differential cardioprotective effects of n-3 PUFAs and their CYP metabolites in the setting of IR injury. Our results demonstrated that perfusion of isolated wild type (WT) mouse hearts, subjected to IR injury in the Langendorff mode, with 19,20-EDP exerted cardioprotection as evidenced by a significant improvement in postischemic functional recovery associated with preserved mitochondrial function and significant attenuation of NLRP3 inflammasome complex activation. Second, we revealed that enhancing the cardiac levels of these epoxy metabolites via genetic deletion or pharmacological inhibition of sEH can also markedly limit mitochondrial dysfunction and attenuate the activation of the NLRP3 inflammasome complex and thus impart cardioprotection against IR injury. Third, we demonstrated that perfusion of mouse hearts with the more chemically and metabolically stable synthetic EDP surrogate, SA-26, significantly improved postischemic recovery and maintained cardiac ATP levels. Finally, we attempted to elucidate whether mitochondrial sirtuin 3 (SIRT3), the primary mitochondrial deacetylase that plays a pivotal role in regulating mitochondrial homeostasis, is directly involved in mediating the protective effects of 19,20-EDP against myocardial IR injury. Importantly, we revealed perfusion of hearts with 19,20-EDP in the isolated working heart model preserved mitochondrial quality and improved cardiac energy metabolism via directly activating SIRT3. Intriguingly, we demonstrated that 19,20-EDP markedly improved mitochondrial respiration and SIRT3 activity in fresh cardiac fibers isolated from human left ventricular tissues obtained from

individuals with ischemic heart disease (IHD) collected through the Human Explanted Heart Program at University of Alberta. Furthermore, using molecular modeling and docking approaches, we proved that 19,20-EDP, via directly binding to the human SIRT3 protein, acts as a positive allosteric modulator (i.e., catalytic enhancer) that triggers SIRT3 activation.

In summary, the data presented in this thesis highlight the beneficial role of 19,20-EDP in limiting IR injury via maintaining mitochondrial homeostasis and limiting NLRP3 inflammasome activation. Moreover, to the best of our knowledge, this work is the first to identify SIRT3 as a potential target for the epoxy lipid 19,20-EDP and to reveal that direct binding of 19,20-EDP to SIRT3 significantly enhances its enzymatic activity. These studies provide new perspectives for the development of novel pharmacological agents, based on the structure of 19,20-EDP, to improve the clinical outcomes in the setting of IR injury.

PREFACE

This thesis is an original work done by Ahmed Mohamed Darwesh Essa. All experimental animal procedures were approved by the University of Alberta Health Sciences Animal Policy and Welfare Committee and conducted according to strict guidelines provided by the Guide to the Care and Use of Experimental Animals (Vol. 1, 2nd ed., 1993, from the Canadian Council on Animal Care). The human research conducted in this thesis forms part of a research collaboration led by Dr. Gavin Oudit from the Faculty of Medicine, with Dr. John Seubert from the Faculty of Pharmacy and Pharmaceutical Sciences. Dr. Oudit is the director of the Human Explanted Heart Program (HELP) and Human Organ Procurement and Exchange Program (HOPE) at the University of Alberta.

Parts of chapter 1 (introduction) have been previously published as **Ahmed M Darwesh**, Deanna K Sosnowski, Tim Yt Lee, Hedieh Keshavarz-Bahaghighat, John M Seubert. “Insights into the cardioprotective properties of n-3 PUFAs against ischemic heart disease via modulation of the innate immune system.” *Chem Biol Interact.* 2019; 308:20-44. I was responsible for reviewing, collecting and summarizing data from the literature and writing the manuscript. Deanna K Sosnowski and Tim Yt Lee were responsible for the design of tables 1.1, 1.2 and 1.3. Hedieh Keshavarz-Bahaghighat was responsible for the design of figures 1.6 and 1.7. John M Seubert was the primary investigator and the supervisory author who was involved in concept formation, reviewing and editing the manuscript.

Chapter 2 of this thesis has been previously published under **Ahmed M. Darwesh**, K. Lockhart Jamieson, Chuying Wang, Victor Samokhvalov, and John M. Seubert. Cardioprotective effects of CYP-derived epoxy metabolites of docosahexaenoic acid involve limiting NLRP3 inflammasome activation. *Can J Physiol Pharmacol.* 2019;97(6):544-556. I was responsible for

designing the research, conducting experiments and performing data analysis as well as writing the manuscript. Lockhart Jamieson and Victor Samokhvalov assisted with the mitochondrial respiration experiments. Chuying Wang aided with the immunoblotting experiments. John M Seubert was the primary investigator and the supervisory author who was involved in concept formation and reviewing and editing the manuscript.

Chapter 3 of this thesis has been previously published under **Ahmed M Darwesh**, Hedieh Keshavarz-Bahaghighat, K Lockhart Jamieson, John M Seubert. Genetic Deletion or Pharmacological Inhibition of Soluble Epoxide Hydrolase Ameliorates Cardiac Ischemia/Reperfusion Injury by Attenuating NLRP3 Inflammasome Activation. *Int J Mol Sci.* 2019;20(14):3502. I was responsible for designing the research, conducting experiments, and manuscript composition. Lockhart Jamieson assisted with the isolation of cardiac fibers in order to run the mitochondrial respiration experiments. Hedieh Keshavarz-Bahaghighat aided with the mitochondrial respiration and immunoblotting experiments. John M Seubert was the primary investigator and the supervisory author who was involved in concept formation and reviewing and editing the manuscript.

Chapter 4 of this thesis has been published as **Ahmed M Darwesh**, Wesam Bassiouni, Adeniyi Michael Adebesein, Abdul Sattar Mohammad, John R Falck, John M Seubert. A Synthetic Epoxydocosapentaenoic Acid Analogue Ameliorates Cardiac Ischemia/Reperfusion Injury: The Involvement of the Sirtuin 3-NLRP3 Pathway. *Int J Mol Sci.* 2020 Jul 24;21(15):5261. I was responsible for designing the research, conducting experiments and performing data analysis as well as writing the manuscript. Wesam Bassiouni aided with the immunoblotting experiments. Both Adeniyi Michael Adebesein and Abdul Sattar Mohammad, under the supervision of John R Falck, were responsible for the synthesis and purification of the EDP surrogates. John M Seubert

was the primary investigator and the supervisory author who was involved in concept formation, reviewing and editing the manuscript as well as coordination of collaborations.

Chapter 5 of this thesis is under revision for submission to Circulation Journal as of November 30th, 2021, as **Ahmed M. Darwesh**, Tariq R. Altamimi, K. Lockhart Jamieson, Wesam Bassiouni, Hao Zhang, Marawan Ahmed, Matthew L. Edin, Darryl C. Zeldin, Khaled Barakat, Gavin Y. Oudit, Gary D. Lopaschuk, John M. Seubert. 19,20-Epoxydocosapentaenoic Acid (19,20-EDP) Ameliorates Cardiac Ischemia-Reperfusion Injury by Directly Activating Mitochondrial Sirtuin 3. I was responsible for designing the research, conducting experiments and performing data analysis as well as writing the manuscript. Tariq R. Altamimi, a member of Gary D. Lopaschuk's research group, performed the working heart experiments. K. Lockhart Jamieson assisted with the isolation of cardiac fibers for the mitochondrial respiration experiments. Wesam Bassiouni aided with the immunoblotting experiments. Hao Zhang, under the supervision of Gavin Y. Oudit, provided the human tissue samples. Marawan Ahmed, from Dr. Khaled Barakat's research group, was responsible for performing the computational structure analyses as well as molecular dynamics trajectories. Matthew L. Edin, a member of Dr. Darryl C. Zeldin's research group, performed the LC-MS/MS used to analyze oxylipid metabolites in human cardiac tissues. John M Seubert was the primary investigator and the supervisory author who was involved in designing the study, reviewing the data and editing the manuscript.

The appendix of this thesis has been published as **Ahmed M. Darwesh**, Wesam Bassiouni, Deanna K. Sosnowski, John M. Seubert. Can N-3 Polyunsaturated Fatty Acids Be Considered A Potential Adjuvant Medication For COVID-19-Associated Cardiovascular Complications? Pharmacol Ther. 2021; 219:107703. I was responsible for screening, collecting and summarizing data from the literature and writing the manuscript. Wesam Bassiouni was responsible for

designing figures 9.1, 9.2, and 9.3. Deanna K Sosnowski was responsible for the design of the tables in this chapter (Tables 9.1, 9.2, 9.3, 9.4, 9.5 and 9.6). John M Seubert was the primary investigator and the supervisory author who was involved in concept formation, reviewing and editing the manuscript.

This dissertation is dedicated with love, appreciation and gratitude to my parents, in-laws, wife, daughter, twin sons, brother, sister and many of my friends.

Thank you for your unconditional love, encouragement, and support

“If I have seen further, it is by standing on the shoulders of Giants.”

Issac Newton

ACKNOWLEDGEMENTS

First and foremost, I would like to profusely thank my distinguished supervisor, Dr. John Seubert, for giving me the opportunity to be part of his excellent research group. His guidance, mentorship, and support throughout my PhD studies helped me a lot during my journey. The vast knowledge and expertise he has, which he is eager to share, proved priceless in developing my research skills and experience. I feel exceedingly lucky to have the chance to learn in Dr. Seubert's lab and I am incredibly grateful for all the opportunities he so generously provided to me.

I am greatly indebted and would like to thank my supervisory committee members Dr. Gary D Lopaschuk and Dr. John R Ussher for their valuable time, enlightening insights and encouragement throughout my graduate studies. Their advice and feedback have been invaluable throughout the course of my training.

I would like to thank Dr. Jason Dyck for his advice, collaboration and mentorship over the years. I would also like to acknowledge Dr. Gavin Oudit whose collaboration was an absolutely invaluable addition to my research project. I must also recognize John R Falck, who so generously provided the synthetic analogues used in my research, as well as Drs. Khaled Barakat, Matthew Edin and Darryl Zeldin, whose contributions were invaluable.

My sincere thanks and appreciation also extend to my past and present lab colleagues. I owe so much to my previous lab "sisters", Dr. Kristi Lockhart Jamieson and Dr. Tomoko Endo for their friendship and their help during my studies. I would also like to thank our previous research associate, Dr. Victor Samokhvalov, who helped me so generously. I am incredibly grateful for all my current lab members, Wesam Bassiouni, Deanna K. Sosnowski, and Robert Valencia for being such great colleagues and peers. I would not have been able to accomplish this work without the support, intellectual input, technical assistance, and teamwork of all my colleagues.

I extend my gratitude to everyone in the Faculty of Graduate Studies and Research and the Faculty of Pharmacy and Pharmaceutical Sciences at University of Alberta. Thanks to the past and present Dean and all the administrative staff for their constant willingness to assist in all my issues.

I am also thankful for the generous financial support provided by the University of Alberta in the form of several scholarships and awards including Izaak Walton Killam Memorial Scholarship (2020-2022), BMO Financial Group Graduate Scholarship (2021), Andrew Stewart Memorial Graduate Prize (2021), Novartis Pharmaceuticals Canada Inc Graduate Scholarship (2021), Alberta Innovates Graduate Student Scholarship (2018-2019), Dr John Samuel Memorial Graduate Scholarship (2018 & 2020), Dr Leonard Wiebe Graduate Award in Pharmaceutical Sciences (2019), among others. I am also thankful to Alberta Innovates for financially supporting me with The Graduate Studentship in Health Innovation (2020-2023). I would like also to recognize the external funding agencies that backed this research work, the Heart and Stroke Foundation (HSF) and Canadian Institutes of Health Research (CIHR).

My deepest gratitude goes to my parents, Nadia Nageida and Mohamed Darwesh. Their unconditional love since the very beginning is the reason why I can chase my goals and realize my dreams. To my sister; Eman Essa, and my brother; Mostafa Essa, the best role models anyone could ask for. I would also like to thank my mother-in-law; Manal Badran, and father-in-law; Ahmed Elgendy, and all of my extended family members for their support throughout my studies.

Finally, I would like to express my genuine gratitude and appreciation to my lovely and caring wife, Ranya Elgendy, and my 3 children, Alya, Yahia, and Selim, who fill my life with hope and happiness. My wife has always been my source of strength throughout this journey. This work would not have been accomplished without the support I receive from her. Thank you for your unwavering love and profuse encouragement.

TABLE OF CONTENTS

1. CHAPTER 1: INTRODUCTION	1
1.1 Ischemic heart disease and reperfusion injury	2
1.2 Bimodal responses to cardiac ischemia.....	3
1.3 Forms of myocardial ischemia reperfusion injury	4
1.3.1 Myocardial stunning	6
1.3.2 Myocardial hibernation.....	6
1.3.3 Lethal myocardial ischemia reperfusion injury	7
1.4 Lethal ischemia reperfusion injury and cardiac remodeling	10
1.5 Mediators of the lethal myocardial ischemia reperfusion injury.....	11
1.5.1 The role of dysregulated mitochondrial homeostasis in the pathogenesis of Ischemia-reperfusion injury	13
1.5.1.1 pH change and mitochondrial calcium overload.....	14
1.5.1.2 Opening of the mitochondrial permeability transition pore (MPTP).....	15
1.5.1.3 Increased mitochondrial ROS production.....	16
1.5.1.4 Aberrant mitochondrial dynamics.....	17
1.5.1.4.1 Dysregulated mitochondrial fusion and fission.....	18
1.5.1.4.2 Dysregulated mitochondrial biogenesis.....	20
1.5.1.5 Alteration of mitochondrial energy metabolism	21
1.5.1.6 Impaired mitochondrial sirtuin 3 function	25

1.5.2	Role of innate immune system in the pathogenesis of ischemia-reperfusion injury..	27
1.5.2.1	Activation of PRRs by damage-associated molecular patterns (DAMPs) (early signaling).....	28
1.5.2.2	Recruitment of different leukocyte populations.....	31
1.5.2.2.1	Neutrophils (1-3 days post death of cardiomyocyte).....	31
1.5.2.2.2	Monocytes (3-5 days post death of cardiomyocyte).....	32
1.5.2.2.3	Macrophages (5-7 days post death of cardiomyocyte).....	32
1.5.2.3	Persistent adverse inflammatory response and LV remodeling	33
1.5.2.4	The interplay between mitochondrial damage and activation of the innate immune system	34
1.5.2.5	Modulation of the innate immune response is cardioprotective	35
1.6	Overview of n-3 and n-6 polyunsaturated fatty acids	37
1.6.1	Cardiovascular benefits of n-3 polyunsaturated fatty acids.....	40
1.6.2	Cardioprotective mechanisms of n-3 PUFAs	59
1.6.2.1	N-3 PUFAs and their metabolites have the potential to reduce inflammatory responses	59
1.6.2.1.1	Metabolite-independent effects	59
1.6.2.1.1.1	Modulation of gene expression of different innate immune components	59
1.6.2.1.1.2	Altering the cell membrane structure	62
1.6.2.1.2	Metabolite-dependent effects	63

1.6.2.1.2.1	Enhancing COX-derived metabolites of n-3 PUFAs	64
1.6.2.1.2.2	LOX-derived metabolites of n-3 PUFAs	65
1.6.2.1.2.3	CYP-derived metabolites of n-3 PUFAs.....	67
1.6.2.1.2.4	Resolvins: The anti-inflammatory and resolving mediators	70
1.6.2.2	N-3 PUFAs and their metabolites have the potential to ameliorate mitochondrial dysfunction under stress conditions	72
1.7	Thesis overview.....	74
1.7.1	Rationale	74
1.7.2	Global hypothesis.....	75
1.7.3	Objectives	76
2.	CHAPTER 2: CARDIOPROTECTIVE EFFECTS OF CYP-DERIVED EPOXY METABOLITES OF DOCOSAHEXAENOIC ACID INVOLVE LIMITING NLRP3 INFLAMMASOME ACTIVATION	77
	Abstract	78
2.1	Introduction	79
2.2	Methods.....	81
2.2.1	Animals and isolated heart perfusion.....	81
2.2.2	Immunoblotting.....	82
2.2.3	Mitochondrial respiration.....	83
2.2.4	Enzymatic Assays	83
2.2.5	Statistics	84

2.3	Results	85
2.3.1	Cardioprotective effects of n3-PUFAs and their CYP-derived epoxy metabolites..	85
2.3.2	Epoxy metabolites limit postischemic mitochondrial injury	89
2.3.3	Effects of n-3 PUFAs and their CYP epoxy metabolites on the assembly and activation of NLRP3 inflammasome	94
2.3.4	Effects of n-3 PUFAs and their CYP epoxy metabolites on Txnip activation and translocation.....	96
2.3.5	Mitofusins	98
2.4	Discussion	100
3.	CHAPTER 3: GENETIC DELETION OR PHARMACOLOGICAL INHIBITION OF SOLUBLE EPOXIDE HYDROLASE AMELIORATES CARDIAC ISCHEMIA/REPERFUSION INJURY BY ATTENUATING NLRP3 INFLAMMASOME ACTIVATION	107
	Abstract	108
3.1	Introduction	109
3.2	Materials and Methods.....	111
3.2.1	Animals.....	111
3.2.2	Isolated heart perfusion.....	112
3.2.3	Immunoblotting.....	113
3.2.4	Enzyme-Linked Immunosorbent Assay.....	114
3.2.5	Measurement of malondialdehyde (MDA) levels.....	114
3.2.6	Mitochondrial respiration.....	115

3.2.7	Enzymatic assays	115
3.2.8	Statistics	116
3.3	Results	117
3.3.1	Deletion or inhibition of sEH improves post-ischemic functional recovery in both males and females.....	117
3.3.2	Deletion or inhibition of sEH limits post-ischemic mitochondrial injury	119
3.3.3	Deletion or inhibition of sEH abrogates the assembly and activation of NLRP3 inflammasome secondary to IR injury.....	123
3.3.4	Deletion or inhibition of sEH blunts the activation and mitochondrial translocation of thioredoxin-interacting protein (Txnip) secondary to IR injury.....	125
3.3.5	Deletion or inhibition of sEH abrogates the IR-Induced upregulation of the mitochondrial protein mitofusin-2.....	127
3.4	Discussion	129
4.	CHAPTER 4: A SYNTHETIC EPOXYDOCOSAPENTAENOIC ACID ANALOGUE AMELIORATES CARDIAC ISCHEMIA/REPERFUSION INJURY: THE INVOLVEMENT OF THE SIRTUIN 3–NLRP3 PATHWAY	137
	Abstract	138
4.1	Introduction	139
4.2	Materials and Methods.....	143
4.2.1	Synthesis of EDP surrogates.....	143
4.2.1.1	Synthesis of SA-26.....	143

4.2.1.2	Synthesis of AS-27.....	145
4.2.1.3	Synthesis of AA-4.....	148
4.2.1.4	¹ H/ ¹³ C NMR.....	149
4.2.2	Animals.....	156
4.2.3	Isolated heart perfusion.....	156
4.2.4	Immunoblotting.....	158
4.2.5	Measurement of malondialdehyde (MDA) levels.....	159
4.2.6	Enzymatic assays.....	159
4.2.7	Measurement of ATP levels in the heart.....	160
4.2.8	Measurement of NAD ⁺ /NADH content in the heart.....	160
4.2.9	Statistics.....	160
4.3	Results.....	161
4.3.1	SA-26 improves post-ischemic functional recovery.....	161
4.3.2	SIRT3 function is preserved in hearts perfused with SA-26.....	163
4.3.3	SA-26 mitigates mitochondrial damage in response to IR injury.....	166
4.3.4	SA-26 inhibits IR-induced NLRP3 assembly on the mitochondrial membrane... ..	169
4.4	Discussion.....	171
5. CHAPTER 5: 19,20-EPOXYDOCOSAPENTAENOIC ACID (19,20-EDP) AMELIORATES CARDIAC ISCHEMIA-REPERFUSION INJURY BY DIRECTLY ACTIVATING MITOCHONDRIAL SIRTUIN 3..179		
	Abstract.....	180

5.1	Introduction	183
5.2	Methods.....	186
5.2.1	Isolated working heart perfusion	186
5.2.2	Isolated Langendorff mouse heart perfusion	187
5.2.3	Analysis of inflammatory cytokines and chemokines in the perfused heart homogenates	190
5.2.4	Human explanted heart tissue	190
5.2.5	Mass spectroscopy (LC-MS/MS)	191
5.2.6	Assessment of mitochondrial respiration in the dissected human myocardial fibers.....	191
5.2.7	Assessment of rate of oxygen consumption in mice cardiac muscle fibers in the presence of different energy substrates	193
5.2.8	Isolation and cultivation of neonatal rat cardiomyocytes	194
5.2.9	Microscopy experiments.....	195
5.2.9.1	Mitochondrial density and morphology	195
5.2.9.2	Mitochondrial membrane potential	196
5.2.9.3	Mitochondrial superoxide levels	196
5.2.10	Immunoblotting.....	196
5.2.11	Enzymatic assays	197
5.2.12	Molecular modeling and docking approaches	198

5.2.12.1	Protein and ligand preparation.....	198
5.2.12.2	Principal component analysis	199
5.2.12.3	Molecular docking simulations	199
5.2.12.4	Molecular Dynamics Simulation and Binding Free Energy Calculation: setup, running & analysis.....	202
5.2.13	Assessment of sirtuin 3 reaction kinetics in the presence and absence of 19,20- EDP.....	205
5.2.14	Statistics	205
5.3	Results	206
5.3.1	19,20-EDP enhanced glucose oxidation and attenuated myocardial ischemia- reperfusion injury in isolated mouse working heart	206
5.3.2	Sirtuin3 mediated the cardioprotective effects of 19,20-EDP against IR injury ..	214
5.3.3	Sirtuin3 is indispensable for preserving glucose energy metabolism in permeabilized mice cardiac fibers.....	219
5.3.4	Preservation of sirtuin 3 activity associated with 19,20-EDP treatment ameliorated the inflammatory surge triggered by IR injury	222
5.3.5	Human left ventricle demonstrated marked changes in the levels of 19,20-EDP and sirtuin 3 activity post-MI.....	226
5.3.6	19,20-EDP improved mitochondrial respiration in fresh fibers isolated from the ischemic human left ventricle.....	228

5.3.7	19,20-EDP ameliorated mitochondrial damage and attenuated ROS production secondary to hypoxia reoxygenation in neonatal rat cardiomyocytes	232
5.3.8	Molecular modeling and docking approaches	235
5.3.8.1	Principal component analysis (PCA) of existing hSIRT3 crystal structures	235
5.3.8.2	19,20-EDP binds to the OP2 site and stabilizes a productive, twisted conformation of NAD ⁺	237
5.3.8.3	19,20-EDP directly enhanced sirtuin 3 activity	239
5.4	Discussion	245
5.4.1	Role of sirtuin 3 in regulating mitochondrial function	246
5.4.2	Role of sirtuin 3 in mitigating ischemia reperfusion injury	247
5.4.3	Role of sirtuin 3 in regulating cardiac energy metabolism	249
5.4.4	Role of sirtuin 3 in ameliorating mitochondrial ROS production.....	250
5.4.5	Role of sirtuin 3 in maintaining mitochondrial respiration.....	252
5.4.6	Role of sirtuin 3 in limiting uncontrolled inflammatory responses	253
5.4.7	Computational structure analyses illustrating the direct binding of 19,20-EDP to sirtuin 3.....	254
5.5	Conclusions and Future directions	256
6.	CHAPTER 6: SUMMARY AND CONCLUSION.....	257
7.	CHAPTER 7: FUTURE RESEARCH DIRECTIONS	262
8.	REFERENCES	266

9. APPENDIX: CAN N-3 POLYUNSATURATED FATTY ACIDS BE CONSIDERED A POTENTIAL ADJUVANT MEDICATION FOR COVID-19-ASSOCIATED CARDIOVASCULAR COMPLICATIONS?.....	335
Abstract	336
9.1 Introduction	337
9.2 COVID-19 and cardiovascular complications	341
9.3 Potential mechanisms of cardiovascular complications in COVID-19 patients	344
9.3.1 Direct pathogen invasion	346
9.3.2 Indirect inflammatory response - Cytokine storm	347
9.3.3 Miscellaneous mechanisms.....	354
9.4 Adverse cardiovascular effects of the proposed empirical/supportive treatments.....	364
9.5 Overview of the n-3 polyunsaturated fatty acids	366
9.5.1 Role of n-3 polyunsaturated fatty acids in patients with respiratory infections and/or sepsis.....	367
9.5.2 Cardiovascular benefits of n-3 polyunsaturated fatty acids.....	369
9.5.3 Potential cardioprotective mechanisms of n-3 PUFAs in the setting of COVID-19.....	370
9.5.3.1 The anti-inflammatory properties of n-3 PUFAs	373
9.5.3.1.1 N-3 PUFAs regulate the expression of several proinflammatory innate immune components and modulate macrophage response	375

9.5.3.1.2	Shifting to the anti-inflammatory COX- and LOX-derived metabolites of n-3 PUFAs.....	378
9.5.3.1.3	Anti-inflammatory features of the n-3 PUFAs-derived specialized pro-resolving mediators (SPMs).....	379
9.5.3.1.4	Role of CYP-mediated metabolites in ameliorating inflammation	381
9.5.3.1.5	N-3 PUFAs alter cell membrane structure and function - modulation of the lipid raft.....	383
9.5.3.2	N-3 PUFAs have the potential to ameliorate mitochondrial dysfunction in the pathogenesis of COVID-19.....	384
9.5.3.3	Direct and indirect effects of n-3 PUFAs on the viral load.....	387
9.5.3.4	Role of n-3 PUFAs in modulating the renin-angiotensin aldosterone system in the setting of COVID-19.....	389
9.5.3.5	N-3 PUFAs possess anti-oxidant properties.....	392
9.5.3.6	N-3 PUFAs have the potential to ameliorate coagulopathy	393
9.5.3.7	Lipid-lowering properties of n-3 PUFAs in the context of COVID-19	395
9.5.4	When and how to intervene with n-3 PUFAs in the context of COVID-19	397
9.6	Summary and conclusion	399

LIST OF TABLES

Table 1. 1: Clinical trials showing positive effect of n-3 PUFAs in the cascade of IHD	43
Table 1. 2: Clinical trials showing no effect of n-3 PUFAs in the cascade of IHD.....	49
Table 1. 3: Examples for the immunomodulatory effects mediated by n-3 PUFA and its metabolites	51
Table 2.1: Respiration was assessed in permeabilized muscle fibers obtained from hearts following ischemia–reperfusion (IR).....	90
Table 3. 1: Mitochondrial respiration was measured in permeabilized cardiac fibers freshly isolated at the end of reperfusion.	120
Table 9. 1: Overview of some proposed pharmacological agents with potential beneficial effects in the setting of COVID-19.....	339
Table 9. 2: Overview of COVID-19-associated cardiovascular complications.....	343
Table 9. 3: Overview of the pharmacological approaches under investigation for ameliorating cytokine storm, hyperinflammatory state, and the associated secondary organ complications in COVID-19 patients.	349
Table 9. 4: Overview of the pharmacological interventions under investigation targeting hypercoagulability and platelet activation in COVID-19 patients.....	355
Table 9. 5: Overview of some proposed pharmacological approaches to attenuate COVID-19 associated cardiovascular injury	358
Table 9. 6: Summary of the ongoing trials investigating pharmacological agents targeting cytokine storm and acute cardiac injury secondary to SARS-CoV-2 infection.	360

LIST OF FIGURES

Figure 1. 1: A schematic illustrating the 3 possible outcomes of myocardial reperfusion based on the magnitude and duration of ischemia.	5
Figure 1. 2: A conceptual illustration of the individual contributions of the acute myocardial ischemia and the reperfusion to the final infarct size..	9
Figure 1. 3: A schematic diagram illustrating the interplay between mitochondrial dysfunction and uncontrolled innate immune reaction in the pathogenesis of myocardial IR injury	12
Figure 1. 4: Alterations in myocardial energy metabolism secondary to IR injury.....	24
Figure 1. 5: Schematic diagram illustrating the inflammatory response secondary to acute cardiac IR injury	29
Figure 1. 6: Overview of n-3 PUFA Metabolism	38
Figure 1. 7: Overview of n-6 PUFA Metabolism	39
Figure 1. 8: Schematic diagram of n-3 PUFAs immunomodulatory effects	61
Figure 1. 9: A schematic illustration of the overall thesis hypothesis and specific objectives....	75
Figure 2. 1: Effects of CYP-derived epoxylipids on postischemic contractile function	88
Figure 2. 2: 19,20-EDP preserved mitochondrial integrity under IR insult	93
Figure 2. 3: 19,20-EDP inhibited cardiac NLRP3 inflammasome activation	95
Figure 2. 4: Postischemic alterations in Txnip, p-Akt, and p-AMPK.	97
Figure 2. 5: Postischemic expression of mitochondrial mitofusins	99
Figure 2. 6: Schematic showing the potential cardioprotective mechanisms	106
Figure 3. 1: Genetic deletion of Epxh2 or pharmacological inhibition (t-AUCB) of soluble epoxide hydrolase (sEH) improved post-ischemic contractile parameters in both males and females....	118

Figure 3. 2: Deficiency of sEH preserved mitochondrial respiratory function following IR injury	120
Figure 3. 3: Deficiency of sEH preserved mitochondrial integrity and limited oxidative stress following ischemia/reperfusion (IR) injury	122
Figure 3. 4: Genetic deletion of <i>Ephx2</i> or pharmacological inhibition of sEH inhibited IR-induced NLRP3 inflammasome activation.....	124
Figure 3. 5: Genetic deletion of <i>Ephx2</i> or pharmacological inhibition of sEH prevented IR-induced activation and translocation of the pro-oxidant Txnip	126
Figure 3. 6: Effect of genetic deletion of <i>Ephx2</i> or pharmacological inhibition of sEH on the post-ischemic expression of mitochondrial mitofusins (Mfns)	128
Figure 3. 7: Schematic showing the potential roles of sEH in IR injury	131
Figure 4. 1: Chemical structures of EDPs and their synthetic analogues	142
Figure 4. 2: Perfusion of hearts with SA-26 improved postischemic contractile parameters. ..	162
Figure 4. 3: Preservation of NAD ⁺ /NADH control ratio and SIRT3 activity limited oxidative stress following IR injury	165
Figure 4. 4: Perfusion of hearts with SA-26 preserved mitochondrial integrity and function under IR insult.....	168
Figure 4. 5: Perfusion of hearts with SA-26 inhibited the IR-induced activation and translocation of the NLRP3 inflammasome to the mitochondria.....	170
Figure 4. 6: Conceptual illustration showing the potential cardioprotective role of the EDP surrogate SA-26 against IR injury	172
Figure 5. 1: Assessment of the sex effect on post-ischemic functional recovery.....	189

Figure 5. 2: Assessment of ex vivo aerobic cardiac function in mice hearts using isolated working heart technique	207
Figure 5. 3: Hearts perfused with 19,20-EDP (10 min before ischemia) in the ex vivo working heart experiment showed improved post-ischemic cardiac recovery	208
Figure 5. 4: Assessment of ex vivo cardiac function in mice hearts using isolated working heart technique	209
Figure 5. 5: Perfusion with 19,20-EDP in the setting of IR injury did not alter palmitate oxidation rate but improved glucose oxidation rate, cardiac efficiency and SIRT3 activity.....	212
Figure 5. 6: Absolute metabolic rates of the mice hearts in the presence of either the vehicle or 19,20-EDP calculated using the isolated working heart technique.....	213
Figure 5. 7: Perfusion of mice hearts with 19,20-EDP in the Langendorff mode improved post-ischemic contractile parameters via maintenance of SIRT3 activity	217
Figure 5. 8: Perfusion of mice hearts with 19,20-EDP in the Langendorff mode improved postischemic contractile parameters	218
Figure 5. 9: Mitochondrial respiration assessed in permeabilized fresh fibers isolated from mice hearts demonstrated reduced capacity for glucose oxidation when SIRT3 is inhibited.	221
Figure 5. 10: Therapeutic effects of 19,20-EDP on cardiac cytokines and chemokines in the setting of IR injury.....	224
Figure 5. 11: Therapeutic effects of 19,20-EDP on cardiac cytokines and chemokines in the setting of IR injury.....	225
Figure 5. 12: Deficiency of 19,20-EDP in human ischemic left ventricular tissues was associated with reduced SIRT3 expression and activity.	227

Figure 5. 13: Treatment with 19,20-EDP improved mitochondrial respiratory function in human ischemic left ventricular tissues 230

Figure 5. 14: Assessment of mitochondrial respiratory function in human ischemic left ventricular tissues..... 231

Figure 5. 15: Treatment of NRCMs, subjected to HR, with 19,20-EDP limited ROS production, preserved mitochondrial density/morphology and maintained mitochondrial membrane potential 234

Figure 5. 16: 19,20-EDP directly binds and enhances the activity of the mitochondrial SIRT..243

Figure 5. 17: Assessment of the effect of direct interaction between SIRT3 and 19,20-EDP...244

Figure 9. 1: Potential mechanisms of SARS-CoV-2-induced cardiovascular complications....345

Figure 9. 2: Potential cardioprotective mechanisms of n-3 PUFAs in the setting of COVID-19.....372

Figure 9. 3: A summary of the anti-inflammatory mechanisms of n-3 PUFAs..... 374

LIST OF ABBREVIATIONS AND SYMBOLS

3-TYP	3-(1H-1,2,3-triazol-4-yl) pyridine
AA	Arachidonic acid
AAR	Area at risk
ACE	Angiotensin converting enzyme
ACS	Acute coronary syndrome
ADP	Adenosine diphosphate
AHA	American Heart Association
ALA	α -Linolenic acid
ALI	Acute lung injury
AMC	7-Amino-4-methylcoumarin
AMPK	5' Adenosine monophosphate-activated protein kinase
Ang II	Angiotensin II
ARB	Angiotensin II receptor blocker
ARDS	Acute respiratory distress syndrome
ASC-1	Apoptosis-associated speck-like protein containing a CARD-1
ASCEND	A Study of Cardiovascular Events in Diabetes
AUDA	12-(3-adamantane-1-yl-ureido)-dodecanoic acid

BMI	Body mass index
BPM	Beats per minute
BSA	Bovine serum albumin
CAD	Coronary artery disease
CaN	Calcineurin
CB2R	Cannabinoid receptor 2
CCL	Chemokine ligand
CCR	Chemokine receptor
CETP	Plasma cholesterol ester transfer protein
CF	Coronary flow
CHD	Coronary heart disease
COLCORONA	Colchicine Coronavirus SARS-CoV2 Trial
COMBOS	Combination of Prescription Omega-3s with Simvastatin
CORIMUNO-19 - SARI	Cohort Multiple Randomized Controlled Trials Open-label of Immune Modulatory Drugs and Other Treatments in COVID-19 Patients - Sarilumab
COX	Cyclooxygenase
COX IV	Cytochrome c oxidase subunit 4
COV-AID	Treatment of COVID-19 Patients with Anti-interleukin Drugs

COVID-19	Coronavirus disease 2019
CRP	C-reactive protein
CS	Citrate Synthase
CVD	Cardiovascular disease
CYP-450	Cytochrome p450
CYS	Cysteine
CysLTs	Cysteinyl leukotrienes
CytoResc	“CytoSorb” Rescue
DAMPs	Damage-associated molecular patterns
DART	Diet and reinfarction trial
DGLA	Dihomo- γ -linolenic acid
DHA	Docosahexaenoic acid
DHDP	Dihydroxydocosapentaenoic acid
DHEQ	Dihydroxyeicosatetraenoic acid
DHET	Dihydroxyeicosatrienoic acid
DiHDPA	Dihydroxydocosapentaneic acid
DiHOME	Dihydroxyoctadecenoic acid
DOIT	Diet and Omega-3 Intervention Trial

Drp-1	Dynamin-related protein-1
DTNB	5,5'-Dithiobis-(2-nitrobenzoic acid)
DTT	Dithiothreitol
EDPs, EpDPE	Epoxydocosapentaenoic acids
EEQ, EpETE	Epoxyeicosatetraenoic acid
EETs	Epoxyeicosatrienoic acids
ELISA	Enzyme-linked immunosorbent assay
EP	E prostanoid
EPA	Eicosapentaenoic acid
<i>EPHX2</i>	Gene encoding soluble epoxide hydrolase enzyme
EPHX4	Epoxide hydrolase 4
EpOME	Epoxyoctadecenoic acid
ER	Endoplasmic reticulum
ERK	Extracellular signal-regulated kinase
ET-1	Endothelin-1
ETC	Electron transport chain
EVOLVE	EpanoVa fOr Lowering Very high triglyceridEs
FA	Fatty acid

FCCP	Carbonyl cyanide p-trifluoromethoxyphenylhydrazone
FFAR4	Free fatty acid receptor 4
Fis1	Fission protein 1
G-CSF	Granulocyte-colony stimulating factor
GAFF	General AMBER Force Field
GAPDH	Glyceraldehyde 3-phosphate dehydrogenase
GISSI-trial	Gruppo Italiano per lo Studio della Sopravvivenza nell'Infarto miocardico
GM-CSF	Granulocyte monocyte-colony stimulating factor
GPR	G-protein coupled receptors
GSH	Glutathione
HDAC	Histone deacetylase
HDHA	Hydroxydocosahexaenoic acid
HDL-c	High density lipoprotein cholesterol
HDoHE	Hydroxy docosaheptaenoic acid
HELP	Human Explanted Heart Program
HEPE	Hydroxyeicosapentaenoic acid
HETE	Hydroxyeicosatetraenoic acid
HF	Heart failure

HFpEF	Heart failure with preserved ejection fraction
HMGB-1	High mobility group box-1
HMPA	Hexamethylphosphoramide
HOPE	Human Organ Procurement and Exchange
HpDHA	Hydroperoxydocosahexaenoic acid
HpETE	Hydroperoxyeicosatetraenoic acid
HR	Hypoxia/reoxygenation
HR	Heart Rate
HR	Hazard ratio
HRP	Horseradish peroxidase
HSaVEC	Human saphenous vein endothelial cells
HSPs	Heat-shock proteins
HUVEC	Human umbilical vein endothelial cells
ICAM-1	Intercellular adhesion molecule-1
ICM	Ischemic cardiomyopathy
ICU	Intensive care unit
IDL-P	Intermediate density lipoprotein
IFD	Induced fit docking

IFN- γ	Interferon- γ
IGF-1	Insulin-like growth factor 1
IHD	Ischemic heart disease
IL	Interleukin
IL-1 β	Interleukin-1beta
IMM	Inner mitochondrial membrane
IR	Ischemia-reperfusion
JELIS	Japan EPA Lipid Intervention Study
JNK	c-Jun NH ₂ -terminal kinase
KHB	Krebs–Henseleit bicarbonate
KC	Keratinocyte chemoattractant chemokine
LA	Linoleic acid
LAD	Left anterior descending coronary artery
LDL	Low-density lipoprotein
Lp-PLA ₂	Lipoprotein phospholipase A ₂
LPS	Lipopolysaccharide
LOX	Lipoxygenases
LT	Leukotriene

LV	Left Ventricle
LVDP	Left ventricular developed pressure
LVEF	Left ventricular ejection fraction
LZD	Lingui Zhugan Decoction
MAHI	Mazankowski Alberta Heart Institute
MaR	Maresin
MCP-1	Monocyte chemoattractant protein-1
MDA	Malondialdehyde
MelCOVID	Melatonin in Patients With COVID-19
MERS-CoV	Middle East respiratory syndrome-related coronavirus
MFF	Mitochondrial fission factor
Mfn1/2	Mitofusin 1 and 2
MHC	Major histocompatibility complex
MI	Myocardial infarction
MID49/51	Mitochondrial dynamics proteins of 49 kDa and 51 kDa
miR	MicroRNA
MMP	Matrix metalloproteinase
MnSOD, SOD2	Manganese superoxide dismutase

MPTP	Mitochondrial permeability transition pore
MSFA	Monounsaturated fatty acids
MSPPOH	N-(methanesulfonyl)-2-(2-propynyloxy)-benzenhexanamide
mtDNA	Mitochondrial DNA
NAC	N-acetylcysteine
NAD ⁺	Nicotinamide adenine dinucleotide
NAM	Nicotinamide
nCoV _s	Novel coronaviruses
NFC	Non-failing control hearts
NF-κB	Nuclear factor kappa-light-chain enhancer activated B-cells
NHE	Na ⁺ /H ⁺ exchanger
NLR	NOD-like receptor
NLRP3	Nucleotide-binding oligomerization domain-like receptor (NLR) family, pyrin domain containing 3
	NOD, LRR and pyrin domains-containing protein 3
	NACHT, LRR and PYD domains-containing protein 3
NMR	Nuclear Magnetic Resonance
NO	Nitric oxide

NRCMs	Neonatal rat cardiomyocytes
NRF	Nuclear respiratory factor
NRVC	Neonatal rat ventricular cardiomyocytes
NYHA	New York Heart Association
OCEAN	Omacor Carotid Endarterectomy Intervention
OMEGA-REMODEL	The Omega-3 Acid Ethyl Esters on Left Ventricular Remodeling After Acute Myocardial Infarction
OMM	Outer mitochondrial membrane
OP2	17-hydroxy-3,6,9,12,15-pentaoxaheptadecan-1-oic acid
Opa-1	Optic atrophy 1
PA	Palmitic acid
PAM	Positive allosteric modulator
PBS	Phosphate-buffered saline
PCA	Principal component analysis
PD	Protectin
PDH	Pyruvate dehydrogenase
PG	Prostaglandin
PGC-1	Peroxisome proliferator-activated receptor gamma coactivator 1.

PGH2	Prostaglandin H2
PKA	Protein kinase A
PKB (AKT)	Protein kinase B
PLA2	Phospholipase A2
PME	Particle Mesh Ewald
PMN	Polymorphonuclear neutrophils
PPAR	Peroxisome proliferator–activated receptor
PPCI	Primary percutaneous coronary intervention
PRR	Pattern recognition receptors
PSP	Peak systolic pressure
PUFAs	Polyunsaturated fatty acids
PVDF	Polyvinylidene difluoride
OR	Odd ratio
ORIGIN	Outcome Reduction with an Initial Glargine Intervention
R&P	Risk and Prevention
RAAS	Renin-angiotensin aldosterone system
RCR	Respiratory control ratio
REDUCE-IT	Reduction of Cardiovascular Events with Icosapent Ethyl–Intervention Trial

RESP	Restrained electrostatic potential
RNA	Ribonucleic acid
ROS	Reactive oxygen species
RUXCOVID	Ruxolitinib in Patients With COVID-19 Associated Cytokine Storm
Rv	Resolvin
SARS-CoV	Severe acute respiratory syndrome coronavirus
SARS-CoV-2	Severe acute respiratory syndrome coronavirus 2
SDH-A	Succinate dehydrogenase subunit A
sEH	Soluble epoxide hydrolase
sEHi	Soluble epoxide hydrolase inhibitor
SERCA	Sarcoplasmic/endoplasmic reticulum calcium ATPase
SFA	Saturated fatty acid
SIRT3	Sirtuin 3
Smad	Suppressor of mothers against decapentaplegic
SEM	Standard error of mean
SPM	Specialized pro-resolving mediators
SR	Sarcoplasmic reticulum
STEMI	ST-Elevation Myocardial Infarction

SU.FOL.OM3	Supplémentation en Folates et Omega-3
T2DM	Type 2 diabetes mellitus
TAC	Transverse aortic constriction
TACTIC-E	mulTi-Arm Therapeutic Study in Pre-ICu Patients Admitted With Covid-19 - Experimental Drugs and Mechanisms
TACTIC-R	mulTi-Arm Therapeutic study in pre-ICu patients admitted with Covid-19 – Repurposed Drugs
TAK1	TGF- β -activated kinase 1
TBA	Thiobarbituric acid
t-AUCB	trans-4-[4-(3-adamantan-1-yl-ureido)-cyclohexyloxy]-benzoic acid
TC	Total cholesterol
TCA	Tricarboxylic acid cycle
Tfam	Mitochondrial transcription factor A.
TG	Triglycerides
TGF- β 1	Transforming growth factor- β 1
THF	Tetrahydrofuran
TIMP	Tissue inhibitor of MMP
TLR	Toll-like receptor

TMAO	Trimethylamine N-oxide
TMB	3,3',5,5'-Tetramethylbenzidine
TMRE	Tetramethylrhodamine ethyl ester
TNB	5-thio-2-nitrobenzoic acid
TNF α	Tumor necrosis factor α
TOC-COVID	Tocilizumab in patients with severe COVID-19 pneumonia
TPPU	1-trifluoromethoxyphenyl-3-(1-propionylpiperidin-4-yl) urea
Trx	Thioredoxin
TrxR	Thioredoxin reductase
TxA2	Thromboxane A2
Txnip	Thioredoxin-interacting protein
VCAM-1	Vascular cell adhesion molecule 1
VDAC	Voltage-dependent anion channel
VEGF	Vascular endothelial growth factor
VITAL	Vitamin D and Omega-3 Trial
VLDL-P	Very low density lipoprotein
VSMC	Vascular smooth muscle cells
WT	Wild-type

CHAPTER 1: INTRODUCTION

This chapter has been adapted from the following published manuscript:

- **Ahmed M Darwesh**, Deanna K Sosnowski, Tim Yt Lee, Hedieh Keshavarz-Bahaghighat, John M Seubert. “Insights into the cardioprotective properties of n-3 PUFAs against ischemic heart disease via modulation of the innate immune system.” Chem Biol Interact. 2019; 308:20-44.

1.1 Ischemic heart disease and reperfusion injury

Ischemic heart disease (IHD) is the most prevalent type of heart disease and a leading cause of cardiovascular morbidity and mortality worldwide [1-4]. The term IHD is applied to a group of closely related syndromes resulting from myocardial ischemia. Ischemia usually arises due to the imbalance or mismatch between myocardial demand and supply of oxygenated blood. Besides insufficiency of oxygen, ischemic events may also result in reduced nutrient availability and impaired removal of metabolic waste products. Several factors contribute to increasing cardiac oxygen demand such as increased heart rate, contractility and elevated blood pressure. While compromised perfusion of the heart is usually attributed to decreased coronary blood flow, coronary vasospasm or hypotension, as well as reduced hematocrit and blood oxygen saturation. In more than 90% of cases, the cause of myocardial ischemia is the reduction in blood flow to the heart due to narrowing or even complete obstruction of the coronary arteries by the formation of atherosclerotic plaques within the vessel walls. Therefore, IHD is often termed coronary artery disease (CAD) or coronary heart diseases (CHD) interchangeably [5-7].

Angina pectoris is a common manifestation of IHD where ischemia is less severe but does not cause cell death in the cardiac muscle, however, it starts to delineate an area at risk (AAR). If the duration and severity of ischemia is prolonged (more than 20 min) a “wave front” of irreversible cardiomyocyte death can occur throughout the myocardium spreading from the subendocardium to the subepicardium, known as myocardial infarction (MI) [8]. Acute MI often results from sudden interruption of blood flow occurring downstream of a blocked vessel due to the rupture or erosion of an unstable atherosclerotic plaque in the coronary arteries, referred to as acute coronary syndrome (ACS) [9-11].

Early and successful myocardial reperfusion or restoration of blood flow to the ischemic myocardium, using either thrombolytic therapy or primary percutaneous coronary intervention (PPCI), is the standard therapeutic intervention to rescue viable myocardial tissue and decrease acute mortality rates. However, reperfusion itself can paradoxically accelerate the death of injured cardiomyocytes, aggravating the damage and increasing the incidence of chronic heart failure (HF). This phenomenon, termed as ischemia-reperfusion (IR) injury, may account for up to 50% of the final infarct size resulting in marked cardiac remodeling leading ultimately to the development of HF [12-14]. The phenomenon of IR injury was initially uncovered over 70 years ago when it was first reported that reperfusion of the dog heart subjected to coronary ligation aggravated the development of cardiac infarction [15].

1.2 Bimodal responses to cardiac ischemia

Most human body tissues can survive short intervals of ischemia that do not produce detectable functional deficits or noticeable injury. However, once a critical duration of ischemia is exceeded, tissue or organ injury develops. Interestingly, it has been demonstrated that exposure of the heart to short bouts of ischemia (< 5 min) and reperfusion (ischemic preconditioning) prior to the prolonged ischemia significantly reduced the infarct size and protected the heart against ischemic injury [16]. Protection induced by ischemic preconditioning stems from the activation of intrinsic cell-survival kinases, such as protein kinase B (AKT, PKB) and extracellular signal-regulated kinase (ERK), early in reperfusion which limits mitochondrial damage [17]. Accordingly, it was concluded that the heart exhibits different responses to ischemia; with longer intervals of ischemia triggering cell damage that is aggravated by reperfusion, short periods of preconditioning ischemia are cardioprotective, reducing the cardiac damage induced by prolonged ischemia that is followed by reperfusion.

1.3 Forms of myocardial ischemia reperfusion injury

The response of tissues to ischemia and reperfusion is determined by the severity and duration of ischemic period, and by the pathological events that originate upon reperfusion [18]. Undoubtedly, prolonged periods of severe ischemia results in greater injury to the heart with postischemic permanent dysfunction as lost cardiomyocytes cannot be replaced due to their limited proliferative capacity. In that sense, restoration of blood flow to the heart at the earliest time possible is obviously of prime importance. Based on the duration and magnitude of ischemia, we can classify myocardial reperfusion injury into 3 major recognized forms, myocardial stunning, myocardial hibernation and lethal ischemia reperfusion injury. The first two are reversible while the third one is irreversible [19] (Figure 1.1).

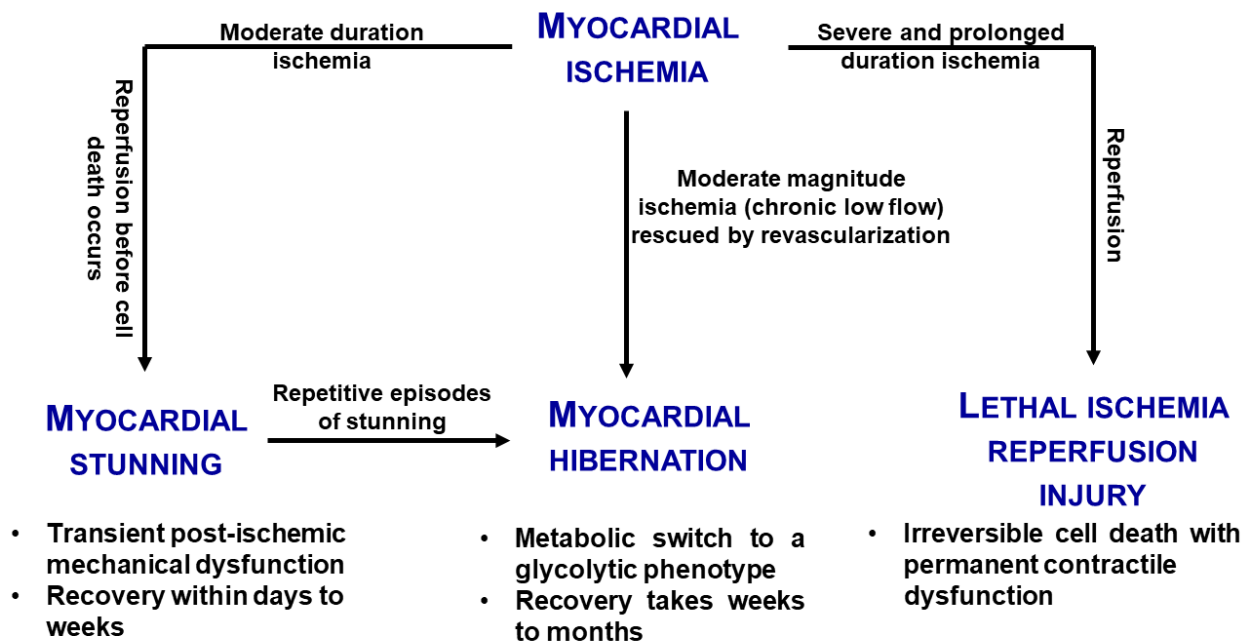


Figure 1. 1: A schematic illustrating the 3 possible outcomes of myocardial reperfusion based on the magnitude and duration of ischemia. Myocardial stunning occurs when the duration and magnitude of myocardial ischemia are not long enough or severe enough to kill cells. Once the heart is reperfused, the myocardium is viable but stunned, exhibiting transient post-ischemic mechanical dysfunction followed by delayed recovery. The second outcome is the myocardial hibernation that occurs secondary to chronic low blood flow to the heart leading to a metabolic shift to a glycolytic phenotype allowing the cardiomyocytes to survive. When the ischemia is relieved by reperfusion, these hibernating cardiomyocytes start to recover within weeks to months. Finally, lethal IR injury is the scenario that occurs secondary to severe and prolonged myocardial ischemia. The myocardial cells die resulting in an infarction and necrotic cells are replaced by scar tissue. Although reperfusion is essential to reduce acute mortality rates, it can paradoxically aggravate the injury leading to a permanent contractile dysfunction. This figure is adapted after [20]

1.3.1 Myocardial stunning

Myocardial stunning is a postischemic mechanical dysfunction that persists for a period of time after reperfusion despite the absence of irreversible damage and despite restoration of normal or near-normal coronary flow [21, 22]. Myocardial stunning results mainly from a relatively short period of ischemia (5–20 min), with reperfusion causing the mechanical dysfunction, followed by delayed recovery. In myocardial stunning, the mechanical dysfunction is not caused by the shortage of myocardial perfusion while it appears to result from reperfusion, which triggers the generation of reactive oxygen species (ROS), transient calcium overload, activation of proteases, such as calpains which proteolyze myofibrils, and altered membrane ion channel activity secondary to rapid restoration of extracellular pH [21-23]. To summarize, myocardial stunning can be considered a relatively mild, sublethal injury that is distinct from MI.

1.3.2 Myocardial hibernation

Cardiomyocytes exposed to extended or repetitive intermittent reductions in the blood supply that are modest in degree followed by a rescue reperfusion, may display an adaptive response termed as myocardial hibernation. Briefly, hibernating heart undergo a metabolic switch to a glycolytic phenotype which favors the use of carbohydrates as an energy source that decreases energy utilization and eventually protects the heart [24, 25]. A plethora of studies reported that myocardial hibernation is associated with upregulation of several stress and angiogenic proteins that also protects the heart from the lethal injury. Overall, myocardial hibernation allows cardiomyocytes to better survive reductions in blood flow associated with subacute levels of ischemia in the absence of irreversible cardiomyocyte injury. Although these adaptive responses reduce myocyte contractile function, reperfusion of the hibernating myocardium reprograms cell

machinery to normalize metabolism and contractile activity leading to cardiac recovery within weeks to months [24, 25].

1.3.3 Lethal myocardial ischemia reperfusion injury

Long duration of severe ischemia followed by reperfusion produce irreversible damage that results in loss of viable myocardium [26]. Reperfusion-induced death of cardiomyocytes that were viable at the end of the ischemic event is defined as lethal myocardial reperfusion injury [13]. The phenomenon of lethal IR injury has been observed in both experimental MI models and in patients with ST-Elevation Myocardial Infarction (STEMI) [14]. Accumulating literature demonstrated that lethal myocardial reperfusion injury may account for up to 50% of the final infarct size and thus represents an important target for cardioprotection in patients undergoing PPCI [27] (Figure 1.2).

Over the past two decades, the use of anti-platelet therapy, β -blockers, statins, and Angiotensin-converting enzyme (ACE) inhibitors together with early reperfusion, have greatly contributed to the reduction in mortality rates after MI [28-30]. However, data from PPCI trials and acute MI registries show that the risk of mortality, particularly in the early phase after STEMI, is still significantly elevated. For instance, in the HEAT-PPCI [31] and HORIZONS-AMI [32] trials, although they excluded high-risk patients and likely underestimated the real mortality risk, mortality rates were 4.7% at 28 days and 2.3% at 30 days, respectively. Moreover, in the OPERA study, the in-hospital mortality rates after STEMI approximates 4.6% [33]. In a more recent cohort of patients with STEMI in Denmark, mortality rate reached 7.9% at 30 days post PPCI [34]. Furthermore, experimental and preclinical observations that some drugs have the potential to limit infarct size secondary to IR injury have encouraged a large number of clinical trials investigating

the therapeutic potential of these agents in the setting of IR injury. However, many of the results of these trials have been negative and inconclusive [35]. Therefore, investigating novel treatment strategies to limit IR injuries becomes imperative.

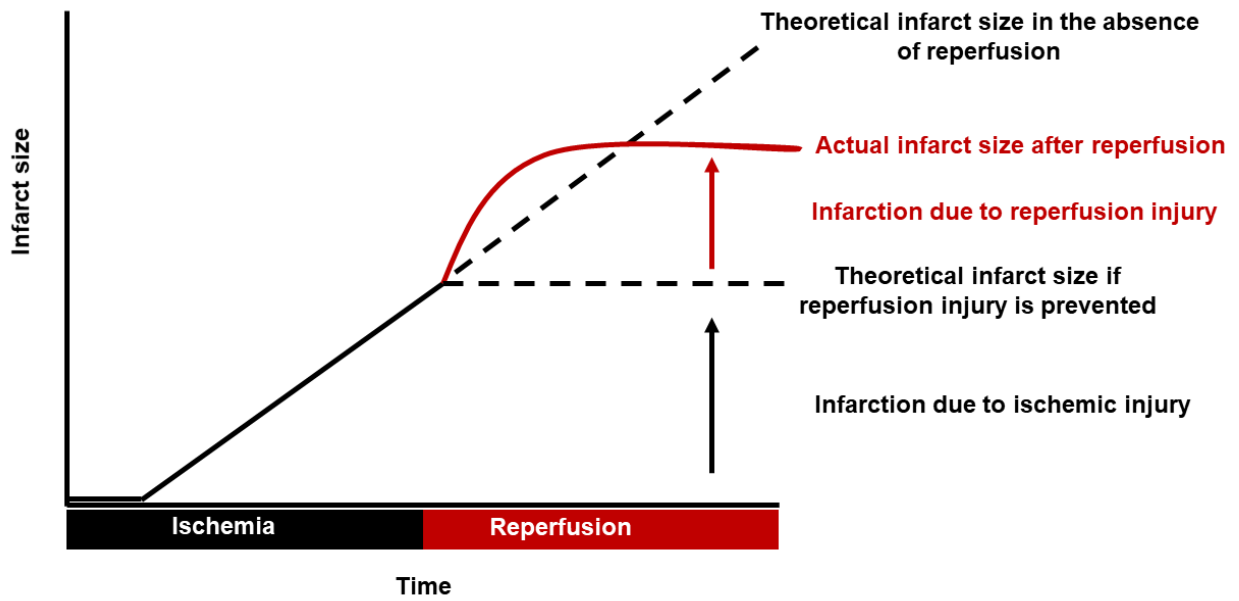


Figure 1. 2: A conceptual illustration of the individual contributions of the acute myocardial ischemia and the reperfusion to the final infarct size. This figure is adapted after [19].

1.4 Lethal ischemia reperfusion injury and cardiac remodeling

The death of cardiomyocytes that occurs in the context of IR injury is associated with a severe decline in cardiac function stemming from marked cardiac remodeling ultimately leading to HF [36-39]. Briefly, it has been demonstrated that the chronic release of mitochondrial reactive oxygen species (ROS) together with persistent inflammation secondary to IR injury not only cause a direct loss of contractile activity but can also trigger geometric changes in the infarcted wall and adaptive changes in the remaining myocardium, which ultimately lead to general dysfunction and dilatation of the ventricle, a process called adverse remodeling [40]. This remodeling leads to impaired left ventricular systolic function, promote the appearance of potentially fatal ventricular arrhythmias, development of left ventricular hypertrophy and progression to HF [41]. Moreover, ROS contribute to fibrosis with phenotypic transformation of fibroblasts to myofibroblasts and collagen deposition which exacerbate the remodeling process [42]. Therefore, development of new pharmacological agents targeting oxidative stress and inflammatory reactions are of supreme importance to protect the heart against the detrimental consequences of the acute myocardial IR injury, and to limit the development of cardiac remodeling and the progression to HF [43, 44].

1.5 Mediators of the lethal myocardial ischemia reperfusion injury

The ultimate cardiac damage secondary to IR injury represents the sum of damage caused by ischemia plus that triggered by reperfusion. Although reperfusion restores the delivery of oxygen and nutrients required for aerobic ATP generation and normalizes extracellular pH, reperfusion itself appears to have detrimental consequences. The mechanisms underlying lethal reperfusion injury are complex, multifactorial, highly integrated and involve mitochondrial dysfunction [45] as evidenced by opening of the mitochondrial permeability transition pore (MPTP) [46], generation of ROS [47], and calcium overload [46, 48-50], in addition to pronounced inflammatory responses [26, 51]. Accordingly, we can summarize the pathways contributing to the pathogenesis of IR injury into the interplay between mitochondrial dysfunction and the exaggerated uncontrolled immune responses which exacerbate and spread the damage throughout the myocardial tissue (Figure 1.3).

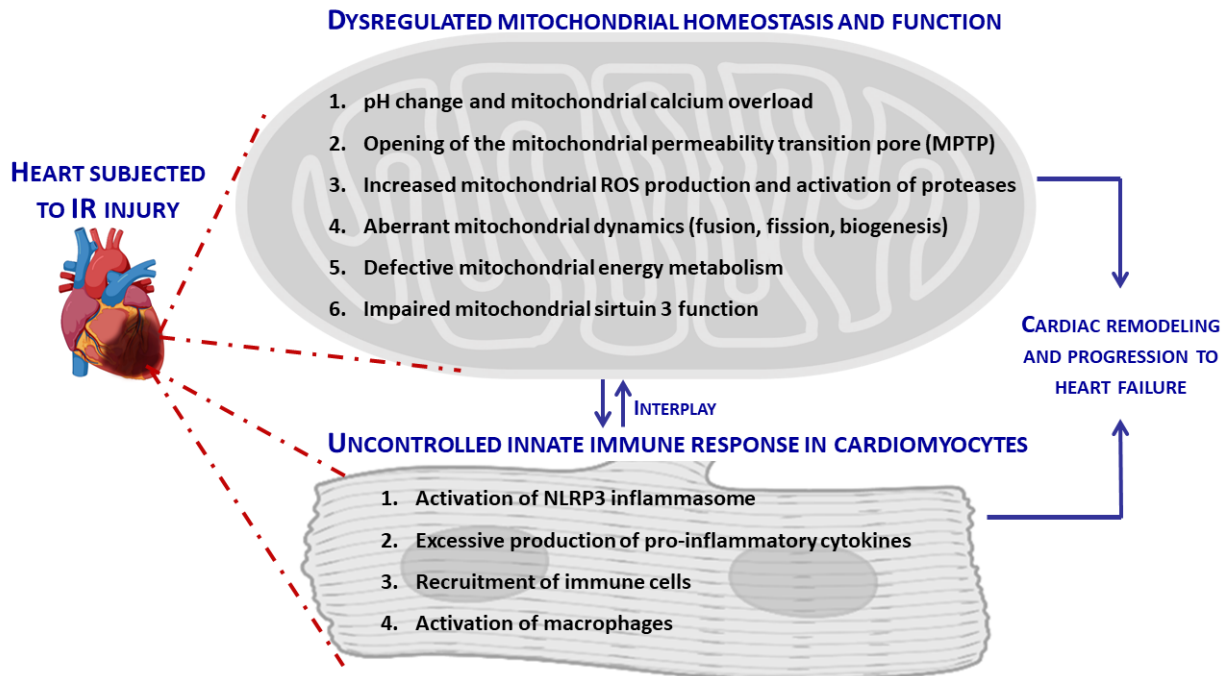


Figure 1. 3: A schematic diagram illustrating the interplay between mitochondrial dysfunction and uncontrolled innate immune reaction in the pathogenesis of myocardial IR injury. Several mechanisms contribute to the impaired mitochondrial homeostasis in the setting of IR injury. These include rapid pH change and the intracellular Ca²⁺ overload, opening of the MPTP, excessive generation of ROS and activation of several proteases, dysregulated mitochondrial dynamics and defective mitochondrial energy metabolism. These effects are associated with uncontrolled immune reactions represented by activation and assembly of NLRP3 inflammasome, excessive production of pro-inflammatory cytokines and chemokines, as well as recruitment and activation of several immune cells. All these changes exacerbate the cardiac damage leading eventually to cardiac remodeling and development of HF.

1.5.1 The role of dysregulated mitochondrial homeostasis in the pathogenesis of ischemia-reperfusion injury

Mitochondria are vital organelles required for healthy cardiac function. In the heart, mitochondria provide the main source of energy that fuels the contractile apparatus [52]. Notably, the heart, which consumes an amount of ATP daily equivalent to approximately 100 times of its weight, does not depend upon stored energy reserves but must constantly be producing it and almost all ATP is generated in the mitochondria of cardiomyocytes. Accordingly, ventricular myocardium is packed full of mitochondria, which account for ~35% of cardiomyocyte volume. Furthermore, the importance of cardiac mitochondrial health and function is beyond ATP synthesis including the regulation of several cellular signaling processes, oxidative stress and many biosynthetic pathways [53]. Therefore, maintaining a healthy mitochondrial pool in the heart is indispensable for preserving cellular homeostasis and sustaining healthy cardiac contractile function.

Mitochondria are vulnerable to significant injury from both ischemia and reperfusion. For instance, IR damages the mitochondrial respiratory chain leading to depletion of ATP, accumulation of mitochondrial ROS, and thus oxidative damage of mitochondrial DNA (mtDNA), proteins and several cellular components, resulting ultimately in myocardial cell death. Importantly, mitochondrial damage is considered a significant sign of the transition of the cardiomyocyte damage from the reversible to the irreversible state [54] as well as the extent or magnitude of mitochondrial damage is a key determinant in the progression of myocardial IR injury towards to HF [55]. Accordingly, new pharmacological agents designed to stabilize or protect mitochondria can provide effective therapeutic approaches to prevent cardiac dysfunction

in response to IR injury. In this section, we will review the main mediators or contributors to mitochondrial dysfunction in the setting of IR injury.

1.5.1.1 pH change and mitochondrial calcium overload

During ischemia, the affected cardiomyocytes become dependent on anaerobic glycolysis for energy supply due to the absence or deficiency of oxygen delivery to the heart. This leads to the accumulation of protons and lactate which, therefore, causes a reduction in the cytosolic pH. Cardiomyocytes then extrudes protons in exchange for sodium via the plasmalemmal Na^+/H^+ exchanger (NHE) in an attempt to reach the standard pH [46, 48, 56, 57]. Afterwards, the sodium ions are exchanged with calcium by the plasmalemmal $\text{Na}^+/\text{Ca}^{2+}$ exchanger leading to the accumulation of calcium in the cytosol. This increase in cytosolic calcium is greatly aggravated by reperfusion, where removal of extracellular protons further increases the proton gradient across the plasmalemma, thereby accelerating NHE exchanger function [46, 56]. Another factor that contributes to the accumulation of cytosolic calcium is the abnormal handling of calcium by the endoplasmic (ER) and sarcoplasmic reticulum (SR) during IR injury. In particular, calcium reuptake into the ER or SR by the sarcoplasmic/endoplasmic reticulum calcium ATPase (SERCA) is compromised during IR injury, whereas calcium release through the ryanodine receptor is enhanced, both of which further exacerbate the lethal elevations in intracellular calcium [49, 50, 58].

Calcium overload plays a crucial role in the deterioration of mitochondrial function and thereby the exacerbation of IR injury. For instance, one of the ways cardiomyocytes deal with this marked increase in the cytosolic calcium is to uptake the calcium into the mitochondria via the mitochondrial calcium uniporter leading to the accumulation of calcium in the mitochondria [50,

58, 59]. Excessive mitochondrial calcium overload inhibits ATP production, exacerbates energy metabolism disorders, triggers MPTP opening and eventually leads to myocardial cell apoptosis [60]. The massive alteration in the calcium homeostasis can also activate a variety of proteins and systems, all of which can contribute to death of cardiomyocytes following IR injury. For instance, calpains, a family of cysteine proteases, are activated by the elevation in calcium levels. Once activated, calpains degrade a wide array of intracellular proteins, including cytoskeletal, ER, and cellular proteins exacerbating the injury [61, 62]. Furthermore, calpastatin, the endogenous inhibitor of calpains, is also often degraded and inhibited in the setting of IR injury which would further increase calpain activation aggravating the cellular injury [63]. Accumulated intracellular calcium can also activate several phospholipases including protein kinase C and phospholipase A (PLA), which destroy the cell membrane skeleton. These reaction produces many toxic products such as leukotrienes (LTs), prostaglandins (PGs), free fatty acids, and oxygen-free radicals which in turn cause mitochondrial dysfunction, increase membrane permeability, and promote massive myocardial cell death [64].

1.5.1.2 Opening of the mitochondrial permeability transition pore (MPTP)

The MPTP is a large nonselective conductance channel in the inner mitochondrial membrane, the opening of which results in mitochondrial membrane depolarization and uncoupling of oxidative phosphorylation, leading to ATP depletion and cell death [65, 66]. In the setting of myocardial IR injury, the MPTP remains closed during ischemia and only opens during reperfusion in response to mitochondrial calcium overload, oxidative stress, ATP depletion, and rapid pH correction [67]. The opening of the MPTP is accompanied by the release of mtDNA and matrix proteins into the cytosol which increases colloid-osmotic pressure in the matrix, triggers the innate immune response, and induces the activation of proteases and lipases, leading to

mitochondrial swelling and cardiomyocyte death [68, 69]. In that sense, several studies demonstrated that preventing MPTP opening during reperfusion reduce infarct size by 40%–50% in small and large animal models [70, 71].

1.5.1.3 Increased mitochondrial ROS production

Mitochondria are considered the largest intracellular source of ROS [72, 73]. Under normal physiological condition, more than 90% of oxygen that enters the cells is reduced to water via the mitochondrial electron transport chain (ETC) in the process of oxidative phosphorylation and about 1– 2% of that oxygen is converted to the superoxide radical, mainly due to “electron leak” at the ETC. In the mitochondria, the superoxide radical is catalytically converted by manganese superoxide dismutase (MnSOD, SOD2), the main mitochondrial antioxidant enzyme, to hydrogen peroxide and molecular oxygen. If accumulated, hydrogen peroxide becomes toxic to body tissues and therefore the antioxidant enzyme Catalase catalyzes the conversion of hydrogen peroxide into water and oxygen, consequently limiting free radical-induced cell damage [74].

Dysregulated mitochondrial ROS production and oxidative stress have been implicated in the pathophysiology of IR injury [75, 76]. During ischemia, not only damage of ETC complexes and electron leakage occurs but also the mitochondrial antioxidant system is highly impacted as evidenced by the impaired activity of the antioxidant enzyme MnSOD and the depletion of several antioxidant substrates such as glutathione, which render cardiomyocytes more susceptible to oxidative stress-induced damage at reperfusion [77, 78]. Restoration of oxygen upon reperfusion exacerbates this pathogenic mechanism as excessive electron leak at the damaged ETC leads to excessive ROS production which exceeds the cells’ antioxidant capacity which is already impaired [79-81].

Elevated ROS levels accelerates and expands myocardial cell death in the setting of IR through oxidative damage to cellular components (such as proteins, lipid and DNA oxidation) [72, 82-85], and activation of MPTP negatively impacting oxidative phosphorylation and energy production [86]. Moreover, toxic ROS can damage mitochondrial respiratory complex I via the oxidation of thiols, which in turn results in the production of excess ROS [87]. This surge of mitochondrial ROS can also initiate a long-term inflammatory response following reperfusion aggravating the injury [88]. Therefore, impaired mitochondrial function associated with excessive ROS production, secondary to IR injury can lead to a vicious cycle of continued injury and reduced cardiac contractile function [46, 47].

1.5.1.4 Aberrant mitochondrial dynamics

Mitochondria are highly dynamic organelles that are constantly moving and undergoing continuous cycles of fusion (forming tubular, intercommunicating networks) and fission (division) to maintain their homeostasis, function, and integrity [89, 90]. For instance, damaged mitochondria are divided by fission into two daughter mitochondria, one healthy and the other is the damaged or the unhealthy one. The healthy mitochondrion can fuse with other healthy mitochondria to exchange lipid membranes and intramitochondrial content. The other defective mitochondrion containing damaged proteins and mutated or flawed mtDNA is removed by lysosome-mediated mitophagy [83, 91-93]. Furthermore, healthy mitochondria can undergo fission to generate two healthy daughter mitochondria for metabolic regulation. This continuous cycle of mitochondrial fission and fusion not only enables a dynamic distribution of mitochondrial proteins and mtDNA through the cellular mitochondrial network, but also regulates the shape, length, and number of mitochondria which is crucial for the maintenance of the optimum function of the mitochondria [85, 94]. This process of mitochondrial dynamics is tightly regulated in the heart in order to

maintain cellular homeostasis as any alterations in the balance of this process can negatively impact mitochondrial morphology and function which, in turn, affects cardiac function and contractility. In the setting of IR injury, it has been shown that dysregulated mitochondrial dynamics is directly linked to the deterioration of cardiac function as, for example, excessive mitochondrial fission and/or impaired fusion and biogenesis could lead to mitochondrial fragmentation and induction of myocardial cell death [95].

1.5.1.4.1 Dysregulated mitochondrial fusion and fission

In mammalian cells, mitochondrial fission is mediated by dynamin-related protein 1 (Drp-1); the outer mitochondrial membrane (OMM)-anchored adapter protein, fission protein 1 (Fis1); mitochondrial fission factor (MFF); and mitochondrial dynamics proteins of 49 kDa and 51 kDa (MID49/51) [96]. Mitochondrial fusion is mediated by the OMM proteins mitofusin 1/2 (Mfn1/2) and the inner mitochondrial membrane (IMM) protein optic atrophy 1 (Opa-1) which maintains the cristae structure [97]. Opa-1 has five isoforms, including two higher molecular weight forms (long-form), referred to as L-Opa-1, and three short-form soluble forms, known as S-Opa-1 [98]. All these proteins are nuclear-encoded and are abundantly expressed in the adult heart [99].

Accumulating literature demonstrated that alteration of proteins involved in mitochondrial fission and fusion is tightly associated with the pathophysiology of several cardiac diseases including IR injury [100-102]. For instance, under normoxic conditions, Drp-1 is located in the cytosol and the phosphorylation at Ser637 residue of Drp-1 by protein kinase A (PKA) inhibits its GTPase activity and its translocation to the mitochondria [103]. During the reperfusion phase, the accumulation of cytosolic calcium activates calcineurin (CaN) that dephosphorylates and consequently activates Drp-1. After that, active Drp-1 translocates to the mitochondria, interacts

with Fis1, Mff, and Mid49/51, oligomerize around OMM and then constricts and cleaves mitochondria by GTP hydrolysis initiating excessive mitochondrial fission and cardiomyocyte death [104, 105]. The excessive activation of the mitochondrial fission protein Drp-1 induces mitochondrial fragmentation, facilitates MPTP opening, aggravates oxidative stress, activates mitochondrial apoptosis, and accelerates cell death. The genetic or pharmacological inhibition of Drp-1 has been shown to reduce the infarct size following MI [106, 107]. Moreover, it has been demonstrated that inhibition of Drp-1 imparts protective effects during myocardial IR by preventing excessive fission [105, 106].

On the other hand, mitochondrial fusion is essential for the physiological functions of mitochondria, including replenishing damaged mitochondrial DNAs and preserving membrane potential [94]. Although both Mfn1 and Mfn2 play a pivotal role in mitochondrial fusion, they exhibit opposite roles in IR injury that could be attributed to the pleiotropic functions of Mfn2 [108]. In the heart, Mfn1 is expressed at a higher level than Mfn2 [109] and is primarily responsible for the fusion of mitochondria. However, Mfn2 acts as a protein stabilizing the interaction because of lower GTPase activity and is involved in other processes including the regulation of mitophagy, altering mitochondrial morphology as well as forming the mitochondria/ER/SR-mitochondrial contact sites [92]. Importantly, it has been shown that, under conditions of ROS-induced stress secondary to IR injury, the down-regulation of Mfn1 disturbs mitochondrial fusion and induces death of cardiomyocytes [110]. Conversely, Mfn2 is upregulated and accumulated in response to the ROS burst and induces the death of cardiomyocytes by inhibiting Akt (protein kinase B) and activating caspase-9 [111, 112]. In the same vein, it has been demonstrated that ablation of Mfn2 delays the opening of MPTP, and consequently mitigates death of cardiomyocytes in the setting of IR injury [113]. Accordingly, it has been concluded that transient inhibition of the accumulation

of Mfn2 in the setting of IR injury limits the damage of mitochondria and renders the cardiomyocytes more resistant to death secondary to IR injury [114]. It is also worth mentioning that ROS also activates the metalloendopeptidase OMA1 that cleaves Opa-1 leading to mitochondrial cristae remodeling, impaired mitochondrial function and consequently cell death [115]. In agreement with this finding, it has been shown that Opa-1^{+/-} mice showed larger infarct sizes compared with wild type, and Opa-1 overexpression results in decreased damage and consequently improved post ischemic cardiac function [116]. Therefore, we can conclude that limiting excessive mitochondrial fission while maintaining mitochondrial fusion could be a potential pharmacological target to reduce myocardial IR injury.

1.5.1.4.2 Dysregulated mitochondrial biogenesis

Mitochondrial biogenesis can be defined as the growth and self-regeneration of mitochondria in which new mitochondria are generated from those existing. Mitochondrial biogenesis is an integral part of mitochondrial homeostasis in which the increase in mitochondrial mass helps compensate for the removal of damaged mitochondria to adapt and respond to the heart's high energetic demand. Furthermore, mitochondrial biogenesis increases the capacity for oxidative phosphorylation, decreases oxidative stress and helps to alleviate mitochondrial dysfunction [117, 118]. There are a large number of transcription factors and regulatory proteins that contribute to the regulation of mitochondrial biogenesis. Among them, the peroxisome proliferator-activated receptor gamma (PPAR γ) coactivator 1 (PGC-1) family of transcriptional coactivators are considered the main regulators of this process. PGC-1 has two types: PGC-1 α and PGC-1 β . PGC-1 α mainly regulates mitochondrial biogenesis by activating nuclear respiratory factor 1 and 2 (NRF1, NRF2), which in turn regulate the ETC complexes' expression and increase the expression of mitochondrial transcription factor A (Tfam). TFAM is not only involved in

enhancing the transcription and replication of mtDNA but also in maintaining the higher structure of mtDNA [119, 120]. Mitochondrial biogenesis was found to be inhibited in a mouse model of cardiac IR injury as it was revealed that oxygen insufficiency induces downregulation of mitochondrial biogenesis by the hypoxia-inducible factor-mediated suppression of PGC-1 α [121]. Yue et al. [122] demonstrated also that IR injury reduces Tfam protein level and exposed mtDNA to oxidative damage associated with excessive production of ROS. Accordingly, preserving and enhancing mitochondrial biogenesis has been considered a promising target to alleviate cardiac IR injury [123, 124].

1.5.1.5 Alteration of mitochondrial energy metabolism

In the heart, mitochondria utilize different energy substrates to generate ATP including fatty acids, glucose, lactate, amino acids, and ketone bodies. Although the contribution of each energy substrate to ATP generation is tightly regulated, there is a significant degree of plasticity and interdependence between the different energy substrates. Under normal physiological conditions, mitochondrial oxidation of fatty acids and carbohydrates produces around 90% - 95% of ATP in the heart and consequently these substrates are considered the major metabolic fuels that sustain the cardiac contractile function [125]. Glycolysis is considered a main contributor to the remainder of ATP content produced in the heart (Figure 1.4A).

In the context of both ischemia and reperfusion, cardiomyocytes suffer from severe stress and damage due to the dramatic alterations that occur in the mitochondrial energy metabolism. During ischemia, mitochondrial oxidative phosphorylation of fatty acids and glucose diminishes due to the deficiency of oxygen and consequently depletion of myocardial ATP occurs [126, 127]. However, rate of anaerobic glycolysis accelerates and becomes the dominant source of energy

during ischemia due to its ability to generate ATP in the absence of oxygen (Figure 1.4B) [126]. As glycolysis only provides a small fraction of ATP compared with that provided by the oxidation of carbohydrates and fatty acids, its ability to maintain normal contractile function and ionic homeostasis is impaired triggering myocardial cells death [128, 129]. Accelerated glycolysis is also associated with increased production of protons, which results in a reduction in the intracellular pH within the ischemic myocardium [130]. Furthermore, because mitochondria cannot oxidize pyruvate during ischemia due to the deficiency of oxygen, it is converted to lactate which also accumulates in the ischemic heart. Importantly, the accumulation of both protons and lactate in the ischemic heart leads eventually to the inhibition of glycolysis in order to prevent further accumulation of these glycolytic by-products which can further deteriorate cardiac function [125]. It is also worth mentioning that during ischemia the ATP synthase runs in reverse order hydrolyzing the remaining amount of ATP in an attempt to maintain the mitochondrial membrane potential and cardiac contractile function [131]. Collectively, the shift of the energy metabolism in the ischemic heart to glycolysis together with the hydrolysis of ATP trigger a rapid fall in ATP content leading to a sharp deterioration in cardiac function. Notably, the inhibition of fatty acid oxidation in the ischemic myocardium results also in the accumulation of toxic fatty acids which can elicit a massive inflammatory response aggravating the cardiac injury [132, 133].

If a previously ischemic myocardium is reperfused in a timely manner, the increased delivery of oxygen to the heart results in restoration of mitochondrial oxidative phosphorylation. However, during this period, rates of fatty acid oxidation recover to a greater extent than rates of glucose oxidation [134, 135] as the heart is exposed to elevated circulating levels of fatty acids as a consequence of ischemic stress [125]. These high levels of fatty acid oxidation reduce the rate of recovery of glucose oxidation, due to the “Randle Cycle” phenomenon (Figure 1.4C) [136].

Importantly, the high rates of fatty acid oxidation are less efficient than glucose as an energy substrate [137], which contributes to a decrease in cardiac efficiency during reperfusion [125, 138]. In addition, the rate of glycolysis remains elevated in the early period of reperfusion which results in continued production of both protons and lactate leading to altered ionic homeostasis and decreased cardiac efficiency during reperfusion [134, 139, 140]. In summary, the high glycolysis and fatty acid oxidation rates accompanied by low mitochondrial glucose oxidation rates and disturbed ionic homeostasis in the post-ischemic reperfused heart result in a decrease in cardiac efficiency and depressed contractile function. Therefore, optimizing energy substrate metabolism during both ischemia and reperfusion is a promising strategy to preserve mechanical function and efficiency and to enhance the recovery of postischemic function.

Contribution of major mitochondrial energy substrates to ATP production

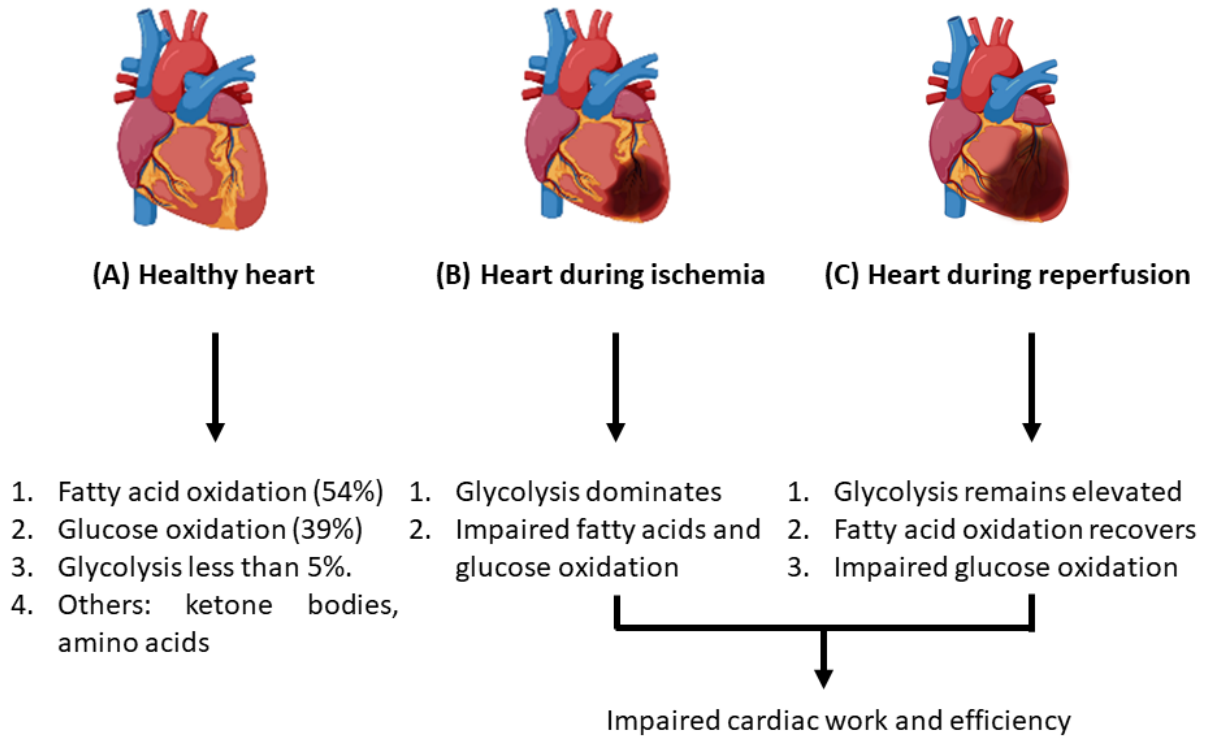


Figure 1. 4: Alterations in myocardial energy metabolism secondary to IR injury. (A) In the aerobic healthy heart, mitochondrial oxidation of fatty acids and glucose is considered the major source of energy production to fuel the contractile function. In contrast, glycolysis provides less than 5% of ATP production. (B) During ischemia, mitochondrial oxidative metabolism of glucose and fatty acid is impaired, and glycolysis becomes a more important source of energy production in response to a decrease in the supply of oxygen. The increase in glycolysis and decrease in glucose oxidation results in the production of both lactate and protons. (C) During reperfusion, mitochondrial oxidative metabolism recovers, but fatty acid oxidation dominates as the source of ATP production, due to increased plasma levels of fatty acids and decreased control of mitochondrial fatty acid uptake. Glucose oxidation rates remain low during reperfusion. Since glycolysis remains elevated, the uncoupling of glycolysis from glucose oxidation persists during reperfusion, leading to an increase in protons and lactate production, which can lead to myocardial acidosis, calcium overload and ultimately decreased cardiac efficiency and function.

1.5.1.6 Impaired mitochondrial sirtuin 3 function

Sirtuins (SIRT1-SIRT7) are highly conserved Nicotinamide Adenine Dinucleotide (NAD⁺)-dependent protein deacetylases that play an essential role in cell homeostasis as energy and redox sensors [141]. Of the SIRT family, SIRT3, SIRT4 and SIRT5 are present in mitochondria [142-145]. Among them, SIRT3 is the only one which exhibits robust deacetylase activity and is considered the primary mitochondrial deacetylase as experimental studies demonstrated that mitochondrial protein acetylation only increases in the heart in the absence of SIRT3 but not the other mitochondrial sirtuins SIRT4 or SIRT5 [142, 146, 147]. SIRT3 regulates mitochondrial function by deacetylating, and thereby activating, numerous mitochondrial proteins involved in energy metabolism [148], oxidative stress responses [149, 150], mitochondrial dynamics [151] and the ETC [152, 153]. Consistently, SIRT3 impairment negatively affects mitochondrial and contractile function in the heart [154]. For instance, it has been shown that SIRT3-knockout mice have 50% less ATP levels than their wild-type littermates and are prone to develop cardiac pathologies at an early age [155, 156].

Accumulating literature has showed that mitochondrial dysfunction secondary to loss or impairment of SIRT3 function has been implicated in several cardiovascular diseases including IR injury. For instance, it has been demonstrated that inhibition or the absence of one or both SIRT3 alleles in the heart (SIRT3^{-/+} or SIRT3^{-/-}) significantly aggravates the reduced cardiac recovery, increased infarct size and cell damage after IR injury. In addition, it has been shown that in the SIRT3^{-/-} hearts, the swelling, breakage, and disarrangement of mitochondria was aggravated in the context of IR injury [157-159]. Moreover, it has been shown that H9c2 cells silenced for SIRT3 expression were more susceptible to IR injury [158]. Therefore, it has been suggested that, in the heart, limiting the loss or activating SIRT3 protects cardiomyocytes from death [158, 160-163]. It

is also worth mentioning that the cofactor NAD^+ is the rate-limiting factor of the functional deacetylase activity of the enzyme SIRT3 [142]. Accordingly, a damaged mitochondrial respiratory chain, as that occurs secondary to IR injury, causes the depletion of NAD^+ which in turn inactivate SIRT3 and disrupts several mitochondrial bioenergetics pathways through the hyperacetylation of many mitochondrial proteins aggravating the injury [164, 165]. In that sense, the development of new pharmacological compounds and approaches that target SIRT3 is essential for preserving normal mitochondrial function and can be considered a novel therapeutic strategy to improve the prognosis of cardiac IR injury.

1.5.2 Role of innate immune system in the pathogenesis of ischemia-reperfusion injury

The innate immune system is considered the first line of the body's defense against injury and insult, which is characterized by an ability to detect and respond quickly to both invading pathogens and sterile cell stressors. The innate response is triggered by the activation of a group of receptors called pattern recognition receptors (PRRs) found on the surface of neutrophils, monocytes/macrophages, endothelial cells and cells in the injured tissue. PRRs are activated following binding of specific microbial motifs or endogenously generated danger signals. Danger signals most commonly stem from cellular debris or intracellular products released early from the injured or damaged cells [166-170]. PRR activation quickly initiates an immune response within the insulted tissue and the whole body by triggering the migration of additional innate immune cells to the affected site, inducing the production of mediators needed for inflammation and repair as well as alerting, instructing and activating the more specific adaptive immune response mediated by T and B lymphocytes [171-175]

Accumulating literature supports the association between the sterile activation of the innate immune system and IHD [176-179]. The incidence of infarction in the myocardium activates the inflammatory reaction which involves two mechanistically distinct phases, the inflammatory phase and the reparatory phase. Death of cardiomyocytes under acute ischemic conditions triggers the initial pro-inflammatory response to first remove necrotic cellular debris from the infarct zone and start the reparative phase. Reperfusion of the ischemic myocardium contributes to tissue loss by accelerating the death of the injured cardiomyocytes exacerbating the pro-inflammatory response and increasing the size of the infarct zone [168, 180-182]. The early pro-inflammatory response is followed by a reparative phase involving resolution of inflammation, myofibroblast proliferation, wound healing and scar formation [183]. Whether these repair mechanisms are beneficial or detrimental to cardiac function is partially dependent upon the amount of tissue damage [184]. Accordingly, persistent or extended inflammatory phase

responses can exaggerate myocardial damage leading to an increase in the infarct size and excessive cardiac remodeling [185]. Treatments targeting the innate immune response may provide a promising therapeutic strategy for limiting infarct size, ameliorating adverse remodeling and improving cardiac function. In this section we will discuss the role the innate immune system has in the pathogenesis and the progression of IHD.

1.5.2.1 Activation of PRRs by damage-associated molecular patterns (DAMPs) (early signaling)

Cardiomyocyte cell death resulting from acute ischemic conditions or reperfusion injury causes the release of cellular debris and contents, referred to as damage-associated molecular patterns (DAMPs, alarmins). Some of these endogenous products can activate the innate immune response in adjacent myocardial cells, myofibroblasts, endothelial cells and migrating immune cells. DAMPs include protein signals such as high mobility group box-1 (HMGB1), S100 proteins or heat-shock proteins (HSPs) and non-protein signals ATP, mitochondrial DNA (mtDNA) and RNA [186-188]. PRRs sense extracellular threats through DAMPs to prime cells for a response to potential injurious conditions. Critical PRRs involved in IHD are toll-like receptors 2 and 4 (TLR2 and TLR4), which are present on various cell types including cardiac, endothelial and circulating immune cells [168, 169, 184, 189-192]. Binding of DAMPs to TLR2 or TLR4 starts the pro-inflammatory phase by activating NF- κ B signaling events. Once activated, NF- κ B translocates to the nucleus driving the expression and release of pro-inflammatory proteins and cytokines including tumor necrosis factor- α (TNF- α), pro-interleukin (IL)-1 β , pro-IL-18, IL-6, IL-8, CXC chemokines (neutrophil chemoattractants), CC chemokines (monocytes and T-lymphocytes chemoattractants) and cell adhesion molecules (e.g., vascular cell adhesion molecule (VCAM), intercellular adhesion molecule (ICAM) and selectins) [193-197]. These mediators promote endothelial activation and permeability, leading to further sequential recruitment of neutrophil and monocytes to the injured myocardium [198, 199] (Figure 1.5).

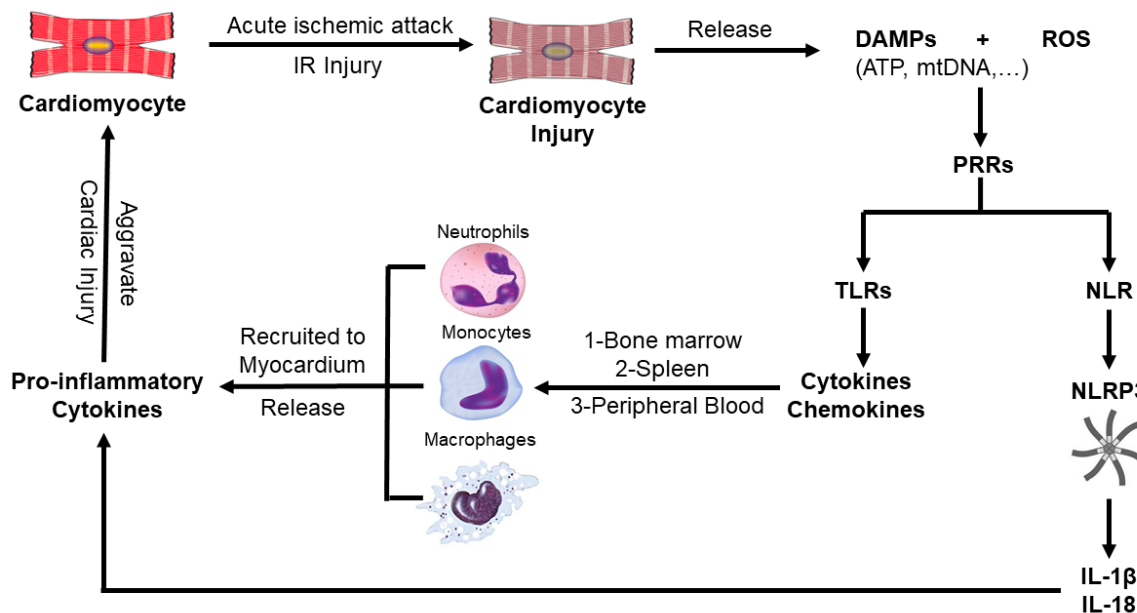


Figure 1. 5: Schematic diagram illustrating the inflammatory response secondary to acute cardiac IR injury. Damage that occurs in cardiomyocytes, in the setting of IR injury, triggers a pro-inflammatory response through the production of DAMPs and ROS, which act on the PRR (TLR, NLR) on the nearby cardiomyocytes, endothelial cells, fibroblasts and resident immune cells. Activation of these receptors stimulate the release of several cytokines and chemokines (such as IL-1 β , IL-18, IL-1 α , IL-6, TNF- α , CCL2, CCL5), which mediate the recruitment and infiltration of inflammatory immune cells (neutrophils, monocytes and macrophages) from the peripheral blood stream, spleen and bone marrow to the injured myocardium. The migration of these cells aggravates the myocardial injury through the release of additional pro-inflammatory cytokines. DAMPs, Damage-associated molecular patterns; IR: Ischemia-Reperfusion; ROS, Reactive oxygen species; mtDNA, mitochondrial DNA; NLRP3, NACHT, LRR and PYD domains-containing protein 3; NLR: NOD-like receptor; PRRs, Pattern recognition receptors; TLRs, Toll-like receptors.

Acute death of cardiomyocytes following acute ischemic and reperfusion conditions can lead to an exaggerated activation of the inflammasome pathway spreading an inflammatory surge to the rest of the myocardium impacting cardiac function [200]. Binding of DAMPs to TLRs or NOD-like receptors (NLR) on cardiac fibroblasts, infiltrating leucocytes and cardiomyocytes will activate the NACHT, LRR and PYD domains-containing protein 3 (NLRP3) inflammasome, a main pro-inflammatory mediator in the setting of IR injury [200-203]. NLRP3 inflammasomes are large multiple protein complex found in the cytosol that consists of a sensor protein (NLR), an adaptor protein (apoptosis-associated speck-like protein containing a CARD-1 (ASC-1)) and a zymogen (procaspase-1) [204]. Once aggregated, NLRs and ASC-1 mediate the cleavage and activation of caspase-1. Active caspase-1 then induces the conversion of pro-IL-1 β and pro-IL-18 to mature IL-1 β and IL-18 respectively, which induces pyroptosis or caspase-1 mediated cell death [203, 205-211]. The release of IL-1 β from cardiac fibroblasts, in response to MI requires two signals: (1) the transcription of pro-IL-1 β by the TLR-NF- κ B pathway, and (2) the activation of pro-IL-1 β to its mature form by the NLRP3 inflammasome. Furthermore, there is now a growing body of evidence suggesting that the NLRP3 inflammasome machinery can be activated through several rapid non-transcriptional pathways triggered by various danger and stress signals such as mitochondrial ROS [212-216]. Once activated, IL-1 β triggers the release of other cytokines and chemokines, which recruit and activate inflammatory cells such as neutrophils and monocytes. In general, IL-1 β is considered a major cytokine mediating the pro-inflammatory response following injury or death of cardiomyocytes [217, 218].

1.5.2.2 Recruitment of different leukocyte populations

The infiltration of the injured myocardium by inflammatory leukocytes is a well-organized process with the chronological recruitment of neutrophils, monocytes and macrophages that has been well documented [219, 220]. The pro-inflammatory and reparative roles of these immune cells in the setting of IHD may have different effects attributable to the functional variation and the amount time the immune cells reside in the injured tissue. As such, the role of leukocytes in the pathogenesis of IHD and post-MI healing may be viewed as a double-edged sword. For example, monocyte/macrophage recruitment is essential for post-MI infarct healing; however, uncontrolled and extensive infiltration may worsen the injury or impair reparative capabilities [221, 222]. Thus, the challenge is how to ameliorate the detrimental effects of these cells, while maintaining their beneficial reparative roles.

1.5.2.2.1 Neutrophils (1-3 days post death of cardiomyocyte)

Neutrophils are the first immune cells to infiltrate the injured myocardium post-infarction. They are recruited from the bone marrow within the first hours of injury and reach a peak after one day before slowly declining [223-225]. Cytokines and chemokines, such as cytokine-induced neutrophil chemoattractant 1 (CINC-1/CXCL1), LTB₄ and IL-8 (CXCL8), produced early in the inflammation cascade promote endothelial activation, permeability and neutrophil recruitment to the infarcted area. The polymorphonuclear neutrophils (PMNs) enter the insulted myocardium by adhering to and rolling on endothelial cells by binding to the cell adhesive molecules P-selectin, E-selectin, VCAM, and ICAMs expressed on activated endothelial cells [198]. Once in the injured myocardium, neutrophils start to remove necrotic cells and tissue debris; however, activated neutrophils can release high levels of ROS, DAMPs, proteolytic enzymes and secrete chemotactic factors further aggravating tissue damage. Excessive neutrophil infiltration and/or their delayed removal may exacerbate myocardial injury by prolonging the pro-inflammatory response [226-

229]. Evidence from clinical studies suggests high levels of neutrophils and their products are correlated to the severity of IHD and infarct size [230].

1.5.2.2.2 Monocytes (3-5 days post death of cardiomyocyte)

Nahrendorf et al. demonstrated a sharp increase in the number of inflammatory monocytes found in blood within the first few hours after coronary blockade reaching a peak 3-5 days post-MI in the injured heart [231]. Monocytes are recruited to the injured myocardium by the increased cardiac and endothelial expression of the chemoattractant chemokine monocyte chemoattractant protein-1 (MCP-1, also called chemokine ligand 2 (CCL2)) and neutrophil-derived granular protein cathelicidin [232-234]. Binding of monocytes and macrophages to CCL2 through their cell surface receptor CC chemokine receptor 2 (CCR2) can induce the expression of other cytokines, MMPs and transforming growth factor- β (TGF- β) causing further cardiac cell death and ventricular dysfunction contributing to injuries [235-237]. IL-1 β is an important stimuli of monocyte recruitment by triggering its production in the spleen and bone marrow following ischemic injury [238-240]. Monocytes and their lineage-descendant macrophages contribute to the resolution of the inflammatory response and ventricular remodeling, yet excessive monocytosis in the post-infarction inflammatory period is deleterious for long-term cardiac function [220, 241, 242]. A large influx of monocytes can contribute to the initial cardiac injury and participate in the release of several inflammatory mediators, proteolytic enzymes and increased ROS production, exacerbating the pro-inflammatory phase.

1.5.2.2.3 Macrophages (5-7 days post death of cardiomyocyte)

The majority of cardiac macrophages are derived and replenished from inflammatory monocytes that differentiate into classical M1 inflammatory macrophages. These cells work to clear the cellular and matrix debris resulting from tissue damage through efferocytosis [243]. Subsequently, reparatory M2 macrophages are formed to promote resolution of inflammation and

contribute to wound healing [231, 244, 245]. Controlled recruitment of macrophages to the injured myocardium is essential for wound healing and tissue repair as defective macrophage clearance of necrotic or apoptotic cells can lead to impaired collagen deposition and scar formation, causing adverse left ventricular remodeling [246-249]. Excessive or prolonged residence of inflammatory M1 macrophages in the infarct myocardium can extend the inflammatory phase and consequently expand the infarcted area, delaying the reparative phase and formation of scar tissue mediated by M2 macrophages and thus aggravating the adverse cardiac remodeling [221, 222, 250].

1.5.2.3 Persistent adverse inflammatory response and LV remodeling

Cardiac remodeling and progression to HF following heart infarction may be influenced by the extent and persistence of the inflammatory response. Following cardiac infarction, an excessive pro-inflammatory response may induce geometric and functional changes in the LV, which includes hypertrophy of the non-infarcted segments and dilatation of the infarcted segments worsening cardiac function [251]. Modulating the persistent or chronic inflammatory response can limit adverse LV remodeling.

During the healing process, the infiltrated macrophages and fibroblasts are responsible for the sustained upregulation of TGF- β , a key mediator in mediating LV remodeling, with its downstream effectors in the myocardium promoting fibrosis and remodeling of the injured cardiac tissue [252, 253]. Active TGF- β binds to its receptor (T β R) at the cell surface and propagates downstream intracellular signals through Smad proteins [254, 255]. Expression of the stimulatory Smad 2, 3, and 4 proteins were shown to be significantly upregulated following cardiac infarction, while expression of the inhibitory Smad7 is decreased in myocardial scars [256, 257]. The activation of the Smad3 signaling pathway mediates extracellular matrix protein synthesis and deposition in the non-infarcted myocardium as well as promotes matrix preservation through increased expression of tissue inhibitors of metalloproteinases (TIMP). TGF- β also activates TGF-

β -activated kinase 1 (TAK1), a potent mediator of cardiomyocyte hypertrophy [252, 258]. Overall, TGF- β -mediated effects contribute to both excessive matrix deposition and pathological hypertrophy post-infarction, leading eventually to dilative cardiac remodeling and severe cardiac dysfunction.

1.5.2.4 The interplay between mitochondrial damage and activation of the innate immune system

Recent studies identified a level of interaction or interplay between mitochondria and innate immune inflammatory responses. Moreover, it has been demonstrated that mitochondrial dysfunction is considered both a trigger and target of uncontrolled inflammatory responses [259-261]. For instance, one explanation of the inflammatory surge secondary to IR injury is that during reperfusion the excessive ROS production from damaged mitochondria triggers the activation of different innate immune cells and induces the formation of inflammasomes, which in turn releases several pro-inflammatory cytokines and chemokines which paradoxically exacerbate myocardial injury [262-264]. It is also well documented that these inflammatory mediators trigger several intracellular cascades that alter mitochondrial metabolism and function. For example, the pro-inflammatory cytokines TNF- α , IL-1 β and IL-6, can impede mitochondrial oxidative phosphorylation and consequently inhibit ATP production [265, 266]. Furthermore, IFN- γ and IL-6 can increase mitochondrial ROS production by directly affecting the ETC exacerbating the cardiac injury [267]. Therefore, therapeutic attempts to protect the mitochondria is considered a promising approach to limit the uncontrolled inflammatory response and to promote survival of the myocardium following IR injury.

1.5.2.5 Modulation of the innate immune response is cardioprotective

Increasing evidence in the literature demonstrates modulating the innate immune system can limit adverse consequences resulting from ischemic injury. Genetic or pharmacological inhibition of TLR2 or TLR4 was demonstrated to blunt the excessive inflammatory response post-MI and attenuate infarct expansion. For example, TLR4-deficient mice sustained smaller infarctions and exhibited less inflammation after myocardial IR injury [268]. Additionally, post-MI hearts in TLR2^{-/-} mice performed better than WT counterparts and were protected against endothelial dysfunction [269]. Interestingly, impaired TLR2 or TLR4 signaling prevented adverse cardiac remodeling and resulted in preserved cardiac function and geometry following MI [270, 271]. Very recently, Yuan et al., showed vaspin, a visceral adipose tissue-derived serine protease inhibitor adipokine, limits the infarct size post IR injury via inhibiting TLR4/NF- κ B signaling pathway both *in vivo* and *in vitro* [272]. In addition, it has been demonstrated that atazanavir, an antiretroviral medication, protects against MI-induced cardiac fibrosis through blocking HMGB1/TLR9 inflammatory signaling pathway in rat hearts [273]. Tanshinone IIA, the main effective component of the Chinese medicine Danshen, has also shown to attenuate MI progression and prevent LV remodeling through inhibition of TLR4/MyD88/NF- κ B signalling pathway in an acute MI rat model [274].

Targeting the NLRP3 inflammasome signaling pathway to inhibit different components (i.e. caspase 1, IL-1 β , ASC-1, or NLRP3 protein) has been demonstrated to reduce infarct size and preserve cardiac function in different models of MI and IR injury [209, 210, 275-278]. Different models support this notion, including evidence demonstrating the cardioprotective effects of cannabinoid receptor 2 (CB2R) agonists involves suppression of NLRP3 inflammasome activation [279]. While Wang et al., provided evidence the hormone Ghrelin protects the heart against IR injury by inhibiting the TLR4/NLRP3 inflammasome pathway [280]. Other research suggests inhibiting CCL2/CCR2 signaling might blunt excessive recruitment of pro-inflammatory

monocyte/macrophage, promote infarct healing, diminish interstitial fibrosis, prevent detrimental remodeling and consequently attenuate contractile dysfunction in the setting of MI [237, 281-283]. Very recently, Wang et al., demonstrated blocking monocyte migration to the infarcted myocardium post-MI with a CCR2 antagonist improved cardiac function and limited the infarct size [284].

Modulating macrophage polarization provides a strategy for reducing infarct size, preventing adverse LV remodeling and preserving cardiac function post-MI. Targeting either pro-inflammatory M1 macrophages or promoting M2 macrophage polarization can facilitate resolution of inflammatory responses and prevent adverse LV remodeling following MI [285-287]. Heinen et al., demonstrated short-term treatment with insulin-like growth factor 1 (IGF1) after acute MI increased the number of the anti-inflammatory M2 macrophages in heart tissue reducing infarct size and improving cardiac function [288]. Moreover, treatment with exogenous IL-19 attenuated acute ischemic injury and improved survival of mice following MI via inhibition of macrophage polarization toward the proinflammatory M1 phenotype while stimulating the polarization and formation of the pro-healing M2 macrophages [289]. Recent evidence suggests the type 2 diabetes mellitus medication, pioglitazone, can limit cardiac remodeling caused by IR injury or ligation of left anterior descending artery (LAD) by antagonizing monocyte/macrophage-mediated acute inflammation promoting cardiac healing. Pioglitazone reduced macrophage recruitment to the injured myocardium and promoted polarization of existing macrophages toward a M2 phenotype [290].

Several lines of evidence indicate that inhibiting the activation of TGF- β and its downstream signaling pathways protects the heart against post-MI cardiac remodeling and fibrosis [291, 292]. For example, the cardioprotective effects of some traditional Chinese medicines, Linggui Zhugan Decoction (LZD) and Qiliqiangxin, are attributed to inhibition of TGF- β 1/Smad-mediated signaling, which reduced myocardial inflammation limiting ventricular

remodeling induced by MI [293]. Further evidence demonstrated downregulating microRNA-330 (miR-330) inhibited the activation of the TGF- β 1/Smad3 signaling pathway suppressing LV remodeling in mice subjected to IR injury [294]. In contrast, microRNA-20b-5p promoted ventricular remodeling following myocardial IR injury in rats by inhibiting the expression of the inhibitory Smad7 by activating TGF- β 1/Smad signaling pathway [295]. Together, these studies highlight a role the innate immune system in the development and progression of MI.

1.6 Overview of n-3 and n-6 polyunsaturated fatty acids

The long-chain n-3 and n-6 polyunsaturated fatty acids (PUFA) are essential fatty acids obtained from dietary sources. They are characterized by the presence of their first double bond at the third (n-3 PUFA) or the sixth position (n-6 PUFA) starting from the omega carbon. The simplest n-3 PUFA is α -linolenic acid (ALA, 18:3 n-3) while linoleic acid (LA, 18:2 n-6) is considered the primary source of the essential n-6 PUFAs. Once inside the body, ALA and LA can be converted into other n-3 and n-6 PUFAs, respectively through a series of elongation and desaturation reactions (Figure 1.6 and 1.7). For instance, ALA is metabolized into eicosapentaenoic acid (EPA, C20:5n-3) which can be further metabolized into docosahexaenoic acid (DHA, C22:6n-3). Using the same series of elongase and delta-4,-5,-6 desaturase enzymes, LA can be converted to dihomo- γ -linolenic acid (20:3n-6; DGLA) and metabolized further to yield arachidonic acid (AA, 20:4n-6). Mammals lack the necessary enzymes (delta-12 and delta-15 desaturase) required to synthesize and interconvert between LA and ALA *de novo*, as such these fatty acids are described as “essential” and must be obtained from the diet [296, 297]. The average daily intake of LA and ALA in Western countries is 10 and 1 g/day, respectively [298]. Importantly, both n-3 and n-6 PUFA compete for the same metabolic enzymes, however, metabolites generated from n-6 PUFAs are predominant as LA is more abundant in western diets than ALA [299-301].

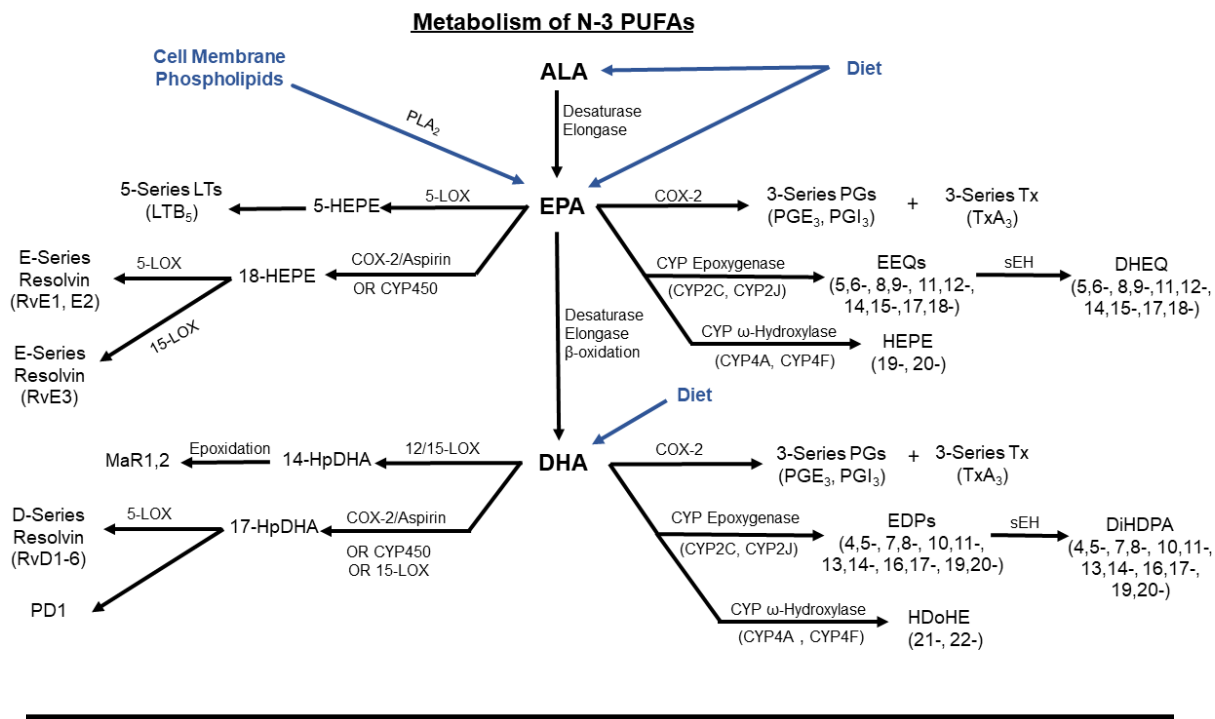


Figure 1. 6: Overview of n-3 PUFA Metabolism. ALA, EPA and DHA are essential fatty acids obtained from dietary sources. EPA and DHA found in cell membrane phospholipids can be released by the enzyme PLA₂. Subsequently, EPA and DHA can be metabolized by COX, LOX and CYP enzymes into a vast array of differing metabolites with numerous physiological functions. ALA, α-Linolenic acid; COX, Cyclooxygenase; CYP, Cytochrome P450; DHA, Docosahexaenoic acid; DiHDDPA, Dihydroxydocosapentaenoic acid; DHEQ, Dihydroxyeicosatetraenoic acid; EDP, Epoxydocosapentaenoic acid; EEQ, Epoxyeicosatetraenoic acid; EPA: Eicosapentaenoic acid; HEPE, Hydroxyeicosapentaenoic acid; HpDHA, Hydroperoxydocosahexaenoic acid; LT, Leukotriene; LOX, Lipoxygenase; MaR, Maresin; PD, Protectin; PG, Prostaglandin; PLA₂, Phospholipase A₂; PUFA, Polyunsaturated fatty acid; Rv, Resolvin; sEH, Soluble epoxide hydrolase; Tx, Thromboxane.

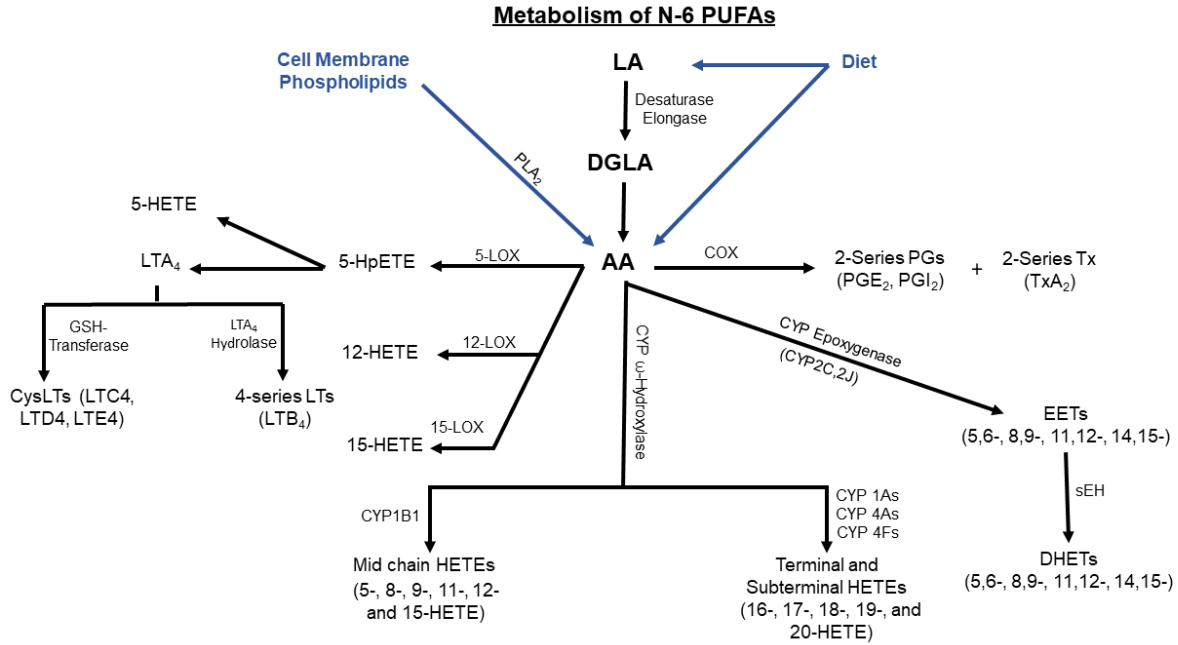


Figure 1. 7: Overview of n-6 PUFA Metabolism. LA and AA are essential fatty acids obtained from dietary sources. AA found in cell membrane phospholipids can be released by the enzyme PLA2. Subsequently, AA can be metabolized by COX, LOX and CYP enzymes into a vast array of differing metabolites with numerous physiological functions. AA, Arachidonic acid; COX, Cyclooxygenase; CYP, Cytochrome p450; CysLTs, Cysteinyl leukotrienes; DHET, Dihydroxyeicosatrienoic acid; DGLA, Dihommo-gamma-linolenic acid; EET, Epoxyeicosatrienoic acids; GSH, Glutathione; HETE, Hydroperoxyeicosatetraenoic acid; HpETE, Hydroperoxyeicosatetraenoic acid; LA, Linoleic acid; LOX, Lipoxygenase; LT, Leukotriene; PG, Prostaglandin; PLA2, Phospholipase A2; PUFA, Polyunsaturated fatty acid; sEH, Soluble epoxide hydrolase; Tx, Thromboxane.

1.6.1 Cardiovascular benefits of n-3 polyunsaturated fatty acids

Early evidence suggesting cardiovascular benefits were associated with n-3 PUFAs originated from epidemiological studies in Greenland Inuit. These studies suggested a higher proportion of EPA compared to AA in their blood was associated with a lower incidence of MI compared to Danish study participants. It was hypothesized that these differences were due to the higher dietary intake of food sources rich in n-3 PUFAs in the Greenland Inuit population [302, 303]. Since then, numerous studies have suggested a role of n-3 PUFA for the prevention of secondary cardiovascular events in patients with documented CAD [304-310] and showed higher intake of n-3 PUFAs lowers the number of mortalities related to cardiovascular diseases (CVD) [311-316]. For example, in a prospective cohort study, Mozaffarian et al. demonstrated higher plasma levels of n-3 PUFA were associated with lower total mortality rates with fewer cardiovascular compared to non-cardiovascular deaths in older adults [317]. In contrast, recent clinical studies challenge the cardiovascular benefits of n-3 PUFAs, indicating a weak or even non-significant relationship between omega-3 fatty acids and reduction in cardiovascular risk, and thus raise questions about the cardiovascular benefits of n-3 PUFAs [318]. Three double-blind trials, the Alpha Omega, the OMEGA and the SU.FOL.OM3, failed to show any additional benefit of n-3 PUFAs on major cardiovascular endpoints [319-321] as well as recent studies have yielded non-significant or less promising results for the cardioprotective effects of n-3 PUFAs [319, 320, 322, 323]. The discrepancies in clinical findings between beneficial and non-beneficial effects might be attributed to several factors, such as overall improved cardiovascular therapy, which includes increased use of beta-blockers, ACEis or ARBs masking any benefits of n-3 PUFAs in more recent studies. Moreover, a lack of standardization of treatment doses, drug formulations and dietary supplementation in the studies impacts bioavailability and cardiovascular effects. For example, marketed products containing the ethyl ester formulation of n-3 PUFAs have been shown to have reduced bioavailability compared to the free fatty acids [324-326].

Overall, there remains uncertainty regarding the beneficial effects n-3 PUFAs toward cardiovascular events and mortality rates (Table 1.1 and 1.2). However, despite these conflicting data, the consumption of n-3 PUFA is recommended by the American Heart Association (AHA) to prevent clinical CVD events in individuals with prevalent CHD, such as a recent MI, to reduce mortality rates and individuals with prevalent HF without preserved left ventricular function to reduce hospitalizations and number of deaths [327, 328]. Importantly, there is a growing understanding of how different metabolites generated from n-3 PUFA impact cellular and organ function, which is providing insight into their potential beneficial role in cardiovascular health [329, 330].

The cardiovascular benefits of n-3 PUFAs may be attributed to their pleiotropic effects on the different components of the cardiovascular system, such as the enrichment of membranes leading to improved organelle and cellular function [331], autonomic tone [332, 333], increasing arrhythmic thresholds [334] and reducing blood pressure [333, 335]. Increased consumption of n-3 PUFAs has a favorable effect on lipid profiles as they replace saturated fatty acids and lower blood triglyceride levels which can stabilize atherosclerotic plaques protecting against IHD [336, 337]. Supplementation with EPA and DHA could also exert a protective effect on the heart through enriching mitochondrial membrane phospholipids composition and thus improving mitochondrial function and increasing the efficiency of ATP generation [338, 339]. Additional cardiovascular benefits of n-3 PUFA stem from their diverse anti-inflammatory properties [340]. For example, the ability of n-3 PUFAs to blunt the excessive activation of the innate immune system was demonstrated to have a positive cardiovascular impact abrogating the progression of IHD [341, 342]. The anti-inflammatory effects of n-3 PUFAs may reduce and stabilize atherosclerotic lesions, which can potentially lead to better outcomes in CAD [343-345]. In addition, growing evidence demonstrates the ability of n-3 PUFAs to reduce circulating levels of inflammatory cytokines, chemokines and pro-inflammatory AA-derived metabolites [338, 346, 347]. The anti-

inflammatory mechanisms of n-3 PUFAs and their metabolites have an important role in regulating and protecting cardiovascular function (Table 1.3).

Table 1. 1: Clinical trials showing positive effect of n-3 PUFAs in the cascade of IHD

Sample criteria and size (n)	Treatment Protocol	Key Findings	Conclusion	Reference
<ul style="list-style-type: none"> - DART Trial: - Prior MI - < 70 years old - (2033) 	<ul style="list-style-type: none"> - Advised to consume 2-3 weekly portions (200-400g) of fatty fish vs. no advice - 2 years 	<ul style="list-style-type: none"> - Significantly reduced death rate (RR=0.71) and reduced IHD event (RR=0.84). 	<ul style="list-style-type: none"> - 2-3 servings of fatty fish per week may reduce all cause mortality and IHD-related deaths in male patients with a history of MI. 	[306]
<ul style="list-style-type: none"> - GISSI – Prevenzione Trial: - Recent MI (≤ 3 months) - (11, 324) 	<ul style="list-style-type: none"> - 0.85-0.882g/day EPA and DHA ethyl esters vs. no treatment control - 3.5 years 	<ul style="list-style-type: none"> - Significantly reduced death, non-fatal MI or stroke (RR=0.85). 	<ul style="list-style-type: none"> - N-3 PUFA supplementation may be effective for secondary prevention of CV events and death. 	[348]
<ul style="list-style-type: none"> - Patients awaiting carotid endarterectomy - (188) 	<ul style="list-style-type: none"> - Fish oil capsules (0.86g/day EPA and 0.52g/day DHA) vs. sunflower oil capsule or placebo control - 42 days 	<ul style="list-style-type: none"> - Significantly higher EPA and DHA in lipid fractions of plaques. - Significantly reduced plaque macrophage infiltration. - No difference in ICAM-1 or VCAM-1 levels and T lymphocytes in plaques. 	<ul style="list-style-type: none"> - N-3 PUFA supplementation may increase carotid plaque stability via reduction of thinning of fibrous caps and plaque inflammation. 	[336]
<ul style="list-style-type: none"> - Autopsy results of deceased Alaskan Natives and Non-natives - Unmatched - (245) 	<ul style="list-style-type: none"> - Observational study. - No intervention 	<ul style="list-style-type: none"> - Significantly higher proportion of EPA and DHA in adipose tissue TG. - Significantly fewer raised atherosclerotic lesions in abdominal LAD coronary artery and right coronary Alaskan Natives. 	<ul style="list-style-type: none"> - Higher dietary intake of n-3 PUFAs may correlate with the observed increase in n-3/n-6 PUFA ratio in adipose tissue and reduced severity of coronary artery plaques. 	[349]

<ul style="list-style-type: none"> - Postmenopausal women - Established CAD - Previous coronary angiography - (288) 	<ul style="list-style-type: none"> - Observational prospective cohort study. - No intervention - 3.2 years 	<ul style="list-style-type: none"> - Significantly reduced mean coronary artery diameter, stenosis, and new lesion development in patients with DHA levels above median values. 	<ul style="list-style-type: none"> - Higher plasma DHA levels may be associated with reduced coronary plaque progression in post-menopausal women with a history of CAD. 	[309]
<ul style="list-style-type: none"> - Confirmed CVD and/or RA and/or OA - Elevated CRP - (99) 	<ul style="list-style-type: none"> - Neptune Krill Oil (NKO) 300mg daily (17% EPA and 10% DHA) vs. placebo - 30 days 	<ul style="list-style-type: none"> - Significantly reduced CRP levels by 7, 14, and 30 days. 	<ul style="list-style-type: none"> - Short term EPA/DHA supplementation may reduce systemic inflammatory response in various chronic inflammatory pathologies and improve overt clinical symptoms. 	[350]
<ul style="list-style-type: none"> - T2DM - Metabolic syndrome - (44) 	<ul style="list-style-type: none"> - 1.8g/day EPA (>98% EPA ethyl ester) + diet intervention vs. diet alone - 3 months 	<ul style="list-style-type: none"> - Significantly reduced CRP, sdLDL, CETP activity, and RLP-TG from baseline. 	<ul style="list-style-type: none"> - EPA supplementation may reduce markers of inflammatory response and improve serum lipid profile in patients suffering from metabolic syndrome at risk for CVD. 	[351]
<ul style="list-style-type: none"> - JELIS Trial: - TC \geq 6.5 mmol/L - LDL-C \geq 4.4mmol/L - Statin treatment - (18,645) 	<ul style="list-style-type: none"> - 1.8g/day EPA vs. statin treatment only - 4.6 years 	<ul style="list-style-type: none"> - Significantly reduced major coronary events (HR=0.81) and unstable angina (HR=0.76). - Reduced fatal and non-fatal MI, coronary events and death. 	<ul style="list-style-type: none"> - Combined EPA and statin therapy in patients with dyslipidemia may reduce the incidence of major coronary events. 	[352]

<ul style="list-style-type: none"> - GISSI-HF Trial: - Chronic heart failure - NYHA class II-IV - (6975) 	<ul style="list-style-type: none"> - 0.85-0.882g/day EPA and DHA ethyl esters vs. placebo - 3.9 years 	<ul style="list-style-type: none"> - Significantly reduced time to death (HR=0.91) and combined time to death or - CV hospital admission (HR=0.92). 	<ul style="list-style-type: none"> - Patients with chronic heart failure supplemented with n-3 PUFAs may experience prolonged survival and reduced CV-associated hospital admissions. 	<p>[353]</p>
<ul style="list-style-type: none"> - COMBOS Trial: - subjects with Residual hypertriglyceridemia despite 8 weeks of diet and simvastatin 40mg/d therapy - (256) 	<ul style="list-style-type: none"> - P-OM3 4 g/d to an ongoing regimen of simvastatin 40 mg/d vs. simvastatin 40mg/day only - 16 weeks 	<ul style="list-style-type: none"> - P-OM3 significantly reduced VLDL-P size and increased low-density LDL-P size without altering HDL-P size. - P-OM3 did not significantly change total VLDL-P or LDL-P concentrations. - P-OM3 significantly lowered large VLDL-P and IDL-P concentrations. - P-OM3 significantly reduced Lp-PLA₂ concentrations. 	<ul style="list-style-type: none"> - High dose n-3 PUFA supplementation in conjunction with statin therapy may improve lipoprotein profiles and reduce inflammatory response in hypertriglyceridemic patients. 	<p>[354]</p>
<ul style="list-style-type: none"> - Hyperlipidemia - (34) 	<ul style="list-style-type: none"> - 7.5g DHA oil (3g DHA)/day vs. placebo - 3 months 	<ul style="list-style-type: none"> - Decreased circulating WBCs, CRP, GM-CSF and IL-6 concentrations. - Increased MMP-2 levels. - No significant change in plasma NO, SAA, G-CSF, IL-1b, IL-2, IL-8, IL-10, TNFα, ICAM-1, VCAM-1, and E-Selectin. 	<ul style="list-style-type: none"> - Short term DHA supplementation may alter the inflammatory response in dyslipidemic male patients by impacting circulating inflammatory biomarker levels which may correlate with improved blood lipid profile and fatty acid composition. 	<p>[355]</p>

<ul style="list-style-type: none"> - OCEAN Trial: - Patients awaiting carotid endarterectomy - (121) 	<ul style="list-style-type: none"> - OMACOR 2g/day (0.81g EPA and 0.675g DHA ethyl esters) vs. placebo - 21 days 	<ul style="list-style-type: none"> - Increased plaque EPA and decreased foam cell composition. - Negative correlation between plaque EPA composition and plaque inflammation, instability and number of plaque T cells. - Significantly lowered plaque MMP-7, MMP-9, MMP-12, IL-6, ICAM-1, and TIMP-2 mRNA levels. 	<ul style="list-style-type: none"> - Increased incorporation of EPA into atherosclerotic plaques in patients with advanced carotid atherosclerosis supplemented with n-3 PUFAs may be associated with reduced plaque inflammation and improved plaque stability. - 	<p>[356]</p>
<ul style="list-style-type: none"> - DOIT Trial: - Cholesterol >6.45 mmol/L - (563) 	<ul style="list-style-type: none"> - 2.4g/day n-3 PUFAs (49% EPA and 35% DHA) vs. placebo - 3 years 	<ul style="list-style-type: none"> - Significantly reduced all-cause mortality (HR=0.53), as well as fatal and non-fatal CV events (HR=0.89). 	<ul style="list-style-type: none"> - Male patients with elevated serum cholesterol supplemented with n-3 PUFAs may experience reduced mortality and incidence of CV events. 	<p>[357]</p>
<ul style="list-style-type: none"> - MARINE Trial: - Elevated TG - (299) 	<ul style="list-style-type: none"> - AMR101 (EPA ethyl ester; icosapent-ethyl) 4g/day and 2g/day vs. placebo - 12 weeks 	<ul style="list-style-type: none"> - Significantly reduced TG levels from baseline <ul style="list-style-type: none"> 1. -33.1% (4g/day) 2. -19.7% (2g/day) 	<ul style="list-style-type: none"> - High and moderate dose EPA supplementation in patients with hypertriglyceridemia may reduce TG levels, improve overall blood lipid profile, and reduce PLA2 activity levels. 	<p>[358]</p>
<ul style="list-style-type: none"> - Previous PPCI - ACS or stable angina - (54) 	<ul style="list-style-type: none"> - Observational study. - No intervention 	<ul style="list-style-type: none"> - Higher colour grade of yellow plaques and number of non-culprit yellow plaques with 	<ul style="list-style-type: none"> - Low serum EPA and EPA/AA ratio may be correlated with 	<p>[359]</p>

		<p>thrombus in patients with low EPA:AA ratio.</p> <ul style="list-style-type: none"> - Association between serum EPA and grade 3 yellow plaques (OR=0.98). 	<p>the observed increase in coronary plaque grade and plaque vulnerability in patients with a history of CVD who have undergone PPCI.</p>	
<ul style="list-style-type: none"> - ANCHOR Trial: - High CVD risk - Statin therapy - Elevated TG - (702) 	<ul style="list-style-type: none"> - AMR101 (EPA ethyl ester; icosapent-ethyl) 4g/day and 2g/day vs. placebo - 12 weeks 	<ul style="list-style-type: none"> - Significantly reduced (A) TG levels <ol style="list-style-type: none"> 1. -21.5% (4g/day) 2. -10.1% (2g/day) (B) Lipoprotein Phospholipase A2 <ol style="list-style-type: none"> 1. -19.0% (4g/day) 2. -18.0% (2g/day) (C) hs-CRP <ol style="list-style-type: none"> 1. -22.0% (4g/day) 2. -6.8% (2g/day) 	<ul style="list-style-type: none"> - In high risk patients on statin therapy with elevated TG, EPA may improve plasma lipid parameters compared to baseline levels as well as reduce markers of systemic inflammation. 	[360]
<ul style="list-style-type: none"> - EVOLVE Trial: - Elevated TG - Untreated dyslipidemia or on stable dose lipid-lowering therapy - BMI \geq 20 - (399) 	<ul style="list-style-type: none"> - EPANOVA (n-3 free fatty acid) 2,3, and 4g/day vs. placebo - 12 weeks 	<ul style="list-style-type: none"> - Significantly reduced (A) TG levels <ol style="list-style-type: none"> 1. -25.9% (2g/day) 2. -25.5% (3g/day) 3. -30.9% (4g/day) (B) Lipoprotein Phospholipase A2 <ol style="list-style-type: none"> 1. -14.9% (2g/day) 2. -11.1% (3g/day) 3. -17.2% (4g/day) - No significant change in hs-CRP 	<ul style="list-style-type: none"> - N-3 PUFA supplementation in conjunction with lifestyle and diet interventions may improve serum lipid parameters but only have a modest effect on inflammatory response. 	[361]
<ul style="list-style-type: none"> - Untreated dyslipidemia with non-culprit thin-cap fibroatheroma (TCFA) lesions - Underwent PPCI or ACS with elevated LDL-C - (30) 	<ul style="list-style-type: none"> - 1.8g/day EPA + rosuvastatin vs. rosuvastatin treatment alone - 9 months 	<ul style="list-style-type: none"> - Greater fibrous cap thickness and decrease in lipid arc and lipid length. - Significantly reduced hs-CRP levels and PTX3 cytokine levels. 	<ul style="list-style-type: none"> - EPA supplementation in addition to statin therapy may enhance fibrous cap stability possibly by reducing plaque 	[362]

		- Lower incidence of macrophage accumulation.	inflammation and systemic inflammatory response compared to statin treatment alone.	
- OMEGA-REMODEL Trial: - Prior MI - (358)	- LOVAZA 4g/day (1.86g EPA and 1.5g DHA ethyl esters) vs. placebo - 6 months	- Significantly reduced 1. LV remodeling 2. hs-CRP 3. Lipoprotein Phospholipase A2 4. Myeloperoxidase levels	- N-3 fatty acids may reduce the extent of myocardial remodeling and fibrosis as well as serum biomarkers of inflammation in patients post-MI.	[363]
- Statin treatment for at least 6 months - Dyslipidemia, stable angina with plan to be treated with bare metal stent - (95)	- 1.8g/day EPA + statin vs. statin alone - 6 months	- Increased EPA:AA ratio from baseline. - Significant increase in fibrous volume and reduction in lipid volume of coronary plaques. - Significant decrease in PTX3 and MCP-1 levels. - Change in lipid volume significantly correlated with PTX3 cytokine and MCP-1 levels.	- Treatment with EPA in conjunction with statin therapy may help improve coronary plaque stability and composition which may be associated with a reduction in local inflammatory biomarker concentrations.	[347]
- REDUCE-IT Trial: - CVD or diabetes - Statin therapy - TG 1.52-5.56 mmol/L - LDL-C 1.06-2.59 mmol/L - (8179)	- VASCEPA (EPA ethyl ester; icosapent-ethyl) 4g/day vs. placebo - 4.9 years	- Significant reduction in CV death, non-fatal MI or stroke, coronary revascularization, or unstable angina (HR=0.75). - Significant reduction in hs-CRP.	- High dose EPA may reduce incidence of major CV events or mortality in patients at high risk for or with established CVD.	[364]

Table 1. 2: Clinical trials showing no effect of n-3 PUFAs in the cascade of IHD

Sample criteria and size (n)	Treatment Protocol	Key Findings	Conclusion	Reference
<ul style="list-style-type: none"> - ALPHA OMEGA Trial: - Prior MI (median 3.7 years) - (4837) 	<ul style="list-style-type: none"> - EPA + DHA 0.4g/day vs. placebo - 3.4 years 	<ul style="list-style-type: none"> - No significant change in major CV events (HR=1.01). 	<ul style="list-style-type: none"> - Low dose dietary supplementation with n-3 PUFAs in patients with previous MI receiving optimized pharmacological therapy may be ineffective for secondary prevention of subsequent major cardiovascular events. 	[319]
<ul style="list-style-type: none"> - OMEGA Trial: - Recent MI (3-14 days) - Received guideline recommended treatment for acute MI - (3851) 	<ul style="list-style-type: none"> - 1g/day (0.46g EPA and 0.38g DHA) vs. placebo - 1 year 	<ul style="list-style-type: none"> - No significant change in sudden cardiac death (OR=0.95). 	<ul style="list-style-type: none"> - Patients receiving guideline-recommended post-MI pharmacological therapy and supplemented with n-3 PUFAs may not receive any additional benefit in prevention of sudden cardiac death, CV events, or total mortality compared to guideline pharmacological therapy alone. 	[320]
<ul style="list-style-type: none"> - Elevated TG - (26) 	<ul style="list-style-type: none"> - High dose n-3 PUFA 3.4g/day EPA+DHA (LOVAZA, 0.465 EPA and 0.375 DHA per 1g capsule) vs. low dose n-3 PUFA 0.85g/day EPA+DHA - 8 weeks 	<ul style="list-style-type: none"> - Decreased TG (-27%). - No significant changes in measures of endothelial function, cholesterol, hs-CRP, IL-1β, IL-6, and TNFα levels or gene expression in lymphocytes. 	<ul style="list-style-type: none"> - Supplementation with high dose n-3 PUFAs may lower TG levels from baseline but have little additional benefit on endothelial function or inflammation compared to low dose n-3 PUFA supplementation. 	[365]
<ul style="list-style-type: none"> - ORIGIN Trial: - High CVD risk 	<ul style="list-style-type: none"> - 0.9g/day EPA and DHA vs. placebo - 6.2 years 	<ul style="list-style-type: none"> - No significant reduction in CV death (HR=0.98). 	<ul style="list-style-type: none"> - N-3 PUFA supplementation in patients with dysglycemia at high risk 	[323]

- Dysglycemia or diabetes - (12,536)			for CVD may not significantly reduce the incidence of major CV events or mortality despite a reduction in TG levels.	
- SU.FOL.OM3 Trial: - Prior MI or ischemic stroke (1-12 months) - (2501)	- 0.6g/day EPA and DHA vs. placebo - 4.2 years	- No significant reduction in CV death, non-fatal MI, or stroke (HR=1.08).	- Secondary prevention of coronary-related events may not be significantly reduced by n-3 PUFAs.	[366]
- R&P Trial: - CV risk factors, - clinical atherosclerosis, - no previous MI - (12,513)	- 1g/day EPA and DHA vs. placebo - 5 years	- No significant reduction in CV death or hospital admission (HR=0.97).	- N-3 PUFAs may not be beneficial for the primary prevention of CV events or death in patients with multiple CV risk factors.	[367]
- ASCEND Trial: - Diabetes - No CVD or atherosclerosis - (15,480)	- 1g/day n-3 PUFAs (460mg EPA and 380mg DHA) vs. placebo - 7.4 years	- No significant difference between first serious CV event rates (RR=0.97).	- N-3 PUFA supplementation may be ineffective as a primary prevention strategy of CV events in patients with type 2 diabetes mellitus.	[368]
- VITAL Trial: - No CV event or cancer history - (25,871)	- OMACOR 1g/day (0.46g EPA and 0.38g DHA) vs. placebo - 5.3 years	- No significant difference in major CV events (HR=0.92).	- N-3 supplementation may not provide any benefit in the primary prevention of major CV events regardless of a patient's CVD risk.	[369]

Table 1. 3: Examples for the immunomodulatory effects mediated by n-3 PUFA and its metabolites

Atherosclerosis and Thrombosis				
N-3 PUFA / Metabolite	Experimental Model	Effects on Different Immune Components	Conclusion	Reference
EPA or DHA	<ul style="list-style-type: none"> - Human platelet-rich plasma - EPA (IC₅₀ = 5.9 μM) or DHA (IC₅₀ = 2.2 μM) added for 90 seconds - Aggregation stimulated using stable TxA₂ mimetic, U46619, fibrinogen and CaCl₂. 	<ul style="list-style-type: none"> - DHA and EPA antagonized TxA₂ and PGH₂ receptor which decreased platelet aggregation. - DHA was found to be more potent than EPA in blocking platelet aggregation. 	<ul style="list-style-type: none"> - EPA and DHA are capable of directly inhibiting agonist interaction with Tx receptor and thus inhibit platelet activation which may serve as a mechanism for their anti-thrombotic effects. 	[370]
DHA	<ul style="list-style-type: none"> - HSAVECs or HUVECs - Pre-treatment with DHA (10 μM) for 24 to 96h - Challenging with the cytokines IL-1α, IL-1β, IL-10, TNF-α, IL-4 or bacterial LPS for an additional 0 to 24h. 	<ul style="list-style-type: none"> - DHA inhibited endothelial activation. - DHA decreased cytokine-induced expression of endothelial and leukocyte adhesion molecules VCAM-1, E-selectin and ICAM-1. - DHA decreased secretion of the inflammatory mediators IL-6 and IL-8. - DHA reduced the adhesion of human monocytes to cytokine-stimulated endothelial cells. 	<ul style="list-style-type: none"> - The anti-inflammatory effects of DHA may contribute to its ability to inhibit the development as well as the progression of atherosclerosis. 	[371]
EPA and DHA	<ul style="list-style-type: none"> - Monocytes obtained from healthy non-smoking adults - Pretreated with a mixture of EPA and DHA at a final ratio 3 EPA : 2 	<ul style="list-style-type: none"> - Mixture inhibited MHC II and ICAM-1. - Mixture reduced CD4 cell activation. 	<ul style="list-style-type: none"> - N-3 PUFAs are efficient in protection against monocyte activation. 	[372]

	<p>DHA (39μM EPA: 26μM DHA) - Challenged with IFN-γ for 48h.</p>			
EPA	<p>- Human monocytic THP-1 cells - Pre-incubated with EPA (60 μM) - Stimulated with LPS for various time periods (6, 12 and 24h)</p>	<p>- EPA attenuated TNF-α production by inhibiting NF-κB activation and binding to DNA.</p>	<p>- EPA might be used for the prevention and alleviation of atherosclerosis as well as the associated-thrombotic episodes.</p>	[373]
Menhaden fish oil (n-3 PUFA: 16% EPA, 19% EPA)	<p>- WT and PPARα-null mice (A) Chronic treatment: Unrestricted access to menhaden fish oil diet for 15 days (B) Acute treatment: Two oral doses of fish oil (0.01 ml/g) at 0 and 12h in a 24h study.</p>	<p>- Fish oil stimulated the secretion of the anti-inflammatory and the anti-atherogenic hormone adiponectin by two folds. - This effect is PPARγ-dependent and PPARα-independent.</p>	<p>N-3 PUFAs possess anti-inflammatory and antiatherogenic properties which could be mediated by stimulation of adiponectin secretion.</p>	[374]
EPA	<p>(A) In vivo experiment: - ApoE$^{-/-}$ or LDL-R$^{-/-}$ mice - Fed on western-type diet \pm 5% EPA (w/w) (5.35 kcal/g) for 13 weeks (B) In vitro experiment: - HUVEC, human monocytic THP-1 cells, and murine</p>	<p>- EPA suppressed the development of atherosclerotic lesions. - EPA stabilized atherosclerotic plaque. - EPA decreased macrophage infiltration in conjunction with increased collagen. - EPA abolished MMP production in macrophage like cells.</p>	<p>- The anti-inflammatory effects of EPA accounts for its ability to prevent the progression and the destabilization of atherosclerotic lesions.</p>	[344]

	<p>macrophage RAW264.7 cells</p> <ul style="list-style-type: none"> - Pre-treated with EPA (1 μM) for 48h - Stimulated with TNF-α (10 ng/ml) for 24h by LPS (10 ng/mL) for 4h. 	<ul style="list-style-type: none"> - EPA upregulated PPARα and thus inhibited NF-kB activation. - EPA attenuated the up-regulation of VCAM-1, ICAM-1 and MCP-1 in HUVECs as well as the expression of MMP-2 and MMP-9 in macrophage-like cells induced by TNF-α. 		
ALA (7.3% w/w)	<ul style="list-style-type: none"> - WT mice - Fed a 0.21% (w/w) cholesterol diet containing either a high (7.3%) or low (0.03%) ALA concentration for 2 weeks - Subjected to photochemical injury for the induction of thrombosis. 	<ul style="list-style-type: none"> - ALA decreased impaired arterial thrombus formation, platelet activation, and NF-κB activity in mice. 	<ul style="list-style-type: none"> - ALA represents an attractive nutritional intervention with direct antithrombotic effects in cardiovascular disorders. 	[375]
EPA	<ul style="list-style-type: none"> - HUVEC - Treated with EPA (3, 10 or 30 μM) in addition to PA (100 μM) for 1 day 	<ul style="list-style-type: none"> - EPA suppressed the PA-induced upregulation of ICAM-1, MCP-1, and IL-6. - EPA inhibited NF-kB pro-inflammatory pathway. 	<ul style="list-style-type: none"> - EPA attenuates saturated fatty acid-induced macrophage cytokine production as well as vascular endothelial dysfunction which explain the anti-atherogenic action of EPA in the clinical setting. 	[376]
RvE1	<ul style="list-style-type: none"> - Female ApoE3 Leiden transgenic mice - Fed an atherogenic diet for 9 weeks 	<ul style="list-style-type: none"> - RvE1 reduced atherosclerotic lesions. - RvE1 did not affect plasma E-selectin, VCAM-1 or MCP-1 levels. 	<ul style="list-style-type: none"> - RvE1 has local anti-inflammatory effects within the aorta and thus attenuates atherogenesis without affecting plasma lipids. 	[377]

	- Treated with either low (1mg/kg/day) or high (5mg/kg/day) RvE1 supplements.	- RvE1 reduced plasma EPHX4 levels. - RvE1 down-regulated the local expression of pro-atherogenic genes in the aorta. RvE1 inactivated IFN- γ and TNF- α signalling pathways in the aorta.		
- EPA alone - DHA alone - EPA+DHA	(A) In vivo: - ApoE -/- mice - Fed western diet supplemented with either 1. EPA (2.5%, w/w), 2. Low-dose EPA + DHA (2.5%, w/w), or 3. High-dose EPA + DHA (5%, w/w) for 20 weeks. (B) In Vitro: - RAW264.7 cells - Pretreated with EPA (3 μ M) or DHA (3 μ M) or their combination for 48h - Challenged by LPS (10 ng/mL) for 4h.	- EPA and DHA additively: 1. Stabilized atherosclerotic plaque 2. Decreased lipid accumulation 3. Attenuated the expression of inflammatory molecules 4. Inhibited macrophage activation 5. Suppressed LPS-induced TLR4 expression in lipid rafts on RAW264.7 cells - Decreased LPS-induced elevation of MCP1, TNF α and MMP9.	- DHA has additional anti-atherosclerotic effects when combined with EPA. - DHA attenuates pro-inflammatory activation of macrophages by inhibiting TLR4 accumulation into lipid rafts.	[378]
Myocardial Infarction				
RvD1	- WT mice - Subjected to the surgical ligation of LAD to induce MI - Injected with either Lipo-RvD1 (3 μ g/kg/day) or free RvD1 (3	- RvD1 reduced neutrophil density in the spleen and discontinued neutrophil recruitment in LV post-MI. - RvD1 stimulated macrophage clearance	- RvD1 exerts potent pro-resolving actions in MI-mediated injury and thereby limited the progression towards LV dysfunction post-MI.	[379]

	<p>µg/kg/day) 3h post-MI and monitored for 5 days.</p>	<p>from infarcted area and promoted early resolution of inflammation post-MI.</p> <ul style="list-style-type: none"> - RvD1 reduced collagen deposition. - RvD1 liposomal formulation offered stability for long-term inflammation resolving effect. 		
Ischemia-Reperfusion Injury				
RvE1	<p>(A) In vivo:</p> <ul style="list-style-type: none"> - Sprague-Dawley rats - Underwent 30 min of ischemia (LAD ligation) and 4h of reperfusion. - Before reperfusion, rats received intravenous RvE1 (0, 0.03, 0.1, or 0.3mg/kg). <p>(B) In vitro:</p> <ul style="list-style-type: none"> - H9c2 cells - Incubated with RvE1 (0, 1, 10, 100, or 1000 nM) - Subjected to 18h normoxia, 16h of hypoxia, or 16h of hypoxia and 2h of reoxygenation. 	<ul style="list-style-type: none"> - RvE1 reduced infarct size. - RvE1 reduced leukocyte infiltration to the ischemic site. 	<ul style="list-style-type: none"> - RvE1 has a direct protective effect on cardiomyocytes against IR injury. 	[380]
EPA	<ul style="list-style-type: none"> - Pigs - Treated with EPA chow (600mg/kg/day) for 3 weeks - Subjected to myocardial ischemia by 90-min occlusion of 	<ul style="list-style-type: none"> - EPA ameliorated myocardial IR injury. - EPA inhibited myocardial Rho-kinase activity. 	<ul style="list-style-type: none"> - Long-term treatment with EPA ameliorates IR injury partly through Rho-kinase pathway inhibition. 	[381]

	the left circumflex coronary artery and subsequent 60-min reperfusion.			
RvD1	<ul style="list-style-type: none"> - Sprague-Dawley rats. - Ischemia: LAD occlusion for 40 min. - Reperfusion for 19 days. - 0.1 µg RvD1 injected into the LV cavity 5 min before ischemia or 5 min after the onset of reperfusion. 	<ul style="list-style-type: none"> - RvD1 decreased neutrophil infiltration into infarcted region. - RvD1 decreased the release of pro-inflammatory cytokines. 	<ul style="list-style-type: none"> - Single RvD1 dose, given 5 min before occlusion or 5 min after the onset of reperfusion, decreases the infarct size post-MI. 	[382]
19,20-EDP	<ul style="list-style-type: none"> - Isolated mouse hearts perfused in the Langendorff mode - Perfused with 1 µM 19,20-EDP - Subjected to 30 min ischemia and followed by 40 min of reperfusion. 	<ul style="list-style-type: none"> - 19,20-EDP inhibited the activation and assembly of NLRP3 inflammasome with its downstream detrimental signals, caspase 1 and IL-1β under IR conditions. 	<ul style="list-style-type: none"> - 19,20-EDP provides protection against IR injury via inhibiting the detrimental NLRP3 inflammasome responses. 	[383]
Cardiac Fibrosis and Remodeling				
EPA	<ul style="list-style-type: none"> - Neonatal rat ventricular cardiomyocytes - Pretreated with 10 µM EPA, - Challenged with 0.1 nM ET-1, on day 5 of culture for 24h 	<ul style="list-style-type: none"> - EPA attenuated TGF-β1 and JNK upregulation caused by ET-1. - EPA reduced ET-1 induced hypertrophy. 	<ul style="list-style-type: none"> - Fish oil may have beneficial protective effects on cardiac hypertrophy. 	[384]
EPA + DHA	<ul style="list-style-type: none"> - WT mice - Fed a fish oil-supplemented diet (12 g menhaden oil + 28 g corn oil 	<ul style="list-style-type: none"> - Fish oil inhibited TGF-β1 induced transformation and proliferation of cardiac fibroblasts and 	<ul style="list-style-type: none"> - N-3 PUFAs prevent cardiac fibrosis and cardiac dysfunction by blocking TGF-β1 - induced phospho- 	[385]

	<p>per kg) for 8 weeks</p> <ul style="list-style-type: none"> - Subjected to TAC surgery - Mice continually fed the fish oil-supplemented diet and euthanized after 3, 7, or 28 days. 	<p>thus reduced cardiac fibrosis.</p>	<p>Smad2/3 nuclear translocation.</p>	
EPA or DHA	<ul style="list-style-type: none"> - WT mice - Started on diets supplemented with 1.9 g/Kg EPA or 1.3 g/Kg DHA for 2 weeks - Subjected to TAC surgery - Diets continued for an additional 6 weeks. 	<ul style="list-style-type: none"> - EPA, not DHA, inhibited TGF-β1 signalling via activation of GRP120 and thus ameliorated cardiac fibrosis. 	<ul style="list-style-type: none"> - EPA-mediated prevention of fibrosis via activation of GRP120 could represent a novel therapy for HFpEF. 	[386]
EPA	<ul style="list-style-type: none"> - DS/obese rat - Fed with low dose (300 mg/kg) or high dose (1g/kg) of EPA for 4 weeks 	<ul style="list-style-type: none"> - EPA increased adiponectin secretion which inactivated NF-κB. - EPA reduced cardiac fibrosis as well as ameliorated LV fibrosis, diastolic dysfunction, oxidative stress and inflammation without lowering blood pressure in DS/obese rats. 	<ul style="list-style-type: none"> - EPA may be suitable for the treatment of cardiac injury associated with metabolic syndrome. 	[387]
EPA	<ul style="list-style-type: none"> - WT mice. - Oral doses of EPA (1g/kg) for 28 days. - Subjected to MI by LAD ligation. - Mice treated again with EPA (1g/kg) once daily for 28 days after MI. 	<ul style="list-style-type: none"> - EPA attenuated fibrosis in the myocardium. - EPA decreased expression of fibrotic genes. - EPA inhibited TGFβ/Smad signalling. 	<ul style="list-style-type: none"> - Long-term administration of EPA improves the prognosis and attenuates chronic cardiac remodeling after MI by modulating the activation of proinflammatory M1 macrophages. 	[388]

<p>DHA or RvD1</p>	<ul style="list-style-type: none"> - Cultured cardiac fibroblasts and peritoneal macrophages isolated from WT and 12/15LOX^{-/-} mice - Treated for 4, 8, 12, and 24h with: <ol style="list-style-type: none"> 1. DHA (50 μM), or 2. RvD1 (10 ng/ml) 	<ul style="list-style-type: none"> - RvD1 showed higher potential than DHA in limiting pro-inflammatory cytokines and chemokine in the absence of 12/15LOX. - RvD1 polarized macrophages towards resolving phenotype (M2) than DHA. - RvD1, but not DHA, diminished expression of COX-2 in 12/15LOX^{-/-} cardiac fibroblast. 	<ul style="list-style-type: none"> - RvD1 possess potent immunomodulating properties, even stronger than DHA, and is a potential candidate for therapeutics in inflammatory diseases including cardiac remodeling. 	<p>[389]</p>
--------------------	--	--	---	--------------

1.6.2 Cardioprotective mechanisms of n-3 PUFAs

1.6.2.1 N-3 PUFAs and their metabolites have the potential to reduce inflammatory responses

Several basic, clinical and epidemiological studies hypothesize that the cardioprotective effects of n-3 PUFAs against IHD are attributed mainly to their immunomodulatory properties [341, 390-393]. The anti-inflammatory effects of EPA, DHA and their biologically active metabolites, are mediated mainly by G-protein coupled receptors (GPR), particularly GPR120 [394], and nuclear receptors particularly peroxisome proliferator-activated receptors (PPAR)- α/γ [395]. This section will highlight the immunomodulatory mechanisms of n-3 PUFAs and the associated cardioprotection against IHD.

1.6.2.1.1 Metabolite-independent effects

1.6.2.1.1.1 Modulation of gene expression of different innate immune components

Emerging evidence demonstrates n-3 PUFAs can regulate the transcription and expression of inflammatory genes such as cytokines, chemokines and adhesion molecules in cardiomyocytes, fibroblasts, endothelial cells, monocytes and macrophages [371, 396-399]. While the exact mechanism(s) remain unknown, n-3 PUFA-mediated events inhibiting NF- κ B pro-inflammatory activity [373, 400-402], or activating PPAR α/γ anti-inflammatory cascades are thought to play a significant role in how they regulate inflammatory genes [395, 403]. The complex cross-talk between transcription factors is exemplified by the activation of PPAR α/γ directly interfering with the activation of NF- κ B preventing translocation to the nucleus reducing the inflammatory burst [404-406]. Interestingly, data from Mishra et al. suggested anti-inflammatory properties of fish oil result from the inhibitory effects of EPA and DHA on NF- κ B activation via a PPAR α -dependent pathway in both human umbilical vein endothelial cells (HUVEC) and microvessel endothelial cells [407]. This idea was further supported by evidence from data

showing treatment of differentiated THP-1 cells and HUVECs with EPA led to the upregulation of PPAR α , which inhibited NF- κ B activation and attenuated TNF α -induced production of MMPs [344]. Another important immunomodulatory mechanism involves activating the GPR120 receptor, which mediates robust and broad anti-inflammatory effects. Research from Oh et al. indicated n-3 PUFAs act on and stimulate GPR120 in both monocytic RAW 264.7 cells and primary intraperitoneal macrophages inhibiting TLR4-mediated inflammatory responses blocking NF- κ B activation [394] (Figure 1.8).

Incorporation of n-3 PUFA such as EPA directly into human atherosclerotic plaques has been associated with a reduced number of foam cells and T cells, less inflammation and increased plaque stability. While the exact mechanism was unknown, the beneficial effects were attributed to suppression of extracellular matrix proteins MMP-7, MMP-9 and MMP-12 involved in remodeling [356]. Limiting adverse left ventricular remodeling and myocardial fibrosis caused by MI or pressure overload stems from an ability of n-3 PUFA to regulate fibrosis and inflammatory signaling. Evidence demonstrates inhibiting the TGF- β 1-induced smad2/3 pathway or activating GPR120 signaling to regulate TAK1 and downstream NF- κ B responses are potential mechanisms [394, 408]. Eclov et al. demonstrated EPA, but not DHA, prevented cardiac fibrosis in a mouse model of pressure overload-induced HF via activation of GPR120 and blocking the TGF- β fibrotic pathway [386]. Long-term administration of EPA in mice for 28 days before and 28 days after experimental MI induction improved the prognosis, reduced the post-MI fibrosis and limited LV remodeling via inhibition of the TGF- β /Smad signaling and promoting macrophage polarization toward the anti-inflammatory M2 phenotype [388]. Further evidence, demonstrated oral administration of EPA to DahlS.Z-Lepr^{fa}/Lepr^{fa} (DS/obese) rats increased adiponectin secretion which inactivated NF- κ B signaling leading to a reduction in cardiac fibrosis and attenuation of diastolic dysfunction [387].

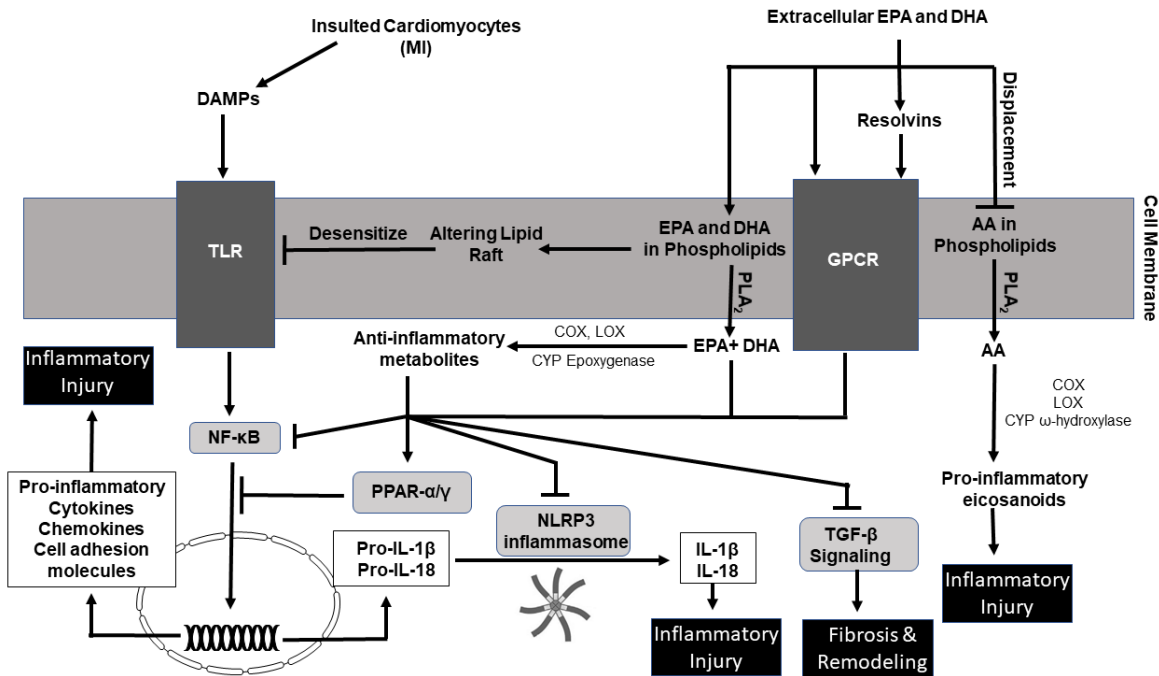


Figure 1. 8: Schematic diagram of n-3 PUFAs immunomodulatory effects. The anti-inflammatory and anti-fibrotic effects of n-3 PUFAs and their metabolites are ascribed to their ability to: (1) incorporate into the cell membrane and displace AA as an alternative substrate for PLA₂, (2) alter the lipid raft restricting the dimerization and pro-inflammatory signaling of TLR, (3) activate GPCR mediated signaling that stimulates PPARs and inhibits NF-κB activity, (4) undergo CYP epoxygenase mediated metabolism into the corresponding anti-inflammatory oxylipins, (5) inhibit the NLRP3 inflammasome cascade, (6) prevent the activation of the pro-fibrotic TGF-β signaling pathway, and, (7) undergo metabolism into anti-inflammatory and pro-resolving lipid mediators resolvins, protectins, and maresins. AA, Arachidonic acid; COX, Cyclooxygenase; CYP, Cytochrome p450; DHA, Docosahexaenoic acid; DAMPs, Damage-associated molecular patterns; EPA, Eicosapentaenoic acid; GPCR, G-protein coupled receptor; IL, Interleukin; LOX, Lipoxygenase; MI, Myocardial infarction; NF-κB, Nuclear factor kappa-light-chain enhancer activated B-cells; NLRP3, NACHT, LRR and PYD domains-containing protein 3; PLA₂, Phospholipase A₂; PPAR, Peroxisome proliferator-activated receptor; TLR, Toll-like receptor; TGF, Transforming growth factor.

1.6.2.1.1.2 Altering the cell membrane structure

Incorporation of n-3 PUFAs into membrane phospholipid bilayers proposes potential insight into the immunomodulatory effects by altering membrane architecture and protein function, which impacts membrane-mediated signaling, generation of bioactive lipids, gene activation, protein trafficking and cytokine secretion [409-413]. The increased membrane incorporation may alter both innate and adaptive immune responses, including the maturation of dendritic cell, macrophage function, as well as T and B cell polarization/activation [414-419]. It was demonstrated that DHA was better than EPA in replacing n-6 PUFAs and cholesterol in plasma membranes of aortic endothelial cells increasing the fluidity of the phospholipid membrane [420]. A change in fluidity can interfere with membrane protein, receptor and transporter function such as the dimerization and expression of the TLR4 subunits, impeding the downstream inflammatory response [378, 421]. Inflammatory cells such as neutrophils, monocytes, macrophages and lymphocytes often contain a large proportion of AA in their membrane. The activation of phospholipase A₂ (PLA₂), the enzyme that liberates AA from the cell membrane, is amongst the earliest biochemical alterations in ischemic myocardium [422-424]. Free AA becomes afterwards a potent source of pro-inflammatory metabolites. However, the substitution of AA with EPA and DHA in the cell membrane, by increasing the consumption of n-3 PUFAs, can alter immune cell reaction in response to inflammatory stimuli by shifting the metabolic profile to less proinflammatory or even anti-inflammatory metabolic profile [425-428].

1.6.2.1.2 Metabolite-dependent effects

As illustrated earlier, the metabolism of n-3 and n-6 PUFAs is closely intertwined as their metabolic pathways compete for the same enzymes. In most cell types, AA is the prevalent PUFA present in membrane phospholipids of cells; for example, in mononuclear cells taken from healthy volunteers consuming a typical Western diet, the mean proportions of LA, DGLA, AA, EPA and DHA were 10, 2, 20, 0.5 and 2.5% of the total fatty acid content [429]. Liberation of AA from the cell membrane by activated PLA₂ under stress conditions generates a wide variety of pro-inflammatory metabolites [430]. The released AA acts as a substrate for cyclooxygenase (COX), lipoxygenase (LOX) and cytochrome P450 (CYP) enzymes to yield a family of oxygenated metabolites. COX converts AA to the 2-series of prostaglandins (PGs) and the 2-series of thromboxanes (TxA), while LOX enzymes metabolize AA to the 4-series LTs and the hydroxyicosatetraenoic acids (HETEs) (Figure 1.7). These metabolites are considered pro-inflammatory mediators that are involved in various pathological processes including IHD [431-434]. Following consumption, n-3 PUFAs compete with n-6 PUFAs for incorporation into cell membranes and for active sites in COX and LOX enzymes to produce less potent pro-inflammatory or even anti-inflammatory metabolites [435]. For example, the production of PGE₂ and LTB₄ by human inflammatory cells was significantly decreased in a diet rich in fish oil [436-439]. N-3 PUFAs can act as a substrate for COX and 5-LOX enzymes resulting in production of the 3-series of PGs and Txs as well as the 5-series LTs, which are a set of less inflammatory or even anti-inflammatory metabolites in comparison to the metabolite family derived from AA [440, 441]. Importantly, 5-, 12- and 15-LOX enzymes are involved in the formation of potent anti-inflammatory mediators derived from the metabolism DHA and EPA called resolvins, protectins and maresins (Figure 1.6). Therefore, the metabolism of n-3 PUFAs by COX and LOX enzymes reduces AA-derived pro-inflammatory metabolites and shifts the metabolic profile toward anti-inflammatory mediators, suggesting a central cardioprotective mechanisms of n-3 PUFAs.

1.6.2.1.2.1 Enhancing COX-derived metabolites of n-3 PUFAs

Numerous studies have shown COX-mediated metabolites of n-6 PUFAs, 2-series PGs and 2-series TxA, play an important role in the pathogenesis of CAD. For instance, TxA₂, a potent vasoconstrictor and platelet aggregator, participates in the initiation and progression of atherogenesis through induction of leukocyte-endothelial cell interaction, platelet activation and thus thrombus formation after the rupture of the atherosclerotic plaque [442]. In addition, a predominant metabolite found in macrophages, PGE₂, induces the expression of MMP enzymes which are crucial in the degradation of atherosclerotic plaque, triggering thrombosis and thus MI induction [443]. However, evidence indicates PGE₂ or its analogues can also protect the heart from IR injury via activation of its receptor subtype E prostanoid receptor 4 (EP₄), suggesting that EP₄ agonists are probably useful for protection against reperfusion-induced cardiac injury [444]. Moreover, Degousee et al. demonstrated PGE₂ could impart a beneficial effect in the infarcted heart by preventing the pathological myocardial remodeling and improve cardiac function after MI [445, 446].

Experimental evidence demonstrates diets rich in n-3 PUFAs shift the balance from TxA₂ to TxA₃ production, increase the levels of PGI₃ and PGE₃ and decrease COX-2 gene expression, reducing the pro-inflammatory mediators and effects attributed to metabolism of AA [447-451]. For example, TxA₃ possesses significantly less potent platelet activation and vasoconstriction properties making it less pro-thrombotic than TxA₂ [452, 453]. Moreover, n-3 PUFAs decrease the affinity of the TxA₂ receptor for TxA₂, thus inhibiting TxA₂-induced platelet aggregation [454]. Research from Tull et al. demonstrated EPA-derived metabolites, PGD₃, can antagonize neutrophil recruitment induced by the AA metabolite, PGD₂, reducing the inflammatory response [455]. 18-hydroxyeicosapentaenoic acids (18-HEPE) is another important metabolite produced

from the metabolism of EPA via either aspirin-acetylated COX-2 [456] or cytochrome P450 monooxygenase [457] enzymes, which possess important anti-inflammatory and anti-fibrotic properties. For example, 18-HEPE was able to prevent macrophage infiltration, cardiac fibrosis and remodeling in a model of transverse aortic constriction (TAC) pressure overload [458]. Together, these studies highlight the complex nature of COX metabolites in the cardiovascular system.

1.6.2.1.2.2 LOX-derived metabolites of n-3 PUFAs

When n-6 PUFAs predominate in cell membranes, proinflammatory mediators such as LTs are produced via the LOX pathways. Conversely, higher ratios of n-3 PUFAs promote secretion of less potent LTs, resulting in a shift to a milieu of less inflammatory mediators. LOX enzymes catalyze the oxidation of AA to produce hydroperoxyeicosatetraenoic acids (HpETEs), which are then reduced to form their HETE derivatives. 5-LOX, 12-LOX and 15-LOX catalyze the metabolism of AA to 5-HETE, 12-HETE and 15-HETE, respectively, which are present in the heart [459-462]. LOX enzymes have a higher affinity for n-3 PUFAs and increased consumption of n-3 PUFAs favors the production of the less pro-inflammatory LTs than the AA-derived inflammatory mediators. For instance, Chapkin et al. illustrated the increased generation of 5-series LTs in macrophages of fish oil-fed mice [450] and neutrophils from humans supplemented with oral fish oil for several weeks [436, 463-466]. Therefore, an increased availability of n-3 PUFAs can shift the metabolism from the detrimental LOX-mediated metabolites of AA, to the less biologically active n-3 PUFA-derived LTB₅ metabolite which possesses 10 to 100 times reduced potency [441, 467-471].

LOX-mediated HETEs are pro-inflammatory and tend to be produced excessively in models of myocardial IR injury [472]. 5-HETE and 12-HETE levels were found to increase significantly in cultured canine myocytes following hypoxia reoxygenation conditions [473].

HETEs play a significant role in the recruitment of leucocytes to damaged areas, production of pro-inflammatory cytokines and contribute to non-resolving inflammation in cardiac pathology [474, 475]. Indeed, elevated expression of 12/15-LOX in mice results in increased pro-inflammatory markers such as MCP-1 and IL-6 and recruitment of monocytes, as well promotes monocyte–endothelial cell interactions that lead to atherogenesis [476-478]. Whereas, 12/15-LOX null mice have significantly lower potential to develop atherosclerosis [479]. Interestingly, reduced plasma levels of 12-HETE in 12/15-LOX null mice resulted in better post-MI survival secondary to the advanced resolution of inflammation [480]. Metabolite products of 12-LOX have a role in the development of cardiac fibrosis and hypertrophy, for example, overexpression of 12-LOX in rat fetal cardiac fibroblasts resulted in growth of cardiac fibroblasts associated with significant elevation of collagen and fibronectin levels, indicative of a fibrotic phenotype [481, 482].

The 5-LOX enzyme catalyzes the conversion of AA to LTA₄, an unstable intermediate, which can be metabolized by LTA₄ hydrolase to LTB₄, a potent chemoattractant, or conjugated to glutathione producing the cysteinyl LTs (CysLTs), including LTC₄, LTD₄, and LTE₄ [483-485]. Interest in the possible involvement of LTs in the development of IHD stems from studies demonstrating robust relationships between LTs and an increased risk of atherosclerotic plaques and development of MI [486, 487]. The 4 series LTs from 5-LOX mediated metabolism are abundantly expressed in arterial walls of patients with atherosclerosis. As 5-LOX is mainly localized in macrophages, dendritic cells, foam cells, mast cells and neutrophilic granulocytes, increased numbers of these cells, and consequently LT production, are associated with atherosclerotic lesions [488-490]. LTs have a role in the migration and infiltration of leukocytes to injured tissues as several reports indicate a correlation between myocardial infarct size with the extent of LT-mediated leukocyte recruitment to the injured myocardium [219, 491].

Involvement of CysLT in the pathogenesis and progression of IHD comes from studies demonstrating increases in LTC₄ and LTD₄-mediated expression of the adhesion molecule P-

selectin in human endothelial cells and enhanced pro-inflammatory signals of IL-8, CXCL-2 and COX-2 correlating with worse outcomes [492-494]. Earlier studies demonstrated increased levels of CysLTs in CAD had numerous aggravating consequences including vasoconstrictive effects on coronary arteries, inducing coronary smooth muscle cell proliferation and inflammation as well as negative inotropic action all of which worsen the prognosis [495, 496]. Ni et al. showed that activation of endothelial and non-endothelial CysLT receptors increases vascular permeability and facilitates the recruitment of leukocytes exacerbating the consequences of IR injury [497]. While the exact mechanisms remain unknown, early work by Hock et al. showed that antagonism of CysLTs receptor reduced the magnitude of myocardial necrosis in a feline model of IR injury [498]. Together, the detrimental effects of CysLT may worsen the clinical manifestation of IHD.

1.6.2.1.2.3 CYP-derived metabolites of n-3 PUFAs

CYP2J and CYP2C isoforms, the constitutively expressed CYP epoxygenases found in the cardiovascular system metabolize EPA into 5 regioisomeric epoxyeicosatetraenoic acids (5,6-, 8,9-, 11,12-, 14,15-, 17,18-EEQ) and DHA into 6 regioisomeric epoxydocosapentaenoic acids (4,5-, 7,8-, 10,11-, 13,14-, 16,17-, 19,20-EDP) [499-503]. CYP epoxygenases preferentially catalyze the epoxidation of the terminal double bond of n-3 PUFAs generating 17,18-EEQ and 19,20-EDP which become the predominant endogenous lipid mediators produced in most tissues, including the lung, kidney, heart and plasma [501, 504, 505]. Of note, these epoxylipids appear to be more effective at lower concentrations compared to their parental n-3 PUFA. For example, Falck et al. showed that 17,18-EEQ was able to protect neonatal rat cardiomyocytes against Ca^{2+} -overload with an $EC_{50} \sim 1-2$ nM, while EPA required prolonged incubation and a ~ 1000 -fold higher concentration to produce the same effect [506]. The epoxy metabolites EEQs and EDPs may then undergo further metabolism by soluble epoxide hydrolase (sEH) enzymes to corresponding inactive diols [507, 508]. Because the ω -3 double bond distinguishing EPA and DHA from AA is the preferred site of attack by human CYPs, n-3 PUFAs compete with AA as

alternate substrates for CYP metabolism. Accordingly, supplementation with EPA and DHA increases the proportion of EEQ and EDP metabolites at the expense of the AA-derived CYP epoxy metabolite, epoxyeicosatrienoic acids (EET) [501].

Recent evidence indicates the CYP-derived metabolites, 17,18-EEQ and 19,20-EDP, are responsible for mediating different anti-inflammatory effects of n-3 PUFAs in various models of injury [501, 509-511]. Fang et al. demonstrated a n-3 PUFA-rich diet given to mice attenuated MI injury by shifting the metabolite profile to more anti-inflammatory mediators, increasing 19,20-EDP and 17,18-EEQ levels while decreasing PGE₂ [512]. In response to cardiac IR injury, the innate immune system triggers inflammatory reactions resulting in both protective and detrimental outcomes, which involves NLRP3 inflammasomes and proinflammatory cytokines. In a mouse model of IR injury, DHA and 19,20-EDP exerted cardioprotective properties resulting in improved postischemic functional recovery associated with attenuation of NLRP3 inflammasome complex activation and preserved mitochondrial function [383]. Interestingly, the attenuation of NLRP3 inflammasome activation was not observed following treatment with EPA or 17,18-EEQ, and importantly inhibition of CYP epoxygenase activity prevented the conversion of DHA to 19,20-EDP abolishing the protective effect [383]. Anti-inflammatory effects of CYP-derived epoxy metabolites have been demonstrated in other conditions, such as 19,20-EDP inhibited TNF α -induced retinal vascular inflammation and intraperitoneal infusions of 17,18-EEQ and 19,20-EDP protected against allergic intestinal inflammation and kidney fibrosis in respective mouse models [513, 514]. 17,18-EEQ inhibited TNF- α -induced inflammation in human bronchi via repression of NF- κ B and activation of the transcription factor PPAR- γ , in which the action of 17,18-EEQ was enhanced by sEH inhibition [515]. Using an animal model of inflammatory pain, Morisseau et al. demonstrated the DHA epoxides, but neither the parent fatty acid nor the corresponding diols, selectively modulate nociceptive pathophysiology [508]. The bacterial endotoxin, lipopolysaccharide (LPS) has a significant role in causing numerous cardiovascular complications

involving adverse inflammatory effects. Recently, it was demonstrated that 19,20-EDP protected HL-1 cardiac cells from LPS-stimulated inflammatory cell injury by preserving mitochondrial integrity and biogenesis [516]. Although the precise molecular mechanisms remain unknown, 19,20-EDP-mediated effects activated SIRT1 signaling to promote mitobiogenesis and attenuate NF- κ B activity [516]. Together, accumulating evidence suggests the anti-inflammatory properties of CYP-epoxygenase metabolites of n-3 PUFAs provide important protective responses in models of cardiovascular injury. However further investigation is required to elucidate their mechanisms and the extent to which they are involved in cardioprotection.

AA can be metabolized by CYP ω -hydroxylases into mid-chain 5-, 8-, 9-, 11-, 12- and 15-HETEs, terminal 20-HETE as well as subterminal 19-, 18-, 17- and 16-HETEs (Figure 1.7) [517, 518]. The ability of mid-chain and terminal HETEs to induce inflammatory responses form part of the basis for their detrimental effects toward IHD and in the development of CVD [519-522]. Kayama et al. showed 12-HETE has a role in the development of HF by increasing MCP-1 expression in cardiac fibroblasts and endothelial cells as well as increasing the infiltration of macrophages into the myocardium leading to cardiac fibrosis [523]. In addition, Maayah et al. demonstrated that 12-HETE, 15-HETE as well as 5-HETE are potent inducers of NF- κ B activation in RL-14 cells, a human ventricular cardiomyocyte cell line [524]. Similarly, 20-HETE activates NF- κ B signaling and induces expression of cellular ICAM-1 adhesion molecules, thereby promoting inflammation leading to vascular endothelial dysfunction, an important component in the pathogenesis of IHD diseases [525]. Coronary plasma concentrations of 20-HETE are markedly increased during ischemia and following reperfusion contributing to infarct size development. Accordingly, the selective inhibitors of CYP4A, the main 20-HETE-forming ω -hydroxylase, reduce ischemic infarct size in IR injury in canine myocardium [526-528]. Consistent with animal studies, the role of HETEs in aggravating CHD has been correlated with human data indicating concentration of HETEs is markedly higher in symptomatic atherosclerotic plaques, as

compared with asymptomatic ones [529, 530]. Importantly, while there is limited data available regarding n-3 PUFAs, CYP ω -hydroxylases preferentially metabolize EPA into hydroxyeicosapentaenoic acids (19- and 20- HEPE) and DHA into hydroxydocosahexaenoic acids (21- and 22-HDoHE) at the expense of AA-derived HETEs, which are thought to possess anti-inflammatory properties [508, 531-533]. Therefore, increasing consumption of n-3 PUFAs will cause a decrease in the levels of the CYP hydroxylase-derived pro-inflammatory metabolites with a concomitant increase in EPA- and DHA-derived anti-inflammatory metabolites which will have a beneficial impact on the cardiovascular health.

1.6.2.1.2.4 Resolvins: The anti-inflammatory and resolving mediators

Important lipid mediators involved in regulating inflammatory responses generated from the metabolism n-3 PUFAs include resolvins, 'resolution phase interaction products' produced from both EPA (E-series, RvE1-2) and DHA (D-series, RvD1-6), as well as protectins and maresins produced from DHA [456, 534, 535]. The synthesis of resolvins, protectins and maresins involve both the COX and LOX pathways, with different epimers being produced in the presence and absence of aspirin [536-539]. Resolvins and protectins, produced from EPA and DHA, were first discovered in inflammatory exudates during the acute inflammatory process indicating their role in inflammation [456, 534, 540]. Several studies demonstrated resolvins, protectins and maresins possess potent anti-inflammatory and inflammation resolving properties indicating an importance in terminating ongoing inflammatory processes. These unique metabolites promote the resolution of acute inflammation by preventing the migration of neutrophils and monocytes across epithelial cells and promoting clearance of PMNs, apoptotic cells, and debris from the site of inflammation [534, 541]. For example, Krishnamoorthy et al. showed that resolvins inhibit neutrophil tissue infiltration by decreasing the production of the chemokine IL-8 and reducing the expression of surface adhesion receptors on the neutrophils, such as CD11b or CD18 [542]. Resolvins also reduced neutrophil-derived ROS production, favored neutrophils apoptosis and

clearance by macrophages, as well as participated in shutting off chemokine signaling [543-545]. The partial agonist/antagonist activity of RvE1 on the LTB₄ receptor on PMNs serves to inhibit NF-κB activation, abolish pro-inflammatory cytokines production and reduce PMN infiltration [534, 535, 546]. Very recently, Sulciner et al. showed that RvD1, RvD2, or RvE1 inhibits debris-stimulated cancer progression by enhancing clearance of debris via macrophage phagocytosis in multiple tumor types. These resolvins suppressed the release of the proinflammatory cytokines/chemokines, including TNFα, IL-6, IL-8, CCL4, and CCL5, by human macrophages cocultured with tumor cell debris [547]. It is believed that E and D-resolvins present a similar function; both can inhibit NF-κB by a mechanism which is PPAR-γ dependent and mediate most of their actions via specific G-protein coupled receptors [450, 548, 549].

Since inflammation has a direct role in the pathogenesis of CVD, particularly IHD, resolvins, due to their anti-inflammatory properties, can improve the prognosis. For example, Morin et al. demonstrated a diet enriched with DHA and monoglycerides significantly increased the levels of RvD2 and RvD3, which correlated with reduced levels of proinflammatory mediators C-reactive protein (CRP), IL-6, TNF-α, and IL-1β in a rat model of hypertension [550]. Several experimental studies illustrated the ability of resolvins to significantly reduce atherosclerotic lesions, as observed in mouse models that lack LOX-12 and LOX-15, the two enzymes responsible of resolvins synthesis, which accelerated atherosclerosis development [551]. Furthermore, Viola et al. showed administration of RvD2 and Maresin 1 in a mouse model of atherosclerosis induces changes in the macrophage profile from an inflammatory (M1) toward a reparative phenotype (M2) which contributes to plaque stability and thus prevents atheroprogession [552]. Consumption of n-3 PUFAs by patients suffering from CAD was able to restore the levels of pro-resolving lipid mediators and promote macrophage phagocytosis of blood clots in vitro [553]. Moreover, RvE1 administration was demonstrated to reduce TNF-α and interferon-γ (IFN-γ) gene expression in aorta, decrease the levels of the inflammatory marker

CRP as well as reduce macrophage infiltration into intima and thus attenuate atherosclerosis and atherosclerotic plaque formation [377, 554, 555]. As a consequence of atherosclerosis, VSMCs become more proliferative, chemotactic and have an enhanced production capacity of pro-inflammatory cytokines [556]. Evidence demonstrates resolvins are capable of reducing the VSMCs responses via local activation of resolution mechanisms and abolishing leukocyte recruitment thereby ameliorating the atheroprogession [557, 558]. Consistent with these effects, oxidative stress levels and NF-kB activation were significantly lower in the RvD1-treated VSMC samples [559, 560].

The role of resolvins in protection against cardiac ischemia and reperfusion injury has been documented to involve numerous mechanisms including anti-inflammatory properties. Both *in vivo* and *in vitro* models of IR injury have demonstrated RvE1 can reduce infarct size, decrease apoptosis and improve cardiomyocyte survival [380]. Similar results were reported for the cardioprotective effects of RvD1, where RvD1 diminished infarct size and neutrophil accumulation in the infarcted myocardium and decreased post-myocardial infarct depression [382, 561, 562]. RvD1 alleviates post-MI inflammation by limiting neutrophil recruitment in the spleen and LV, increasing resolving lipid mediators, altering macrophage phenotype post-MI and reducing the expression of pro-fibrotic genes and collagen deposition. Together, these results indicated that RvD1 can modulate the pathophysiology of resolution in order to limit cardiac remodeling and thus prevent the progression of HF following MI [379].

1.6.2.2 N-3 PUFAs and their metabolites have the potential to ameliorate mitochondrial dysfunction under stress conditions

Under normal physiological conditions, it is essential for all body organs and physiological systems, particularly the cardiovascular system, to maintain a large number of functional mitochondria to provide energy, as well as preserve and regulate different cellular functions [52].

Maintaining a healthy pool of mitochondria depends upon a delicate balance between the formation of newly generated mitochondria by the process of “mitochondrial biogenesis”, to meet the increased energy demand, and the efficient elimination of irreversibly damaged mitochondria through mitophagy [563, 564]. Mitochondrial damage, decreased biogenesis and impaired mitophagy has been implicated in several pathologies including IR injury [565-569].

Numerous studies have demonstrated cardioprotective properties of n-3 PUFA, and their epoxy lipid metabolites, involve an ability to preserve a healthy mitochondrial pool, attenuate exaggerated inflammatory responses and maintain cardiomyocyte viability under stress conditions [570-572]. The cited studies indicate that CYP-epoxyeicosanoids exert (i) acute anti-apoptotic effects by slowing the loss of mitochondrial membrane potential and preventing opening of the MPTP and (ii) long-term effects that improve mitochondrial quality by promoting the removal of damaged mitochondria and stimulating mitochondrial biogenesis. Interestingly, earlier data demonstrated 19,20-EDP protected HL-1 cardiac cells from the bacterial endotoxin, LPS, cell injury by preserving mitochondrial biogenesis and integrity [516]. Furthermore, n-3 PUFAs could impart a cardioprotective effect via enriching mitochondrial membrane phospholipid composition, which enhances mitochondrial function promoting efficient ATP generation [338, 339]. This unique capacity of CYP epoxyeicosanoids in maintaining mitochondrial quality is of potential clinical interest, considering that mitochondria are the organelles, where all paths converge that lead to cardioprotection against IR injury [573]. However, further research is required to investigate the potential mechanism by which these epoxy metabolites mediate cardioprotection in the context of IR injury.

1.7 Thesis overview

1.7.1 Rationale

While success with early reperfusion strategies and adjuvant therapies has decreased acute mortality rates following myocardial ischemic attacks, development of reperfusion injury and subsequent chronic HF remains a major clinical concern. Although the intrinsic mechanism(s) involved in the pathogenesis of IR injury are not fully understood, deterioration of mitochondria is considered a major contributing factor. Damaged mitochondria not only lead to increased cellular stress but also triggers adverse innate immune responses aggravating IR injury. In that sense, as cardiomyocytes are terminally differentiated post-mitotic cells, preservation of a healthy pool of mitochondria is critical in maintaining cellular homeostasis, mitigating uncontrolled innate immune reactions and consequently limit the cardiac damage secondary to IR injury.

Dietary long-chain n-3 PUFAs are essential constituents of the body, which have numerous benefits including protection against CVD. There is growing evidence indicating ‘epoxylipids’, which are a class of novel lipid mediators generated endogenously from PUFA, mediate many of the beneficial biological responses in both cardiac and extra-cardiac tissues, but the underlying mechanisms have not been fully elucidated. For instance, DHA, the main n-3 PUFA, can be metabolized by CYP epoxygenases to generate the epoxy lipid 19,20-EDP. Importantly, data generated from our lab demonstrated that the epoxy metabolite 19,20-EDP is a very active lipid mediator that has the ability to limit cardiac damage under stress conditions however, the mechanism remains elusive.

1.7.2 Global hypothesis

We hypothesize that enhancing the cardiac levels of the epoxy lipid 19,20-EDP will protect against IR injury by regulating mitochondrial quality, and consequently limiting the uncontrolled innate immune response. Moreover, we hypothesize that 19,20-EDP maintains mitochondrial quality via directly activating the mitochondrial SIRT3 protein. The protected mitochondria, associated with attenuated inflammatory responses, result in better functioning cardiomyocytes and accordingly improved cardiac function in the setting of IR injury (Figure 1.9).

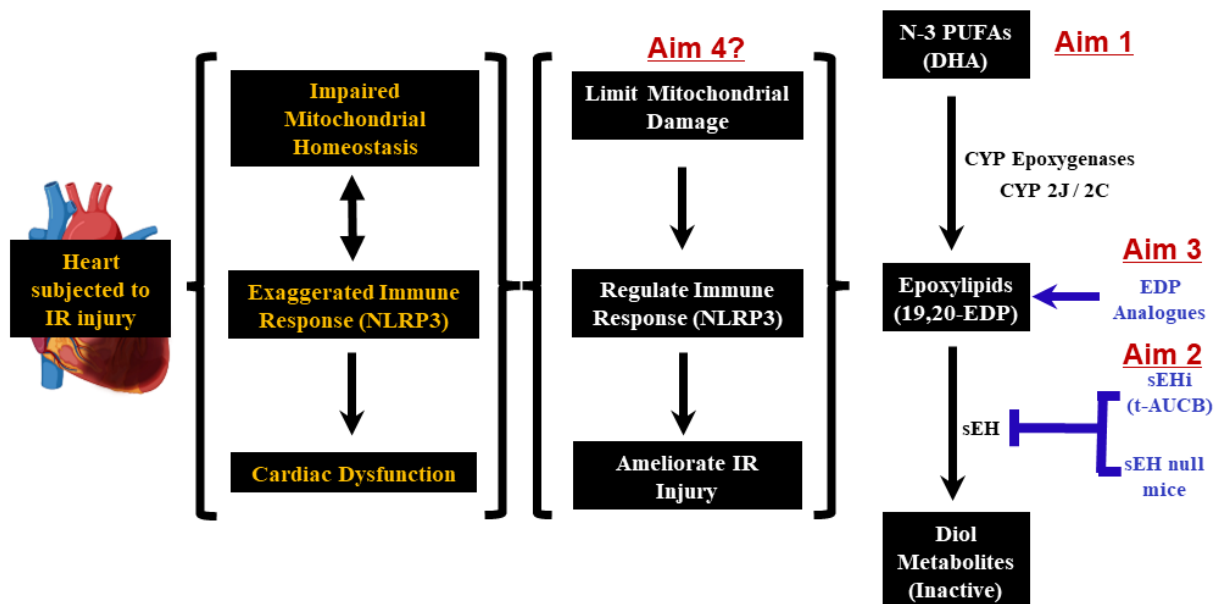


Figure 1. 9: A schematic illustration of the overall thesis hypothesis and specific objectives.

1.7.3 Objectives

- 1- To investigate the differential cardioprotective effects of the primary n-3 PUFAs (DHA and EPA) and their corresponding CYP metabolites (19,20-EDP and 17,18-EEQ) in the setting of IR injury.
- 2- To investigate whether enhancing the cardiac levels of the epoxy metabolites of n-3 PUFAs, via genetic or pharmacologic inhibition of sEH, can ameliorate IR injury.
- 3- To develop novel pharmaceutical compounds based on the structure of EDPs that have both mimetic and sEH inhibitory properties, and consequently increased stability and efficacy, and test their cardioprotective properties in the context of IR injury.
- 4- To obtain mechanistic insight on how 19,20-EDP mediate mitochondrial protection in the setting of IR injury.

CHAPTER 2

Cardioprotective Effects of CYP-Derived Epoxy Metabolites of Docosahexaenoic Acid Involve Limiting NLRP3 Inflammasome Activation

This chapter has been adapted from the following published manuscript:

- **Ahmed M. Darwesh**, K. Lockhart Jamieson, Chuying Wang, Victor Samokhvalov, and John M. Seubert. Cardioprotective effects of CYP-derived epoxy metabolites of docosahexaenoic acid involve limiting NLRP3 inflammasome activation. *Can J Physiol Pharmacol.* 2019;97(6):544-556.

Abstract

Impaired mitochondrial function and activation of NLRP3 inflammasome cascade has a significant role in the pathogenesis of myocardial ischemia reperfusion (IR) injury. The current study investigated whether eicosapentaenoic acid (EPA), docosahexaenoic acid (DHA), or their corresponding CYP epoxygenase metabolites 17,18-epoxyeicosatetraenoic acid (17,18-EEQ) and 19,20-epoxydocosapentaenoic acid (19,20-EDP) protect against IR injury. Isolated mouse hearts were perfused in the Langendorff mode with vehicle, DHA, 19,20-EDP, EPA, or 17,18-EEQ and subjected to 30 min of ischemia and followed by 40 min of reperfusion. In contrast with EPA and 17,18-EEQ, DHA and 19,20-EDP exerted cardioprotection, as shown by a significant improvement in postischemic functional recovery associated with significant attenuation of NLRP3 inflammasome complex activation and preserved mitochondrial function. Hearts perfused with DHA or 19,20-EDP displayed a marked reduction in localization of mitochondrial Drp-1 and Mfn-2 as well as maintained Opa-1 levels. DHA and 19,20-EDP preserved the activities of both the cytosolic Trx-1 and mitochondrial Trx-2. DHA cardioprotective effect was attenuated by the CYP epoxygenase inhibitor N-(methanesulfonyl)-2-(2-propynyloxy)-benzenhexanamide (MSPPOH). In conclusion, our data indicate a differential cardioprotective response between DHA, EPA, and their active metabolites toward IR injury. Interestingly, 19,20-EDP provided the best protection against IR injury via maintaining mitochondrial function and thereby reducing the detrimental NLRP3 inflammasome responses.

2.1 Introduction

Myocardial ischemia-reperfusion (IR) injury remains one of the leading causes of cardiovascular morbidity and mortality worldwide. Damage to the heart begins to occur after it has been deprived of oxygen; while the restoration of coronary blood flow is essential for survival, reperfusion itself can cause injury. Mitochondrial damage and associated activation of highly specific immune responses during reperfusion are contributing factors to declining heart function following injury [209, 574, 575].

It is well established that within the first minutes of myocardial reperfusion, the reactive oxygen species (ROS) burst from damaged mitochondria triggers inflammatory reactions, inducing formation of inflammasomes, which paradoxically exacerbate myocardial injury [262, 263]. Inflammasomes are large cytosolic macromolecular structures assembled in response to pro-inflammatory stimuli like cellular debris and microbial products, which lead to local or systemic inflammatory responses. Several types of the inflammasome platforms have been described, of which the nucleotide-binding oligomerization domain-like receptor (NLR) family pyrin domain containing 3 (NLRP3) is considered to be the prominent participant in response to noninfectious stimuli such as myocardial IR injury [576, 577]. The oligomerization and assembly of NLRP3 inflammasomes after myocardial IR injury promotes the autocatalytic activation of caspase-1, production of active cytokines notably IL-1 β and promotes cell death via pyroptosis [200, 211, 262]. Therapeutic attempts to protect the mitochondria and thereby limit the NLRP3 inflammasome response is a promising approach to promote survival of the myocardium following IR injury.

Dietary long-chain omega-3 polyunsaturated fatty acids (n-3 PUFA) are essential constituents of the body, which have been attributed to numerous benefits including protection against cardiovascular disease (CVD). However, our understanding of the precise protective mechanism(s) of action is extremely limited and conflicted in the literature [327, 330, 578]. Importantly, there is growing evidence indicating ‘epoxy lipids’, which are a class of novel lipid mediators generated endogenously from PUFA, mediate many of the effects [329, 330]. Eicosapentaenoic acid (EPA) and docosahexaenoic acid (DHA) can be metabolized by cyclooxygenases (COX), lipoxygenases (LOX) and cytochrome P450 (CYP) enzymes to a vast array of lipid mediators with some known cellular functions. CYP epoxygenases add oxygen across one of the double bonds of EPA or DHA to generate three-membered ethers known as epoxides. There are five regioisomeric metabolites of EPA termed epoxyeicosatetraenoic acids (5,6-, 8,9-, 11,12-, 14,15-, 17,18-EEQ) and six regioisomeric metabolites of DHA termed epoxydocosapentaenoic acids (4,5-, 7,8-, 10,11-, 13,14-, 16,17-, 19,20-EDP) [501]. Recent evidence has demonstrated CYP-derived epoxy metabolites of EPA and DHA, particularly 19,20-EDP and 17,18-EEQ, are potent lipid mediators having cellular protective effects limiting mitochondrial injury [339, 501, 516, 579]. The current study builds upon our previous data to hypothesize that CYP-derived epoxy metabolites of EPA and DHA could attenuate myocardial IR injury through maintaining mitochondrial function and consequently limiting NLRP3 inflammasome activation.

2.2 Methods

2.2.1 Animals and isolated heart perfusion

Commercially available C57BL/6 mice were purchased from Charles River Laboratories (Pointe Claire, PQ). All studies were carried out using 2-3 month-old male and female mice weighing 25-30g. Mice were euthanized intraperitoneally with sodium pentobarbital (Euthanyl, 100mg/kg) and following non-responsiveness to external stimulation hearts were isolated and perfused in the Langendorff mode [580-583]. Briefly, mouse hearts were perfused in the retrograde mode at a constant flow-rate for 40 min of baseline (stabilization) and then subjected to 30 min of global no flow ischemia followed by 40 min of reperfusion. Hearts were perfused with either DHA (10 μ M), 19,20 EDP (1 μ M), EPA (10 μ M), 17,18 EEQ (1 μ M), N-(methanesulfonyl)-2-(2-propynyloxy)-benzenehexanamide (MSPPOH), (CYP epoxygenase inhibitor, 50 μ M) (Cayman Chemicals, Ann Arbor, MI, USA), DHA + MSPPOH or EPA + MSPPOH. The concentrations utilized in the current study were based on previously published data from cell culture experiments and experience working with CYP-derived epoxy metabolites of arachidonic acid, which demonstrate cardioprotective effects at similar concentrations [580, 581]. In all experiments, chemicals were added 20 min before ischemia and were present in the heart throughout the reperfusion period. The percentage of left ventricular developed pressure (%LVDP) at 40 min of reperfusion (R40), as compared to baseline LVDP, was taken as a marker for recovery of contractile function. After 40 min of reperfusion, hearts were immediately frozen and stored below -80°C . Haemodynamic parameters were acquired and analyzed using ADI software from (Holliston, MA, USA). Collection of the heart effluent was taken during both pre- and postischemic protocols to determine coronary flow (CF) rates. All animal experimental protocols were approved by the University of Alberta Health Sciences Welfare Committee and conducted

according to strict guidelines provided by the Guide to the Care and Use of Experimental Animals (Vol. 1, 2nd ed., 1993, from the Canadian Council on Animal Care).

2.2.2 Immunoblotting

Crude mitochondrial and cytosolic fractions were prepared from frozen mouse hearts as previously described [582, 583]. Briefly, heart tissues were ground with mortar and pestle on dry ice and then homogenized in ice-cold homogenization buffer (20 mmol/L Tris-HCl, 50 mmol/L NaCl, 50 mmol/L NaF, 5 mmol/L sodium pyrophosphate, 1 mmol/L EDTA and 250 mmol/L sucrose added on the day of the experiment, pH 7.0). Samples were first centrifuged at 800xg for 10 min at 4°C and the supernatant was then centrifuged at 10,000xg for 20min. The pellet was resuspended in 100µl homogenization buffer to obtain a mitochondrial-enriched fraction. The supernatant was ultra-centrifuged at 105,000xg for 60min and the subsequent supernatant was used as the cytosolic fraction. Protein concentrations in both cytosolic and mitochondrial fractions were measured by the Bradford assay. Western blotting was done as previously described [584]. Protein (30-50µg) was resolved by electrophoresis on (10–15%) SDS-polyacrylamide gels and transferred onto polyvinylidene difluoride (PVDF) membranes (BioRad Laboratories, Hercules, CA, USA). Immunoblots were probed with antibodies to total- Akt (Cat#: 9272) or phospho-(Ser⁴⁷³) Akt (Cat#: 4060), total- αAMPK (Cat#: 2532) or phospho-(Thr¹⁷²) αAMPK (Cat#: 2535), Mfn-2 (Cat#: 9482), Drp-1 (Cat#: 5391), GAPDH (Cat#: 51745), Prohibitin (Cat#: 2426) (1:1000, Cell Signaling Technology, Inc., MA, USA), NLRP3 protein (1:500) (Cat#: ab214185), IL-1β (Cat#: ab9722), Mfn-1 (ab104274), (1:1000, Abcam, Burlingame, CA, USA), and Txnip (Cat#: K0205-3, 1:500, MBL International Co., Woburn, MA, USA). After washing, membranes were incubated with the corresponding secondary antibodies (1:5000). The blots were visualized with ECL

reagent. Relative band intensities were expressed as fold of the control assessed using Image J software (NIH, USA).

2.2.3 Mitochondrial respiration

Mitochondrial oxygen consumption was measured in permeabilized cardiac fibers using a Clark electrode connected to an Oxygraph Plus recorder (Hansatech Instruments Ltd., Norfolk, England). Cardiac fibers were directly isolated from the left ventricles of experimental mice as previously described [584, 585]. Hearts were dissected under a dissecting microscope in ice-cold isolation buffer (2.77 mM Ca KEGTA, 7.23 mM K₂EGTA, 20 mM imidazole, 20 mM taurine, 49 mM K-MES, 3 mM K₂HPO₄, 9.5 mM MgCl₂, 5.7 mM ATP, 1 μM leupeptin, 15 mM phosphocreatine). A 2–5 mm strip of the anterior left ventricle was isolated then remaining fats and vessels were removed. Myocardial strips were dissected into bundles containing 6–8 fibers each, 1 mm wide and 3–4 mm long. Fresh fibers were permeabilized in isolation buffer containing 100 μg/ml saponin, rinsed three times for 5 min in ice-cold respiration buffer and immediately added to the respiration chamber. Respiration rates were measured at 30°C before and after addition of 0.5 mM adenosine diphosphate (ADP) in the presence of 5 mM malate and 10 mM glutamate as respiratory substrates. Respiratory control ratio (RCR) was calculated as the ratio between basal and ADP-stimulated respiration rates to estimate mitochondrial respiration efficiency.

2.2.4 Enzymatic Assays

Caspase-1 activity was assessed in cytosolic fractions using a fluorometric assay method according to a previously described protocol [586]. The assay quantitated 7-Amino-4-methylcoumarin (AMC) fluorescence after cleavage of Ac-YVAD-AMC (Cat #: ALX-260-024-

M005) fluorogenic substrates by caspase-1 (Enzo life Sciences, NY, USA) in heart homogenates. The fluorescence was monitored by a fluorometer at wavelengths of 380 (excitation) and 460 nm (emission). The activity was calculated by using a linear standard curve created with AMC.

The insulin disulfide reduction assay, where thioredoxin (Trx) after reduction by thioredoxin reductase (TrxR) enzyme is used to reduce insulin disulfides, was performed to measure Trx activity as described previously [587, 588]. Briefly, equal amounts of mitochondrial or cytosolic protein (30 μ g) were preincubated at 37 °C for 15 min with 2 μ L of dithiothreitol (DTT) activation buffer (100 mM HEPES (pH 7.6), 2 mM EDTA, 1 mg/ml bovine serum albumin (BSA), 2 mM DTT) to reduce and activate endogenous Trx. Then, 20 μ L of reaction mixture containing 100 mM HEPES pH 7.6, 2 mM EDTA, 0.2 mM NADPH, and 140 μ M insulin were added. The reaction was started by the addition of 0.5 U mammalian TrxR (Cayman Chemicals, Ann Arbor, MI, USA) or an equal volume of water for negative controls and maintained at 37 °C for 30 min. The reaction was stopped by the addition of 125 μ l of stop solution consisting of 10 M guanidine hydrochloride and 1.7 mM (5,5-dithio-bis-(2-nitrobenzoic acid) (DTNB) in 0.2 M Tris-HCl (pH 8.0). Reduction of DTNB to 5-thio-2-nitrobenzoic acid (TNB) was detected by optical density at 412 nm. Changes in the absorbance in the absence of TrxR were subtracted from those in the presence of the reductase.

2.2.5 Statistics

Values are expressed as mean \pm standard error of mean (SEM). Statistical significance was determined by one-way ANOVA with a Tukey post hoc test to assess differences between groups; $p < 0.05$ was considered statistically significant.

2.3 Results

2.3.1 Cardioprotective effects of n3-PUFAs and their CYP-derived epoxy metabolites

To demonstrate whether CYP epoxy metabolites of n-3 PUFA have comparable cardioprotective effects, we first compared DHA, EPA and their corresponding CYP epoxy metabolites 19,20-EDP and 17,18-EEQ. Preischemic cardiac parameters were similar between all treatment groups (Figure 2.1). No significant differences were observed in the heart rate at the end of reperfusion between the different groups (Figure 2.1D). Moreover, there were no differences between male and female mice in either pre- or postischemic recovery in any treatment group, as such data from both sexes were combined. Hearts perfused with DHA or 19,20-EDP had significantly improved postischemic recovery of LVDP compared with control mice (Figure 2.1A and C). This protective effect was blocked when hearts were co-perfused with a CYP epoxygenase inhibitor MSPPOH together with DHA (Figure 2.1A and C). Thus, suggesting the cardioprotective effect of DHA was attributable to its CYP epoxy metabolite 19,20-EDP. In contrast, hearts perfused with either EPA or 17,18-EEQ failed to provide better postischemic recovery compared to control hearts (Figure 2.1 B and C). Consistent with improved postischemic functional recovery, hearts perfused with DHA or 19,20-EDP demonstrated better rates of contraction (dP/dt max) and relaxation (dP/dt min) in comparison to the control mice (Figure 2.1 E and G). While again no marked improvement was recognized in contraction or relaxation rates in hearts perfused with either EPA or 17,18-EEQ (Figure 2.1 F and H). Evidence in the literature has demonstrated n-3 PUFAs can improve vascular function as elucidated by their ability to reduce arterial stiffness, increase blood flow and lower elevated blood pressure [314, 589-592]. Interestingly, the coronary flow rates did not significantly differ between pre-ischemic (2.32 ± 0.4 ml/min) and postischemic perfused hearts (2.06 ± 0.5 ml/min) in our model. Importantly, no differences were observed in

pre- and postischemic flow rates in any of the treatment groups (Figure 2.11). Together, these data suggest pretreatment with either n-3 PUFAs, DHA or EPA, or their metabolites, 17,18-EEQ or 19,20-EDP, did not alter the coronary flow rates indicating the cardioprotective effect was not attributable to alterations in hemodynamics in the perfused heart model.

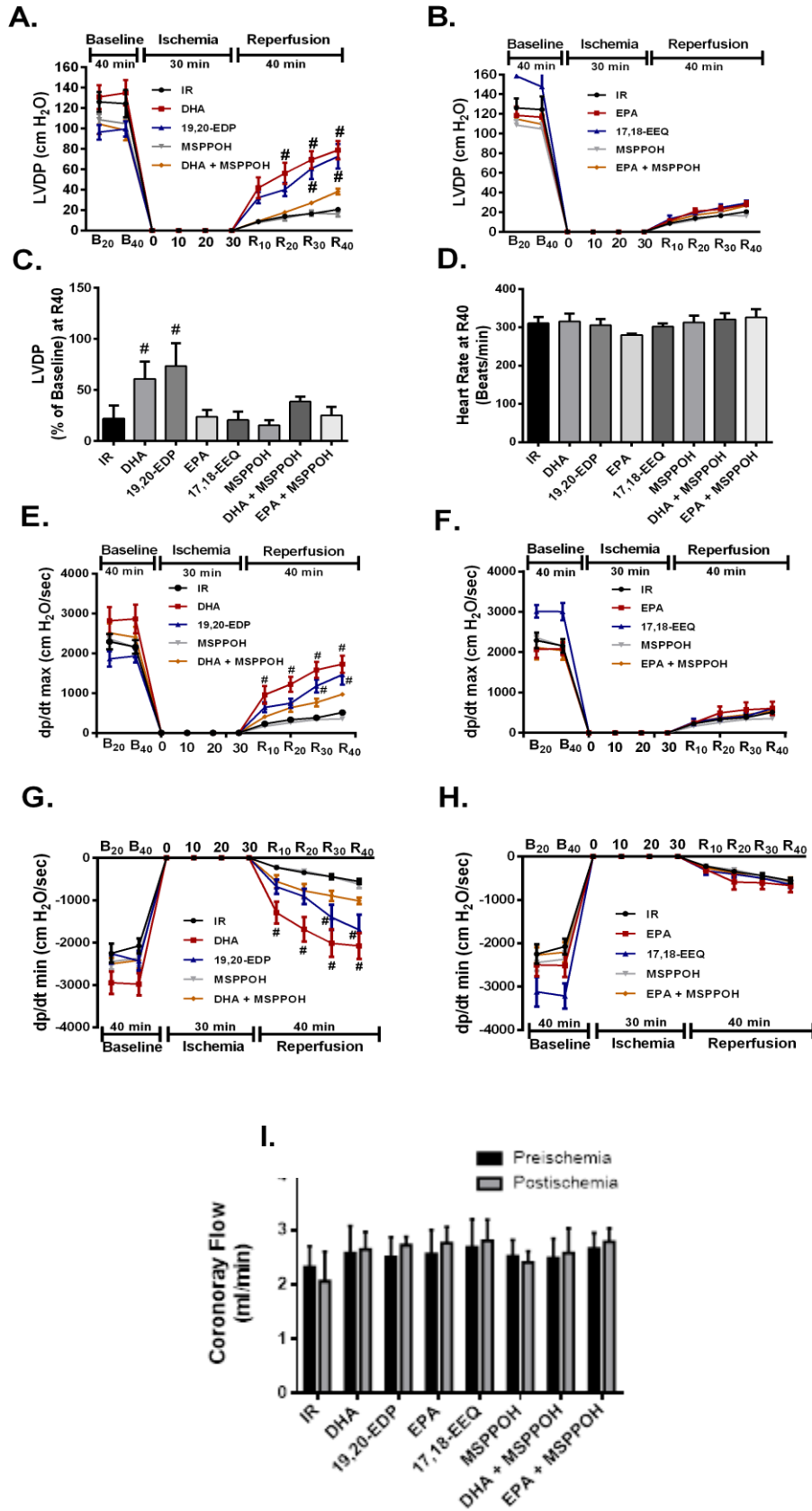


Figure 2. 1: Effects of CYP-derived epoxylipids on postischemic contractile function. (A and B) LVDP at the baseline before (B20) and after (B40) drug treatment, at ischemia, and at 10, 20, 30, and 40 min reperfusion (R10, R20, R30, and R40). (C) LVDP recovery at 40 min of reperfusion as a percentage of baseline. (D) Heart rate assessed as beats per minute at the end of reperfusion (R40). (E and F) Rate of contraction and (G and H) rate of relaxation in hearts at the baseline before (B20) and after (B40) drug treatment, at ischemia, and at 10, 20, 30, and 40 min reperfusion (R10, R20, R30, and R40). (I) Coronary flow rates from perfused hearts. Values represent mean \pm SE; n = 6–8 per group. #p < 0.05 versus IR. LVDP; left ventricular developed pressure; IR, ischemia–reperfusion; DHA, docosahexaenoic acid; 19,20-EDP, 19,20-epoxydocosapentaenoic acid; EPA, eicosapentaenoic acid; 17,18-EEQ, 17,18-epoxyeicosatetraenoic acid; MSPPOH, N-(methanesulfonyl)-2-(2-propynyloxy)-benzenhexanamide.

2.3.2 Epoxy metabolites limit postischemic mitochondrial injury

Decreased mitochondrial quality stemming from IR injury leads to a vicious cycle of continued injury and reduced cardiac function. Importantly, mitochondrial dysfunction has been shown to directly activate the NLRP3 inflammasome [260, 575]. Previously, using *in vitro* models we demonstrated that 19,20-EDP limit mitochondrial injury and can enhance respiration [339, 516]. As such, we investigated mitochondrial respiration in hearts perfused with 19,20-EDP compared to control mice as a marker of mitochondrial function. Basal respiration rates did not differ significantly between all groups, however, ADP-stimulated respiration was significantly reduced in postischemic hearts from vehicle control mice (Table 2.1). Perfusion with 19,20-EDP did not alter ADP-stimulated respiration relative to aerobic controls but did preserve postischemic respiration compared to vehicle control (Table 2.1). Indeed, the RCR, a marker of mitochondrial efficiency, significantly decreased in vehicle group compared to aerobic CT. However, the RCR values were maintained in fibers separated from hearts treated with 19,20-EDP either aerobic or exposed to IR injury, suggesting better mitochondrial function in postischemic hearts.

Table 2.1: Respiration was assessed in permeabilized muscle fibers obtained from hearts following ischemia–reperfusion (IR).

	Basal Respiration (nmol O ₂ .min ⁻¹ .mg ⁻¹)	ADP-stimulated (nmol O ₂ .min ⁻¹ .mg ⁻¹)	Respiratory Control Ratio (RCR)
Aerobic Control	2.4 ± 0.74	7.53 ± 1.33	3.52 ± 0.59
19,20-EDP Aerobic Control	2.363 ± 0.30	7.59 ± 0.74 [#]	3.34 ± 0.36 [#]
IR	2.85 ± 1.03	2.26 ± 0.93 [*]	0.78 ± 0.12 [*]
19,20-EDP	2.01 ± 0.69	6.083 ± 0.7 [#]	3.00 ± 0.46 [#]

Respiration was measured using a Clark electrode-based chamber connected to an oxygraph where malate and glutamate were used to initiate basal respiration. Rates were expressed as respiratory control ratio, which is a ratio of ADP-stimulated to basal respiration. Values represent mean ± SE; *P < 0.05 versus aerobic control and #P < 0.05 versus IR, n = 4–5 per group.

Postischemic mitochondrial dysfunction often results in marked elevations in cellular ROS production, which are regulated by various antioxidant mechanisms. Thioredoxins (Trxs) are cellular antioxidant proteins that have multiple functions in maintaining the reducing environment in the cell, reducing oxidative stress and thus inhibiting apoptosis [593]. Two major isoforms of Trx have been identified in mammalian cells, cytoplasmic Trx-1 and mitochondrial Trx-2 [593-595]. Postischemic control hearts had a marked reduction in both cytosolic Trx-1 and mitochondrial Trx-2 catalytic activities, suggesting increased ROS levels, which is consistent with decreased mitochondrial function (Figure 2.2 A and B). We observed hearts perfused with 19,20-EDP maintained both Trx-1 and Trx-2 catalytic activities relative to aerobic controls and significantly higher than postischemic IR groups (Figure 2.2 A and B), suggesting better antioxidant levels and reduced ROS production. Although Trx-1 and Trx-2 antioxidant activities were maintained at a comparable level to the aerobic control in hearts perfused with DHA, they did not reach significance compared to the IR groups. Similarly, EPA showed a trend to maintain Trx-1 and Trx-2 activities, however, their levels were not significantly maintained compared to the aerobic control group. The levels of Trx-1 and Trx-2 activities were significantly reduced in case of 17,18-EEQ pretreatment compared to the aerobic control similar to IR hearts and worse functional outcomes. Intriguingly, adding MSPPOH to DHA in the perfusion solution blocked its beneficial trend on maintaining the activity of Trx-1/2 proteins indicating again the role of its CYP epoxy metabolite, 19,20-EDP, in mediating the cardioprotective properties of DHA (Figure 2.2 A and B).

Reports have shown that proteins regulating mitochondrial dynamics, particularly dynamin-related protein 1 (Drp-1) and optic atrophy 1 (Opa-1), are involved in the cascade of myocardial IR injury [101]. An increased mitochondrial localization of the active form Drp-1

following significant damage caused but stressors such as IR injury results in fission of mitochondria. Often IR injury is associated with a marked reduction in mitochondrial Opa-1 levels leading to a significant reduction in oxygen consumption rates and cardiomyocyte cell death [596-598]. Consistent with decreased mitochondrial function observed in postischemic vehicle control IR hearts, we noticed a marked increase in mitochondrial expression of Drp-1 and decrease in mitochondrial Opa-1 levels (Figure 2.2 C and D). Perfusion of hearts with either DHA or 19,20-EDP limited the mitochondrial localization of Drp-1 and limited the loss of Opa-1 protein (Figure 2.2 C and D), which supports the notion of reduced mitochondrial injury. However, neither EPA nor 17,18-EEQ prevented the mitochondrial localization of Drp-1 and resulted in marked decreases of Opa-1 levels compared to the vehicle groups (Figure 2.2 C and D). Co-perfusion with the CYP epoxygenase inhibitor, MSPPOH, with DHA significantly blocked the beneficial effects suggesting a role for the metabolite 19,20-EDP in the protective responses.

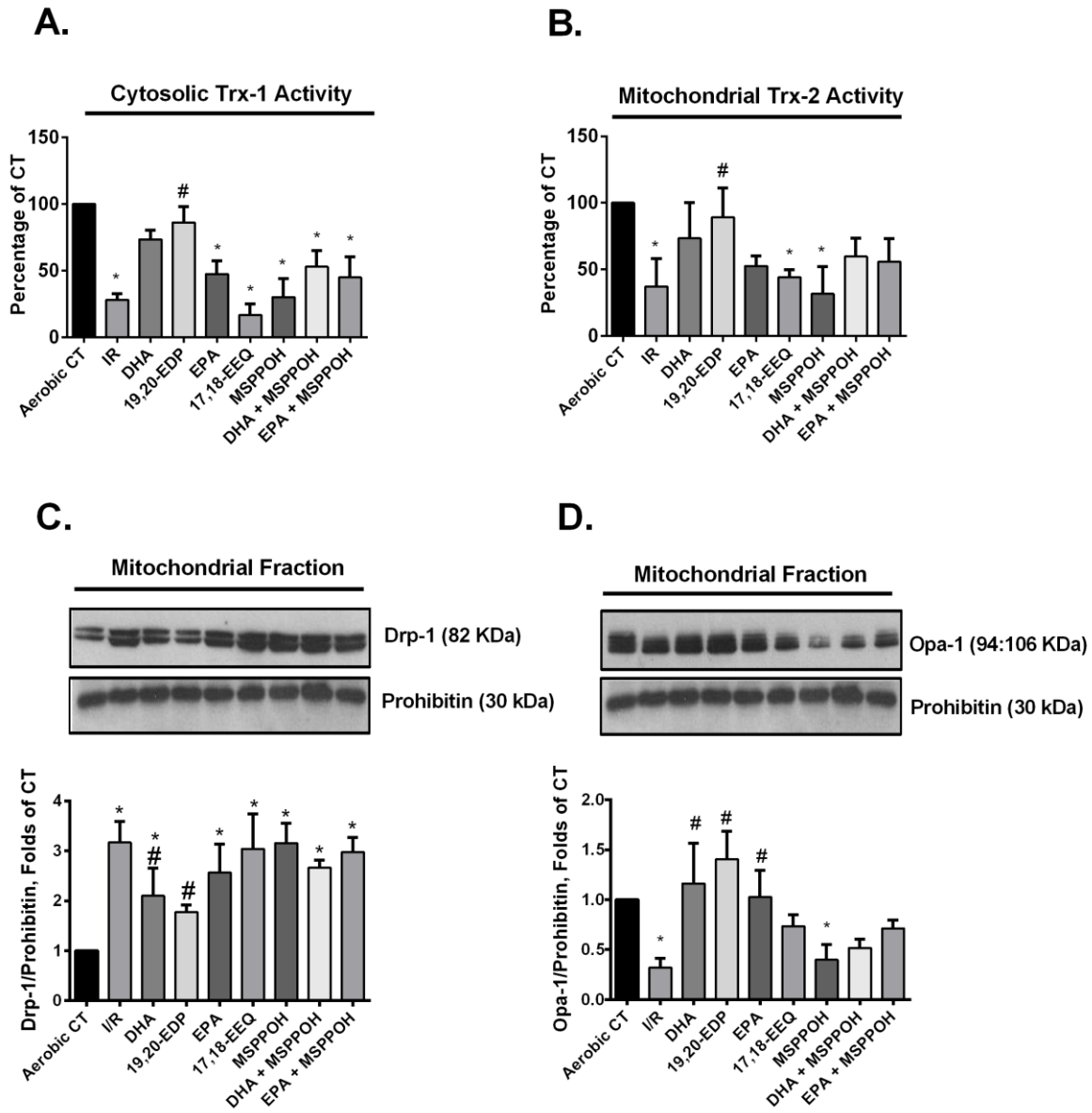


Figure 2. 2: 19,20-EDP preserved mitochondrial integrity under IR insult. Cardiac (A) cytosolic Trx-1 and (B) mitochondrial Trx-2 activities were assessed in mice hearts following 30 min of ischemia and 40 min of reperfusion. Representative immunoblots and densitometric quantification of the mitochondrial protein expression of (C) Drp-1 and (D) Opa-1 proteins in mice hearts after 30 min of ischemia and 40 min of reperfusion. All expression was normalized to prohibitin loading control. Values represent mean \pm SE. * $p < 0.05$ versus aerobic CT, # $p < 0.05$ versus IR (n = 3–5 per group). CT, control; IR, ischemia–reperfusion; DHA, docosahexaenoic acid; 19,20-EDP, 19,20-epoxydocosapentaenoic acid; EPA, eicosapentaenoic acid; 17,18-EEQ, 17,18-epoxyeicosatetraenoic acid; MSPPOH, N-(methylsulfonyl)-2-(2-propynyloxy) benzenehexanamide.

2.3.3 Effects of n-3 PUFAs and their CYP epoxy metabolites on the assembly and activation of NLRP3 inflammasome

To determine the ability of different n-3 PUFAs to interfere with the NLRP3 inflammasome cascade activation in the current experimental model, the expression levels of the inflammasome components NLRP3 and IL-1 β proteins as well as the activity of caspase 1 enzyme were assessed. As shown in Figure 2.3, immunoblot analysis revealed that IR injury significantly up-regulated both active NLRP3 and mature-IL-1 β expressions, as well as increased the activity of caspase1 enzyme compared to the aerobic control. Hearts perfused with either DHA, 19,20-EDP or EPA prevented the IR-induced upregulation of NLRP3 protein compared to the aerobic control (Figure 2.3A). However, only 19,20-EDP pretreatment was able to significantly inhibit the IR-induced IL-1 β activation after 40min of reperfusion (Figure 2.3B). Hearts perfused with DHA or 19,20-EDP was able to maintain the aerobic control levels of caspase-1 activity (Figure 2.3C). Although pretreatment with EPA significantly inhibited the IR-induced activation of caspase 1 activity, caspase 1 activity showed an increased trend compared to the aerobic control (Figure 2.3C), which was reflected in the significant increase the expression levels of IL-1 β (Figure 2.3B). Perfusion with 17,18-EEQ failed to attenuate postischemic NLRP3 or IL-1 β expression as well as caspase-1 activity (Figure 2.3A, B and C). Hearts perfused with the CYP epoxygenase inhibitor, MSPPOH, attenuated the postischemic effects of DHA and EPA on NLRP3 and IL-1 β expression as well as caspase-1 activity (Figure 2.3A, B and C), suggesting the epoxy metabolites are the important mediators triggering the observed postischemic responses.

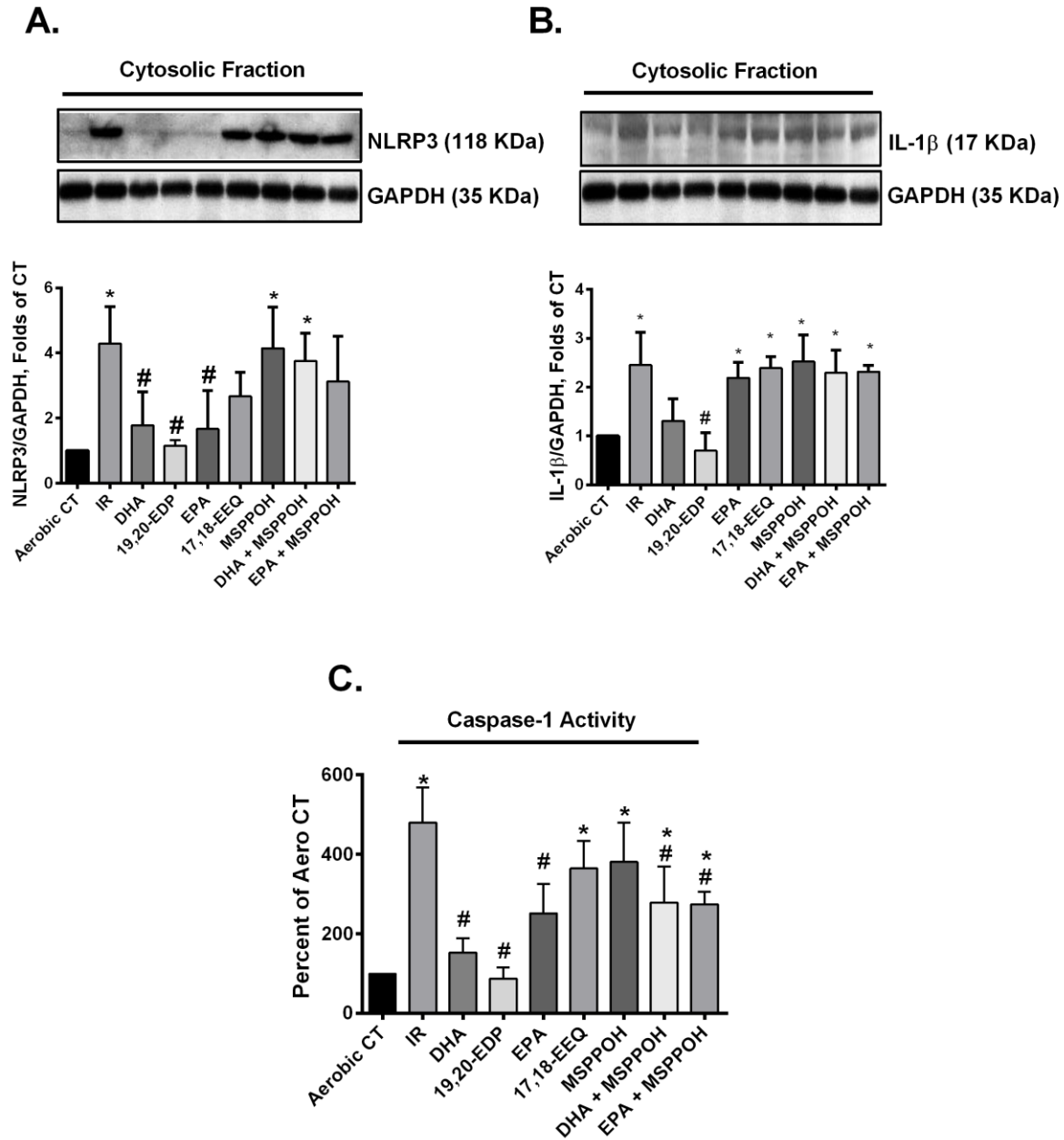


Figure 2.3: 19,20-EDP inhibited cardiac NLRP3 inflammasome activation. Representative immunoblots and densitometric quantification of the cytosolic protein expression of (A) NLRP3 and (B) IL-1 β in mice hearts after 30 min of ischemia and 40 min of reperfusion. All expression was normalized to GAPDH loading control (n = 3–4). Cardiac (C) caspase-1 activity assessed in the cytosolic fraction following 30 min of ischemia and 40 min of reperfusion. Values represent mean \pm SE. *p < 0.05 versus aerobic CT, #p < 0.05 versus IR (n = 5–6 per group). CT, control; IR, ischemia–reperfusion; DHA, docosahexaenoic acid; 19,20-EDP, 19,20-epoxydocosapentaenoic acid; EPA, eicosapentaenoic acid; 17,18-EEQ, 17,18-epoxyeicosatetraenoic acid; MSPPOH, N-(methanesulfonyl)-2-(2-propynyloxy) benzenehexanamide.

2.3.4 Effects of n-3 PUFAs and their CYP epoxy metabolites on Txnip activation and translocation

The thioredoxin-interacting protein (Txnip) links oxidative stress and the NLRP3 activation and inflammasome formation [599]. In the current experiments, postischemic hearts had a marked increase of both cytosolic and mitochondrial Txnip protein expression consistent with increased inflammasome formation (Figure 2.4 A and B). Txnip accumulation correlated with the reduction in the antioxidant activities of both Trx-1 and -2. Considering Txnip preferentially binds to the thiol active sites of reduced but not oxidized Trx, these data suggest it would prevent Trx ability to work as an antioxidant. In contrast, hearts perfused with DHA, 19,20-EDP or EPA had significantly blunted localization of Txnip in cytosolic and mitochondrial fractions compared to IR group (Figure 2.4 A and B). Perfusion with 17,18-EEQ failed to block the mitochondrial localization of Txnip. It is well-established that both p-AMPK and p-Akt can phosphorylate Txnip at the same site, causing its degradation, and thus protecting cardiomyocytes from apoptosis and ischemic injury [600, 601]. Therefore, we assessed the phosphorylation of AMPK at Thr-172 and Akt at Ser-473 in the heart after the IR injury. Hearts perfused with either DHA, 19,20-EDP or EPA markedly increased the phosphorylation of Akt compared to the IR vehicle group (Figure 2.4C). Similarly, hearts perfused with DHA or 19,20-EDP significantly increased the expression of p-AMPK compared to IR vehicle group (Figure 2.4D), while perfusion with EPA did not increase p-AMPK levels. Consistently, perfusion with 17,18-EEQ failed to significantly increase p-AMPK or p-AKT levels. The co-perfusion of MSPPOH and DHA attenuated the activation of AMPK and AKT. Together, these data suggest 19,20-EDP activates AMPK and AKT, which correlates with decreased Txnip cytosolic and mitochondrial accumulation.

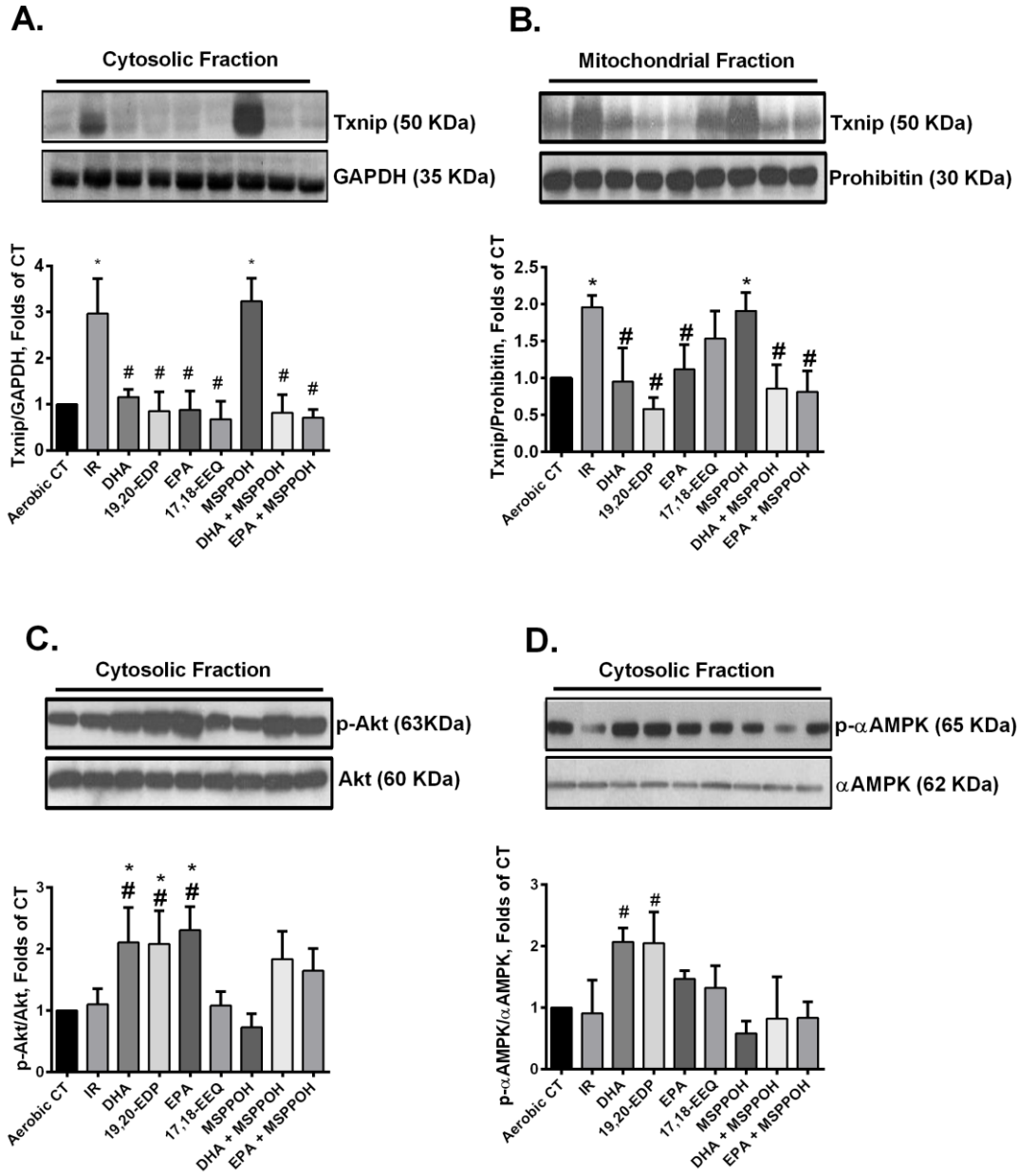


Figure 2. 4: Postischemic alterations in Txnip, p-Akt, and p-AMPK. Representative immunoblots and densitometric quantification of the (A) cytosolic Txnip, (B) mitochondrial Txnip, (C) phospho-(Ser473) Akt, and (D) phospho-(Thr172) AMPK protein expressions in hearts after 30 min of ischemia and 40 min of reperfusion (n = 3–4 per group). Cytosolic protein expression was normalized to GAPDH, while mitochondrial Txnip expression was normalized to prohibitin (n = 5–6 per group). Values represent mean ± SE. *p < 0.05 versus aerobic CT, #p < 0.05 versus IR. CT, control; IR, ischemia–reperfusion; DHA, docosahexaenoic acid; 19,20-EDP, 19,20-epoxydocosapentaenoic acid; EPA, eicosapentaenoic acid; 17,18-EEQ, 17,18-epoxyeicosatetraenoic acid; MSPPOH, N-(methylsulfonyl)-2-(2-propynyloxy)-benzenehexanamide.

2.3.5 Mitofusins

Mitofusins (Mfn)-1 and -2 are integral proteins found on the outer mitochondrial membrane commonly known for their role in mitochondrial fusion. Emerging evidence in the literature has demonstrated non-canonical roles for Mfn-2 within specific cell types, such as being involved in cardiomyocyte cell death and activation of the NLRP3 inflammasome [113, 602]. In the current study, we observed no significant differences in mitochondrial expression of Mfn-1 (Figure 2.5A). However, there were marked increases in mitochondrial expression of Mfn-2 in postischemic hearts, which was attenuated when perfused with DHA or 19,20-EDP (Figure 2.5B). Perfusion with EPA or 17,18-EEQ failed to block the increased postischemic expression of mitochondrial Mfn-2. Moreover, perfusion with MSPPOH appeared to block the DHA-mediated effect on Mfn-2 expression. Overall, these data correlate with an increased expression of postischemic Mfn-2, which potentially signals activation of NLRP3 inflammasomes that is attenuated by DHA and 19,20-EDP thus limiting cardiac injury.

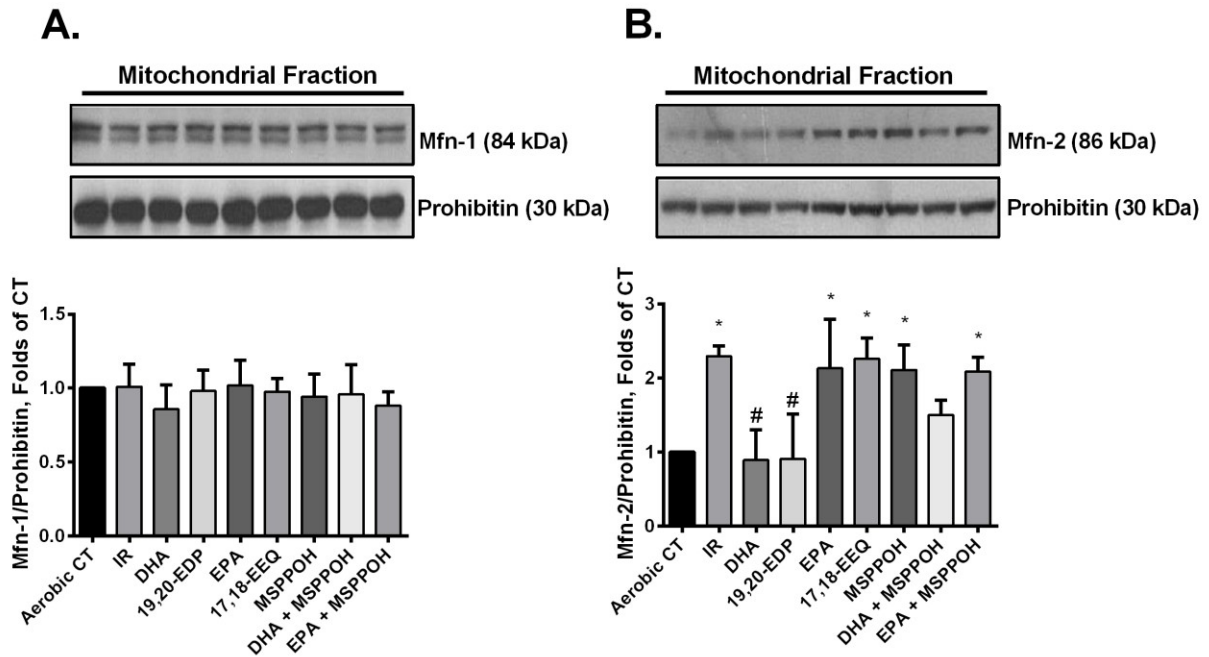


Figure 2. 5: Postischemic expression of mitochondrial mitofusins. Representative immunoblot and densitometric quantification of (A) Mfn-1 and (B) Mfn-2 in mice hearts following 30 min of ischemia and 40 min of reperfusion. Values represent mean \pm SE. * $p < 0.05$ versus aerobic CT, # $p < 0.05$ versus IR (n = 3–4 per group).

2.4 Discussion

Numerous epidemiological, clinical and animal studies have demonstrated n-3 PUFAs, primarily EPA and DHA, have significant cardiovascular benefits [327, 329, 603-605]. These beneficial effects include protection against coronary heart disease [578, 606], myocardial infarction [307, 320], IR-induced arrhythmias [607] and sudden cardiac death [307, 608]. Evidence from such studies support the notion that n-3 PUFAs are promising bioactive compounds, which can reduce the risk of cardiac death and confer general health benefits [314]. However, emerging evidence has identified CYP-derived epoxygenase metabolites, 17,18-EEQ and 19,20-EDP, as important lipid mediators obtained from n-3 PUFA metabolism, which may be responsible for many of the beneficial effects, including protection against cardiac arrhythmia, promotion of angiogenesis and amelioration of inflammatory responses [329, 330, 599, 609]. Previously, we demonstrated 19,20-EDP provides protective effects against hypoxia-reoxygenation injury in HL-1 cardiac cells [339]. In the current study, we report that CYP-derived epoxy metabolites of DHA attenuate IR injury by protecting mitochondrial function and inhibiting NLRP3 inflammasome activation in mice. Interestingly, neither the n-3 PUFA, EPA or the epoxy lipid 17,18-EEQ provided protection against IR injury in the mouse model. Taken together, the data suggest 19,20-EDP is an effective lipid mediate that protects hearts against IR injury.

In response to cardiac IR injury, the immune system triggers inflammatory reactions resulting in both protective and detrimental outcomes. The innate immune system uses pattern-recognition receptors to detect pathogen-associated or damage-associated molecular patterns to surmount a response involving NLRP3 inflammasomes and proinflammatory cytokines [205, 211, 610]. NLRP3 inflammasomes integrate stress signals that activate caspase-1 and IL-1 β , a prominent and early mediator, amplifying the inflammatory reaction within the ischemic heart

causing further damage [168, 577, 611]. Genetic deletion of the NLRP3 gene or pharmacological inhibitors of inflammasome activation result in decreased myocardial infarct size and restore heart function after IR injury [205, 599, 610]. Several studies showed that the upregulation of the NLRP3 protein, the main component of NLRP3 inflammasome, after IR injury is attributed to the cross-talk between NLRP3 inflammasome and mitochondria, whereby NLRP3 senses ROS produced by dysfunctional mitochondria [200, 575]. Increasing evidence from both human and animal studies demonstrate that n-3 PUFAs can suppress inflammation and inhibit the production of proinflammatory cytokines including IL-1 β and thus may have a beneficial role in various human inflammatory diseases such as diabetes, atherosclerosis, and arthritis [394, 612-614]. In agreement with these reports, we demonstrated that DHA, EPA as well as 19,20-EDP not only significantly suppressed the accumulation of the active NLRP3 protein in the cytosol after IR injury but also suppressed the IR-induced activation of caspase-1. However, only 19,20-EDP was able to maintain IL-1 β at aerobic control levels. Interestingly, Yan et al., demonstrated that other oxygenated metabolites of DHA, including Protectin D1 (PD1), Resolvin D1 (RvD1) and aspirin-triggered Resolvin D1 (ATRvD1), produced by arachidonic acid-lipoxygenases and aspirin-acetylated COX-2 metabolic pathways were not involved in n-3 PUFA mediated inflammasome inhibition [613] supporting our findings that CYP epoxy metabolites are important for mediating its anti-inflammatory properties.

Ischemia dramatically alters mitochondrial efficiency by impacting oxidative phosphorylation, acidosis, and ionic gradients resulting in osmotic swelling and membrane depolarization. Although reperfusion therapy greatly enhances survivability, reperfusion itself may lead to further complications. The sudden re-introduction of oxygen causes re-energization of the mitochondria and reactivation of the electron transport chain. The electrons swiftly flow into

the mitochondria but cannot be used for oxidative phosphorylation because of a loss of cytochrome oxidase and dismutase enzymatic activity, leading to formation of ROS. Mitochondria gradually lose their ability to produce energy while continuing to emit higher amounts of ROS. Ultimately, the damage contributes to contractile dysfunction and cell death. Mitochondrial dysfunction results in decreased cardiac function, however, recent evidence indicates the role of mitochondria in regulating inflammasome activation and the subsequent responses [209]. Previously, we published data demonstrating CYP epoxygenase metabolites of DHA, such as 19,20-EDP, protect mitochondria from injury limiting cardiac cell death [339, 516, 579]. Similarly, in the current study, we demonstrate that cardioprotective effects of 19,20-EDP involve reduced mitochondrial injury as observed by the better postischemic respiration. Several reports show that proteins regulating mitochondrial dynamics are involved in myocardial IR injury [101, 102]. Under normal conditions, Drp-1 is found in the cytosol in an inactive form, however following cellular stress Drp-1 translocates to the outer mitochondrial membrane initiating mitochondrial fission and reducing the number of functional mitochondria, which accelerates myocardial death. Studies using genetic or pharmacological approaches to limit the accumulation of Drp-1 in the mitochondria protected cardiomyocytes against IR injury and improved cardiac contractile function [105, 106, 615]. Our data supports these findings where increased mitochondrial Drp-1 in the IR group had reduced mitochondrial function and impaired cardiac functional recovery. Both DHA and 19,20-EDP significantly inhibited the translocation of Drp-1 to the mitochondria, correlating with improved cardiac functional recovery. Further evidence indicating that 19,20-EDP limited mitochondrial injury was reflected in the expression of Opa-1. The Opa-1 protein is localized in the inner mitochondrial membrane and is considered an important determinant of mitochondrial integrity and function [97, 616]. It has been shown that during myocardial IR injury,

the excessive mitochondrial fission as well as the increased ROS production induce Opa-1 proteolysis leading to mitochondrial fragmentation, reduction in oxygen consumption rates and accordingly cardiomyocytes apoptosis. Moreover, reduced levels of Opa-1 have been reported in samples from human hearts with ischemic cardiomyopathy [616-619]. Consistently, our data suggest the cardioprotective effects of 19,20-EDP maintained levels of Opa-1 and consequently better mitochondrial respiratory function.

Studies suggest the involvement of Txnip as an activator of NLRP3 inflammasome and a pro-oxidant in the IR injury cascade [620, 621]. Under normal physiological conditions, Txnip is localized primarily in the nucleus, and upon IR stress, it translocates to the cytosol inhibiting the antioxidant activity of Trx-1 and activates NLRP3 inflammasome formation. Activated NLRP3 inflammasomes shuttle Txnip to the mitochondria inhibiting Trx-2 activity and initiating cell death processes in the cardiac cells [263, 622-624]. Our findings demonstrate IR injury results in increased cytosolic and mitochondrial Txnip as well as reduced Trx-1 and Trx-2 activities correlating with worse postischemic functional recovery. Yoshioka et al. demonstrated genetic deletion of Txnip protects the myocardium from IR injury [625]. Consistent with this notion, our results indicate 19,20-EDP is able to inhibit the translocation of Txnip to the cytosol and mitochondria under IR conditions. This maintains Trx-1 and -2 activities, which can act as antioxidant enzymes and consequently improve postischemic functional recovery. Importantly, both Akt and AMPK have been shown to inhibit IR-induced Txnip cardiac inflammation and injury [600, 601]. The increased p~Akt and p~AMPK observed following post-ischemic functional recovery in hearts perfused with 19,20-EDP provide a potential cardioprotective mechanism.

Mitochondria are dynamic organelles which are involved in a variety of cellular functions, including a link with the innate immune response. Interestingly, recent evidence indicates Mfn-2

has a role in NLRP3 inflammasome activation [602]. These data suggested a mitochondrial membrane potential-dependent association with NLRP3 and Mfn-2 in inflammasome activation following RNA virus infection. Our current study demonstrated elevated markers of NLRP3 inflammasome formation were associated with increased mitochondrial Mfn-2 expression in hearts following IR injury and the cardioprotective effects DHA or 19,20-EDP might involve limiting this response. Evidence indicates mitochondrial dysfunction will trigger an increased Mfn-2 expression and activation of NLRP3 inflammasomes beginning an innate immune response. There are multiple lines of evidence suggesting that the pro-apoptotic Mfn phenotype might be a unique function of Mfn-2 and not shared by Mfn-1 [108, 112, 626, 627]. We did not observe any changes the expression levels of Mfn-1 following IR injury. We believe DHA and/or EDPs limit the mitochondrial response to injury; however, our understanding of the connection between Mfn-2 and the protective mechanism(s) is unknown. While our data suggest DHA and/or EDP attenuate NLRP3 inflammasome activation, a potential process might involve mitochondrial and endoplasmic reticulum coupling. For example, Mfn-2 acts as a tether between the mitochondria and endoplasmic reticulum to facilitate Ca^{2+} transfer required for maintaining mitochondrial bioenergetics; under ischemic conditions this tether leads to mitochondrial Ca^{2+} overload accelerating mitochondrial degradation [615, 628]. Moreover, acute ablation of cardiac Mfn-2 reduces mitochondrial Ca^{2+} overload, rendering the heart resistant to acute infarction following IR [114]. Therefore, DHA and/or EDP might be working to regulate Ca^{2+} overload, as such further studies are required to understand the potential mechanisms.

In the current study, pretreatment with CYP epoxygenase inhibitor MSPPOH abrogated the effect of DHA on Mfn-2 and Opa-1, significantly blocked the ability of DHA to inhibit Drp-1 mitochondrial translocation, abolished the inhibitory effect of DHA on the expression levels of

NLRP3 and IL-1 β and consequently limited caspase-1 activity, indicating that the cardioprotective effects of DHA are mainly mediated by its metabolite 19,20-EDP (Figure 2.6). In conclusion, our results demonstrate that the CYP epoxygenase metabolite of DHA, 19,20-EDP, could protect against myocardial IR injury by preserving mitochondrial function and inhibiting NLRP3 inflammasome activation. However, neither EPA nor 17,18-EEQ provide sufficient protection against IR injury. Although the precise molecular mechanisms remain unknown, we propose that 19,20-EDP-mediated cardioprotective effects preserve the mitochondrial pool, reduce IR induced inflammasome activation and promote cell survival, which ultimately results in better cardiac functional recovery.

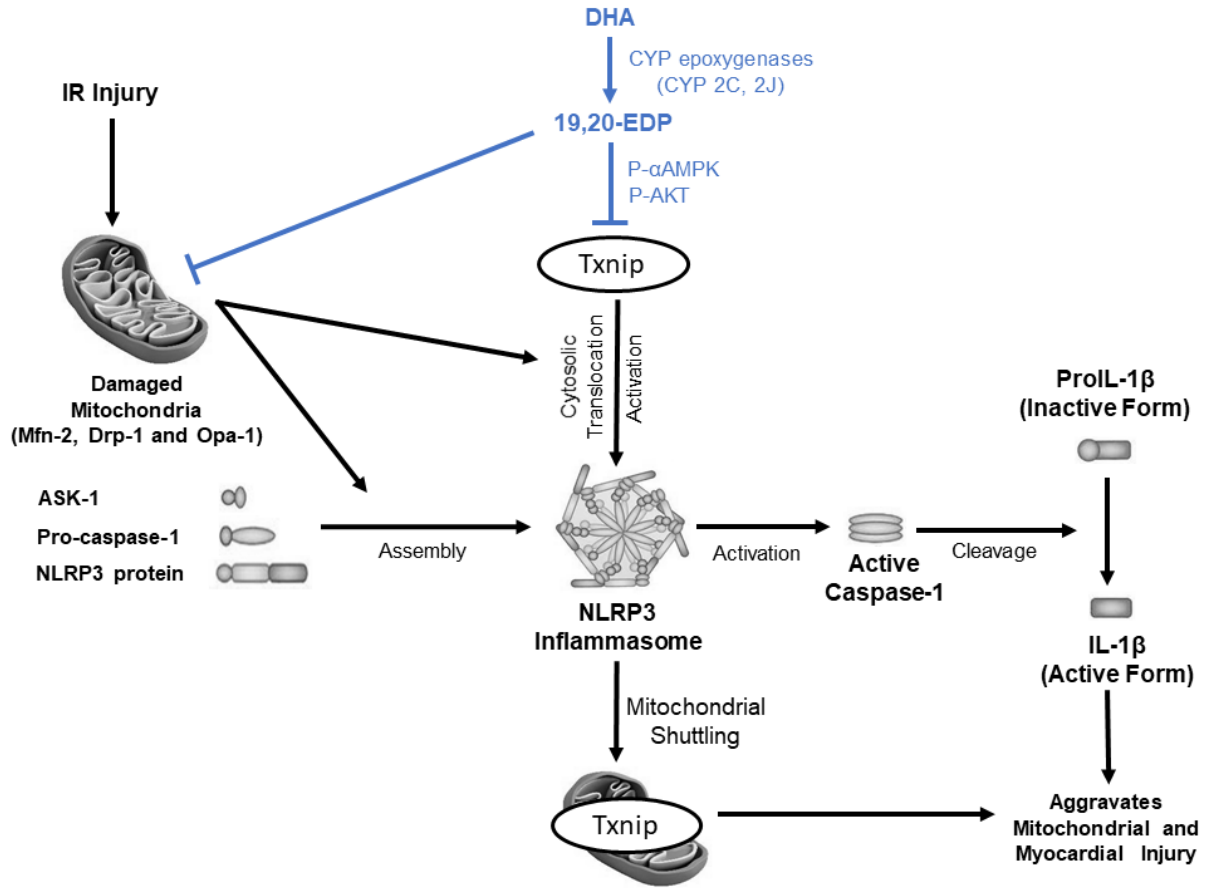


Figure 2. 6: Schematic showing the potential cardioprotective mechanisms. Hearts perfused with 19,20-EDP had preserved mitochondrial quality and consequently reduced NLRP3 activation protecting the heart against the IR insult. IR induces mitochondrial damage through the translocation of Drp-1 to the outer mitochondrial membrane initiating mitochondrial fission and thereby accelerating the proteolysis of the fusion protein Opa-1. These changes are associated with excessive ROS production from the damaged mitochondria activating the assembly of NLRP3 inflammasome and its downstream signal caspase-1 enzyme, which activates the formation of IL-1 β aggravating myocardial death. In addition, ROS are involved in the activation and translocation of Txnip to the cytosol, an important step in NLRP3 inflammasome formation, which then become shuttled to the mitochondria exacerbating mitochondrial damage. Often, these changes are associated with a marked accumulation of Mfn-2 on the mitochondria, an important signal for the translocation of NLRP3 and Txnip to the mitochondria. 19,20-EDP acts as a cardioprotective agent against these detrimental changes through yet to be identified molecular mechanisms. Under IR insult conditions, 19,20-EDP can (i) maintain mitochondrial integrity and function, (ii) activate α AMPK and Akt and thereby accelerate Txnip degradation, and consequently (iii) inhibit the activation and assembly of NLRP3 inflammasomes with its downstream detrimental signals, caspase-1 and IL-1 β . In summary, 19,20-EDP protective effects toward the mitochondria inhibit the activation of NLRP3 inflammasomes resulting in improved postischemic functional recovery following myocardial IR injury. IR, ischemia–reperfusion; DHA, docosahexaenoic acid; 19,20-EDP, 19,20-epoxydocosapentaenoic acid.

Chapter 3

Genetic Deletion or Pharmacological Inhibition of Soluble Epoxide Hydrolase Ameliorates Cardiac Ischemia/Reperfusion Injury by Attenuating NLRP3 Inflammasome Activation

This chapter has been adapted from the following published manuscript:

- **Ahmed M Darwesh**, Hedieh Keshavarz-Bahaghighat, K Lockhart Jamieson, John M Seubert. Genetic Deletion or Pharmacological Inhibition of Soluble Epoxide Hydrolase Ameliorates Cardiac Ischemia/Reperfusion Injury by Attenuating NLRP3 Inflammasome Activation. *Int J Mol Sci.* 2019;20(14):3502.

Abstract

Activation of the nucleotide-binding oligomerization domain-like receptor (NLR) family pyrin domain containing 3 (NLRP3) inflammasome cascade has a role in the pathogenesis of ischemia/reperfusion (IR) injury. There is growing evidence indicating cytochrome p450 (CYP450)-derived metabolites of n-3 and n-6 polyunsaturated fatty acids (PUFAs) possess both adverse and protective effects in the heart. CYP-derived epoxy metabolites are rapidly hydrolyzed by the soluble epoxide hydrolase (sEH). The current study hypothesized that the cardioprotective effects of inhibiting sEH involves limiting activation of the NLRP3 inflammasome. Isolated hearts from young wild-type (WT) and sEH null mice were perfused in the Langendorff mode with either vehicle or the specific sEH inhibitor trans-4-[4-(3-adamantan-1-yl-ureido)-cyclohexyloxy]-benzoic acid (t-AUCB). Improved post-ischemic functional recovery and better mitochondrial respiration were observed in both sEH null hearts or WT hearts perfused with t-AUCB. Inhibition of sEH markedly attenuated the activation of the NLRP3 inflammasome complex and limited the mitochondrial localization of the fission protein dynamin-related protein-1 (Drp-1) triggered by IR injury. Cardioprotective effects stemming from the inhibition of sEH included preserved activities of both cytosolic thioredoxin (Trx)-1 and mitochondrial Trx-2 antioxidant enzymes. Together, these data demonstrate that inhibiting sEH imparts cardioprotection against IR injury via maintaining post-ischemic mitochondrial function and attenuating a detrimental innate inflammatory response.

3.1 Introduction

Ischemic heart disease is a leading cause of cardiovascular death and disability worldwide [3, 629]. In patients who experience an ischemic event, early and successful restoration of blood flow to the ischemic myocardium, a process known as reperfusion, is critical to maintain viable myocardial tissue, limit infarct size and reduce acute mortality rates. However, reperfusion paradoxically can induce and exacerbate tissue injury resulting in increased incidence of chronic heart failure. Several studies demonstrated that up to 50% of the final infarct size could be attributed to the ischemia/reperfusion (IR) insult [14, 630]. While the mechanisms underlying IR injury are complex, activation of an inflammatory response associated with excessive mitochondrial damage contributes to deteriorating heart function [26].

Experimental evidence has demonstrated that during reperfusion a surge of reactive oxygen species (ROS) is rapidly generated from damaged mitochondria. This ROS burst triggers a series of inflammatory reactions, which induce the formation and activation of inflammasomes aggravating myocardial injury [209, 262, 575]. Inflammasomes are large cytosolic inflammatory protein scaffolds assembled in response to cellular danger signals in order to activate several innate immune defenses [631, 632]. The most widely characterized inflammasome platform in the heart that becomes activated in response to aseptic stimuli, such as myocardial IR injury, is the nucleotide-binding oligomerization domain-like receptor (NLR) family pyrin domain containing 3 (NLRP3) [576, 577]. In the setting of a myocardial IR insult, activation of the NLRP3 inflammasome spreads an inflammatory surge to the rest of the myocardium triggering further damage by promoting the autocatalytic activation of pro-caspase-1. Active caspase-1 subsequently cleaves inactive pro-interleukin-1beta (pro-IL-1 β) into to the mature pro-inflammatory cytokine IL-1 β triggering pyroptosis or caspase-1 mediated cell death [200, 207-209]. Accordingly, limiting

mitochondrial damage and blunting the activation of a NLRP3 inflammasome cascade is a promising therapeutic strategy to promote recovery and alleviate adverse cardiac injury following IR insult.

Soluble epoxide hydrolase (sEH) catalyzes the hydrolysis of lipid epoxides to their corresponding diol derivatives by the addition of water [633]. sEH is highly expressed in the mammalian heart tissue and has a pivotal role in metabolizing cytochrome P450 (CYP450)-derived epoxy metabolites of both n-3 and n-6 polyunsaturated fatty acids (PUFAs) to their corresponding diol derivatives [507]. For example, sEH rapidly degrades the cardioprotective lipids epoxydocosapentaenoic acids (EDPs) and epoxyeicosatrienoic acids (EETs) into their less bioactive corresponding diol products [634, 635]. In contrast, the CYP-derived epoxy metabolites of linoleic acid (LA), epoxyoctadecenoic acids (EpOMEs), are rapidly converted by sEH into their corresponding bioactive diols, dihydroxyoctadecenoic acid (DiHOME) [636, 637], which have been shown to have cardiotoxic effects [581, 638-640]. Altogether, the detrimental outcomes associated with the activation of sEH in response to cardiovascular insult could be attributed to the excessive degradation of protective epoxy lipids (i.e., EDPs and EETs) and enhanced production of toxic diol-metabolites (i.e., DiHOMEs).

Inhibition of sEH has emerged as an intriguing approach to limit cardiac damage in different cardiovascular settings [641, 642]. Despite all the promising findings associated with the inhibition of sEH in the heart, the effect of sEH inhibition on mitochondrial degeneration and the associated NLRP3 inflammasome activation in the setting of IR injury has not been investigated. Results from the current study builds upon our previous findings [570, 643] and demonstrates that deletion of the gene encoding sEH (*Ephx2*) or pharmacological inhibition of sEH enzyme could attenuate myocardial IR injury through maintaining mitochondrial function and consequently

limiting NLRP3 inflammasome activation. To the best of our knowledge, the current study also provides the first evidence that the cardioprotective effects associated with sEH inhibition against IR injury is sex-independent in young subjects.

3.2 Materials and Methods

3.2.1 Animals

Mice with targeted disruption of *EPHX2* (sEH null) and wild-type (WT) littermates on a C57/Bl6 background were maintained in a colony at the University of Alberta [581] and used in the current study. All studies were carried out using 2–3 month-old male and female mice weighing 25–30 g. Mice were fed on a standard rodent chow diet ad libitum (fat 11.3%, fiber 4.6%, protein 21% (w/w)), more specifically linoleic acid (2.12%), linolenic acid (0.27%), arachidonic acid (0.01%), omega-3 fatty acid (0.45%), total saturated fatty acid (SFA) (0.78%) and total monounsaturated fatty acids (MSFA) (0.96%) (PicoLab® Rodent Diet 20 Cat. No 5053, LabDiets, Inc., St. Louis, MO, USA) and housed under conditions of constant temperature and humidity with a 12:12-h light–dark cycle. All animal experimental protocols were approved by the University of Alberta Health Sciences Welfare Committee (University of Alberta Animal Welfare, ACUC, study ID#AUP330, Renewal June, 2019) and conducted according to strict guidelines provided by the Guide to the Care and Use of Experimental Animals (Vol. 1, 2nd ed., 1993, from the Canadian Council on Animal Care).

3.2.2 Isolated heart perfusion

Soluble epoxide hydrolase null (sEH^{-/-}) and wild-type (WT) mice of both sexes (equal ratios) were anesthetized by an intraperitoneal injection of sodium pentobarbital (Euthanyl, 100 mg/kg). Following complete non-responsiveness to external stimulation, hearts were quickly excised and perfused in the Langendorff mode with Krebs–Henseleit buffer containing (in mM) 120 NaCl, 25 NaHCO₃, 10 Dextrose, 1.75 CaCl₂, 1.2 MgSO₄, 1.2 KH₂PO₄, 4.7 KCL, 2 Sodium Pyruvate (pH 7.4) and bubbled with 95% O₂ and 5% CO₂ at 37 °C [383, 581, 583]. The left atrium was then excised, and a water-filled balloon made of saran plastic wrap was inserted into the left ventricle through the mitral valve. The balloon was connected to a pressure transducer for continuous measurement of left ventricular developed pressure (LVDP) and heart rate (HR). Hearts with persistent arrhythmias or LVDP less than 80 cm H₂O were excluded from the experiment. Mouse hearts were perfused in the retrograde mode at a constant flow rate for 40 min of baseline (stabilization) and then subjected to 30 min of global no flow ischemia followed by 40 min of reperfusion. In a group of WT mice, the specific sEH inhibitor trans-4-[4-(3-adamantan-1-yl-ureido)-cyclohexyloxy]-benzoic acid (t-AUCB) (0.1 μM) (Cayman Chemicals, Ann Arbor, MI, USA) [643] was added 20 min before ischemia and was present in the heart until the end of the reperfusion period. The percentage of LVDP at 40 min of reperfusion (R40), as compared to baseline LVDP, was taken as a marker for recovery of contractile function. At the end of reperfusion, hearts were immediately flash frozen in liquid nitrogen and stored below -80 °C. Contractile and hemodynamic parameters were acquired and analyzed using ADI software from (Holliston, MA, USA). Collection of the heart effluent was done during both pre- and post-ischemic protocols to determine coronary flow (CF) rates.

3.2.3 Immunoblotting

Frozen mouse hearts were ground, homogenized and then fractionated into mitochondrial and cytosolic fractions as previously described [582, 583]. Briefly, frozen cardiac tissues were ground with mortar and pestle on dry ice and then homogenized in ice-cold homogenization buffer (20 mmol/L Tris-HCL, 50 mmol/L NaCl, 50 mmol/L NaF, 5 mmol/L sodium pyrophosphate, 1 mmol/L EDTA, and 250 mmol/L sucrose added on the day of the experiment, pH 7.0). Samples were first centrifuged at 800× g for 10 min at 4 °C to separate the cellular debris. The collected supernatant was then centrifuged at 10,000× g for 20min. The pellet was resuspended in homogenization buffer to obtain a mitochondrial-enriched fraction. The supernatant was ultracentrifuged at 105,000× g for 60 min and the subsequent supernatant was used as the cytosolic fraction. Protein concentrations in both cytosolic and mitochondrial fractions were measured by the Bradford assay. Western blotting was done as previously described [383, 584]. Protein (30–50 µg) was resolved by electrophoresis on (10–15%) SDS-polyacrylamide gels and transferred onto polyvinylidene difluoride (PVDF) membranes (BioRad Laboratories, Hercules, CA, USA). Immunoblots were probed with antibodies to Drp-1 (Cat#: 5391), glyceraldehyde 3-phosphate dehydrogenase (GAPDH) (Cat#: 51745), heat shock protein 60 (Hsp60) (Cat#: 4870) (1:1000, Cell Signaling Technology, Inc., Danvers, city, MA, USA), NLRP3 protein (1:500) (Cat#: ab214185), Mitofusin (Mfn)-1 (ab104274), Mfn-2 (ab50838) (1:1000, Abcam, Burlingame, CA, USA), sEH (Cat#: E-AB-60489, 1:250, Elabscience Biotechnology Co., Wuhan, China), and thioredoxin interacting protein (Txnip) (Cat#: K0205-3, 1:500, MBL International Co., Woburn, MA, USA). After washing, membranes were incubated with the corresponding secondary antibodies (1:5000). The blots were visualized with ECL reagent. Relative band intensities were expressed as fold of the control assessed using ImageJ software (Version 1.47v, NIH, USA).

3.2.4 Enzyme-Linked Immunosorbent Assay

Enzyme-linked immunosorbent assay (ELISA) was used to quantify the cardiac cytosolic levels of the cytokine IL-1 β where mouse IL-1 β ELISA kit (ab100705, Abcam) was used according to the manufacturer's recommendations. Briefly, cytosolic samples were pipetted into a 96-well plate where IL-1 β present in a sample became attached to the wells by the immobilized antibody specific for mouse IL-1 β that is coated on the wells. The wells were then washed, and biotinylated anti-mouse IL-1 β antibody was added. Horseradish peroxidase (HRP) conjugated streptavidin was added to the wells after washing away unbound biotinylated antibody. A 3,3',5,5'-Tetramethylbenzidine (TMB) substrate solution was then added to the wells. Afterwards, the stop solution was pipetted into the wells and the intensity of the color was measured at 450 nm. IL-1 β concentration in the different samples was calculated by using a linear standard curve created with different concentrations of the standard IL-1 β .

3.2.5 Measurement of malondialdehyde (MDA) levels

The level of malondialdehyde (MDA) was assessed in the cardiac tissue using a lipid peroxidation (MDA) colorimetric assay kit (Abcam, Burlingame, CA, USA) according to manufacturer's instructions [644]. In this assay, free MDA present in the sample reacts with thiobarbituric acid (TBA) and generates a MDA-TBA adduct which was quantified colorimetrically at wavelength 532 nm. MDA levels were expressed as nmole MDA per mg protein.

3.2.6 Mitochondrial respiration

Clark electrode connected to an Oxygraph Plus recorder (Hansatech Instruments Ltd., Norfolk, England) was used to measure mitochondrial oxygen consumption in permeabilized cardiac fibers. Fresh cardiac fibers were isolated from the left ventricles of the perfused hearts at the end of reperfusion as previously described [584, 585]. Briefly, heart tissues were dissected under a dissecting microscope in ice-cold isolation buffer (2.77 mM Ca KEGTA, 7.23 mM K₂EGTA, 20 mM imidazole, 20 mM taurine, 49 mM K-MES, 3 mM K₂HPO₄, 9.5 mM MgCl₂, 5.7 mM ATP, 1 μM leupeptin, 15 mM phosphocreatine). A 3–5 mm strip of the anterior left ventricle was isolated and the remaining fats and vessels were removed. Afterwards, myocardial strips were disassembled into bundles containing 6–8 fibers each, 1 mm wide and 3–4 mm long. Fresh fibers were then permeabilized in isolation buffer containing 100 μg/mL saponin, washed three times for 5 min in ice-cold respiration buffer and immediately added to the respiration chamber containing 1.8 mL respiration buffer. The rate of oxygen consumption was measured at 30 °C before and after addition of 0.5 mM adenosine diphosphate (ADP) in the presence of 5 mM malate and 10 mM glutamate as respiratory substrates to initiate basal respiration. RCR was calculated as the ratio between basal and ADP-stimulated respiration rates to estimate mitochondrial respiration efficiency.

3.2.7 Enzymatic assays

Cleavage of the caspase-1 specific fluorogenic substrate Ac-YVAD-AMC (Cat #: ALX-260-024-M005, Enzo life Sciences, Farmingdale,, NY, USA) was used to assess functional caspase-1 activity in cytosolic fractions of the heart homogenates [586]. The assay quantitated the fluorescence intensity of the cleaved 7-Amino-4-methylcoumarin (AMC) using a fluorometer (at

excitation 380 nm, and emission 460 nm wavelengths). The activity was calculated by using a linear standard curve created with AMC.

The insulin disulfide reduction assay was conducted to measure thioredoxin (Trx) activity as previously described [587, 588]. In this assay, Trx is first reduced by TrxR enzyme and then is used to reduce insulin disulfides. Briefly, equal amounts of mitochondrial or cytosolic protein (30 μ g) were preincubated with 2 μ L of dithiothreitol (DTT) activation buffer (100 mM HEPES (pH 7.6), 2 mM EDTA, 1 mg/mL bovine serum albumin (BSA), 2 mM DTT at 37 °C for 15 min to reduce and activate endogenous Trx. Afterwards, 20 μ L of reaction mixture containing 100 mM HEPES pH 7.6, 2 mM EDTA, 0.2 mM NADPH, and 140 μ M insulin were added. The reaction was then started by the addition of 0.5 U mammalian TrxR (Cayman Chemicals, Ann Arbor, MI, USA) or an equal volume of water for negative controls. The samples were incubated at 37 °C for 30 min. The reaction was stopped by the addition of 125 μ L of stop solution containing 10 M guanidine hydrochloride and 1.7 mM (5,5-dithio-bis-(2-nitrobenzoic acid) (DTNB) in 0.2 M Tris-HCl (pH 8.0). Reduction of DTNB to 5-thio-2-nitrobenzoic acid (TNB) was detected by optical density at 412 nm. Changes in the absorbance in the absence of TrxR were subtracted from those in the presence of the reductase.

3.2.8 Statistics

Values are expressed as mean \pm standard error of mean (SEM). Statistical significance was determined by one-way analysis of variance (ANOVA) with a Tukey post hoc test to assess differences between groups; $p < 0.05$ was considered statistically significant.

3.3 Results

3.3.1 Deletion or inhibition of sEH improves post-ischemic functional recovery in both males and females

Although accumulating literature suggests that sEH enzyme is a good target to ameliorate IR injury [581, 583, 641], the differential response of both males and females to sEH inhibition has not been investigated. Notably, preischemic cardiac parameters were similar between males and females in all young treatment groups. sEH null hearts or WT hearts perfused with the sEH inhibitor t-AUCB and subjected to IR showed significantly improved post-ischemic recovery of LVDP compared to the WT IR control group (Figure 3.1A). Importantly, both male and female hearts respond similarly to the genetic deletion of *Ephx2* or pharmacological inhibition of sEH as there were no significant differences between both sexes in terms of post-ischemic functional recovery (Figure 3.1A). Moreover, no significant differences were observed in the heart rate at the end of reperfusion between all the study groups (Figure 3.1B). Consistent with improved post-ischemic functional recovery, both male and female sEH null hearts or WT hearts perfused with t-AUCB demonstrated better rates of contraction (dP/dt max) and relaxation (dP/dt min) in comparison to the corresponding IR control mice (Figure 3.1 C and D). Interestingly, the coronary flow rates did not significantly differ between pre- and post-ischemic perfused heart in any of the treatment groups in our model indicating the cardioprotective effect was not attributable to alterations in hemodynamics in the perfused heart model (Figure 3.1E). Together, these data suggest that the genetic deletion of *Ephx2* or pharmacological inhibition of sEH similarly improve post-ischemic functional recovery in both males and females and as such data from both sexes were combined in the rest of the experiments.

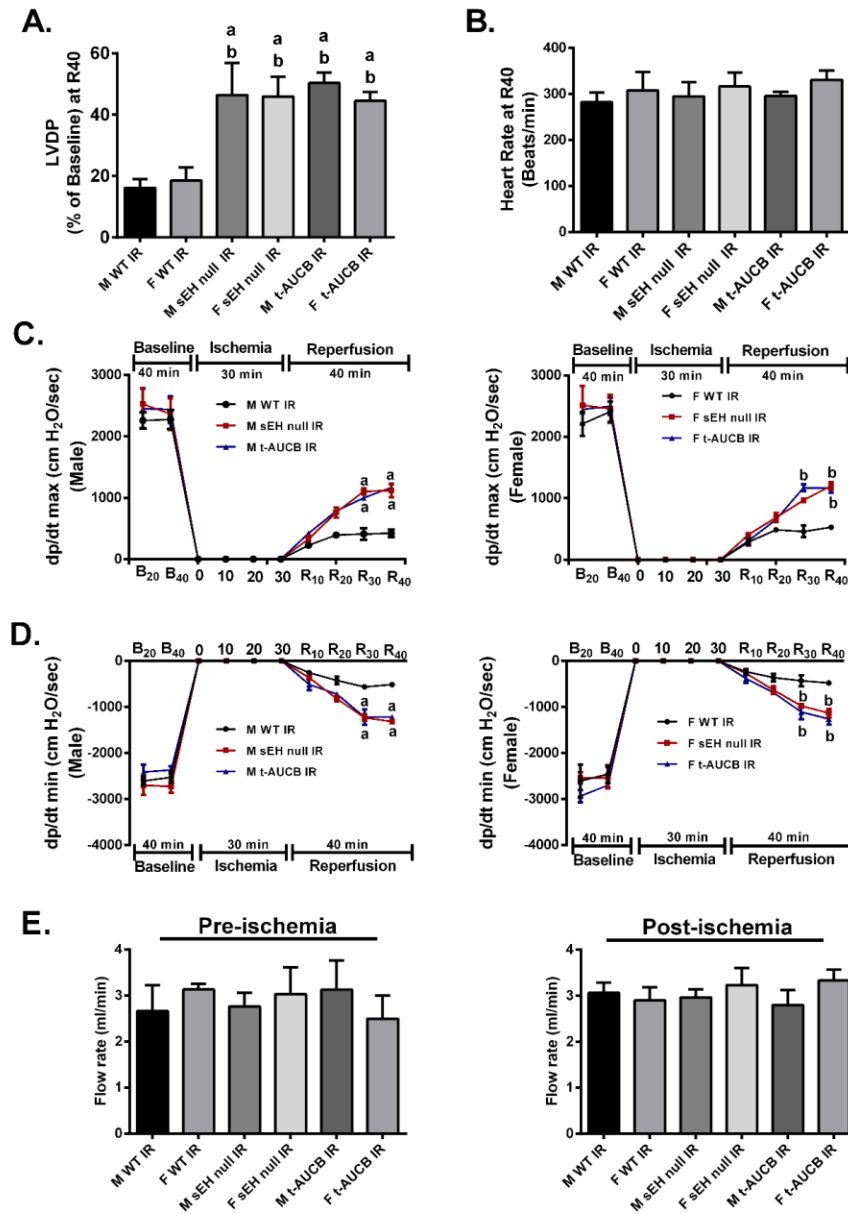


Figure 3. 1: Genetic deletion of *Ephx2* or pharmacological inhibition (t-AUCB) of soluble epoxide hydrolase (sEH) improved post-ischemic contractile parameters in both males and females. (A) Left ventricular developed pressure (LVDP) recovery at 40 min of reperfusion as a percentage of baseline, (B) heart rate assessed as beats per minute (BPM) at the end of reperfusion (R40), (C) rate of contraction (dp/dt max), (D) rate of relaxation (dp/dt min) in both male and female hearts at the baseline before (B₂₀) and after (B₄₀) drug treatment, at ischemia, and at 10, 20, 30 and 40 min reperfusion (R₁₀, R₂₀, R₃₀, and R₄₀), and (E) coronary flow rates from perfused hearts both pre- and post-ischemia. Values represent mean \pm standard error of mean (SEM); a $p < 0.05$ vs. M WT IR, b $p < 0.05$ vs. F WT IR (n = 4–7 per group). F; Female, LVDP; Left ventricular developed pressure, M; Male.

3.3.2 Deletion or inhibition of sEH limits post-ischemic mitochondrial injury

Mitochondria serve as the important arbiters of cardiomyocyte life and death [645]. Impaired mitochondrial function, associated with excessive ROS production, secondary to IR injury leads to a vicious cycle of continued injury and reduced cardiac contractile function [46, 47]. Accordingly, we investigated the effect of the genetic deletion of *Ephx2* or pharmacological inhibition (t-AUCB) of sEH on the mitochondrial respiration in fibers separated from hearts subjected to IR injury. Notably, basal respiration rates did not differ significantly between all groups (Table 3.1), however, respiratory control ratio (RCR), a marker of mitochondrial efficiency, was significantly reduced in post-ischemic WT vehicle control hearts compared to both the WT and sEH null aerobic controls (Figure 3.2). However, genetic deletion of *Ephx2* or pharmacological inhibition of sEH preserved post-ischemic ADP-stimulated respiration and RCR values, suggesting better mitochondrial function in post-ischemic hearts (Table 3.1).

Table 3. 1: Mitochondrial respiration was measured in permeabilized cardiac fibers freshly isolated at the end of reperfusion.

Groups	Basal Respiration (nmol O ₂ /min/mg)	ADP-stimulated (nmol O ₂ /min/mg)	Respiratory Control Ratio (RCR)
WT Aerobic	0.64 ± 0.12	3.36 ± 0.81	5.26 ± 0.49
sEH null Aerobic	0.58 ± 0.15	2.70 ± 0.71	4.90 ± 0.75
WT IR	0.75 ± 0.18	1.02 ± 0.21	1.43 ± 0.11 *†
sEH null IR	0.97 ± 0.36	3.95 ± 1.37	4.03 ± 0.31 #
t-AUCB IR	0.88 ± 0.18	2.92 ± 0.49	3.87 ± 0.59 #

Oxygen consumption was assessed using a Clark electrode connected to an Oxygraph Plus recorder where malate and glutamate were used to stimulate basal respiration. Rates were presented as Respiratory Control Ratio (RCR), which is a ratio of adenosine diphosphate (ADP)-stimulated to basal respiration. Values represent mean ± SEM, * p < 0.05 vs. WT Aerobic CT, † p < 0.05 vs. sEH null Aerobic, # p < 0.05 vs. WT IR (n = 4–8 per group).

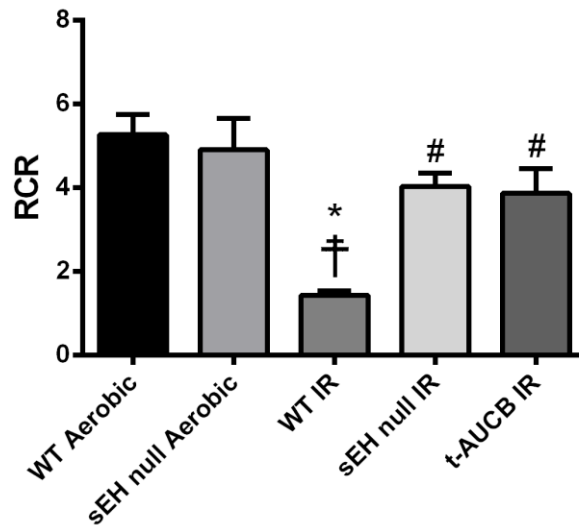


Figure 3. 2: Deficiency of sEH preserved mitochondrial respiratory function following IR injury. Histogram demonstrating changes in respiratory control ratio (RCR) values in both wild-type (WT) and sEH null mice under aerobic conditions or following 30 min ischemia and 40 min reperfusion. Values represent mean ± SEM, * p < 0.05 vs. WT Aerobic CT, † p < 0.05 vs. sEH null Aerobic, # p < 0.05 vs. WT IR (n = 4–8 per group).

Several studies demonstrated that proteins regulating mitochondrial dynamics, such as Drp-1, play a role in the cascade of myocardial IR injury [101, 105]. In response to IR injury, Drp-1 translocates from the cytosol to the mitochondria resulting in uncontrolled and exaggerated fission inducing myocardial cell death [106]. Consistent with this notion, we observed a significant increase in mitochondrial expression of Drp-1 in hearts from WT IR mice (Figure 3.3A). This finding is consistent with the decreased mitochondrial respiration/function observed in post-ischemic vehicle WT IR hearts. Genetic deletion of *Ephx2* or pharmacological inhibition of sEH limited the post-ischemic mitochondrial localization of Drp-1 (Figure 3.3A), supporting the notion of reduced mitochondrial injury.

Excessive mitochondrial damage, in response to IR injury, often results in significant elevations in cellular ROS levels. Thioredoxins (Trxs) are important antioxidant proteins that play a cytoprotective role against various oxidative stresses in a variety of systems. Trxs are important for maintaining the reducing environment in the cell, protecting against oxidative stress and thus limiting cardiomyocyte cell death [593, 646]. In mammalian cells, there are two major isoforms of Trxs, cytosolic Trx-1 and mitochondrial Trx-2 [593-595]. In the current study, we observed a marked reduction in both cytosolic Trx-1 and mitochondrial Trx-2 antioxidant activities in WT hearts subjected to IR injury, suggesting increased ROS levels (Figure 3.3 B and C). Moreover, the cardiac levels of MDA, the main end product of lipid peroxidation and a key marker of oxidative stress [644, 647], were significantly elevated following IR injury (Figure 3.3D). However, genetic deletion of *Ephx2* or pharmacological inhibition of sEH preserved both Trx-1 and Trx-2 catalytic activities as well as significantly blunted the accumulation of MDA in post-ischemic hearts (Figure 3.3 B, C and D), suggesting less ROS production.

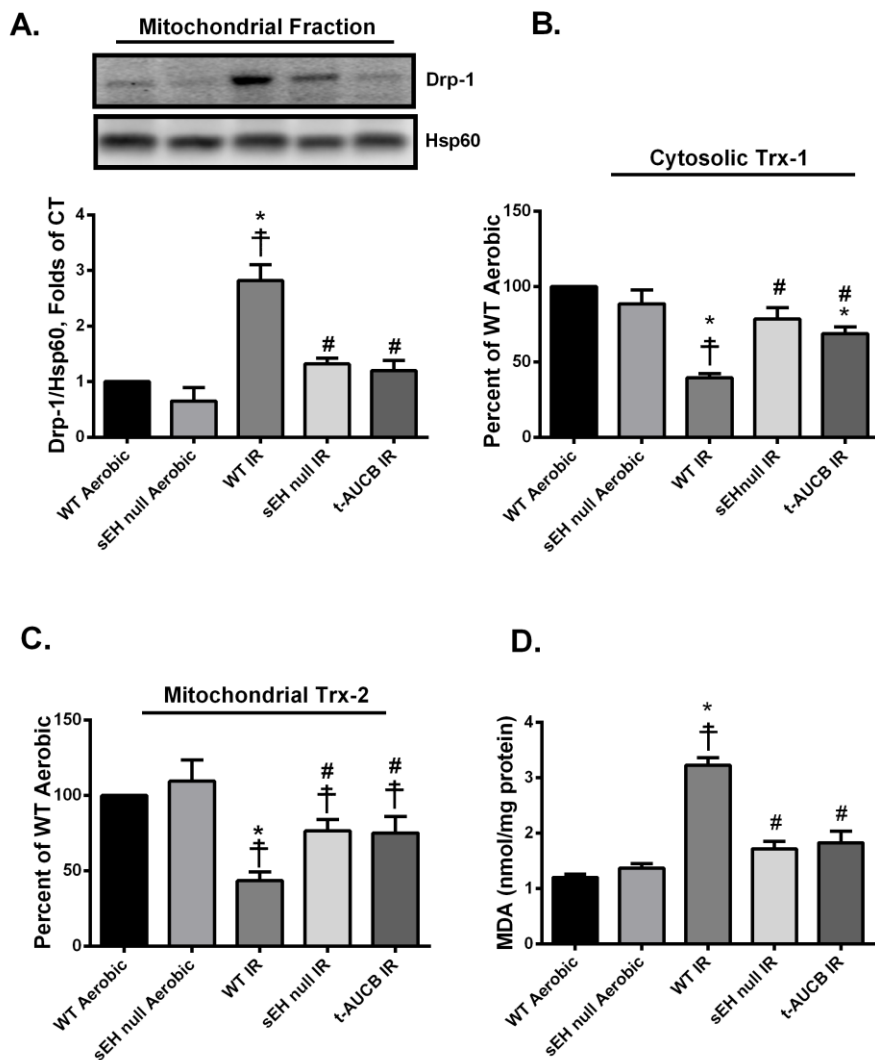


Figure 3. 3: Deficiency of sEH preserved mitochondrial integrity and limited oxidative stress following ischemia/reperfusion (IR) injury. (A) Representative immunoblots and densitometric quantification of the expression of mitochondrial protein Drp-1 in mice hearts after 30 min ischemia and 40 min reperfusion. Protein expression was normalized to heat shock protein 60 (Hsp60) used as a loading control. Cardiac (B) cytosolic thioredoxin (Trx)-1 and (C) mitochondrial Trx-2 activities were assessed in hearts following 30 min ischemia and 40 min reperfusion. Trx activity was assessed using the insulin disulfide reduction assay. In this assay, by using an excess of NADPH and thioredoxin reductase (TrxR) enzyme, Trx activity was measured via the oxidation of NADPH and the generation of free SH groups in reduced insulin by 5,5'-dithiobis-(2-nitrobenzoic acid) (DTNB) after stopping the reaction with guanidine-HCl. (D) Cardiac MDA levels assessed using a lipid peroxidation (MDA) colorimetric assay kit in mice hearts following 30 min ischemia and 40 min reperfusion. Values represent mean \pm SEM, * $p < 0.05$ vs. WT Aerobic CT, † $p < 0.05$ vs. sEH null Aerobic, # $p < 0.05$ vs. WT IR (n = 3–5 per group).

3.3.3 Deletion or inhibition of sEH abrogates the assembly and activation of NLRP3 inflammasome secondary to IR injury

Immunoblotting confirmed the complete ablation of the gene encoding sEH (*Ephx2*) in sEH null animals (Figure 3.4A). Furthermore, there was no marked change in the expression of sEH protein in WT mice subjected to IR injury compared to their counterparts under aerobic conditions (Figure 3.4A). A direct correlation between mitochondrial dysfunction, excessive ROS production and the activation of NLRP3 inflammasome cascade has been well-established in several reports [260, 575]. To determine the effect of the genetic deletion of *Ephx2* or pharmacological inhibition of sEH on the activation of the NLRP3 inflammasome, we assessed the expression levels of NLRP3 and IL-1 β proteins as well as caspase-1 activity. Immunoblot analyses showed that IR injury markedly up-regulated NLRP3 protein expression (Figure 3.4B), which correlated with increased catalytic activity of caspase-1 in WT hearts (Figure 3.4C). Moreover, enzyme-linked immunosorbent assay (ELISA) results revealed that active cytokine IL-1 β was increased following IR injury in WT hearts (Figure 3.4D). Genetic ablation of *Ephx2* or perfusing with t-AUCB markedly abrogated the IR-induced upregulation of NLRP3 and IL-1 β protein expression and prevented the increase of caspase-1 activity (Figure 3.4 B, C and D). Altogether, these data suggest inhibition of sEH limits NLRP3 inflammasome activation correlated with reduced cardiac IR injury.

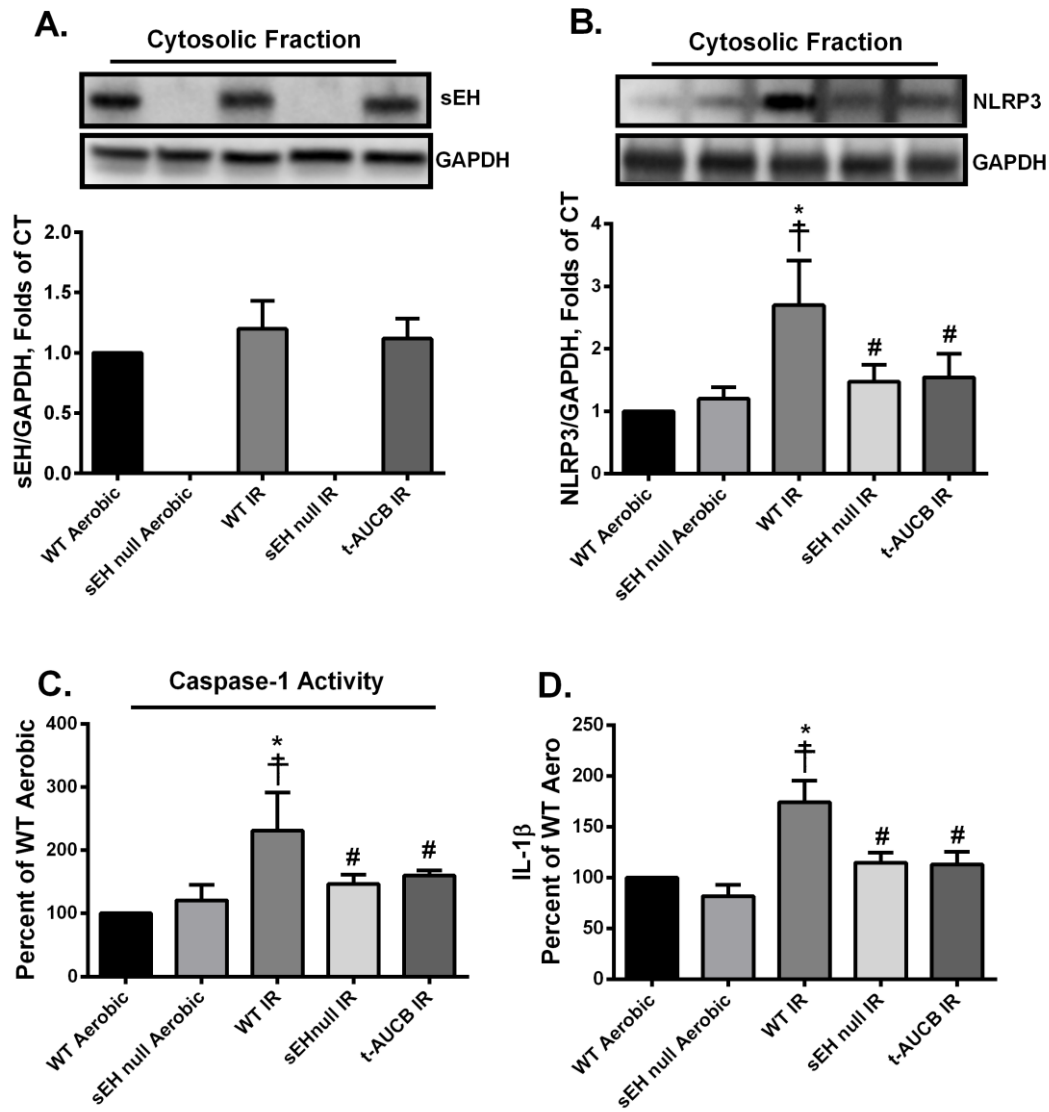


Figure 3. 4: Genetic deletion of *Ephx2* or pharmacological inhibition of sEH inhibited IR-induced NLRP3 inflammasome activation. Representative immunoblots and densitometric quantification of the expression of the cytosolic proteins (A) sEH and (B) NLRP3 in mice hearts after 30 min ischemia and 40 min reperfusion. All expressions were normalized to glyceraldehyde 3-phosphate dehydrogenase (GAPDH) loading control. (C) Cardiac caspase-1 enzymatic activity assessed in the cytosolic fraction following 30min ischemia and 40min reperfusion. The assay quantitated the fluorescence intensity resulting from the cleavage of the caspase-1 specific fluorogenic substrate Ac-YVAD-AMC by the cytosolic heart homogenates. (D) Cardiac IL-1 β protein levels assessed by enzyme-linked immunosorbent assay (ELISA) in the cytosolic fraction following 30 min ischemia and 40 min reperfusion. Values represent mean \pm SEM, * $p < 0.05$ vs. WT Aerobic CT, † $p < 0.05$ vs. sEH null Aerobic, # $p < 0.05$ vs. WT IR (n = 3–5 per group).

3.3.4 Deletion or inhibition of sEH blunts the activation and mitochondrial translocation of thioredoxin-interacting protein (Txnip) secondary to IR injury.

Thioredoxin-interacting protein (Txnip) is an upstream trigger in the NLRP3 inflammasome cascade that binds these two proteins together, which is essential for downstream activation. Furthermore, Txnip acts as a pro-oxidant protein by preferentially binding to and inhibiting the antioxidant activities of both Trx-1 and -2. Thus, Txnip serves as a central protein linking oxidative stress to NLRP3 inflammasome formation [599, 620, 624]. In the current study, post-ischemic WT hearts had a significant increase of both cytosolic and mitochondrial Txnip protein expression consistent with increased inflammasome formation and mitochondrial dysfunction (Figure 3.5 A and B). Interestingly, the accumulation of Txnip correlates with the significant reduction in the antioxidant activities of both Trx-1 and -2 in WT hearts following IR injury (Figure 3.3 B and C). In contrast, hearts perfused with t-AUCB or isolated from sEH null mice demonstrated significantly lower post-ischemic localization of Txnip in both cytosolic and mitochondrial fractions (Figure 3.5 A and B).

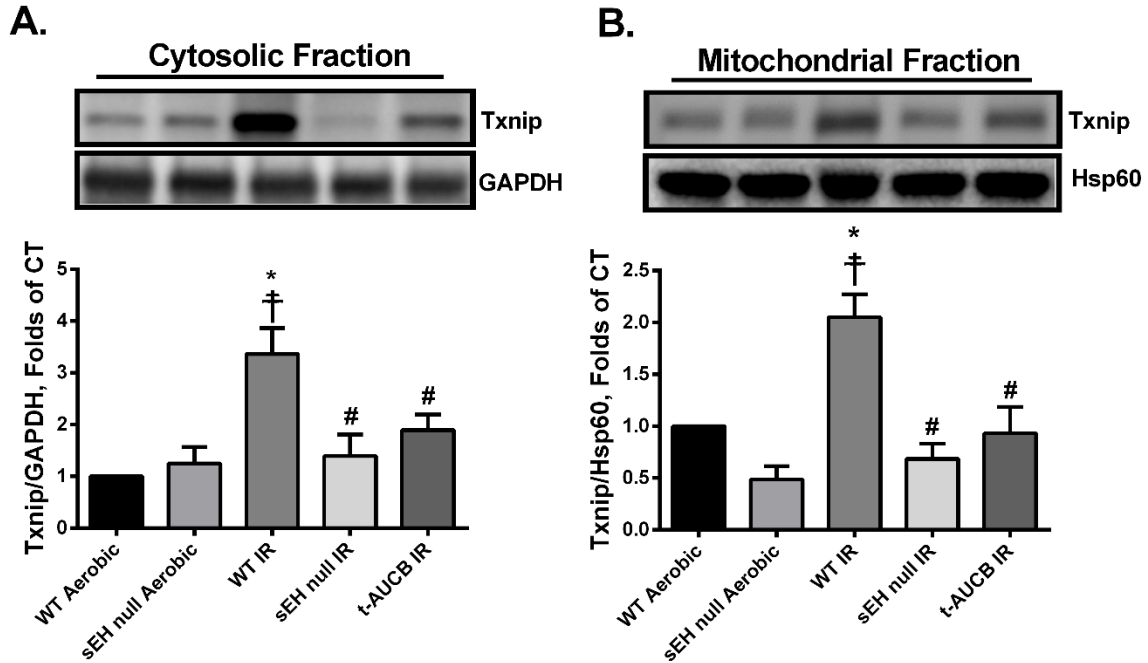


Figure 3. 5: Genetic deletion of *Ephx2* or pharmacological inhibition of sEH prevented IR-induced activation and translocation of the pro-oxidant Txnip. Representative immunoblots and densitometric quantification of protein expression of (A) cytosolic Txnip and (B) mitochondrial Txnip in hearts after 30 min ischemia and 40 min reperfusion. Cytosolic protein expression was normalized to GAPDH while mitochondrial Txnip expression was normalized to Hsp60. Values represent mean \pm SEM, * $p < 0.05$ vs. WT Aerobic CT, † $p < 0.05$ vs. sEH null Aerobic, # $p < 0.05$ vs. WT IR (n = 3–4 per group).

3.3.5 Deletion or inhibition of sEH abrogates the IR-Induced upregulation of the mitochondrial protein mitofusin-2

Mitofusins (Mfn)-1 and -2 are integral proteins that localize to the outer mitochondrial membrane and have a role in dynamic events regulating mitochondrial quality [648]. In the mammalian heart, Mfn-1 expression is higher than Mfn-2 and is primarily responsible for mitochondrial fusion [109]. However, emerging evidence indicates non-canonical roles for Mfn-2 within specific cell types include activation of the NLRP3 inflammasome and cardiomyocyte cell death [112, 602]. In the current study, we observed no significant differences in mitochondrial expression of Mfn-1 among the different study groups (Figure 3.6A). However, there were significant increases in mitochondrial expression of Mfn-2 in post-ischemic WT hearts, which were attenuated when *Ephx2* was genetically deleted (Figure 3.6B). Although pharmacological inhibition of sEH showed a trend to limit mitochondrial expression of Mfn-2, it did not reach statistical significance compared to WT IR hearts (Figure 3.6B). Overall, these data correlate with deteriorated mitochondrial function and activated NLRP3 inflammasome cascade observed in post-ischemic WT hearts and are also consistent with the reduced cardiac injury in sEH null or pharmacologically treated mice.

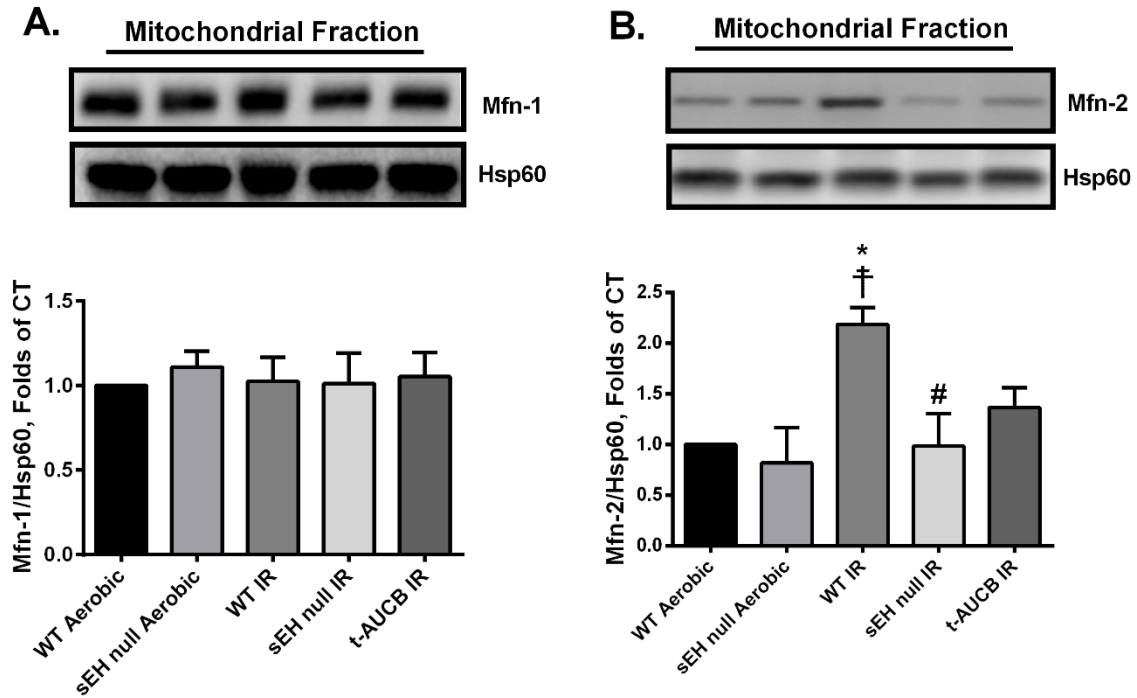


Figure 3. 6: Effect of genetic deletion of *Ephx2* or pharmacological inhibition of sEH on the post-ischemic expression of mitochondrial mitofusins (Mfns). Representative immunoblot and densitometric quantification of the mitochondrial expression of (A) Mfn-1 and (B) Mfn-2 proteins in mice hearts following 30 min ischemia and 40 min reperfusion. Values represent mean \pm SEM, * $p < 0.05$ vs. WT Aerobic CT, † $p < 0.05$ vs. sEH null Aerobic, # $p < 0.05$ vs. WT IR (n = 3–4 per group).

3.4 Discussion

In the current study, we demonstrate that genetic deletion of *Ephx2* or pharmacological inhibition of sEH enzyme with t-AUCB limits mitochondrial damage, abrogates activation of the NLRP3 inflammasome cascade, improves post-ischemic functional recovery and thus imparts cardioprotection in the setting of IR injury. The cardioprotective effects associated with sEH inhibition were independent of sex or hemodynamic changes in young mice. Together, the current data suggest a novel cardioprotective mechanism for inhibition of sEH that limits an innate inflammatory response.

The gene encoding mammalian sEH (*Ephx2*) has been identified in numerous species such as mouse [649], rat [650] and human [651], as well as bacteria [652, 653] and plants [654, 655]. Importantly, sEH catalytic activity supports both advantageous and deleterious reactions in its role to metabolize endogenous or exogenous epoxides. Under normal physiological conditions, endothelial sEH plays a pivotal role in the metabolism of epoxy lipids into diol metabolites, a function that modulates the biological effects of the lipids within the cardiovascular system [656]. Moreover, in healthy individuals, there is likely an equilibrium between the anti-inflammatory metabolites generated by CYP450 and the sEH-derived pro-inflammatory ones [657]. However, under many pathophysiological states, such as diabetes, obesity, IR injury and aging, there is a shift in equilibrium favoring more sEH-dependent inflammatory pathways [658]. Therefore, blocking sEH activity has become a promising therapeutic approach to limit adverse inflammatory responses and the associated injury.

Inhibition of sEH has emerged over the last few years as an attractive therapeutic approach for the treatment and prevention of several cardiovascular disorders [571, 580, 581, 583, 641, 642, 659-661]. In the mammalian heart, there is a mounting evidence that CYP-derived epoxy lipids

EETs and EDPs mediate many beneficial effects by maintaining mitochondrial quality and reducing adverse inflammatory reactions [329, 580-583, 662, 663]. Importantly, the rapid hydrolysis of the bioactive oxylipins by sEH limits their beneficial cardiovascular effects while increasing adverse effects [635]. Previous data has demonstrated deficiency of sEH is associated with improved post-ischemic functional recovery with smaller infarct size [641, 664]. These beneficial effects were attributed in part to the stabilization of protective epoxy-metabolites EETs and EDPs [570, 584, 665]. In contrast, CYP-derived epoxylipids EpOMEs are metabolized by sEH to DiHOMEs, which possess more cytotoxic effects [581, 638, 639, 666, 667]. Early evidence has demonstrated that the cardiac levels of DiHOMEs are increased in models of myocardial IR injury [668]. Recent data indicates both 12,13-EpOME and 12,13-DiHOME diminish post-ischemic cardiac functional recovery, however, inhibition of sEH prevented the detrimental effect of 12,13-EpOME suggesting 12,13-DiHOME was the active metabolite [640]. Moreover, Edin et al. reported that increased post-ischemic functional recovery in sEH-deficient mice was associated with higher concentrations of EETs and lower concentrations of LA diols [669]. The exact cardiotoxic mechanisms of DiHOMEs are unknown but are most likely attributable to several different effects. For example, accumulation of DiHOMEs in the heart is associated with impaired mitochondrial function, uncoupled oxidative phosphorylation and altered ion channel kinetics resulting in extensive cardiac injury [638, 664, 669-671]. Taken together, these reports indicate that inhibition of sEH could serve as a dual cardioprotective strategy to preserve the levels of cardioprotective epoxylipids while simultaneously decreasing the production of the cardiotoxic LA diols, ultimately protecting cardiac mitochondria and preserving cardiac function (Figure 3.7).

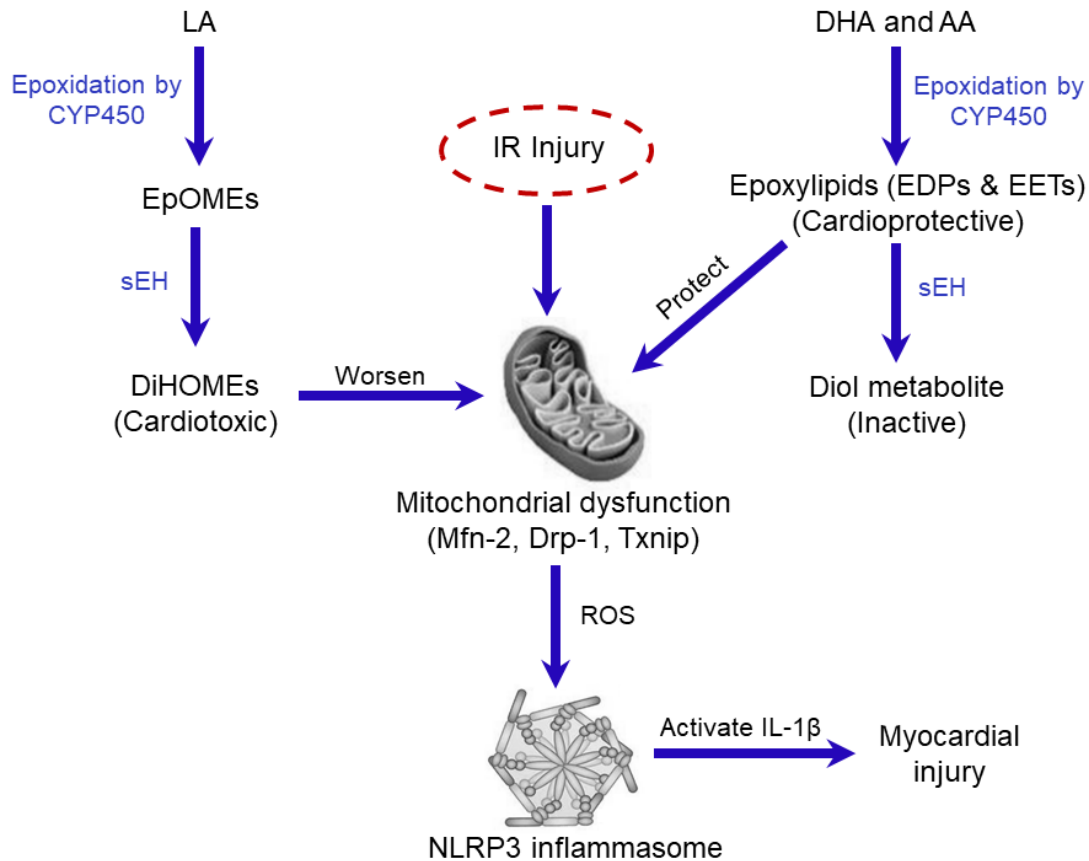


Figure 3. 7: Schematic showing the potential roles of sEH in IR injury. Cellular injury in response to IR insult is associated with the release of polyunsaturated fatty acids (PUFAs) from the cell membrane which can be metabolized via epoxidation by cytochrome P450 (CYP450) isoenzymes to linoleic acid (LA) metabolites epoxyoctadecenoic acids (EpOMEs), which are further metabolized by sEH to dihydroxyoctadecenoic acid (DiHOMEs) with cardiotoxic effects targeting mitochondria resulting in injury. In contrast, sEH rapidly degrades the cardioprotective epoxylipids, epoxydocosapentaenoic acids (EDPs) and epoxyeicosatrienoic acids (EETs), generated from the CYP-mediated metabolism of the n-3 docosahexaenoic acid (DHA) and n-6 arachidonic acid (AA), respectively. These biologically active epoxy metabolites mediate many of the beneficial cardiovascular effects of the parent PUFAs by maintaining mitochondrial quality and reducing adverse inflammatory reactions. IR injury triggers the translocation of dynamin-related protein-1 (Drp-1) from the cytosol to the mitochondria initiating events that lead to the assembly and oligomerization of NLRP3 inflammasome. Active NLRP3 shuttles Txnip to the mitochondria aggravating mitochondrial damage as well the formation of the pro-inflammatory cytokine IL-1 β triggering cardiomyocyte cell death.

Excessive activation of the innate immune system and the associated inflammatory response plays a pivotal role in aggravating myocardial IR injury [168, 195]. Recently, the innate NLRP3 inflammasome cascade has been found to be a major contributor to the pathology [205, 672]. Briefly, the death of cardiomyocytes resulting from acute ischemic conditions or reperfusion injury causes the release of cellular debris and contents, referred to as damage-associated molecular patterns (DAMPs) [186, 188]. Binding of DAMPs to the pattern recognition NOD-like receptors (NLR) on cardiac fibroblasts, infiltrating leucocytes and cardiomyocytes will activate the oligomerization and formation of NLRP3 inflammasomes [205, 211]. Moreover, several studies demonstrated that the activation of the NLRP3 protein, the main component of NLRP3 inflammasome, after IR injury is attributed to the cross-talk between NLRP3 inflammasome and mitochondria, whereby NLRP3 senses ROS produced by dysfunctional mitochondria [200, 575]. Once aggregated, NLRP3 inflammasome mediates the cleavage and activation of caspase-1. Active caspase-1 then induces the conversion of pro-IL-1 β to mature IL-1 β [205-209, 211]. IL-1 β triggers the release of other cytokines and chemokines, which recruit and activate inflammatory cells such as neutrophils and monocytes driving a severe inflammatory process aggravating cellular injury [631]. Accumulating literature demonstrates the main role of IL-1 β involves initiating the inflammatory cascade, however evidence suggests it may have a direct detrimental effect on the myocardium. For instance, it has been reported IL-1 β acts as a cardio-depressant cytokine where single or multiple injections of IL-1 β causes systolic dysfunction and reduces LV contractility reserve in healthy mice and human subjects in the absence of ischemia [673-676]. Furthermore, IL-1 β induces direct negative inotropic effects in isolated perfused rat hearts [677]. Moreover, *in vitro* experiments have demonstrated IL-1 β stimulation activates apoptotic pathways in neonatal rat cardiomyocytes [678]. Our current understanding indicates IL-1 β triggers cardiac

damage in IR injury through either recruitment of a pro-inflammatory cells, such as leukocytes, causing adverse response or direct action on cardiac cells [168, 217, 218, 577].

Deletion of the NLRP3 gene or pharmacological inhibition of inflammasome formation post-MI is associated with cardiovascular protection resulting in smaller infarct size and better functional recovery [205-210, 277, 599, 610, 679]. Increasing evidence from both human and animal studies demonstrate some CYP-derived epoxylipids, such as EDPs and EETs, possess anti-inflammatory properties. Therefore, therapeutic approaches to elevate the levels of these lipid mediators, as in the case of sEH inhibition, are useful for treating different inflammatory disorders such as diabetes, atherosclerosis, and arthritis [613, 614, 663, 680, 681]. Zhou et al., demonstrated inhibition of sEH can attenuate lipopolysaccharide (LPS)-induced acute lung injury and improve survival in mice by suppressing the activation of NLRP3 inflammasome and the expression of its downstream effector IL-1 β [682]. Recently, we demonstrated EDPs can suppress NLRP3 inflammasome activation thereby inhibiting production of proinflammatory cytokines including IL-1 β following IR injury [383]. The current study provides supporting evidence whereby the cardioprotective effects following pharmacological inhibition of sEH or genetic deletion of Ephx2 are attributable to a reduced innate immune response.

Mitochondria are important organelles required for healthy cardiac function but are susceptible to significant injury from ischemia and reperfusion. IR-induced injury causes damage to the electron transport chain (ETC) mainly during the ischemic period [86]. As such, re-introduction of oxygen to the ischemic myocardium that contains injured mitochondria leads to mitochondrial-driven injury with excessive production of ROS and accumulation of calcium, which contributes to contractile dysfunction and cell death [81]. Recent evidence suggests mitochondria play a key role in regulating NLRP3 inflammasome activation and the subsequent

responses [209]. The current study demonstrates cardioprotective effects associated with sEH inhibition involve reduced mitochondrial injury, which is attributed to an altered balance between CYP-derived epoxylipids, EETs and EDPs, with sEH cardiotoxic diols, DiHOMEs.

Proteins regulating mitochondrial dynamics are involved in the pathogenesis of myocardial IR injury. Under normal conditions, Drp-1 is localized in the cytosol in an inactive phosphorylated form, which becomes dephosphorylated following a stress event and translocates to the outer mitochondrial membrane initiating mitochondrial fission, reducing the number of functional mitochondria and accelerating myocardial injury [101, 102]. Several studies show genetic deletion or pharmacological inhibition of Drp-1 protects cardiomyocytes against IR injury and improves cardiac contractile function [105, 106]. Data generated from the current study support these reports where increased mitochondrial Drp-1 in the IR group correlates with reduced mitochondrial respiration and impaired cardiac functional recovery. Both genetic deletion of *Ephx2* and pharmacological inhibition of sEH enzyme significantly inhibited the translocation of Drp-1 to the mitochondria, correlating with improved cardiac functional recovery. These results support our previous findings demonstrating post-MI mitochondrial ultrastructure and function in young WT mice displayed a complete loss of cellular organization, cristae and function that was maintained in the young sEH null mice [570, 584].

Evidence demonstrates Txnip, a pro-oxidant and a well-known activator of NLRP3 inflammasome, has a negative role in the pathogenesis of IR injury [620, 621]. Under normal physiological conditions, Txnip is confined primarily to the nucleus, however, following IR stress and excessive ROS production, it translocates to the cytosol inhibiting the antioxidant activity of Trx-1 and activates the oligomerization of NLRP3 inflammasome. Active NLRP3 inflammasome in turn shuttles and translocates Txnip to the mitochondria inhibiting the main mitochondrial

antioxidant Trx-2 initiating the process of cardiomyocyte cell death [622-624]. Similarly, the current study demonstrates IR injury is associated with increased cytosolic and mitochondrial Txnip, reduced Trx-1 and Trx-2 activities as well as accumulated MDA levels, the main lipid peroxidation end product suggesting increased ROS production [647, 683]. Yoshioka et al. demonstrated that genetic deletion of Txnip protects the myocardium from IR injury [625]. Consistent with this notion, our results indicate deficiency of sEH inhibited the translocation of Txnip to the cytosol and mitochondria under IR conditions, limited the loss of the antioxidant activities of both Trx-1 and -2 proteins, ameliorated the accumulation of MDA and correlated with improved post-ischemic functional recovery.

Emerging evidence for the non-canonical roles of Mfn-2 in the activation of different innate immune components and pathogenesis of IR injury indicates that mitochondrial dysfunction is associated with increased Mfn-2 expression, which accelerates cardiomyocyte death [684, 685]. The exact mechanisms remain unknown, Mfn-2 mediated tethering of mitochondria and endoplasmic reticulum facilitate the transfer of calcium to the mitochondria. Under ischemic conditions, this phenomenon accumulates calcium in the mitochondria accelerating degradation [615, 628]. Indeed, acute ablation of cardiac Mfn-2 reduces mitochondrial calcium overload, rendering the heart resistant to acute infarction following IR [114]. The current study demonstrated myocardial IR injury was associated with increased mitochondrial Mfn-2 protein expression but was prevented by inhibition of sEH. Altogether, we believe that deficiency of sEH limits the mitochondrial damage in response to injury; however, the connection between Mfn-2 and the protective mechanism(s) needs further investigation.

In conclusion, our results demonstrate that inhibition of sEH protects against myocardial IR injury by preserving mitochondrial function and inhibiting NLRP3 inflammasome activation. Although the exact molecular mechanisms remain unknown, we propose inhibiting sEH results in altered cardiac levels of bioactive epoxylipids EDPs and EETs together with reduced DiHOME levels, which collectively maintain an optimally functioning mitochondrial pool, inhibit a detrimental innate inflammasome response and thereby promote cell survival. It is recognized the current study was limited by not directly assessing changes in the levels of epoxylipids (EETs, EDPs, EpOMEs) as well as the diol metabolites (DiHOMEs) in response to IR injury. However, it has been shown that cardiac ischemic insults decrease levels of the cardioprotective epoxylipids EETs and EDPs and cardiotoxic DiHOMEs accumulate aggravating the injury [668, 686]. Therefore, future characterization of how IR injury alters the levels of these metabolites will provide more insight into the complex responses and pathobiology.

Chapter 4

A Synthetic Epoxydocosapentaenoic Acid Analogue Ameliorates Cardiac Ischemia/Reperfusion Injury: The Involvement of the Sirtuin 3–NLRP3 Pathway

This chapter has been adapted from the following published manuscript:

- **Ahmed M Darwesh**, Wesam Bassiouni, Adeniyi Michael Adebesein, Abdul Sattar Mohammad, John R Falck, John M Seubert. A Synthetic Epoxydocosapentaenoic Acid Analogue Ameliorates Cardiac Ischemia/Reperfusion Injury: The Involvement of the Sirtuin 3-NLRP3 Pathway. *Int J Mol Sci.* 2020 Jul 24;21(15):5261.

Abstract

While survival rates have markedly improved following cardiac ischemia-reperfusion (IR) injury, the resulting heart damage remains an important issue. Preserving mitochondrial quality and limiting NLRP3 inflammasome activation is an approach to limit IR injury, in which the mitochondrial deacetylase sirtuin 3 (SIRT3) has a role. Recent data demonstrate cytochrome P450 (CYP450)-derived epoxy metabolites of docosahexaenoic acid (DHA), epoxydocosapentaenoic acids (EDPs), attenuate cardiac IR injury. EDPs undergo rapid removal and inactivation by enzymatic and non-enzymatic processes. The current study hypothesizes that the cardioprotective effects of the synthetic EDP surrogates AS-27, SA-26 and AA-4 against IR injury involve activation of SIRT3. Isolated hearts from wild type (WT) mice were perfused in the Langendorff mode with vehicle, AS-27, SA-26 or AA-4. Improved postischemic functional recovery, maintained cardiac ATP levels, reduced oxidative stress and attenuation of NLRP3 activation were observed in hearts perfused with the analogue SA-26. Assessment of cardiac mitochondria demonstrated SA-26 preserved SIRT3 activity and reduced acetylation of manganese superoxide dismutase (MnSOD) suggesting enhanced antioxidant capacity. Together, these data demonstrate that the cardioprotective effects of the EDP analogue SA-26 against IR injury involve preservation of mitochondrial SIRT3 activity, which attenuates a detrimental innate NLRP3 inflammasome response.

4.1 Introduction

Ischemic heart disease remains one of the primary causes of death worldwide [3, 629]. In patients with an ischemic event, early and successful reperfusion or restoration of blood flow to the ischemic myocardium is the most effective treatment to reduce myocardial damage and acute mortality rates [687, 688]. However, the benefit of reperfusion is partly attenuated by paradoxical damage to cardiomyocytes that were still viable at the end of the ischemic period, a process known as “ischemia reperfusion” (IR) injury [14, 19]. Evidence indicates cardiac dysfunction resulting from IR injury can be linked to mitochondrial dysfunction, excessive oxidative stress and the activation of an inflammatory response [72, 689]. Strategies preserving mitochondrial integrity and function have been shown to attenuate IR injury and improve cardiac function [690, 691].

Sirtuins (SIRT1-SIRT7) are a class of nicotinamide adenine dinucleotide (NAD⁺)-dependent deacetylase proteins targeted therapeutically for modulating cardiovascular disease (CVD) [692, 693]. In the heart, SIRT3 is highly expressed and localized in the mitochondria where it is essential for regulating mitochondrial homeostasis [694, 695]. Importantly, more than 60% of mitochondrial proteins are acetylated due to the high pH and the high concentration of acetyl-CoA [696, 697]. SIRT3 regulates mitochondrial function by deacetylating, and thereby activating, numerous mitochondrial proteins involved in energy metabolism [148], oxidative stress responses [149, 150], mitochondrial dynamics [151] and the electron transport chain (ETC) [152, 153]. Studies demonstrate that limiting the loss of SIRT3 following IR injury provides cardioprotective responses and highlight its importance [158, 161].

The nucleotide-binding oligomerization domain-like receptor (NLR) family pyrin domain containing 3 (NLRP3) inflammasomes have been shown to play an essential role in the pathogenesis of myocardial IR injury [205, 277]. NLRP3 inflammasomes are a large cytosolic

platform assembled and activated in response to cellular stress, which can exacerbate inflammatory reactions. During reperfusion, the reactive oxygen species (ROS) burst resulting from damaged mitochondria activates NLRP3 inflammasomes. The oligomerization and assembly of NLRP3 inflammasomes promotes the autocatalytic activation of caspase-1, which in turn exacerbates mitochondrial damage and myocardial injury via pyroptosis [211, 698]. Therefore, mitochondrial damage is both a trigger and a target of NLRP3 inflammasome activation [259, 699]. Recent evidence reports attempts to preserve SIRT3 activity under stress conditions can block the activation of NLRP3 inflammasome ameliorating the inflammatory insult [700].

Long-chain n-3 polyunsaturated fatty acids (n-3 PUFA) are essential constituents of the body which have a role in cellular homeostasis and protection against CVD [327, 330]. Docosahexaenoic acid (DHA), an abundant n-3 PUFA found in mammalian tissues, can be metabolized by cyclooxygenases (COX), lipoxygenases (LOX) and cytochromes P450 (CYP) to a vast range of lipid mediators with different cellular functions [300, 330, 701]. CYP epoxygenases add oxygen across one of the double bonds of DHA to generate three-membered ethers known as epoxylipids. There are six regioisomeric epoxylipids of DHA termed epoxydocosapentaenoic acids (4,5-, 7,8-, 10,11-, 13,14-, 16,17-, 19,20-EDP) [501]. There is growing evidence indicating that EDPs mediate many of the salutary effects of the parent compound DHA [329, 330, 339]. Previously, we demonstrated that EDPs can maintain mitochondrial quality and limit NLRP3 inflammasome activation providing a cardioprotective response toward IR injury [339, 383, 681, 702]. However, EDPs are rapidly converted to the corresponding and less biologically active vicinal diol by soluble epoxide hydrolase (sEH) or can be metabolized by other pathways including β -oxidation, chain shortening and chain elongation [507, 703]. Accordingly, there is interest in developing methods to enhance their bioavailability [704]. In the current study, we synthesize and

investigate the cardioprotective properties of the 19,20-EDP analogue AS-II-75-27 (AS-27) as well as the 16,17-EDP analogues AA-XII-52-4 (AA-4) and SA-II-109-26 (SA-26) against IR injury. The chemical structure of these EDP surrogates possess several key features: (i) a partially saturated carbon backbone to avoid autooxidation and improve physical stability; and (ii) for AS-27, a disubstituted urea that obviates epoxide hydrolysis by sEH and prolongs the half-life (Figure 4.1) [665, 705]. Building upon previous data, we explore the hypothesis that EDP surrogates will attenuate myocardial IR injury through the activation of SIRT3 and subsequent inhibition of NLRP3 inflammasome cascade.

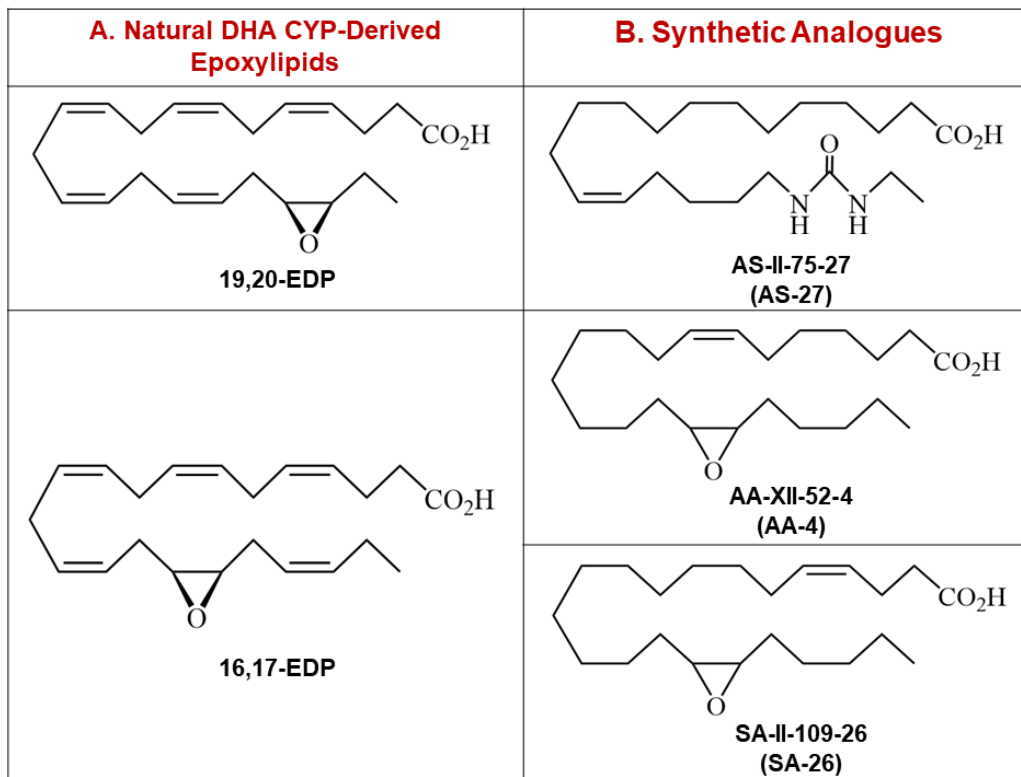


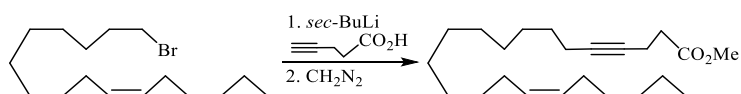
Figure 4. 1: Chemical structures of EDPs and their synthetic analogues. (A) Chemical structures of the 2 most abundant natural metabolites of DHA, 19,20-EDP and 16,17-EDP. (B) Chemical structures of AS-27, the synthetic analogue of 19,20-EDP, as well as AA-4 and SA-26, synthetic analogues of 16,17-EDP. DHA: Docosahexaenoic acid, EDP: Epoxydocosapentaenoic acid.

4.2 Materials and Methods

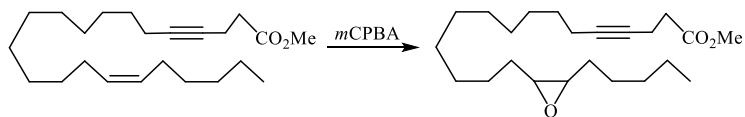
4.2.1 Synthesis of EDP surrogates

The EDP analogs were prepared in the Falck lab using standard synthetic methods as previously described [706, 707]. All analogs were fully characterized by $^1\text{H}/^{13}\text{C}$ Nuclear Magnetic Resonance (NMR) and mass spectroscopy and were $\geq 95\%$ pure. Details of synthesis of the compounds and $^1\text{H}/^{13}\text{C}$ NMR and mass spectra are shown below.

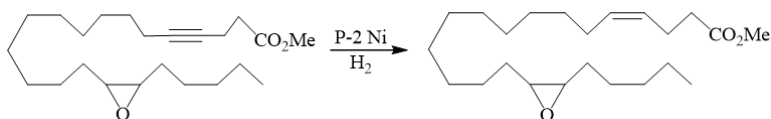
4.2.1.1 Synthesis of SA-26



To a stirring, $-78\text{ }^\circ\text{C}$ solution of 4-pentynoic acid (Gas–solid two-phase flow (GSF), 341 mg, 3.47 mmol) in anhydrous tetrahydrofuran/ hexamethylphosphoramide (THF/HMPA) (4:1, 10 mL) under an argon atmosphere was added dropwise *sec*-BuLi (5.79 mL, 1.4 M hexane solution). The reaction mixture was warmed over 40 min to $0\text{ }^\circ\text{C}$. After an additional 3 h at the same temperature, a solution of 16-bromohexadec-6(Z)-ene1 (920 mg, 2.89 mmol) in THF (5 mL) was added and the whole was allowed to stir at rt overnight. Following quenching with aq. 1 N HCl, the reaction mixture was extracted with EtOAc ($3 \times 50\text{ mL}$) and the combined extracts were dried over Na_2SO_4 , filtered, and concentrated in vacuo. The crude was treated with excess diazomethane in Et₂O at 0 ° for 2 h, then purified by SiO₂ column chromatography to give methyl docos-16(Z)-en-4-ynoate (465 mg, 48% over 2 steps) as a colorless oil. TLC: $R_f \sim 0.43$ (5% EtOAc/hexanes). ^1H NMR (300 MHz, CDCl_3) δ 5.43–5.26 (m, 2H), 3.69 (s, 3H), 2.57–2.41 (m, 4H), 2.17–2.06 (m, 2H), 2.06–1.92 (m, 4H), 1.53–1.18 (m, 22H), 0.88 (t, $J = 6.6\text{ Hz}$, 3H).

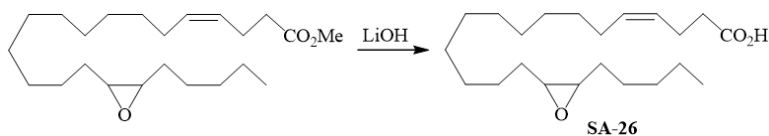


m-Chloroperbenzoic acid (77%, 132 mg, 0.76 mmol) was added portionwise to a stirring, 0 °C solution of the above ester (223 mg, 0.64 mmol) in anhydrous CH₂Cl₂ (5 mL). After 1 h at rt, the reaction mixture was quenched with sat. Na₂SO₃ solution, extracted with EtOAc, and concentrated and the residue purified by SiO₂ column chromatography to give methyl 15-(3-pentyloxiran-2-yl)pentadec-4-ynoate (191 mg, 82%) as an oil. TLC: R_f ~ 0.5 (10% EtOAc/hexanes). ¹H NMR (300 MHz, CDCl₃) δ 3.69 (s, 3H), 2.90 (t, J = 3 Hz, 2H), 2.57–2.38 (m, 4H), 2.16–2.04 (m, 2H), 1.58–1.16 (m, 28H), 0.89 (t, J = 6.6 Hz, 3H).



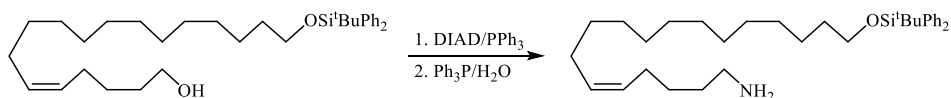
NaBH₄ (10 mg, 0.27 mmol) was added to stirring solution of Ni(OAc)₂·4H₂O (68 mg, 0.27 mmol) in absolute EtOH (5 mL) under a hydrogen atmosphere (1 atm). After 10 min, distilled ethylenediamine (25 mg, 0.54 mmol) was added to the resultant black suspension followed after another 10 min by a solution of methyl 15-(3-pentyloxiran-2-yl)pentadec-4-ynoate in ab. EtOH (2 mL). After 1 h, the reaction mixture was passed through a bed of SiO₂ that was washed by EtOAc (5 mL). The combined eluates were concentrated and purified via SiO₂ column chromatography to give methyl 15-(3-pentyloxiran-2-yl)pentadec-4(Z)-enoate (188 mg, 98%) as an oil. TLC: R_f ~ 0.52 (10% EtOAc/hexanes). ¹H NMR (300 MHz, CDCl₃) δ 5.43–5.29 (m, 2H), 3.66 (s, 3H), 2.89 (t, J = 3 Hz, 2H), 2.35–2.34 (m, 4H), 2.03–1.99 (m, 2H), 1.48–1.26 (m, 24H), 0.89 (t, J = 6.6 Hz,

3H); ^{13}C NMR (CDCl_3 , 75 MHz) δ 173.75, 131.69, 127.37, 57.31, 51.60, 34.27, 31.85, 29.75, 29.71, 29.68, 29.66, 29.41, 27.95, 27.91, 27.30, 26.73, 26.41, 22.91, 22.72, 13.11.



To a solution of methyl 15-(3-pentoxiran-2-yl)pentadec-4(Z)-enoate (119 mg, 0.32 mmol) in THF/ H_2O (4:1, 5 mL) was added LiOH (1 m aq. soln, 1 mL) at 0 °C. After stirring at rt for 12 h, the mixture was acidified to pH 4.5 using 1 M aq. oxalic acid and extracted with EtOAc (3×20 mL). The combined extracts were washed with brine, concentrated in vacuo, and the residue purified via SiO_2 chromatography to give SA-26 (100 mg, 88%) as a colorless oil. TLC: $R_f \sim 0.45$ (30% EtOAc/hexanes). ^1H NMR (300 MHz, CDCl_3) δ 5.47–5.42 (m, 1H), 5.37–5.32 (m, 1H), 2.92 (t, $J = 3.3$, 2H), 2.41–2.35 (m, 4H), 2.06–2.01 (m, 2H), 1.50–1.27 (m, 26H), 0.90 (t, $J = 5.4$ Hz, 3H).

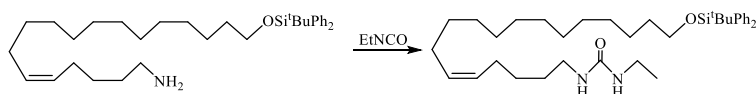
4.2.1.2 Synthesis of AS-27



Diphenylphosphoryl azide (DIAD, 1.15 g, 4.1 mmol) was added dropwise to a 0 °C solution of the known 18-((tert-butyldiphenylsilyl)oxy)octadec-5(Z)-en-1-ol (1.82 g, 3.4 mmol) and Ph_3P (1.02 g, 4.1 mmol) in anhydrous THF (50 mL). After stirring at rt for 22 h, water (10 mL) was added and the reaction mixture was extracted with EtOAc (2×20 mL). The combined

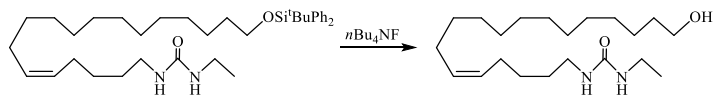
extracts were dried over Na₂SO₄, filtered, and concentrated in vacuo. The residue was used for next step without further purification.

Ph₃P (0.9 g, 3.54 mmol) was added to a stirring, rt solution of the above crude azide (1.82 g, 2.3 mmol) in anhydrous THF (30 mL). After 2 h, water (2 mL) was added and allowed to stir an additional 48 h. The reaction mixture was diluted with water (10 mL), extracted with EtOAc (2 × 30 mL), and the combined extracts were dried over Na₂SO₄, filtered, and concentrated in vacuo. Purification of the residue by SiO₂ column chromatography using a gradient of 25-35% EtOAc/hexanes afforded 18-((tert-butyldiphenylsilyl)oxy)octadec-5(Z)-en-1-amine (1.06 g, 71% over 2 steps) as an oil. TLC: R_f ~ 0.2 (50% EtOAc/hexanes). ¹H NMR (400 MHz, CDCl₃) δ 7.67 (dt, J = 7.8, 1.6 Hz, 4H), 7.40 (dt, J = 10.7, 1.5 Hz, 6H), 5.44–5.31 (m, 2H), 3.65 (td, J = 6.5, 1.4 Hz, 2H), 2.72 (t, J = 7.0 Hz, 2H), 2.24–1.94 (m, 6H), 1.63–1.18 (m, 24H), 1.05 (d, J = 1.4 Hz, 9H); ¹³C NMR (101 MHz, CDCl₃) δ 135.56, 134.16, 130.35, 129.45, 129.30, 127.54, 64.01, 32.59, 29.76, 29.70, 29.67, 29.63, 29.59, 29.40, 29.35, 27.26, 26.99, 26.96, 26.86, 26.78, 25.77, 19.22.

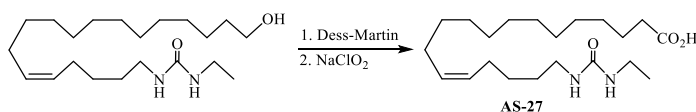


A solution of the above amine (0.75 g, 1.36 mmol) and EtNCO (0.1 g, 1.4 mmol) was stirred at rt in dry THF (20 mL) for 18 h, then all volatiles were removed in vacuo. The residue was purified by SiO₂ column chromatography using 5% methanol/CH₂Cl₂ and dichloromethane as eluent to provide 1-(18-((tert-butyldiphenylsilyl)oxy)octadec-5(Z)-en-1-yl)-3-ethylurea (0.6 g, 79 % yield) as an oil. TLC: R_f ~ 0.3 (50% EtOAc/hexanes). ¹H NMR (400 MHz, CDCl₃) δ 7.74–7.55 (m, 4H), 7.47–7.29 (m, 6H), 5.42–5.23 (m, 2H), 4.18 (s, 2H), 3.65 (t, J = 6.5 Hz, 2H), 3.21–3.19 (m, 4H), 2.05–2.02 (m, 4H), 1.66–1.17 (m, 24H), 1.13 (t, J = 7.2 Hz, 3H), 1.04 (s, 9H); ¹³C NMR (101 MHz, CDCl₃) δ 170.56, 135.24, 133.85, 130.19, 129.13, 128.77, 127.21, 63.69, 40.24,

35.10, 32.26, 29.50, 29.43, 29.35, 29.30, 29.26, 29.07, 29.03, 26.95, 26.64, 26.54, 26.50, 25.45, 18.89, 15.16.



TBAF (1 M THF soln, 1 mL, 1.04 mmol) was added to a stirring, 0 °C solution of the above urea (0.65 g, 1.04 mmol) in dry THF (15 mL). After stirring at RT for 12 h, water (10 mL) was added and the reaction mixture was extracted with EtOAc (2 × 20 mL). The combined extracts were dried over Na₂SO₄, filtered, and concentrated in vacuum. The residue was purified SiO₂ column chromatography using a gradient of 30-45% EtOAc/hexanes to give 1-ethyl-3-(18-hydroxyoctadec-5(Z)-en-1-yl) urea (300 mg, 81%) as a white semi-solid. TLC: R_f ~0.5 (80% EtOAc/hexanes). ¹H NMR (400 MHz, CDCl₃) δ 5.41–5.28 (m, 2H), 4.30 (d, J = 8.2 Hz, 2H), 3.63 (t, J = 6.7 Hz, 2H), 3.23–3.13 (m, 4H), 2.01 (dt, J = 5.6, 7.0 Hz, 4H), 1.60–1.44 (m, 5H), 1.43–1.22 (m, 21H), 1.13 (t, J = 7.2 Hz, 3H); ¹³C NMR (101 MHz, CDCl₃) δ 158.14, 130.48, 129.12, 63.05, 40.53, 35.39, 32.79, 29.84, 29.66, 29.56, 29.52, 29.46, 29.40, 29.23, 27.20, 26.98, 26.83, 25.72, 15.47.



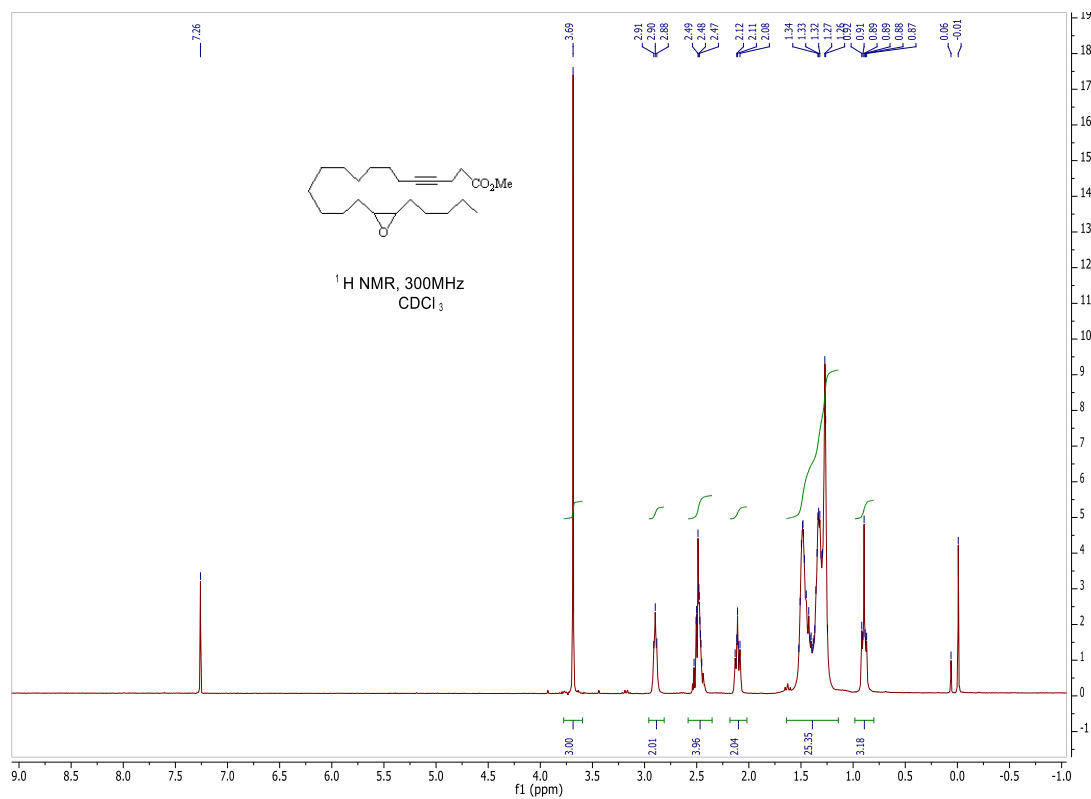
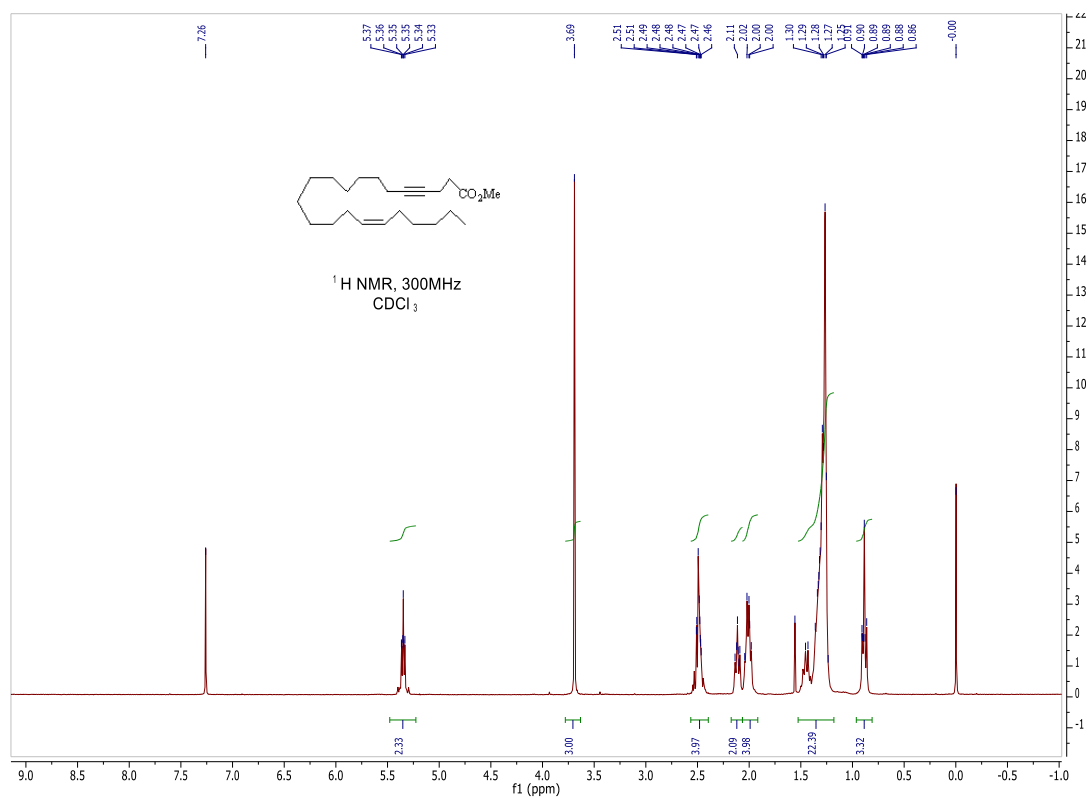
Dess-Martin periodinane (167 mg, 0.39 mmol) and NaHCO₃ (44 mg, 0.52 mmol) were added sequentially to a stirring, 0 °C solution of the above alcohol (100 mg, 0.26 mmol) in CH₂Cl₂ (20 mL). After stirring for 3 h at rt, the reaction mixture was quenched with a saturated aq. solution of sodium thiosulfate (10 mL) and extracted with CH₂Cl₂ (2 × 20 mL). The combined extracts were dried over Na₂SO₄, concentrated in vacuo and the crude 1-ethyl-3-(18-oxooctadec-5(Z)-en-1-yl)urea was used in the next step without purification.

To a stirring, 0 °C solution of the above aldehyde (80 mg, 0.21 mmol) in tert-BuOH and water (1:1, 8 mL) were added sequentially 2-methyl-2-butene (147 mg, 2.1 mmol), NaH₂PO₄ (58 mg, 0.42 mmol), and NaClO₂ (28 mg, 0.31 mmol). After 4 h, saturated aq. NH₄Cl (10 mL) added to the reaction mixture which was then extracted with EtOAc (2 × 20 mL). The combined organic extracts were dried over Na₂SO₄, concentrated in vacuo and the residue purified by SiO₂ column chromatography using a gradient of 5-10% methanol/CH₂Cl₂ to give 18-(3-ethylureido)octadec-13(Z)-enoic acid (AS-27, 54 mg, 63% over two steps) as a white powder. TLC: R_f ~ 0.5 (10% MeOH/CH₂Cl₂). ¹H NMR (400 MHz, CDCl₃) δ 5.45–5.26 (m, 2H), 4.93–4.40 (m, 2H), 3.20 (q, J = 7.3 Hz, 2H), 3.10 (t, J = 7.1 Hz, 2H), 2.32 (t, J = 7.1 Hz, 2H), 2.05–2.01 (m, 4H), 1.57 (dq, J = 6.3, 7.2 Hz, 4H), 1.44–1.21 (m, 18H), 1.15 (t, J = 7.2 Hz, 3H); ¹³C NMR (101 MHz, CDCl₃) δ 177.75, 159.14, 130.58, 129.09, 77.32, 77.00, 76.68, 40.80, 35.46, 34.06, 29.36, 29.34, 29.09, 28.93, 28.87, 28.84, 28.78, 28.71, 26.87, 26.79, 24.68, 15.27.

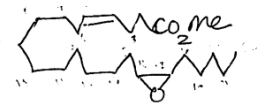
4.2.1.3 Synthesis of AA-4

This analog was prepared from the known 1-bromoundec-5(Z)-ene as described for SA-26 in 10% overall yield. ¹H NMR (500 MHz, C₆D₆) δ 5.57 – 5.33 (m, 2H), 2.84 – 2.73 (m, 2H), 2.18 – 1.90 (m, 7H), 1.60 – 1.08 (m, 31H), 0.87 (t, J = 7.0 Hz, 3H).

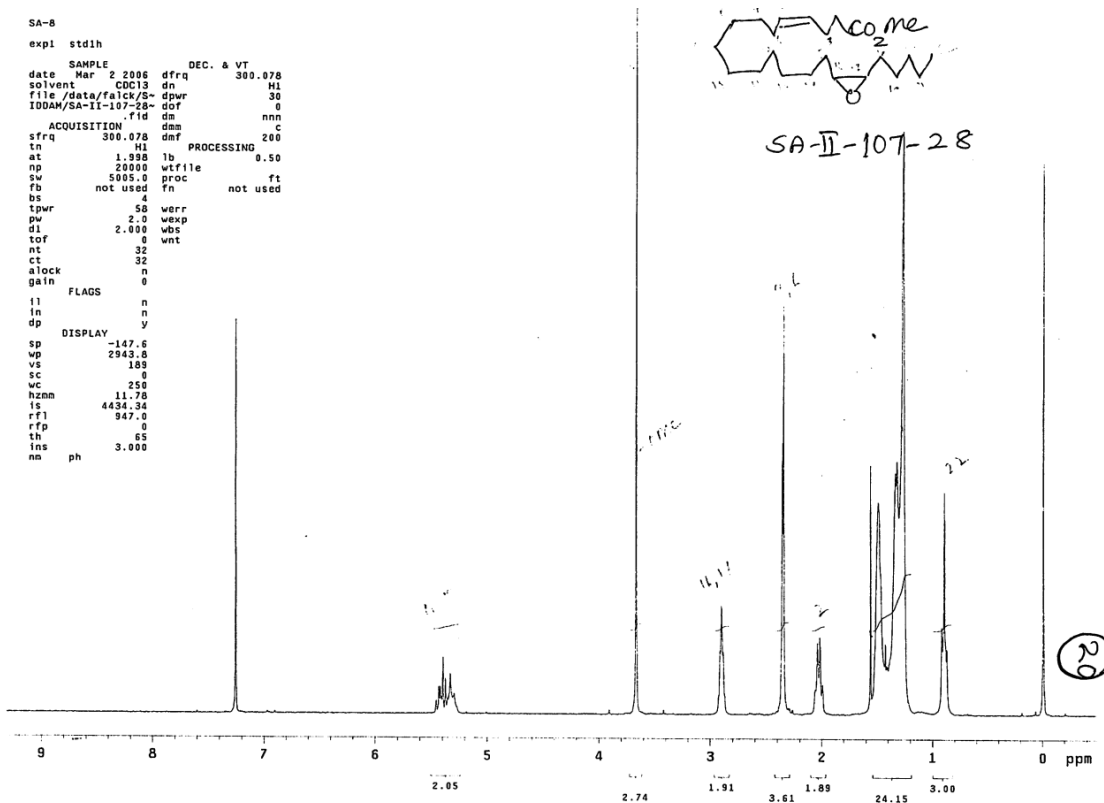
4.2.1.4 $^1\text{H}/^{13}\text{C}$ NMR



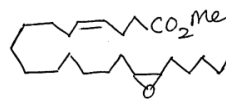
SA-8
 expl std1h
 SAMPLE DEC. & VT
 date Mar 2 2006 dfrq 300.078
 solvent CDCl3 dn H1
 file /data/falk/S- dpwr 30
 IDDM/SA-II-107-28- dof 0
 - rid dm nnn
 ACQUISITION dmm c
 sfrq 300.078 dmf 200
 tn H1 PROCESSING
 at 1.998 lb 0.50
 np 2000 wfile
 sw 5005.0 proc ft
 fb not used fn not used
 bs 4
 tpwr 58 werr
 pw 2.0 wexp
 d1 2.000 wbs
 tof 0 wnt
 nt 32
 ct 32
 alock n
 gain 0
 FLAGS
 fl n
 in n
 dp y
 DISPLAY
 sp -147.6
 wp 2943.8
 vs 189
 sc 0
 wc 250
 hznm 11.76
 is 4434.34
 rfl 947.0
 rfp 0
 th 65
 ins 3.000
 nm ph



SA-II-107-28

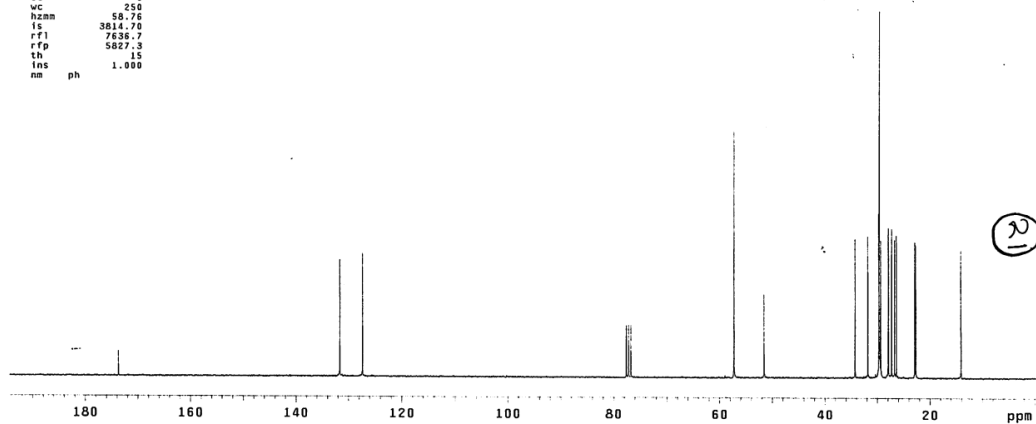


SA-31C
 PPS 2
 sequence: s2pu1
 expl std13c
 SAMPLE DEC. & VT
 date Mar 2 2006 dfrq 300.078
 solvent CDCl3 dn H1
 file /data/falk/S- dpwr 37
 IDDM/SA-II-107-28- dof 0
 - rid dm nnn
 ACQUISITION dmm c
 sfrq 75.462 dm nvy
 tn C13 dnm w
 at 1.815 dmf 10400
 np 68096 PROCESSING
 fb 18781.7 lb 1.00
 bs 10400 wfile
 tpwr 56 fn not used
 pw 7.6
 d1 2.000 werr react
 tof 0 wbs procpot
 nt 2000 wnt testen
 ct 400
 alock n
 gain 30
 FLAGS
 fl n
 in n
 dp y
 DISPLAY
 sp -25.2
 wp 14890.5
 vs 80
 sc 0
 wc 250
 hznm 58.76
 is 3814.70
 rfl 7538.7
 rfp 5827.3
 th 15
 ins 1.000
 nm ph



SA-II-107-28

No of carbons = 23

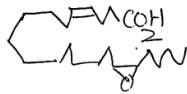


STANDARD 1H OBSERVE

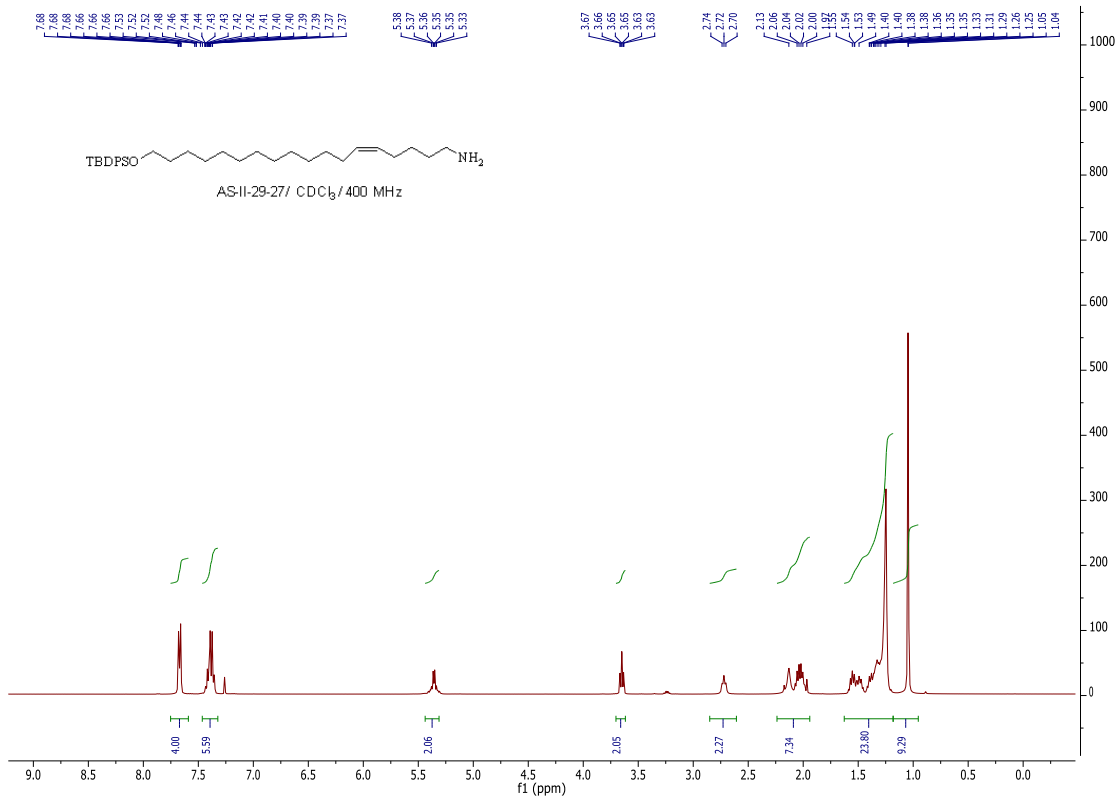
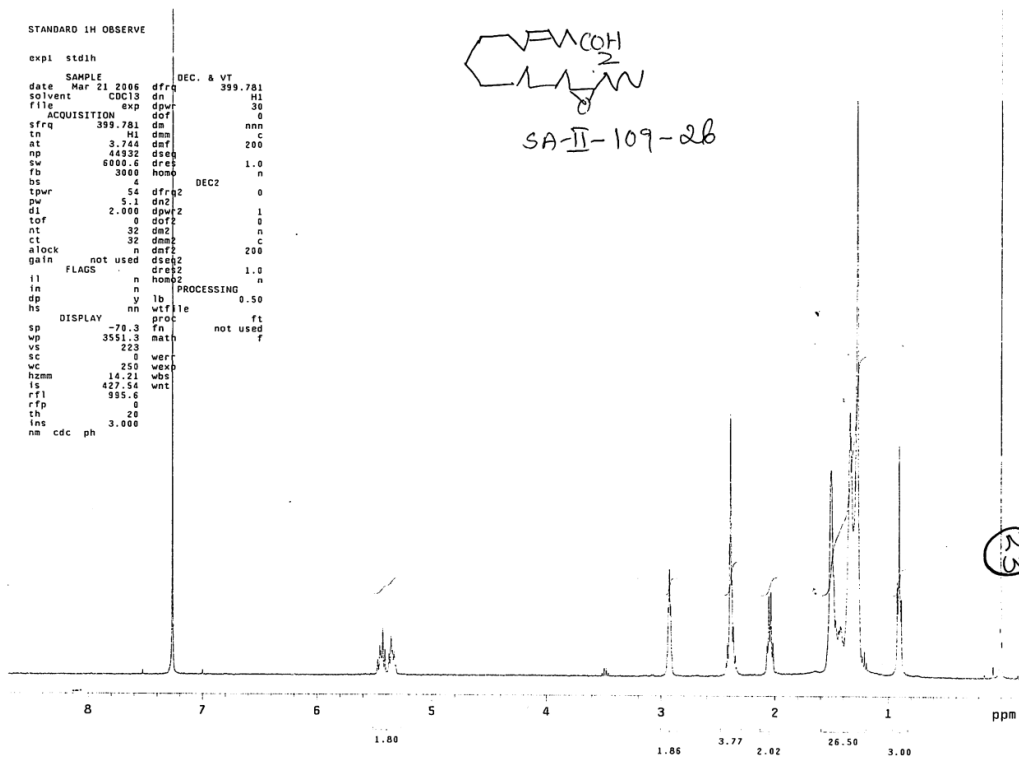
```

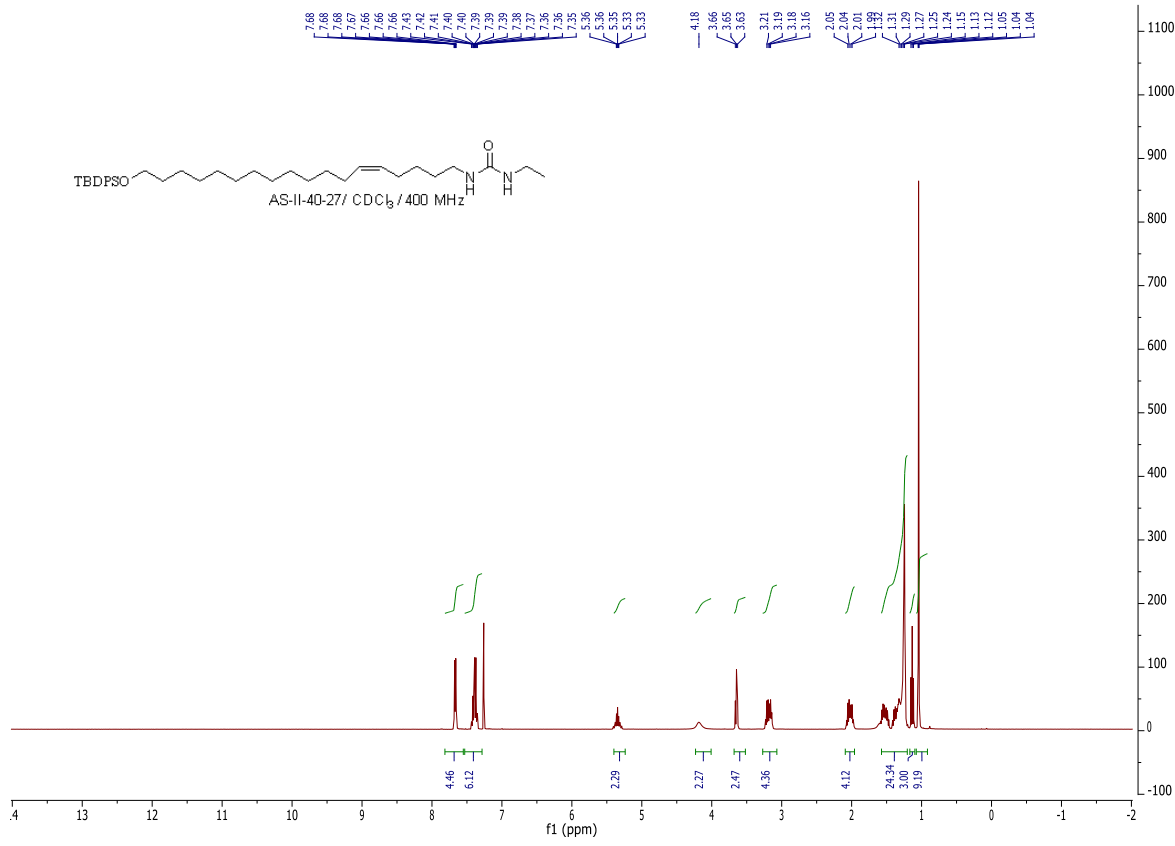
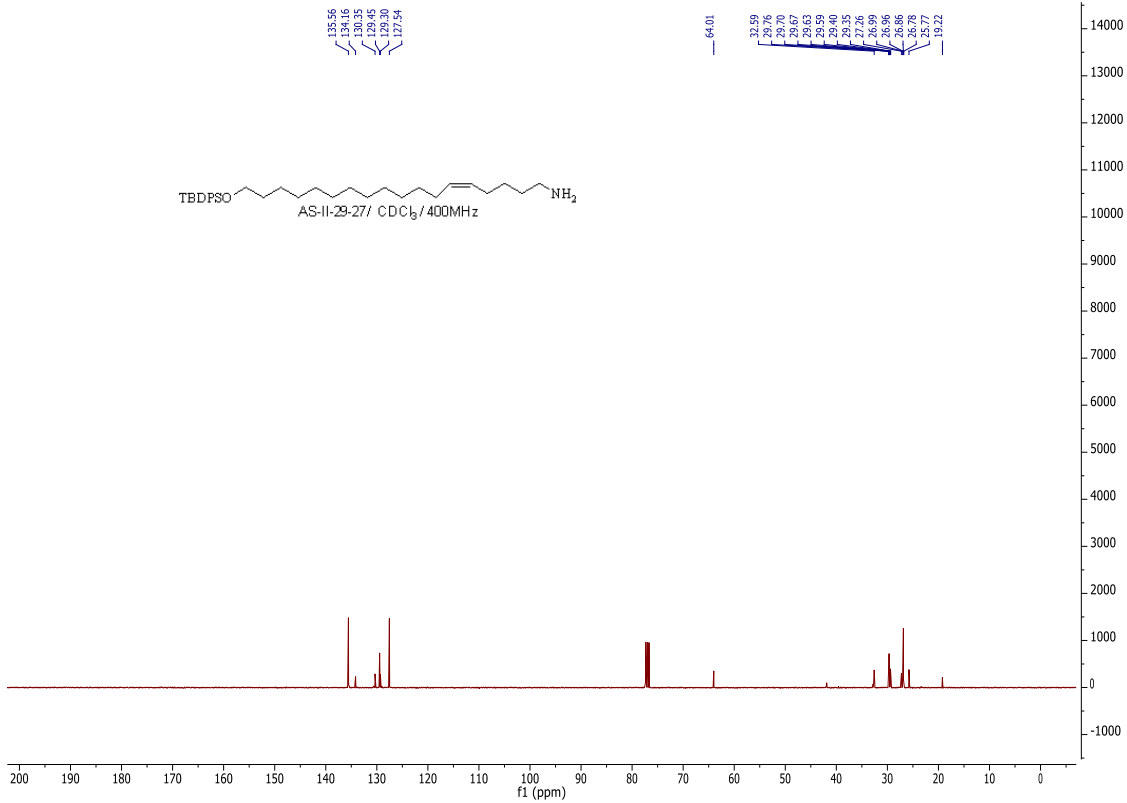
expl stdih
SAMPLE
date Mar 21 2006 dfr 399.781
solvent CDC13 dn H1
file exp dpr 30
ACQUISITION dpr 0
sfrq 399.781 dm nnn
in H1 dm c
at 3.744 daf 200
mp 44332 dseg
sw 6000.6 dres 1.0
fb 3000 hoap n
bs 4 DECZ
tpwr 54 dfrq2 0
pw 5.1 daz
d1 2.000 dpwz 1
tof 0 dofz 0
ot 32 do2 n
ct 32 dmz c
alock n dafz 200
gain not used dseg2
FLAGS n dres2 1.0
in n hoap2
in n PROCESSING
dp y lb 0.50
ns nm wfile
DISPLAY -70.3 fa n not used
sp 3551.3 math f
vc 223 wer
sc 0 wex
wc 250 wps
hnm 14.21 wnt
is 427.54 wnt
rf1 955.6
th 26
ins 3.000
nm cdc ph

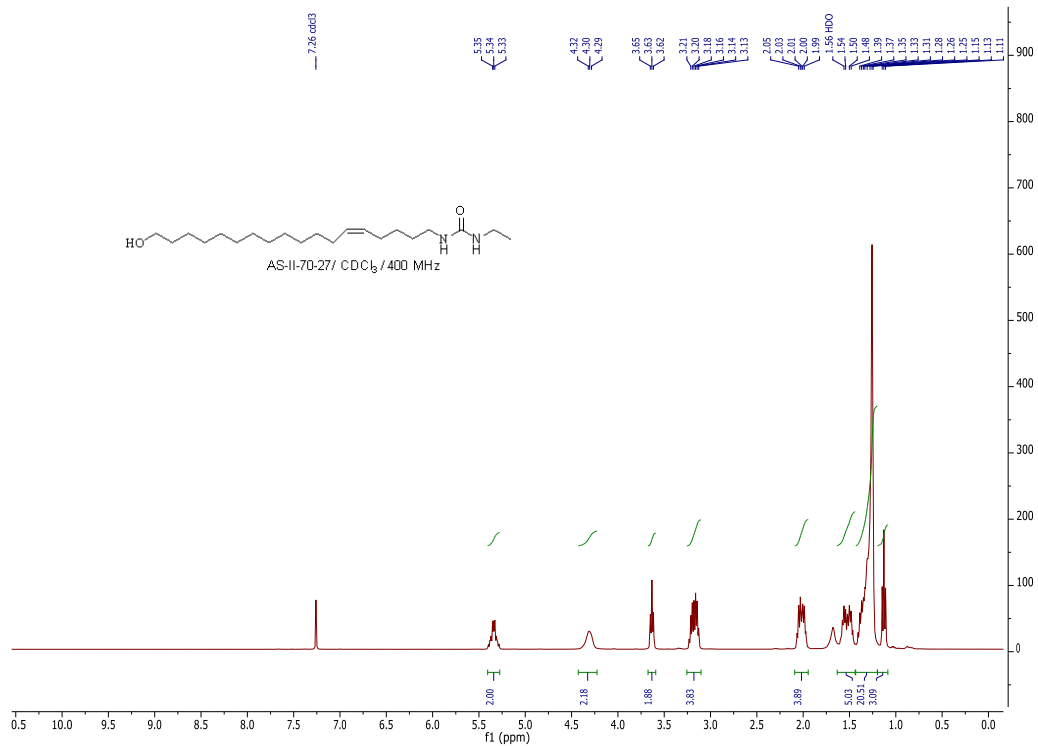
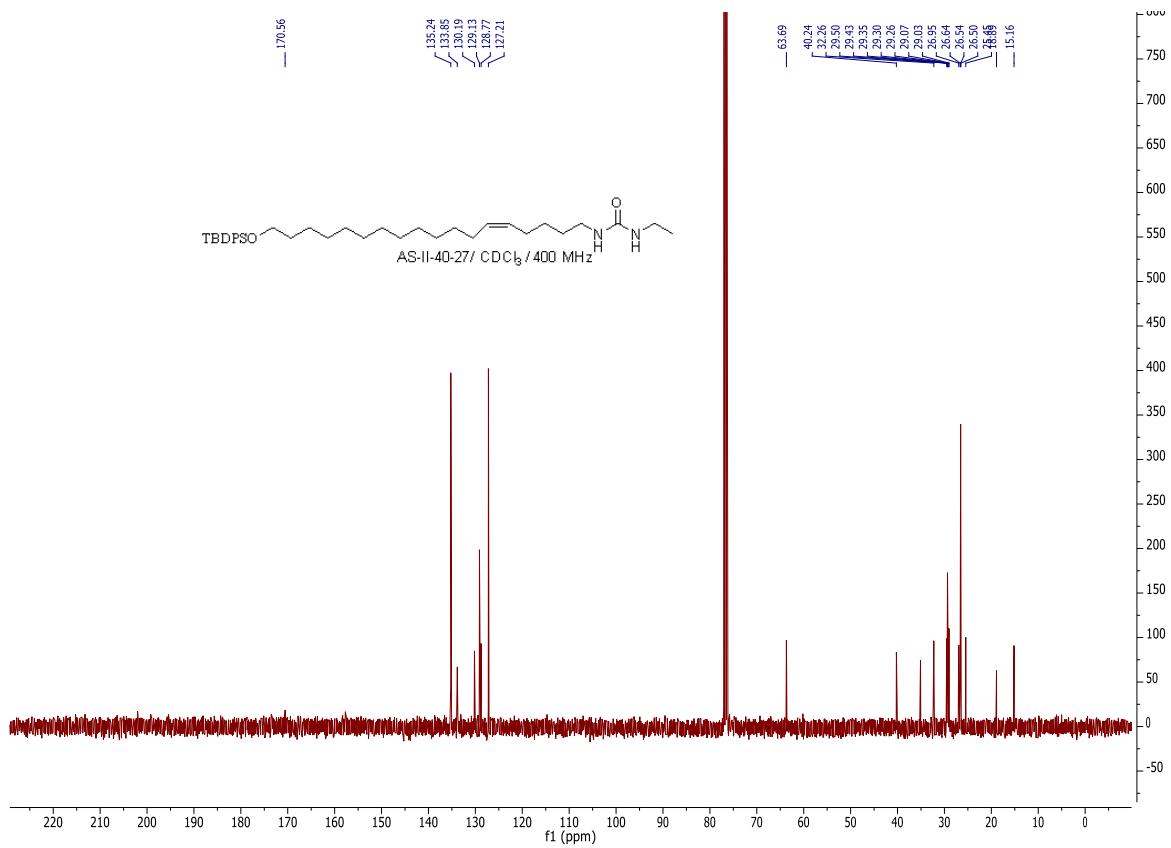
```

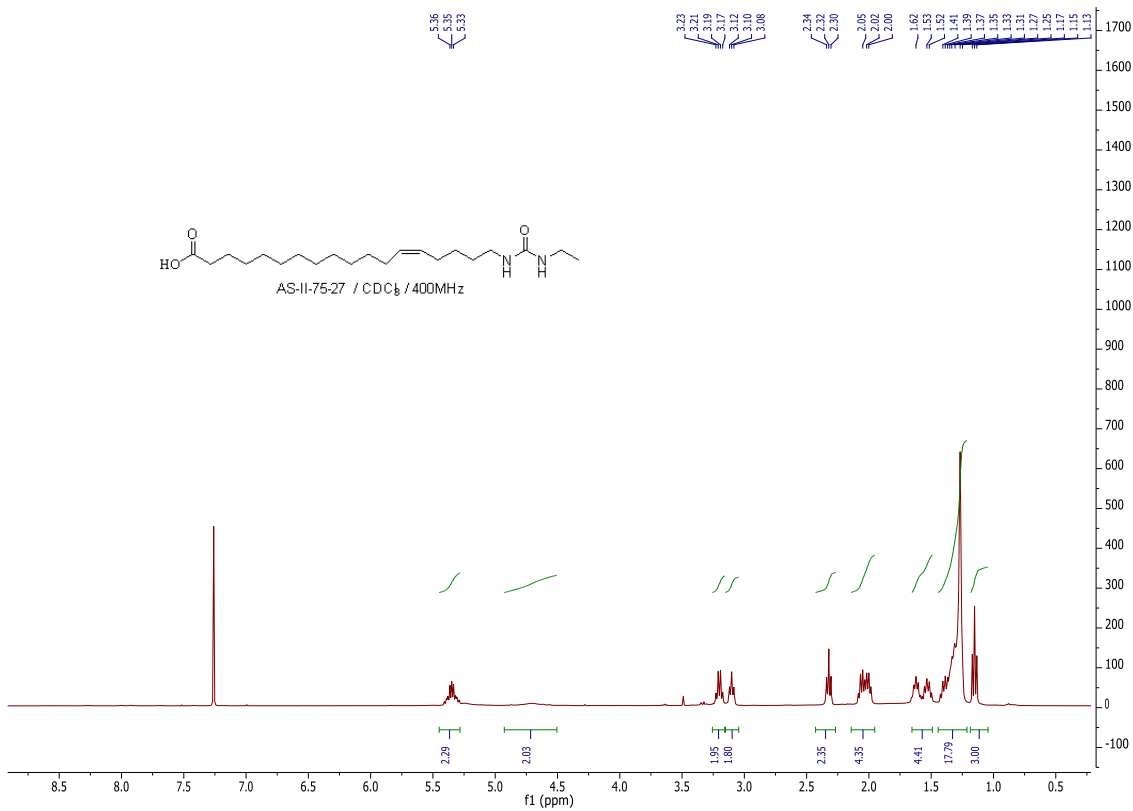
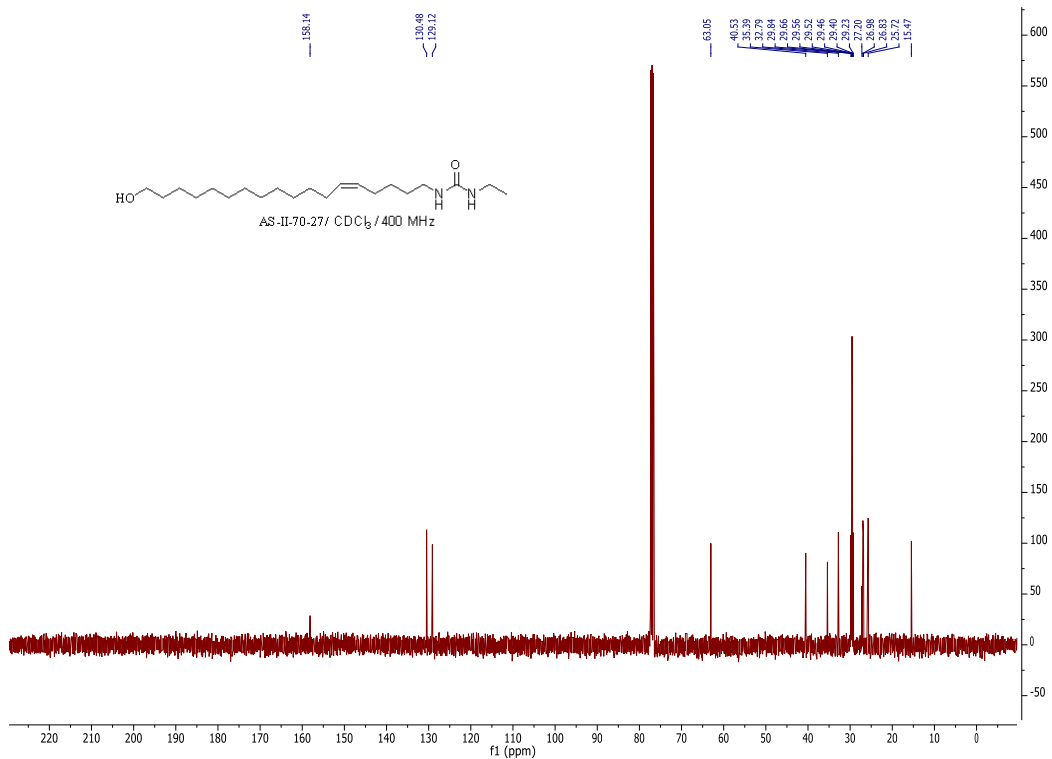


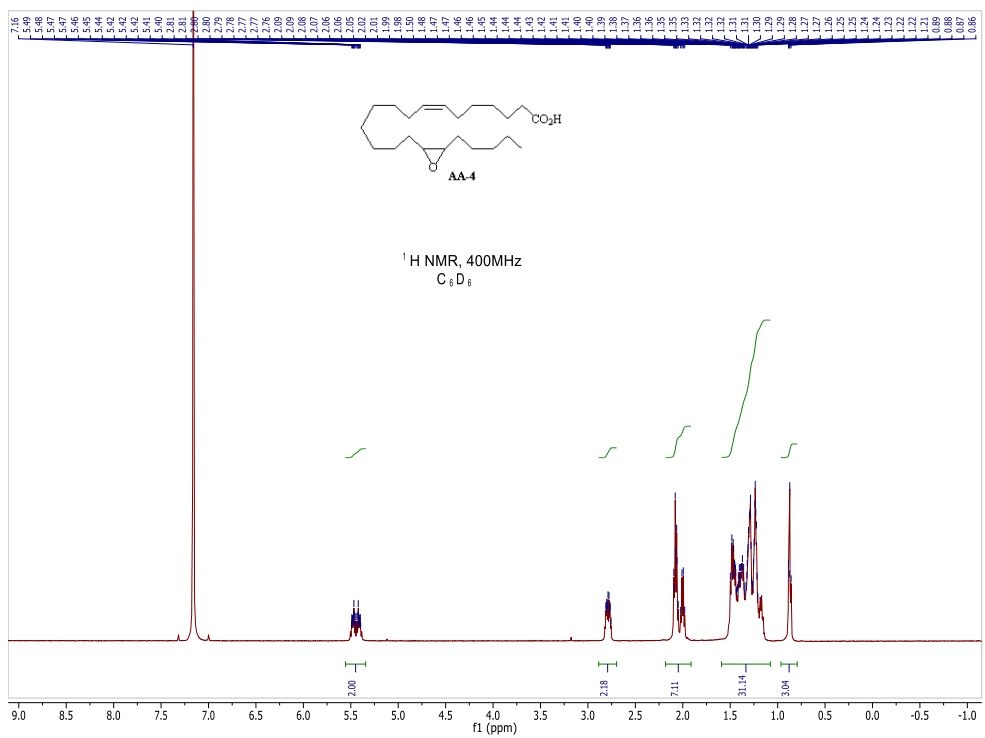
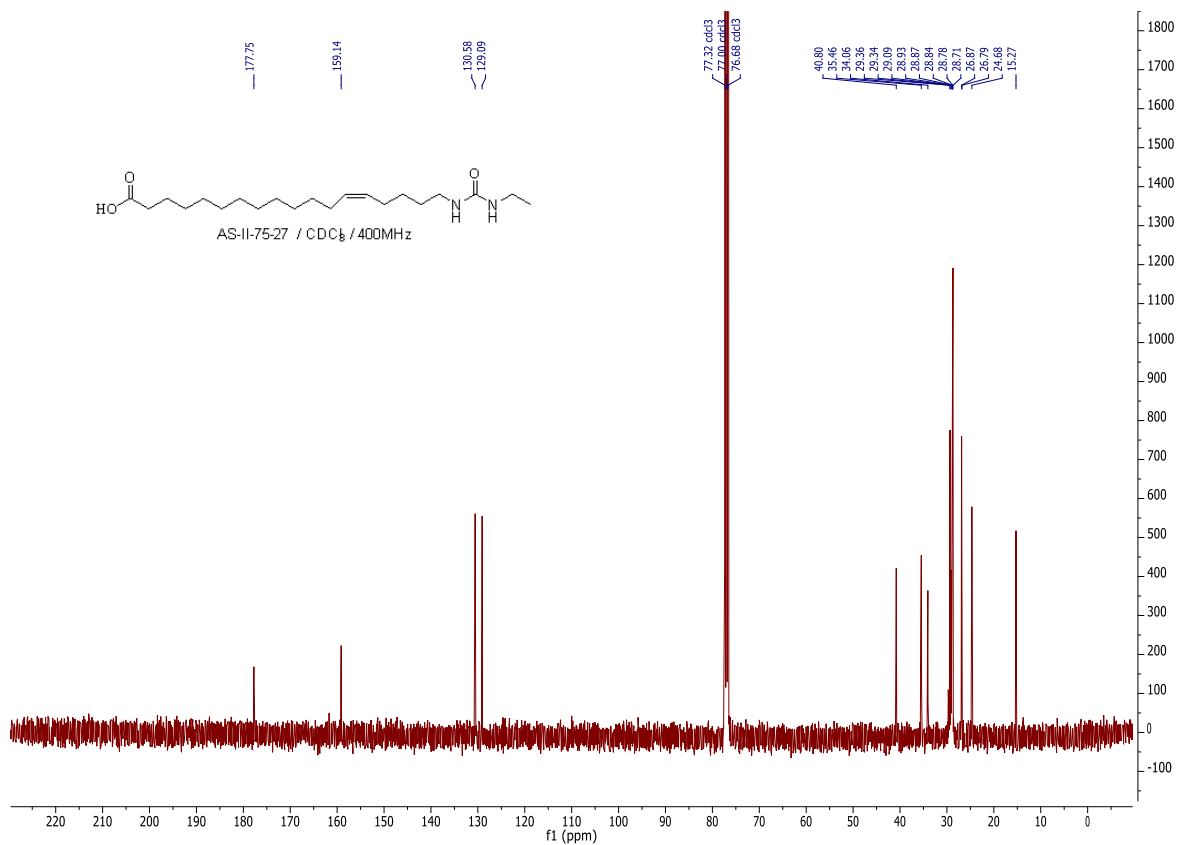
SA-II-109-2b











4.2.2 Animals

All studies were carried out using 2–3-month-old male and female wild-type (WT) C57/Bl6 mice weighing 25–30 g. Mice were maintained in a colony at the University of Alberta and housed under conditions of constant temperature and humidity with a 12:12-h light–dark cycle. Mice were fed on a standard rodent chow diet ad libitum (fat 11.3%, fiber 4.6%, protein 21% (w/w)). The composition of the diet includes linolenic acid (0.27%), linoleic acid (2.12%), arachidonic acid (0.01%), omega-3 fatty acid (0.45%), total saturated fatty acids (SFA) (0.78%) and total monounsaturated fatty acids (MSFA) (0.96%) (PicoLab® Rodent Diet 20 Cat. No 5053, LabDiets, Inc., St. Louis, MO, USA). All animal experimental protocols were approved by the University of Alberta Health Sciences Welfare Committee (University of Alberta Animal Welfare, ACUC, study ID#AUP330) and conducted according to strict guidelines provided by the Guide to the Care and Use of Experimental Animals (Voloum. 1, 2nd ed., 1993, from the Canadian Council on Animal Care).

4.2.3 Isolated heart perfusion

Wild-type (WT) mice of both sexes (equal ratios) were anesthetized by an intraperitoneal injection of sodium pentobarbital (Euthanyl, 100 mg/kg). Following complete non-responsiveness to external stimulation, hearts were quickly excised and perfused in the Langendorff mode [383] with Krebs-Henseleit buffer containing (in mM) 120 NaCl, 25 NaHCO₃, 10 Dextrose, 1.75 CaCl₂, 1.2 MgSO₄, 1.2 KH₂PO₄, 4.7 KCL, 2 Sodium Pyruvate (pH 7.4) and bubbled with 95% O₂ and 5% CO₂ at 37 °C. The left atrium was then excised, and a water-filled balloon made of saran plastic wrap was inserted into the left ventricle through the mitral valve. The balloon was connected to a pressure transducer for continuous measurement of left ventricular developed pressure (LVDP)

and heart rate (HR). Hearts with persistent arrhythmias or LVDP less than 80 cm H₂O were excluded from the experiment. Mouse hearts were perfused in the retrograde mode at a constant flow rate for 20 min of baseline (stabilization) and then subjected to 30 min of global no flow ischemia followed by 40 min of reperfusion. Hearts were perfused with either AS-27 (1 μM), SA-26 (1 μM), or AA-4 (1 μM). The concentrations utilized in the current study were based on previously published data from cell culture experiments and experience working with CYP-derived epoxy metabolites of n-3 PUFAs, which demonstrate cardioprotective effects at similar concentrations [580, 581]. In all experiments, chemicals were added at the beginning of reperfusion and were present in the heart throughout the reperfusion period. The percentage of left ventricular developed pressure (%LVDP) at 40 min of reperfusion (R40), as compared to baseline LVDP, was taken as a marker for recovery of contractile function. After 40 min of reperfusion, hearts were immediately frozen and stored below -80 °C. Haemodynamic parameters were acquired and analyzed using ADI software from (Holliston, MA, USA). Collection of the heart effluent was taken during both pre- and postischemic protocols to determine of coronary flow (CF) rates.

4.2.4 Immunoblotting

Frozen mouse hearts were ground, homogenized and then fractionated into mitochondrial and cytosolic fractions as previously described [702]. Briefly, frozen cardiac tissues were ground with mortar and pestle on dry ice and then homogenized in ice-cold homogenization buffer (20 mmol/L Tris-HCL, 50 mmol/L NaCl, 50 mmol/L NaF, 5 mmol/L sodium pyrophosphate, 1 mmol/L EDTA, and 250 mmol/L sucrose added on the day of the experiment, pH 7.0). Samples were first centrifuged at 800× g for 10 min at 4 °C to separate the cellular debris. The collected supernatant was then centrifuged at 10,000× g for 20 min. The pellet was resuspended in homogenization buffer to obtain a mitochondrial-enriched fraction. The supernatant was ultracentrifuged at 105,000× g for 60 min and the subsequent supernatant was used as the cytosolic fraction. Protein concentrations in both cytosolic and mitochondrial fractions were measured by the Bradford assay. Western blotting was carried out as previously described [702]. Protein (30–50 µg) was resolved by electrophoresis on (10–15%) SDS-polyacrylamide gels and transferred onto polyvinylidene difluoride (PVDF) membranes (BioRad Laboratories, Hercules, CA, USA). Immunoblots were probed with antibodies against citrate synthase (CS, ab129095), caspase 1 (ab179515), total manganese superoxide dismutase (MnSOD, ab13533), acetyl-MnSOD (ab137037), VDAC (ab14734) (Abcam, Burlingame, CA, USA), succinate dehydrogenase subunit A (SDH-A, 5839), cytochrome c oxidase subunit IV (COX IV, 11967), SIRT3 (5490), NLRP3 (15101), dynamin related protein-1 (Drp-1, 5391) (Cell Signaling Technology, Inc., MA, USA) and optic atrophy-1 (Opa-1, 612606) (Becton Dickinson Canada Inc, Mississauga, ON, CAN). After washing, membranes were incubated with the corresponding secondary antibodies. The blots were visualized with ECL reagent. Relative band intensities were expressed as fold of the control assessed using Image J software (NIH, USA).

4.2.5 Measurement of malondialdehyde (MDA) levels

The level of MDA was assessed in the cardiac tissue using a lipid peroxidation (MDA) colorimetric assay kit (ab118970, Abcam, Burlingame, CA, USA) according to manufacturer's instructions [644, 702]. In this assay, free MDA present in the sample reacts with thiobarbituric acid (TBA) and generate a MDA-TBA adduct which was quantified colorimetrically at wavelength 532 nm. MDA levels were expressed as nmole MDA per mg protein.

4.2.6 Enzymatic assays

Cleavage of the caspase-1 specific fluorogenic substrate Ac-YVAD-AMC (ALX-260-024-M005, Enzo life Sciences, NY, USA) was used to assess functional caspase-1 activity in cytosolic fractions of the heart homogenates [702]. The assay quantitated the fluorescence intensity of the cleaved 7-Amino-4-methylcoumarin (AMC) using a fluorometer (at excitation 380 nm, and emission 460 nm wavelengths). The activity was calculated by using a linear standard curve created with AMC.

SIRT3 activity was detected in the isolated mitochondrial fractions using a SIRT3 fluorescent assay kit (50088, BPS Bioscience, San Diego, CA, United States), according to the manufacturer's instructions [708]. In this assay, heart mitochondrial fractions were mixed with the specific histone deacetylase (HDAC) fluorogenic substrate, bovine serum albumin, NAD^+ and assay buffer. The deacetylation process induced by SIRT3 in the sample sensitizes the HDAC substrate so that subsequent treatment with the SIRT3 assay developer produces a fluorescence product that was measured using a fluorescence plate reader at 350/460 nm excitation/emission wavelengths.

4.2.7 Measurement of ATP levels in the heart

ATP levels in the heart tissue were measured using a fluorometric based assay kit (ab83355, Abcam Inc, Toronto, ON, Canada). Briefly, heart powders were homogenized in ice-cold assay buffer and centrifuged at $15,000\times g$ for 2 min. The supernatant was used to quantitate ATP at 535 nm excitation and 587 nm emission with a Biotek plate reader (Winooski, VT, USA).

4.2.8 Measurement of NAD⁺/NADH content in the heart

NAD⁺ and NADH contents were measured in whole heart homogenates using a colorimetric NAD/NADH Assay Kit according to the manufacturer's protocol (ab65348, Abcam, Burlingame, CA, USA). Samples were split into 2 fractions to separately measure total amount of nicotinamide adenine dinucleotides (NAD⁺ + NADH = NAD_{total}) in one fraction and NADH in the other fraction after decomposition of NAD⁺ by heating the samples at 60 °C for 30 min. Levels of NAD⁺ were estimated by subtracting NADH from NAD_{total}. Absorbance was measured at 450 nm using microplate reader.

4.2.9 Statistics

Values are expressed as mean \pm standard error of mean (SEM). Statistical significance was determined by one-way ANOVA with a Tukey post hoc test to assess differences between groups; $p < 0.05$ was considered statistically significant.

4.3 Results

4.3.1 SA-26 improves post-ischemic functional recovery

Our previous data suggest that EDPs ameliorate cardiac IR injury [383], however, these natural metabolites are rapidly degraded which limit their prolonged use [507]. Therefore, the current study investigates the cardioprotective properties of more chemically and metabolically stable synthetic analogues which were obtained through reducing the number of double bonds and replacing the epoxy-group with a urea group. Notably, preischemic cardiac parameters were similar among all treatment groups. Hearts perfused with SA-26 during the reperfusion period significantly improved postischemic recovery of LVDP compared to vehicle IR group (Figure 4.2 A and B). Consistent with improved postischemic functional recovery, hearts perfused with SA-26 demonstrated better rates of contraction (dP/dt max) and relaxation (dP/dt min) in comparison to the corresponding vehicle IR group (Figure 4.2 C and D). However, perfusion of mouse hearts with either AS-27 or AA-4 did not improve LVDP (Figure 4.2 A and B), rates of contraction (dP/dt max) or relaxation (dP/dt min) (Figure 4.2 C and D) in comparison to the corresponding vehicle IR group. No significant differences were observed in the heart rate at the end of reperfusion between all the study groups (Figure 4.2E). Interestingly, no differences were observed in postischemic coronary flow rates in any of the treatment groups indicating the cardioprotective effect was not attributable to alterations in hemodynamics in the perfused heart model (Figure 4.2F). Together, these data suggest that perfusion of hearts with the EDP analogue SA-26 improves post-ischemic functional recovery and ameliorate IR injury.

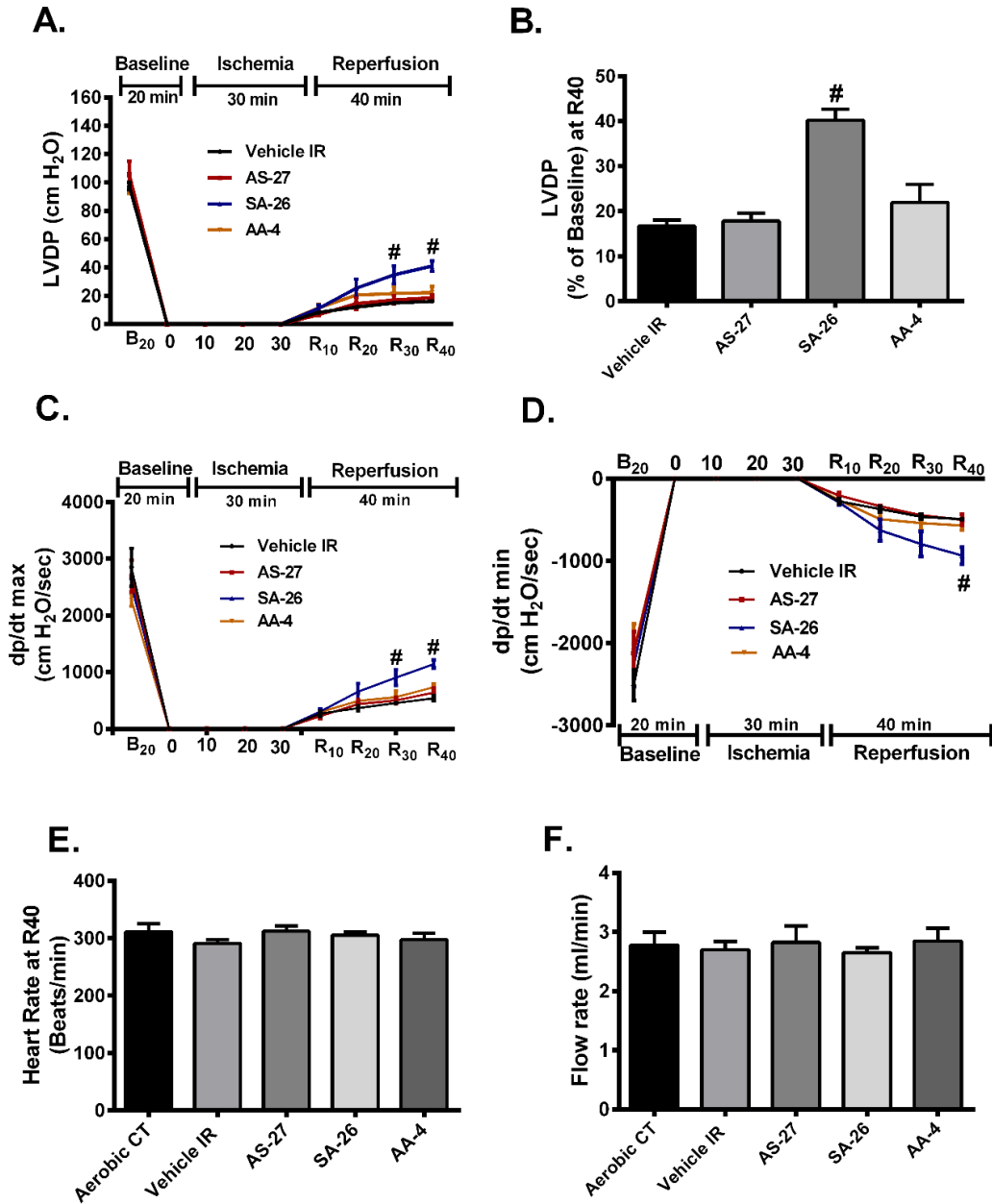


Figure 4. 2: Perfusion of hearts with SA-26 improved postischemic contractile parameters. (A) LVDP at the baseline before drug treatment (B₂₀), during ischemia, and at 10, 20, 30 and 40 min reperfusion (R₁₀, R₂₀, R₃₀, and R₄₀). (B) LVDP recovery at 40 min of reperfusion as a percentage of baseline. (C) Rate of contraction (dp/dt max), and (D) rate of relaxation (dp/dt min) at baseline before drug treatment (B₂₀), ischemia, and 10, 20, 30 and 40 min reperfusion (R₁₀, R₂₀, R₃₀, and R₄₀). (E) Heart rate assessed as beats per minute (BPM) in vehicle treated aerobic hearts and hearts subjected to ischemia-reperfusion (IR) injury at the end of reperfusion (R₄₀). (F) Coronary flow rates from vehicle treated aerobic hearts as well as hearts subjected to IR injury assessed post-ischemia. Values represent mean \pm SEM; #p < 0.05 vs. Vehicle IR (n = 4–7 per group). LVDP; left ventricular developed pressure.

4.3.2 SIRT3 function is preserved in hearts perfused with SA-26

Increased mitochondrial ROS production is implicated in the development of the oxidative damage triggered by IR injury [709]. Over 90% of cellular ROS produced during IR injury is generated by mitochondria as electrons escape the disrupted ETC to combine with molecular O₂ producing superoxide anions (O^{•-2}) [710, 711]. SIRT3 can protect the heart against oxidative stress by directly deacetylating and activating the antioxidant enzyme manganese superoxide dismutase (MnSOD) in mitochondria, significantly enhancing its ability to scavenge ROS [149, 712]. MnSOD is the primary mitochondrial antioxidant enzyme that converts O^{•-2} to H₂O₂, which is further converted to water by catalase [713]. We observed no significant differences in mitochondrial expression of SIRT3 among different groups (Figure 4.3A). However, SIRT3 activity was significantly decreased in vehicle control hearts subjected to IR injury (Figure 4.3B). The IR-induced reduction in SIRT3 activity resulted in significantly elevated acetylation and thus decline in the level of activated MnSOD (Figure 4.3C). Hearts perfused with the analogue SA-26 demonstrated significantly enhanced SIRT3 activity and reduced MnSOD acetylation levels compared to the vehicle control IR group (Figure 4.3 B and C). These data suggest perfusion of hearts with SA-26 confers protection against IR-induced oxidative damage by preserving SIRT3 activity accompanied with decreased acetylation and hence maintained MnSOD antioxidant capacity. This was partially supported by assessment of the cardiac levels of MDA, the main end product of lipid peroxidation and a key biomarker of oxidative stress [644, 647]. MDA cardiac levels were significantly elevated following IR injury (Figure 4.3D). However, perfusing with SA-26 significantly blunted the accumulation of MDA in post-ischemic hearts (Figure 4.3D), suggesting less ROS production. In contrast, hearts perfused with the analogues AS-27 and AA-4

neither maintained SIRT3 activity, nor limited the reduction in levels of activated MnSOD nor abrogated the accumulation of MDA compared to the vehicle control IR group.

Sirtuins are a family of NAD⁺-dependent histone deacetylases. Therefore, the rate-limiting factors of SIRT3 activity are the availability of the co-factor NAD⁺ and the ratio of oxidized to the reduced NAD⁺ [142, 714]. We measured NAD⁺ and NADH levels and their relative ratio in the setting of IR injury. There were no significant differences in the total NAD content between any of the study groups (Figure 4.3 E). However, NAD⁺ content and NAD⁺/NADH ratio were markedly lower in hearts subjected to IR injury compared to aerobic CT (Figure 4.3 F and G). Interestingly, perfusion of mice hearts with the analogue SA-26 maintained NAD⁺ levels and thus restored NAD⁺/NADH ratio compared to the vehicle IR (Figure 4.3 G and H). On the other hand, hearts perfused with the EDP analogues AS-27 or AA-4 did not restore the NAD⁺/NADH ratio compared to the vehicle IR group (Figure 4.3 G and H). These findings well correlate with the observed reduction in SIRT3 activity and the impaired post-ischemic recovery in the hearts perfused with these analogues.

Collectively, these data provide evidence that SA-26 prevents cardiac mitochondrial dysfunction and protects the heart against IR-induced oxidative injury via maintaining SIRT3 activity and consequently activating the major mitochondrial antioxidant enzyme MnSOD.

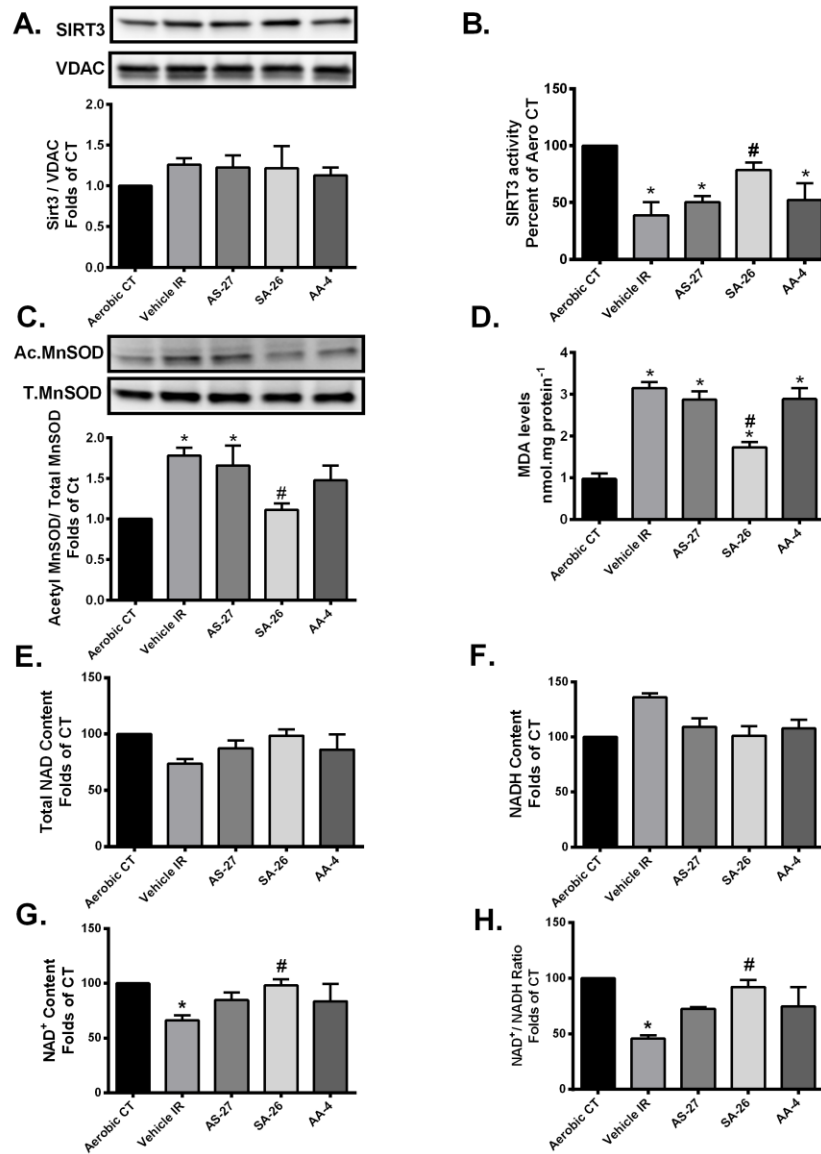


Figure 4. 3: Preservation of NAD⁺/NADH control ratio and SIRT3 activity limited oxidative stress following IR injury. (A) Representative immunoblots and densitometric quantification of the expression of mitochondrial protein SIRT3 in mice hearts after 30 min ischemia and 40 min reperfusion. Protein expression was normalized to voltage-dependent anion channel (VDAC) protein used as a loading control. (B) Cardiac SIRT3 activity was determined in mitochondrial fractions in mice hearts after 30 min ischemia and 40 min reperfusion using a SIRT3 fluorescent assay kit. (C) Representative immunoblots and densitometric quantification of the relative protein expression of AcMnSOD normalized to total manganese superoxide dismutase (MnSOD) in mice hearts after 30 min ischemia and 40 min reperfusion. (D) Cardiac malondialdehyde (MDA) levels assessed using a lipid peroxidation (MDA) colorimetric assay kit in mice hearts following 30 min ischemia and 40 min reperfusion. Cardiac levels of (E) Total NAD, (F) NADH, (G) NAD⁺ and (H) NAD⁺/NADH ratio expressed as nmol per g dry weight assessed in mice hearts after 30 min ischemia and 40 min reperfusion. Values represent mean ± SEM, *p < 0.05 vs. Aerobic CT, #p < 0.05 vs. Vehicle IR (n = 4–5 per group).

4.3.3 SA-26 mitigates mitochondrial damage in response to IR injury

Accumulating literature revealed that cardiac dysfunction resulting from IR injury can be directly linked to mitochondrial damage [690, 691]. We investigated the changes in the protein levels of the ETC components SDH-A (Complex II) and COX IV, the terminal enzyme of the mitochondrial respiratory chain (Complex IV). Immunoblotting results revealed that no significant differences in the protein expression of SDH-A or COX IV among different treatment groups (Figure 4.4 A and B). Additionally, there were no significant changes in the expression level of citrate synthase (CS) suggesting differences were not attributable to changes in mitochondrial biomass (Figure 4.4C).

Mitochondrial dysfunction resulting from IR injury could stem from aberrations in proteins regulating mitochondrial dynamics, particularly Drp-1 and Opa-1 [101]. An increased mitochondrial localization of the active Drp-1 following marked mitochondrial damage results in excessive mitochondrial fission [715, 716]. Opa-1, a protein localized in the inner mitochondrial membrane, is considered an important determinant of mitochondrial integrity, fusion and function [97, 616]. Loss of Opa-1 impairs mitochondrial fusion, perturbs cristae structure, and increases the susceptibility of cell death [151, 717]. In the current study, we observed a marked increase in mitochondrial expression of Drp-1 and a significant decrease in mitochondrial Opa-1 levels in the vehicle IR group compared to the aerobic CT (Figure 4.4 D and E). However, perfusion of hearts with SA-26 limited the mitochondrial localization of Drp-1 and limited the loss of Opa-1 protein compared to the IR group (Figure 4.4 D and E), which supports the notion of reduced mitochondrial injury. However, neither AS-27 nor AA-4 prevented the mitochondrial localization of Drp-1 compared to the vehicle IR group (Figure 4.4 D and E). Notably, the level of Opa-1 protein was not significantly reduced in hearts perfused with either AS-27, SA-26 or AA-4

compared to the aerobic CT. However, only hearts perfused with the EDP analogue SA-26 maintained Opa-1 protein at a significantly higher level compared to the IR group.

To further assess the effect of these changes on the mitochondrial function, we evaluated cardiac ATP levels in the different study groups. Cardiac ATP levels were significantly lower in the vehicle IR group as well as hearts perfused with the analogues AS-27 or AA-4 compared to the aerobic group. Interestingly, hearts perfused with the analogue SA-26 maintained ATP content at a significantly higher level than the vehicle IR group (Figure 4.4F). Altogether, these findings demonstrate that SA-26 could improve cardiac recovery following IR injury via ameliorating mitochondrial dysfunction and consequently maintaining adequate supply of cellular energy.

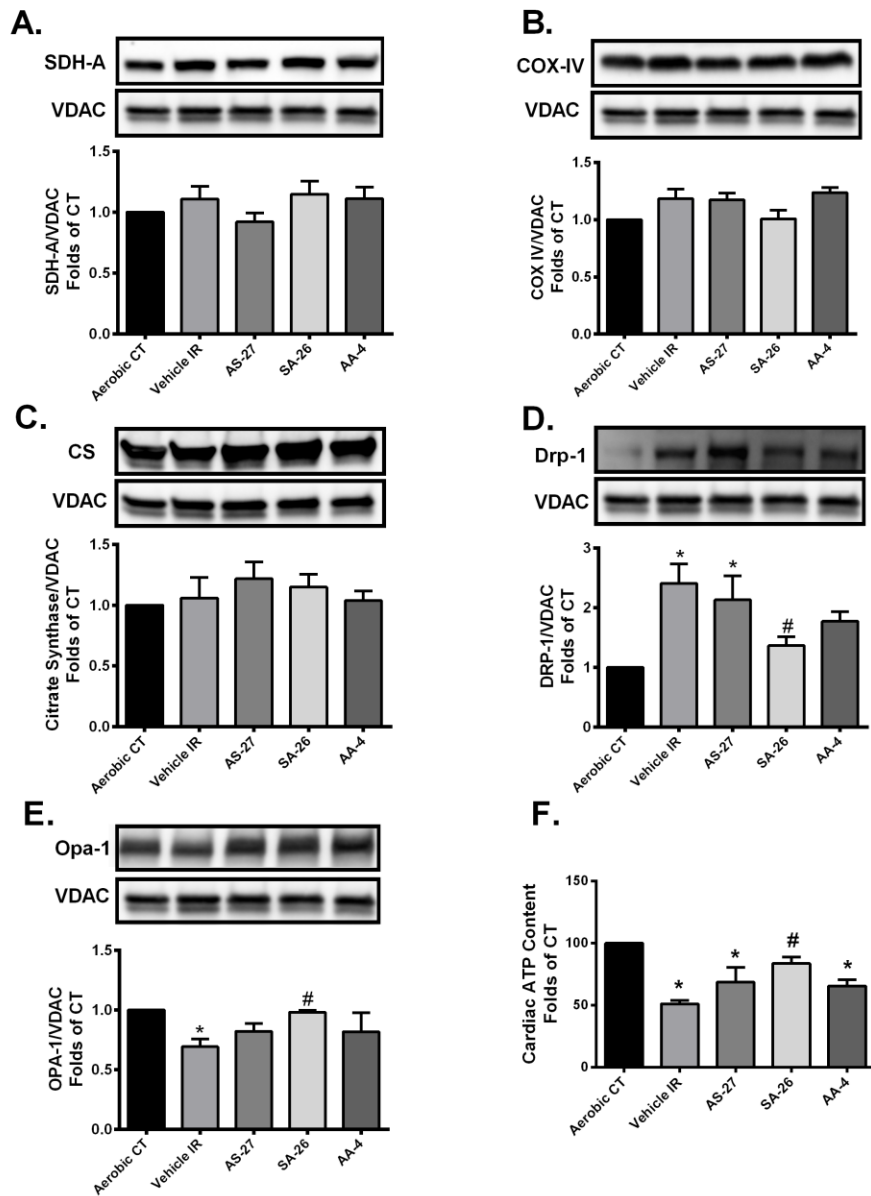


Figure 4. 4: Perfusion of hearts with SA-26 preserved mitochondrial integrity and function under IR insult. Representative immunoblots and densitometric quantification of the mitochondrial protein expression of (A) succinate dehydrogenase subunit A (SDH-A), (B) cytochrome c oxidase subunit IV (COX IV), (C) citrate synthase (CS), (D) dynamin-related protein 1 (Drp-1) and (E) optic atrophy 1 (Opa-1) proteins observed in mice hearts following 30 min ischemia and 40 min reperfusion. All expressions were normalized to VDAC loading control. (F) Cardiac ATP levels were measured in mice hearts using a fluorometric based assay kit assessed following 30 min ischemia and 40 min reperfusion. Values represent mean \pm SEM, * $p < 0.05$ vs. Aerobic CT, # $p < 0.05$ vs. Vehicle IR (n = 4 – 5 per group).

4.3.4 SA-26 inhibits IR-induced NLRP3 assembly on the mitochondrial membrane

Growing evidence demonstrates mitochondrial damage can be both a trigger and a target of NLRP3 inflammasome cascade [259, 260]. Briefly, assembly of the NLRP3 inflammasome complex requires recruitment of NLRP3 and pro-caspase 1 to mitochondria in the perinuclear region, leading to increased co-localization of NLRP3 on mitochondrial membrane [575, 718, 719]. Afterwards, the activated NLRP3 inflammasome induces cleavage of pro-caspase-1 to generate the active caspase 1 [259]. To determine the ability of different analogues to interfere with the NLRP3 inflammasome cascade activation in the current experimental model, expression levels of NLRP3 and cleaved caspase 1 proteins were determined in the mitochondrial fractions and caspase-1 activity was assessed in cytosolic fractions. As shown in Figure 4.5, immunoblot analysis revealed hearts subjected to IR injury or even perfused with the analogue AS-27 showed significantly higher protein levels of both NLRP3 and caspase-1 in mitochondrial fractions (Figure 4.5 A and C) and demonstrated higher caspase-1 activity compared to aerobic control (Figure 4.5B). Perfusion with SA-26 significantly prevented the IR-induced upregulation of NLRP3 protein and caspase-1 in mitochondrial fractions (Figure 4.5 A and C). Moreover, active caspase-1 levels were the same between aerobic controls and hearts perfused with SA-26 (Figure 4.5B). Perfusion of mice hearts with the analogue AA-4 failed to attenuate postischemic NLRP3 or caspase-1 activation compared to the vehicle IR group (Figure 4.3A–C). Cumulatively, these data demonstrate that the analogue SA-26 limited the activation of NLRP3 inflammasomes in response to IR injury.

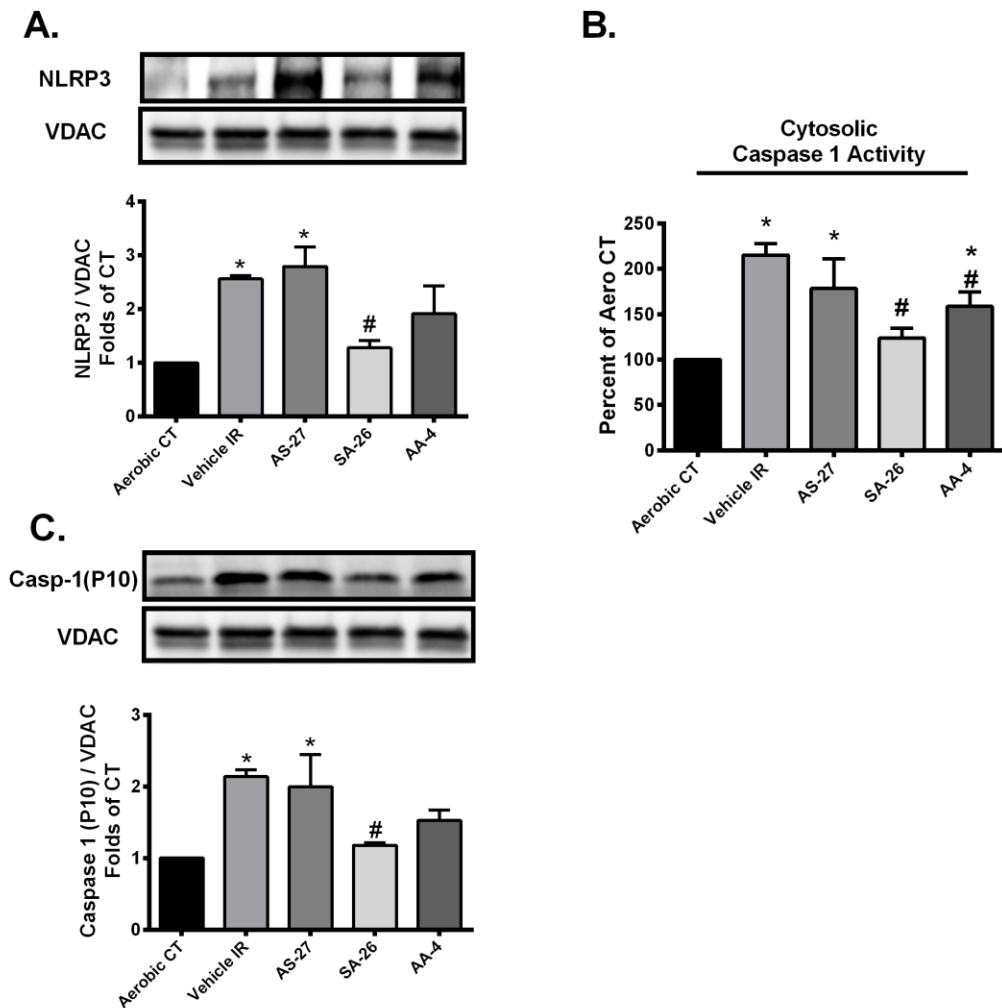


Figure 4. 5: Perfusion of hearts with SA-26 inhibited the IR-induced activation and translocation of the NLRP3 inflammasome to the mitochondria. (A) Representative immunoblots and densitometric quantification of the mitochondrial expression of NLRP3 protein in mice hearts after 30 min ischemia and 40 min reperfusion. Protein expression was normalized to VDAC loading control. (B) Cardiac caspase-1 enzymatic activity assessed in the cytosolic fraction following 30 min ischemia and 40 min reperfusion. The assay quantitated the fluorescence intensity resulting from the cleavage of the caspase-1 specific fluorogenic substrate Ac-YVAD-AMC by the cytosolic heart homogenates. (C) Representative immunoblots and densitometric quantification of the mitochondrial expression of cleaved caspase-1 (P10) in mice hearts after 30 min ischemia and 40 min reperfusion. Protein expression was normalized to VDAC protein used as a loading control. Values represent mean \pm SEM, * $p < 0.05$ vs. Aerobic CT, # $p < 0.05$ vs. Vehicle IR (n = 4–5 per group).

4.4 Discussion

In the current study, we provide evidence for a novel cardioprotective mechanism of the newly synthetic EDP surrogate SA-26. Our results suggest that the perfusion of hearts with SA-26 during the reperfusion period ameliorates IR injury by maintaining mitochondrial integrity and function. Hearts perfused with SA-26 showed improved SIRT3 activity, enhanced antioxidant capacity and limited oxidative injury. This effect was associated with the inhibition of the assembly and mitochondrial translocation of NLRP3 inflammasomes. To the best of our knowledge, this is the first study reporting the involvement of SIRT3 in mediating the cardioprotective properties of the CYP-derived epoxylipids of n-3 PUFAs or their analogues against IR injury (Figure 4.6).

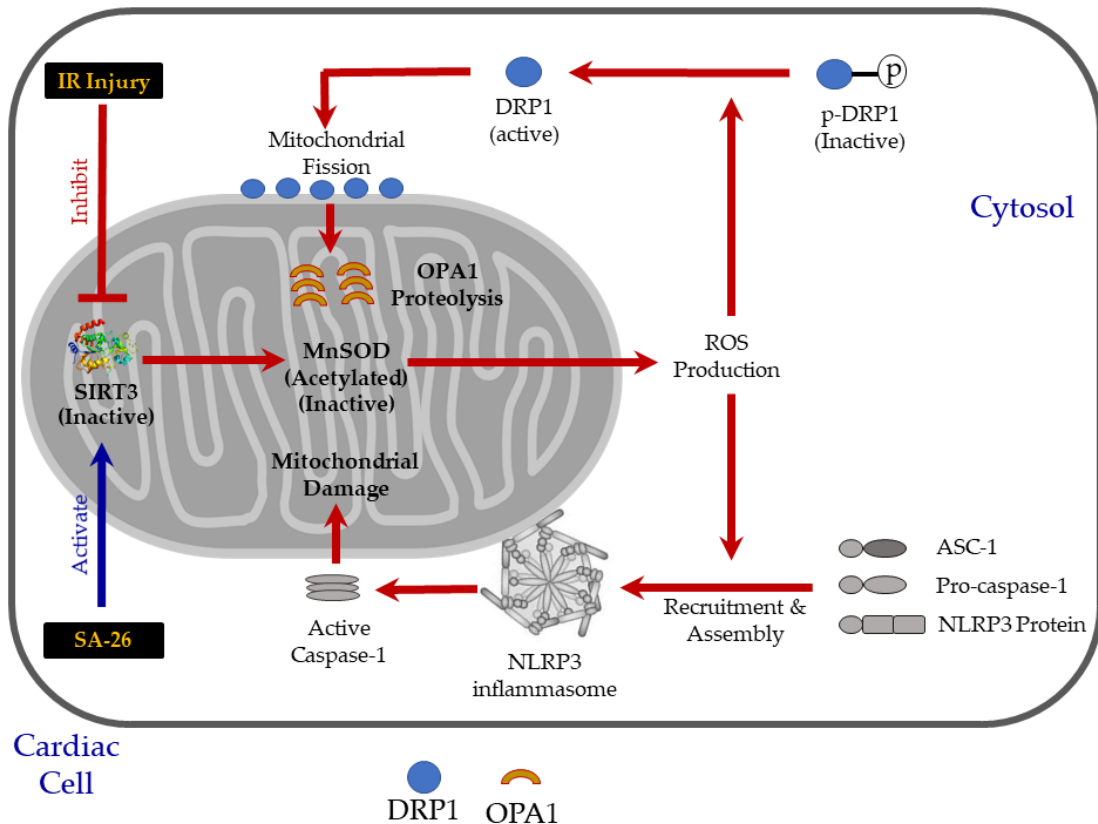


Figure 4. 6: Conceptual illustration showing the potential cardioprotective role of the EDP surrogate SA-26 against IR injury. Hearts subjected to IR injury showed decreased SIRT3 activity and increased acetylation of MnSOD, suggesting diminished antioxidant capacity. Accordingly, the reactive oxygen species (ROS) burst from damaged mitochondria triggers excessive activation and recruitment of Drp-1 on the mitochondrial outer membrane, inducing Opa-1 proteolysis which impairs mitochondrial fusion, perturbs cristae structure, and prompts mitochondrial fragmentation. Furthermore, the excessive ROS production from the damaged mitochondria activates the assembly of NLRP3 inflammasome on mitochondrial membrane leading to the activation of caspase-1 which in turn, aggravates mitochondrial damage. Perfusion of hearts with SA-26 during the reperfusion period ameliorates IR injury by maintaining mitochondrial integrity and function. Hearts perfused with SA-26 showed improved SIRT3 activity, enhanced antioxidant capacity and limited oxidative injury. This effect was associated with the inhibition of the assembly and mitochondrial translocation of the detrimental NLRP3 inflammasome and consequently improved postischemic functional recovery.

Emerging evidence has identified EDPs, a group of epoxylipids generated endogenously through the CYP-metabolism of the n-3 PUFA DHA, as potent lipid mediators with better beneficial effects than its parent compound, including protection against CVDs [329, 330, 609]. Although the precise mechanism(s) remains elusive, our group and others have demonstrated that pathways targeting the mitochondria and NLRP3 inflammasome activation are involved [339, 383, 516]. As such, elevation of intracellular EDPs has been hypothesized to impart cardioprotective effects against several CVDs. However, EDPs are considered chemically and metabolically labile mediators which limit their use as therapeutic or pharmacological agents [501]. For instance, the peak plasma concentration of these metabolites occurred 1 min post intraperitoneal injection, indicating a relatively short half-life for these metabolites [720, 721]. Moreover, EDPs may slowly darken and polymerize upon exposure to light, heat or oxygen because of the presence of their multiple double bonds [704]. Considerable interest has arisen in developing methods or surrogates to enhance the bioavailability of EDPs, particularly 16,17-EDP and 19,20-EDP, the two most abundant and potent regioisomers [722, 723]. One of the approaches to enhance the bioavailability and consequently the beneficial effects of these metabolites would be combining EDPs with an sEH inhibitor (sEHi) to limit their degradation. For instance, Capozzi et al. demonstrated the exogenous addition of 19,20-EDP combined with the sEHi 12-(3-adamantane-1-yl-ureido)-dodecanoic acid (AUDA) in an inflammation model of tumor necrosis factor alpha (TNF α)-stimulated human retinal microvascular endothelial cells, significantly inhibited the expression of the inflammatory markers vascular cell adhesion molecule 1 (VCAM-1) and intercellular adhesion molecule-1 (ICAM-1). In contrast, the diol metabolites of 19,20-EDP hydrolysis, 19,20-dihydroxydocosapentaenoic acid (19,20-DHDP), aggravated VCAM1 and ICAM1 expression suggesting an opposing effect of the diol to the epoxy lipid [724]. Furthermore, Ulu et al.

demonstrated 19,20-EDP contributed to the antihypertensive actions of DHA in angiotensin II-induced hypertension. Importantly, the combination of 19,20-EDP with the sEHi TPPU (1-trifluoromethoxyphenyl-3-(1-propionylpiperidin-4-yl) urea) significantly lowered blood pressure as compared to angiotensin-II infused animals [511]. The current study was designed to first demonstrate the cardioprotective properties of AS-27 (19,20-EDP analogue), AA-4 and SA-26 (16,17-EDP analogues) as potential drug leads for IR injury and future experiments combining these compounds with sEHi are warranted.

SIRT3, the primary mitochondrial deacetylase [694], has a key role in regulating mitochondrial function including regulating energy metabolism, ATP production, antioxidant defense and inflammatory signaling [149, 697, 725]. SIRT3 directly deacetylates and activates the mitochondrial antioxidant MnSOD significantly enhancing its ability to scavenge ROS [149, 712, 713]. SIRT3 promotes effective electron transport via the deacetylation of ETC complex components, the main source of more than 90% of cellular ROS, which indirectly reduces ROS production [710, 711]. Experimental studies demonstrate that cardiac SIRT3 levels and/or activity are decreased in response to acute IR injury [161]. This is supported by evidence in H9c2 cells or adult mouse hearts where knocking down SIRT3 aggravated IR injury and mitochondrial dysfunction [158]. Furthermore, *ex vivo* studies using hearts isolated from SIRT3^{-/-} mice subjected to global IR exhibited significantly less recovery of cardiac function [157]. Approaches to upregulate SIRT3 expression and activity, such as administration of melatonin prior to reperfusion resulted in decreased acetylation of MnSOD, improved postischemic cardiac contractile function and limited oxidative damage [726]. In agreement with these reports, the current study demonstrated that hearts subjected to IR injury had decreased SIRT3 activity, increased acetylation of MnSOD, reduced ATP content and accumulation of MDA. Interestingly, the perfusion of hearts

with the EDP analogue SA-26 during the reperfusion period was able to maintain SIRT3 activity, reduced acetylation of MnSOD and ameliorated the accumulation of MDA which correlated with improved post-ischemic functional recovery. These effects were associated with improved cardiac ATP levels. Together, these data indicate maintenance and promotion of SIRT3 activity can protect cardiomyocytes from oxidative stress-mediated cell death and limit cardiac injury.

The rate-limiting factor of SIRT3 activity is the availability of NAD^+ , a required cofactor for functional deacetylase activity of the enzyme [142, 714]. The observed reduction of SIRT3 activity in hearts subjected to IR injury could be attributed to the reduction of NAD^+/NADH ratio. Di Lisa et al. reported that NAD^+ depletion during IR injury is partly due to the opening of the mitochondrial permeability transition pore (MPTP) leading to a release of mitochondrial NAD^+ into the cytosol where it is degraded by glycohydrolase [727, 728]. Furthermore, during IR injury, ROS-induced damage leads to the production of single-strand breaks in the DNA which increases catabolism of NAD^+ , resulting in reduced level of NAD^+ [729]. The reduction of NAD^+ content limits the activation of SIRT3, thereby leading to a hyper-acetylation of MnSOD and thus further ROS production. This hypothesis is supported by the recent finding of Fu et al. demonstrating trans-viniferin, a natural derivative stilbenic antioxidant, can activate SIRT3 by increasing the NAD^+/NADH ratio in a cell model of Huntington's disease [730]. Consistent with this notion, our results revealed IR injury depleted NAD^+ levels and consequently the NAD^+/NADH ratio in the heart. However, hearts perfused with the analogue SA-26 maintained significantly higher NAD^+/NADH ratio which could explain the improved SIRT3 activity and the enhanced post-ischemic cardiac recovery.

Proteins regulating mitochondrial dynamics, particularly Drp-1 and Opa-1, are involved in modulating mitochondrial function following myocardial IR injury [101]. Under healthy conditions, Drp-1 is predominantly found in the cytosol in an inactive phosphorylated form. Following cellular stress, Drp-1 shuttles to the outer mitochondrial membrane initiating fission events reducing the number of functional mitochondria accelerating myocardial cell death [716]. Moreover, several reports reveal limiting mitochondrial accumulation of Drp-1 will protect cardiomyocytes against IR injury and improve cardiac function [105, 106]. Conversely, Opa-1 is localized in the inner mitochondrial membrane and has a critical role in maintaining cristae structure [97, 616]. Damage from IR injury can induce Opa-1 proteolysis which impairs mitochondrial function, perturbs cristae structure, induces fragmentation, thereby increasing susceptibility of cell death [616, 619, 717]. Data generated from the current study support these reports where we observed a marked increase in mitochondrial Drp-1 expression and decrease in mitochondrial Opa-1 levels associated with impaired cardiac functional recovery in hearts subjected to IR injury. However, the perfusion of hearts with SA-26 significantly limited this response, which supports the notion of reduced mitochondrial injury. However, neither AA-4 nor AS-27 prevented the mitochondrial localization of Drp-1, which resulted in marked decreases of Opa-1 levels.

The relationship between SIRT3 and proteins regulating mitochondrial dynamics is well-documented in other disease models, where the SIRT3-dependent inhibition of fission is accompanied by the maintenance and activation of fusion. For example, in a cisplatin-induced acute kidney injury model, the reduction of SIRT3 mRNA and protein expression is associated with a marked mitochondrial accumulation of Drp-1, severe mitochondrial damage and severe injury than WT animals [731]. Hyperacetylated Opa-1 exhibits reduced activity correlating with

pathological hypertrophy observed in mouse hearts subjected to either angiotensin-II treatment or transverse aortic constriction. Enhanced activation or overexpression of SIRT3 protected these hearts by directly binding to and deacetylating Opa-1 thereby augmenting its GTPase activity [151]. Together, these studies suggest SIRT3 is a crucial regulator of mitochondrial integrity and is essential to maintain fitness of mitochondrial population under stress conditions.

Mounting evidence suggests that mitochondrial damage can trigger the activation of the NLRP3 inflammasome cascade which in turn aggravates mitochondrial dysfunction leading to a vicious cycle of continued injury and reduced cardiac function [259, 699]. The assembly of the NLRP3 inflammasome requires recruitment of NLRP3 protein to mitochondria in the perinuclear region resulting in dissipation of membrane potential, decreased oxidative phosphorylation and mitochondrial damage exacerbating cardiac damage [575, 719, 732]. Interestingly, Chen et al. demonstrated SIRT3 overexpression significantly diminished NLRP3 inflammasome activation induced by trimethylamine n-oxide (TMAO) in endothelial cells [700]. Additionally, Liu et al. showed SIRT3-deficient macrophages display impaired autophagy associated with accelerated NLRP3 inflammasome activation and endothelial dysfunction [733]. Our data support these findings where increased NLRP3 and cleaved caspase-1 protein levels were observed in the mitochondrial fractions of hearts subjected to IR injury. However, hearts perfused with the analogue SA-26 showed significantly lower levels of NLRP3 and cleaved caspase-1 as well as caspase 1 activity consistent with the maintained SIRT3 activity and improved cardiac functional recovery. Neither AS-27 nor AA-4 significantly inhibited the activation and translocation of either NLRP3 or mature caspase-1 to the mitochondria which matched the impaired SIRT3 activity and the compromised cardiac recovery observed in these hearts.

Considering the numerous promising and salutary biological actions of EDPs, one goal of this study was to provide proof of concept that more stable, synthetic analogs of DHA epoxides could mimic the biological actions of the natural CYP metabolites. We developed EDP analogues because of the limited stability and storage conditions of endogenous EDPs. Our results demonstrate the EDP surrogate SA-26 protects against myocardial IR injury by limiting NLRP3 inflammasome activation, while other structurally similar compounds, AS-27 and AA-4, did not provide sufficient protection. Although the precise molecular mechanisms remain unknown, we propose that SA-26 mediates its cardioprotection by preserving SIRT3 function. This study provides new perspectives for the development of pharmacological agents based on the EDP structure and suggest SA-26 is a strong lead scaffold for future development of a clinical drug candidate. Importantly, the increased stability of SA-26 may serve as a potential therapeutic agent in limiting mitochondrial damage and myocardial injury in response to IR injury. Future studies are still required to assess the bioavailability of these analogues, and to identify how changing the parent EDP chemical structure via altering the number and/or the position of the double bonds as well as the inclusion of different substituted groups will affect the stability and potency of the generated compounds.

Chapter 5

19,20-Epoxydocosapentaenoic Acid (19,20-EDP) Ameliorates Cardiac Ischemia-Reperfusion Injury by Directly Activating Mitochondrial Sirtuin 3

A manuscript based on this chapter is pending submission:

- **Ahmed M. Darwesh**, Tariq R. Altamimi, K. Lockhart Jamieson, Wesam Bassiouni, Hao Zhang, Marawan Ahmed, Matthew L. Edin, Darryl C. Zeldin, Khaled Barakat, Gavin Y. Oudit, Gary D. Lopaschuk, John M. Seubert. 19,20-Epoxydocosapentaenoic Acid (19,20-EDP) Ameliorates Cardiac Ischemia-Reperfusion Injury by Directly Activating Mitochondrial Sirtuin 3

Abstract

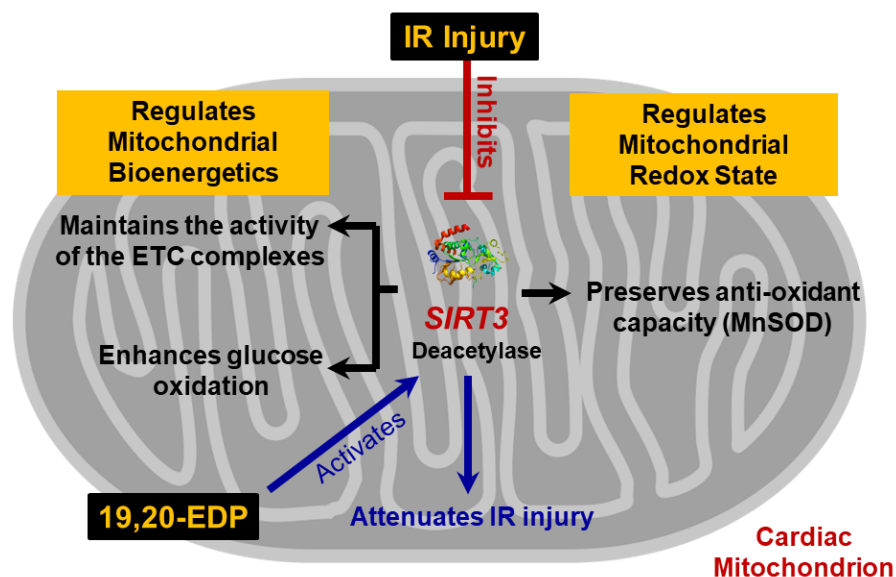
Background: Although acute reperfusion therapies following cardiac ischemic attacks have improved patient outcomes, mortality rates secondary to ischemia reperfusion (IR) injury remains high. Our recent data demonstrates that 19,20-epoxydocosapentaenoic acid (19,20-EDP), a cytochrome P450-derived epoxy metabolite of docosahexaenoic acid (DHA), attenuates cardiac IR injury; however, the mechanism remains elusive. Maintaining mitochondrial quality is essential to limit myocardial damage following IR injury. The mitochondrial deacetylase sirtuin 3 (SIRT3) plays a pivotal role in regulating mitochondrial function and cardiac energy metabolism. In the current study, we hypothesize that 19,20-EDP attenuates cardiac IR injury via stimulating mitochondrial SIRT3.

Methods: Langendorff and isolated working heart perfusions were performed in C57BL/6 mice to assess the effect of 19,20-EDP on cardiac function and energy metabolism secondary to IR injury. Mitochondrial SIRT3 downstream targets and mitochondrial respiration were assessed in human left ventricular (LV) tissues obtained from individuals with ischemic heart disease (IHD) collected through the Human Explanted Heart Program and compared to non-failing control hearts (NFC) collected from unused transplant donors through the Human Organ Procurement and Exchange Program at the University of Alberta. We also investigated the binding affinity of 19,20-EDP to human SIRT3 using molecular modeling and docking approaches.

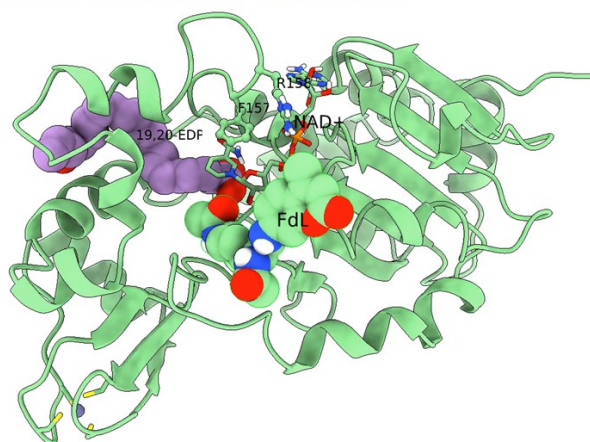
Results: Hearts perfused with 19,20-EDP demonstrated improved post-ischemic functional recovery, better glucose oxidation rate and enhanced cardiac efficiency compared to the control group. The cardioprotective effects were associated with enhanced mitochondrial SIRT3 activity and reduced global protein acetylation. Mitochondrial fractions obtained from the LVs of human myocardium with IHD showed decreased SIRT3 protein and increased acetylation of manganese

superoxide dismutase (MnSOD) suggesting decreased antioxidant capacity. Interestingly, treatment with 19,20-EDP markedly improved mitochondrial respiration and SIRT3 activity in cardiac fibers obtained from human LV with IHD. Moreover, an *in vitro* SIRT3 assay demonstrated that SIRT3, in the presence of 19,20-EDP, was able to deacetylate a specific substrate at much lower concentrations of nicotinamide adenine dinucleotide (NAD⁺). Moreover, the molecular modeling data demonstrated that 19,20-EDP binds to the human SIRT3 protein enhancing the NAD⁺-complex stabilization leading to improved SIRT3 de-acetylation activity. Importantly, the beneficial effects of 19,20-EDP were abolished using the SIRT3 inhibitors.

Conclusion: These data demonstrate that 19,20-EDP-mediated cardioprotective mechanisms against IR injury involve preservation and activation of mitochondrial SIRT3, which results in improved cardiac efficiency.



hSIRT3 complex with NAD⁺, 19,20-EDP and FdL dye molecule



Graphical abstract: (A) A schematic model illustrating the proposed mechanism of 19,20-EDP in ameliorating IR injury. SIRT3 activity is suppressed following IR injury resulting in hyperacetylation of several key mitochondrial proteins. This in turn contributes to impaired mitochondrial energy metabolism and function leading to cardiac dysfunction. The current study identifies SIRT3 as a potential target for the epoxy lipid 19,20-EDP and revealed that direct binding of 19,20-EDP to SIRT3 significantly enhances its enzymatic activity. 19,20-EDP, via directly activating SIRT3, attenuated IR injury through preventing mitochondrial damage and improving mitochondrial quality as evidenced by enhanced antioxidant capacity, limited oxidative injury, stimulated glucose oxidation, improved mitochondrial respiration, and increased ATP production. (B) Molecular docking result illustrating a model structure of the full reaction ready complex of hSIRT3 with bound allosteric modulator (19,20-EDP), cofactor (NAD⁺) and a model substrate (FdL).

5.1 Introduction

Ischemic heart disease (IHD) is the leading cause of cardiovascular morbidity and mortality worldwide [3, 629]. Early reperfusion or restoration of the blood flow to the ischemic myocardium is crucial and considered the primary and most effective intervention to reduce myocardial damage due to a prolonged ischemic insult [734]. However, reperfusion of the jeopardized myocardium can accelerate the damage of cardiomyocytes that were still viable at the end of the ischemic period contributing to up to 50% of the final infarct size and increasing the incidence of chronic heart failure (HF), a process termed as ischemia-reperfusion (IR) injury [13, 14, 19]. This explains why despite optimal myocardial reperfusion, the 1-year cardiovascular mortality in clinical trials of coronary reperfusion strategies still approximates 11% [28]. Therefore, adjunct cardioprotective interventions, in addition to reperfusion, are still needed.

Evidence indicates cardiac dysfunction resulting from IR injury can be linked to mitochondrial dysfunction, excessive oxidative stress and the activation of an inflammatory response [72, 689]. As mitochondria play a key role in mediating cellular homeostasis, mitochondrial dysfunction during IR injury induces an impaired energy supply resulting in heart dysfunction. Therefore, investigating novel targets and therapeutic strategies to restore and preserve mitochondrial integrity and function is essential for cardiomyocyte survival and to attenuate IR injury [690, 691, 735-738]. Sirtuins (SIRT1-SIRT7) are highly conserved nicotinamide adenine dinucleotide (NAD⁺)-dependent protein deacetylases that play an essential role in cell homeostasis as energy and redox sensors [141]. Of the SIRT family, SIRT3, SIRT4 and SIRT5 are present in mitochondria [142-145]. Among them, SIRT3 is the only one which exhibits robust deacetylase activity and is considered the primary mitochondrial deacetylase [142, 147]. In the heart, SIRT3 is indispensable for regulating mitochondrial homeostasis and

maintaining cardiac contractile function and therefore has been targeted therapeutically for modulating cardiovascular disease (CVD) [693-695]. Importantly, more than 60% of mitochondrial proteins are acetylated due to the high pH and the high concentration of acetyl-CoA [696, 739]. Protein acetylation in the mitochondria has mostly an inhibitory role, and consequently, an acetylated mitochondrial proteome would result in inhibition of mitochondrial metabolism and ATP synthesis. SIRT3 regulates mitochondrial function by deacetylating, and thereby activating, numerous mitochondrial proteins involved in energy metabolism [148], oxidative stress responses [149], and cellular respiration [152, 153]. Consistently, SIRT3 impairment negatively affects mitochondrial and contractile function in the heart [154]. For instance, it has been shown that SIRT3-knockout mice have 50% less ATP levels than their wild-type (WT) littermates and are prone to develop cardiac pathologies at an early age [155, 156]. Studies demonstrate that limiting the loss of SIRT3 following IR injury provides cardioprotective responses [158, 161-163]. In that sense, the development of new pharmacological compounds that target SIRT3 is essential for preserving normal mitochondrial function and can be considered a novel strategy in improving the prognosis of cardiac IR injury.

The long-chain n-3 polyunsaturated fatty acids (PUFA) are essential fatty acids obtained from dietary sources. Several basic, clinical and epidemiological studies demonstrate that n-3 PUFAs have a fundamental role in regulating cellular homeostasis and protection against CVD [327, 330]. Docosahexaenoic acid (DHA), an abundant n-3 PUFA found in mammalian tissues, can be metabolized by cytochromes P450 (CYP) to generate three-membered ethers known as epoxylipids [300, 330, 701]. There are six regioisomeric epoxylipids of DHA termed epoxydocosapentaenoic acids (4,5-, 7,8-, 10,11-, 13,14-, 16,17-, 19,20-EDP) [501]. There is growing evidence indicating that EDPs mediate many of the salutary effects of the parent

compound DHA [329, 330, 339]. Preservation of mitochondrial quality and function has been increasingly recognized as the main mechanism by which CYP-epoxy lipids maintain cardiomyocyte viability under stress conditions [339, 383, 570-572, 681, 702, 740]. Although a plethora of preclinical studies have tried to investigate how these CYP-derived epoxy lipids affect mitochondrial function within the cardiovascular system, the identity of the specific receptor or target involved remains unknown [330]. Accordingly, in the current study and building upon our previous data, we attempted to elucidate whether the mitochondrial SIRT3, the master regulator of mitochondrial functions, is involved in mediating the protective effects of 19,20-EDP against myocardial IR injury. In this study, we report that the epoxy lipid 19,20-EDP maintains mitochondrial quality, improves energy metabolism and reduces oxidative stress via directly activating SIRT3 improving the prognosis of cardiac IR injury. To the best of our knowledge, this is the first report to identify a molecular target for the CYP-derived epoxy lipid 19,20-EDP.

5.2 Methods

5.2.1 Isolated working heart perfusion

C57Bl/6 WT mice (2-3 months of age) of both sexes in equal proportions were anaesthetized using a 12 mg sodium pentobarbital intraperitoneal injection and their hearts were freshly excised and immersed in ice-cold Krebs–Henseleit bicarbonate (KHB) solution. Subsequently, the aorta was quickly cannulated and hearts perfused in the working heart mode as previously described [741] with minor modifications. Oxygenated KHB containing 1.2 mM palmitate bound to 3% fatty acid-free bovine serum albumin, 5 mM glucose, and insulin (100 mU/mL), was delivered to the left atrium at a preload pressure of 11.5 mmHg and ejected by the heart against an afterload pressure of 50 mmHg. Hearts were perfused aerobically for 30 min, followed by 20 min of global no-flow ischemia, and 40 min of reperfusion. The perfusate contained either vehicle or 19,20-EDP (1 μ M) added 10 min before ischemia and was present in the heart throughout the reperfusion period.

Heart rate and aortic pressure (mmHg) were measured with a pressure transducer (Harvard Apparatus) connected to the aortic outflow line. Cardiac output and aortic flow (mL/min) were measured with T206 flow probes (Transonic Systems, Inc) in the preload and afterload lines, respectively. Coronary flow (mL/min) was calculated as the difference between the cardiac output and the aortic flow. Cardiac work was calculated as the product of cardiac output and peak systolic pressure (minus the preload pressure). Cardiac function data were collected through an MP100 system from AcqKnowledge (BIOPAC Systems, Inc., USA). Glucose, and palmitate oxidation rates were measured by perfusing hearts with radiolabeled [14 C] glucose and [$^{9,10-3}$ H] palmitate and measuring 14 CO₂ and 3 H₂O production, respectively, as previously described [741, 742]. Efficiency was assessed by normalizing cardiac work for total acetyl-CoA production rates as

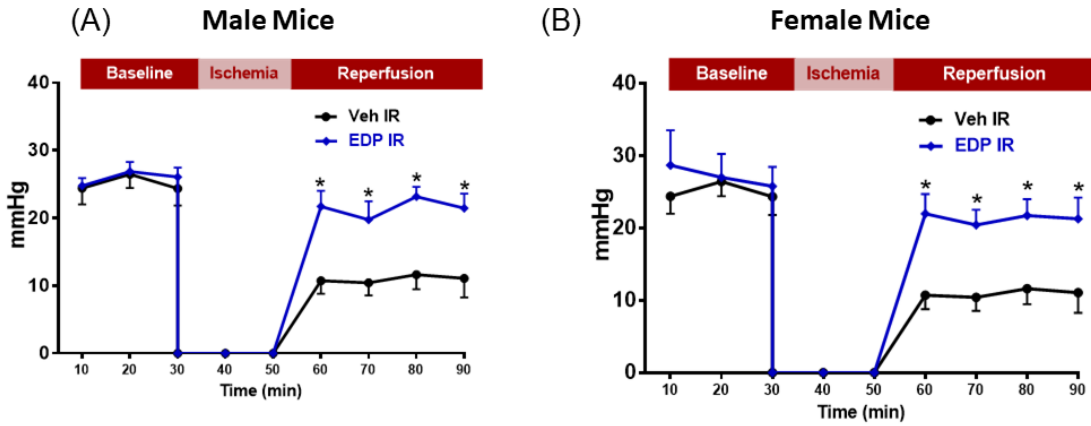
calculated from glucose and palmitate oxidation rates. At the end of reperfusion, hearts were freeze-clamped in liquid nitrogen using Wollenberger tongs and stored at -80°C for further biochemical analysis.

5.2.2 Isolated Langendorff mouse heart perfusion

C57Bl/6 WT mice (2-3 months of age) of both sexes in equal proportions were anesthetized by an intraperitoneal injection of sodium pentobarbital (Euthanyl, 100 mg/kg). Following complete non-responsiveness to external stimulation, hearts were quickly excised and perfused in the Langendorff mode with Krebs-Henseleit buffer containing (in mM) 120 NaCl, 25 NaHCO₃, 10 Dextrose, 1.75 CaCl₂, 1.2 MgSO₄, 1.2 KH₂PO₄, 4.7 KCL, 2 Sodium Pyruvate (pH 7.4) and bubbled with 95% O₂ and 5% CO₂ at 37 °C [162, 702]. The left atrium was then excised, and a water-filled balloon made of saran plastic wrap was inserted into the left ventricle through the mitral valve. The balloon was connected to a pressure transducer for continuous measurement of LVDP and heart rate (HR). Hearts with persistent arrhythmias or LVDP less than 80 cm H₂O were excluded from the experiment. Mouse hearts were perfused in the retrograde mode at a constant flow rate for 20 min of baseline (stabilization) and then with either vehicle, 19,20-EDP (1 μM) [383] with or without either of the SIRT3 inhibitors nicotinamide (NAM, 30 μM) [743, 744] or 3-(1H-1,2,3-triazol-4-yl) pyridine (3-TYP, 50 nM) [745] for 20 min of baseline and subjected to 30 min of global no flow ischemia followed by 40 min of reperfusion. The percentage of left ventricular developed pressure (%LVDP) at 40 min of reperfusion (R40), as compared to baseline LVDP, was taken as a marker for recovery of contractile function. After 40 min of reperfusion, hearts were immediately frozen and stored below -80°C . Haemodynamic parameters were acquired and analyzed using ADI software from (Holliston, MA, USA). Collection of the heart effluent was taken during both pre- and postischemic protocols to determine of coronary flow (CF) rates.

Importantly, 19,20-EDP similarly improved post-ischemic functional recovery, almost equally, in both males and females (Figure 5.1) and as such data from both sexes were combined.

Isolated working heart: Developed pressure



Langendorff perfusion: Left ventricular developed pressure (LVDP)

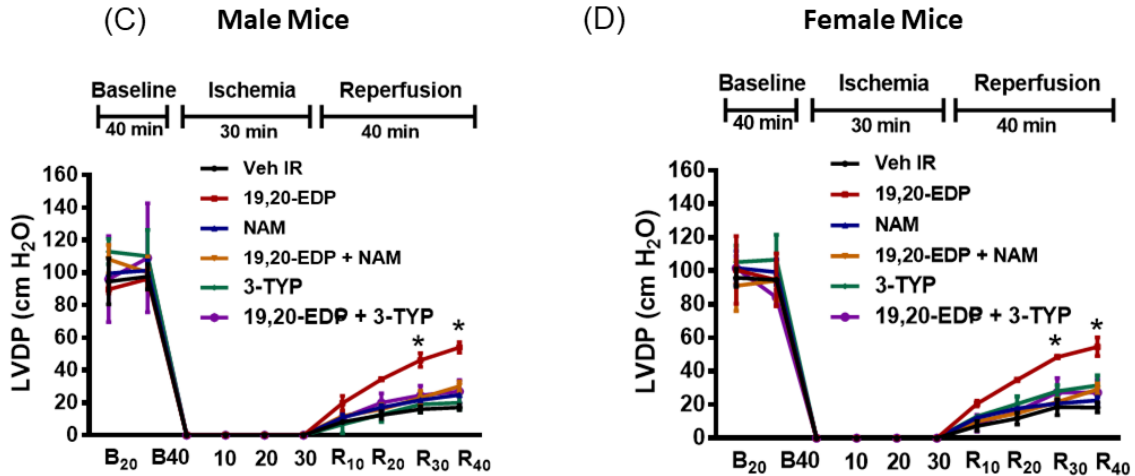


Figure 5. 1: Assessment of the sex effect on post-ischemic functional recovery. Assessment of developed pressure obtained from the isolated working heart experiment at the baseline, during ischemia, and at 10, 20, 30 and 40 min reperfusion (R10, R20, R30, and R40) in (A) male mice and (B) female mice. Assessment of left ventricular developed pressure (LVDP) obtained from Langendorff experiment at the baseline, during ischemia, and at 10, 20, 30 and 40 min reperfusion (R10, R20, R30, and R40) in (C) male mice and (D) female mice. Values represent mean \pm SEM; The significance of differences was determined by the use of a two-way ANOVA followed by a Tukey post hoc analysis; * $p < 0.05$ vs. Vehicle IR.

5.2.3 Analysis of inflammatory cytokines and chemokines in the perfused heart homogenates

Frozen mouse hearts obtained from the Langendorff experiment were ground with mortar and pestle on dry ice and then homogenized in ice-cold homogenization buffer (20 mmol/L Tris-HCL, 50 mmol/L NaCl, 50 mmol/L NaF, 5 mmol/L sodium pyrophosphate, 1 mmol/L EDTA, and 250 mmol/L sucrose added on the day of the experiment, pH 7.0). Samples were then centrifuged at 800× g for 10 min at 4 °C to separate the cellular debris. Afterwards, inflammatory cytokines and chemokines were measured in heart homogenates by analytical services at Eve Technologies (Calgary, Alberta, Canada).

5.2.4 Human explanted heart tissue

Human heart tissues were acquired under protocols approved by the Health Research Ethics Board of the University of Alberta. Prior to transplantation or donation, all participants or next of kin have given informed consent. Adult non-failing control (NFC) heart tissues (Left ventricular ejection fraction (LVEF) \geq 60%) were collected from donors with no cardiovascular history when transplants were unsuitable due to medical or technical issues, as part of the Human Organ Procurement and Exchange (HOPE) at the University of Alberta. Ischemic heart samples were obtained from patients with end-stage heart failure secondary to ischemic cardiomyopathy (ICM) as part of the Human Explanted Heart Program (HELP) at the University of Alberta. Collections were performed in the operating room during cardiac transplantations at the Mazankowski Alberta Heart Institute (MAHI). All myocardium samples were excised from the left ventricular free wall avoiding epicardial adipose tissue within 5-10 minutes of its excision following cold cardioplegia. Three samples from each ICM heart were obtained from the non-infarct (remote region, viable tissue), peri-infarct (border region containing viable and non-viable

tissue) and infarct (direct injury) regions. The biopsy samples were then cut into several pieces in ice-cold mitochondria preserving isolation buffer (in mmol/L: 2.77 Ca-K₂EGTA, 7.23 K₂EGTA, 3 K₂HPO₄, 9.5 MgCl₂, 5.7 Na₂ATP, 15 phosphocreatine, 20 imidazole, 20 taurine, 0.5 dithiothreitol, and 49 K-methanesulfonate, 1 μM leupeptin, pH 7.1, at 0°C) and distributed into three parts. One part that was immediately transferred to the laboratory within 15 min in the isolation buffer and used for mitochondrial respiration measurements. The second fresh part was incubated in the isolation buffer containing the vehicle, 19,20-EDP (1 μM), NAM (30 μM) or 19,20-EDP (1 μM) + NAM (30 μM) on ice for 2 h for the assessment of SIRT3 activity. The third part was immediately flash-frozen in liquid nitrogen and stored in ultra-low (-80°C) freezers for later analyses.

5.2.5 Mass spectroscopy (LC-MS/MS)

NFC and ischemic human heart tissues were ground using mortar and pestle on dry ice pre-cooled with liquid nitrogen and stored at – 80°C until processing. LC-MS/MS methods were used to quantify 19,20-EDP levels in NFC, non-infarct, peri-infarct and infarct tissues as previously described [644, 746].

5.2.6 Assessment of mitochondrial respiration in the dissected human myocardial fibers

At the end of the heart transplantation procedure, fresh cardiac fibers were dissected out from both the non- and peri-infarct regions of the ischemic heart and from the NFC and promptly placed into ice-cold isolation buffer as previously described. Briefly, after removing the fats and vessels, the fresh myocardial biopsy was finely dissected into pieces and teased using forceps to separate fibers (1 mm wide and 3–4 mm long) under a dissecting microscope in ice-cold isolation buffer. The fibers were then permeabilized at 4°C in isolation buffer containing 50 μg/mL saponin

for 30 min, washed three times for 5 min each in ice-cold respiration buffer (0.5 mM EGTA, 3 mM MgCl₂.6H₂O, 20 mM taurine, 10 mM KH₂PO₄, 20 mM HEPES, 1 g liter⁻¹ BSA, 60 mM potassium-lactobionate, 110 mM mannitol, 0.3 mM dithiothreitol) and immediately added to the respiration chamber at 30°C containing 1.8 mL respiration buffer [585]. The fibers were then treated with either the vehicle, 19,20-EDP (1 μM), NAM (30 μM) or 19,20-EDP + NAM before starting the experiment.

Clark electrode connected to an Oxygraph Plus recorder (Hansatech Instruments Ltd., Norfolk, England) was used to measure mitochondrial oxygen consumption in the saponin-permeabilized human explanted cardiac fiber using a stepwise protocol to evaluate various components of the electron transport system in non and peri-infarct regions as well as NFC fibers. Respiratory parameters and indices were calculated as described by previous authors [747-750]. First, standard protocols were followed for calibration of the electrode in the respiration chamber, with a saturated oxygen concentration and equipped with magnetic stirring. The following parameters were measured to assess the functional state of mitochondrial electron transport chain (ETC) [751]. (a) State 4 respiration, defined as basal respiration, was assessed in presence of 10 mM glutamate + 5 mM malate (b) State 3 respiration, defined as maximal adenosine diphosphate (ADP)-stimulated respiration, was measured after the addition of 2 mM ADP that resembles the basal respiration of the tissue at saturating concentrations of substrates and ADP [752] (c) Oligomycin-resistant respiration, also known as ATP-independent respiration, oxygen consumption rate was measured after inhibiting ATP synthase with oligomycin (2 μM). This occurs as a result of proton leak or transport of charged molecules across the inner mitochondrial membrane. (d) Maximum respiratory rate: obtained after dissipation of the proton gradient after uncoupling oxidative phosphorylation by the uncoupler, carbonyl cyanide

pttrifluoromethoxyphenylhydrazone (FCCP, 4 μ M). This depends on the activity of the electron transport complexes and the quantity of mitochondria in the tissue. This also may be associated with oxidation reactions mediated by reactive oxygen species (ROS) or oxidases. (e) Spare respiratory capacity was calculated as the difference between the maximum respiratory rate and state 3 respiration. This parameter represents the ability of the ETC to respond to a rise in energy demands and/or to resist an insult [748]. (f) The respiratory control ratio (RCR) was calculated as the ratio between state 3 and state 4 respiration rates to estimate mitochondrial respiration efficiency. A high ratio represents strong coupling between ATP synthesis and electron transport. Similar information can be obtained by calculating (g) the coupling efficiency ratio which is the difference between ADP-stimulated respiration and oligomycin resistant respiration divided by ADP stimulated respiration [748]. Oxygen flux rates were normalized per milligram of tissue dry weight and mitochondrial respiration rate is expressed in nmol O₂/minute/mg of tissue.

Samples from respiration buffer were collected at the end of state 3 respiration and the level of ATP in the respiration buffer was measured using the fluorometric assay kit (ab83355, Abcam Inc, Toronto, ON, Canada). Results were expressed as nmol of ATP per minute per mg of dry weight. ATP/O ratio was calculated as ATP/state 3 respiration.

5.2.7 Assessment of rate of oxygen consumption in mice cardiac muscle fibers in the presence of different energy substrates

The effect of acute *in vitro* exposure of cardiac mitochondria to 19,20-EDP and NAM on glucose and fatty acid oxidation was also determined using permeabilized mice cardiac fibers. For this purpose, fresh cardiac fibers were isolated from the left ventricles of mice hearts under a dissecting microscope in ice-cold isolation buffer as previously described. Fresh fibers were then permeabilized in isolation buffer containing 50 μ g/mL saponin, washed three times for 5 min in

ice-cold respiration buffer and immediately added to the respiration chamber containing 1.8 mL respiration buffer containing either the vehicle, 19,20-EDP (1 μ M), NAM (30 Mm) or 19,20-EDP + NAM at same concentrations. Clark electrode connected to an Oxygraph Plus recorder (Hansatech Instruments Ltd., Norfolk, England) was also used to measure mitochondrial oxygen consumption in permeabilized mice cardiac fibers.

Fatty acid oxidation was assessed using palmitoyl carnitine as a substrate (40 μ M) in the presence of 5mM malate (M + PC) and carbohydrate oxidation was assessed by providing mitochondria with pyruvate (10 mM) and malate (5 mM) (M + Py). Tissue oxygen consumption was recorded at 30 °C in the presence of substrates only (state 4) and following the addition of saturating amounts of ADP (2 mM; state 3) and then the uncoupler FCCP (4 μ M). Mitochondrial respiratory control ratio (RCR), which is an indicator of coupling between phosphorylation and oxygen consumption, was calculated for each metabolic substrate as a proportion of state 3/state 4 respiration to estimate mitochondrial respiration efficiency.

5.2.8 Isolation and cultivation of neonatal rat cardiomyocytes

Primary cultures of cardiac myocytes were prepared from neonatal rat hearts. Briefly, hearts from 2–3-day-old neonatal rat pups (Sprague-Dawley rats, both sexes) were isolated and placed in ice-cold 1X phosphate-buffered saline solution (PBS). After repeated rinsing, the atria were removed, and the ventricles were minced with scissors. The minced tissue was washed three times in ice-cold PBS solution and then placed in a T25 tissue culture flask containing ice-cold 1X PBS, DNase (0.025% w/v), collagenase (0.10% w/v), and trypsin (0.05% w/v). The tissue was digested on rotary shaker at 37 °C for 20 min, then transferred to a 50-mL tube containing 20 mL DMEM/F12 media supplemented with 20% fetal bovine serum (FBS), and 50 μ g/ml gentamicin.

Tissues were centrifuged at $114 \times g$ for 1 min at 4 °C and the supernatant was discarded. Digestions were repeated two more times, collecting supernatant fractions. After the final digestion, digested tissue and supernatant fractions were pooled and centrifuged at $300 \times g$ for 7 min at 4 °C. The resulting pellet was resuspended in 10-20 ml of plating media (DMEM/F12 media supplemented with 10% horse serum, 5% FBS, 50 µg/ml gentamicin and 100 U/mL penicillin/streptomycin) and passed through a 70 µm nylon mesh strainer. Cells were plated on laminin coated dishes (Sigma-Aldrich, Oakville, ON, Canada) and cardiomyocytes cultures were used for experiments after 48h of plating.

5.2.9 Microscopy experiments

Neonatal rat cardiomyocytes (NRCMs) were plated in the plating media in 6-well glass bottom plate suitable for fluorescent microscopy (MatTek, Ashland, MA, USA). NRCMs were placed in a computer-controlled humidified hypoxic chamber (0.9% O₂, 5%CO₂, and 94% N₂) for 24 h followed by reoxygenation under normal (normoxic) conditions for 6 h. Deoxygenated medium was used in all hypoxic experiments. The control cells were exposed to 30 h of normoxia. NRCMs were treated with either the vehicle, 19,20-EDP (1 µM), NAM (30 µM) or 19,20-EDP + NAM at same concentrations before hypoxia and present throughout the experiment. In all experiments, the NRCMs were imaged by Zeiss Axio Observer Z1 inverted epifluorescence microscope using Zeiss Zen software with 63x oil objective lens and maintained at 37°C.

5.2.9.1 Mitochondrial density and morphology

For the assessment of mitochondrial density and morphology, NRCMs were incubated with the Mitotracker Green dye (250 nM, Life technologies, product #M-7514) and the nuclear stain Hoechst dye (1 µM, Life technologies, product #H3570) for 30 min before running the microscopy

experiment. For each treated group, 5 fields of cells were randomly selected to delineate the shape of mitochondria.

5.2.9.2 Mitochondrial membrane potential

Mitochondrial membrane potential was determined by staining the cells with the mitochondrial TMRE (tetramethylrhodamine, ethyl ester) dye (100 nM, Sigma, product #87917) and the nuclear stain Hoechst dye (1 μ M) for 30 min before running the microscopy experiment. For each treated group, 5 fields of cells were randomly selected to address the changes in mitochondrial potential.

5.2.9.3 Mitochondrial superoxide levels

Mitochondrial ROS production was assessed in NRCM after being subjected to 24hr hypoxia. Cardiomyocytes were incubated with both the nuclear stain (Hoechst 33342, 1 μ M) and the specific mitochondrial superoxide indicator MitoSOX Red stain (1 μ M, ThermoFischer, product #M36008) for 10-15 min at the beginning of reoxygenation and imaged at 30 min of reoxygenation using a Zeiss Axio Observer Z1 inverted epifluorescence microscope with 63x oil objective lens and maintained at 37°C throughout the experiment.

5.2.10 Immunoblotting

Frozen mouse and human hearts were ground, homogenized and then fractionated into mitochondrial and cytosolic fractions as previously described [702]. Briefly, frozen cardiac tissues were ground with mortar and pestle on dry ice and then homogenized in ice-cold homogenization buffer (20 mmol/L Tris-HCL, 50 mmol/L NaCl, 50 mmol/L NaF, 5 mmol/L sodium pyrophosphate, 1 mmol/L EDTA, and 250 mmol/L sucrose added on the day of the experiment,

pH 7.0). Samples were first centrifuged at 800× g for 10 min at 4 °C to separate the cellular debris. The collected supernatant was then centrifuged at 10,000× g for 20 min. The pellet was resuspended in homogenization buffer to obtain a mitochondrial-enriched fraction. The supernatant was ultra-centrifuged at 105,000× g for 60 min and the subsequent supernatant was used as the cytosolic fraction. Protein concentrations in both cytosolic and mitochondrial fractions were measured by the Bradford assay. Western blotting was carried out as previously described [702]. Protein (30–50 µg) was resolved by electrophoresis on (10–15%) SDS-polyacrylamide gels and transferred onto polyvinylidene difluoride (PVDF) membranes (BioRad Laboratories, Hercules, CA, USA). Immunoblots were probed with antibodies against citrate synthase (CS, ab129095), total manganese superoxide dismutase (MnSOD, ab13533), acetyl-MnSOD (acetyl K68, ab137037), VDAC (ab14734) (Abcam, Burlingame, CA, USA), acetyl-MnSOD (acetyl K122, PA5105107, Life Technologies), succinate dehydrogenase subunit A (SDH-A, 5839), Cytochrome c oxidase subunit 4 (COX IV, 11967), SIRT3 (5490) (Cell Signaling Technology, Inc., MA, USA). After washing, membranes were incubated with the corresponding secondary antibodies. The blots were visualized with ECL or ECL prime reagent. Relative band intensities were expressed as fold of the control assessed using Image J software (NIH, USA).

5.2.11 Enzymatic assays

SIRT3 activity was assessed in the isolated mitochondrial fractions using a SIRT3 fluorescent assay kit (50088, BPS Bioscience, San Diego, CA, United States), according to the manufacturer's instructions. In this assay, heart mitochondrial fractions were mixed with the specific histone deacetylase (HDAC) fluorogenic substrate, bovine serum albumin, NAD⁺ and assay buffer. The deacetylation process induced by SIRT3 in the sample sensitizes the HDAC substrate so that subsequent treatment with the SIRT3 assay developer produces a fluorescence

product that was measured using a fluorescence plate reader at 350/460 nm excitation/emission wavelengths.

In another set of experiments, isolated fibers from NFC, non- and peri- infarct regions of human ischemic hearts were incubated in isolation buffer with either the vehicle, 19,20-EDP (1 μ M), NAM (30 μ M) or 19,20-EDP + NAM at same concentrations for 2 h on ice. Afterwards, tissues were minced by using scissors and homogenized to isolate mitochondrial fractions. SIRT3 activity was assessed in mitochondrial fractions using the same previously mentioned assay.

5.2.12 Molecular modeling and docking approaches

5.2.12.1 Protein and ligand preparation

The atomic coordinates of all deposited hSIRT3 crystal structures (31 crystal structures) were downloaded from the protein data bank. Structures were prepared using the protein preparation wizard in Maestro, the Schrodinger suite [753]. The protein preparation step included the addition of missing residues, missing heavy atoms and hydrogen atoms. The ionization states of the titratable residues were predicted using Propka at pH 8.0. At this pH, all histidine residues were protonated at the epsilon and the delta nitrogens (charge +1). However, the epsilon protonated form (HIE) of binding site Histidine (HIS248, according to the hSIRT3 numbering scheme) was adopted. Binding site histidine has been shown to serve as a proton carrier during the de-acetylation reaction in other Sirtuins [754]. Another histidine (HIS95) was shown to coordinate a Na^{+1} ion at the C-pocket and was modelled as HID (delta nitrogen protonated). The propka predicted protonation states of all other residues were preserved for the rest of the computational structural analysis, including the molecular dynamics simulations as well as the binding free energy calculations. Finally, constrained minimization was performed using the OPLS3 [755] force field to a maximum heavy atoms displacement of 0.3 Å.

As we will discuss in the following sections, three ligand molecules were used for the docking simulations. These are the 19,20-EDP, NAD⁺, and FdL substrate. The chemical structures of these molecules are given in Figure 5.16A. The chemical structure of 19,20-EDP was downloaded from the PubChem database as an sdf file and prepared using the ligprep module, the Schrodinger suite [756]. 19,20-EDP preparation includes adding missing hydrogens, optimizing initial ligand geometries and assigning a de-protonated carboxylate protonation state. The chemical structures of FdL (without the long peptide chain) and NAD⁺ were extracted from the prepared 5H4D crystal structure, which represents a hSIRT3 structure co-crystallized with NAD⁺, FdL substrate and a hSIRT3 activator (amiodarone).

5.2.12.2 Principal component analysis

Individual chains of selected structures for structural analysis were saved as PDB files upon completing the necessary the structure preparation. All hetero residues (bound ligands/co-factors/co-substrates, ions, water molecules) were removed. Principal component analysis was conducted using the BIO3D structural bio-informatics library in R studio [757]. The analysis started by superposing all protein C α atoms through RMS fitting.

5.2.12.3 Molecular docking simulations

For the purpose of the molecular docking simulations, the 4BN4 crystal structure [758] was selected for two reasons. First, the structure represents a nearly active reaction complex containing a NAD⁺ analogue (AR6, Adenosine-5-Diphosphoribose) and an empty cavity for the acetylated peptide co-substrate. Second, our principal component analysis (PCA) identified a prominent shift of the α 3 helix as one of the major conformational changes observed in few hSIRT3 crystal structures. In particular, this helical shift opens a hydrophobic pocket adjacent to

the NAD⁺ binding site. In addition to being completely open, this pocket is occupied by OP2 (17-hydroxy-3,6,9,12,15-pentaoxaheptadecan-1-oic acid, Figure 5.16A) in the 4BN4 crystal structure. The linear structure of the OP2 carboxylic acid (Figure 5.16A) suggests that linear chain fatty acids, such as 19,20-EDP (Figure 5.16A) are good candidates to bind the same site. Besides being not-interfering with acetylated peptide substrate binding site, the proximity of this site from the reaction complex binding site (NAD⁺ & acetylated peptide substrate) suggests a role of this site to trigger hSIRT3 activation and/or reaction complex stabilization, allosterically. It is noteworthy to mention that the designated pocket partially overlaps with a binding pocket that was previously shown to bind 4'-bromo-resveratrol, a potent hSIRT3 inhibitor (PDB ID: 4C7B) [759]. Moreover, as has been previously shown in a study by Gai et al., this pocket, enclosed by the helices by the α_3 , α_4 , α_6 -helices, and α_2 - α_3 loop, opens upon complex formation of Sirtuins with certain long-chain acyl lysine substrates that reach the proximity of the C-pocket [760].

Our docking simulations were conducted in three consecutive steps including six molecular entities; these steps are i) docking 19,20-EDP to the apo 4BN4 crystal structure, (ii) take the output of step 1 and use as a receptor for docking NAD⁺, and finally (iii) take the relaxed structural complexes from step 2 and use it as a receptor to dock the FdL dye (with the accompanying peptide chain removed) as a representative for acetylated peptide hSIRT3 substrates. In the following paragraph, we will give a detailed overview of each docking step.

First, using rigid receptor flexible ligand docking in Glide [761] and Smina [762], the structure of 19,20-EDP was docked to the 4BN4 crystal structure at the OP2 binding site. In this run, the OP2 molecule was removed while the AR6 structure (a NAD⁺ analogue) was kept as is. The standard precision glide-docking module was used (Glide SP). The docking box was centered on the OP2 binding site with a box size of 15 Å across the XYZ dimension. To gauge the robustness

of the adopted docking protocol, we initially tried to re-dock the OP2 molecule to its own binding site to see if the selected protocol can reproduce the co-crystallized OP2 bound conformation. The co-crystallized pose of OP2 exhibited a characteristic binding mode where the carboxylate group is buried within a slightly hydrophilic region of the hSIRT3 structure (residues: SER149, ASN229, ASP231 and GLU234) and is bridged to the surrounding residues by the aid of a conserved water molecule. Interestingly, neither Glide (XP or SP) nor Smina were able to reproduce the experimentally observed binding mode without including this water molecule as part of the receptor during the docking simulation. All poses were found to be flipped by 180° from the co-crystallized pose such that the carboxylate group are pointing outside the binding cavity, i.e. solvent exposed. After including the water molecule, Glide was able to regenerate the observed binding mode within an RMSD ~ 0.5 Å from the OP2 co-crystallized pose. In our 19,20-EDP docking, this water molecule was kept during the necessary grid generation step. With the exception of the expanded sampling criteria for docking setup, all other docking parameters were left to the default values. Only the top docked complex was saved from this run for further analysis.

Second, the saved docked complex produced from the first docking simulation was used as an input receptor for NAD⁺ docking. To account for the large molecular size of NAD⁺ that requires certain degree of receptor flexibility, the induced fit docking module of Schrodinger (IFD module) was used [763, 764]. In general, the IFD module of Schrodinger takes place at three steps, first; rigid receptor docking with a reduced atomic vdW radii scaling as a workaround to account for protein flexibility. This is followed by side chain reorganization in Prime and finally a re-docking step. For the first docking step in IFD, the standard precision docking module of Glide (Glide SP) was used, for the second step, we used the Glide extra precision docking [765]. The top 9 poses generated from the IFD docking were saved and thoroughly analyzed to select the most

probable model of the NAD⁺/19,20-EDP/hSIRT3 complex structure. For reasons that will become clear later, we focused our analysis to a single complex (complex #2, according to the generated IFD score) where the nicotinamide motif of NAD⁺ is twisted around the glycosidic bond to occupy the canonical C pocket (see below). This NAD⁺ conformation is known as the “productive” NAD⁺ conformation. In the remaining complexes, NAD⁺ adopts an extended conformation where the nicotinamide motif occupies the acetyl-LYS peptide substrate-binding site. This NAD⁺ conformation is usually designated as the “non-productive” NAD⁺ conformation [744, 766].

For the last docking simulation, 10 representative PDB frames from the MD simulations of the selected model (complex #2) for NAD⁺/19,20-EDP/hSIRT3 complex were evenly sampled across the 100 ns production MD trajectory, and used as inputs for the last docking simulation, that is docking a model acetylated peptide substrate (FdL) to the NAD⁺/19,20-EDP/hSIRT3 complex in an ensemble based docking fashion. The standard precision module of glide (Glide SP) was used with enhanced search parameters. A representative pose where the acetyl-LYS motif of FdL occupies the known substrate-binding site was saved for further structural analysis.

5.2.12.4 Molecular Dynamics Simulation and Binding Free Energy Calculation: setup, running & analysis

MD simulations for the modelled complexes were performed using the program AMBER18 [767, 768]. All simulation input files were generated using the tleap utility in AMBER18. In total, we have conducted 19 MD simulations for approximately 100 ns each. Of these simulations, 9 simulations were performed for the NAD⁺/19,20-EDP/hSIRT3 complexes generated from the induced fit docking, and 9 for the same IFD generated complexes but with the 19,20-EDP structure being removed, i.e. NAD⁺/hSIRT3 complexes. The last simulation was performed for the full reaction complex, i.e. FdL/NAD⁺/19,20-EDP/hSIRT3.

The three-dimensional (3D) structures of each complex were immersed in a cubic box of TIP3P water molecules with a minimum distance of 12 Å between any atom and box boundaries, and neutralized by counter-ions. Bonded and non-bonded parameters of the protein residues were assigned with the AMBER ff14SB force field [769] using tleap. The parameters for the OP2 and the FdL molecules were determined with the General AMBER Force Field (GAFF). Atomic partial charges were assigned through the restrained electrostatic potential method (RESP) using the AM1 output generated by antechamber [770-772]. NAD⁺ parameters were extracted from the AMBER library without modifications. Four ZN⁺² coordinating cysteine residues (CYS141, CYS144, CYS165 and CYS168) were modelled as CYM residues, i.e. de-protonated cysteine.

Each solvated system was energy-minimized, heated and equilibrated according to a standard multi-stage protocol. For the minimization phase, 4 consecutive stages of minimization of 4000 steepest decent minimization cycles followed by 1000 cycles of conjugate gradient minimization cycles each were performed. In the first minimization stage, a 100 kcal/mol/Å² positional restraints were applied on the protein and ligand/co-factors heavy atoms using harmonic potential. In the next two minimization stages, positional restraints of 50 kcal/mol/Å², 5 kcal/mol/Å² were applied for the second and third minimization, respectively. Final minimization was conducted for the entire system without restraints. Subsequently, each system was gradually heated to 300K over 50 ps and the dynamics time step was set to 1 fs. Heating stage was conducted in the NVT ensemble (constant number of particles, constant volume and constant temperature). NPT (constant number of particles, constant pressure and constant temperature) equilibration was performed in three consecutive steps. In the first equilibration, each system was simulated for 50,000 steps of 1 fs time steps, to give a total of 50 ps, and with positional restraints of 1 kcal/mol/Å² applied on protein and ligands/co-factors/substrate heavy atoms. In the second

equilibration, each system was simulated for 50,000 steps of 2 fs time steps, to give a total of 100 ps, and with positional restraints of 0.1 kcal/mol/Å² applied on protein and ligands/co-factors/substrate heavy atoms. Final NPT equilibration was performed for 5,000,000 steps using 2fs integration time steps, i.e. total equilibration time of 10 ns, without restraints.

Production MD simulations were performed under the NPT ensemble. Production trajectories were performed in 5 chunks of 20 ns each with random velocity initiation to improve the statistical sampling, giving total simulation trajectories of 100 ns for each system. In all MD runs, the temperature was maintained at 300 K using the langevin thermostat in AMBER (ntt=3) [773]. Long-range electrostatic interactions were estimated through the particle mesh Ewald (PME) summation method [774], and with a cut-off of 9 Å for non-bonded interactions. An atmospheric pressure of 1 bar was maintained through the Berendsen barostat in NPT equilibration and production simulations. All MD simulations were performed using the GPU-accelerated MD code, pmemd.cuda in AMBER18 [775]. Unless otherwise specified, analyses of the generated MD trajectories were performed using the CPPTRAJ [776] utility in AMBER18.

End-point binding free energies of NAD⁺ in the 19,20-EDP-included & 19,20-EDP-deleted complexes were calculated through the standard AMBER/molecular mechanics generalized Born surface area (MM-GBSA) protocol using the generated MD trajectories. The AMBER/MM-GBSA protocol has been successfully applied in several biomolecular interaction studies, including protein–ligand binding [777-780], protein–protein interaction studies [781, 782]. We have included the closest 20 water molecules from NAD⁺ molecule as part of the receptor atoms, instead of the default settings where the MD trajectories are completely desolvated. Approximately 6250 frames were evenly sampled from each 100 ns MD trajectory and used for the calculation. For more details about the protocol, readers are encouraged to consult recent reviews [777, 783].

5.2.13 Assessment of sirtuin 3 reaction kinetics in the presence and absence of 19,20-EDP

To explore whether SIRT3 activity is enhanced after binding to 19,20-EDP, we tested affinity of SIRT3 for NAD^+ in the presence and absence of 19,20-EDP and used Michaelis Menten equation to calculate V_{\max} , k_{cat} , K_{mNAD^+} and the catalytic efficiency of SIRT3 ($k_{\text{cat}}/k_{\text{m}}$ ratio). In this experiment, SIRT3 recombinant enzyme was incubated with acetylated HDAC fluorogenic substrate with decreasing concentration of NAD^+ in the presence or absence of 19,20-EDP or the analogue OP2. The fluorescence intensity of the produced deacetylated HDAC fluorogenic substrate was measured at Ex/Em (350/460 nm). Reactions without NAD^+ served as negative controls (Figure 5.17A).

5.2.14 Statistics

Values are expressed as mean \pm standard error of mean (SEM). Statistical significance was determined by the use of an unpaired, two-tailed Student's t-test, one-way analysis of variance (ANOVA) or two-way ANOVA with a Tukey post hoc test to assess differences between groups; $p < 0.05$ was considered statistically significant.

5.3 Results

5.3.1 19,20-EDP enhanced glucose oxidation and attenuated myocardial ischemia-reperfusion injury in isolated mouse working heart

To investigate the cardioprotective actions of 19,20-EDP in a physiologically relevant model, we utilized the isolated working heart system and monitored pre- and post-ischemic cardiac function. Hearts perfused aerobically for 90-min with either the vehicle or 19,20-EDP showed comparable heart function (Figure 5.2A-H). Moreover, baseline heart function in both vehicle and 19,20-EDP perfused hearts subjected to IR insult was comparable. However, perfusion of the mouse heart with 19,20-EDP, added 10 min before ischemia, resulted in a better recovery of cardiac function in isolated working hearts subjected to 20 min of global ischemia and 40 min reperfusion. The enhanced functional recovery was evident as a significantly higher cardiac output, cardiac work, developed pressure, peak systolic pressure (PSP), rate pressure product and similar heart rate, compared with vehicle controls (Figure 5.3A-F, Figure 5.4A-F). This improvement in cardiac function resulted in an increase in both coronary and aortic flow (Figure 5.3 G and H, Figure 5.4 G and H). Importantly, the coronary flow was comparable during the aerobic and baseline perfusion, indicating that an increase in myocardial oxygenation or flow before the ischemic insult was not responsible for the improved function during reperfusion.

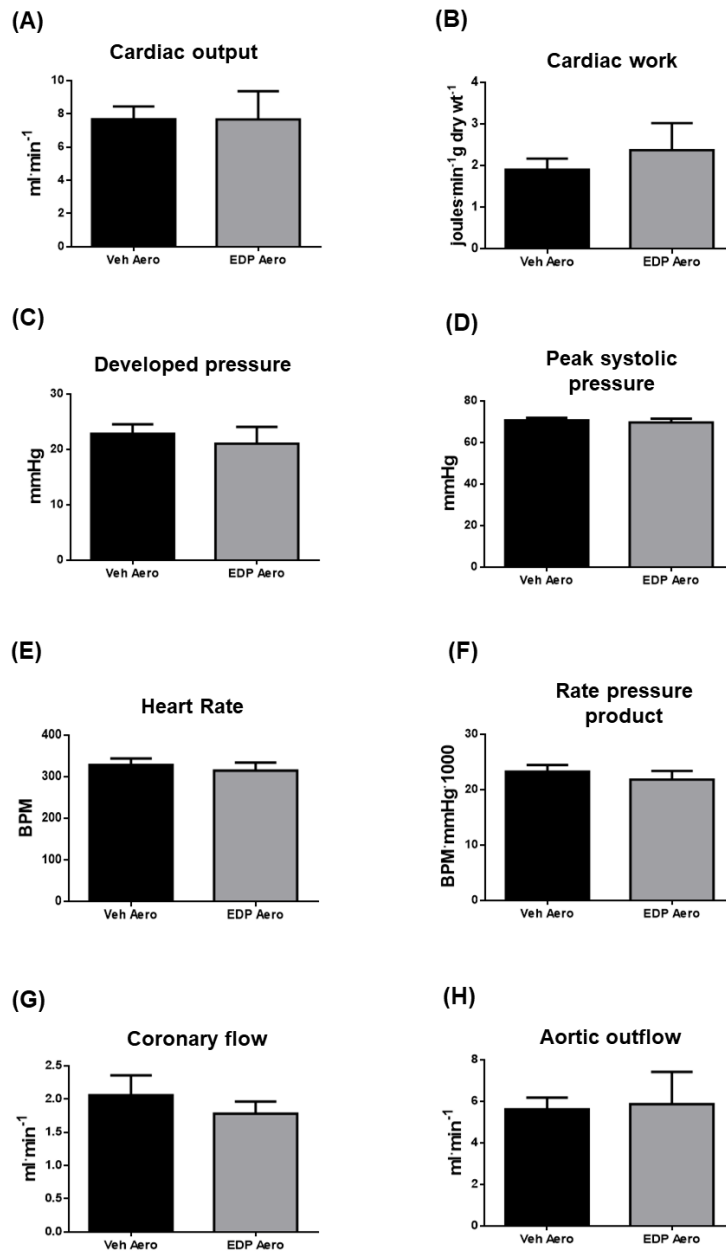


Figure 5. 2: Assessment of *ex vivo* aerobic cardiac function in mice hearts using isolated working heart technique. (A) Cardiac output, (B) Cardiac work, (C) Developed pressure, (D) Peak systolic pressure, (E) Heart rate, (F) Rate pressure product, (G) Coronary flow and (H) Aortic outflow, were calculated after 90 min of aerobic perfusion in hearts treated with either the vehicle or 19,20-EDP. Values represent mean ± SEM; The significance of differences was determined by the use of a two-tailed Student's t-test; * $p < 0.05$ vs. Vehicle IR (n = 5–8 per group).

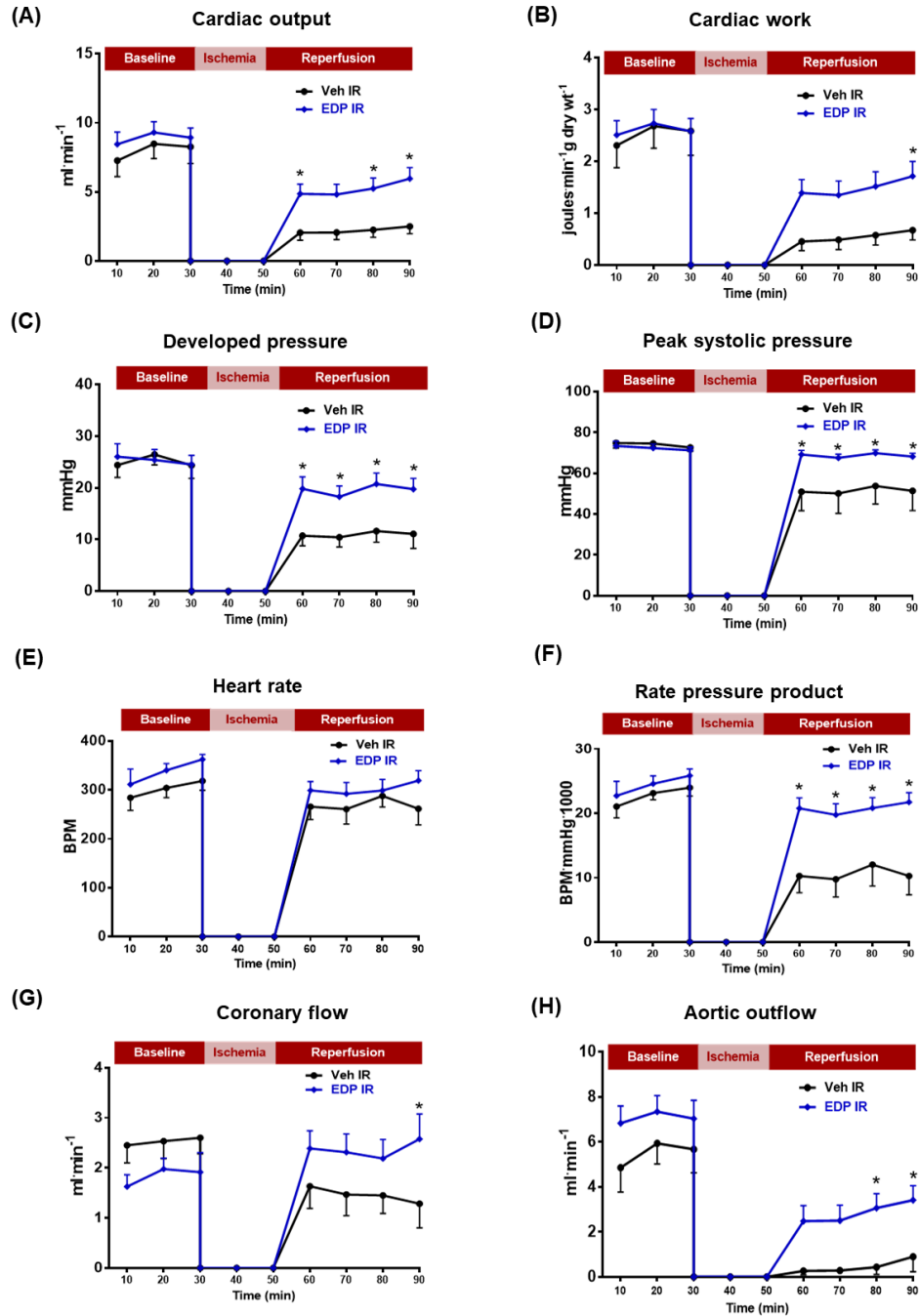


Figure 5. 3: Hearts perfused with 19,20-EDP (10 min before ischemia) in the *ex vivo* working heart experiment showed improved post-ischemic cardiac recovery. (A) Cardiac output, (B) Cardiac work, (C) Developed pressure, (D) Peak systolic pressure, (E) Heart rate (F) Rate pressure product (G) Coronary flow and (H) Aortic outflow assessed at the baseline before drug treatment (10 and 20 min), during drug treatment (30 min), during ischemia, and at 10-, 20-, 30- and 40-min of reperfusion. Values represent mean \pm SEM; The significance of differences was determined by the use of a two-way ANOVA followed by a Tukey post hoc analysis; * $p < 0.05$ vs. Vehicle IR ($n = 5 - 8$ per group).

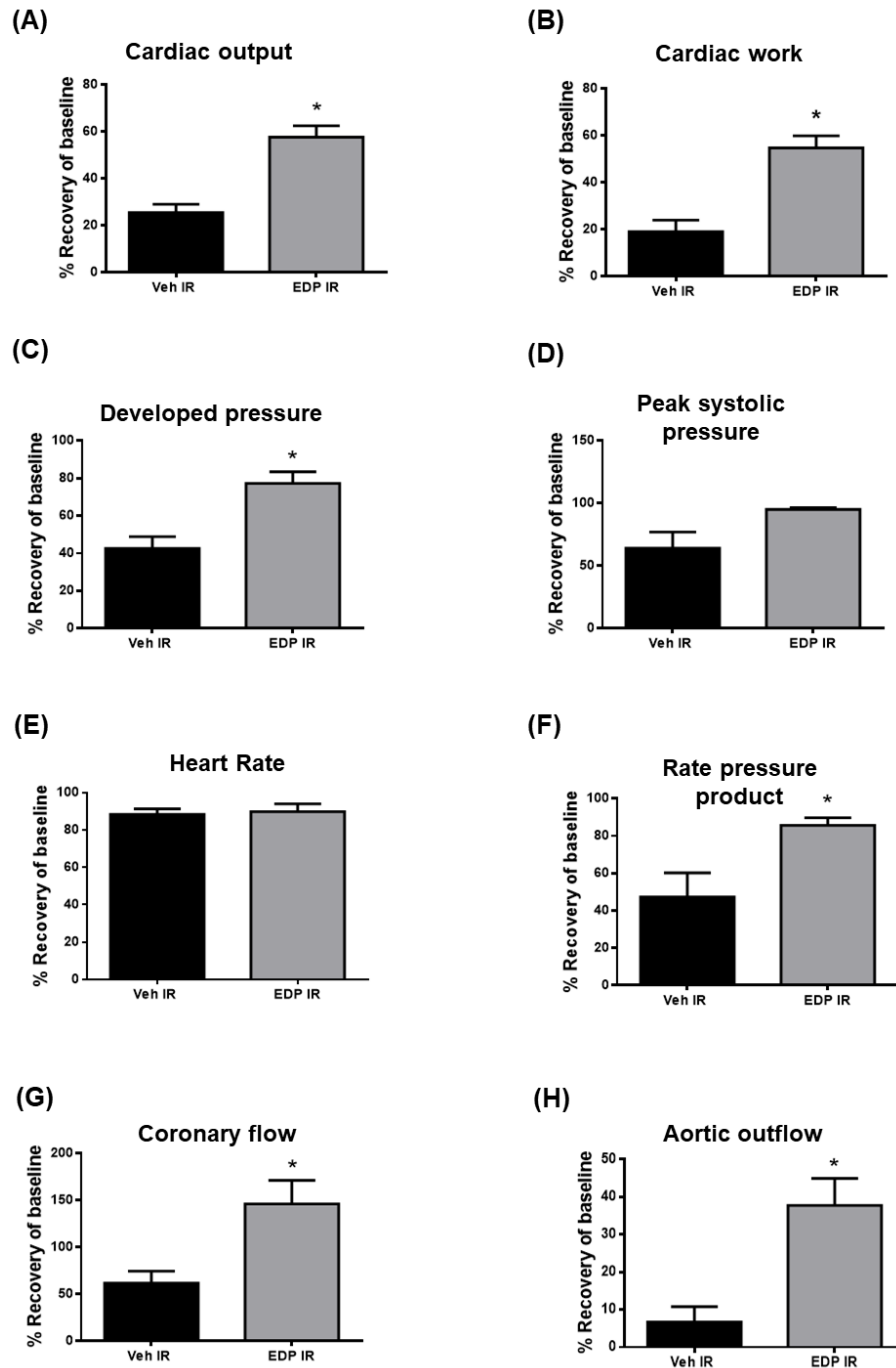


Figure 5. 4: Assessment of *ex vivo* cardiac function in mice hearts using isolated working heart technique. Recovery of (A) Cardiac output, (B) Cardiac work, (C) Developed pressure, (D) Peak systolic pressure, (E) Heart rate (F) Rate pressure product (G) Coronary flow and (G) Aortic outflow, were calculated at the end of the 40 min reperfusion as a percentage of the baseline values. Values represent mean \pm SEM; The significance of differences was determined by the use of a two-tailed Student's t-test; * $p < 0.05$ vs. Vehicle IR (n = 5–8 per group).

Many studies have associated cardiac dysfunction during and following myocardial IR injury with the balance between the major energy substrates utilized by the heart [134, 784]. Reportedly, during reperfusion of the ischemic myocardium, fatty acid oxidation rates quickly recover, while glucose oxidation rates remain suppressed. Excessive reliance on fatty acid oxidation contributes to cardiac dysfunction [134, 785], while inhibiting glucose oxidation rates in the heart, thereby decreasing cardiac efficiency [134, 786]. Accordingly, counteracting fatty acid oxidation-induced inhibition of glucose oxidation in the heart (either by directly stimulating glucose oxidation [134, 787], or by inhibiting fatty acid oxidation), [788-790] has been shown to improve recovery of post-ischemic hearts. In this regard, we investigated the effect of 19,20-EDP on cardiac energy metabolism in the setting of IR injury.

To assess energy substrate preference in hearts perfused with 19,20-EDP in the setting of IR injury, we utilized a radioisotope-based method coupled with working heart perfusion to simultaneously assess the oxidation of fatty acids and glucose, the two major energy substrates used by the heart. No marked changes in the rate of glucose or palmitate oxidation were observed in hearts perfused aerobically for 90 minutes with either the vehicle or 19,20-EDP (Figure 5.6 A and B). Furthermore, basal fatty acid and glucose oxidation rates were comparable in hearts perfused with either 19,20-EDP or the vehicle. However, hearts perfused with 19,20-EDP showed significantly enhanced glucose oxidation rates at reperfusion, contributing to higher rates of acetyl-CoA generated from glucose oxidation, while palmitate oxidation rates were comparable to the vehicle IR control (Figure 5.5 A and B, Figure 5.6 C and D). The higher post-ischemic cardiac work in 19,20-EDP-perfused hearts, compared with vehicle treated hearts, did not require a parallel increase in total acetyl CoA production from exogenous substrates. This translates to a significantly higher cardiac efficiency at reperfusion of 19,20-EDP-treated hearts compared with

vehicle controls (Figure 5.5C). Meanwhile, control hearts subjected to IR injury struggled to produce sufficient magnitude of cardiac work and the rates of acetyl-CoA generated from glucose oxidation remained at a significant low level leading to a significant decline in cardiac efficiency (Figure 5.5C). In summary, the higher cardiac work and improved cardiac efficiency seen in hearts perfused with 19,20-EDP correlates well with the enhanced glucose oxidation in these hearts in the setting of IR injury.

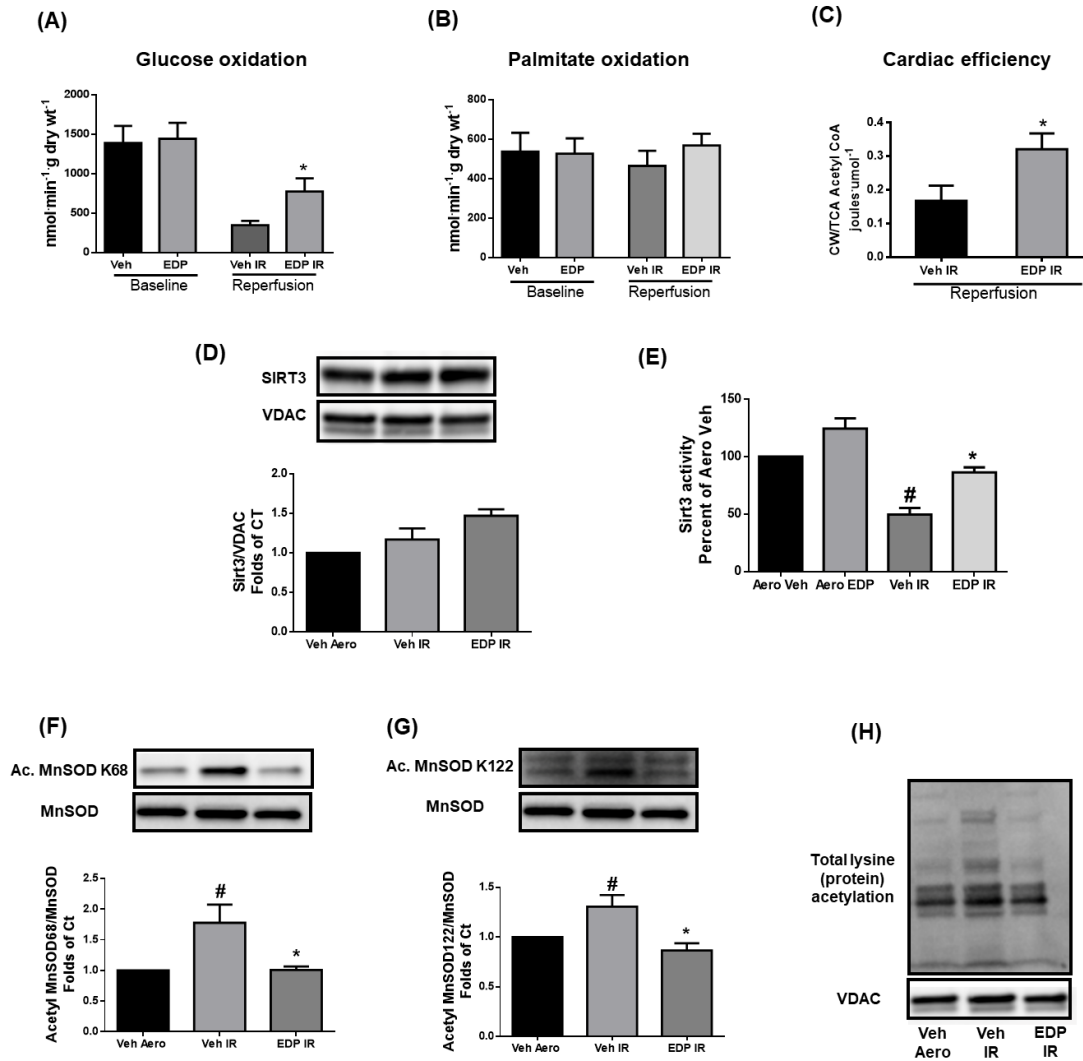


Figure 5. 5: Perfusion with 19,20-EDP in the setting of IR injury did not alter palmitate oxidation rate but improved glucose oxidation rate, cardiac efficiency and SIRT3 activity. (A) Glucose oxidation rate, (B) Palmitate (fatty acid) oxidation rate, and (C) Cardiac efficiency in hearts subjected to IR injury at the baseline and during reperfusion. (D) Representative immunoblot and densitometric quantification of the expression of mitochondrial protein SIRT3 in mice hearts. Protein expression was normalized to voltage-dependent anion channel (VDAC) protein used as a loading control. (E) Cardiac SIRT3 activity was determined in mitochondrial fractions in mice hearts after 20 min ischemia and 40 min reperfusion using a SIRT3 fluorescent assay kit. Representative immunoblots and densitometric quantification of the relative protein expression of (F) Acetyl MnSOD K68 and (G) Acetyl MnSOD K122 normalized to total manganese superoxide dismutase (MnSOD) in mice hearts after 20 min ischemia and 40 min reperfusion. (H) Overall cardiac protein (lysine) acetylation in mice hearts after 20 min ischemia and 40 min reperfusion. Values represent mean \pm SEM; The significance of differences was determined by the use of either one-way analysis of variance followed by a Tukey post hoc analysis or unpaired, two-tailed Student's t-test; * $p < 0.05$ vs. Vehicle IR, # $p < 0.05$ vs. Vehicle aerobic (n = 5–8 per group).

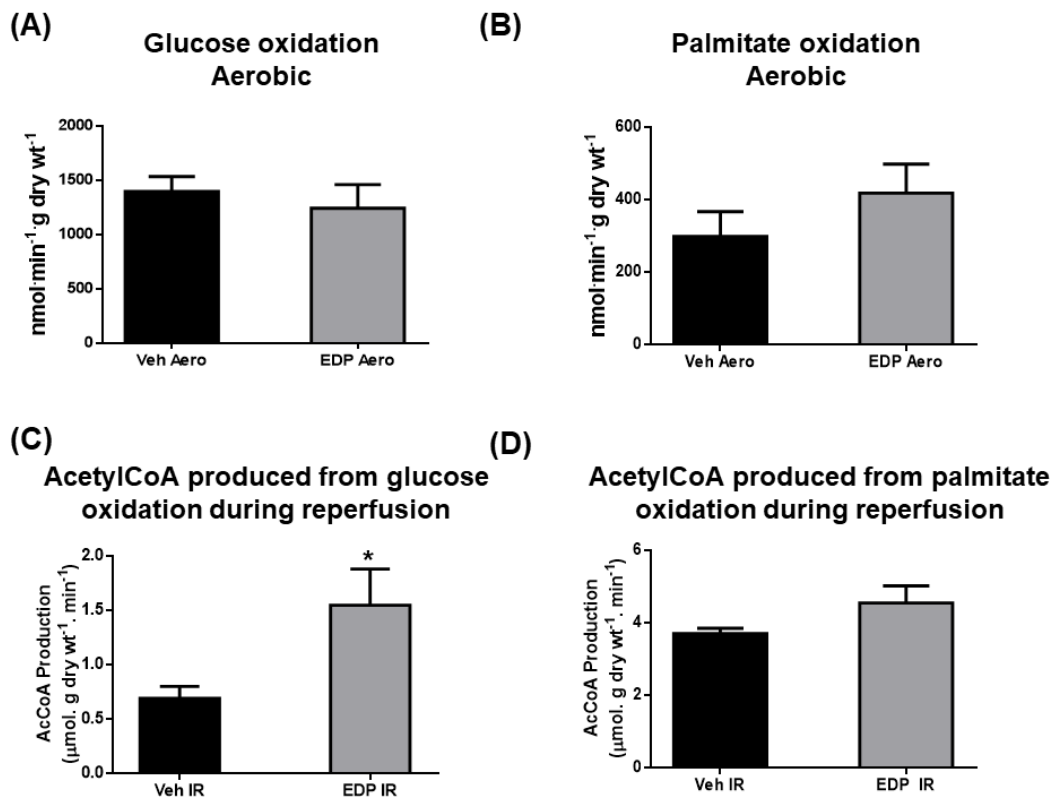


Figure 5. 6: Absolute metabolic rates of the mice hearts in the presence of either the vehicle or 19,20-EDP calculated using the isolated working heart technique. (A) Glucose oxidation rate and (B) Palmitate oxidation rate were calculated after 90 min of aerobic perfusion in hearts treated with either the vehicle or 19,20-EDP. (C) Acetyl-CoA produced from glucose oxidation and (D) Acetyl-CoA produced from palmitate oxidation were calculated during the 40-min reperfusion. Values represent mean \pm SEM; The significance of differences was determined by the use of a two-tailed Student's t-test; * $p < 0.05$ vs. Vehicle IR (n = 5–8 per group).

5.3.2 Sirtuin3 mediated the cardioprotective effects of 19,20-EDP against IR injury

Accumulating literature showed that SIRT3 can protect the heart against oxidative stress induced by IR injury by directly deacetylating and activating mitochondrial antioxidant enzyme manganese superoxide dismutase (MnSOD) [149, 712] and preserving the function of ETC complex components, the main source of more than 90% of cellular ROS [152]. Moreover, it has been demonstrated that SIRT3 promotes, from within the mitochondria, glucose uptake and oxidation [697] and that SIRT3 KO muscle undergoes a fuel switch, whereby the mitochondria rely more on fatty acids as substrates for oxidative phosphorylation [791]. In that sense, we aimed in the current study to investigate whether 19,20-EDP improves post-ischemic recovery, associated with improved glucose utilization via directly affecting SIRT3 expression and/or activity.

In the isolated working heart model, we observed no significant differences in mitochondrial expression of SIRT3 among different groups (Figure 5.5D). However, SIRT3 activity was significantly reduced in vehicle control hearts subjected to IR injury (Figure 5.5E). The IR-induced reduction in SIRT3 activity resulted in significantly elevated acetylation of MnSOD at both lysine residues in the highly conserved catalytic center 68 (K68) and 122 (K122) [792] inhibiting its enzymatic activity (Figure 5.5 F and G) as well as increased total protein acetylation (Figure 5.5H). Intriguingly, hearts perfused with 19,20-EDP demonstrated preserved SIRT3 activity, reduced MnSOD acetylation at both lysine sites and lower global protein acetylation levels compared to the vehicle control IR group (Figure 5.5 E-H). These data suggest perfusion of hearts with 19,20-EDP confers protection against IR-induced oxidative damage and enhances glucose oxidation by preserving SIRT3 activity.

These results were confirmed by using the SIRT3 inhibitors NAM and 3-TYP in the Langendorff model. In this experiment, hearts subjected to IR injury were either perfused with the vehicle, 19,20-EDP, NAM, 3-TYP, 19,20-EDP + NAM or 19,20-EDP + 3-TYP. Notably, preischemic cardiac parameters were similar among all treatment groups. Consistent with the previous findings, hearts perfused with 19,20-EDP showed significantly improved postischemic recovery of LVDP compared to vehicle IR group (Figure 5.7A, Figure 5.8A). Moreover, hearts perfused with 19,20-EDP demonstrated better rates of contraction (dP/dt max) and relaxation (dP/dt min) in comparison to the corresponding vehicle IR group (Figures 5.7 B and C). Interestingly, the protective effect of 19,20-EDP was blocked when hearts were co-perfused with either of the SIRT3 inhibitors NAM or 3-TYP (Figure 5.7 A-C). Importantly, no significant differences were observed in the heart rate at the end of reperfusion between all the study groups (Figure 5.8B). Furthermore, no differences were observed in pre-ischemic coronary flow rates in any of the treatment groups indicating the cardioprotective effect was not attributable to alterations in hemodynamics (Figure 5.8 C and D).

Accumulating literature revealed that cardiac dysfunction resulting from IR injury can be directly linked to mitochondrial damage [690, 691]. We investigated the changes in the protein levels of the ETC components succinate dehydrogenase subunit A (SDH-A, Complex II) and cytochrome c oxidase subunit IV (COX IV), the terminal enzyme of the mitochondrial respiratory chain (Complex IV). Immunoblotting results revealed no significant differences in the protein expression of SDH-A or COX IV among different treatment groups (Figure 5.8 E and F). Additionally, there were no significant changes in the expression level of citrate synthase (CS) (Figure 5.8G) suggesting that differences were not attributable to changes in mitochondrial biomass.

On the other hand, and in agreement with the working heart findings, we observed no significant differences in mitochondrial expression of SIRT3 among different groups (Figure 5.7D). However, SIRT3 activity was significantly declined in the vehicle control hearts subjected to IR injury (Figure 5.7E). The IR-induced reduction in SIRT3 activity was associated with significant elevation in the K68 and K122 acetylated MnSOD leading to reduced activity (Figure 5.7 F and G). Intriguingly, hearts perfused with 19,20-EDP, compared to the vehicle control IR group, demonstrated preserved SIRT3 activity as well as MnSOD function as evidenced by reduced acetylation at both lysine catalytic sites K68 and K122 (Figure 5.7D-G). Consistently, hearts perfused with 19,20-EDP plus either of the SIRT3 inhibitors NAM or 3-TYP neither maintained SIRT3 activity, nor limited the reduction in levels of activated MnSOD compared to the vehicle control IR group. Therefore, these data confirm the involvement of SIRT3 in mediating the cardioprotective effects of 19,20-EDP against IR injury.

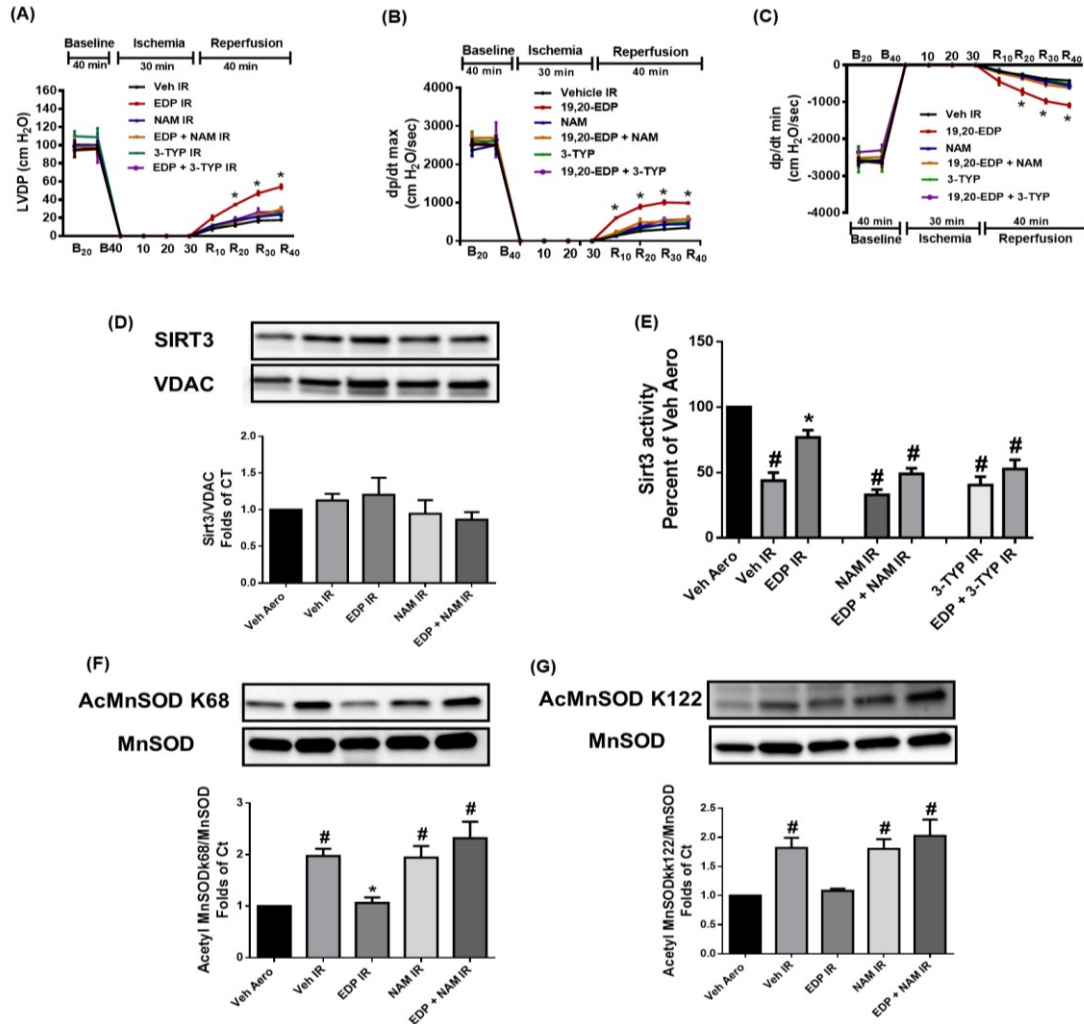


Figure 5. 7: Perfusion of mice hearts with 19,20-EDP in the Langendorff mode improved post-ischemic contractile parameters via maintenance of SIRT3 activity. (A) LVDP at the baseline before drug treatment (B₂₀), after drug treatment (B₄₀), during ischemia, and at 10-, 20, 30- and 40-min reperfusion (R₁₀, R₂₀, R₃₀, and R₄₀). (B) Rate of contraction (dp/dt max), and (C) rate of relaxation (dp/dt min) at baseline before drug treatment (B₂₀), after drug treatment (B₄₀), during ischemia, and at 10-, 20-, 30- and 40-min reperfusion (R₁₀, R₂₀, R₃₀, and R₄₀). (D) Representative immunoblot and densitometric quantification of the expression of mitochondrial protein SIRT3 in mice hearts after 30 min ischemia and 40 min reperfusion. Protein expression was normalized to voltage-dependent anion channel (VDAC) protein used as a loading control. (E) Cardiac SIRT3 activity was determined in mitochondrial fractions in mice hearts after 30 min ischemia and 40 min reperfusion using a SIRT3 fluorescent assay kit. Representative immunoblots and densitometric quantification of the relative protein expression of (F) Acetyl MnSOD K68 and (G) Acetyl MnSOD K122 normalized to total manganese superoxide dismutase (MnSOD) in mice hearts after 30 min ischemia and 40 min reperfusion. Values represent mean ± SEM; The significance of differences was determined by the use of either two-way or one-way ANOVA followed by a Tukey post hoc analysis; * p < 0.05 vs. Vehicle IR, # p < 0.05 vs. Vehicle aerobic (n = 5–8 per group). LVDP; left ventricular developed pressure.

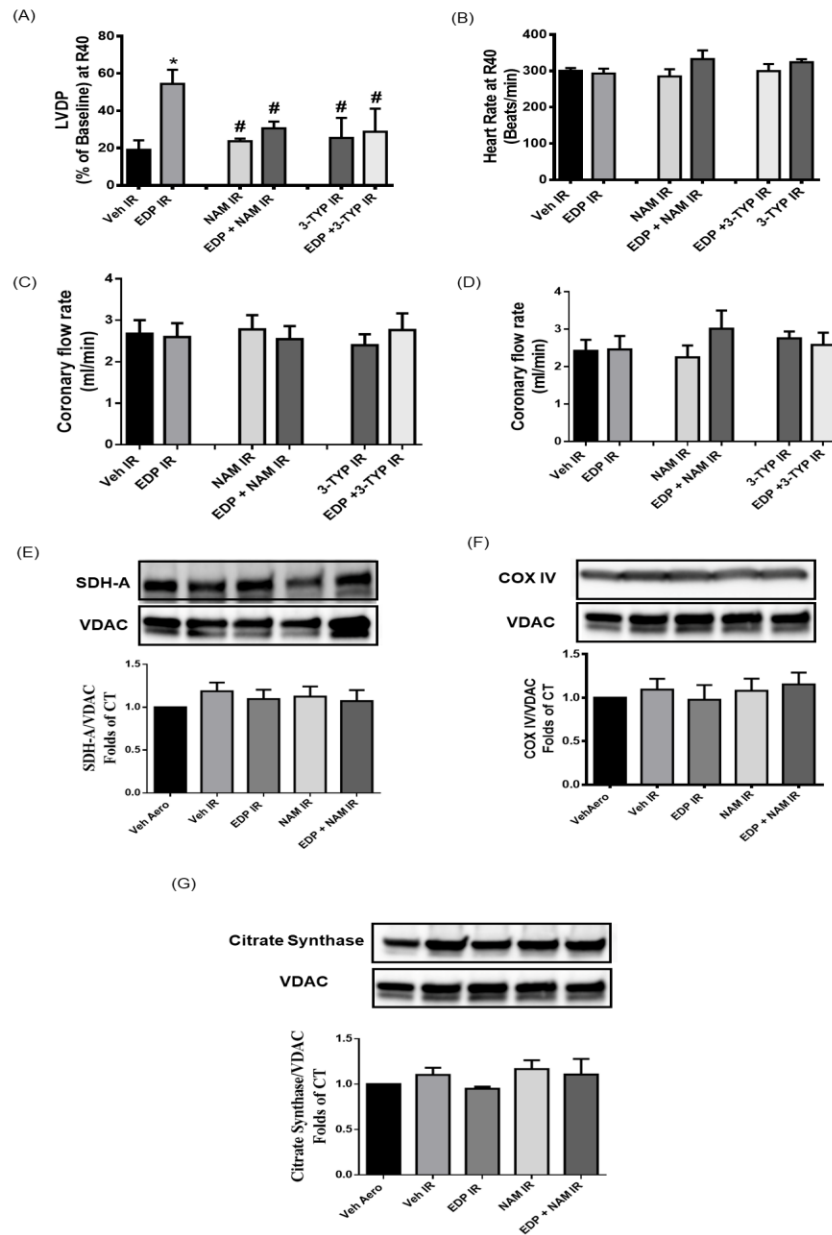


Figure 5. 8: Perfusion of mice hearts with 19,20-EDP in the Langendorff mode improved postischemic contractile parameters. (A) Left ventricular developed pressure (LVDP) recovery at 40 min of reperfusion as a percentage of baseline, (B) heart rate assessed as beats per minute (BPM) at the end of reperfusion (R40), (C) Pre- ischemic and (D) Post-ischemic coronary flow rates. Representative immunoblots and densitometric quantification of the mitochondrial protein expression of (E) succinate dehydrogenase subunit A (SDH-A), (F) cytochrome c oxidase subunit IV (COX IV), (G) citrate synthase (CS). Values represent mean \pm SEM; The significance of differences was determined by the use of one-way ANOVA followed by a Tukey post hoc analysis; * $p < 0.05$ vs. vehicle IR, # $p < 0.05$ vs. EDP IR (n = 5 - 8).

5.3.3 Sirtuin3 is indispensable for preserving glucose energy metabolism in permeabilized mice cardiac fibers

Significant impairment in mitochondrial energy metabolism and function and consequently the occurrence of metabolic disorders has been demonstrated in the heart during IR injury. Therefore, metabolic modulation is considered a well-established therapy for IR injury [134, 787, 788, 790, 793, 794]. The objective of metabolic modulation in patients with IHD is to enhance glucose oxidation due to the fact that oxidizing one molecule of glucose consumes less oxygen than one molecule of a fatty acid such as palmitate [134, 784, 787, 788, 795]. Moreover, the fact that metabolic modulation yields its effects independent of changes in cardiac hemodynamics makes it a promising strategy as an adjunct therapy for patients with IR injury.

To further explore the direct effect of 19,20-EDP on the modulation of mitochondrial energy metabolism and to determine if inhibition of SIRT3 might alter this response, we assessed the rate of mitochondrial respiration in cardiac muscle fibers freshly isolated from mice left ventricle in the presence of different energy substrates. Fatty acid oxidation was assessed using malate (5 mM) + palmitoyl carnitine (40 μ M) (M + Pc) substrates while carbohydrate oxidation was assessed by providing mitochondria with malate (5 mM) + pyruvate (10 mM) (M + Py) [796]. Treatment of cardiac fibers with 19,20-EDP did not significantly affect basal respiration, ADP-stimulated respiration or FCCP state in the presence of either fatty acid (M + Pc) or carbohydrate (M + Py) substrates (Figure 5.9). However, addition of NAM, either alone or in combination with 19,20-EDP, significantly impaired mitochondrial respiration induced by ADP and FCCP as well as RCR in the presence of the carbohydrate substrates (M + Py) (Figure 5.9B-D). Importantly, we observed no significant effect of NAM addition on these parameters in the presence of the fatty acid substrates (M + Pc) (Figure 5.9 E-H). Interestingly, these findings are consistent with our

working heart findings as well as with previous findings showing that muscle fibers of SIRT3 KO mice are characterized by impaired mitochondrial carbohydrate-based substrate oxidation and have increased reliance on fatty acids to provide substrates for the respiratory chain to compensate for reduced glycolytic substrates [791]. Taken together, these results highlight the role of SIRT3 in regulating energy substrate preference in cardiac energy metabolism.

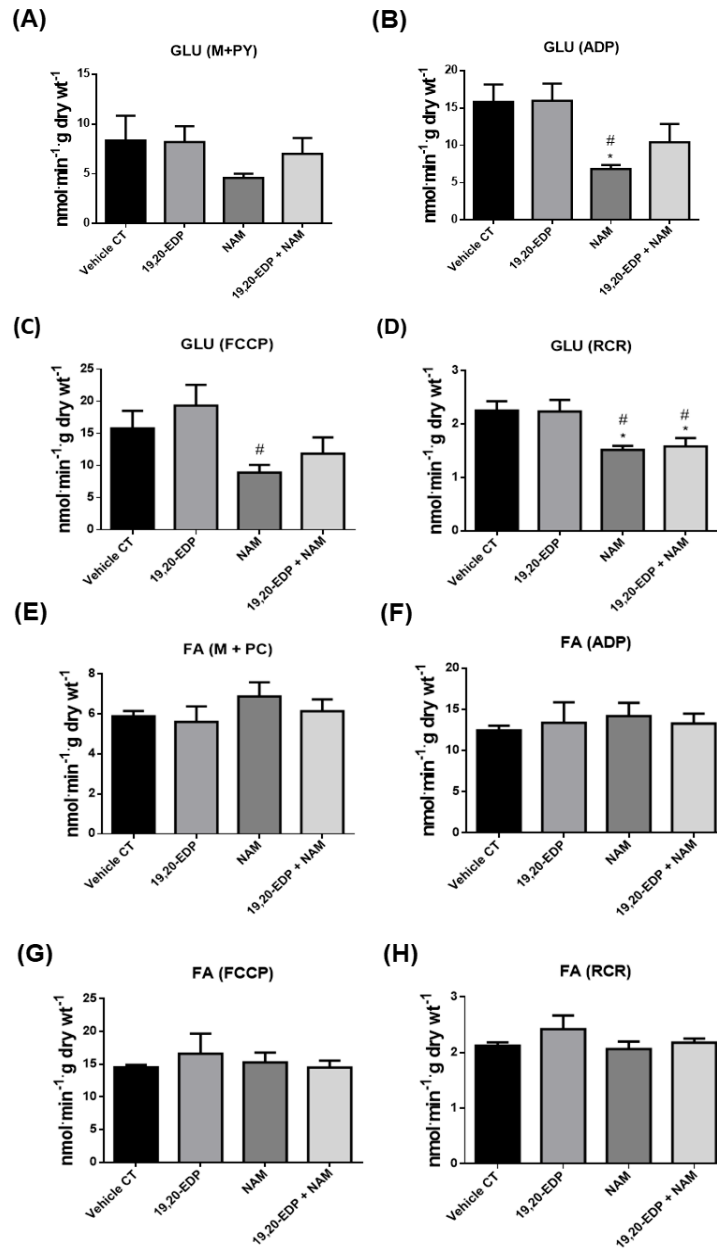


Figure 5. 9: Mitochondrial respiration assessed in permeabilized fresh fibers isolated from mice hearts demonstrated reduced capacity for glucose oxidation when SIRT3 is inhibited.

Mitochondrial oxidation of carbohydrates was assessed upon subsequent addition of (A) Malate and Pyruvate (M+Py), (B) ADP, (C) FCCP, (D) RCR was calculated as the ratio of mitochondrial respiration in the presence of ADP to mitochondrial respiration in the presence of M+Py. Mitochondrial oxidation of fatty acids was assessed upon subsequent addition of (E) Malate and Palmitoyl-carnitine (M+Pc) (F) ADP, (G) FCCP, (H) RCR was calculated as the ratio of mitochondrial respiration in the presence of ADP to mitochondrial respiration in the presence of M+Pc. Values represent mean \pm SEM; The significance of differences was determined by the use of one-way analysis of variance followed by a Tukey post hoc analysis; * $p < 0.05$ vs. vehicle IR, # $p < 0.05$ vs. EDP IR (n = 5).

5.3.4 Preservation of sirtuin 3 activity associated with 19,20-EDP treatment ameliorated the inflammatory surge triggered by IR injury

Aggravation and persistence of inflammation is an integral component of the host response to tissue injury and have been shown to contribute significantly to IR injury [797]. Cytokines such as tumor necrosis factor- α (TNF- α) and interleukin-6 (IL-6) increase promptly after myocardial IR injury where they locally enhance inflammation through their pleiotropic autocrine effect and trigger additional cellular inflammatory response leading to the development and progression of cardiac pathologies [197, 798, 799]. Several studies have revealed multiple critical links between impaired SIRT3 function and occurrence of inflammatory reactions. For instance, it has been shown that SIRT3 plays a key role in modulating the inflammatory response in cardiomyocytes where preservation of SIRT3 plays a key role in ameliorating inflammatory responses attenuating the development of cardiac hypertrophy and the progression of heart failure while loss or inhibition of SIRT3 is associated with uncontrolled cardiac inflammation and fibrosis [800]. In that sense, we aimed in the current study to investigate whether the enhanced SIRT3 activity, noticed in hearts perfused with 19,20-EDP, is associated with ameliorated inflammatory response secondary to IR injury.

We assessed the levels of these inflammatory cytokines in the homogenates of hearts collected from the Langendorff experiment (Figure 5.10 and Figure 5.11). Importantly, control hearts subjected to IR injury exhibited significantly elevated levels of the pro-inflammatory cytokines IL-6, TNF- α , IL-5 and the keratinocyte chemoattractant (KC) chemokine compared to the aerobic group (Figure 5.10A-D). On the other hand, the levels these inflammatory markers in hearts perfused with 19,20-EDP were not significantly different from the aerobic group. Again, the addition of the SIRT3 inhibitor NAM abolished the ameliorating effect of 19,20-EDP against

these cytokines highlighting the role of SIRT3 in mediating the protective effect of 19,20-EDP against this detrimental response (Figure 5.10A-D). It is also worth mentioning that, perfusion of hearts with 19,20-EDP was accompanied with a significant increase in the levels of vascular endothelial growth factor (VEGF) in these hearts, a signaling factor that promotes angiogenesis, and protect against myocardial IR injury [801] (Figure 5.10E). Moreover, 19,20-EDP perfused hearts showed a trend to increase the levels of IL-15 (Figure 5.10F), a cytokine with cardioprotective properties that has the potential to protect cardiomyocytes against hypoxia-induced cell death [802].

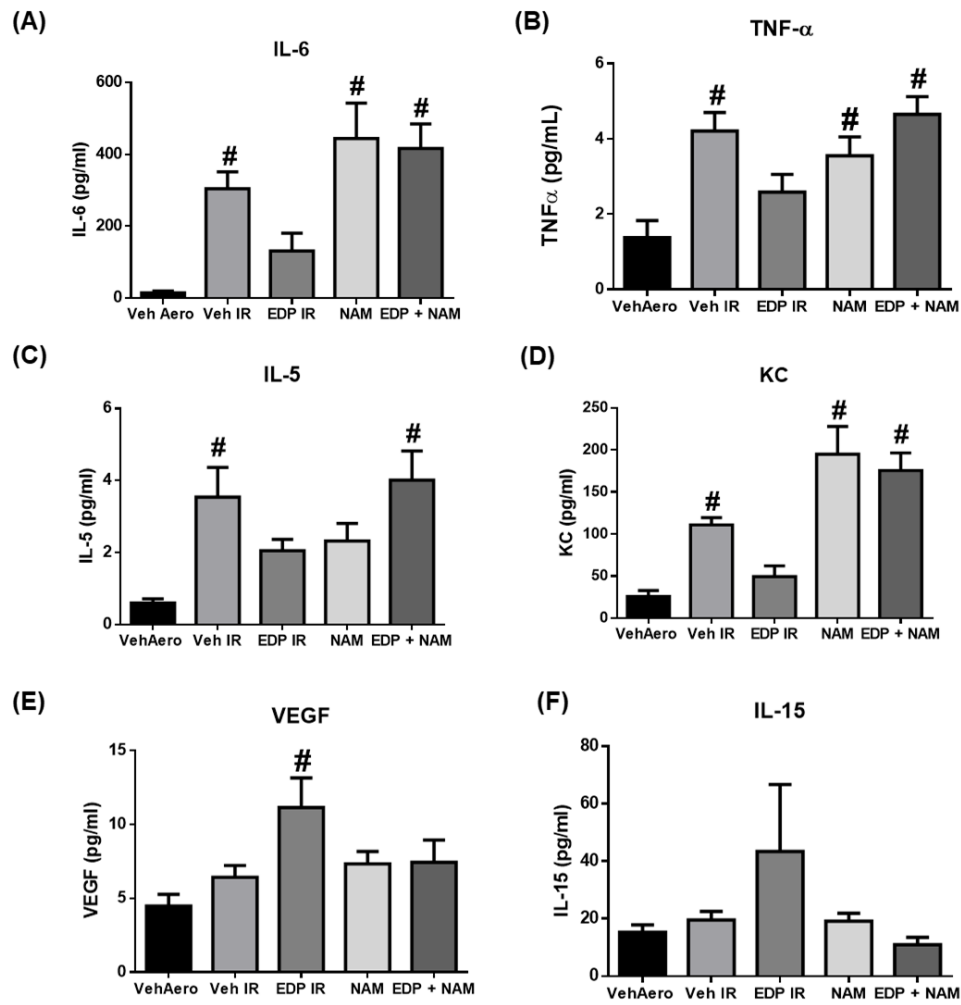


Figure 5. 10: Therapeutic effects of 19,20-EDP on cardiac cytokines and chemokines in the setting of IR injury. (A) IL-6, (B) TNF- α , (C) IL-5, (D) KC, (E) VEGF, and (F) IL-15 were determined in heart homogenates at the end of Langendorff reperfusion. Values represent mean \pm SEM; The significance of differences was determined by the use of one-way ANOVA followed by a Tukey post hoc analysis; # $p < 0.05$ vs. Vehicle aerobic ($n = 4 - 6$ per group).

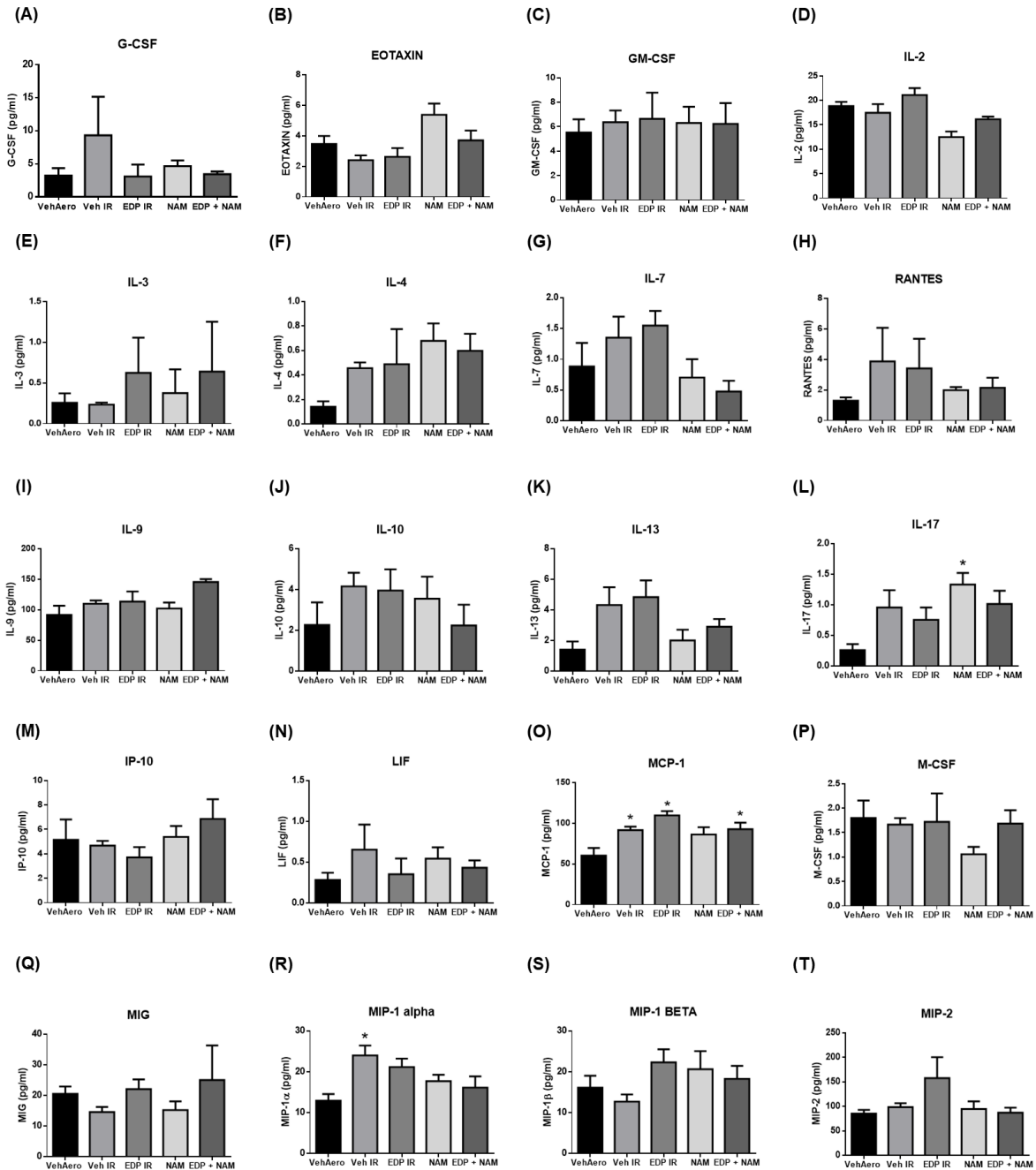


Figure 5. 11: Therapeutic effects of 19,20-EDP on cardiac cytokines and chemokines in the setting of IR injury. (A) G-CSF, (B) Eotaxin (C) GM-CSF (D) IL-2 (E) IL-3 and (F) IL-4 (G) IL-7 (H) RANTES (I) IL-9 (J) IL-10 (K) IL-13 (L) IL-17 (M) IP-10 (N) LIF (O) MCP-1 (P) M-CSF (Q) MIG (R) MIP-1alpha (S) MIP-1beta (T) MIP-2 were determined in heart homogenates at the end of reperfusion. Values represent mean \pm SEM; The significance of differences was determined by the use of one-way analysis of variance followed by a Tukey post hoc analysis; * $p < 0.05$ vs. Vehicle aerobic ($n = 4 - 6$ per group)

5.3.5 Human left ventricle demonstrated marked changes in the levels of 19,20-EDP and sirtuin 3 activity post-MI

Consistent with our findings, assessment of oxylipin levels in human LV tissue using LC-MS/MS demonstrated significantly decreased amounts of 19,20-EDP in the non-, peri- and infarct regions compared to the NFC (Figure 5.12A). Afterwards, we assessed the expression and activity of SIRT3 in both NFC and non- and peri-infarct regions of human hearts post-MI. Interestingly, assessment of LV mitochondria demonstrated a significant decline in SIRT3 expression and activity in hearts post-MI particularly in the peri and infarct regions compared to the NFC (Figure 5.12 B and C). The reduction in SIRT3 activity resulted in significantly elevated acetylation of the antioxidant MnSOD at both sites K68 and K122 leading to a reduction in its catalytic activity (Figure 5.12 D and E) as well as elevated total lysine acetylation (Figure 5.12 F). We then investigated the direct effect of 19,20-EDP on the SIRT3 activity levels on human cardiac tissues post-MI. Interestingly, incubation of the freshly isolated non- or peri-infarct biopsy with 1 μ M 19,20-EDP for 2 h significantly enhanced SIRT3 activity. However, addition of SIRT3 inhibitor NAM abolished this effect (Figure 5.12 G and H)

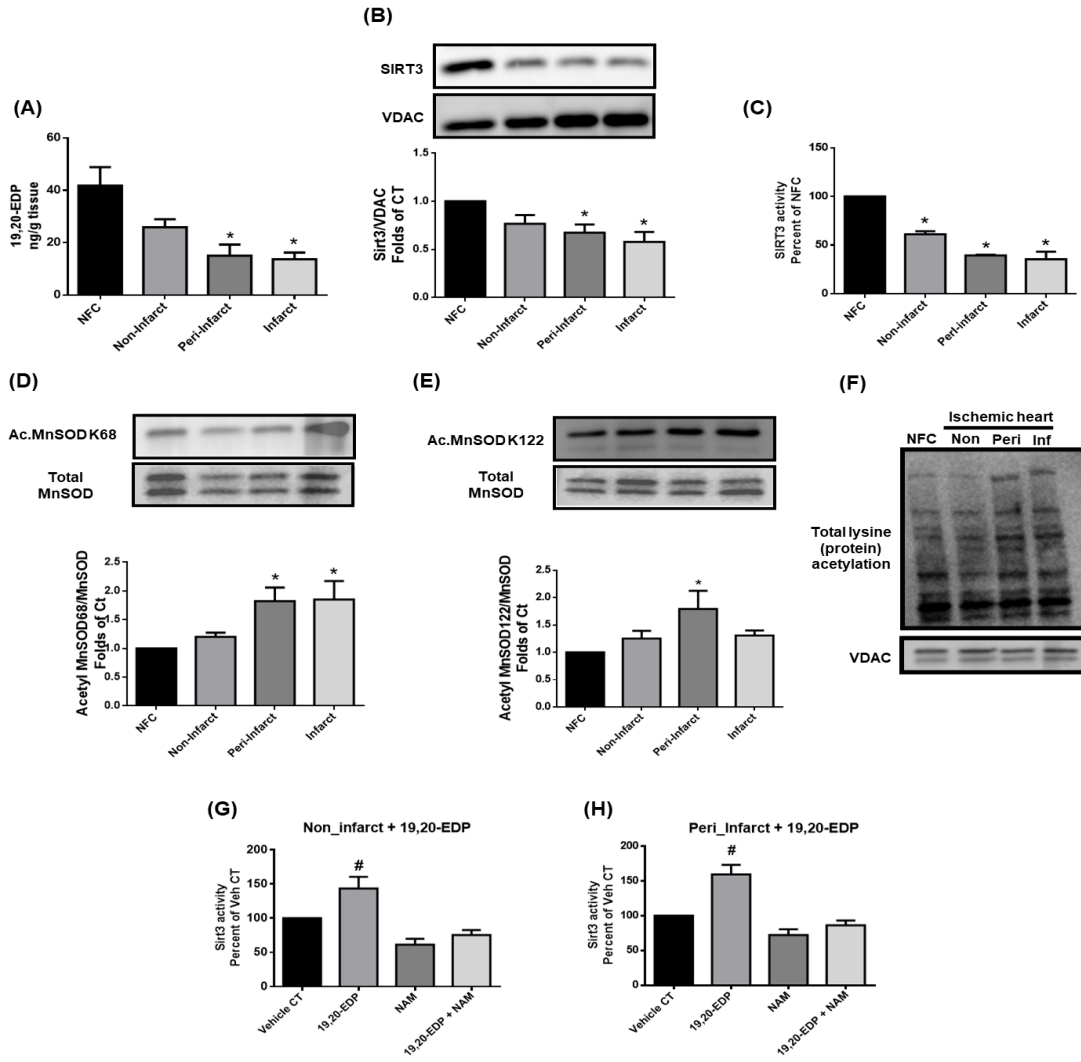


Figure 5. 12: Deficiency of 19,20-EDP in human ischemic left ventricular tissues was associated with reduced SIRT3 expression and activity. (A) 19,20-EDP levels in human left ventricle (LV) tissue (ng/g tissue) was measured by LC–MS/MS. (B) Representative immunoblot and densitometric quantification of the expression of mitochondrial protein SIRT3 and (C) SIRT3 activity in non-failing control hearts as well as non-infarct, peri-infarct and infarct regions of human ischemic left ventricular tissues. Representative immunoblots and densitometric quantification of the relative protein expression of the mitochondrial (D) AcMnSOD K68, (E) AcMnSOD K122, and (F) Overall cardiac protein (lysine) acetylation in non-failing control hearts as well as non-infarct, peri-infarct and infarct regions of human ischemic left ventricular tissues. SIRT3 and overall cardiac protein (lysine) acetylation were normalized to VDAC, AcMnSOD K68 and AcMnSOD K122 were normalized to total manganese superoxide dismutase (MnSOD). Assessment of SIRT3 activity in (G) non-infarct and (H) Peri-infarct regions of human ischemic left ventricular tissues after incubation with the vehicle, 19,20-EDP, NAM or 19,20-EDP + NAM. Values represent mean \pm SEM; The significance of differences was determined by the use of one-way ANOVA followed by a Tukey post hoc analysis; * $p < 0.05$ vs. NFC, # $p < 0.05$ vs. vehicle control (n = 3 – 5 per group).

5.3.6 19,20-EDP improved mitochondrial respiration in fresh fibers isolated from the ischemic human left ventricle

It has been previously established that inhibition or loss of SIRT3 would impair mitochondrial respiration and that SIRT3-KO mice exhibit decreased oxygen consumption rate and develop oxidative stress as SIRT3 tightly regulates respiration in isolated mitochondria [156, 803]. In the same vein, overexpression of SIRT3 is associated with increased oxygen consumption rate and reduced oxidative stress [143]. Therefore, we assessed the rate of mitochondrial respiration in permeabilized fibers isolated from NFC, non-, and peri-infarct regions of the human left ventricle in the presence or absence of 19,20-EDP and the SIRT3 inhibitor NAM. Quantitation of the results of all samples is shown in figure 5.13 and figure 5.14. First, we observed that NFC fibers showed preserved mitochondrial respiration as represented by RCR and spare respiratory capacity. In contrast, mitochondrial respiration was significantly impaired in non-infarct and peri-infarct sections of the ischemic human heart compared to NFC as evidenced by reduced RCR, coupling efficiency, spare respiratory capacity, and rate of ATP production (Figure 5.13 A-D, and Figure 5.14). These results are in agreement with previous reports demonstrating decreased mitochondrial respiration in both adjacent (peri-infarct) and remote (non-infarct) regions of ischemic cardiac muscle [752]. This reduction in ETC complex activities and mitochondrial respiration could be attributed to the loss of SIRT3 in these regions as illustrated previously in figure 5.12 [156, 804-807]. Afterwards, we assessed the effect of 19,20-EDP \pm NAM on the respiratory parameters in each region separately. In the NFC permeabilized fibers, addition of 19,20-EDP did not significantly alter mitochondrial oxygen flux or any of the assessed respiratory values compared to the control. However, incubation of the non-infarct fibers with 19,20-EDP significantly enhanced RCR, coupling efficiency, spare respiratory capacity, and the rate of ATP

production (Figure 5.13). Similar findings were obtained after treating the peri-infarct regions with 19,20-EDP except that coupling efficiency did not reach significant levels (figure 5.14C-D). Interestingly, addition of the SIRT3 inhibitor NAM to the NFC fibers significantly reduced RCR, coupling efficiency, spare respiratory capacity, and the levels of ATP. Moreover, the addition of NAM abolished the improvement in mitochondrial respiratory parameters induced by 19,20-EDP in both non- and peri-infarct regions. These results are consistent with our data showing that loss of SIRT3 in these tissues is associated with acetylation and decrease of activity and function of ETC components resulting in decreased mitochondrial respiration and ATP production and that 19,20-EDP can potentially improve mitochondrial respiration via directly affecting SIRT3.

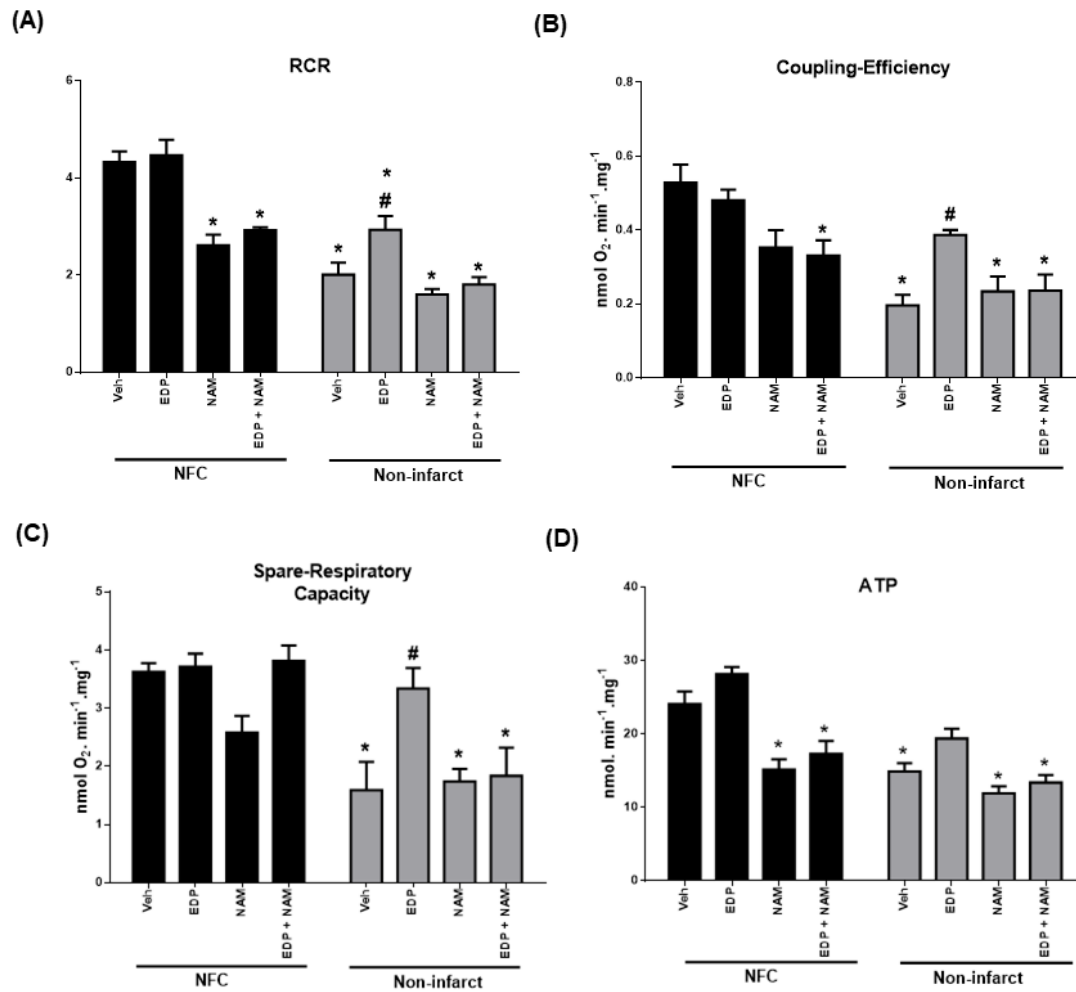


Figure 5.13: Treatment with 19,20-EDP improved mitochondrial respiratory function in human ischemic left ventricular tissues. Bar charts demonstrating changes in the values of (A) Respiratory control ratio (RCR), (B) Coupling efficiency, (C) Spare respiratory capacity, and (D) Rate of ATP production in respiration medium in both NFC hearts and non-infarct regions of human ischemic left ventricular tissues. Values represent mean ± SEM; The significance of differences was determined by the use of one-way ANOVA followed by a Tukey post hoc analysis; * $p < 0.05$ vs. Vehicle NFC, # $p < 0.05$ vs. vehicle non-infarct region (n = 4 - 6 per group).

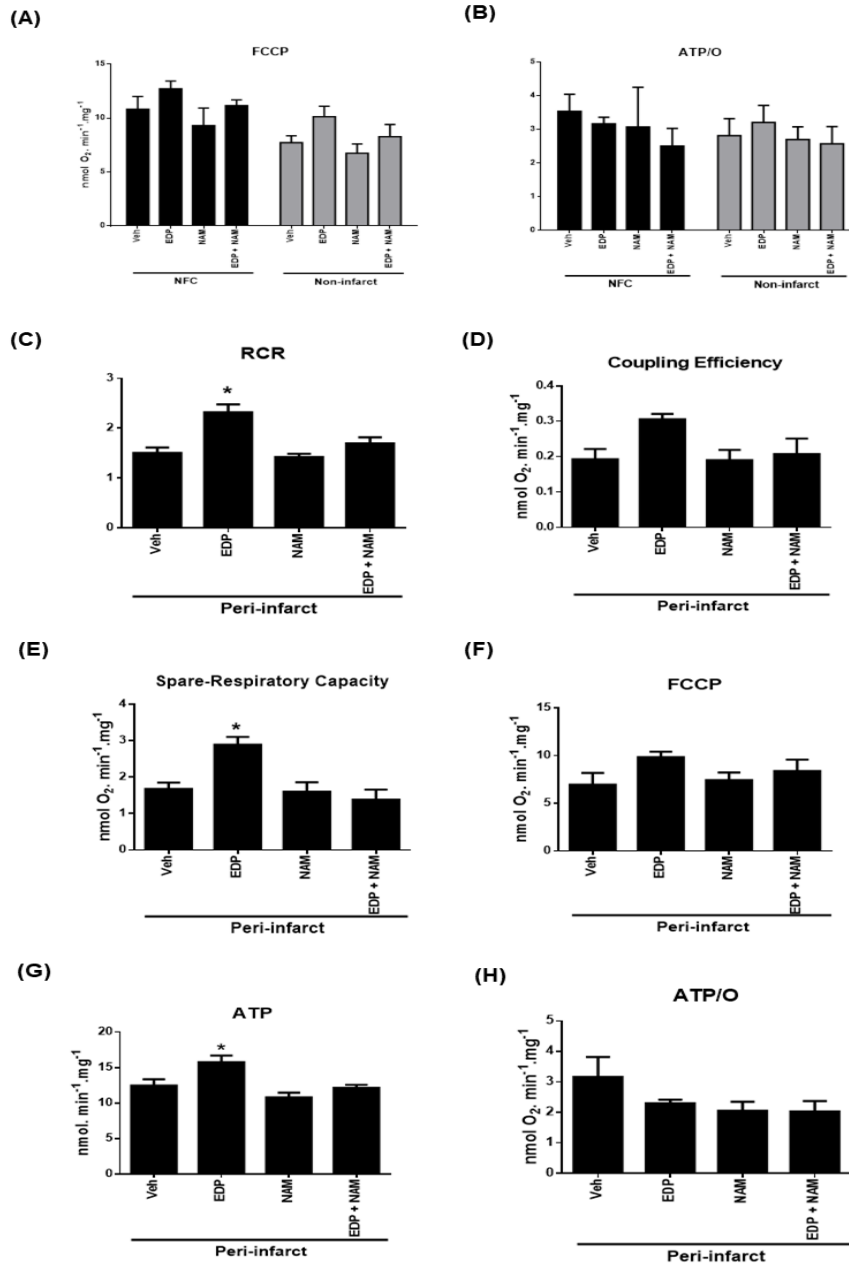


Figure 5. 14: Assessment of mitochondrial respiratory function in human ischemic left ventricular tissues. Bar charts demonstrating the values of (A) FCCP and (B) ATP/O in both NFC hearts and non-infarct regions of human ischemic left ventricular tissues. Bar charts demonstrating the values of (C) Respiratory control ratio (RCR), (D) Coupling efficiency, (E) Spare respiratory capacity, (F) FCCP-stimulated respiration, (I) Rate of ATP production in respiration medium and (J) ATP/O in peri-infarct regions of human ischemic left ventricular tissues. Values represent mean \pm SEM; The significance of differences was determined by the use of one-way ANOVA followed by a Tukey post hoc analysis; * $p < 0.05$ vs. Vehicle control (n = 4 - 6 per group).

5.3.7 19,20-EDP ameliorated mitochondrial damage and attenuated ROS production secondary to hypoxia reoxygenation in neonatal rat cardiomyocytes

To further examine the effect of 19,20-EDP on mitochondrial ROS production under stress conditions, NRCM were subjected to hypoxia reoxygenation (HR) and stained with MitoSOX to assess alterations in mitochondrial ROS production. Microscopy analysis demonstrated that under aerobic conditions, treatment of NRCM with 19,20-EDP did not affect the levels of ROS production compared to the control. However, addition of the SIRT3 inhibitor NAM either alone or combined with 19,20-EDP was associated with significantly increased ROS production as evidenced by increased MitoSOX red fluorescence intensity (a specific indicator of mitochondrial superoxide) (Figure 5.15A). Moreover, mitochondrial ROS generation was significantly increased in NRCM after HR, compared to the aerobic control group. Interestingly, treatment with 19,20-EDP, significantly reduced HR-induced MitoSOX fluorescence. However, the addition of the SIRT3 inhibitor NAM abolished the ROS reducing effect of 19,20-EDP in the setting of HR conditions (Figure 5.15A).

In another set of experiments to assess the effect of 19,20-EDP on alterations in mitochondrial morphology/density and membrane potential, NRCM were subjected to HR and stained with the corresponding dyes Mitotracker Green and TMRE. NRCM treated with the vehicle or the 19,20-EDP under aerobic conditions demonstrated healthy mitochondrial morphology that is characterized by filamentous and tubular shape as evidenced by mitotracker green staining (highlighted by white arrows) as well as preservation of the mitochondrial voltage membrane potential as evidenced by TMRE red fluorescence (Figure 5.15 B and C). On the other hand, a 24-hour hypoxia and 6h reoxygenation caused a significant loss of mitochondrial structure as evidenced by significant punctate and fragmented mitochondrial morphology (highlighted by

yellow arrows) as well as loss of mitochondrial membrane potential (Figure 5.15 B and C). Intriguingly, treatment of neonatal cardiomyocytes with 1 μ M 19,20-EDP maintained both Mitotracker Green and TMRE fluorescence under HR conditions. Importantly, NRCM treated with NAM, either alone or combined with 19,20-EDP, under either aerobic or HR conditions, exhibited significant punctate and fragmented mitochondrial morphology as indicated by mitotracker green dye that was associated with a loss in TMRE staining, indicating a decrease/distortion in mitochondrial density/morphology and loss of mitochondrial membrane voltage (Figure 5.15 B and C). Again, these results indicate the importance of SIRT3 in mediating the protective effects of 19,20-EDP on mitochondrial integrity and quality and consequently its cardioprotective effects against IR injury.

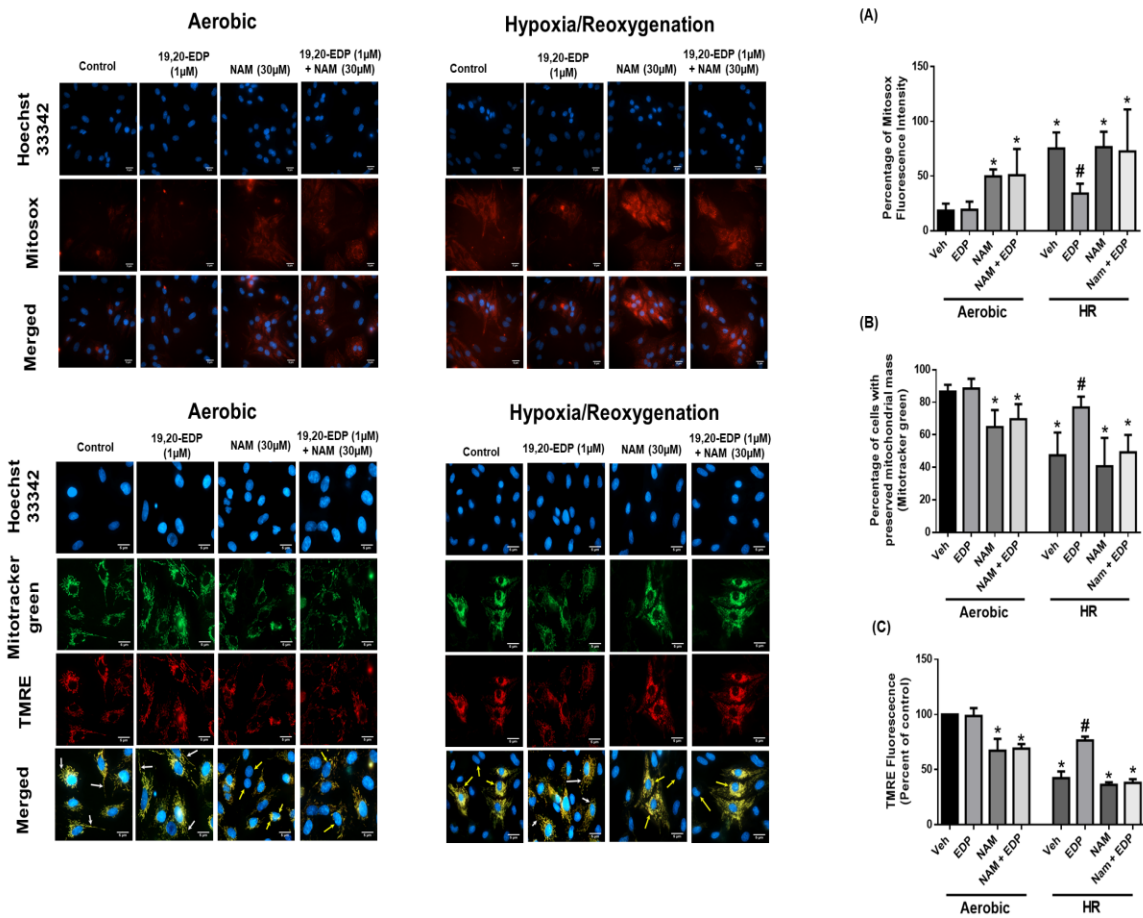


Figure 5. 15: Treatment of NRCMs, subjected to HR, with 19,20-EDP limited ROS production, preserved mitochondrial density/morphology and maintained mitochondrial membrane potential. Representative images of NRCMs stained with either (MitoSOX and Hoechst 33342 dyes), or (Mitotracker green, TMRE and Hoechst 33342 dyes). Histograms representing the (A) the quantification of percentage of MitoSOX fluorescence intensity (B) quantification of percentage of NRCMs with preserved mitochondrial mass as evidenced by mitotracker green stain, (C) the relative quantification of TMRE fluorescence intensity. Normal mitochondrial morphology (filamentous and tubular shape) are highlighted by white arrows. In contrast, punctate and fragmented mitochondrial morphology are highlighted by yellow arrows. Values represent mean \pm SEM; The significance of differences was determined by the use of one-way ANOVA followed by a Tukey post hoc analysis; * $p < 0.05$ vs. Aerobic vehicle, # $p < 0.05$ vs. HR vehicle (n = 3 per group, 5 fields each).

5.3.8 Molecular modeling and docking approaches

5.3.8.1 Principal component analysis (PCA) of existing hSIRT3 crystal structures

We started our structural analysis by collecting all available Human SIRT3 (hSIRT3) crystal structures. As of June 2020, there were 31 crystal structures of hSIRT3 deposited in the Protein Data Bank. Some of these structures represent apo structures; others represent hSIRT3 co-crystallized with NAD⁺, NAD⁺ analogues, small molecule inhibitors, small molecule activators, acetylated peptide substrates, or combinations of these molecular entities. As the main goal from this initial analysis was to identify flexible regions and to determine the location of the most suitable binding sites for 19,20-EDP, we decided to limit the analysis to structures that have no internal missing protein segments (24 crystal structures). The majority of missing regions in the incomplete structures were mostly from the flexible α 3 helix region.

The presence of crystal structure representatives of hSIRT3 bound to different molecular entities and in different activation/conformational states have made the PCA analysis of these crystal structures particularly appealing. As shown in Figure 5.16b, the first two principal components could explain approximately 86.3% of the variations in the crystal structures. Our PCA analysis showed that whereas residues from the α 3 helix (residues ~ASP156-LEU173) and the nearby zinc binding domain (residues ~GLY249-ILE291) are the main contributors to the first principal component, second principal component exhibited an almost exclusive contribution from the α 3 helix residues (Figure 5.16C). A scatter plot for the largest two principal components (PC1 & PC2) of these crystal structures is also given in Figure 5.16B and is labelled by the PDB codes of the corresponding structures. Along the top two PCs, it is possible to cluster nearby structures according to their relative locations on the PC scatter plot. As shown in the figure 5.16, we can identify three major groups of structures. In particular, two interesting groups of structures can be

identified with respect to the relative position of the $\alpha 3$ helix. These groups of structures are (i) structures where the allosteric pocket (the OP2 pocket in the 4BN4 structure) is fully or partially open, and (ii) structures where the pocket is closed/partially closed by the $\alpha 3$ helix.

The overlay of the investigated X ray structures shows large positional variations of the $\alpha 3$ helix. As an illustration, we have superposed the structure of the 4BN4 (a representative from the first group with an open pocket) over the 5Z93 structure (as a representative from the second group for the closed pocket). The superposition is given in Figure 5.16E and it is clear from the figure that a significant clockwise-like rotation of the $\alpha 3$ helix in the 5Z93 structure is a pre-requisite to open the cavity required to bind OP2 as observed in the 4BN4 crystal structure. Based on the presence of hetero-residues/cofactors/inhibitors/activators, crystallization conditions and activation states, other crystal structures in the studied set can occupy intermediate states along the PC1/PC2 spaces. It was also observed that inhibitors that bind to the C-pocket and extend to the acetyl-LYS substrate-binding site form a unique cluster of conformations (PDB codes: 4JSR, 4JT8, 4JT9). A closer analysis of these structures showed their close similarity with the first cluster of conformations, i.e. those with the OP2 pocket is partially or fully open. It was also observed that the presence of productive $\text{NAD}^+/\text{NAD}^+$ analogues conformations in the studied set of structures favors the closure of the designated hydrophobic pocket, as in the 5H4D & 4FVT structures. Similar observations could be drawn from analyzing the generated MD trajectories where we observed that in the absence of 19,20-EDP, there was a spontaneous transition of the $\alpha 3$ helix to close the pocket. It is therefore likely that the binding of 19,20-EDP requires the presence of hSIRT3 either in the NAD^+ free protein or the presence of NAD^+ in the extended, non-productive conformation. Another possibility is the existence of an un-characterized breathing motion of the productive- NAD^+ bound hSIRT3 conformation that allows the binding of 19,20-

EDP. This will be the subject of future studies. It is apparent from this analysis how the conformational structure of hSIRT3 is tightly coupled to type of interactions involved by the co-crystallized ligands/co-factors.

5.3.8.2 19,20-EDP binds to the OP2 site and stabilizes a productive, twisted conformation of NAD⁺

As explained in the methods, the OP2 binding site was utilized as the most potential binding site of 19,20-EDP to carry out the docking simulation. In order to investigate the structural stabilities of the resulting complexes from the docking simulations, we performed MD simulations for 100 ns simulation time in explicit water (5 trajectories of 20 ns each, restarted from different initial velocities to improve the statistical sampling). As a reminder, MD simulations were performed for the 19,20-EDP-included & 19,20-EDP-deleted complexes. Structural and energetic analyses of the generated MD simulation trajectories were then conducted. Unless otherwise specified, all structural analyses, including RMSD and H-bonds occupancy analyses were performed through the CPPTRAJ utility in AMBER18. The binding free energy of NAD⁺ was estimated through the AMBER/MM-GBSA approach using the same parameters in the 19,20-EDP free and the 19,20-EDP included complexes. The closet 20 water molecules from the NAD⁺ molecule were treated as part of the receptor structure.

In principle, previous crystal structures of hSIRT3 as well as other members of the Sirtuins family of deacetylases have indicated that a bound NAD⁺ molecule exists in two distinct categories of conformations, (i) an extended non-productive conformation where the nicotinamide motif occupies the acetyl-Lys substrate (Figure 5.16F) binding site, and (ii) a twisted productive conformations where the nicotinamide motif occupies the C-pocket (Figure 5.16F), exposing the reactive anomeric carbon (C1'') of NAD⁺ to the acetyl-Lys binding site [744, 766]. While the

twisted NAD⁺ conformation allows the binding of the acetyl-Lys substrate and facilitates the nucleophilic attack by the acetyl-oxygen of the acetyl-Lys, followed by the formation alkylamide intermediate, extended NAD⁺ conformation blocks the binding of the acetyl-Lys substrate. This nucleophilic attack is the first step of a concerted SN2 reaction that ends by the formation of deacetylated peptide substrate and the liberation of nicotinamide and O-acetyl-ADP-ribose as by-products [808-810]. Studies have also shown that occupying the C-pocket with small molecule ligands (including free nicotinamide itself) abolishes the catalytic activity of hSIRT3 as it pushes the nicotinamide motif of NAD⁺ to occupy the acetyl-Lys binding site, forcing NAD⁺ to adopt the extended conformation [766]. One can then hypothesize that it is possible to positively modulate the NAD⁺ involved deacetylation reaction by doing the opposite, i.e. by forcing NAD⁺ to adopt the twisted conformation where the nicotinamide motif is held fixed to the C-pocket by the help of an external anchor.

As has been discussed in a number of studies [744, 766] concerned with Sirtuins deacetylation activities, interactions formed by conserved residues at the C-pocket, in particular the interactions with conserved ASP231 and ASN229 (according to hSIRT3 numbering scheme) to the carboxamide group of the nicotinamide motif of NAD⁺ is responsible for holding the nicotinamide to the C pocket, forcing NAD⁺ to adopt a twisted conformation. The studies have indicated that this twisted conformation is a prerequisite for the acetyl-LYS substrate to bind to the active site, otherwise the nicotinamide motif in the extended, non-productive NAD⁺ conformation will block the substrate-binding site. Our MD simulations showed that in the absence of 19,20-EDP, NAD⁺ forms stable H-bonds with ASN229 (71% of the simulation time, with an average distance of 2.85 Å and an average D(donor)-H(hydrogen)-A(acceptor) angle of 162.0°). In the presence of 19,20-EDP, the interaction formed by the carboxamide group gets stronger due

to the presence of free 19,20-EDP carboxylate group anchored at the C-pocket cavity, which offers additional possibilities of charge assisted H-bonding interactions. Tracing the H-bonding involved the carboxamide hydrogens of the nicotinamide motif of NAD⁺ and the carboxylate group of 19,20-EDP showed that 19,20-EDP forms strong charge assisted H-bonding with a total occupancy value of 63.21% of the simulation time. This stabilization was also manifested by stronger binding affinities according to the AMBER/MM-GBSA protocol (-142.68±9.24 kcal/mol in the presence of 19,20-EDP, versus -129.57±10.05 kcal/mol in the absence of 19,20-EDP), and a slightly more stable NAD⁺ heavy atom average RMSD values (1.04 Å in the presence of 19,20-EDP, versus 1.2 Å in the absence of 19,20-EDP, Figure 5.16G). It should be noted that this improved NAD⁺ affinity is not originating only from direct interactions with 19,20-EDP. Our binding energy decomposition showed improved interactions with the flexible loop residues (PHE157 & ARG158). For example, the total binding energies provided by PHE157 improved from -1.23±0.69 kcal/mol to -4.66±1.19 kcal/mol, and that of ARG158 improved from -6.80±3.80 kcal/mol to -9.03±1.61 kcal/mol.

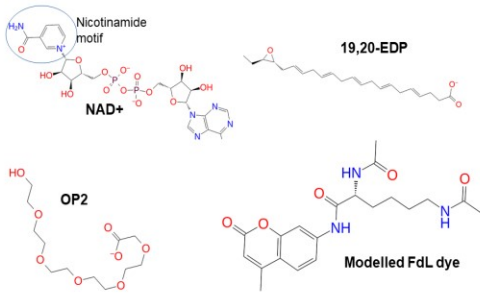
5.3.8.3 19,20-EDP directly enhanced sirtuin 3 activity

To understand the mechanism through which 19,20-EDP enhances SIRT3 activity, we tested the affinity of SIRT3 for NAD⁺ in the presence and absence of 19,20-EDP. In this experiment, acetylated HDAC substrate was incubated with increasing concentrations of NAD⁺ in the presence or absence of different concentrations of 19,20-EDP (Figure 5.17A). Reactions without NAD⁺ served as negative controls. The result of this experiment demonstrated that SIRT3, in the presence of 19,20-EDP, was able to deacetylate HDAC substrate at much lower concentrations of NAD⁺, than in the absence of 19,20-EDP (Figure 5.17B). To determine which kinetic parameters were enhanced by 19,20-EDP-induced SIRT3 activation, steady-state kinetic analyses were performed by measuring rates of reaction across varying NAD⁺ concentrations in

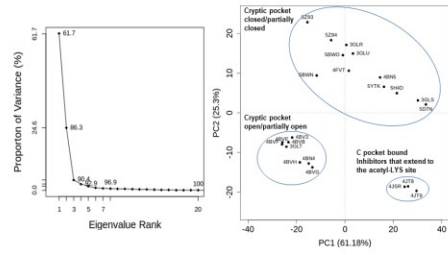
the presence or absence of 19,20-EDP and monitoring the formation of the deacylated product. Data were fitted to the Michaelis-Menten equation to solve for the intrinsic kinetic parameters of SIRT3 and to calculate V_{\max} , K_{mNAD^+} , k_{cat} and k_{cat}/K_{mNAD^+} (Figure 5.17C). Of these parameters, V_{\max} represents the maximum rate of reaction when the enzyme is saturated with substrate, k_{cat} is the turnover number that describes how many substrate molecules are transformed into products per unit time by a single enzyme, the K_{mNAD^+} value denotes the concentration of NAD^+ at half V_{\max} of SIRT3 activity and gives us a description of the affinity of the NAD^+ to SIRT3. Putting these two together to obtain the ratio k_{cat}/K_{mNAD^+} "catalytic efficiency" ratio allows a way to test how effective SIRT3 is on acetylated HDAC in the presence of different concentrations of NAD^+ or in other words measures the apparent rate of enzyme capture of the substrate to form a productive complex destined to form products. The greater the catalytic efficiency ratio, the higher the rate of catalysis is; conversely, the lower the ratio, the slower the catalysis is. Interestingly, we found that incubation of 19,20-EDP with SIRT3 resulted in a significantly enhanced SIRT3 activity in a concentration-dependent manner, but not OP2, as represented by a significant decrease in K_{mNAD^+} with no marked change in K_{cat} and consequently, a marked increase in the catalytic efficiency (k_{cat}/K_{mNAD^+}). This significant decrease in K_{mNAD^+} implies that 19,20-EDP significantly enhances SIRT3 activity mainly by improving its ability to capture its main co-factor NAD^+ , a finding that matches our docking and modelling results (Figure 5.16I). Importantly, the conducted hSIRT3 competition assay and kinetic analysis showed that OP2 blocks the enzymatic modulation exerted by 19,20-EDP, justifying our choice of this site as the most probable binding site for 19,20-EDP.

Afterwards, we assessed if 19,20-EDP can activate SIRT3 in a time-dependent manner. NRCMs were treated with 1 μ M 19,20-EDP and the mitochondrial SIRT3 activity was determined at different time points (1, 4, 16 and 30 hours). The results showed that 19,20-EDP can rapidly enhances SIRT3 activity within the first hour (Figure 5.17D). Collectively, these data indicated that 19,20-EDP is capable of enhancing mitochondrial SIRT3 activity within a short time period which was confirmed using the modelling and docking approaches.

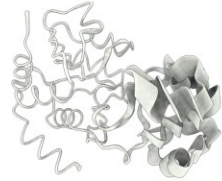
(A)



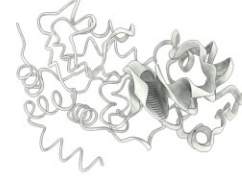
(B)



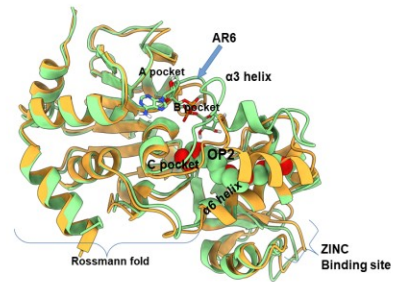
(C) PC1



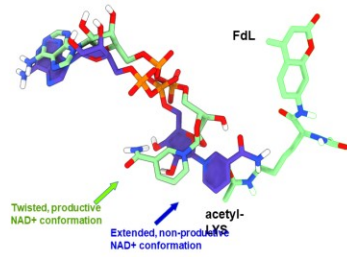
(D) PC2



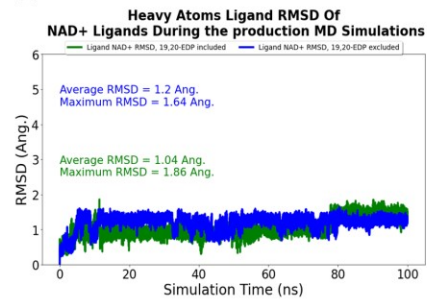
(E)



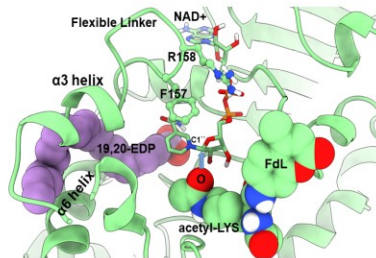
(F)



(G)



(H)



(I)

Parameter	Control	19,20-EDP (1 μ M)	OP2 (1 μ M)	19,20-EDP + OP2
V_{max} (AFU/min)	2644	2457	2365	2405
$K_{M_{NAD^+}}$ (μ M)	186.3	89.48	184	151
K_{cat} (min^{-1})	26.44	24.57	23.65	24.05
$K_{cat} / K_{M_{NAD^+}}$ ($min^{-1}\mu M^{-1}$) (Catalytic efficiency)	0.14	0.275	0.128	0.159

Figure 5. 16: 19,20-EDP directly binds and enhances the activity of the mitochondrial SIRT3. (A) The chemical structures of the molecules studied in the manuscript; NAD⁺, 19-20-EDP, OP2 and the modelled FdL dye. (B) Left panel, a scree plot showing the proportion of variance against its eigenvalue rank of the studied set of X-ray structures. In the right panel, a scatters plot showing the projection of the studied set of crystal structures on the top two largest eigenvectors in the PC space. Structures that are located at close proximity are grouped based on the corresponding values in the PC space. (C&D) Coil representations to visualize the motions along PC1 (left) and PC2 (right). (E) A structure superposition of the 4BN4 structure (light-green cartoon representation) as a representative for structures with an open allosteric pocket over the crystal structures of 5Z93 (orange cartoon representation) as a representative of structures with closed pocket. The 4BN4 structure is co-crystallized with AR6 (a NAD⁺ analogue without the nicotinamide motif), OP2 (shown as vdW spheres, with light-green carbon and red oxygen atoms) that binds the allosteric pocket and whose binding requires an apparent clock-wise motion of the α 3 helix, (F) A superposition for the 3 dimensional structures of NAD⁺ in the twisted productive conformation overlaid on the extended non-productive conformation. The extended conformation exhibits steric clashes with the acetyl-LYS binding site of the modelled FdL dye, (G) ligand heavy-atoms RMSD plot of NAD⁺ in the presence and in the absence of 19,20-EDP during the 100 ns production MD simulations, and (H) A model structure of the full reaction ready complex of hSIRT3 (shown in light-green cartoons) with bound allosteric modulator (19,20-EDP, shown as vdW spheres, with purple carbons and red oxygen atoms), cofactor (NAD⁺, shown in stick representation with light-green carbon, orange phosphorous, red oxygen, blue nitrogen, and white hydrogen atoms) and a model substrate (FdL, shown as vdW spheres with light-green carbons, red oxygen, blue nitrogen, and white hydrogen atoms). The side chains of critical flexible linker residues those are important for NAD⁺ binding (PHE157 & ARG158) are shown in ball and stick representations, with light-green carbon, yellow nitrogen and white hydrogen atoms. The first step of the proposed catalysis is the nucleophilic attack of the acetyl oxygen of the substrate on the electron-deficient anomeric C1'' atom of the NAD⁺ molecule. (I) SIRT3 kinetic values obtained using a Michaelis–Menten fit in the presence of the vehicle, 19,20-EDP, OP2 or 19,20-EDP + OP2.

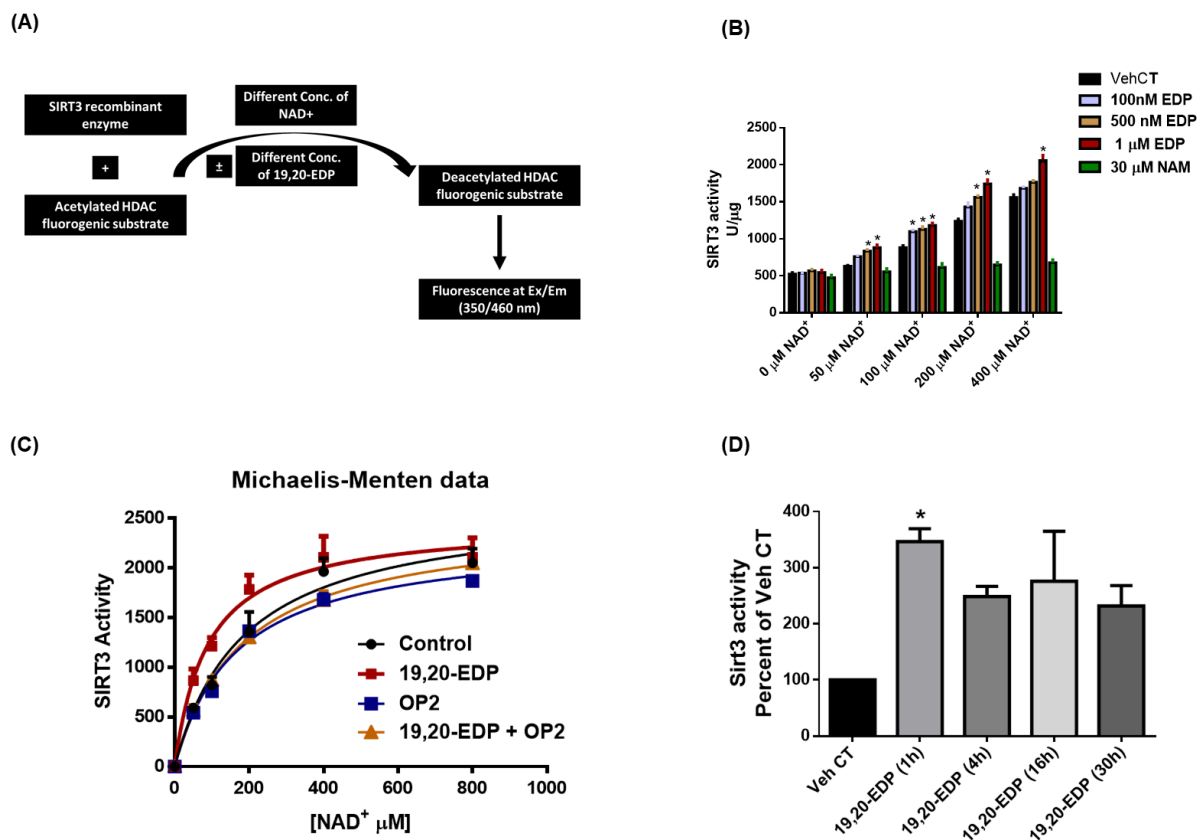


Figure 5. 17: Assessment of the effect of direct interaction between SIRT3 and 19,20-EDP. (A) A schematic diagram illustrating the experiment used for the assessment of the direct effect of 19,20-EDP on the activity SIRT3. (B) Bar chart showing the effect of different concentrations of 19,20-EDP on the activity of SIRT3 in the presence of different concentrations of the co-factor NAD⁺. (C) Michaelis–Menten fit for SIRT3 and its cofactor NAD⁺ in the presence of the vehicle, 19,20-EDP (1 μM), OP2 (1 μM) or 19,20-EDP (1 μM) + OP2 (1 μM). (D) Bar chart demonstrating the time-dependent effect of 19,20-EDP (1 μM) on SIRT3 activity in NRCMs. Values represent mean ± SEM; The significance of differences was determined by the use of one-way analysis of variance followed by a Tukey post hoc analysis; * p < 0.05 vs. vehicle control (n = 3 - 5).

5.4 Discussion

Despite the high number of studies and intense research describing the multiple biological and cardioprotective effects of the CYP-derived epoxylipids of n-3 PUFAs, there is still currently no known receptor or specific target for these metabolites [329, 811]. There have been candidates suggested for the receptor, however the identification of definite cellular targets remains elusive [329, 812, 813]. To the best of our knowledge, this study is the first to identify SIRT3 as a potential target for the epoxylipid 19,20-EDP and to reveal that direct binding of 19,20-EDP to SIRT3 significantly enhances its enzymatic activity. Beside the molecular modeling and docking approaches, we have proved this finding using several *in vitro*, *in situ* and *ex vivo* methods using NRCM, mouse and human cardiac tissues. This comprehensive analysis provides additional insight into the mechanism by which 19,20-EDP improves mitochondrial function and imparts cardioprotection against IR injury.

The current study demonstrated that SIRT3 function is suppressed not only secondary to IR injury but also in ischemic human myocardium resulting in hyperacetylation of several key mitochondrial proteins. This in turn contributes to impaired mitochondrial function and altered energy metabolism resulting in cardiac dysfunction. Therefore, activation and/or maintenance of SIRT3 activity, the master regulator of mitochondrial homeostasis, is indispensable for the preservation of mitochondrial quality and for limiting IR injury. In this study, the epoxylipid 19,20-EDP, as a direct SIRT3 activator, attenuated IR injury in mouse hearts through preventing mitochondrial damage as evidenced by enhanced antioxidant capacity, limited oxidative injury, stimulated glucose oxidation, and increased rates of ATP production. Moreover, 19,20-EDP treatment ameliorated ROS production and maintained mitochondrial density and membrane potential in NRCMs in the setting of HR. Interestingly, we have demonstrated that acute treatment

with 19,20-EDP is capable of improving impaired mitochondrial function (respiration) in explanted human ischemic heart tissue, a finding highly applicable to clinical settings. Importantly, inhibition of SIRT3 with the SIRT3 inhibitor NAM or 3-TYP blocked the cardioprotective effects of 19,20-EDP toward IR injury. In summary, 19,20-EDP, through direct activation of SIRT3, is capable of maintaining mitochondrial quality and consequently ameliorating IR injury.

5.4.1 Role of sirtuin 3 in regulating mitochondrial function

In the heart, mitochondria provide the main source of energy that fuels the contractile apparatus [52]. However, the importance of cardiac mitochondrial health and function is beyond ATP synthesis including cellular signaling, oxidative stress and biosynthetic pathways. Therefore, maintaining a healthy mitochondrial pool in the heart is indispensable for the maintenance of cellular homeostasis. The mitochondrial deacetylase SIRT3, through regulating the mitochondrial acetylome, plays a pivotal role in the maintenance of mitochondrial function including regulating energy metabolism, ATP production, antioxidant defense and inflammatory signaling [149, 694, 697, 725]. Accordingly, it has been shown that excessive lysine acetylation, associated with impaired SIRT3 function, disrupts protein function and mitochondrial quality, thereby compromising metabolic and respiratory reserve and increasing organ susceptibility to energetic stress and energy depletion [739]. For instance, it has been demonstrated recently that failing human myocardium is characterized by decreased expression of the mitochondrial deacetylase SIRT3 that was associated with increased global protein acetylation and enzymatic inhibition leading to impaired cardiac energy metabolism [814]. Therefore, it is plausible to conclude that preserving and enhancing SIRT3 enzymatic activity in the heart is essential for the maintenance of a healthy mitochondrial pool and thus ameliorating cardiovascular disorders. It is worth mentioning that experimental studies demonstrated that mitochondrial protein acetylation only

increases in the heart in the absence of SIRT3 but not the other mitochondrial sirtuins SIRT4 or SIRT5 [146].

5.4.2 Role of sirtuin 3 in mitigating ischemia reperfusion injury

Accumulating literature has showed that mitochondrial dysfunction secondary to loss or impairment of SIRT3 function has been implicated in several cardiovascular diseases including IR injury. For instance, it has been demonstrated that inhibition or the absence of one or both SIRT3 alleles in the heart (SIRT3^{-/+} or SIRT3^{-/-}) significantly aggravates the reduced cardiac recovery, increased infarct size and cell damage after IR injury. In addition, it has been shown that in the Sirt3^{-/-} hearts, the swelling, breakage, and disarrangement of mitochondria was aggravated after IR injury [157-159]. Moreover, it has been shown that H9c2 cells silenced for SIRT3 expression were more susceptible to IR injury [158]. Therefore, it has been suggested that, in the heart, overexpression or activation of SIRT3 protects cardiomyocytes from death [160]. In the same vein, we noticed in the current study that SIRT3 activity and/or expression was consistently reduced not only in isolated hearts subjected to IR injury but also in human ischemic LV tissues which was associated with increased acetylation and consequently decreased activity of the antioxidant MnSOD. However, perfusion or treatment with 19,20-EDP significantly improved SIRT3 function, enhanced mitochondrial quality and increased post-ischemic cardiac recovery. Conversely, 19,20-EDP-treatment did not improve cardiac function when SIRT3 was inhibited. These results strongly suggest that the beneficial cardiac effects of 19,20-EDP could be mediated through activation of SIRT3.

The availability of the cofactor NAD^+ is the rate-limiting factor of the functional deacetylase activity of SIRT3 [142]. In the current study, we proved that the physical interaction of hSIRT3 with 19,20-EDP may enhance SIRT3 deacetylase activity by stabilizing and increasing affinity of SIRT3 to NAD^+ . This increased affinity for NAD^+ could be vital in combating IR injury as it has been previously demonstrated that reduction of SIRT3 activity in hearts subjected to IR injury could be attributed to the reduction of NAD^+ . Di Lisa et al. reported that NAD^+ depletion during IR injury is partly due to the opening of the mitochondrial permeability transition pore (MPTP) leading to a release of mitochondrial NAD^+ into the cytosol where it is degraded by glycohydrolase [727]. Furthermore, during IR injury, ROS-induced damage leads to the production of single-strand breaks in the DNA which increases catabolism of NAD^+ , resulting in reduced level of NAD^+ [729]. The reduction of NAD^+ content limits the activation of SIRT3, thereby leading to a hyper-acetylation and inactivation of several mitochondrial proteins including MnSOD and complexes of ETC impairing mitochondrial function leading to cardiac dysfunction. Therefore, direct activation of SIRT3 by 19,20-EDP by increasing its affinity for NAD^+ help SIRT3 remain active under IR conditions. In agreement with this, we found that treatment with 19,20-EDP not only improved post-ischemic cardiac recovery in hearts subjected to IR injury but also improved mitochondrial respiration in human hearts with pre-existing MI.

Activation of SIRT3 by 19,20-EDP in the mitochondria can also replenish the lost NAD^+ levels. NADH generated in the glyceraldehyde 3 phosphate dehydrogenase reactions can be deoxidized to NAD^+ via the pyruvate dehydrogenase, the citric acid cycle and the mitochondrial ETC particularly that the activities of the enzymes involved in these pathways are regulated by acetylation controlled by SIRT3 [815-817]. These findings suggest that direct activation of SIRT3 by 19,20-EDP can have immediate consequences on the survival of cells under stress conditions.

5.4.3 Role of sirtuin 3 in regulating cardiac energy metabolism

Numerous studies have validated metabolic modulation as a promising therapy for improving cardiac efficiency secondary to IR injury [134, 784, 787, 788]. Following ischemia and during reperfusion, increased rates of fatty acid oxidation result in the subsequent inhibition of glucose oxidation rates contributing to cardiac dysfunction [134, 784]. Moreover, during reperfusion, myocardial glycolysis rates quickly recover, whereas glucose oxidation rates remains suppressed, resulting in the accumulation of lactate and protons [134]. Therefore, a plethora of studies showed that modulating metabolic changes by overcoming fatty acid oxidation-induced inhibition of glucose oxidation improves the recovery of post-ischemic cardiac function [134, 784, 787, 788, 795, 818]. Notably, it has been shown that enhancement of glucose oxidation is more crucial than the inhibition of fatty acid oxidation for metabolic modulation-induced cardiac protection [784]. Stimulation of glucose oxidation improves cardiac efficiency not only via decreasing oxygen consumption, as one molecule of glucose consumes less oxygen than one molecule of a fatty acid, but also by decreasing intracellular acidosis through improved coupling between glycolysis and glucose oxidation [134, 787, 795, 819] and consequently limiting cytosolic Ca^{2+} overload [820, 821]. Such approach is advantageous and a desirable strategy as an adjunct therapy for patients with IHD mainly due to the fact that metabolic modulation produces its effects independent of changes in cardiac hemodynamics [125, 793, 822].

Accumulating literature demonstrated that SIRT3 could be considered as a main regulator of the metabolic pathways and a key coordinator of global metabolic shifts that mediates beneficial effects in energy homeostasis within the mitochondria, through the deacetylation of numerous mitochondrial proteins involved in energy metabolism [153, 156, 697, 816, 817, 823]. Analysis of the mitochondrial acetylome revealed that over 60% of mitochondrial proteins contain

acetylation sites and that most of these proteins are involved in regulating energy metabolism, particularly fatty acid metabolism and tricarboxylic acid cycle (TCA) [739, 824-826]. In that sense, it has been demonstrated that the absence or inhibition of SIRT3 contributes to a dramatic hyperacetylation of mitochondrial proteins leading to severe metabolic perturbations [146, 697]. For instance, it has been demonstrated that SIRT3-deficient muscle exhibits mitochondrial dysfunction with a fuel switch characterized by increased reliance on fatty acid substrates and decreased reliance on glycolytic substrates [791]. Importantly, it has also been shown that loss of SIRT3 leads to the hyperacetylation of pyruvate dehydrogenase, the rate-limiting enzyme for glucose oxidation that contributed to a decrease in enzymatic activity leading to impaired glucose oxidation and ATP deprivation [814]. These aberrant changes in the metabolic pathways can exacerbate and accelerate the progression of IHDs. Accordingly, stimulating or maintaining the activity of SIRT3 might potentially ameliorate IR injury through mediating reprogramming in cardiac energy metabolism by promoting glucose utilization that fuels TCA and facilitates ETC-mediated ATP production to overcome the low energy input [146, 827]. Interestingly, in the current study, hearts perfused with 19,20-EDP ameliorated IR-induced SIRT3 loss, and improved glucose oxidation which could explain the improved cardiac efficiency observed in these hearts. In conclusion, we here show a novel regulatory pathway of the epoxy lipid 19,20-EDP in the hearts subjected to IR injury that involves activation of SIRT3. These findings might provide novel insights into the mechanism by which 19,20-EDP ameliorates IR injury.

5.4.4 Role of sirtuin 3 in ameliorating mitochondrial ROS production

Manganese superoxide dismutase (MnSOD) is the primary mitochondrial antioxidant enzyme [713]. Acetylation of MnSOD at the highly conserved catalytic center lysines 68 (K68) and 122 (K122) represents a major post-translational regulation that inhibits its enzymatic activity

[792]. SIRT3 can directly activates MnSOD in mitochondria by mediating its deacetylation at both catalytic sites (K68 and K122) significantly enhancing its antioxidant capacity and its ability to scavenge ROS [149, 712]. However, under IR conditions, the impairment of SIRT3 activity is associated with acetylation-induced inactivation of mitochondrial MnSOD rendering the enzyme inactive leading to excessive ROS production likely exceeds the antioxidant capacity of the mitochondria. Accordingly, the increased mitochondrial ROS production is implicated in the development of the oxidative damage [709]. For instance, it has been shown MnSOD activity was reduced in the heart of SIRT3^{+/-} mice [158] and SIRT3^{-/-} [157] hearts after oxidative stress induced by *ex vivo* IR. The reduced MnSOD activity was associated with increased oxidative damage to mitochondrial proteins [157]. Indeed, SIRT3 deficient cardiomyocytes produced double the levels of ROS than WT cells [155]. Conversely, activation of SIRT3 recovered MnSOD activity in WT hearts after IR [159] and abolished phenylephrine-induced ROS stimulation in NRCM [828]. Consistent with these studies, we observed in the current study that the IR-induced reduction in SIRT3 activity resulted in significantly elevated K68 and K122 acetylation and thus decline in the level of activated MnSOD. Intriguingly, hearts perfused with 19,20-EDP demonstrated preserved SIRT3 activity and reduced K68 and K122 MnSOD acetylation levels compared to the vehicle control IR group. This was also supported by assessment of ROS production in NRCMs after exposure to HR where treatment with 19,20-EDP significantly reduced ROS levels and maintained mitochondrial density and membrane potential. These effects of 19,20-EDP were absent when SIRT3 inhibitor NAM was added. These data thus demonstrated involvement of Sirt3-mediated signaling in the cardioprotective effects of 19,20-EDP against IR injury.

5.4.5 Role of sirtuin 3 in maintaining mitochondrial respiration

SIRT3 activity has been shown to positively correlate with oxygen consumption in isolated muscle mitochondria and to regulate mitochondrial respiration and ATP production in the heart through the deacetylation of mitochondrial complexes and subunits of the respiratory ETC [156, 803, 804, 829]. Accordingly, in several cardiac pathologies where SIRT3 is deficient or impaired, ATP levels were reduced which could be attributed to defective mitochondrial respiration portraying SIRT3 as a key player [156, 804, 817, 830, 831]. For instance, it has been shown SIRT3^{-/-} hearts have increased complex I and II acetylation which correlates with decreased mitochondrial respiration [152, 154, 156, 832, 833]. Also, there is evidence that SIRT3 interacts with subunits of complex V, ATP synthase, where SIRT3 downregulation increased the acetylation of complex V resulting in decreased enzymatic activity, impaired mitochondrial respiration and reduced ATP level [152, 834, 835]. Therefore, it has been hypothesized that activation of SIRT3 could activate mitochondrial respiration and increase ATP production through deacetylating different ETC complexes [814, 836]. In the current study and in agreement with these studies, the observed impaired mitochondrial respiration in human cardiac ischemic tissues in both non- and peri-infarct regions could be attributed to impaired SIRT3 activity. Importantly, this finding is in line with the research study conducted by Galan et al. where they demonstrated that after MI, reduction of mitochondrial respiration and oxidative phosphorylation occur in all LV regions including both MIadjacent and MIremote regions that was not substrate specific [752]. Interestingly, the addition of 19,20-EDP, through activating SIRT3, increased oxygen consumption and improved mitochondrial respiration in both non- and peri-infarct regions. 19,20-EDP could not alleviate these aberrant changes when SIRT3 is inhibited. Together, these results again suggest the cellular effects of 19,20-EDP could be mediated through activation of SIRT3.

5.4.6 Role of sirtuin 3 in limiting uncontrolled inflammatory responses

Sterile inflammatory responses and activation of innate immune system are considered hallmark and among the main pathological mechanisms contributing to myocardial IR injury [220, 837]. During reperfusion, the restoration of blood flow to the endangered myocardial region is followed by a sterile inflammatory response induced by the release of pro-inflammatory chemokines and cytokines, including several interleukins and tumor necrosis factor α (TNF α), among others [19, 88, 220, 838-840]. This uncontrolled inflammatory response is detrimental to the heart as it contributes to LV remodeling, induces the activation of proapoptotic signaling pathways and exacerbates cardiomyocyte death leading to poor clinical outcomes [197]. One explanation of this inflammatory surge secondary to IR injury is that during reperfusion the excessive ROS production from damaged mitochondria triggers the activation of different innate immune cells which in turn releases several pro-inflammatory cytokines and chemokines [264]. Therefore, it has been postulated that maintaining mitochondrial integrity and quality in the context of IR injury could limit this uncontrolled inflammatory response. Accordingly, it is reasonable to hypothesize that preserving SIRT3 activity, the master regulator of mitochondrial function and redox state, could limit this inflammatory response secondary to IR injury. Along the same line of evidence, it has been demonstrated that macrophages isolated from SIRT3 knockout mice exhibits significant changes in mitochondrial redox homeostasis, which are accompanied by pro-inflammatory-like phenotype alterations as a result of the activation of the NF- κ B pathway [841]. In the current study, we observed that perfusing the hearts subjected to IR injury with 19,20-EDP limited the inflammatory response and this effect was abolished by the addition of the SIRT3 inhibitor NAM. Again, these findings support that hypothesis that the cardioprotective effect of 19,20-EDP against IR injury involve the maintenance and activation of the mitochondrial SIRT3.

5.4.7 Computational structure analyses illustrating the direct binding of 19,20-EDP to sirtuin3

One major goal of the study was to unveil the mechanism by which 19,20-EDP modulates the enzymatic activity of hSIRT3. To achieve this goal, a series of computational structure analyses of available X-ray structures as well as molecular dynamics trajectories were performed. Our findings establish a direct connection between 19,20-EDP binding and the *in vitro* observed activation of the hSIRT3 catalyzed deacetylation reaction mediated by NAD⁺. In brief, the data suggests that 19,20-EDP is a positive allosteric modulator (PAM, i.e., catalytic enhancer). Previous structural studies have shown that ligands that occupy to the C-pocket (e.g. NAM) [744, 766] prevent the formation of the twisted, productive conformation of NAD⁺. However, through structural and energetic analysis, we have unambiguously shown that 19,20-EDP binds a hydrophobic cleft at the proximity of the C-pocket, stabilizing a productive, reaction-ready & twisted NAD⁺ conformation that otherwise will have a reduced population with respect to the non-productive extended NAD⁺ conformation. The reactive anomeric carbon (C1'') of the twisted NAD⁺ conformation is optimally poised toward the acetyl group of the simulated model substrate (FdL dye). A representative snapshot showing a hypothetical nearly reactive structure for the full complex (FdL/NAD⁺/19,20-EDP/hSIRT3) is given in Figure 5.16h. Conducted hSIRT3 competition assay and kinetic analysis showed that OP2 is a competitive inhibitor of the enzymatic modulation exerted by 19,20-EDP, justifying our choice of this site as the most probable binding site for 19,20-EDP.

Unlike the traditional view of allostery where the binding of a modulator results in wave-like propagation of strain energy to reach the binding site of the orthosteric ligand, affecting its conformations and/or dynamics [842], 19,20-EDP forms physical contacts (electrostatics &

H-bonding) with the nicotinamide motif of NAD⁺ in its twisted, productive conformation. 19,20-EDP augments the structural stabilization role played by some conserved C-pocket residues, such as ASP231 & ASN229 (according to hSIRT3 numbering scheme) as suggested by previous studies, including experimental mutational studies of members of the Sirtuins family of enzymes, including Sir2Tm. Example of these mutational studies is the one conducted by Avalos et al. who mutated C-pocket aspartate to asparagine (D103N mutation, according to the Sir2Tm numbering) to examine the importance of ASP residue on the presumed catalytic pathway. The results of that study strongly suggested that conserved acidic residues, typified by ASP231, play critical role in enzymatic activation, possibly through NAD⁺ stabilization [744]. The results also indicated that the twisted NAD⁺ conformation required for catalysis is strained and could be only accessible provided that an external stabilizer is involved; which is the role played by C-pocket aspartate, and we suggest here that 19,20-EDP is another potential stabilizer. Furthermore, our binding energy decomposition analysis showed that 19,20-EDP improve the binding affinities of critical residues to NAD⁺, such as PHE157 & ARG158. Taken together, 19,20-EDP can be grouped with other traditional NAD⁺ boosters, including NAD⁺ degradation inhibitors, pharmacological activators like Honokiol [836], NAD⁺ synthesis boosters and precursors [843, 844]. This opens an entire new range of possibilities for the longevity field where hSIRT3, and Sirtuins in general, are key players.

Although these structural and energetic analyses suggest that 19,20-EDP offers improved stabilities of the NAD⁺ molecule in the productive conformation, justifying hSIRT3 modulation by 19,20-EDP, other mechanisms of positive modulations are not entirely excluded. Examples of these mechanisms are stabilization of transition states (e.g. the O-alkyl amidate intermediate and the released nicotinamide), stabilizing local and global protein structures and lowering reaction barriers [845]. Investigating these potential mechanisms using higher resolution computational

methods, such as QM and QM/MM simulations, require validation from several experiments, including nuclear magnetic resonance (NMR), kinetic isotope and mutational experiments, and this will be the subject of future studies.

Our analysis provides a framework to discover other more potent positive modulators for hSIRT3. In principle, we believe that structural modifications for future positive modulators should leave the free carboxylate group of 19,20-EDP intact. Modifications on other sites of 19,20-EDP to enhance the acidity of the carboxylate group, i.e. lowering pKa, or increase the surface contacts with lipophilic residues lining the cavity should be attempted.

5.5 Conclusions and Future directions

A central approach to limit IR injury is the maintenance of mitochondrial integrity and function to help the heart adequately meet its own metabolic demands and consequently improve post-ischemic cardiac function. The current study highlighted 19,20-EDP as a promising new pharmacological agent for ameliorating IR injury. To the best of our knowledge, this study is the first to identify a target for the epoxy lipid 19,20-EDP and to report that direct physical binding of 19,20-EDP to SIRT3 significantly enhances its enzymatic activity improving mitochondrial function, enhancing cardiac energy metabolism and imparting cardioprotection against IR injury. We also demonstrated that acute treatment with 19,20-EDP, through activation of SIRT3, is capable of improving mitochondrial function in human cardiac tissues with pre-existing ischemic disease, a finding highly relevant to clinical cardiology. Therefore, 19,20-EDP holds tremendous promise as novel potential therapy that improve efficiency of mitochondrial energy production in ischemic cardiac tissue and that improve post-ischemic cardiac recovery via activation of SIRT3.

Chapter 6

Summary and conclusion

The main goal of the research work conducted in this thesis was to investigate the cardioprotective effects of the CYP-derived epoxy metabolites, particularly 19,20-EDP, in the setting of IR injury. Moreover, we aimed to explore the mechanism underlying these potential cardioprotective properties particularly that there is still currently no identified receptor or specific target for these metabolites. Furthermore, working with our collaborators, we attempted to generate and identify more chemically, and metabolically stable analogues based on the structure of 19,20-EDP, which have both mimetic and sEH inhibitory properties. The overall goal is to develop new therapies to mitigate cardiac IR injury and consequently improve the long-term clinical outcomes.

First, we investigated the differential cardioprotective effects of the n-3 PUFAs DHA and EPA as well as their corresponding CYP metabolites 19,20-EDP and 17,18-EEQ in the setting of IR injury. Furthermore, we examined their effects on the mitochondrial quality and the associated inflammatory response in the *ex vivo* Langendorff model of IR injury. Our data demonstrated that 19,20-EDP not only significantly suppressed the accumulation of the active NLRP3 protein in the cytosol after IR injury but also suppressed the IR-induced activation of caspase-1 and IL-1 β . Moreover, we showed that the cardioprotective effects of 19,20-EDP involve reduced mitochondrial injury as observed by the maintenance of Opa-1 levels, inhibition of the translocation of Drp-1 to the mitochondria and consequently better mitochondrial respiratory function. In addition, we provided evidence that the cardioprotective effects of DHA are mainly mediated by its metabolite 19,20-EDP. Collectively, the main findings in this study revealed a differential cardioprotective response between DHA, EPA, and their active metabolites toward IR injury. Interestingly, 19,20-EDP provided the best protection against IR injury via maintaining mitochondrial function and thereby reducing the detrimental NLRP3 inflammasome responses.

The results of the previous study have encouraged us to perform another study to investigate whether enhancing the cardiac levels of the CYP-derived epoxy metabolites, particularly 19,20-EDP, via genetic deletion or pharmacological inhibition of the sEH enzyme would also attenuate IR injury. Accordingly, isolated hearts from wild-type (WT) and sEH null mice were perfused in the Langendorff mode with either vehicle or the specific sEH inhibitor t-AUCB. Intriguingly, improved post-ischemic functional recovery and better mitochondrial respiration were observed in both sEH null hearts and WT hearts perfused with t-AUCB. Inhibition of sEH markedly attenuated the activation of the NLRP3 inflammasome complex and limited the mitochondrial localization of the fission protein Drp-1 triggered by IR injury. Together, these data consistently demonstrated that inhibiting sEH imparts cardioprotection against IR injury via maintaining post-ischemic mitochondrial function and attenuating a detrimental innate inflammatory response.

Despite the revealed salutary cardioprotective effects of 19,20-EDP, they are metabolically labile agents and accordingly have poor stability. This would limit their usefulness as a possible pharmacological or therapeutic modality clinically. Therefore, in a third study we tested the potential cardioprotective properties of synthetic 19,20-EDP analogs, that have enhanced chemical and metabolic stability, in the context of IR injury. The results showed that the perfusion of mouse hearts with the EDP surrogate, SA-26, significantly improved postischemic recovery, maintained cardiac ATP levels and attenuated activation of the NLRP3 inflammasome. Importantly, assessment of mitochondria in these hearts showed that SA-26 preserved the activity of sirtuin 3 (SIRT3) enzyme, the primary mitochondrial deacetylase that plays a pivotal role in regulating mitochondrial homeostasis and maintaining cardiac contractile function. These findings proposes that the novel synthetic analogues of 19,20-EDP offer new insights for the establishment of

pharmacological agents based on 19,20-EDP structure that could serve as a future clinical drug candidate.

Finally, we attempted to elucidate the mechanism by which 19,20-EDP maintains mitochondrial function and consequently limits the inflammatory response and attenuates the cardiac injury secondary to IR. Based on the findings from the previous studies, we proposed that the mitochondrial enzyme SIRT3, the main mitochondrial deacetylase, is involved in mediating the cardioprotective effects of 19,20-EDP against myocardial IR injury. In this study, we examined the effect of 19,20-EDP, in the presence and absence of SIRT3 inhibitors, on the activity of SIRT3, mitochondrial function, cardiac energy metabolism, and post-ischemic cardiac function using both the *ex vivo* Langendorff and the isolated working heart IR injury models. Interestingly, we revealed that perfusion of hearts with 19,20-EDP in the isolated working heart model preserved mitochondrial quality and improved cardiac energy metabolism via directly activating SIRT3 which resulted in improved post-ischemic cardiac recovery. Mitochondrial SIRT3 downstream targets and mitochondrial respiration were also assessed in human LV tissues obtained from individuals with IHD collected through the Human Explanted Heart Program and compared to NFC collected from unused transplant donors through the Human Organ Procurement and Exchange Program at the University of Alberta. Importantly, mitochondrial fractions obtained from the ischemic human myocardium showed decreased SIRT3 protein levels and activity while incubation of the fresh human ischemic cardiac fibers with 19,20-EDP markedly improved mitochondrial respiration and SIRT3 activity. Furthermore, an *in vitro* SIRT3 assay demonstrated that SIRT3, in the presence of 19,20-EDP, was able to deacetylate a specific substrate at much lower concentrations of NAD⁺. Consistently, using molecular modeling and docking approaches, we proved that 19,20-EDP, via directly binding to the human SIRT3 protein, acts as a positive

allosteric modulator (i.e., catalytic enhancer) that triggers SIRT3 activation. Importantly, the beneficial effects of 19,20-EDP were abolished by the use SIRT3 inhibitors. In conclusion, these data demonstrate that 19,20-EDP-mediated cardioprotective mechanisms against IR injury involve preservation and activation of mitochondrial SIRT3, which results in improved cardiac efficiency.

In summary, the data presented in this thesis highlight the beneficial role of the 19,20-EDP in limiting IR injury via activating SIRT3, maintaining mitochondrial homeostasis and limiting NLRP3 inflammasome activation. Moreover, to the best of our knowledge, this work is the first to identify SIRT3 as a potential target for the epoxy lipid 19,20-EDP and to reveal that direct binding of 19,20-EDP to SIRT3 significantly enhances its enzymatic activity. These studies provide new perspectives for the development of novel pharmacological agents, based on the 19,20-EDP structure, to improve the clinical outcomes in the setting of IR injury. All these findings add up to our understanding of the beneficial role of the CYP-derived epoxy metabolites on the cardiac mitochondrial quality and function and therefore underlines the need for continuing research in this field.

Chapter 7

Future Research Directions

The current thesis has focused on investigating the cardioprotective effects of 19,20-EDP and its synthetic analogues in the setting of IR injury. A fundamental consideration of this dissertation has been to investigate the molecular target and consequently the underlying cardioprotective mechanism of 19,20-EDP. In this thesis research work we provided evidence that 19,20-EDP, via directly activating SIRT3, maintains mitochondrial quality, limits uncontrolled immune responses, and consequently mitigates cardiac IR injury. This comprehensive analysis provides additional insight into the mechanism by which 19,20-EDP improves mitochondrial function and imparts cardioprotection against IR injury. The data presented in this thesis raises the potential for considerable amount of future research in order to elaborate more on the underlying mechanisms and translate these findings into clinical practice. Of importance, more research is required to investigate the following interesting points:

- 7.1 Assess the potential cardioprotective effects triggered by intervention with 19,20-EDP and its analogues at different time points during ischemia and after reperfusion in order to allow for further elucidation of the potential prophylactic and/or treatment properties of these epoxylipids as practically it is not always possible to predict when an individual will experience a heart attack. Understanding and exploring the effects of different time points administration/intervention is fundamental for the translational research of these metabolites.
- 7.2 Define the effective dose or concentration of 19,20-EDP that can be used against IR injury in the *in vivo* models by establishing a dose response curve particularly that most of the experiments were performed in heart tissue in isolation and consequently concentrations of 19,20-EDP in the *ex vivo* experiments cannot be extrapolated to *in vivo* models.

- 7.3 Determine the influence of chronic treatment with 19,20-EDP, versus acute settings, on the cardiac mitochondrial and contractile function as well as the associated long-term clinical outcomes secondary to IR injury.
- 7.4 Examine the ability of 19,20-EDP and its synthetic analogues to prevent the progression of cardiac injury secondary to IR to heart failure using different *in vivo* models.
- 7.5 Investigate whether treatment with 19,20-EDP could ameliorate the progression of other established CVD as heart failure and dilated cardiomyopathy.
- 7.6 Investigate whether systemic administration of 19,20-EDP could affect other mitochondrial-containing tissues and produce off-target effects not measured in the current experiments.
- 7.7 Study the possible differential effects of 19,20-EDP in protecting aged vs young myocardium against IR injury, focusing on possible sex differences.

As elderly population is considered the fastest growing age group worldwide, there is an increased interest in age-related diseases, particularly cardiac diseases. Of note, the pathophysiological progression of IR injury in elderly population is made more difficult by the multiple changes to cardiovascular structure and function that occur during normal aging. Moreover, evidence from animal models and humans indicate a decreased ability of the aged heart to tolerate stress compared to young counterparts [2, 846]. It is also worth mentioning that aged-associated changes to cardiac physiology may differ between females and males. Furthermore, several studies report clear sex discrepancies in clinical outcomes for patients with hearts subjected to IR injury. Therefore, exploring the effect of sex and/or age on the cardioprotective role of 19,20-EDP against IR injury becomes imperative.

- 7.8 Examine the cardioprotective effects of 19,20-EDP against IR injury in different animal models experiencing other concurrent diseases such as diabetes and hyperlipidemia. This will be fundamental studies in order to translate our findings in clinical settings as many human patients who experience IR injury suffer from comorbidities such as diabetes and hyperlipidemia. There is now growing evidence that many diseases such as hyperlipidemia and diabetes can affect the pathophysiology and development of IR injury independent of the vascular aspects [847, 848].
- 7.9 Test the binding affinity of the 19,20-EDP synthetic analogues to SIRT3 and whether this binding affects SIRT3 activity.
- 7.10 Examine whether 19,20-EDP is a ligand of another undiscovered cell membrane receptor, or if it binds to an already known receptor of possibly similar ligands.

REFERENCES

1. Wong, N.D., *Epidemiological studies of CHD and the evolution of preventive cardiology*. Nat Rev Cardiol, 2014. **11**(5): p. 276-89.
2. Paneni, F., et al., *The Aging Cardiovascular System: Understanding It at the Cellular and Clinical Levels*. J Am Coll Cardiol, 2017. **69**(15): p. 1952-1967.
3. Benjamin, E.J., et al., *Heart Disease and Stroke Statistics-2017 Update: A Report From the American Heart Association*. Circulation, 2017. **135**(10): p. e146-e603.
4. Roth, G.A., et al., *Demographic and epidemiologic drivers of global cardiovascular mortality*. N Engl J Med, 2015. **372**(14): p. 1333-41.
5. Ashley, E.A. and J. Niebauer, in *Cardiology Explained*. 2004: London.
6. Antman, E.M., et al., *ACC/AHA guidelines for the management of patients with ST-elevation myocardial infarction; A report of the American College of Cardiology/American Heart Association Task Force on Practice Guidelines (Committee to Revise the 1999 Guidelines for the Management of patients with acute myocardial infarction)*. J Am Coll Cardiol, 2004. **44**(3): p. E1-E211.
7. Libby, P. and P. Theroux, *Pathophysiology of coronary artery disease*. Circulation, 2005. **111**(25): p. 3481-8.
8. Alpert, J.S., et al., *Myocardial infarction redefined--a consensus document of The Joint European Society of Cardiology/American College of Cardiology Committee for the redefinition of myocardial infarction*. J Am Coll Cardiol, 2000. **36**(3): p. 959-69.
9. Jiang, S.L., X.P. Ji, and Y. Zhang, *[Introduction to ACC/AHA guidelines for the management of patients with ST-elevation myocardial infarction(2004 revision)]*. Zhonghua Yi Xue Za Zhi, 2005. **85**(1): p. 62-4.
10. Reimer, K.A., et al., *The wavefront phenomenon of ischemic cell death. 1. Myocardial infarct size vs duration of coronary occlusion in dogs*. Circulation, 1977. **56**(5): p. 786-94.
11. Frangogiannis, N.G., *Pathophysiology of Myocardial Infarction*. Compr Physiol, 2015. **5**(4): p. 1841-75.
12. Braunwald, E. and R.A. Kloner, *Myocardial reperfusion: a double-edged sword?* J Clin Invest, 1985. **76**(5): p. 1713-9.
13. Piper, H.M., D. Garcia-Dorado, and M. Ovize, *A fresh look at reperfusion injury*. Cardiovasc Res, 1998. **38**(2): p. 291-300.

14. Yellon, D.M. and D.J. Hausenloy, *Myocardial reperfusion injury*. N Engl J Med, 2007. **357**(11): p. 1121-35.
15. Jennings, R.B., et al., *Myocardial necrosis induced by temporary occlusion of a coronary artery in the dog*. Arch Pathol, 1960. **70**: p. 68-78.
16. Murry, C.E., R.B. Jennings, and K.A. Reimer, *Preconditioning with ischemia: a delay of lethal cell injury in ischemic myocardium*. Circulation, 1986. **74**(5): p. 1124-36.
17. Downey, J.M., A.M. Davis, and M.V. Cohen, *Signaling pathways in ischemic preconditioning*. Heart Fail Rev, 2007. **12**(3-4): p. 181-8.
18. Bulkley, G.B., *Free radical-mediated reperfusion injury: a selective review*. Br J Cancer Suppl, 1987. **8**: p. 66-73.
19. Hausenloy, D.J. and D.M. Yellon, *Myocardial ischemia-reperfusion injury: a neglected therapeutic target*. J Clin Invest, 2013. **123**(1): p. 92-100.
20. Kloner, R.A., *Stunned and Hibernating Myocardium: Where Are We Nearly 4 Decades Later?* J Am Heart Assoc, 2020. **9**(3): p. e015502.
21. Bolli, R. and E. Marban, *Molecular and cellular mechanisms of myocardial stunning*. Physiol Rev, 1999. **79**(2): p. 609-34.
22. Depre, C. and S.F. Vatner, *Cardioprotection in stunned and hibernating myocardium*. Heart Fail Rev, 2007. **12**(3-4): p. 307-17.
23. Kloner, R.A., et al., *Medical and cellular implications of stunning, hibernation, and preconditioning: an NHLBI workshop*. Circulation, 1998. **97**(18): p. 1848-67.
24. Depre, C. and S.F. Vatner, *Mechanisms of cell survival in myocardial hibernation*. Trends Cardiovasc Med, 2005. **15**(3): p. 101-10.
25. Slezak, J., et al., *Hibernating myocardium: pathophysiology, diagnosis, and treatment*. Can J Physiol Pharmacol, 2009. **87**(4): p. 252-65.
26. Kalogeris, T., et al., *Cell biology of ischemia/reperfusion injury*. Int Rev Cell Mol Biol, 2012. **298**: p. 229-317.
27. Weman, S.M., et al., *Reperfusion injury associated with one-fourth of deaths after coronary artery bypass grafting*. Ann Thorac Surg, 2000. **70**(3): p. 807-12.

28. Jernberg, T., et al., *Association between adoption of evidence-based treatment and survival for patients with ST-elevation myocardial infarction*. JAMA, 2011. **305**(16): p. 1677-84.
29. Gallone, G., et al., *Medical Therapy for Long-Term Prevention of Atherothrombosis Following an Acute Coronary Syndrome: JACC State-of-the-Art Review*. J Am Coll Cardiol, 2018. **72**(23 Pt A): p. 2886-2903.
30. Hennekens, C.H., et al., *Adjunctive drug therapy of acute myocardial infarction--evidence from clinical trials*. N Engl J Med, 1996. **335**(22): p. 1660-7.
31. Shahzad, A., et al., *Unfractionated heparin versus bivalirudin in primary percutaneous coronary intervention (HEAT-PPCI): an open-label, single centre, randomised controlled trial*. Lancet, 2014. **384**(9957): p. 1849-1858.
32. Stone, G.W., et al., *Bivalirudin during primary PCI in acute myocardial infarction*. N Engl J Med, 2008. **358**(21): p. 2218-30.
33. Montalescot, G., et al., *STEMI and NSTEMI: are they so different? 1 year outcomes in acute myocardial infarction as defined by the ESC/ACC definition (the OPERA registry)*. Eur Heart J, 2007. **28**(12): p. 1409-17.
34. Pedersen, F., et al., *Short- and long-term cause of death in patients treated with primary PCI for STEMI*. J Am Coll Cardiol, 2014. **64**(20): p. 2101-8.
35. Dirksen, M.T., et al., *Reperfusion injury in humans: a review of clinical trials on reperfusion injury inhibitory strategies*. Cardiovasc Res, 2007. **74**(3): p. 343-55.
36. Pfeffer, M.A. and E. Braunwald, *Ventricular remodeling after myocardial infarction. Experimental observations and clinical implications*. Circulation, 1990. **81**(4): p. 1161-72.
37. White, P.D., G.K. Mallory, and J. Salcedo-Salgar, *The Speed of Healing of Myocardial Infarcts*. Trans Am Clin Climatol Assoc, 1936. **52**: p. 97-104 1.
38. Mouton, A.J., O.J. Rivera, and M.L. Lindsey, *Myocardial infarction remodeling that progresses to heart failure: a signaling misunderstanding*. Am J Physiol Heart Circ Physiol, 2018. **315**(1): p. H71-H79.
39. Jones, A., S. Abramson, and J. Romanelli, *Simultaneous rupture of ventricular septum and papillary muscle as a mechanical complication of acute myocardial infarction*. J Am Coll Cardiol, 2011. **57**(7): p. e13.

40. Gajarsa, J.J. and R.A. Kloner, *Left ventricular remodeling in the post-infarction heart: a review of cellular, molecular mechanisms, and therapeutic modalities*. Heart Fail Rev, 2011. **16**(1): p. 13-21.
41. Gaudron, P., et al., *Progressive left ventricular dysfunction and remodeling after myocardial infarction. Potential mechanisms and early predictors*. Circulation, 1993. **87**(3): p. 755-63.
42. Sorescu, D. and K.K. Griendling, *Reactive oxygen species, mitochondria, and NAD(P)H oxidases in the development and progression of heart failure*. Congest Heart Fail, 2002. **8**(3): p. 132-40.
43. Daiber, A., et al., *Discovery of new therapeutic redox targets for cardioprotection against ischemia/reperfusion injury and heart failure*. Free Radic Biol Med, 2021. **163**: p. 325-343.
44. Heusch, G., *Myocardial ischaemia-reperfusion injury and cardioprotection in perspective*. Nat Rev Cardiol, 2020. **17**(12): p. 773-789.
45. Di Lisa, F., et al., *Mitochondrial pathways for ROS formation and myocardial injury: the relevance of p66(Shc) and monoamine oxidase*. Basic Res Cardiol, 2009. **104**(2): p. 131-9.
46. Baines, C.P., *The mitochondrial permeability transition pore and ischemia-reperfusion injury*. Basic Res Cardiol, 2009. **104**(2): p. 181-8.
47. Raedschelders, K., D.M. Ansley, and D.D. Chen, *The cellular and molecular origin of reactive oxygen species generation during myocardial ischemia and reperfusion*. Pharmacol Ther, 2012. **133**(2): p. 230-55.
48. Murphy, E. and C. Steenbergen, *Ion transport and energetics during cell death and protection*. Physiology (Bethesda), 2008. **23**: p. 115-23.
49. Sanada, S., I. Komuro, and M. Kitakaze, *Pathophysiology of myocardial reperfusion injury: preconditioning, postconditioning, and translational aspects of protective measures*. Am J Physiol Heart Circ Physiol, 2011. **301**(5): p. H1723-41.
50. Talukder, M.A., J.L. Zweier, and M. Periasamy, *Targeting calcium transport in ischaemic heart disease*. Cardiovasc Res, 2009. **84**(3): p. 345-52.
51. Kvietys, P.R. and D.N. Granger, *Role of reactive oxygen and nitrogen species in the vascular responses to inflammation*. Free Radic Biol Med, 2012. **52**(3): p. 556-592.

52. Murphy, E., et al., *Mitochondrial Function, Biology, and Role in Disease: A Scientific Statement From the American Heart Association*. *Circ Res*, 2016. **118**(12): p. 1960-91.
53. Page, E. and L.P. McCallister, *Quantitative electron microscopic description of heart muscle cells. Application to normal, hypertrophied and thyroxin-stimulated hearts*. *Am J Cardiol*, 1973. **31**(2): p. 172-81.
54. Williams, G.S., L. Boyman, and W.J. Lederer, *Mitochondrial calcium and the regulation of metabolism in the heart*. *J Mol Cell Cardiol*, 2015. **78**: p. 35-45.
55. Niemann, B., M. Schwarzer, and S. Rohrbach, *Heart and Mitochondria: Pathophysiology and Implications for Cardiac Surgeons*. *Thorac Cardiovasc Surg*, 2018. **66**(1): p. 11-19.
56. Baines, C.P., *The molecular composition of the mitochondrial permeability transition pore*. *J Mol Cell Cardiol*, 2009. **46**(6): p. 850-7.
57. Baines, C.P., *How and when do myocytes die during ischemia and reperfusion: the late phase*. *J Cardiovasc Pharmacol Ther*, 2011. **16**(3-4): p. 239-43.
58. Szydlowska, K. and M. Tymianski, *Calcium, ischemia and excitotoxicity*. *Cell Calcium*, 2010. **47**(2): p. 122-9.
59. Contreras, L., et al., *Mitochondria: the calcium connection*. *Biochim Biophys Acta*, 2010. **1797**(6-7): p. 607-18.
60. Dorn, G.W., 2nd and C. Maack, *SR and mitochondria: calcium cross-talk between kissing cousins*. *J Mol Cell Cardiol*, 2013. **55**: p. 42-9.
61. Croall, D.E. and K. Ersfeld, *The calpains: modular designs and functional diversity*. *Genome Biol*, 2007. **8**(6): p. 218.
62. Hernando, V., et al., *Calpain translocation and activation as pharmacological targets during myocardial ischemia/reperfusion*. *J Mol Cell Cardiol*, 2010. **49**(2): p. 271-9.
63. Sorimachi, Y., et al., *Downregulation of calpastatin in rat heart after brief ischemia and reperfusion*. *J Biochem*, 1997. **122**(4): p. 743-8.
64. Hausenloy, D.J. and D.M. Yellon, *Ischaemic conditioning and reperfusion injury*. *Nat Rev Cardiol*, 2016. **13**(4): p. 193-209.
65. Hausenloy, D.J. and D.M. Yellon, *The mitochondrial permeability transition pore: its fundamental role in mediating cell death during ischaemia and reperfusion*. *J Mol Cell Cardiol*, 2003. **35**(4): p. 339-41.

66. Heusch, G., K. Boengler, and R. Schulz, *Inhibition of mitochondrial permeability transition pore opening: the Holy Grail of cardioprotection*. Basic Res Cardiol, 2010. **105**(2): p. 151-4.
67. Griffiths, E.J. and A.P. Halestrap, *Mitochondrial non-specific pores remain closed during cardiac ischaemia, but open upon reperfusion*. Biochem J, 1995. **307** (Pt 1): p. 93-8.
68. Carraro, M. and P. Bernardi, *Calcium and reactive oxygen species in regulation of the mitochondrial permeability transition and of programmed cell death in yeast*. Cell Calcium, 2016. **60**(2): p. 102-7.
69. Martin, J.L., et al., *Mitochondrial mechanisms and therapeutics in ischaemia reperfusion injury*. Pediatr Nephrol, 2019. **34**(7): p. 1167-1174.
70. Hausenloy, D.J., et al., *Inhibiting mitochondrial permeability transition pore opening: a new paradigm for myocardial preconditioning?* Cardiovasc Res, 2002. **55**(3): p. 534-43.
71. Hausenloy, D.J., M.R. Duchon, and D.M. Yellon, *Inhibiting mitochondrial permeability transition pore opening at reperfusion protects against ischaemia-reperfusion injury*. Cardiovasc Res, 2003. **60**(3): p. 617-25.
72. Perrelli, M.G., P. Pagliaro, and C. Penna, *Ischemia/reperfusion injury and cardioprotective mechanisms: Role of mitochondria and reactive oxygen species*. World J Cardiol, 2011. **3**(6): p. 186-200.
73. Lee, H.L., et al., *Biphasic modulation of the mitochondrial electron transport chain in myocardial ischemia and reperfusion*. Am J Physiol Heart Circ Physiol, 2012. **302**(7): p. H1410-22.
74. Peoples, J.N., et al., *Mitochondrial dysfunction and oxidative stress in heart disease*. Exp Mol Med, 2019. **51**(12): p. 1-13.
75. Misra, M.K., et al., *Oxidative stress and ischemic myocardial syndromes*. Med Sci Monit, 2009. **15**(10): p. RA209-219.
76. Stowe, D.F. and A.K. Camara, *Mitochondrial reactive oxygen species production in excitable cells: modulators of mitochondrial and cell function*. Antioxid Redox Signal, 2009. **11**(6): p. 1373-414.
77. Arduini, A., et al., *Effect of ischemia and reperfusion on antioxidant enzymes and mitochondrial inner membrane proteins in perfused rat heart*. Biochim Biophys Acta, 1988. **970**(2): p. 113-21.

78. Jassem, W., et al., *Glyoxalase II and glutathione levels in rat liver mitochondria during cold storage in Euro-Collins and University of Wisconsin solutions*. *Transplantation*, 1996. **61**(9): p. 1416-20.
79. Dalton, T.P., H.G. Shertzer, and A. Puga, *Regulation of gene expression by reactive oxygen*. *Annu Rev Pharmacol Toxicol*, 1999. **39**: p. 67-101.
80. Solaini, G. and D.A. Harris, *Biochemical dysfunction in heart mitochondria exposed to ischaemia and reperfusion*. *Biochem J*, 2005. **390**(Pt 2): p. 377-94.
81. Halestrap, A.P., S.J. Clarke, and S.A. Javadov, *Mitochondrial permeability transition pore opening during myocardial reperfusion--a target for cardioprotection*. *Cardiovasc Res*, 2004. **61**(3): p. 372-85.
82. Richardson, A.G. and E.E. Schadt, *The role of macromolecular damage in aging and age-related disease*. *J Gerontol A Biol Sci Med Sci*, 2014. **69 Suppl 1**: p. S28-32.
83. Kuznetsov, A.V., et al., *The Role of Mitochondria in the Mechanisms of Cardiac Ischemia-Reperfusion Injury*. *Antioxidants (Basel)*, 2019. **8**(10).
84. Murphy, M.P., *How mitochondria produce reactive oxygen species*. *Biochem J*, 2009. **417**(1): p. 1-13.
85. Tahrir, F.G., et al., *Mitochondrial quality control in cardiac cells: Mechanisms and role in cardiac cell injury and disease*. *J Cell Physiol*, 2019. **234**(6): p. 8122-8133.
86. Chen, Q., et al., *Modulation of electron transport protects cardiac mitochondria and decreases myocardial injury during ischemia and reperfusion*. *Am J Physiol Cell Physiol*, 2007. **292**(1): p. C137-47.
87. Lesnefsky, E.J., et al., *Mitochondrial Dysfunction and Myocardial Ischemia-Reperfusion: Implications for Novel Therapies*. *Annu Rev Pharmacol Toxicol*, 2017. **57**: p. 535-565.
88. Eltzschig, H.K. and T. Eckle, *Ischemia and reperfusion--from mechanism to translation*. *Nat Med*, 2011. **17**(11): p. 1391-401.
89. Detmer, S.A. and D.C. Chan, *Functions and dysfunctions of mitochondrial dynamics*. *Nat Rev Mol Cell Biol*, 2007. **8**(11): p. 870-9.
90. Chen, L. and A.A. Knowlton, *Mitochondria and heart failure: new insights into an energetic problem*. *Minerva Cardioangiol*, 2010. **58**(2): p. 213-29.

91. Dorn, G.W., 2nd, *Mitochondrial dynamics in heart disease*. Biochim Biophys Acta, 2013. **1833**(1): p. 233-41.
92. Wang, W., C. Fernandez-Sanz, and S.S. Sheu, *Regulation of mitochondrial bioenergetics by the non-canonical roles of mitochondrial dynamics proteins in the heart*. Biochim Biophys Acta Mol Basis Dis, 2018. **1864**(5 Pt B): p. 1991-2001.
93. Song, M., et al., *Mitochondrial fission and fusion factors reciprocally orchestrate mitophagic culling in mouse hearts and cultured fibroblasts*. Cell Metab, 2015. **21**(2): p. 273-286.
94. Ono, T., et al., *Human cells are protected from mitochondrial dysfunction by complementation of DNA products in fused mitochondria*. Nat Genet, 2001. **28**(3): p. 272-5.
95. Chen, L. and A.A. Knowlton, *Mitochondrial dynamics in heart failure*. Congest Heart Fail, 2011. **17**(6): p. 257-61.
96. Kraus, F. and M.T. Ryan, *The constriction and scission machineries involved in mitochondrial fission*. J Cell Sci, 2017. **130**(18): p. 2953-2960.
97. Song, Z., et al., *Mitofusins and OPA1 mediate sequential steps in mitochondrial membrane fusion*. Mol Biol Cell, 2009. **20**(15): p. 3525-32.
98. Ishihara, N., et al., *Regulation of mitochondrial morphology through proteolytic cleavage of OPA1*. EMBO J, 2006. **25**(13): p. 2966-77.
99. Hoppins, S., L. Lackner, and J. Nunnari, *The machines that divide and fuse mitochondria*. Annu Rev Biochem, 2007. **76**: p. 751-80.
100. Sabbah, H.N., *Targeting the Mitochondria in Heart Failure: A Translational Perspective*. JACC Basic Transl Sci, 2020. **5**(1): p. 88-106.
101. Maneechote, C., et al., *Roles of mitochondrial dynamics modulators in cardiac ischaemia/reperfusion injury*. J Cell Mol Med, 2017. **21**(11): p. 2643-2653.
102. Vasquez-Trincado, C., et al., *Mitochondrial dynamics, mitophagy and cardiovascular disease*. J Physiol, 2016. **594**(3): p. 509-25.
103. Kim, H., et al., *Fine-tuning of Drp1/Fis1 availability by AKAP121/Siah2 regulates mitochondrial adaptation to hypoxia*. Mol Cell, 2011. **44**(4): p. 532-44.

104. Ingerman, E., et al., *Dnm1 forms spirals that are structurally tailored to fit mitochondria*. J Cell Biol, 2005. **170**(7): p. 1021-7.
105. Sharp, W.W., et al., *Dynamin-related protein 1 (Drp1)-mediated diastolic dysfunction in myocardial ischemia-reperfusion injury: therapeutic benefits of Drp1 inhibition to reduce mitochondrial fission*. FASEB J, 2014. **28**(1): p. 316-26.
106. Ong, S.B., et al., *Inhibiting mitochondrial fission protects the heart against ischemia/reperfusion injury*. Circulation, 2010. **121**(18): p. 2012-22.
107. Din, S., et al., *Pim-1 preserves mitochondrial morphology by inhibiting dynamin-related protein 1 translocation*. Proc Natl Acad Sci U S A, 2013. **110**(15): p. 5969-74.
108. Ishihara, N., Y. Eura, and K. Mihara, *Mitofusin 1 and 2 play distinct roles in mitochondrial fusion reactions via GTPase activity*. J Cell Sci, 2004. **117**(Pt 26): p. 6535-46.
109. Santel, A., et al., *Mitofusin-1 protein is a generally expressed mediator of mitochondrial fusion in mammalian cells*. J Cell Sci, 2003. **116**(Pt 13): p. 2763-74.
110. Li, J., et al., *Mitofusin 1 is negatively regulated by microRNA 140 in cardiomyocyte apoptosis*. Mol Cell Biol, 2014. **34**(10): p. 1788-99.
111. Nan, J., et al., *Molecular regulation of mitochondrial dynamics in cardiac disease*. Biochim Biophys Acta Mol Cell Res, 2017. **1864**(7): p. 1260-1273.
112. Shen, T., et al., *Mitofusin-2 is a major determinant of oxidative stress-mediated heart muscle cell apoptosis*. J Biol Chem, 2007. **282**(32): p. 23354-61.
113. Papanicolaou, K.N., et al., *Mitofusin-2 maintains mitochondrial structure and contributes to stress-induced permeability transition in cardiac myocytes*. Mol Cell Biol, 2011. **31**(6): p. 1309-28.
114. Hall, A.R., et al., *Hearts deficient in both Mfn1 and Mfn2 are protected against acute myocardial infarction*. Cell Death Dis, 2016. **7**: p. e2238.
115. Zhang, K., H. Li, and Z. Song, *Membrane depolarization activates the mitochondrial protease OMA1 by stimulating self-cleavage*. EMBO Rep, 2014. **15**(5): p. 576-85.
116. Boengler, K., G. Lochnit, and R. Schulz, *Mitochondria "THE" target of myocardial conditioning*. Am J Physiol Heart Circ Physiol, 2018. **315**(5): p. H1215-H1231.

117. Kubli, D.A., et al., *Bnip3 functions as a mitochondrial sensor of oxidative stress during myocardial ischemia and reperfusion*. Am J Physiol Heart Circ Physiol, 2008. **295**(5): p. H2025-31.
118. Hamacher-Brady, A., et al., *Response to myocardial ischemia/reperfusion injury involves Bnip3 and autophagy*. Cell Death Differ, 2007. **14**(1): p. 146-57.
119. Virbasius, J.V. and R.C. Scarpulla, *Activation of the human mitochondrial transcription factor A gene by nuclear respiratory factors: a potential regulatory link between nuclear and mitochondrial gene expression in organelle biogenesis*. Proc Natl Acad Sci U S A, 1994. **91**(4): p. 1309-13.
120. Kanki, T., et al., *Architectural role of mitochondrial transcription factor A in maintenance of human mitochondrial DNA*. Mol Cell Biol, 2004. **24**(22): p. 9823-34.
121. Thomas, L.W. and M. Ashcroft, *Exploring the molecular interface between hypoxia-inducible factor signalling and mitochondria*. Cell Mol Life Sci, 2019. **76**(9): p. 1759-1777.
122. Yue, R., et al., *Mitochondrial DNA oxidative damage contributes to cardiomyocyte ischemia/reperfusion-injury in rats: cardioprotective role of lycopene*. J Cell Physiol, 2015. **230**(9): p. 2128-41.
123. Yang, J., et al., *HDAC inhibition induces autophagy and mitochondrial biogenesis to maintain mitochondrial homeostasis during cardiac ischemia/reperfusion injury*. J Mol Cell Cardiol, 2019. **130**: p. 36-48.
124. Sanz, M.N., et al., *Cardioprotective reperfusion strategies differentially affect mitochondria: Studies in an isolated rat heart model of donation after circulatory death (DCD)*. Am J Transplant, 2019. **19**(2): p. 331-344.
125. Lopaschuk, G.D., et al., *Myocardial fatty acid metabolism in health and disease*. Physiol Rev, 2010. **90**(1): p. 207-58.
126. Neely, J.R., et al., *Effects of ischemia on function and metabolism of the isolated working rat heart*. Am J Physiol, 1973. **225**(3): p. 651-8.
127. Fedele, F.A., et al., *Metabolic response to prolonged reduction of myocardial blood flow distal to a severe coronary artery stenosis*. Circulation, 1988. **78**(3): p. 729-35.
128. Ussher, J.R. and G.D. Lopaschuk, *The malonyl CoA axis as a potential target for treating ischaemic heart disease*. Cardiovasc Res, 2008. **79**(2): p. 259-68.

129. Harmancey, R., et al., *Decreased long-chain fatty acid oxidation impairs postischemic recovery of the insulin-resistant rat heart*. FASEB J, 2013. **27**(10): p. 3966-78.
130. Hochachka, P.W. and T.P. Mommsen, *Protons and anaerobiosis*. Science, 1983. **219**(4591): p. 1391-7.
131. Di Lisa, F., et al., *Mitochondria and cardioprotection*. Heart Fail Rev, 2007. **12**(3-4): p. 249-60.
132. Van der Vusse, G.J., R.S. Reneman, and M. van Bilsen, *Accumulation of arachidonic acid in ischemic/reperfused cardiac tissue: possible causes and consequences*. Prostaglandins Leukot Essent Fatty Acids, 1997. **57**(1): p. 85-93.
133. Di Paola, M. and M. Lorusso, *Interaction of free fatty acids with mitochondria: coupling, uncoupling and permeability transition*. Biochim Biophys Acta, 2006. **1757**(9-10): p. 1330-7.
134. Liu, Q., et al., *High levels of fatty acids delay the recovery of intracellular pH and cardiac efficiency in post-ischemic hearts by inhibiting glucose oxidation*. J Am Coll Cardiol, 2002. **39**(4): p. 718-25.
135. Liedtke, A.J., S. Nellis, and J.R. Neely, *Effects of excess free fatty acids on mechanical and metabolic function in normal and ischemic myocardium in swine*. Circ Res, 1978. **43**(4): p. 652-61.
136. Randle, P.J., et al., *The glucose fatty-acid cycle. Its role in insulin sensitivity and the metabolic disturbances of diabetes mellitus*. Lancet, 1963. **1**(7285): p. 785-9.
137. How, O.J., et al., *Influence of substrate supply on cardiac efficiency, as measured by pressure-volume analysis in ex vivo mouse hearts*. Am J Physiol Heart Circ Physiol, 2005. **288**(6): p. H2979-85.
138. McCormack, J.G., et al., *Ranolazine stimulates glucose oxidation in normoxic, ischemic, and reperfused ischemic rat hearts*. Circulation, 1996. **93**(1): p. 135-42.
139. Lee, S., et al., *Energy-wasteful total Ca(2+) handling underlies increased O(2) cost of contractility in canine stunned heart*. Am J Physiol Heart Circ Physiol, 2000. **278**(5): p. H1464-72.
140. Trines, S.A., et al., *Oxygen wastage of stunned myocardium in vivo is due to an increased oxygen cost of contractility and a decreased myofibrillar efficiency*. Cardiovasc Res, 2001. **51**(1): p. 122-30.

141. Kim, S.C., et al., *Substrate and functional diversity of lysine acetylation revealed by a proteomics survey*. Mol Cell, 2006. **23**(4): p. 607-18.
142. Onyango, P., et al., *SIRT3, a human SIR2 homologue, is an NAD-dependent deacetylase localized to mitochondria*. Proc Natl Acad Sci U S A, 2002. **99**(21): p. 13653-8.
143. Shi, T., et al., *SIRT3, a mitochondrial sirtuin deacetylase, regulates mitochondrial function and thermogenesis in brown adipocytes*. J Biol Chem, 2005. **280**(14): p. 13560-7.
144. Schwer, B., et al., *The human silent information regulator (Sir)2 homologue hSIRT3 is a mitochondrial nicotinamide adenine dinucleotide-dependent deacetylase*. J Cell Biol, 2002. **158**(4): p. 647-57.
145. Michishita, E., et al., *Evolutionarily conserved and nonconserved cellular localizations and functions of human SIRT proteins*. Mol Biol Cell, 2005. **16**(10): p. 4623-35.
146. Lombard, D.B., et al., *Mammalian Sir2 homolog SIRT3 regulates global mitochondrial lysine acetylation*. Mol Cell Biol, 2007. **27**(24): p. 8807-14.
147. Bao, J., et al., *Characterization of the murine SIRT3 mitochondrial localization sequence and comparison of mitochondrial enrichment and deacetylase activity of long and short SIRT3 isoforms*. J Cell Biochem, 2010. **110**(1): p. 238-47.
148. Newman, J.C., W. He, and E. Verdin, *Mitochondrial protein acylation and intermediary metabolism: regulation by sirtuins and implications for metabolic disease*. J Biol Chem, 2012. **287**(51): p. 42436-43.
149. Qiu, X., et al., *Calorie restriction reduces oxidative stress by SIRT3-mediated SOD2 activation*. Cell Metab, 2010. **12**(6): p. 662-7.
150. Lin, S., et al., *Sirtuins in mitochondrial stress: Indispensable helpers behind the scenes*. Ageing Res Rev, 2018. **44**: p. 22-32.
151. Samant, S.A., et al., *SIRT3 deacetylates and activates OPA1 to regulate mitochondrial dynamics during stress*. Mol Cell Biol, 2014. **34**(5): p. 807-19.
152. Finley, L.W., et al., *Succinate dehydrogenase is a direct target of sirtuin 3 deacetylase activity*. PLoS One, 2011. **6**(8): p. e23295.
153. Cimen, H., et al., *Regulation of succinate dehydrogenase activity by SIRT3 in mammalian mitochondria*. Biochemistry, 2010. **49**(2): p. 304-11.

154. Koentges, C., et al., *SIRT3 deficiency impairs mitochondrial and contractile function in the heart*. Basic Res Cardiol, 2015. **110**(4): p. 36.
155. Sundaresan, N.R., et al., *Sirt3 blocks the cardiac hypertrophic response by augmenting Foxo3a-dependent antioxidant defense mechanisms in mice*. J Clin Invest, 2009. **119**(9): p. 2758-71.
156. Ahn, B.H., et al., *A role for the mitochondrial deacetylase Sirt3 in regulating energy homeostasis*. Proc Natl Acad Sci U S A, 2008. **105**(38): p. 14447-52.
157. Parodi-Rullan, R.M., et al., *High Sensitivity of SIRT3 Deficient Hearts to Ischemia-Reperfusion Is Associated with Mitochondrial Abnormalities*. Front Pharmacol, 2017. **8**: p. 275.
158. Porter, G.A., et al., *SIRT3 deficiency exacerbates ischemia-reperfusion injury: implication for aged hearts*. Am J Physiol Heart Circ Physiol, 2014. **306**(12): p. H1602-9.
159. Zhang, Y., et al., *Exogenous NAD(+) administration significantly protects against myocardial ischemia/reperfusion injury in rat model*. Am J Transl Res, 2016. **8**(8): p. 3342-50.
160. Sundaresan, N.R., et al., *SIRT3 is a stress-responsive deacetylase in cardiomyocytes that protects cells from stress-mediated cell death by deacetylation of Ku70*. Mol Cell Biol, 2008. **28**(20): p. 6384-401.
161. Klishadi, M.S., et al., *Losartan protects the heart against ischemia reperfusion injury: sirtuin3 involvement*. J Pharm Pharm Sci, 2015. **18**(1): p. 112-23.
162. Darwesh, A.M., et al., *A Synthetic Epoxydocosapentaenoic Acid Analogue Ameliorates Cardiac Ischemia/Reperfusion Injury: The Involvement of the Sirtuin 3-NLRP3 Pathway*. Int J Mol Sci, 2020. **21**(15).
163. Wei, L., et al., *Dihydromyricetin Ameliorates Cardiac Ischemia/Reperfusion Injury through Sirt3 Activation*. Biomed Res Int, 2019. **2019**: p. 6803943.
164. Wagner, G.R. and M.D. Hirschey, *Nonenzymatic protein acylation as a carbon stress regulated by sirtuin deacylases*. Mol Cell, 2014. **54**(1): p. 5-16.
165. Lee, C.F., et al., *Normalization of NAD+ Redox Balance as a Therapy for Heart Failure*. Circulation, 2016. **134**(12): p. 883-94.
166. Janeway, C.A., Jr. and R. Medzhitov, *Innate immune recognition*. Annu Rev Immunol, 2002. **20**: p. 197-216.

167. Medzhitov, R., *Innate immunity: quo vadis?* Nat Immunol, 2010. **11**(7): p. 551-3.
168. Arslan, F., D.P. de Kleijn, and G. Pasterkamp, *Innate immune signaling in cardiac ischemia*. Nat Rev Cardiol, 2011. **8**(5): p. 292-300.
169. Mann, D.L., *The emerging role of innate immunity in the heart and vascular system: for whom the cell tolls*. Circ Res, 2011. **108**(9): p. 1133-45.
170. Matzinger, P., *The danger model: a renewed sense of self*. Science, 2002. **296**(5566): p. 301-5.
171. Iwasaki, A. and R. Medzhitov, *Regulation of adaptive immunity by the innate immune system*. Science, 2010. **327**(5963): p. 291-5.
172. Iwasaki, A. and R. Medzhitov, *Control of adaptive immunity by the innate immune system*. Nat Immunol, 2015. **16**(4): p. 343-53.
173. Antonelli, M. and I. Kushner, *It's time to redefine inflammation*. FASEB J, 2017. **31**(5): p. 1787-1791.
174. Manthiram, K., et al., *The monogenic autoinflammatory diseases define new pathways in human innate immunity and inflammation*. Nat Immunol, 2017. **18**(8): p. 832-842.
175. Clark, R. and T. Kupper, *Old meets new: the interaction between innate and adaptive immunity*. J Invest Dermatol, 2005. **125**(4): p. 629-37.
176. Willerson, J.T. and P.M. Ridker, *Inflammation as a cardiovascular risk factor*. Circulation, 2004. **109**(21 Suppl 1): p. II2-10.
177. Zakyntinos, E. and N. Pappa, *Inflammatory biomarkers in coronary artery disease*. J Cardiol, 2009. **53**(3): p. 317-33.
178. Kaptoge, S., et al., *Inflammatory cytokines and risk of coronary heart disease: new prospective study and updated meta-analysis*. Eur Heart J, 2014. **35**(9): p. 578-89.
179. Golia, E., et al., *Inflammation and cardiovascular disease: from pathogenesis to therapeutic target*. Curr Atheroscler Rep, 2014. **16**(9): p. 435.
180. Zhao, Z.Q., et al., *Reperfusion induces myocardial apoptotic cell death*. Cardiovasc Res, 2000. **45**(3): p. 651-60.

181. Zhao, Z.Q., et al., *Progressively developed myocardial apoptotic cell death during late phase of reperfusion*. *Apoptosis*, 2001. **6**(4): p. 279-90.
182. Ong, S.B., et al., *Inflammation following acute myocardial infarction: Multiple players, dynamic roles, and novel therapeutic opportunities*. *Pharmacol Ther*, 2018. **186**: p. 73-87.
183. Prabhu, S.D. and N.G. Frangogiannis, *The Biological Basis for Cardiac Repair After Myocardial Infarction: From Inflammation to Fibrosis*. *Circ Res*, 2016. **119**(1): p. 91-112.
184. Arslan, F., et al., *Bridging innate immunity and myocardial ischemia/reperfusion injury: the search for therapeutic targets*. *Curr Pharm Des*, 2008. **14**(12): p. 1205-16.
185. Kain, V., S.D. Prabhu, and G.V. Halade, *Inflammation revisited: inflammation versus resolution of inflammation following myocardial infarction*. *Basic Res Cardiol*, 2014. **109**(6): p. 444.
186. Chan, J.K., et al., *Alarmins: awaiting a clinical response*. *J Clin Invest*, 2012. **122**(8): p. 2711-9.
187. Bliksoen, M., et al., *Increased circulating mitochondrial DNA after myocardial infarction*. *Int J Cardiol*, 2012. **158**(1): p. 132-4.
188. van Hout, G.P., et al., *Targeting danger-associated molecular patterns after myocardial infarction*. *Expert Opin Ther Targets*, 2016. **20**(2): p. 223-39.
189. Frantz, S., et al., *Toll4 (TLR4) expression in cardiac myocytes in normal and failing myocardium*. *J Clin Invest*, 1999. **104**(3): p. 271-80.
190. Ding, H.S., et al., *The HMGB1-TLR4 axis contributes to myocardial ischemia/reperfusion injury via regulation of cardiomyocyte apoptosis*. *Gene*, 2013. **527**(1): p. 389-93.
191. Chao, W., *Toll-like receptor signaling: a critical modulator of cell survival and ischemic injury in the heart*. *Am J Physiol Heart Circ Physiol*, 2009. **296**(1): p. H1-12.
192. Ionita, M.G., et al., *Endogenous inflammatory molecules engage Toll-like receptors in cardiovascular disease*. *J Innate Immun*, 2010. **2**(4): p. 307-15.
193. Riva, M., et al., *Induction of nuclear factor-kappaB responses by the S100A9 protein is Toll-like receptor-4-dependent*. *Immunology*, 2012. **137**(2): p. 172-82.
194. Scaffidi, P., T. Misteli, and M.E. Bianchi, *Release of chromatin protein HMGB1 by necrotic cells triggers inflammation*. *Nature*, 2002. **418**(6894): p. 191-5.

195. Marchant, D.J., et al., *Inflammation in myocardial diseases*. Circ Res, 2012. **110**(1): p. 126-44.
196. Coggins, M. and A. Rosenzweig, *The fire within: cardiac inflammatory signaling in health and disease*. Circ Res, 2012. **110**(1): p. 116-25.
197. Nian, M., et al., *Inflammatory cytokines and postmyocardial infarction remodeling*. Circ Res, 2004. **94**(12): p. 1543-53.
198. Ryckman, C., et al., *Proinflammatory activities of S100: proteins S100A8, S100A9, and S100A8/A9 induce neutrophil chemotaxis and adhesion*. J Immunol, 2003. **170**(6): p. 3233-42.
199. Bujak, M., et al., *Interleukin-1 receptor type I signaling critically regulates infarct healing and cardiac remodeling*. Am J Pathol, 2008. **173**(1): p. 57-67.
200. Mastrocola, R., et al., *Pharmacological Inhibition of NLRP3 Inflammasome Attenuates Myocardial Ischemia/Reperfusion Injury by Activation of RISK and Mitochondrial Pathways*. Oxid Med Cell Longev, 2016. **2016**: p. 5271251.
201. Bauernfeind, F.G., et al., *Cutting edge: NF-kappaB activating pattern recognition and cytokine receptors license NLRP3 inflammasome activation by regulating NLRP3 expression*. J Immunol, 2009. **183**(2): p. 787-91.
202. Mangan, M.S.J., et al., *Targeting the NLRP3 inflammasome in inflammatory diseases*. Nat Rev Drug Discov, 2018. **17**(8): p. 588-606.
203. Mezzaroma, E., S. Toldo, and A. Abbate, *Role of NLRP3 (cryopyrin) in acute myocardial infarction*. Cardiovasc Res, 2013. **99**(1): p. 225-6.
204. Mariathasan, S., et al., *Differential activation of the inflammasome by caspase-1 adaptors ASC and Ipaf*. Nature, 2004. **430**(6996): p. 213-8.
205. Kawaguchi, M., et al., *Inflammasome activation of cardiac fibroblasts is essential for myocardial ischemia/reperfusion injury*. Circulation, 2011. **123**(6): p. 594-604.
206. Mezzaroma, E., et al., *The inflammasome promotes adverse cardiac remodeling following acute myocardial infarction in the mouse*. Proc Natl Acad Sci U S A, 2011. **108**(49): p. 19725-30.
207. Qiu, Z., et al., *NLRP3 Inflammasome Activation-Mediated Pyroptosis Aggravates Myocardial Ischemia/Reperfusion Injury in Diabetic Rats*. Oxid Med Cell Longev, 2017. **2017**: p. 9743280.

208. Sandanger, O., et al., *The NLRP3 inflammasome is up-regulated in cardiac fibroblasts and mediates myocardial ischaemia-reperfusion injury*. Cardiovasc Res, 2013. **99**(1): p. 164-74.
209. Toldo, S. and A. Abbate, *The NLRP3 inflammasome in acute myocardial infarction*. Nat Rev Cardiol, 2018. **15**(4): p. 203-214.
210. van Hout, G.P., et al., *The selective NLRP3-inflammasome inhibitor MCC950 reduces infarct size and preserves cardiac function in a pig model of myocardial infarction*. Eur Heart J, 2017. **38**(11): p. 828-836.
211. Martinon, F., K. Burns, and J. Tschopp, *The inflammasome: a molecular platform triggering activation of inflammatory caspases and processing of proIL-beta*. Mol Cell, 2002. **10**(2): p. 417-26.
212. Juliana, C., et al., *Non-transcriptional priming and deubiquitination regulate NLRP3 inflammasome activation*. J Biol Chem, 2012. **287**(43): p. 36617-22.
213. Paik, S., et al., *An update on the regulatory mechanisms of NLRP3 inflammasome activation*. Cell Mol Immunol, 2021. **18**(5): p. 1141-1160.
214. Py, B.F., et al., *Deubiquitination of NLRP3 by BRCC3 critically regulates inflammasome activity*. Mol Cell, 2013. **49**(2): p. 331-8.
215. Shen, J., et al., *Membrane nanotubes facilitate the propagation of inflammatory injury in the heart upon overactivation of the beta-adrenergic receptor*. Cell Death Dis, 2020. **11**(11): p. 958.
216. Xin, J.Z., et al., *alpha1-AR overactivation induces cardiac inflammation through NLRP3 inflammasome activation*. Acta Pharmacol Sin, 2020. **41**(3): p. 311-318.
217. Saxena, A., et al., *IL-1 induces proinflammatory leukocyte infiltration and regulates fibroblast phenotype in the infarcted myocardium*. J Immunol, 2013. **191**(9): p. 4838-48.
218. Orn, S., et al., *Increased interleukin-1beta levels are associated with left ventricular hypertrophy and remodelling following acute ST segment elevation myocardial infarction treated by primary percutaneous coronary intervention*. J Intern Med, 2012. **272**(3): p. 267-76.
219. Swirski, F.K. and M. Nahrendorf, *Leukocyte behavior in atherosclerosis, myocardial infarction, and heart failure*. Science, 2013. **339**(6116): p. 161-6.

220. Nahrendorf, M., M.J. Pittet, and F.K. Swirski, *Monocytes: protagonists of infarct inflammation and repair after myocardial infarction*. *Circulation*, 2010. **121**(22): p. 2437-45.
221. Murray, P.J. and T.A. Wynn, *Protective and pathogenic functions of macrophage subsets*. *Nat Rev Immunol*, 2011. **11**(11): p. 723-37.
222. ter Horst, E.N., et al., *Modulators of Macrophage Polarization Influence Healing of the Infarcted Myocardium*. *Int J Mol Sci*, 2015. **16**(12): p. 29583-91.
223. Yan, X., et al., *Temporal dynamics of cardiac immune cell accumulation following acute myocardial infarction*. *J Mol Cell Cardiol*, 2013. **62**: p. 24-35.
224. Ma, Y., et al., *Temporal neutrophil polarization following myocardial infarction*. *Cardiovasc Res*, 2016. **110**(1): p. 51-61.
225. Engler, R.L., et al., *Accumulation of polymorphonuclear leukocytes during 3-h experimental myocardial ischemia*. *Am J Physiol*, 1986. **251**(1 Pt 2): p. H93-100.
226. Vinten-Johansen, J., *Involvement of neutrophils in the pathogenesis of lethal myocardial reperfusion injury*. *Cardiovasc Res*, 2004. **61**(3): p. 481-97.
227. Duilio, C., et al., *Neutrophils are primary source of O₂ radicals during reperfusion after prolonged myocardial ischemia*. *Am J Physiol Heart Circ Physiol*, 2001. **280**(6): p. H2649-57.
228. Engler, R.L., et al., *Role of leukocytes in response to acute myocardial ischemia and reflow in dogs*. *Am J Physiol*, 1986. **251**(2 Pt 2): p. H314-23.
229. Siminiak, T., N.A. Flores, and D.J. Sheridan, *Neutrophil interactions with endothelium and platelets: possible role in the development of cardiovascular injury*. *Eur Heart J*, 1995. **16**(2): p. 160-70.
230. Carbone, F., et al., *Pathophysiological role of neutrophils in acute myocardial infarction*. *Thromb Haemost*, 2013. **110**(3): p. 501-14.
231. Nahrendorf, M., et al., *The healing myocardium sequentially mobilizes two monocyte subsets with divergent and complementary functions*. *J Exp Med*, 2007. **204**(12): p. 3037-47.
232. Wantha, S., et al., *Neutrophil-derived cathelicidin promotes adhesion of classical monocytes*. *Circ Res*, 2013. **112**(5): p. 792-801.

233. Kumar, A.G., et al., *Induction of monocyte chemoattractant protein-1 in the small veins of the ischemic and reperfused canine myocardium*. *Circulation*, 1997. **95**(3): p. 693-700.
234. Birdsall, H.H., et al., *Complement C5a, TGF-beta 1, and MCP-1, in sequence, induce migration of monocytes into ischemic canine myocardium within the first one to five hours after reperfusion*. *Circulation*, 1997. **95**(3): p. 684-92.
235. Morimoto, H. and M. Takahashi, *Role of monocyte chemoattractant protein-1 in myocardial infarction*. *Int J Biomed Sci*, 2007. **3**(3): p. 159-67.
236. White, G.E., A.J. Iqbal, and D.R. Greaves, *CC chemokine receptors and chronic inflammation--therapeutic opportunities and pharmacological challenges*. *Pharmacol Rev*, 2013. **65**(1): p. 47-89.
237. Frangogiannis, N.G., et al., *Critical role of monocyte chemoattractant protein-1/CC chemokine ligand 2 in the pathogenesis of ischemic cardiomyopathy*. *Circulation*, 2007. **115**(5): p. 584-92.
238. Sager, H.B., et al., *Targeting Interleukin-1beta Reduces Leukocyte Production After Acute Myocardial Infarction*. *Circulation*, 2015. **132**(20): p. 1880-90.
239. Swirski, F.K., et al., *Identification of splenic reservoir monocytes and their deployment to inflammatory sites*. *Science*, 2009. **325**(5940): p. 612-6.
240. Leuschner, F., et al., *Rapid monocyte kinetics in acute myocardial infarction are sustained by extramedullary monocytopoiesis*. *J Exp Med*, 2012. **209**(1): p. 123-37.
241. Lambert, J.M., E.F. Lopez, and M.L. Lindsey, *Macrophage roles following myocardial infarction*. *Int J Cardiol*, 2008. **130**(2): p. 147-58.
242. Dutta, P. and M. Nahrendorf, *Monocytes in myocardial infarction*. *Arterioscler Thromb Vasc Biol*, 2015. **35**(5): p. 1066-70.
243. Epelman, S., et al., *Embryonic and adult-derived resident cardiac macrophages are maintained through distinct mechanisms at steady state and during inflammation*. *Immunity*, 2014. **40**(1): p. 91-104.
244. Hanna, R.N., et al., *The transcription factor NR4A1 (Nur77) controls bone marrow differentiation and the survival of Ly6C- monocytes*. *Nat Immunol*, 2011. **12**(8): p. 778-85.
245. Hilgendorf, I., et al., *Ly-6Chigh monocytes depend on Nr4a1 to balance both inflammatory and reparative phases in the infarcted myocardium*. *Circ Res*, 2014. **114**(10): p. 1611-22.

246. van Amerongen, M.J., et al., *Macrophage depletion impairs wound healing and increases left ventricular remodeling after myocardial injury in mice*. Am J Pathol, 2007. **170**(3): p. 818-29.
247. Leblond, A.L., et al., *Systemic and Cardiac Depletion of M2 Macrophage through CSF-1R Signaling Inhibition Alters Cardiac Function Post Myocardial Infarction*. PLoS One, 2015. **10**(9): p. e0137515.
248. Frantz, S. and M. Nahrendorf, *Cardiac macrophages and their role in ischaemic heart disease*. Cardiovasc Res, 2014. **102**(2): p. 240-8.
249. Fujiu, K., J. Wang, and R. Nagai, *Cardioprotective function of cardiac macrophages*. Cardiovasc Res, 2014. **102**(2): p. 232-9.
250. Dewald, O., et al., *CCL2/Monocyte Chemoattractant Protein-1 regulates inflammatory responses critical to healing myocardial infarcts*. Circ Res, 2005. **96**(8): p. 881-9.
251. Westman, P.C., et al., *Inflammation as a Driver of Adverse Left Ventricular Remodeling After Acute Myocardial Infarction*. J Am Coll Cardiol, 2016. **67**(17): p. 2050-60.
252. Bujak, M. and N.G. Frangogiannis, *The role of TGF-beta signaling in myocardial infarction and cardiac remodeling*. Cardiovasc Res, 2007. **74**(2): p. 184-95.
253. Deten, A., et al., *Changes in extracellular matrix and in transforming growth factor beta isoforms after coronary artery ligation in rats*. J Mol Cell Cardiol, 2001. **33**(6): p. 1191-207.
254. Shi, Y. and J. Massague, *Mechanisms of TGF-beta signaling from cell membrane to the nucleus*. Cell, 2003. **113**(6): p. 685-700.
255. Schiller, M., D. Javelaud, and A. Mauviel, *TGF-beta-induced SMAD signaling and gene regulation: consequences for extracellular matrix remodeling and wound healing*. J Dermatol Sci, 2004. **35**(2): p. 83-92.
256. Wang, B., et al., *Decreased Smad 7 expression contributes to cardiac fibrosis in the infarcted rat heart*. Am J Physiol Heart Circ Physiol, 2002. **282**(5): p. H1685-96.
257. Hao, J., et al., *Elevation of expression of Smads 2, 3, and 4, decorin and TGF-beta in the chronic phase of myocardial infarct scar healing*. J Mol Cell Cardiol, 1999. **31**(3): p. 667-78.

258. Matsumoto-Ida, M., et al., *Activation of TGF-beta1-TAK1-p38 MAPK pathway in spared cardiomyocytes is involved in left ventricular remodeling after myocardial infarction in rats*. Am J Physiol Heart Circ Physiol, 2006. **290**(2): p. H709-15.
259. Yu, J., et al., *Inflammasome activation leads to Caspase-1-dependent mitochondrial damage and block of mitophagy*. Proc Natl Acad Sci U S A, 2014. **111**(43): p. 15514-9.
260. Gurung, P., J.R. Lukens, and T.D. Kanneganti, *Mitochondria: diversity in the regulation of the NLRP3 inflammasome*. Trends Mol Med, 2015. **21**(3): p. 193-201.
261. Mohanty, A., R. Tiwari-Pandey, and N.R. Pandey, *Mitochondria: the indispensable players in innate immunity and guardians of the inflammatory response*. J Cell Commun Signal, 2019. **13**(3): p. 303-318.
262. Takahashi, M., *NLRP3 inflammasome as a novel player in myocardial infarction*. Int Heart J, 2014. **55**(2): p. 101-5.
263. Tschopp, J. and K. Schroder, *NLRP3 inflammasome activation: The convergence of multiple signalling pathways on ROS production?* Nat Rev Immunol, 2010. **10**(3): p. 210-5.
264. Pantazi, E., et al., *Role of sirtuins in ischemia-reperfusion injury*. World J Gastroenterol, 2013. **19**(43): p. 7594-602.
265. Jo, E.K., et al., *Molecular mechanisms regulating NLRP3 inflammasome activation*. Cell Mol Immunol, 2016. **13**(2): p. 148-59.
266. Naik, E. and V.M. Dixit, *Mitochondrial reactive oxygen species drive proinflammatory cytokine production*. J Exp Med, 2011. **208**(3): p. 417-20.
267. Li, X., et al., *Targeting mitochondrial reactive oxygen species as novel therapy for inflammatory diseases and cancers*. J Hematol Oncol, 2013. **6**: p. 19.
268. Oyama, J., et al., *Reduced myocardial ischemia-reperfusion injury in toll-like receptor 4-deficient mice*. Circulation, 2004. **109**(6): p. 784-9.
269. Favre, J., et al., *Toll-like receptors 2-deficient mice are protected against postischemic coronary endothelial dysfunction*. Arterioscler Thromb Vasc Biol, 2007. **27**(5): p. 1064-71.
270. Shishido, T., et al., *Toll-like receptor-2 modulates ventricular remodeling after myocardial infarction*. Circulation, 2003. **108**(23): p. 2905-10.

271. Timmers, L., et al., *Toll-like receptor 4 mediates maladaptive left ventricular remodeling and impairs cardiac function after myocardial infarction*. *Circ Res*, 2008. **102**(2): p. 257-64.
272. Yuan, L., et al., *Vaspin protects rats against myocardial ischemia/reperfusion injury (MIRI) through the TLR4/NF-kappaB signaling pathway*. *Eur J Pharmacol*, 2018. **835**: p. 132-139.
273. Zhang, G., et al., *Long-term oral atazanavir attenuates myocardial infarction-induced cardiac fibrosis*. *Eur J Pharmacol*, 2018. **828**: p. 97-102.
274. Wu, D.M., et al., *Tanshinone IIA prevents left ventricular remodeling via the TLR4/MyD88/NF-kappaB signalling pathway in rats with myocardial infarction*. *J Cell Mol Med*, 2018. **22**(6): p. 3058-3072.
275. Coll, R.C., et al., *A small-molecule inhibitor of the NLRP3 inflammasome for the treatment of inflammatory diseases*. *Nat Med*, 2015. **21**(3): p. 248-55.
276. Marchetti, C., et al., *A novel pharmacologic inhibitor of the NLRP3 inflammasome limits myocardial injury after ischemia-reperfusion in the mouse*. *J Cardiovasc Pharmacol*, 2014. **63**(4): p. 316-322.
277. Toldo, S., et al., *Inhibition of the NLRP3 inflammasome limits the inflammatory injury following myocardial ischemia-reperfusion in the mouse*. *Int J Cardiol*, 2016. **209**: p. 215-20.
278. Pomerantz, B.J., et al., *Inhibition of caspase 1 reduces human myocardial ischemic dysfunction via inhibition of IL-18 and IL-1beta*. *Proc Natl Acad Sci U S A*, 2001. **98**(5): p. 2871-6.
279. Yu, W., et al., *Selective Activation of Cannabinoid Receptor 2 Attenuates Myocardial Infarction via Suppressing NLRP3 Inflammasome*. *Inflammation*, 2018.
280. Wang, Q., et al., *Ghrelin protects the heart against ischemia/reperfusion injury via inhibition of TLR4/NLRP3 inflammasome pathway*. *Life Sci*, 2017. **186**: p. 50-58.
281. Hayashidani, S., et al., *Anti-monocyte chemoattractant protein-1 gene therapy attenuates left ventricular remodeling and failure after experimental myocardial infarction*. *Circulation*, 2003. **108**(17): p. 2134-40.
282. Kaikita, K., et al., *Targeted deletion of CC chemokine receptor 2 attenuates left ventricular remodeling after experimental myocardial infarction*. *Am J Pathol*, 2004. **165**(2): p. 439-47.

283. Liehn, E.A., et al., *A new monocyte chemotactic protein-1/chemokine CC motif ligand-2 competitor limiting neointima formation and myocardial ischemia/reperfusion injury in mice*. J Am Coll Cardiol, 2010. **56**(22): p. 1847-57.
284. Wang, J., et al., *Effect of CCR2 inhibitor-loaded lipid micelles on inflammatory cell migration and cardiac function after myocardial infarction*. Int J Nanomedicine, 2018. **13**: p. 6441-6451.
285. Weirather, J., et al., *Foxp3+ CD4+ T cells improve healing after myocardial infarction by modulating monocyte/macrophage differentiation*. Circ Res, 2014. **115**(1): p. 55-67.
286. Courties, G., et al., *In vivo silencing of the transcription factor IRF5 reprograms the macrophage phenotype and improves infarct healing*. J Am Coll Cardiol, 2014. **63**(15): p. 1556-66.
287. Harel-Adar, T., et al., *Modulation of cardiac macrophages by phosphatidylserine-presenting liposomes improves infarct repair*. Proc Natl Acad Sci U S A, 2011. **108**(5): p. 1827-32.
288. Heinen, A., et al., *IGF1 Treatment Improves Cardiac Remodeling after Infarction by Targeting Myeloid Cells*. Mol Ther, 2019. **27**(1): p. 46-58.
289. An, W., et al., *Exogenous IL-19 attenuates acute ischaemic injury and improves survival in male mice with myocardial infarction*. Br J Pharmacol, 2018.
290. Tokutome, M., et al., *PPARgamma-targeting Nanomedicine Promotes Cardiac Healing After Acute Myocardial Infarction by Skewing Monocyte/Macrophage Polarization in Preclinical Animal Models*. Cardiovasc Res, 2018.
291. Bujak, M., et al., *Essential role of Smad3 in infarct healing and in the pathogenesis of cardiac remodeling*. Circulation, 2007. **116**(19): p. 2127-38.
292. Tan, S.M., et al., *Targeted inhibition of activin receptor-like kinase 5 signaling attenuates cardiac dysfunction following myocardial infarction*. Am J Physiol Heart Circ Physiol, 2010. **298**(5): p. H1415-25.
293. Han, A., et al., *Qiliqiangxin Attenuates Cardiac Remodeling via Inhibition of TGF-beta1/Smad3 and NF-kappaB Signaling Pathways in a Rat Model of Myocardial Infarction*. Cell Physiol Biochem, 2018. **45**(5): p. 1797-1806.
294. Liu, Z.Y., et al., *Downregulated microRNA-330 suppresses left ventricular remodeling via the TGF-beta1/Smad3 signaling pathway by targeting SRY in mice with myocardial ischemia-reperfusion injury*. J Cell Physiol, 2018.

295. Liang, Z.G., et al., *MicroRNA20b5p promotes ventricular remodeling by targeting the TGFbeta/Smad signaling pathway in a rat model of ischemiareperfusion injury*. Int J Mol Med, 2018. **42**(2): p. 975-987.
296. Sprecher, H., *Biochemistry of essential fatty acids*. Prog Lipid Res, 1981. **20**: p. 13-22.
297. Burdge, G.C. and P.C. Calder, *Introduction to fatty acids and lipids*. World Rev Nutr Diet, 2015. **112**: p. 1-16.
298. Baker, E.J., et al., *Metabolism and functional effects of plant-derived omega-3 fatty acids in humans*. Prog Lipid Res, 2016. **64**: p. 30-56.
299. Lattka, E., et al., *Genetic variants of the FADS1 FADS2 gene cluster as related to essential fatty acid metabolism*. Curr Opin Lipidol, 2010. **21**(1): p. 64-9.
300. Arterburn, L.M., E.B. Hall, and H. Oken, *Distribution, interconversion, and dose response of n-3 fatty acids in humans*. Am J Clin Nutr, 2006. **83**(6 Suppl): p. 1467S-1476S.
301. Burr, M.L., *Lessons from the story of n-3 fatty acids*. Am J Clin Nutr, 2000. **71**(1 Suppl): p. 397S-8S.
302. Dyerberg, J., et al., *Eicosapentaenoic acid and prevention of thrombosis and atherosclerosis?* Lancet, 1978. **2**(8081): p. 117-9.
303. Bang, H.O., J. Dyerberg, and A.B. Nielsen, *Plasma lipid and lipoprotein pattern in Greenlandic West-coast Eskimos*. Lancet, 1971. **1**(7710): p. 1143-5.
304. Bucher, H.C., et al., *N-3 polyunsaturated fatty acids in coronary heart disease: a meta-analysis of randomized controlled trials*. Am J Med, 2002. **112**(4): p. 298-304.
305. Studer, M., et al., *Effect of different antilipidemic agents and diets on mortality: a systematic review*. Arch Intern Med, 2005. **165**(7): p. 725-30.
306. Burr, M.L., et al., *Effects of changes in fat, fish, and fibre intakes on death and myocardial reinfarction: diet and reinfarction trial (DART)*. Lancet, 1989. **2**(8666): p. 757-61.
307. Marchioli, R., et al., *Early protection against sudden death by n-3 polyunsaturated fatty acids after myocardial infarction: time-course analysis of the results of the Gruppo Italiano per lo Studio della Sopravvivenza nell'Infarto Miocardico (GISSI)-Prevenzione*. Circulation, 2002. **105**(16): p. 1897-903.

308. Kromhout, D., E.B. Bosschieter, and C. de Lezenne Coulander, *The inverse relation between fish consumption and 20-year mortality from coronary heart disease*. N Engl J Med, 1985. **312**(19): p. 1205-9.
309. Erkkila, A.T., et al., *Higher plasma docosahexaenoic acid is associated with reduced progression of coronary atherosclerosis in women with CAD*. J Lipid Res, 2006. **47**(12): p. 2814-9.
310. Mozaffarian, D., R. Micha, and S. Wallace, *Effects on coronary heart disease of increasing polyunsaturated fat in place of saturated fat: a systematic review and meta-analysis of randomized controlled trials*. PLoS Med, 2010. **7**(3): p. e1000252.
311. Lee, J.H., et al., *Omega-3 fatty acids for cardioprotection*. Mayo Clin Proc, 2008. **83**(3): p. 324-32.
312. Kris-Etherton, P.M., et al., *Fish consumption, fish oil, omega-3 fatty acids, and cardiovascular disease*. Arterioscler Thromb Vasc Biol, 2003. **23**(2): p. e20-30.
313. Mozaffarian, D., *JELIS, fish oil, and cardiac events*. Lancet, 2007. **369**(9567): p. 1062-3.
314. Mozaffarian, D. and J.H. Wu, *Omega-3 fatty acids and cardiovascular disease: effects on risk factors, molecular pathways, and clinical events*. J Am Coll Cardiol, 2011. **58**(20): p. 2047-67.
315. Swedberg, K., *n-3 Fatty acids in cardiovascular disease*. N Engl J Med, 2011. **365**(12): p. 1159; author reply 1159.
316. Lee, J.H., et al., *Omega-3 fatty acids: cardiovascular benefits, sources and sustainability*. Nature Reviews Cardiology, 2009. **6**: p. 753.
317. Mozaffarian, D., et al., *Plasma phospholipid long-chain omega-3 fatty acids and total and cause-specific mortality in older adults: a cohort study*. Ann Intern Med, 2013. **158**(7): p. 515-25.
318. Hooper, L., et al., *Risks and benefits of omega 3 fats for mortality, cardiovascular disease, and cancer: systematic review*. BMJ, 2006. **332**(7544): p. 752-60.
319. Kromhout, D., et al., *n-3 fatty acids and cardiovascular events after myocardial infarction*. N Engl J Med, 2010. **363**(21): p. 2015-26.
320. Rauch, B., et al., *OMEGA, a randomized, placebo-controlled trial to test the effect of highly purified omega-3 fatty acids on top of modern guideline-adjusted therapy after myocardial infarction*. Circulation, 2010. **122**(21): p. 2152-9.

321. Galan, P., et al., *Effects of B vitamins and omega 3 fatty acids on cardiovascular diseases: a randomised placebo controlled trial*. *BMJ*, 2010. **341**: p. c6273.
322. Galan, P., et al., *The SU.FOL.OM3 Study: a secondary prevention trial testing the impact of supplementation with folate and B-vitamins and/or Omega-3 PUFA on fatal and non fatal cardiovascular events, design, methods and participants characteristics*. *Trials*, 2008. **9**: p. 35.
323. Investigators, O.T., et al., *n-3 fatty acids and cardiovascular outcomes in patients with dysglycemia*. *N Engl J Med*, 2012. **367**(4): p. 309-18.
324. Offman, E., et al., *Steady-state bioavailability of prescription omega-3 on a low-fat diet is significantly improved with a free fatty acid formulation compared with an ethyl ester formulation: the ECLIPSE II study*. *Vasc Health Risk Manag*, 2013. **9**: p. 563-73.
325. Davidson, M.H., et al., *A novel omega-3 free fatty acid formulation has dramatically improved bioavailability during a low-fat diet compared with omega-3-acid ethyl esters: the ECLIPSE (Epanova((R)) compared to Lovaza((R)) in a pharmacokinetic single-dose evaluation) study*. *J Clin Lipidol*, 2012. **6**(6): p. 573-84.
326. Dyerberg, J., et al., *Bioavailability of marine n-3 fatty acid formulations*. *Prostaglandins Leukot Essent Fatty Acids*, 2010. **83**(3): p. 137-41.
327. Siscovick, D.S., et al., *Omega-3 Polyunsaturated Fatty Acid (Fish Oil) Supplementation and the Prevention of Clinical Cardiovascular Disease: A Science Advisory From the American Heart Association*. *Circulation*, 2017. **135**(15): p. e867-e884.
328. Sacks, F.M., et al., *Dietary Fats and Cardiovascular Disease: A Presidential Advisory From the American Heart Association*. *Circulation*, 2017. **136**(3): p. e1-e23.
329. Schunck, W.H., et al., *Therapeutic potential of omega-3 fatty acid-derived epoxyeicosanoids in cardiovascular and inflammatory diseases*. *Pharmacol Ther*, 2018. **183**: p. 177-204.
330. Jamieson, K.L., et al., *Cytochrome P450-derived eicosanoids and heart function*. *Pharmacol Ther*, 2017. **179**: p. 47-83.
331. Din, J.N., et al., *Dietary intervention with oil rich fish reduces platelet-monocyte aggregation in man*. *Atherosclerosis*, 2008. **197**(1): p. 290-6.
332. Abuissa, H., et al., *Autonomic function, omega-3, and cardiovascular risk*. *Chest*, 2005. **127**(4): p. 1088-91.

333. O'Keefe, J.H., Jr., et al., *Effects of omega-3 fatty acids on resting heart rate, heart rate recovery after exercise, and heart rate variability in men with healed myocardial infarctions and depressed ejection fractions*. Am J Cardiol, 2006. **97**(8): p. 1127-30.
334. Anand, R.G., et al., *The role of fish oil in arrhythmia prevention*. J Cardiopulm Rehabil Prev, 2008. **28**(2): p. 92-8.
335. Geleijnse, J.M., et al., *Blood pressure response to fish oil supplementation: metaregression analysis of randomized trials*. J Hypertens, 2002. **20**(8): p. 1493-9.
336. Thies, F., et al., *Association of n-3 polyunsaturated fatty acids with stability of atherosclerotic plaques: a randomised controlled trial*. Lancet, 2003. **361**(9356): p. 477-85.
337. Plutzky, J., *Atherosclerotic plaque rupture: emerging insights and opportunities*. Am J Cardiol, 1999. **84**(1A): p. 15J-20J.
338. Duda, M.K., K.M. O'Shea, and W.C. Stanley, *omega-3 polyunsaturated fatty acid supplementation for the treatment of heart failure: mechanisms and clinical potential*. Cardiovasc Res, 2009. **84**(1): p. 33-41.
339. Samokhvalov, V., et al., *SIRT Is Required for EDP-Mediated Protective Responses toward Hypoxia-Reoxygenation Injury in Cardiac Cells*. Front Pharmacol, 2016. **7**: p. 124.
340. Calder, P.C., *N-3 polyunsaturated fatty acids and inflammation: from molecular biology to the clinic*. Lipids, 2003. **38**(4): p. 343-52.
341. Calder, P.C., *Omega-3 polyunsaturated fatty acids and inflammatory processes: nutrition or pharmacology?* Br J Clin Pharmacol, 2013. **75**(3): p. 645-62.
342. Kromhout, D., et al., *Fish oil and omega-3 fatty acids in cardiovascular disease: do they really work?* Eur Heart J, 2012. **33**(4): p. 436-43.
343. Yasuda, S. and H. Shimokawa, *Potential usefulness of fish oil in the primary prevention of acute coronary syndrome*. Eur Heart J, 2010. **31**(1): p. 15-6.
344. Matsumoto, M., et al., *Orally administered eicosapentaenoic acid reduces and stabilizes atherosclerotic lesions in ApoE-deficient mice*. Atherosclerosis, 2008. **197**(2): p. 524-33.
345. Ueeda, M., et al., *Serum N-3 polyunsaturated fatty acid levels correlate with the extent of coronary plaques and calcifications in patients with acute myocardial infarction*. Circ J, 2008. **72**(11): p. 1836-43.

346. Zhao, G., et al., *Dietary alpha-linolenic acid inhibits proinflammatory cytokine production by peripheral blood mononuclear cells in hypercholesterolemic subjects*. *Am J Clin Nutr*, 2007. **85**(2): p. 385-91.
347. Niki, T., et al., *Effects of the Addition of Eicosapentaenoic Acid to Strong Statin Therapy on Inflammatory Cytokines and Coronary Plaque Components Assessed by Integrated Backscatter Intravascular Ultrasound*. *Circ J*, 2016. **80**(2): p. 450-60.
348. Investigators, G.-P., *Dietary supplementation with n-3 polyunsaturated fatty acids and vitamin E after myocardial infarction: results of the GISSI-Prevenzione trial*. *Gruppo Italiano per lo Studio della Sopravvivenza nell'Infarto miocardico*. *Lancet*, 1999. **354**(9177): p. 447-55.
349. McLaughlin, J., et al., *Adipose tissue triglyceride fatty acids and atherosclerosis in Alaska Natives and non-Natives*. *Atherosclerosis*, 2005. **181**(2): p. 353-62.
350. Deutsch, L., *Evaluation of the effect of Neptune Krill Oil on chronic inflammation and arthritic symptoms*. *J Am Coll Nutr*, 2007. **26**(1): p. 39-48.
351. Satoh, N., et al., *Purified eicosapentaenoic acid reduces small dense LDL, remnant lipoprotein particles, and C-reactive protein in metabolic syndrome*. *Diabetes Care*, 2007. **30**(1): p. 144-6.
352. Yokoyama, M., et al., *Effects of eicosapentaenoic acid on major coronary events in hypercholesterolaemic patients (JELIS): a randomised open-label, blinded endpoint analysis*. *Lancet*, 2007. **369**(9567): p. 1090-8.
353. Tavazzi, L., et al., *Effect of n-3 polyunsaturated fatty acids in patients with chronic heart failure (the GISSI-HF trial): a randomised, double-blind, placebo-controlled trial*. *Lancet*, 2008. **372**(9645): p. 1223-30.
354. Davidson, M.H., et al., *Effects of prescription omega-3-acid ethyl esters on lipoprotein particle concentrations, apolipoproteins AI and CIII, and lipoprotein-associated phospholipase A(2) mass in statin-treated subjects with hypertriglyceridemia*. *J Clin Lipidol*, 2009. **3**(5): p. 332-40.
355. Kelley, D.S., et al., *DHA supplementation decreases serum C-reactive protein and other markers of inflammation in hypertriglyceridemic men*. *J Nutr*, 2009. **139**(3): p. 495-501.
356. Cawood, A.L., et al., *Eicosapentaenoic acid (EPA) from highly concentrated n-3 fatty acid ethyl esters is incorporated into advanced atherosclerotic plaques and higher plaque EPA is associated with decreased plaque inflammation and increased stability*. *Atherosclerosis*, 2010. **212**(1): p. 252-9.

357. Einvik, G., et al., *A randomized clinical trial on n-3 polyunsaturated fatty acids supplementation and all-cause mortality in elderly men at high cardiovascular risk*. Eur J Cardiovasc Prev Rehabil, 2010. **17**(5): p. 588-92.
358. Bays, H.E., et al., *Eicosapentaenoic acid ethyl ester (AMR101) therapy in patients with very high triglyceride levels (from the Multi-center, placebo-controlled, Randomized, double-blIND, 12-week study with an open-label Extension [MARINE] trial)*. Am J Cardiol, 2011. **108**(5): p. 682-90.
359. Kashiyama, T., et al., *Relationship between coronary plaque vulnerability and serum n-3/n-6 polyunsaturated fatty acid ratio*. Circ J, 2011. **75**(10): p. 2432-8.
360. Ballantyne, C.M., et al., *Efficacy and safety of eicosapentaenoic acid ethyl ester (AMR101) therapy in statin-treated patients with persistent high triglycerides (from the ANCHOR study)*. Am J Cardiol, 2012. **110**(7): p. 984-92.
361. Kastelein, J.J., et al., *Omega-3 free fatty acids for the treatment of severe hypertriglyceridemia: the EpanoVa fOr Lowering Very high triglyceridEs (EVOLVE) trial*. J Clin Lipidol, 2014. **8**(1): p. 94-106.
362. Nishio, R., et al., *Stabilizing effect of combined eicosapentaenoic acid and statin therapy on coronary thin-cap fibroatheroma*. Atherosclerosis, 2014. **234**(1): p. 114-9.
363. Heydari, B., et al., *Effect of Omega-3 Acid Ethyl Esters on Left Ventricular Remodeling After Acute Myocardial Infarction: The OMEGA-REMODEL Randomized Clinical Trial*. Circulation, 2016. **134**(5): p. 378-91.
364. Bhatt, D.L., et al., *Cardiovascular Risk Reduction with Icosapent Ethyl for Hypertriglyceridemia*. N Engl J Med, 2018.
365. Skulas-Ray, A.C., et al., *Dose-response effects of omega-3 fatty acids on triglycerides, inflammation, and endothelial function in healthy persons with moderate hypertriglyceridemia*. Am J Clin Nutr, 2011. **93**(2): p. 243-52.
366. Blacher, J., et al., *Cardiovascular effects of B-vitamins and/or N-3 fatty acids: the SU.FOL.OM3 trial*. Int J Cardiol, 2013. **167**(2): p. 508-13.
367. Risk, et al., *n-3 fatty acids in patients with multiple cardiovascular risk factors*. N Engl J Med, 2013. **368**(19): p. 1800-8.
368. Bowman, L., et al., *Effects of n-3 Fatty Acid Supplements in Diabetes Mellitus*. N Engl J Med, 2018. **379**(16): p. 1540-1550.

369. Manson, J.E., et al., *Marine n-3 Fatty Acids and Prevention of Cardiovascular Disease and Cancer*. N Engl J Med, 2018.
370. Swann, P.G., D.L. Venton, and G.C. Le Breton, *Eicosapentaenoic acid and docosahexaenoic acid are antagonists at the thromboxane A2/prostaglandin H2 receptor in human platelets*. FEBS Lett, 1989. **243**(2): p. 244-6.
371. De Caterina, R., et al., *The omega-3 fatty acid docosahexaenoate reduces cytokine-induced expression of proatherogenic and proinflammatory proteins in human endothelial cells*. Arterioscler Thromb, 1994. **14**(11): p. 1829-36.
372. Hughes, D.A. and A.C. Pinder, *N-3 polyunsaturated fatty acids modulate the expression of functionally associated molecules on human monocytes and inhibit antigen-presentation in vitro*. Clin Exp Immunol, 1997. **110**(3): p. 516-23.
373. Zhao, Y., et al., *Eicosapentaenoic acid prevents LPS-induced TNF-alpha expression by preventing NF-kappaB activation*. J Am Coll Nutr, 2004. **23**(1): p. 71-8.
374. Neschen, S., et al., *Fish oil regulates adiponectin secretion by a peroxisome proliferator-activated receptor-gamma-dependent mechanism in mice*. Diabetes, 2006. **55**(4): p. 924-8.
375. Holy, E.W., et al., *Dietary alpha-linolenic acid inhibits arterial thrombus formation, tissue factor expression, and platelet activation*. Arterioscler Thromb Vasc Biol, 2011. **31**(8): p. 1772-80.
376. Ishida, T., et al., *Eicosapentaenoic Acid Prevents Saturated Fatty Acid-Induced Vascular Endothelial Dysfunction: Involvement of Long-Chain Acyl-CoA Synthetase*. J Atheroscler Thromb, 2015. **22**(11): p. 1172-85.
377. Salic, K., et al., *Resolvin E1 attenuates atherosclerosis in absence of cholesterol-lowering effects and on top of atorvastatin*. Atherosclerosis, 2016. **250**: p. 158-65.
378. Takashima, A., et al., *Combination of n-3 polyunsaturated fatty acids reduces atherogenesis in apolipoprotein E-deficient mice by inhibiting macrophage activation*. Atherosclerosis, 2016. **254**: p. 142-150.
379. Kain, V., et al., *Resolvin D1 activates the inflammation resolving response at splenic and ventricular site following myocardial infarction leading to improved ventricular function*. J Mol Cell Cardiol, 2015. **84**: p. 24-35.
380. Keyes, K.T., et al., *Resolvin E1 protects the rat heart against reperfusion injury*. Am J Physiol Heart Circ Physiol, 2010. **299**(1): p. H153-64.

381. Gao, J.Y., et al., *Long-term treatment with eicosapentaenoic acid ameliorates myocardial ischemia-reperfusion injury in pigs in vivo. -Involvement of Rho-kinase pathway inhibition.* Circ J, 2011. **75**(8): p. 1843-51.
382. Gilbert, K., et al., *Resolvin D1, a metabolite of omega-3 polyunsaturated fatty acid, decreases post-myocardial infarct depression.* Mar Drugs, 2014. **12**(11): p. 5396-407.
383. Darwesh, A.M., et al., *Cardioprotective effects of CYP-derived epoxy metabolites of docosahexaenoic acid involve limiting NLRP3 inflammasome activation.* Can J Physiol Pharmacol, 2019. **97**(6): p. 544-556.
384. Shimojo, N., et al., *Eicosapentaenoic acid prevents endothelin-1-induced cardiomyocyte hypertrophy in vitro through the suppression of TGF-beta 1 and phosphorylated JNK.* Am J Physiol Heart Circ Physiol, 2006. **291**(2): p. H835-45.
385. Chen, J., et al., *Omega-3 fatty acids prevent pressure overload-induced cardiac fibrosis through activation of cyclic GMP/protein kinase G signaling in cardiac fibroblasts.* Circulation, 2011. **123**(6): p. 584-93.
386. Eclöv, J.A., et al., *EPA, not DHA, prevents fibrosis in pressure overload-induced heart failure: potential role of free fatty acid receptor 4.* J Lipid Res, 2015. **56**(12): p. 2297-308.
387. Ito, S., et al., *Highly purified eicosapentaenoic acid ameliorates cardiac injury and adipose tissue inflammation in a rat model of metabolic syndrome.* Obes Sci Pract, 2016. **2**(3): p. 318-329.
388. Takamura, M., et al., *Long-Term Administration of Eicosapentaenoic Acid Improves Post-Myocardial Infarction Cardiac Remodeling in Mice by Regulating Macrophage Polarization.* J Am Heart Assoc, 2017. **6**(2).
389. Kain, V. and G.V. Halade, *Immune responsive resolvin D1 programs peritoneal macrophages and cardiac fibroblast phenotypes in diversified metabolic microenvironment.* J Cell Physiol, 2018.
390. Jung, U.J., et al., *n-3 Fatty acids and cardiovascular disease: mechanisms underlying beneficial effects.* Am J Clin Nutr, 2008. **87**(6): p. 2003S-9S.
391. Calder, P.C., *Omega-3 fatty acids and inflammatory processes: from molecules to man.* Biochem Soc Trans, 2017. **45**(5): p. 1105-1115.
392. Calder, P.C. and R.F. Grimble, *Polyunsaturated fatty acids, inflammation and immunity.* Eur J Clin Nutr, 2002. **56 Suppl 3**: p. S14-9.

393. Endo, J. and M. Arita, *Cardioprotective mechanism of omega-3 polyunsaturated fatty acids*. J Cardiol, 2016. **67**(1): p. 22-7.
394. Oh, D.Y., et al., *GPR120 is an omega-3 fatty acid receptor mediating potent anti-inflammatory and insulin-sensitizing effects*. Cell, 2010. **142**(5): p. 687-98.
395. Gani, O.A. and I. Sylte, *Molecular recognition of docosahexaenoic acid by peroxisome proliferator-activated receptors and retinoid-X receptor alpha*. J Mol Graph Model, 2008. **27**(2): p. 217-24.
396. Hughes, D.A., S. Southon, and A.C. Pinder, *(n-3) Polyunsaturated fatty acids modulate the expression of functionally associated molecules on human monocytes in vitro*. J Nutr, 1996. **126**(3): p. 603-10.
397. Collie-Duguid, E.S. and K.W. Wahle, *Inhibitory effect of fish oil N-3 polyunsaturated fatty acids on the expression of endothelial cell adhesion molecules*. Biochem Biophys Res Commun, 1996. **220**(3): p. 969-74.
398. Miles, E.A., F.A. Wallace, and P.C. Calder, *Dietary fish oil reduces intercellular adhesion molecule 1 and scavenger receptor expression on murine macrophages*. Atherosclerosis, 2000. **152**(1): p. 43-50.
399. Sanderson, P. and P.C. Calder, *Dietary fish oil diminishes lymphocyte adhesion to macrophage and endothelial cell monolayers*. Immunology, 1998. **94**(1): p. 79-87.
400. Lo, C.J., et al., *Fish oil decreases macrophage tumor necrosis factor gene transcription by altering the NF kappa B activity*. J Surg Res, 1999. **82**(2): p. 216-21.
401. Novak, T.E., et al., *NF-kappa B inhibition by omega -3 fatty acids modulates LPS-stimulated macrophage TNF-alpha transcription*. Am J Physiol Lung Cell Mol Physiol, 2003. **284**(1): p. L84-9.
402. Kumar, A., et al., *Nuclear factor-kappaB: its role in health and disease*. J Mol Med (Berl), 2004. **82**(7): p. 434-48.
403. Zapata-Gonzalez, F., et al., *Human dendritic cell activities are modulated by the omega-3 fatty acid, docosahexaenoic acid, mainly through PPAR(gamma):RXR heterodimers: comparison with other polyunsaturated fatty acids*. J Leukoc Biol, 2008. **84**(4): p. 1172-82.
404. Poynter, M.E. and R.A. Daynes, *Peroxisome proliferator-activated receptor alpha activation modulates cellular redox status, represses nuclear factor-kappaB signaling, and*

- reduces inflammatory cytokine production in aging.* J Biol Chem, 1998. **273**(49): p. 32833-41.
405. Ricote, M., et al., *The peroxisome proliferator-activated receptor(PPARgamma) as a regulator of monocyte/macrophage function.* J Leukoc Biol, 1999. **66**(5): p. 733-9.
406. Vanden Berghe, W., et al., *A paradigm for gene regulation: inflammation, NF-kappaB and PPAR.* Adv Exp Med Biol, 2003. **544**: p. 181-96.
407. Mishra, A., A. Chaudhary, and S. Sethi, *Oxidized omega-3 fatty acids inhibit NF-kappaB activation via a PPARalpha-dependent pathway.* Arterioscler Thromb Vasc Biol, 2004. **24**(9): p. 1621-7.
408. Im, D.S., *Omega-3 fatty acids in anti-inflammation (pro-resolution) and GPCRs.* Prog Lipid Res, 2012. **51**(3): p. 232-7.
409. Katagiri, Y.U., N. Kiyokawa, and J. Fujimoto, *A role for lipid rafts in immune cell signaling.* Microbiol Immunol, 2001. **45**(1): p. 1-8.
410. Yaqoob, P., *The nutritional significance of lipid rafts.* Annu Rev Nutr, 2009. **29**: p. 257-82.
411. Chapkin, R.S., et al., *Docosahexaenoic acid alters the size and distribution of cell surface microdomains.* Biochim Biophys Acta, 2008. **1778**(2): p. 466-71.
412. Turk, H.F. and R.S. Chapkin, *Membrane lipid raft organization is uniquely modified by n-3 polyunsaturated fatty acids.* Prostaglandins Leukot Essent Fatty Acids, 2013. **88**(1): p. 43-7.
413. Stillwell, W. and S.R. Wassall, *Docosahexaenoic acid: membrane properties of a unique fatty acid.* Chem Phys Lipids, 2003. **126**(1): p. 1-27.
414. McMurray, D.N., D.L. Bonilla, and R.S. Chapkin, *n-3 Fatty acids uniquely affect anti-microbial resistance and immune cell plasma membrane organization.* Chem Phys Lipids, 2011. **164**(7): p. 626-35.
415. Shaikh, S.R. and M. Edidin, *Polyunsaturated fatty acids, membrane organization, T cells, and antigen presentation.* Am J Clin Nutr, 2006. **84**(6): p. 1277-89.
416. Kong, W., J.H. Yen, and D. Ganea, *Docosahexaenoic acid prevents dendritic cell maturation, inhibits antigen-specific Th1/Th17 differentiation and suppresses experimental autoimmune encephalomyelitis.* Brain Behav Immun, 2011. **25**(5): p. 872-82.

417. Kim, W., et al., *Regulatory activity of polyunsaturated fatty acids in T-cell signaling*. Prog Lipid Res, 2010. **49**(3): p. 250-61.
418. Rockett, B.D., et al., *n-3 PUFA improves fatty acid composition, prevents palmitate-induced apoptosis, and differentially modifies B cell cytokine secretion in vitro and ex vivo*. J Lipid Res, 2010. **51**(6): p. 1284-97.
419. Shaikh, S.R. and M. Edidin, *Polyunsaturated fatty acids and membrane organization: elucidating mechanisms to balance immunotherapy and susceptibility to infection*. Chem Phys Lipids, 2008. **153**(1): p. 24-33.
420. Hashimoto, M., et al., *Effects of eicosapentaenoic acid and docosahexaenoic acid on plasma membrane fluidity of aortic endothelial cells*. Lipids, 1999. **34**(12): p. 1297-304.
421. Ciesielska, A. and K. Kwiatkowska, *Modification of pro-inflammatory signaling by dietary components: The plasma membrane as a target*. Bioessays, 2015. **37**(7): p. 789-801.
422. Hazen, S.L., D.A. Ford, and R.W. Gross, *Activation of a membrane-associated phospholipase A2 during rabbit myocardial ischemia which is highly selective for plasmalogen substrate*. J Biol Chem, 1991. **266**(9): p. 5629-33.
423. Ford, D.A., et al., *The rapid and reversible activation of a calcium-independent plasmalogen-selective phospholipase A2 during myocardial ischemia*. J Clin Invest, 1991. **88**(1): p. 331-5.
424. Mancuso, D.J., et al., *Cardiac ischemia activates calcium-independent phospholipase A2beta, precipitating ventricular tachyarrhythmias in transgenic mice: rescue of the lethal electrophysiologic phenotype by mechanism-based inhibition*. J Biol Chem, 2003. **278**(25): p. 22231-6.
425. Brouard, C. and M. Pascaud, *Effects of moderate dietary supplementations with n-3 fatty acids on macrophage and lymphocyte phospholipids and macrophage eicosanoid synthesis in the rat*. Biochim Biophys Acta, 1990. **1047**(1): p. 19-28.
426. Faber, J., et al., *Supplementation with a fish oil-enriched, high-protein medical food leads to rapid incorporation of EPA into white blood cells and modulates immune responses within one week in healthy men and women*. J Nutr, 2011. **141**(5): p. 964-70.
427. Gibney, M.J. and B. Hunter, *The effects of short- and long-term supplementation with fish oil on the incorporation of n-3 polyunsaturated fatty acids into cells of the immune system in healthy volunteers*. Eur J Clin Nutr, 1993. **47**(4): p. 255-9.

428. Grando, F.C., et al., *Modulation of peritoneal macrophage activity by the saturation state of the fatty acid moiety of phosphatidylcholine*. Braz J Med Biol Res, 2009. **42**(7): p. 599-605.
429. Yaqoob, P., et al., *Encapsulated fish oil enriched in alpha-tocopherol alters plasma phospholipid and mononuclear cell fatty acid compositions but not mononuclear cell functions*. Eur J Clin Invest, 2000. **30**(3): p. 260-74.
430. Leslie, C.C., *Cytosolic phospholipase A(2): physiological function and role in disease*. J Lipid Res, 2015. **56**(8): p. 1386-402.
431. Lewis, R.A., K.F. Austen, and R.J. Soberman, *Leukotrienes and other products of the 5-lipoxygenase pathway. Biochemistry and relation to pathobiology in human diseases*. N Engl J Med, 1990. **323**(10): p. 645-55.
432. Tilley, S.L., T.M. Coffman, and B.H. Koller, *Mixed messages: modulation of inflammation and immune responses by prostaglandins and thromboxanes*. J Clin Invest, 2001. **108**(1): p. 15-23.
433. Kalinski, P., *Regulation of immune responses by prostaglandin E2*. J Immunol, 2012. **188**(1): p. 21-8.
434. Levy, B.D., et al., *Lipid mediator class switching during acute inflammation: signals in resolution*. Nat Immunol, 2001. **2**(7): p. 612-9.
435. Surette, M.E., *The science behind dietary omega-3 fatty acids*. CMAJ, 2008. **178**(2): p. 177-80.
436. Lee, T.H., et al., *Effect of dietary enrichment with eicosapentaenoic and docosahexaenoic acids on in vitro neutrophil and monocyte leukotriene generation and neutrophil function*. N Engl J Med, 1985. **312**(19): p. 1217-24.
437. Caughey, G.E., et al., *The effect on human tumor necrosis factor alpha and interleukin 1 beta production of diets enriched in n-3 fatty acids from vegetable oil or fish oil*. Am J Clin Nutr, 1996. **63**(1): p. 116-22.
438. von Schacky, C., et al., *n-3 fatty acids and cysteinyl-leukotriene formation in humans in vitro, ex vivo, and in vivo*. J Lab Clin Med, 1993. **121**(2): p. 302-9.
439. Prescott, S.M., *The effect of eicosapentaenoic acid on leukotriene B production by human neutrophils*. J Biol Chem, 1984. **259**(12): p. 7615-21.

440. Corey, E.J., C. Shih, and J.R. Cashman, *Docosahexaenoic acid is a strong inhibitor of prostaglandin but not leukotriene biosynthesis*. Proc Natl Acad Sci U S A, 1983. **80**(12): p. 3581-4.
441. Lee, T.H., et al., *Effects of exogenous arachidonic, eicosapentaenoic, and docosahexaenoic acids on the generation of 5-lipoxygenase pathway products by ionophore-activated human neutrophils*. J Clin Invest, 1984. **74**(6): p. 1922-33.
442. Kobayashi, T., et al., *Roles of thromboxane A(2) and prostacyclin in the development of atherosclerosis in apoE-deficient mice*. J Clin Invest, 2004. **114**(6): p. 784-94.
443. Cipollone, F. and M.L. Fazio, *COX-2 and atherosclerosis*. J Cardiovasc Pharmacol, 2006. **47 Suppl 1**: p. S26-36.
444. Xiao, C.Y., et al., *Prostaglandin E2 protects the heart from ischemia-reperfusion injury via its receptor subtype EP4*. Circulation, 2004. **109**(20): p. 2462-8.
445. Degousee, N., et al., *Microsomal prostaglandin E2 synthase-1 deletion leads to adverse left ventricular remodeling after myocardial infarction*. Circulation, 2008. **117**(13): p. 1701-10.
446. Degousee, N., et al., *Lack of microsomal prostaglandin E(2) synthase-1 in bone marrow-derived myeloid cells impairs left ventricular function and increases mortality after acute myocardial infarction*. Circulation, 2012. **125**(23): p. 2904-13.
447. Lee, S.A., et al., *DHA and EPA Down-regulate COX-2 Expression through Suppression of NF-kappaB Activity in LPS-treated Human Umbilical Vein Endothelial Cells*. Korean J Physiol Pharmacol, 2009. **13**(4): p. 301-7.
448. Gryglewski, R.J., et al., *Effects of all cis-5,8,11,14,17 eicosapentaenoic acid and PGH3 on platelet aggregation*. Prostaglandins, 1979. **18**(3): p. 453-78.
449. Yaqoob, P. and P. Calder, *Effects of dietary lipid manipulation upon inflammatory mediator production by murine macrophages*. Cell Immunol, 1995. **163**(1): p. 120-8.
450. Chapkin, R.S., C.C. Akoh, and C.C. Miller, *Influence of dietary n-3 fatty acids on macrophage glycerophospholipid molecular species and peptidoleukotriene synthesis*. J Lipid Res, 1991. **32**(7): p. 1205-13.
451. Peterson, L.D., et al., *Eicosapentaenoic and docosahexaenoic acids alter rat spleen leukocyte fatty acid composition and prostaglandin E2 production but have different effects on lymphocyte functions and cell-mediated immunity*. Lipids, 1998. **33**(2): p. 171-80.

452. Cohen, M.G., et al., *Insights into the inhibition of platelet activation by omega-3 polyunsaturated fatty acids: beyond aspirin and clopidogrel*. *Thromb Res*, 2011. **128**(4): p. 335-40.
453. Harris, W.S., et al., *Omega-3 fatty acids and coronary heart disease risk: clinical and mechanistic perspectives*. *Atherosclerosis*, 2008. **197**(1): p. 12-24.
454. Karanian, J.W., H.Y. Kim, and N. Salem, Jr., *The structure-activity relationship of lipoxygenase products of long-chain polyunsaturated fatty acids: effects on human platelet aggregation*. *Lipids*, 1996. **31 Suppl**: p. S305-8.
455. Tull, S.P., et al., *Omega-3 Fatty acids and inflammation: novel interactions reveal a new step in neutrophil recruitment*. *PLoS Biol*, 2009. **7**(8): p. e1000177.
456. Serhan, C.N., et al., *Novel functional sets of lipid-derived mediators with antiinflammatory actions generated from omega-3 fatty acids via cyclooxygenase 2-nonsteroidal antiinflammatory drugs and transcellular processing*. *J Exp Med*, 2000. **192**(8): p. 1197-204.
457. Arita, M., C.B. Clish, and C.N. Serhan, *The contributions of aspirin and microbial oxygenase to the biosynthesis of anti-inflammatory resolvins: novel oxygenase products from omega-3 polyunsaturated fatty acids*. *Biochem Biophys Res Commun*, 2005. **338**(1): p. 149-57.
458. Endo, J., et al., *18-HEPE, an n-3 fatty acid metabolite released by macrophages, prevents pressure overload-induced maladaptive cardiac remodeling*. *J Exp Med*, 2014. **211**(8): p. 1673-87.
459. Breitbart, E., et al., *Lipoxygenase activity in heart cells*. *FEBS Lett*, 1996. **395**(2-3): p. 148-52.
460. Chen, X.S., et al., *cDNA cloning, expression, mutagenesis of C-terminal isoleucine, genomic structure, and chromosomal localizations of murine 12-lipoxygenases*. *J Biol Chem*, 1994. **269**(19): p. 13979-87.
461. Haeggstrom, J.Z. and C.D. Funk, *Lipoxygenase and leukotriene pathways: biochemistry, biology, and roles in disease*. *Chem Rev*, 2011. **111**(10): p. 5866-98.
462. Mashima, R. and T. Okuyama, *The role of lipoxygenases in pathophysiology; new insights and future perspectives*. *Redox Biol*, 2015. **6**: p. 297-310.

463. Endres, S., et al., *The effect of dietary supplementation with n-3 polyunsaturated fatty acids on the synthesis of interleukin-1 and tumor necrosis factor by mononuclear cells.* N Engl J Med, 1989. **320**(5): p. 265-71.
464. Sperling, R.I., et al., *Dietary omega-3 polyunsaturated fatty acids inhibit phosphoinositide formation and chemotaxis in neutrophils.* J Clin Invest, 1993. **91**(2): p. 651-60.
465. Rola-Pleszczynski, M. and I. Lemaire, *Leukotrienes augment interleukin 1 production by human monocytes.* J Immunol, 1985. **135**(6): p. 3958-61.
466. Dinarello, C.A., et al., *The influence of lipoxygenase inhibitors on the in vitro production of human leukocytic pyrogen and lymphocyte activating factor (interleukin-1).* Int J Immunopharmacol, 1984. **6**(1): p. 43-50.
467. Simopoulos, A.P., *Omega-3 fatty acids in inflammation and autoimmune diseases.* J Am Coll Nutr, 2002. **21**(6): p. 495-505.
468. Gil, A., *Polyunsaturated fatty acids and inflammatory diseases.* Biomed Pharmacother, 2002. **56**(8): p. 388-96.
469. Terano, T., J.A. Salmon, and S. Moncada, *Biosynthesis and biological activity of leukotriene B5.* Prostaglandins, 1984. **27**(2): p. 217-32.
470. Goldman, D.W., W.C. Pickett, and E.J. Goetzl, *Human neutrophil chemotactic and degranulating activities of leukotriene B5 (LTB5) derived from eicosapentaenoic acid.* Biochem Biophys Res Commun, 1983. **117**(1): p. 282-8.
471. Lee, T.H., et al., *Characterization and biologic properties of 5,12-dihydroxy derivatives of eicosapentaenoic acid, including leukotriene B5 and the double lipoxygenase product.* J Biol Chem, 1984. **259**(4): p. 2383-9.
472. Hughes, H., et al., *Gas chromatographic-mass spectrometric analysis of lipoxygenase products in post-ischemic rabbit myocardium.* Prostaglandins Leukot Essent Fatty Acids, 1991. **42**(4): p. 225-31.
473. Kuzuya, T., et al., *Free radical generation coupled with arachidonate lipoxygenase reaction relates to reoxygenation induced myocardial cell injury.* Cardiovasc Res, 1993. **27**(6): p. 1056-60.
474. Kuhn, H. and V.B. O'Donnell, *Inflammation and immune regulation by 12/15-lipoxygenases.* Prog Lipid Res, 2006. **45**(4): p. 334-56.

475. Lopez, E.F., et al., *Obesity superimposed on aging magnifies inflammation and delays the resolving response after myocardial infarction*. *Am J Physiol Heart Circ Physiol*, 2015. **308**(4): p. H269-80.
476. Wen, Y., et al., *Role of 12/15-lipoxygenase in the expression of MCP-1 in mouse macrophages*. *Am J Physiol Heart Circ Physiol*, 2008. **294**(4): p. H1933-8.
477. Dwarakanath, R.S., et al., *Viral vector-mediated 12/15-lipoxygenase overexpression in vascular smooth muscle cells enhances inflammatory gene expression and migration*. *J Vasc Res*, 2008. **45**(2): p. 132-42.
478. Reilly, K.B., et al., *12/15-Lipoxygenase activity mediates inflammatory monocyte/endothelial interactions and atherosclerosis in vivo*. *J Biol Chem*, 2004. **279**(10): p. 9440-50.
479. Cyrus, T., et al., *Disruption of the 12/15-lipoxygenase gene diminishes atherosclerosis in apo E-deficient mice*. *J Clin Invest*, 1999. **103**(11): p. 1597-604.
480. Kain, V., et al., *Genetic deletion of 12/15 lipoxygenase promotes effective resolution of inflammation following myocardial infarction*. *J Mol Cell Cardiol*, 2018. **118**: p. 70-80.
481. Wen, Y., et al., *Overexpression of 12-lipoxygenase causes cardiac fibroblast cell growth*. *Circ Res*, 2001. **88**(1): p. 70-6.
482. Wen, Y., et al., *Overexpression of 12-lipoxygenase and cardiac fibroblast hypertrophy*. *Trends Cardiovasc Med*, 2003. **13**(4): p. 129-36.
483. Funk, C.D., *Prostaglandins and leukotrienes: advances in eicosanoid biology*. *Science*, 2001. **294**(5548): p. 1871-5.
484. Peters-Golden, M. and W.R. Henderson, Jr., *Leukotrienes*. *N Engl J Med*, 2007. **357**(18): p. 1841-54.
485. Back, M., *Studies of receptors and modulatory mechanisms in functional responses to cysteinyl-leukotrienes in smooth muscle*. *Acta Physiol Scand Suppl*, 2002. **648**: p. 1-55.
486. Helgadottir, A., et al., *The gene encoding 5-lipoxygenase activating protein confers risk of myocardial infarction and stroke*. *Nat Genet*, 2004. **36**(3): p. 233-9.
487. Dwyer, J.H., et al., *Arachidonate 5-lipoxygenase promoter genotype, dietary arachidonic acid, and atherosclerosis*. *N Engl J Med*, 2004. **350**(1): p. 29-37.

488. Spanbroek, R., et al., *Expanding expression of the 5-lipoxygenase pathway within the arterial wall during human atherogenesis*. Proc Natl Acad Sci U S A, 2003. **100**(3): p. 1238-43.
489. Cipollone, F., et al., *Association between 5-lipoxygenase expression and plaque instability in humans*. Arterioscler Thromb Vasc Biol, 2005. **25**(8): p. 1665-70.
490. Mehrabian, M., et al., *Identification of 5-lipoxygenase as a major gene contributing to atherosclerosis susceptibility in mice*. Circ Res, 2002. **91**(2): p. 120-6.
491. Jolly, S.R., et al., *Reduction of myocardial infarct size by neutrophil depletion: effect of duration of occlusion*. Am Heart J, 1986. **112**(4): p. 682-90.
492. Papayianni, A., C.N. Serhan, and H.R. Brady, *Lipoxin A4 and B4 inhibit leukotriene-stimulated interactions of human neutrophils and endothelial cells*. J Immunol, 1996. **156**(6): p. 2264-72.
493. Pedersen, K.E., B.S. Bochner, and B.J. Udem, *Cysteinyl leukotrienes induce P-selectin expression in human endothelial cells via a non-CysLT1 receptor-mediated mechanism*. J Pharmacol Exp Ther, 1997. **281**(2): p. 655-62.
494. Uzonyi, B., et al., *Cysteinyl leukotriene 2 receptor and protease-activated receptor 1 activate strongly correlated early genes in human endothelial cells*. Proc Natl Acad Sci U S A, 2006. **103**(16): p. 6326-31.
495. Allen, S.P., et al., *Enhanced excretion of urinary leukotriene E4 in coronary artery disease and after coronary artery bypass surgery*. Coron Artery Dis, 1993. **4**(10): p. 899-904.
496. Allen, S., et al., *Differential leukotriene constrictor responses in human atherosclerotic coronary arteries*. Circulation, 1998. **97**(24): p. 2406-13.
497. Ni, N.C., et al., *Multiple-site activation of the cysteinyl leukotriene receptor 2 is required for exacerbation of ischemia/reperfusion injury*. Arterioscler Thromb Vasc Biol, 2014. **34**(2): p. 321-30.
498. Hock, C.E., L.D. Beck, and L.A. Papa, *Peptide leukotriene receptor antagonism in myocardial ischaemia and reperfusion*. Cardiovasc Res, 1992. **26**(12): p. 1206-11.
499. Konkel, A. and W.H. Schunck, *Role of cytochrome P450 enzymes in the bioactivation of polyunsaturated fatty acids*. Biochim Biophys Acta, 2011. **1814**(1): p. 210-22.

500. Westphal, C., A. Konkel, and W.H. Schunck, *Cytochrome p450 enzymes in the bioactivation of polyunsaturated Fatty acids and their role in cardiovascular disease*. Adv Exp Med Biol, 2015. **851**: p. 151-87.
501. Arnold, C., et al., *Arachidonic acid-metabolizing cytochrome P450 enzymes are targets of {omega}-3 fatty acids*. J Biol Chem, 2010. **285**(43): p. 32720-33.
502. Fisslthaler, B., et al., *Cytochrome P450 2C is an EDHF synthase in coronary arteries*. Nature, 1999. **401**(6752): p. 493-7.
503. Rosolowsky, M. and W.B. Campbell, *Synthesis of hydroxyeicosatetraenoic (HETEs) and epoxyeicosatrienoic acids (EETs) by cultured bovine coronary artery endothelial cells*. Biochim Biophys Acta, 1996. **1299**(2): p. 267-77.
504. Fer, M., et al., *Metabolism of eicosapentaenoic and docosahexaenoic acids by recombinant human cytochromes P450*. Arch Biochem Biophys, 2008. **471**(2): p. 116-25.
505. Lucas, D., et al., *Stereoselective epoxidation of the last double bond of polyunsaturated fatty acids by human cytochromes P450*. J Lipid Res, 2010. **51**(5): p. 1125-33.
506. Falck, J.R., et al., *17(R),18(S)-epoxyeicosatetraenoic acid, a potent eicosapentaenoic acid (EPA) derived regulator of cardiomyocyte contraction: structure-activity relationships and stable analogues*. J Med Chem, 2011. **54**(12): p. 4109-18.
507. Harris, T.R. and B.D. Hammock, *Soluble epoxide hydrolase: gene structure, expression and deletion*. Gene, 2013. **526**(2): p. 61-74.
508. Morisseau, C., et al., *Naturally occurring monoepoxides of eicosapentaenoic acid and docosahexaenoic acid are bioactive antihyperalgesic lipids*. J Lipid Res, 2010. **51**(12): p. 3481-90.
509. Wang, R.X., et al., *Activation of vascular BK channels by docosahexaenoic acid is dependent on cytochrome P450 epoxygenase activity*. Cardiovasc Res, 2011. **90**(2): p. 344-52.
510. Agbor, L.N., et al., *Elevated blood pressure in cytochrome P4501A1 knockout mice is associated with reduced vasodilation to omega-3 polyunsaturated fatty acids*. Toxicol Appl Pharmacol, 2012. **264**(3): p. 351-60.
511. Ulu, A., et al., *An omega-3 epoxide of docosahexaenoic acid lowers blood pressure in angiotensin-II-dependent hypertension*. J Cardiovasc Pharmacol, 2014. **64**(1): p. 87-99.

512. Fang, X., et al., *Omega-3 PUFA attenuate mice myocardial infarction injury by emerging a protective eicosanoid pattern*. Prostaglandins Other Lipid Mediat, 2018. **139**: p. 1-9.
513. Kunisawa, J., et al., *Dietary omega3 fatty acid exerts anti-allergic effect through the conversion to 17,18-epoxyeicosatetraenoic acid in the gut*. Sci Rep, 2015. **5**: p. 9750.
514. Sharma, A., et al., *Novel Omega-3 Fatty Acid Epoxygenase Metabolite Reduces Kidney Fibrosis*. Int J Mol Sci, 2016. **17**(5).
515. Morin, C., et al., *17,18-epoxyeicosatetraenoic acid targets PPARgamma and p38 mitogen-activated protein kinase to mediate its anti-inflammatory effects in the lung: role of soluble epoxide hydrolase*. Am J Respir Cell Mol Biol, 2010. **43**(5): p. 564-75.
516. Samokhvalov, V., et al., *CYP-epoxygenase metabolites of docosahexaenoic acid protect HL-1 cardiac cells against LPS-induced cytotoxicity Through SIRT1*. Cell Death Discov, 2015. **1**.
517. Kroetz, D.L. and D.C. Zeldin, *Cytochrome P450 pathways of arachidonic acid metabolism*. Curr Opin Lipidol, 2002. **13**(3): p. 273-83.
518. Spector, A.A. and A.W. Norris, *Action of epoxyeicosatrienoic acids on cellular function*. Am J Physiol Cell Physiol, 2007. **292**(3): p. C996-1012.
519. Dolegowska, B., et al., *Platelets arachidonic acid metabolism in patients with essential hypertension*. Platelets, 2009. **20**(4): p. 242-9.
520. El-Sherbeni, A.A. and A.O. El-Kadi, *Alterations in cytochrome P450-derived arachidonic acid metabolism during pressure overload-induced cardiac hypertrophy*. Biochem Pharmacol, 2014. **87**(3): p. 456-66.
521. Shoieb, S.M. and A.O.S. El-Kadi, *S-Enantiomer of 19-Hydroxyeicosatetraenoic Acid Preferentially Protects Against Angiotensin II-Induced Cardiac Hypertrophy*. Drug Metab Dispos, 2018. **46**(8): p. 1157-1168.
522. Elshenawy, O.H., A. Anwar-Mohamed, and A.O. El-Kadi, *20-Hydroxyeicosatetraenoic acid is a potential therapeutic target in cardiovascular diseases*. Curr Drug Metab, 2013. **14**(6): p. 706-19.
523. Kayama, Y., et al., *Cardiac 12/15 lipoxygenase-induced inflammation is involved in heart failure*. J Exp Med, 2009. **206**(7): p. 1565-74.

524. Maayah, Z.H. and A.O. El-Kadi, 5-, 12- and 15-Hydroxyeicosatetraenoic acids induce cellular hypertrophy in the human ventricular cardiomyocyte, RL-14 cell line, through MAPK- and NF-kappaB-dependent mechanism. *Arch Toxicol*, 2016. **90**(2): p. 359-73.
525. Ishizuka, T., et al., 20-Hydroxyeicosatetraenoic acid stimulates nuclear factor-kappaB activation and the production of inflammatory cytokines in human endothelial cells. *J Pharmacol Exp Ther*, 2008. **324**(1): p. 103-10.
526. Nithipatikom, K., et al., Inhibition of cytochrome P450omega-hydroxylase: a novel endogenous cardioprotective pathway. *Circ Res*, 2004. **95**(8): p. e65-71.
527. Gross, E.R., et al., Cytochrome P450 omega-hydroxylase inhibition reduces infarct size during reperfusion via the sarcolemmal KATP channel. *J Mol Cell Cardiol*, 2004. **37**(6): p. 1245-9.
528. Nithipatikom, K., et al., Determination of cytochrome P450 metabolites of arachidonic acid in coronary venous plasma during ischemia and reperfusion in dogs. *Anal Biochem*, 2001. **292**(1): p. 115-24.
529. Shishehbor, M.H., et al., Systemic elevations of free radical oxidation products of arachidonic acid are associated with angiographic evidence of coronary artery disease. *Free Radic Biol Med*, 2006. **41**(11): p. 1678-83.
530. Mallat, Z., et al., The relationship of hydroxyeicosatetraenoic acids and F2-isoprostanes to plaque instability in human carotid atherosclerosis. *J Clin Invest*, 1999. **103**(3): p. 421-7.
531. VanRollins, M., Epoxygenase metabolites of docosahexaenoic and eicosapentaenoic acids inhibit platelet aggregation at concentrations below those affecting thromboxane synthesis. *J Pharmacol Exp Ther*, 1995. **274**(2): p. 798-804.
532. Yokokura, Y., et al., Identification of 14,20-dihydroxy-docosahexaenoic acid as a novel anti-inflammatory metabolite. *J Biochem*, 2014. **156**(6): p. 315-21.
533. Weylandt, K.H., et al., Suppressed liver tumorigenesis in fat-1 mice with elevated omega-3 fatty acids is associated with increased omega-3 derived lipid mediators and reduced TNF-alpha. *Carcinogenesis*, 2011. **32**(6): p. 897-903.
534. Serhan, C.N., et al., Resolvins: a family of bioactive products of omega-3 fatty acid transformation circuits initiated by aspirin treatment that counter proinflammation signals. *J Exp Med*, 2002. **196**(8): p. 1025-37.

535. Serhan, C.N., N. Chiang, and T.E. Van Dyke, *Resolving inflammation: dual anti-inflammatory and pro-resolution lipid mediators*. Nat Rev Immunol, 2008. **8**(5): p. 349-61.
536. Serhan, C.N. and N. Chiang, *Resolution phase lipid mediators of inflammation: agonists of resolution*. Curr Opin Pharmacol, 2013. **13**(4): p. 632-40.
537. Bannenberg, G. and C.N. Serhan, *Specialized pro-resolving lipid mediators in the inflammatory response: An update*. Biochim Biophys Acta, 2010. **1801**(12): p. 1260-73.
538. Oh, S.F., et al., *Pro-resolving actions and stereoselective biosynthesis of 18S E-series resolvins in human leukocytes and murine inflammation*. J Clin Invest, 2011. **121**(2): p. 569-81.
539. Mas, E., et al., *Resolvins D1, D2, and other mediators of self-limited resolution of inflammation in human blood following n-3 fatty acid supplementation*. Clin Chem, 2012. **58**(10): p. 1476-84.
540. Hong, S., et al., *Novel docosatrienes and 17S-resolvins generated from docosahexaenoic acid in murine brain, human blood, and glial cells. Autacoids in anti-inflammation*. J Biol Chem, 2003. **278**(17): p. 14677-87.
541. Campbell, E.L., et al., *Resolvin E1 promotes mucosal surface clearance of neutrophils: a new paradigm for inflammatory resolution*. FASEB J, 2007. **21**(12): p. 3162-70.
542. Krishnamoorthy, S., et al., *Resolvin D1 binds human phagocytes with evidence for proresolving receptors*. Proc Natl Acad Sci U S A, 2010. **107**(4): p. 1660-5.
543. Ariel, A., et al., *Apoptotic neutrophils and T cells sequester chemokines during immune response resolution through modulation of CCR5 expression*. Nat Immunol, 2006. **7**(11): p. 1209-16.
544. Schwab, J.M., et al., *Resolvin E1 and protectin D1 activate inflammation-resolution programmes*. Nature, 2007. **447**(7146): p. 869-74.
545. Serhan, C.N. and N. Chiang, *Novel endogenous small molecules as the checkpoint controllers in inflammation and resolution: entree for resoleomics*. Rheum Dis Clin North Am, 2004. **30**(1): p. 69-95.
546. Arita, M., et al., *Resolvin E1 selectively interacts with leukotriene B4 receptor BLT1 and ChemR23 to regulate inflammation*. J Immunol, 2007. **178**(6): p. 3912-7.

547. Sulciner, M.L., et al., *Resolvins suppress tumor growth and enhance cancer therapy*. J Exp Med, 2018. **215**(1): p. 115-140.
548. Arita, M., et al., *Stereochemical assignment, antiinflammatory properties, and receptor for the omega-3 lipid mediator resolvin E1*. J Exp Med, 2005. **201**(5): p. 713-22.
549. Liao, Z., et al., *Resolvin D1 attenuates inflammation in lipopolysaccharide-induced acute lung injury through a process involving the PPARgamma/NF-kappaB pathway*. Respir Res, 2012. **13**: p. 110.
550. Morin, C., et al., *Effect of docosahexaenoic acid monoacylglyceride on systemic hypertension and cardiovascular dysfunction*. Am J Physiol Heart Circ Physiol, 2015. **309**(1): p. H93-H102.
551. Merched, A.J., et al., *Atherosclerosis: evidence for impairment of resolution of vascular inflammation governed by specific lipid mediators*. FASEB J, 2008. **22**(10): p. 3595-606.
552. Viola, J.R., et al., *Resolving Lipid Mediators Maresin 1 and Resolvin D2 Prevent Atheroprogession in Mice*. Circ Res, 2016. **119**(9): p. 1030-1038.
553. Elajami, T.K., et al., *Specialized proresolving lipid mediators in patients with coronary artery disease and their potential for clot remodeling*. FASEB J, 2016. **30**(8): p. 2792-801.
554. Hasturk, H., et al., *Resolvin E1 (RvE1) Attenuates Atherosclerotic Plaque Formation in Diet and Inflammation-Induced Atherogenesis*. Arterioscler Thromb Vasc Biol, 2015. **35**(5): p. 1123-33.
555. Libby, P. and P.M. Ridker, *Inflammation and atherosclerosis: role of C-reactive protein in risk assessment*. Am J Med, 2004. **116 Suppl 6A**: p. 9S-16S.
556. Bennett, M.R., S. Sinha, and G.K. Owens, *Vascular Smooth Muscle Cells in Atherosclerosis*. Circ Res, 2016. **118**(4): p. 692-702.
557. Miyahara, T., et al., *D-series resolvin attenuates vascular smooth muscle cell activation and neointimal hyperplasia following vascular injury*. FASEB J, 2013. **27**(6): p. 2220-32.
558. Akagi, D., et al., *Systemic delivery of proresolving lipid mediators resolvin D2 and maresin 1 attenuates intimal hyperplasia in mice*. FASEB J, 2015. **29**(6): p. 2504-13.
559. Wu, B., et al., *Perivascular delivery of resolvin D1 inhibits neointimal hyperplasia in a rat model of arterial injury*. J Vasc Surg, 2017. **65**(1): p. 207-217 e3.

560. Chatterjee, A., et al., *Biosynthesis of proresolving lipid mediators by vascular cells and tissues*. FASEB J, 2017. **31**(8): p. 3393-3402.
561. Gilbert, K., et al., *Metabolites derived from omega-3 polyunsaturated fatty acids are important for cardioprotection*. Eur J Pharmacol, 2015. **769**: p. 147-53.
562. Gilbert, K., et al., *Resolvin D1 Reduces Infarct Size Through a Phosphoinositide 3-Kinase/Protein Kinase B Mechanism*. J Cardiovasc Pharmacol, 2015. **66**(1): p. 72-9.
563. Meyers, D.E., H.I. Basha, and M.K. Koenig, *Mitochondrial cardiomyopathy: pathophysiology, diagnosis, and management*. Tex Heart Inst J, 2013. **40**(4): p. 385-94.
564. Bayeva, M., M. Gheorghide, and H. Ardehali, *Mitochondria as a therapeutic target in heart failure*. J Am Coll Cardiol, 2013. **61**(6): p. 599-610.
565. Srivastava, S., *The Mitochondrial Basis of Aging and Age-Related Disorders*. Genes (Basel), 2017. **8**(12).
566. Wu, N.N., Y. Zhang, and J. Ren, *Mitophagy, Mitochondrial Dynamics, and Homeostasis in Cardiovascular Aging*. Oxid Med Cell Longev, 2019. **2019**: p. 9825061.
567. Rovira-Llopis, S., et al., *Mitochondrial dynamics in type 2 diabetes: Pathophysiological implications*. Redox Biol, 2017. **11**: p. 637-645.
568. Cho, D.H., J.K. Kim, and E.K. Jo, *Mitophagy and Innate Immunity in Infection*. Mol Cells, 2020. **43**(1): p. 10-22.
569. Kim, S.J., et al., *The essential role of mitochondrial dynamics in antiviral immunity*. Mitochondrion, 2018. **41**: p. 21-27.
570. Akhnokh, M.K., et al., *Inhibition of Soluble Epoxide Hydrolase Limits Mitochondrial Damage and Preserves Function Following Ischemic Injury*. Front Pharmacol, 2016. **7**: p. 133.
571. Batchu, S.N., et al., *Novel soluble epoxide hydrolase inhibitor protects mitochondrial function following stress*. Can J Physiol Pharmacol, 2012. **90**(6): p. 811-23.
572. Katragadda, D., et al., *Epoxyeicosatrienoic acids limit damage to mitochondrial function following stress in cardiac cells*. J Mol Cell Cardiol, 2009. **46**(6): p. 867-75.
573. Walters, A.M., G.A. Porter, Jr., and P.S. Brookes, *Mitochondria as a drug target in ischemic heart disease and cardiomyopathy*. Circ Res, 2012. **111**(9): p. 1222-36.

574. Linde, A., et al., *Innate immunity and inflammation--New frontiers in comparative cardiovascular pathology*. Cardiovasc Res, 2007. **73**(1): p. 26-36.
575. Zhou, R., et al., *A role for mitochondria in NLRP3 inflammasome activation*. Nature, 2011. **469**(7329): p. 221-5.
576. Stutz, A., D.T. Golenbock, and E. Latz, *Inflammasomes: too big to miss*. J Clin Invest, 2009. **119**(12): p. 3502-11.
577. Takahashi, M., *Role of the inflammasome in myocardial infarction*. Trends Cardiovasc Med, 2011. **21**(2): p. 37-41.
578. Harris, W.S., L. Del Gobbo, and N.L. Tintle, *The Omega-3 Index and relative risk for coronary heart disease mortality: Estimation from 10 cohort studies*. Atherosclerosis, 2017. **262**: p. 51-54.
579. Qadhi, R., et al., *Differential responses to docosahexaenoic acid in primary and immortalized cardiac cells*. Toxicol Lett, 2013. **219**(3): p. 288-97.
580. Seubert, J., et al., *Enhanced postischemic functional recovery in CYP2J2 transgenic hearts involves mitochondrial ATP-sensitive K⁺ channels and p42/p44 MAPK pathway*. Circ Res, 2004. **95**(5): p. 506-14.
581. Seubert, J.M., et al., *Role of soluble epoxide hydrolase in postischemic recovery of heart contractile function*. Circ Res, 2006. **99**(4): p. 442-50.
582. Batchu, S.N., et al., *Epoxyeicosatrienoic acid prevents postischemic electrocardiogram abnormalities in an isolated heart model*. J Mol Cell Cardiol, 2009. **46**(1): p. 67-74.
583. Chaudhary, K.R., et al., *Role of B-type natriuretic peptide in epoxyeicosatrienoic acid-mediated improved post-ischaemic recovery of heart contractile function*. Cardiovasc Res, 2009. **83**(2): p. 362-70.
584. Jamieson, K.L., et al., *Genetic deletion of soluble epoxide hydrolase provides cardioprotective responses following myocardial infarction in aged mice*. Prostaglandins Other Lipid Mediat, 2017. **132**: p. 47-58.
585. Kuznetsov, A.V., et al., *Analysis of mitochondrial function in situ in permeabilized muscle fibers, tissues and cells*. Nat Protoc, 2008. **3**(6): p. 965-76.
586. Seubert, J.M., et al., *Apoptosis in murine hepatoma hepa 1c1c7 wild-type, C12, and C4 cells mediated by bilirubin*. Mol Pharmacol, 2002. **62**(2): p. 257-64.

587. Holmgren, A. and M. Bjornstedt, *Thioredoxin and thioredoxin reductase*. *Methods Enzymol*, 1995. **252**: p. 199-208.
588. Arner, E.S. and A. Holmgren, *Measurement of thioredoxin and thioredoxin reductase*. *Curr Protoc Toxicol*, 2001. **Chapter 7**: p. Unit 7 4.
589. Tousoulis, D., et al., *Omega-3 PUFAs improved endothelial function and arterial stiffness with a parallel antiinflammatory effect in adults with metabolic syndrome*. *Atherosclerosis*, 2014. **232**(1): p. 10-6.
590. Wang, Q., et al., *Effect of omega-3 fatty acids supplementation on endothelial function: a meta-analysis of randomized controlled trials*. *Atherosclerosis*, 2012. **221**(2): p. 536-43.
591. Miller, P.E., M. Van Elswyk, and D.D. Alexander, *Long-chain omega-3 fatty acids eicosapentaenoic acid and docosahexaenoic acid and blood pressure: a meta-analysis of randomized controlled trials*. *Am J Hypertens*, 2014. **27**(7): p. 885-96.
592. Minihane, A.M., et al., *Consumption of Fish Oil Providing Amounts of Eicosapentaenoic Acid and Docosahexaenoic Acid That Can Be Obtained from the Diet Reduces Blood Pressure in Adults with Systolic Hypertension: A Retrospective Analysis*. *J Nutr*, 2016. **146**(3): p. 516-23.
593. Powis, G. and W.R. Montfort, *Properties and biological activities of thioredoxins*. *Annu Rev Biophys Biomol Struct*, 2001. **30**: p. 421-55.
594. Tao, L., et al., *Thioredoxin reduces post-ischemic myocardial apoptosis by reducing oxidative/nitrative stress*. *Br J Pharmacol*, 2006. **149**(3): p. 311-8.
595. Tanaka, T., et al., *Thioredoxin-2 (TRX-2) is an essential gene regulating mitochondria-dependent apoptosis*. *EMBO J*, 2002. **21**(7): p. 1695-703.
596. Le Page, S., et al., *Increase in Cardiac Ischemia-Reperfusion Injuries in *Opal* +/- Mouse Model*. *PLoS One*, 2016. **11**(10): p. e0164066.
597. Chen, L., et al., *Mitochondrial OPA1, apoptosis, and heart failure*. *Cardiovasc Res*, 2009. **84**(1): p. 91-9.
598. Chen, H., A. Chomyn, and D.C. Chan, *Disruption of fusion results in mitochondrial heterogeneity and dysfunction*. *J Biol Chem*, 2005. **280**(28): p. 26185-92.
599. Liu, Y., et al., *TXNIP mediates NLRP3 inflammasome activation in cardiac microvascular endothelial cells as a novel mechanism in myocardial ischemia/reperfusion injury*. *Basic Res Cardiol*, 2014. **109**(5): p. 415.

600. Wu, N., et al., *AMPK-dependent degradation of TXNIP upon energy stress leads to enhanced glucose uptake via GLUT1*. Mol Cell, 2013. **49**(6): p. 1167-75.
601. Waldhart, A.N., et al., *Phosphorylation of TXNIP by AKT Mediates Acute Influx of Glucose in Response to Insulin*. Cell Rep, 2017. **19**(10): p. 2005-2013.
602. Ichinohe, T., et al., *Mitochondrial protein mitofusin 2 is required for NLRP3 inflammasome activation after RNA virus infection*. Proc Natl Acad Sci U S A, 2013. **110**(44): p. 17963-8.
603. Kris-Etherton, P.M., et al., *Fish consumption, fish oil, omega-3 fatty acids, and cardiovascular disease*. Circulation, 2002. **106**(21): p. 2747-57.
604. Lavie, C.J., et al., *Omega-3 polyunsaturated fatty acids and cardiovascular diseases*. J Am Coll Cardiol, 2009. **54**(7): p. 585-94.
605. Mozaffarian, D., *Fish and n-3 fatty acids for the prevention of fatal coronary heart disease and sudden cardiac death*. Am J Clin Nutr, 2008. **87**(6): p. 1991S-6S.
606. Calder, P.C. and P. Yaqoob, *Marine omega-3 fatty acids and coronary heart disease*. Curr Opin Cardiol, 2012. **27**(4): p. 412-9.
607. Matthan, N.R., et al., *A systematic review and meta-analysis of the impact of omega-3 fatty acids on selected arrhythmia outcomes in animal models*. Metabolism, 2005. **54**(12): p. 1557-65.
608. Leaf, A., et al., *Clinical prevention of sudden cardiac death by n-3 polyunsaturated fatty acids and mechanism of prevention of arrhythmias by n-3 fish oils*. Circulation, 2003. **107**(21): p. 2646-52.
609. Zhang, G., S. Kodani, and B.D. Hammock, *Stabilized epoxygenated fatty acids regulate inflammation, pain, angiogenesis and cancer*. Prog Lipid Res, 2014. **53**: p. 108-23.
610. Wang, Y., et al., *Naoxintong attenuates Ischaemia/reperfusion Injury through inhibiting NLRP3 inflammasome activation*. J Cell Mol Med, 2017. **21**(1): p. 4-12.
611. Rider, P., et al., *IL-1alpha and IL-1beta recruit different myeloid cells and promote different stages of sterile inflammation*. J Immunol, 2011. **187**(9): p. 4835-43.
612. Fritsche, K., *Fatty acids as modulators of the immune response*. Annu Rev Nutr, 2006. **26**: p. 45-73.

613. Yan, Y., et al., *Omega-3 fatty acids prevent inflammation and metabolic disorder through inhibition of NLRP3 inflammasome activation*. *Immunity*, 2013. **38**(6): p. 1154-63.
614. Robinson, D.R., et al., *Dietary marine lipids suppress continuous expression of interleukin-1 beta gene transcription*. *Lipids*, 1996. **31 Suppl**: p. S23-31.
615. Cereghetti, G.M., et al., *Dephosphorylation by calcineurin regulates translocation of Drp1 to mitochondria*. *Proc Natl Acad Sci U S A*, 2008. **105**(41): p. 15803-8.
616. Olichon, A., et al., *The human dynamin-related protein OPA1 is anchored to the mitochondrial inner membrane facing the inter-membrane space*. *FEBS Lett*, 2002. **523**(1-3): p. 171-6.
617. Meeusen, S., et al., *Mitochondrial inner-membrane fusion and crista maintenance requires the dynamin-related GTPase Mgm1*. *Cell*, 2006. **127**(2): p. 383-95.
618. Civiletto, G., et al., *Opal overexpression ameliorates the phenotype of two mitochondrial disease mouse models*. *Cell Metab*, 2015. **21**(6): p. 845-54.
619. Varanita, T., et al., *The OPA1-dependent mitochondrial cristae remodeling pathway controls atrophic, apoptotic, and ischemic tissue damage*. *Cell Metab*, 2015. **21**(6): p. 834-44.
620. Wang, Y., G.W. De Keulenaer, and R.T. Lee, *Vitamin D(3)-up-regulated protein-1 is a stress-responsive gene that regulates cardiomyocyte viability through interaction with thioredoxin*. *J Biol Chem*, 2002. **277**(29): p. 26496-500.
621. Su, H., et al., *Acute hyperglycaemia enhances oxidative stress and aggravates myocardial ischaemia/reperfusion injury: role of thioredoxin-interacting protein*. *J Cell Mol Med*, 2013. **17**(1): p. 181-91.
622. Zhang, R., et al., *Thioredoxin-2 inhibits mitochondria-located ASK1-mediated apoptosis in a JNK-independent manner*. *Circ Res*, 2004. **94**(11): p. 1483-91.
623. Saxena, G., J. Chen, and A. Shalev, *Intracellular shuttling and mitochondrial function of thioredoxin-interacting protein*. *J Biol Chem*, 2010. **285**(6): p. 3997-4005.
624. Zhou, R., et al., *Thioredoxin-interacting protein links oxidative stress to inflammasome activation*. *Nat Immunol*, 2010. **11**(2): p. 136-40.
625. Yoshioka, J., et al., *Deletion of thioredoxin-interacting protein in mice impairs mitochondrial function but protects the myocardium from ischemia-reperfusion injury*. *J Clin Invest*, 2012. **122**(1): p. 267-79.

626. Detmer, S.A. and D.C. Chan, *Complementation between mouse Mfn1 and Mfn2 protects mitochondrial fusion defects caused by CMT2A disease mutations*. J Cell Biol, 2007. **176**(4): p. 405-14.
627. Cipolat, S., et al., *OPA1 requires mitofusin 1 to promote mitochondrial fusion*. Proc Natl Acad Sci U S A, 2004. **101**(45): p. 15927-32.
628. Archer, S.L., *Mitochondrial dynamics--mitochondrial fission and fusion in human diseases*. N Engl J Med, 2013. **369**(23): p. 2236-51.
629. Anderson, J.L. and D.A. Morrow, *Acute Myocardial Infarction*. N Engl J Med, 2017. **376**(21): p. 2053-2064.
630. Menees, D.S., et al., *Door-to-balloon time and mortality among patients undergoing primary PCI*. N Engl J Med, 2013. **369**(10): p. 901-9.
631. Schroder, K. and J. Tschopp, *The inflammasomes*. Cell, 2010. **140**(6): p. 821-32.
632. Guo, H., J.B. Callaway, and J.P. Ting, *Inflammasomes: mechanism of action, role in disease, and therapeutics*. Nat Med, 2015. **21**(7): p. 677-87.
633. Hammock, B.D., M. Ratcliff, and D.A. Schooley, *Hydration of an 18O epoxide by a cytosolic epoxide hydrolase from mouse liver*. Life Sci, 1980. **27**(18): p. 1635-41.
634. Yu, Z., et al., *Soluble epoxide hydrolase regulates hydrolysis of vasoactive epoxyeicosatrienoic acids*. Circ Res, 2000. **87**(11): p. 992-8.
635. Fang, X., et al., *Effect of soluble epoxide hydrolase inhibition on epoxyeicosatrienoic acid metabolism in human blood vessels*. Am J Physiol Heart Circ Physiol, 2004. **287**(6): p. H2412-20.
636. Mabalirajan, U., et al., *Linoleic acid metabolite drives severe asthma by causing airway epithelial injury*. Sci Rep, 2013. **3**: p. 1349.
637. Lynes, M.D., et al., *The cold-induced lipokine 12,13-diHOME promotes fatty acid transport into brown adipose tissue*. Nat Med, 2017. **23**(5): p. 631-637.
638. Siegfried, M.R., et al., *Direct cardiovascular actions of two metabolites of linoleic acid*. Life Sci, 1990. **46**(6): p. 427-33.
639. Sugiyama, S., et al., *Leukotoxin, 9, 10-epoxy-12-octadecenoate, causes cardiac failure in dogs*. Life Sci, 1987. **40**(3): p. 225-31.

640. Bannehr, M., et al., *Linoleic Acid Metabolite DiHOME Decreases Post-ischemic Cardiac Recovery in Murine Hearts*. *Cardiovasc Toxicol*, 2019.
641. Motoki, A., et al., *Soluble epoxide hydrolase inhibition and gene deletion are protective against myocardial ischemia-reperfusion injury in vivo*. *Am J Physiol Heart Circ Physiol*, 2008. **295**(5): p. H2128-34.
642. Imig, J.D. and B.D. Hammock, *Soluble epoxide hydrolase as a therapeutic target for cardiovascular diseases*. *Nat Rev Drug Discov*, 2009. **8**(10): p. 794-805.
643. Chaudhary, K.R., et al., *Inhibition of soluble epoxide hydrolase by trans-4- [4-(3-adamantan-1-yl-ureido)-cyclohexyloxy]-benzoic acid is protective against ischemia-reperfusion injury*. *J Cardiovasc Pharmacol*, 2010. **55**(1): p. 67-73.
644. Samokhvalov, V., et al., *Deficiency of Soluble Epoxide Hydrolase Protects Cardiac Function Impaired by LPS-Induced Acute Inflammation*. *Front Pharmacol*, 2018. **9**: p. 1572.
645. Honda, H.M., P. Korge, and J.N. Weiss, *Mitochondria and ischemia/reperfusion injury*. *Ann N Y Acad Sci*, 2005. **1047**: p. 248-58.
646. Tao, L., et al., *Cardioprotective effects of thioredoxin in myocardial ischemia and reperfusion: role of S-nitrosation [corrected]*. *Proc Natl Acad Sci U S A*, 2004. **101**(31): p. 11471-6.
647. Ozer, M.K., et al., *Ischemia-reperfusion leads to depletion of glutathione content and augmentation of malondialdehyde production in the rat heart from overproduction of oxidants: can caffeic acid phenethyl ester (CAPE) protect the heart?* *Mol Cell Biochem*, 2005. **273**(1-2): p. 169-75.
648. Chan, D.C., *Mitochondria: dynamic organelles in disease, aging, and development*. *Cell*, 2006. **125**(7): p. 1241-52.
649. Grant, D.F., D.H. Storms, and B.D. Hammock, *Molecular cloning and expression of murine liver soluble epoxide hydrolase*. *J Biol Chem*, 1993. **268**(23): p. 17628-33.
650. Knehr, M., et al., *Isolation and characterization of a cDNA encoding rat liver cytosolic epoxide hydrolase and its functional expression in Escherichia coli*. *J Biol Chem*, 1993. **268**(23): p. 17623-7.
651. Beetham, J.K., T. Tian, and B.D. Hammock, *cDNA cloning and expression of a soluble epoxide hydrolase from human liver*. *Arch Biochem Biophys*, 1993. **305**(1): p. 197-201.

652. Misawa, E., et al., *Characterisation of a catabolic epoxide hydrolase from a Corynebacterium sp.* Eur J Biochem, 1998. **253**(1): p. 173-83.
653. Rink, R., et al., *Primary structure and catalytic mechanism of the epoxide hydrolase from Agrobacterium radiobacter AD1.* J Biol Chem, 1997. **272**(23): p. 14650-7.
654. Stapleton, A., et al., *Cloning and expression of soluble epoxide hydrolase from potato.* Plant J, 1994. **6**(2): p. 251-8.
655. Kiyosue, T., et al., *Characterization of an Arabidopsis cDNA for a soluble epoxide hydrolase gene that is inducible by auxin and water stress.* Plant J, 1994. **6**(2): p. 259-69.
656. Weintraub, N.L., et al., *Epoxide hydrolases regulate epoxyeicosatrienoic acid incorporation into coronary endothelial phospholipids.* Am J Physiol, 1999. **277**(5): p. H2098-108.
657. Luria, A., et al., *Compensatory mechanism for homeostatic blood pressure regulation in Ephx2 gene-disrupted mice.* J Biol Chem, 2007. **282**(5): p. 2891-8.
658. Williams, J.M., et al., *20-hydroxyeicosatetraenoic acid: a new target for the treatment of hypertension.* J Cardiovasc Pharmacol, 2010. **56**(4): p. 336-44.
659. Imig, J.D., *Cardiovascular therapeutic aspects of soluble epoxide hydrolase inhibitors.* Cardiovasc Drug Rev, 2006. **24**(2): p. 169-88.
660. Marino, J.P., Jr., *Soluble epoxide hydrolase, a target with multiple opportunities for cardiovascular drug discovery.* Curr Top Med Chem, 2009. **9**(5): p. 452-63.
661. Gross, G.J. and K. Nithipatikom, *Soluble epoxide hydrolase: a new target for cardioprotection.* Curr Opin Investig Drugs, 2009. **10**(3): p. 253-8.
662. Seubert, J.M., et al., *Role of epoxyeicosatrienoic acids in protecting the myocardium following ischemia/reperfusion injury.* Prostaglandins Other Lipid Mediat, 2007. **82**(1-4): p. 50-9.
663. Node, K., et al., *Anti-inflammatory properties of cytochrome P450 epoxygenase-derived eicosanoids.* Science, 1999. **285**(5431): p. 1276-9.
664. Chaudhary, K.R., et al., *Differential effects of soluble epoxide hydrolase inhibition and CYP2J2 overexpression on postischemic cardiac function in aged mice.* Prostaglandins Other Lipid Mediat, 2013. **104-105**: p. 8-17.

665. Batchu, S.N., et al., *Cardioprotective effect of a dual acting epoxyeicosatrienoic acid analogue towards ischaemia reperfusion injury*. Br J Pharmacol, 2011. **162**(4): p. 897-907.
666. Li, N., et al., *Beneficial effects of soluble epoxide hydrolase inhibitors in myocardial infarction model: Insight gained using metabolomic approaches*. J Mol Cell Cardiol, 2009. **47**(6): p. 835-45.
667. Moghaddam, M.F., et al., *Bioactivation of leukotoxins to their toxic diols by epoxide hydrolase*. Nat Med, 1997. **3**(5): p. 562-6.
668. Dudda, A., G. Spiteller, and F. Kobelt, *Lipid oxidation products in ischemic porcine heart tissue*. Chem Phys Lipids, 1996. **82**(1): p. 39-51.
669. Edin, M.L., et al., *Endothelial expression of human cytochrome P450 epoxygenase CYP2C8 increases susceptibility to ischemia-reperfusion injury in isolated mouse heart*. FASEB J, 2011. **25**(10): p. 3436-47.
670. Harrell, M.D. and J.R. Stimers, *Differential effects of linoleic Acid metabolites on cardiac sodium current*. J Pharmacol Exp Ther, 2002. **303**(1): p. 347-55.
671. Sisemore, M.F., et al., *Cellular characterization of leukotoxin diol-induced mitochondrial dysfunction*. Arch Biochem Biophys, 2001. **392**(1): p. 32-7.
672. Guo, Z., et al., *NLRP3 Is Involved in Ischemia/Reperfusion Injury*. CNS Neurol Disord Drug Targets, 2016. **15**(6): p. 699-712.
673. Van Tassell, B.W., et al., *Enhanced interleukin-1 activity contributes to exercise intolerance in patients with systolic heart failure*. PLoS One, 2012. **7**(3): p. e33438.
674. Kumar, A., et al., *Tumor necrosis factor alpha and interleukin 1beta are responsible for in vitro myocardial cell depression induced by human septic shock serum*. J Exp Med, 1996. **183**(3): p. 949-58.
675. Van Tassell, B.W., et al., *Interleukin-1beta induces a reversible cardiomyopathy in the mouse*. Inflamm Res, 2013. **62**(7): p. 637-40.
676. Cain, B.S., et al., *Tumor necrosis factor-alpha and interleukin-1beta synergistically depress human myocardial function*. Crit Care Med, 1999. **27**(7): p. 1309-18.
677. Hosenpud, J.D., S.M. Campbell, and D.J. Mendelson, *Interleukin-1-induced myocardial depression in an isolated beating heart preparation*. J Heart Transplant, 1989. **8**(6): p. 460-4.

678. Ing, D.J., et al., *Modulation of cytokine-induced cardiac myocyte apoptosis by nitric oxide, Bak, and Bcl-x*. *Circ Res*, 1999. **84**(1): p. 21-33.
679. Nazir, S., et al., *Cytoprotective activated protein C averts Nlrp3 inflammasome-induced ischemia-reperfusion injury via mTORC1 inhibition*. *Blood*, 2017. **130**(24): p. 2664-2677.
680. Inceoglu, B., et al., *Inhibition of soluble epoxide hydrolase reduces LPS-induced thermal hyperalgesia and mechanical allodynia in a rat model of inflammatory pain*. *Life Sci*, 2006. **79**(24): p. 2311-9.
681. Darwesh, A.M., et al., *Insights into the cardioprotective properties of n-3 PUFAs against ischemic heart disease via modulation of the innate immune system*. *Chem Biol Interact*, 2019. **308**: p. 20-44.
682. Zhou, Y., et al., *Soluble Epoxide Hydrolase Inhibitor Attenuates Lipopolysaccharide-Induced Acute Lung Injury and Improves Survival in Mice*. *Shock*, 2017. **47**(5): p. 638-645.
683. Liu, F.C., H.I. Tsai, and H.P. Yu, *Organ-Protective Effects of Red Wine Extract, Resveratrol, in Oxidative Stress-Mediated Reperfusion Injury*. *Oxid Med Cell Longev*, 2015. **2015**: p. 568634.
684. Seth, R.B., et al., *Identification and characterization of MAVS, a mitochondrial antiviral signaling protein that activates NF-kappaB and IRF 3*. *Cell*, 2005. **122**(5): p. 669-82.
685. Xu, L.G., et al., *VISA is an adapter protein required for virus-triggered IFN-beta signaling*. *Mol Cell*, 2005. **19**(6): p. 727-40.
686. Xu, M., et al., *Cardiotonic Pill Reduces Myocardial Ischemia-Reperfusion Injury via Increasing EET Concentrations in Rats*. *Drug Metab Dispos*, 2016. **44**(7): p. 878-87.
687. O'Gara, P.T., et al., *2013 ACCF/AHA guideline for the management of ST-elevation myocardial infarction: a report of the American College of Cardiology Foundation/American Heart Association Task Force on Practice Guidelines*. *J Am Coll Cardiol*, 2013. **61**(4): p. e78-e140.
688. Maroko, P.R., et al., *Coronary artery reperfusion. I. Early effects on local myocardial function and the extent of myocardial necrosis*. *J Clin Invest*, 1972. **51**(10): p. 2710-6.
689. Cadenas, S., *ROS and redox signaling in myocardial ischemia-reperfusion injury and cardioprotection*. *Free Radic Biol Med*, 2018. **117**: p. 76-89.

690. Jassem, W., et al., *The role of mitochondria in ischemia/reperfusion injury*. Transplantation, 2002. **73**(4): p. 493-9.
691. Di Lisa, F. and P. Bernardi, *Mitochondria and ischemia-reperfusion injury of the heart: fixing a hole*. Cardiovasc Res, 2006. **70**(2): p. 191-9.
692. Bugger, H., C.N. Witt, and C. Bode, *Mitochondrial sirtuins in the heart*. Heart Fail Rev, 2016. **21**(5): p. 519-28.
693. Winnik, S., et al., *Protective effects of sirtuins in cardiovascular diseases: from bench to bedside*. Eur Heart J, 2015. **36**(48): p. 3404-12.
694. Pillai, V.B., et al., *Mitochondrial SIRT3 and heart disease*. Cardiovasc Res, 2010. **88**(2): p. 250-6.
695. Koentges, C., C. Bode, and H. Bugger, *SIRT3 in Cardiac Physiology and Disease*. Front Cardiovasc Med, 2016. **3**: p. 38.
696. Rardin, M.J., et al., *Label-free quantitative proteomics of the lysine acetylome in mitochondria identifies substrates of SIRT3 in metabolic pathways*. Proc Natl Acad Sci U S A, 2013. **110**(16): p. 6601-6.
697. Hirschey, M.D., et al., *SIRT3 deficiency and mitochondrial protein hyperacetylation accelerate the development of the metabolic syndrome*. Mol Cell, 2011. **44**(2): p. 177-90.
698. Wen, H., E.A. Miao, and J.P. Ting, *Mechanisms of NOD-like receptor-associated inflammasome activation*. Immunity, 2013. **39**(3): p. 432-41.
699. Horng, T., *Calcium signaling and mitochondrial destabilization in the triggering of the NLRP3 inflammasome*. Trends Immunol, 2014. **35**(6): p. 253-61.
700. Chen, M.L., et al., *Trimethylamine-N-Oxide Induces Vascular Inflammation by Activating the NLRP3 Inflammasome Through the SIRT3-SOD2-mtROS Signaling Pathway*. J Am Heart Assoc, 2017. **6**(9).
701. Jump, D.B., *The biochemistry of n-3 polyunsaturated fatty acids*. J Biol Chem, 2002. **277**(11): p. 8755-8.
702. Darwesh, A.M., et al., *Genetic Deletion or Pharmacological Inhibition of Soluble Epoxide Hydrolase Ameliorates Cardiac Ischemia/Reperfusion Injury by Attenuating NLRP3 Inflammasome Activation*. Int J Mol Sci, 2019. **20**(14).

703. Morisseau, C. and B.D. Hammock, *Epoxide hydrolases: mechanisms, inhibitor designs, and biological roles*. *Annu Rev Pharmacol Toxicol*, 2005. **45**: p. 311-33.
704. Cinelli, M.A., et al., *Enzymatic synthesis and chemical inversion provide both enantiomers of bioactive epoxydocosapentaenoic acids*. *J Lipid Res*, 2018. **59**(11): p. 2237-2252.
705. Falck, J.R., et al., *14,15-Epoxyeicosa-5,8,11-trienoic acid (14,15-EET) surrogates containing epoxide bioisosteres: influence upon vascular relaxation and soluble epoxide hydrolase inhibition*. *J Med Chem*, 2009. **52**(16): p. 5069-75.
706. Zhang, H.Y., et al., *Synthesis of long-chain fatty acid derivatives as a novel anti-Alzheimer's agent*. *Bioorg Med Chem Lett*, 2014. **24**(2): p. 604-8.
707. Falck, J.R., et al., *14,15-Epoxyeicosa-5,8,11-trienoic Acid (14,15-EET) surrogates: carboxylate modifications*. *J Med Chem*, 2014. **57**(16): p. 6965-72.
708. Jamieson, K.L., et al., *Age and Sex Differences in Hearts of Soluble Epoxide Hydrolase Null Mice*. *Front Physiol*, 2020. **11**: p. 48.
709. Tompkins, A.J., et al., *Mitochondrial dysfunction in cardiac ischemia-reperfusion injury: ROS from complex I, without inhibition*. *Biochim Biophys Acta*, 2006. **1762**(2): p. 223-31.
710. Finkel, T. and N.J. Holbrook, *Oxidants, oxidative stress and the biology of ageing*. *Nature*, 2000. **408**(6809): p. 239-47.
711. Balaban, R.S., S. Nemoto, and T. Finkel, *Mitochondria, oxidants, and aging*. *Cell*, 2005. **120**(4): p. 483-95.
712. Tao, R., et al., *Sirt3-mediated deacetylation of evolutionarily conserved lysine 122 regulates MnSOD activity in response to stress*. *Mol Cell*, 2010. **40**(6): p. 893-904.
713. Spitz, D.R. and L.W. Oberley, *An assay for superoxide dismutase activity in mammalian tissue homogenates*. *Anal Biochem*, 1989. **179**(1): p. 8-18.
714. Imai, S. and L. Guarente, *NAD⁺ and sirtuins in aging and disease*. *Trends Cell Biol*, 2014. **24**(8): p. 464-71.
715. Palmer, C.S., et al., *The regulation of mitochondrial morphology: intricate mechanisms and dynamic machinery*. *Cell Signal*, 2011. **23**(10): p. 1534-45.
716. Otera, H., et al., *Mff is an essential factor for mitochondrial recruitment of Drp1 during mitochondrial fission in mammalian cells*. *J Cell Biol*, 2010. **191**(6): p. 1141-58.

717. Signorile, A., et al., *Mitochondrial cAMP prevents apoptosis modulating Sirt3 protein level and OPA1 processing in cardiac myoblast cells*. *Biochim Biophys Acta Mol Cell Res*, 2017. **1864**(2): p. 355-366.
718. Subramanian, N., et al., *The adaptor MAVS promotes NLRP3 mitochondrial localization and inflammasome activation*. *Cell*, 2013. **153**(2): p. 348-61.
719. Misawa, T., et al., *Microtubule-driven spatial arrangement of mitochondria promotes activation of the NLRP3 inflammasome*. *Nat Immunol*, 2013. **14**(5): p. 454-60.
720. Hasegawa, E., et al., *Cytochrome P450 monooxygenase lipid metabolites are significant second messengers in the resolution of choroidal neovascularization*. *Proc Natl Acad Sci U S A*, 2017. **114**(36): p. E7545-E7553.
721. Shen, H.C., *Soluble epoxide hydrolase inhibitors: a patent review*. *Expert Opin Ther Pat*, 2010. **20**(7): p. 941-56.
722. Wang, W., et al., *omega-3 polyunsaturated fatty acids-derived lipid metabolites on angiogenesis, inflammation and cancer*. *Prostaglandins Other Lipid Mediat*, 2014. **113-115**: p. 13-20.
723. Shearer, G.C., et al., *Detection of omega-3 oxylipins in human plasma and response to treatment with omega-3 acid ethyl esters*. *J Lipid Res*, 2010. **51**(8): p. 2074-81.
724. Capozzi, M.E., et al., *Epoxygenated Fatty Acids Inhibit Retinal Vascular Inflammation*. *Sci Rep*, 2016. **6**: p. 39211.
725. Bell, E.L. and L. Guarente, *The SirT3 divining rod points to oxidative stress*. *Mol Cell*, 2011. **42**(5): p. 561-8.
726. Zhai, M., et al., *Melatonin ameliorates myocardial ischemia reperfusion injury through SIRT3-dependent regulation of oxidative stress and apoptosis*. *J Pineal Res*, 2017. **63**(2).
727. Di Lisa, F., et al., *Opening of the mitochondrial permeability transition pore causes depletion of mitochondrial and cytosolic NAD⁺ and is a causative event in the death of myocytes in postischemic reperfusion of the heart*. *J Biol Chem*, 2001. **276**(4): p. 2571-5.
728. Hill, B.G., et al., *Myocardial ischaemia inhibits mitochondrial metabolism of 4-hydroxy-trans-2-nonenal*. *Biochem J*, 2009. **417**(2): p. 513-24.
729. Lindahl, T., et al., *Post-translational modification of poly(ADP-ribose) polymerase induced by DNA strand breaks*. *Trends Biochem Sci*, 1995. **20**(10): p. 405-11.

730. Fu, J., et al., *trans-(-)-epsilon-Viniferin increases mitochondrial sirtuin 3 (SIRT3), activates AMP-activated protein kinase (AMPK), and protects cells in models of Huntington Disease*. J Biol Chem, 2012. **287**(29): p. 24460-72.
731. Morigi, M., et al., *Sirtuin 3-dependent mitochondrial dynamic improvements protect against acute kidney injury*. J Clin Invest, 2015. **125**(2): p. 715-26.
732. Shimada, K., et al., *Oxidized mitochondrial DNA activates the NLRP3 inflammasome during apoptosis*. Immunity, 2012. **36**(3): p. 401-14.
733. Liu, P., et al., *Sirtuin 3-induced macrophage autophagy in regulating NLRP3 inflammasome activation*. Biochim Biophys Acta Mol Basis Dis, 2018. **1864**(3): p. 764-777.
734. Blondheim, D.S., et al., *Characteristics, Management, and Outcome of Transient ST-elevation Versus Persistent ST-elevation and Non-ST-elevation Myocardial Infarction*. Am J Cardiol, 2018. **121**(12): p. 1449-1455.
735. Lin, B., et al., *DUSP14 knockout accelerates cardiac ischemia reperfusion (IR) injury through activating NF-kappaB and MAPKs signaling pathways modulated by ROS generation*. Biochem Biophys Res Commun, 2018. **501**(1): p. 24-32.
736. Fan, D., et al., *Sesamin Protects Against Cardiac Remodeling Via Sirt3/ROS Pathway*. Cell Physiol Biochem, 2017. **44**(6): p. 2212-2227.
737. Lemieux, H., et al., *Mitochondrial respiratory control and early defects of oxidative phosphorylation in the failing human heart*. Int J Biochem Cell Biol, 2011. **43**(12): p. 1729-38.
738. Muntean, D.M., et al., *The Role of Mitochondrial Reactive Oxygen Species in Cardiovascular Injury and Protective Strategies*. Oxid Med Cell Longev, 2016. **2016**: p. 8254942.
739. Baeza, J., M.J. Smallegan, and J.M. Denu, *Mechanisms and Dynamics of Protein Acetylation in Mitochondria*. Trends Biochem Sci, 2016. **41**(3): p. 231-244.
740. El-Sikhry, H.E., et al., *Novel Roles of Epoxyeicosanoids in Regulating Cardiac Mitochondria*. PLoS One, 2016. **11**(8): p. e0160380.
741. Altamimi, T.R., et al., *A novel role of endothelial autophagy as a regulator of myocardial fatty acid oxidation*. J Thorac Cardiovasc Surg, 2019. **157**(1): p. 185-193.

742. Altamimi, T.R., et al., *Cytosolic carnitine acetyltransferase as a source of cytosolic acetyl-CoA: a possible mechanism for regulation of cardiac energy metabolism*. *Biochem J*, 2018. **475**(5): p. 959-976.
743. Bitterman, K.J., et al., *Inhibition of silencing and accelerated aging by nicotinamide, a putative negative regulator of yeast sir2 and human SIRT1*. *J Biol Chem*, 2002. **277**(47): p. 45099-107.
744. Avalos, J.L., K.M. Bever, and C. Wolberger, *Mechanism of sirtuin inhibition by nicotinamide: altering the NAD(+) cosubstrate specificity of a Sir2 enzyme*. *Mol Cell*, 2005. **17**(6): p. 855-68.
745. Xu, H., et al., *Caffeine Targets SIRT3 to Enhance SOD2 Activity in Mitochondria*. *Front Cell Dev Biol*, 2020. **8**: p. 822.
746. Jamieson, K.L., et al., *Soluble Epoxide Hydrolase in Aged Female Mice and Human Explanted Hearts Following Ischemic Injury*. *Int J Mol Sci*, 2021. **22**(4).
747. Salabei, J.K., A.A. Gibb, and B.G. Hill, *Comprehensive measurement of respiratory activity in permeabilized cells using extracellular flux analysis*. *Nat Protoc*, 2014. **9**(2): p. 421-38.
748. Brand, M.D. and D.G. Nicholls, *Assessing mitochondrial dysfunction in cells*. *Biochem J*, 2011. **435**(2): p. 297-312.
749. Pesta, D. and E. Gnaiger, *High-resolution respirometry: OXPHOS protocols for human cells and permeabilized fibers from small biopsies of human muscle*. *Methods Mol Biol*, 2012. **810**: p. 25-58.
750. Hill, B.G., et al., *Integration of cellular bioenergetics with mitochondrial quality control and autophagy*. *Biol Chem*, 2012. **393**(12): p. 1485-1512.
751. Amerand, A., et al., *In vitro effect of hydrostatic pressure exposure on hydroxyl radical production in fish red muscle*. *Redox Rep*, 2005. **10**(1): p. 25-8.
752. Galan, D.T., et al., *Reduced mitochondrial respiration in the ischemic as well as in the remote nonischemic region in postmyocardial infarction remodeling*. *Am J Physiol Heart Circ Physiol*, 2016. **311**(5): p. H1075-H1090.
753. Schrödinger Suite 2015-1 Protein Preparation Wizard; Epik version 3.1, S., LLC, New York, NY, 2015; Impact version 6.6, Schrödinger, LLC, New York, NY, 2015; Prime version 3.9, Schrödinger, LLC, New York, NY, 2015., *Schrödinger Suite 2015-1 Protein Preparation Wizard; Epik version 3.1, Schrödinger, LLC, New York, NY, 2015; Impact*

version 6.6, Schrödinger, LLC, New York, NY, 2015; Prime version 3.9, Schrödinger, LLC, New York, NY, 2015.

754. Shi, Y., et al., *Sirtuin Deacetylation Mechanism and Catalytic Role of the Dynamic Cofactor Binding Loop*. J Phys Chem Lett, 2013. **4**(3): p. 491-495.
755. Harder, E., et al., *OPLS3: A Force Field Providing Broad Coverage of Drug-like Small Molecules and Proteins*. J Chem Theory Comput, 2016. **12**(1): p. 281-96.
756. Schrödinger Release 2017-3: LigPrep, S., LLC, New York, NY, 2020., *Schrödinger Release 2017-3: LigPrep, Schrödinger, LLC, New York, NY, 2020*.
757. Grant, B.J., L. Skjærven, and X.-Q. Yao, *The Bio3D packages for structural bioinformatics*. Protein Science. **n/a**(n/a).
758. Nguyen, G.T., et al., *Structures of human sirtuin 3 complexes with ADP-ribose and with carba-NAD⁺ and SRTI720: binding details and inhibition mechanism*. Acta Crystallogr D Biol Crystallogr, 2013. **69**(Pt 8): p. 1423-32.
759. Nguyen, G.T., M. Gertz, and C. Steegborn, *Crystal structures of Sirt3 complexes with 4'-bromo-resveratrol reveal binding sites and inhibition mechanism*. Chem Biol, 2013. **20**(11): p. 1375-85.
760. Gai, W., et al., *Crystal structures of SIRT3 reveal that the alpha2-alpha3 loop and alpha3-helix affect the interaction with long-chain acyl lysine*. FEBS Lett, 2016. **590**(17): p. 3019-28.
761. Repasky, M.P., M. Shelley, and R.A. Friesner, *Flexible ligand docking with Glide*. Curr Protoc Bioinformatics, 2007. **Chapter 8**: p. Unit 8 12.
762. Koes, D.R., M.P. Baumgartner, and C.J. Camacho, *Lessons learned in empirical scoring with smina from the CSAR 2011 benchmarking exercise*. J Chem Inf Model, 2013. **53**(8): p. 1893-904.
763. Sherman, W., et al., *Novel procedure for modeling ligand/receptor induced fit effects*. J Med Chem, 2006. **49**(2): p. 534-53.
764. Sherman, W., H.S. Beard, and R. Farid, *Use of an induced fit receptor structure in virtual screening*. Chem Biol Drug Des, 2006. **67**(1): p. 83-4.
765. Friesner, R.A., et al., *Extra precision glide: docking and scoring incorporating a model of hydrophobic enclosure for protein-ligand complexes*. J Med Chem, 2006. **49**(21): p. 6177-96.

766. Guan, X., et al., *Mechanism of inhibition of the human sirtuin enzyme SIRT3 by nicotinamide: computational and experimental studies*. PLoS One, 2014. **9**(9): p. e107729.
767. Case, D.A., et al., *The Amber biomolecular simulation programs*. J Comput Chem, 2005. **26**(16): p. 1668-88.
768. D.A. Case, I.Y.B.-S., S.R. Brozell, D.S. Cerutti, T.E. Cheatham, III, V.W.D. Cruzeiro, T.A. Darden, R.E. Duke, D. Ghoreishi, M.K. Gilson, H. Gohlke, A.W. Goetz, D. Greene, R. Harris, N. Homeyer, Y. Huang, S. Izadi, A. Kovalenko, T. Kurtzman, T.S. Lee, S. LeGrand, P. Li, C. Lin, J. Liu, T. Luchko, R. Luo, D.J.Mermelstein, K.M. Merz, Y. Miao, G. Monard, C. Nguyen, H. Nguyen, I. Omelyan, A. Onufriev, F. Pan, R.Qi, D.R. Roe, A. Roitberg, C. Sagui, S. Schott-Verdugo, J. Shen, C.L. Simmerling, J. Smith, R. SalomonFerrer, J. Swails, R.C. Walker, J. Wang, H. Wei, R.M. Wolf, X. Wu, L. Xiao, D.M. York and P.A. Kollman (2018), AMBER 2018, University of California, San Francisco., *D.A. Case, I.Y. Ben-Shalom, S.R. Brozell, D.S. Cerutti, T.E. Cheatham, III, V.W.D. Cruzeiro, T.A. Darden, R.E. Duke, D. Ghoreishi, M.K. Gilson, H. Gohlke, A.W. Goetz, D. Greene, R. Harris, N. Homeyer, Y. Huang, S. Izadi, A. Kovalenko, T. Kurtzman, T.S. Lee, S. LeGrand, P. Li, C. Lin, J. Liu, T. Luchko, R. Luo, D.J.Mermelstein, K.M. Merz, Y. Miao, G. Monard, C. Nguyen, H. Nguyen, I. Omelyan, A. Onufriev, F. Pan, R.Qi, D.R. Roe, A. Roitberg, C. Sagui, S. Schott-Verdugo, J. Shen, C.L. Simmerling, J. Smith, R. SalomonFerrer, J. Swails, R.C. Walker, J. Wang, H. Wei, R.M. Wolf, X. Wu, L. Xiao, D.M. York and P.A. Kollman (2018), AMBER 2018, University of California, San Francisco.*
769. Maier, J.A., et al., *ff14SB: Improving the Accuracy of Protein Side Chain and Backbone Parameters from ff99SB*. J Chem Theory Comput, 2015. **11**(8): p. 3696-713.
770. Duan, Y., et al., *A point-charge force field for molecular mechanics simulations of proteins based on condensed-phase quantum mechanical calculations*. J Comput Chem, 2003. **24**(16): p. 1999-2012.
771. Cerutti, D.S., et al., *Derivation of fixed partial charges for amino acids accommodating a specific water model and implicit polarization*. J Phys Chem B, 2013. **117**(8): p. 2328-38.
772. Bayly, C.I., et al., *A well-behaved electrostatic potential based method using charge restraints for deriving atomic charges: the RESP model*. The Journal of Physical Chemistry, 1993. **97**(40): p. 10269-10280.
773. Davidchack, R.L., R. Handel, and M.V. Tretyakov, *Langevin thermostat for rigid body dynamics*. J Chem Phys, 2009. **130**(23): p. 234101.
774. Darden, T., D. York, and L. Pedersen, *Particle mesh Ewald: An $N \cdot \log(N)$ method for Ewald sums in large systems*. The Journal of chemical physics, 1993. **98**(12): p. 10089-10092.

775. Salomon-Ferrer, R., et al., *Routine Microsecond Molecular Dynamics Simulations with AMBER on GPUs. 2. Explicit Solvent Particle Mesh Ewald*. Journal of Chemical Theory and Computation, 2013. **9**(9): p. 3878-3888.
776. Roe, D.R. and T.E. Cheatham, *PTRAJ and CPPTRAJ: Software for Processing and Analysis of Molecular Dynamics Trajectory Data*. Journal of Chemical Theory and Computation, 2013. **9**(7): p. 3084-3095.
777. Wang, E., et al., *End-Point Binding Free Energy Calculation with MM/PBSA and MM/GBSA: Strategies and Applications in Drug Design*. Chem Rev, 2019. **119**(16): p. 9478-9508.
778. Ahmed, M., et al., *A Comprehensive Computational Analysis for the Binding Modes of Hepatitis C Virus NS5A Inhibitors: The Question of Symmetry*. ACS Infect Dis, 2016. **2**(11): p. 872-881.
779. Elsayed, N.M.Y., et al., *Design, synthesis, biological evaluation and dynamics simulation of indazole derivatives with antiangiogenic and antiproliferative anticancer activity*. Bioorg Chem, 2019. **82**: p. 340-359.
780. Ahmed, M., et al., *Structure-based screening and validation of potential dengue virus inhibitors through classical and QM/MM affinity estimation*. J Mol Graph Model, 2019. **90**: p. 128-143.
781. Ivanisenko, N.V., et al., *Exploring interaction of TNF and orthopoxviral CrmB protein by surface plasmon resonance and free energy calculation*. Protein Pept Lett, 2014. **21**(12): p. 1273-81.
782. Viricel, C., M. Ahmed, and K. Barakat, *Human PD-1 binds differently to its human ligands: a comprehensive modeling study*. J Mol Graph Model, 2015. **57**: p. 131-42.
783. Genheden, S. and U. Ryde, *The MM/PBSA and MM/GBSA methods to estimate ligand-binding affinities*. Expert Opin Drug Discov, 2015. **10**(5): p. 449-61.
784. Ussher, J.R., et al., *Stimulation of glucose oxidation protects against acute myocardial infarction and reperfusion injury*. Cardiovasc Res, 2012. **94**(2): p. 359-69.
785. Lopaschuk, G.D., et al., *Glucose and palmitate oxidation in isolated working rat hearts reperfused after a period of transient global ischemia*. Circ Res, 1990. **66**(2): p. 546-53.
786. Saddik, M. and G.D. Lopaschuk, *Myocardial triglyceride turnover and contribution to energy substrate utilization in isolated working rat hearts*. J Biol Chem, 1991. **266**(13): p. 8162-70.

787. Liu, B., et al., *Cardiac efficiency is improved after ischemia by altering both the source and fate of protons*. *Circ Res*, 1996. **79**(5): p. 940-8.
788. Dyck, J.R., et al., *Malonyl coenzyme a decarboxylase inhibition protects the ischemic heart by inhibiting fatty acid oxidation and stimulating glucose oxidation*. *Circ Res*, 2004. **94**(9): p. e78-84.
789. Dyck, J.R., et al., *Absence of malonyl coenzyme A decarboxylase in mice increases cardiac glucose oxidation and protects the heart from ischemic injury*. *Circulation*, 2006. **114**(16): p. 1721-8.
790. Lopaschuk, G.D., et al., *Beneficial effects of trimetazidine in ex vivo working ischemic hearts are due to a stimulation of glucose oxidation secondary to inhibition of long-chain 3-ketoacyl coenzyme a thiolase*. *Circ Res*, 2003. **93**(3): p. e33-7.
791. Lantier, L., et al., *SIRT3 Is Crucial for Maintaining Skeletal Muscle Insulin Action and Protects Against Severe Insulin Resistance in High-Fat-Fed Mice*. *Diabetes*, 2015. **64**(9): p. 3081-92.
792. Tao, R., et al., *Regulation of MnSOD enzymatic activity by Sirt3 connects the mitochondrial acetylome signaling networks to aging and carcinogenesis*. *Antioxid Redox Signal*, 2014. **20**(10): p. 1646-54.
793. Opie, L.H., *Metabolic management of acute myocardial infarction comes to the fore and extends beyond control of hyperglycemia*. *Circulation*, 2008. **117**(17): p. 2172-7.
794. Stanley, W.C., *Partial fatty acid oxidation inhibitors for stable angina*. *Expert Opin Investig Drugs*, 2002. **11**(5): p. 615-29.
795. Dyck, J.R. and G.D. Lopaschuk, *Malonyl CoA control of fatty acid oxidation in the ischemic heart*. *J Mol Cell Cardiol*, 2002. **34**(9): p. 1099-109.
796. Ljubkovic, M., et al., *Disturbed Fatty Acid Oxidation, Endoplasmic Reticulum Stress, and Apoptosis in Left Ventricle of Patients With Type 2 Diabetes*. *Diabetes*, 2019. **68**(10): p. 1924-1933.
797. Pluijmert, N.J., et al., *Effects on cardiac function, remodeling and inflammation following myocardial ischemia-reperfusion injury or unreperfused myocardial infarction in hypercholesterolemic APOE*3-Leiden mice*. *Sci Rep*, 2020. **10**(1): p. 16601.
798. Gupta, S., et al., *Prevention of cardiac hypertrophy and heart failure by silencing of NF-kappaB*. *J Mol Biol*, 2008. **375**(3): p. 637-49.

799. Jones, W.K., et al., *NF-kappaB as an integrator of diverse signaling pathways: the heart of myocardial signaling?* Cardiovasc Toxicol, 2003. **3**(3): p. 229-54.
800. Palomer, X., et al., *SIRT3-mediated inhibition of FOS through histone H3 deacetylation prevents cardiac fibrosis and inflammation.* Signal Transduct Target Ther, 2020. **5**(1): p. 14.
801. Luo, Z., et al., *Vascular endothelial growth factor attenuates myocardial ischemia-reperfusion injury.* Ann Thorac Surg, 1997. **64**(4): p. 993-8.
802. Yeghiazarians, Y., et al., *IL-15: a novel prosurvival signaling pathway in cardiomyocytes.* J Cardiovasc Pharmacol, 2014. **63**(5): p. 406-11.
803. Jing, E., et al., *Sirtuin-3 (Sirt3) regulates skeletal muscle metabolism and insulin signaling via altered mitochondrial oxidation and reactive oxygen species production.* Proc Natl Acad Sci U S A, 2011. **108**(35): p. 14608-13.
804. Vassilopoulos, A., et al., *SIRT3 deacetylates ATP synthase F1 complex proteins in response to nutrient- and exercise-induced stress.* Antioxid Redox Signal, 2014. **21**(4): p. 551-64.
805. Kim, H.S., et al., *Hepatic-specific disruption of SIRT6 in mice results in fatty liver formation due to enhanced glycolysis and triglyceride synthesis.* Cell Metab, 2010. **12**(3): p. 224-36.
806. Walker, J.E. and V.K. Dickson, *The peripheral stalk of the mitochondrial ATP synthase.* Biochim Biophys Acta, 2006. **1757**(5-6): p. 286-96.
807. Kim, H.S., et al., *SIRT3 is a mitochondria-localized tumor suppressor required for maintenance of mitochondrial integrity and metabolism during stress.* Cancer Cell, 2010. **17**(1): p. 41-52.
808. Hu, P., S. Wang, and Y. Zhang, *Highly Dissociative and Concerted Mechanism for the Nicotinamide Cleavage Reaction in Sir2Tm Enzyme Suggested by Ab Initio QM/MM Molecular Dynamics Simulations.* Journal of the American Chemical Society, 2008. **130**(49): p. 16721-16728.
809. Shi, Y., et al., *Sirtuin Deacetylation Mechanism and Catalytic Role of the Dynamic Cofactor Binding Loop.* The Journal of Physical Chemistry Letters, 2013. **4**(3): p. 491-495.
810. Kincaid, B. and E. Bossy-Wetzels, *Forever young: SIRT3 a shield against mitochondrial meltdown, aging, and neurodegeneration.* Front Aging Neurosci, 2013. **5**: p. 48.

811. Spector, A.A., *Arachidonic acid cytochrome P450 epoxygenase pathway*. J Lipid Res, 2009. **50 Suppl**: p. S52-6.
812. Spector, A.A., et al., *Epoxyeicosatrienoic acids (EETs): metabolism and biochemical function*. Prog Lipid Res, 2004. **43**(1): p. 55-90.
813. Wagner, K., et al., *The role of long chain fatty acids and their epoxide metabolites in nociceptive signaling*. Prostaglandins Other Lipid Mediat, 2014. **113-115**: p. 2-12.
814. Zhang, X., et al., *MicroRNA-195 Regulates Metabolism in Failing Myocardium Via Alterations in Sirtuin 3 Expression and Mitochondrial Protein Acetylation*. Circulation, 2018. **137**(19): p. 2052-2067.
815. Houtkooper, R.H., et al., *The secret life of NAD⁺: an old metabolite controlling new metabolic signaling pathways*. Endocr Rev, 2010. **31**(2): p. 194-223.
816. Schwer, B., et al., *Reversible lysine acetylation controls the activity of the mitochondrial enzyme acetyl-CoA synthetase 2*. Proc Natl Acad Sci U S A, 2006. **103**(27): p. 10224-10229.
817. Hirschey, M.D., et al., *SIRT3 regulates mitochondrial fatty-acid oxidation by reversible enzyme deacetylation*. Nature, 2010. **464**(7285): p. 121-5.
818. Soltys, C.L., S. Kovacic, and J.R. Dyck, *Activation of cardiac AMP-activated protein kinase by LKB1 expression or chemical hypoxia is blunted by increased Akt activity*. Am J Physiol Heart Circ Physiol, 2006. **290**(6): p. H2472-9.
819. Clanachan, A.S., *Contribution of protons to post-ischemic Na⁽⁺⁾ and Ca⁽²⁺⁾ overload and left ventricular mechanical dysfunction*. J Cardiovasc Electrophysiol, 2006. **17 Suppl 1**: p. S141-S148.
820. Jeremy, R.W., et al., *The functional recovery of post-ischemic myocardium requires glycolysis during early reperfusion*. J Mol Cell Cardiol, 1993. **25**(3): p. 261-76.
821. Moro, M.A., et al., *Paradoxical fate and biological action of peroxynitrite on human platelets*. Proc Natl Acad Sci U S A, 1994. **91**(14): p. 6702-6.
822. Ciapponi, A., R. Pizarro, and J. Harrison, *Trimetazidine for stable angina*. Cochrane Database Syst Rev, 2005(4): p. CD003614.
823. Sol, E.M., et al., *Proteomic investigations of lysine acetylation identify diverse substrates of mitochondrial deacetylase sirt3*. PLoS One, 2012. **7**(12): p. e50545.

824. Guan, K.L. and Y. Xiong, *Regulation of intermediary metabolism by protein acetylation*. Trends Biochem Sci, 2011. **36**(2): p. 108-16.
825. Foster, D.B., et al., *The cardiac acetyl-lysine proteome*. PLoS One, 2013. **8**(7): p. e67513.
826. Hebert, A.S., et al., *Calorie restriction and SIRT3 trigger global reprogramming of the mitochondrial protein acetylome*. Mol Cell, 2013. **49**(1): p. 186-99.
827. Schlicker, C., et al., *Substrates and regulation mechanisms for the human mitochondrial sirtuins Sirt3 and Sirt5*. J Mol Biol, 2008. **382**(3): p. 790-801.
828. Pillai, V.B., et al., *Exogenous NAD blocks cardiac hypertrophic response via activation of the SIRT3-LKB1-AMP-activated kinase pathway*. J Biol Chem, 2010. **285**(5): p. 3133-44.
829. Jing, E., et al., *Sirt3 regulates metabolic flexibility of skeletal muscle through reversible enzymatic deacetylation*. Diabetes, 2013. **62**(10): p. 3404-17.
830. Zoll, J., et al., *ACE inhibition prevents myocardial infarction-induced skeletal muscle mitochondrial dysfunction*. J Appl Physiol (1985), 2006. **101**(2): p. 385-91.
831. Koentges, C., et al., *Preserved recovery of cardiac function following ischemia-reperfusion in mice lacking SIRT3*. Can J Physiol Pharmacol, 2016. **94**(1): p. 72-80.
832. Canto, C., et al., *The NAD(+) precursor nicotinamide riboside enhances oxidative metabolism and protects against high-fat diet-induced obesity*. Cell Metab, 2012. **15**(6): p. 838-47.
833. Horton, J.L., et al., *Mitochondrial protein hyperacetylation in the failing heart*. JCI Insight, 2016. **2**(1).
834. Wu, Y.T., et al., *Regulation of mitochondrial F(o)F(1)ATPase activity by Sirt3-catalyzed deacetylation and its deficiency in human cells harboring 4977bp deletion of mitochondrial DNA*. Biochim Biophys Acta, 2013. **1832**(1): p. 216-27.
835. Yang, W., et al., *Mitochondrial Sirtuin Network Reveals Dynamic SIRT3-Dependent Deacetylation in Response to Membrane Depolarization*. Cell, 2016. **167**(4): p. 985-1000 e21.
836. Pillai, V.B., et al., *Honokiol blocks and reverses cardiac hypertrophy in mice by activating mitochondrial Sirt3*. Nat Commun, 2015. **6**: p. 6656.

837. Liu, J., H. Wang, and J. Li, *Inflammation and Inflammatory Cells in Myocardial Infarction and Reperfusion Injury: A Double-Edged Sword*. Clin Med Insights Cardiol, 2016. **10**: p. 79-84.
838. Slegtenhorst, B.R., et al., *Ischemia/reperfusion Injury and its Consequences on Immunity and Inflammation*. Curr Transplant Rep, 2014. **1**(3): p. 147-154.
839. Chen, G.Y. and G. Nunez, *Sterile inflammation: sensing and reacting to damage*. Nat Rev Immunol, 2010. **10**(12): p. 826-37.
840. Frangogiannis, N.G., *Chemokines in ischemia and reperfusion*. Thromb Haemost, 2007. **97**(5): p. 738-47.
841. Kurundkar, D., et al., *SIRT3 diminishes inflammation and mitigates endotoxin-induced acute lung injury*. JCI Insight, 2019. **4**(1).
842. Nussinov, R. and C.J. Tsai, *The different ways through which specificity works in orthosteric and allosteric drugs*. Curr Pharm Des, 2012. **18**(9): p. 1311-6.
843. Rajman, L., K. Chwalek, and D.A. Sinclair, *Therapeutic Potential of NAD-Boosting Molecules: The In Vivo Evidence*. Cell Metab, 2018. **27**(3): p. 529-547.
844. Guan, X., et al., *Biophysical characterization of hit compounds for mechanism-based enzyme activation*. PLoS One, 2018. **13**(3): p. e0194175.
845. Hu, P., S. Wang, and Y. Zhang, *Highly dissociative and concerted mechanism for the nicotinamide cleavage reaction in Sir2Tm enzyme suggested by ab initio QM/MM molecular dynamics simulations*. J Am Chem Soc, 2008. **130**(49): p. 16721-8.
846. Lesnefsky, E.J., P. Minkler, and C.L. Hoppel, *Enhanced modification of cardiolipin during ischemia in the aged heart*. J Mol Cell Cardiol, 2009. **46**(6): p. 1008-15.
847. Boengler, K., R. Schulz, and G. Heusch, *Loss of cardioprotection with ageing*. Cardiovasc Res, 2009. **83**(2): p. 247-61.
848. Ferdinandy, P., R. Schulz, and G.F. Baxter, *Interaction of cardiovascular risk factors with myocardial ischemia/reperfusion injury, preconditioning, and postconditioning*. Pharmacol Rev, 2007. **59**(4): p. 418-58.

Appendix

Can N-3 Polyunsaturated Fatty Acids Be Considered A Potential Adjuvant Medication For COVID-19-Associated Cardiovascular Complications?

This chapter has been adapted from the following published manuscript:

- **Ahmed M. Darwesh**, Wesam Bassiouni, Deanna K. Sosnowski, John M. Seubert. Can N-3 Polyunsaturated Fatty Acids Be Considered A Potential Adjuvant Medication For COVID-19-Associated Cardiovascular Complications? *Pharmacol Ther.* 2021; 219:107703

Abstract

Coronavirus disease 2019 (COVID-19), caused by the Severe Acute Respiratory Syndrome Coronavirus 2 (SARS-CoV-2), has currently led to a global pandemic with millions of confirmed and increasing cases around the world. The novel SARS-CoV-2 not only affects the lungs causing severe acute respiratory dysfunction but also leads to significant dysfunction in multiple organs and physiological systems including the cardiovascular system. A plethora of studies have shown the viral infection triggers an exaggerated immune response, hypercoagulation and oxidative stress, which contribute significantly to poor cardiovascular outcomes observed in COVID-19 patients. To date, there are no approved vaccines or therapies for COVID-19. Accordingly, cardiovascular protective and supportive therapies are urgent and necessary to the overall prognosis of COVID-19 patients. Accumulating literature has demonstrated the beneficial effects of n-3 polyunsaturated fatty acids (n-3 PUFA) toward the cardiovascular system, which include ameliorating uncontrolled inflammatory reactions, reduced oxidative stress and mitigating coagulopathy. Moreover, it has been demonstrated the n-3 PUFAs, eicosapentaenoic acid (EPA) and docosahexaenoic acid (DHA), are precursors to a group of potent bioactive lipid mediators, generated endogenously, which mediate many of the beneficial effects attributed to their parent compounds. Considering the favorable safety profile for n-3 PUFAs and their metabolites, it is reasonable to consider n-3 PUFAs as potential adjuvant therapies for the clinical management of COVID-19 patients. In this article, we provide an overview of the pathogenesis of cardiovascular complications secondary to COVID-19 and focus on the mechanisms that may contribute to the likely benefits of n-3 PUFAs and their metabolites.

9.1 Introduction

The first outbreak of the novel coronaviruses was triggered by severe and acute respiratory syndrome coronavirus (SARS-CoV) in China in 2002, which was followed in 2012 by the Middle East respiratory syndrome-related coronavirus (MERS-CoV). Both SARS-CoV and MERS-CoV are infectious, lethal and accounted for thousands of deaths over the past two decades [1, 2]. The Coronavirus Study Group of the International Committee on Taxonomy of Viruses evaluated the novelty of the coronavirus responsible for the recent outbreak in 2019 (COVID-19) and formally considered it related to SARS-CoV, as they share about 79% nucleotide identity and accordingly named it as severe acute respiratory syndrome coronavirus 2 (SARS-CoV-2) or 2019-novel coronavirus [3-5]. The recent eruption of COVID-19 was first reported in Wuhan, Hubei Province, China in late December 2019 when a series of pneumonia cases of unknown cause were detected [6]. Highly contagious, COVID-19 spread rapidly throughout China and most countries across the world. On March 11th, the spread of COVID-19 was declared by the World Health Organization as a global pandemic and by September 18th, 2020, the cumulative number of diagnosed patients internationally was 30,217,420 with 946,847 global deaths [7].

Coronaviruses infect both animals and humans affecting their respiratory, gastrointestinal, cardiovascular and central nervous systems [8]. Consistently, SARS-CoV-2 primarily targets the lungs but it can affect many other organs and systems, including the kidneys, heart, blood vessels, gastrointestinal tract and brain [9]. Symptoms of COVID-19 are manifested as myalgia, fatigue, fever and dry cough, together with lower respiratory tract disease. In some cases, the severe progression of the disease leads to acute lung injury (ALI), acute respiratory distress syndrome (ARDS), respiratory failure, sepsis, heart failure (HF) and sudden cardiac arrest within a few days. Importantly, there is significant morbidity and mortality in the elderly and individuals with

underlying health conditions [10, 11]. Although treatment with corticosteroids, antiviral therapy and mechanical respiratory support have been employed, there is still no specific treatment for COVID-19 and therefore supportive care is of paramount importance [10, 12] (Table 9.1).

Table 9. 1: Overview of some proposed pharmacological agents with potential beneficial effects in the setting of COVID-19.

Pharmacological intervention	Conclusion	Reference
Antioxidants including Vitamin C and E	<ul style="list-style-type: none"> • Antioxidant effects may ameliorate cardiac injuries of critically ill COVID-19 patients 	[13]
Melatonin	<ul style="list-style-type: none"> • May have preventive effect against septic cardiomyopathy. • Has benefits in myocardial infarction, cardiomyopathy, hypertensive heart diseases, and pulmonary hypertension 	[14]
Anti-interleukin-6	<ul style="list-style-type: none"> • Tocilizumab (anti-IL-6 receptor), siltuximab (anti-IL-6), and sirukumab (anti-IL-6) are proposed as possible treatments to manage cytokine storm and elevated IL-6 levels 	[15-17]
Anti-TNF α	<ul style="list-style-type: none"> • Infliximab, adalimumab, etanercept, golimumab, certolizumab as TNFα neutralizing therapies suggested as potential agents for COVID-19 hyperinflammatory state which may ameliorate organ damage including acute cardiac injury 	[18]
Janus kinase (JAK) inhibitors	<ul style="list-style-type: none"> • Ruxolitinib, tofacitinib, baricitinib are proposed to be beneficial in controlling excessive IL-6 signaling through STAT-1 and STAT-3 pathways 	[15, 18-20]
Anti-interleukin-1	<ul style="list-style-type: none"> • Anakinra, a modified IL-1 receptor antagonist protein, is suggested to have therapeutic potential in cytokine storm, given its effectiveness on patient survival in severe sepsis 	[15, 20]
Granulocyte-macrophage-colony stimulating factor (GM-CSF) inhibition	<ul style="list-style-type: none"> • GM-CSF can play a pro-inflammatory role signaling to macrophages • COVID-19 patients have been demonstrated to have elevated GM-CSF levels • Literature proposes that targeting GM-CSF upstream of inflammatory cytokines ex. gimsilumab, may be useful to blunt cytokine storm 	[15]
Statins	<ul style="list-style-type: none"> • Anti-inflammatory properties, including reduction in cytokines, may benefit in COVID-19 hyperinflammatory states in addition to their conventional cardioprotective properties 	[15, 20]
ACEi/ARBs	<ul style="list-style-type: none"> • Proposed that treatment with RAAS antagonists may theoretically be beneficial by upregulating ACE2 and compensating for ACE2 receptors lost due to COVID-19 	[16]
N-acetylcysteine (NAC)	<ul style="list-style-type: none"> • Anti-oxidant and anti-inflammatory properties of NAC proposed as an adjuvant therapy for COVID-19 and secondary cardiovascular complications • Suggested role for NAC in prevention of hypertension, atherosclerosis-associated inflammation, acute heart failure, thrombo-inflammation, and myocardial ischemia 	[21, 22]
Eicosanoids and soluble epoxide	<ul style="list-style-type: none"> • Epoxyeicosatrienoic acids (EETs) are cardioprotective, anti-inflammatory and pro-resolving 	[23]

hydrolase (sEH) inhibitors	<ul style="list-style-type: none">• Inhibition of their metabolizing enzyme, sEH, may be beneficial by maintaining eicosanoid levels and reducing endoplasmic reticulum (ER) stress• Potential to limit inflammatory storm and resolve inflammation in addition to their established cardioprotective properties• Co-treatment with sEH inhibitors and omega-3 fatty acids may provide synergistic effects	
-------------------------------	--	--

9.2 COVID-19 and cardiovascular complications

The correlation between pneumonia, an inflammatory condition of lung alveoli compromising the ability for gas exchange, and cardiovascular complications has been well established [24, 25]. For example, patients with underlying cardiovascular disease are more likely to develop community-acquired pneumonia [26] and about 8 to 25% of patients with community acquired pneumonia develop at least one cardiac complication during their hospital stay. The exaggerated cardiovascular episodes after pneumonia have been associated with increased mortality [27, 28]. In line with these observations, cardiac complications have been reported in patients with novel coronavirus infections such as tachycardia and hypotension, which are common in SARS patients. Moreover, arrhythmia, cardiomegaly and diastolic dysfunction have been reported in SARS patients [29, 30]. In addition, infection with MERS-CoV was associated with acute myocarditis, myocardial edema and severe left ventricular dysfunction [31].

In the context of COVID-19, both patients with and without underlying cardiovascular comorbidities can develop cardiovascular complications secondary to SARS-CoV-2 infection. For example, Wang et al., reported that among 138 hospitalized patients with COVID-19 in Wuhan, China, cardiac injury, as evidenced by new ECG or echocardiographic abnormalities or elevated high-sensitivity cardiac troponin I, was present in 7.2% of all patients and 22% of patients who required intensive care unit (ICU) care [6]. Moreover, the National Health Commission of China reported that 12% of patients infected with SARS-CoV-2 and without known cardiovascular disease (CVD) had elevated troponin levels or cardiac arrest during hospitalization, 17% had coronary heart disease and 35% of patients had hypertension [32, 33]. However, there is accumulating evidence that COVID-19 patients with underlying CVD are at higher risk for developing severe complications [6, 10]. For instance, older patients with underlying CVD who

are infected with SARS-CoV-2 are more prone to become severely ill, develop cardiac injury or require intensive care [34, 35]. The death rate among patients with underlying CVD has been stated as 10.5%, which is much higher than that of the general population [12, 36]. Furthermore, according to an epidemiological study conducted in China, 4.2% of the confirmed cases and 22.7% of mortalities have cardiovascular comorbidities [36]. Many COVID-19 patients suffer from persistent hypotension, myocardial injury, myocarditis, left ventricular dysfunction, arrhythmia and HF [33, 35, 37, 38]. Importantly, cardiac biopsy samples collected from patients with COVID-19 demonstrated increased interstitial infiltration of mononuclear inflammatory cells providing extra evidence of myocarditis in COVID-19 patients [39]. Therefore, cardiovascular damage secondary to COVID-19 is now drawing growing attention in clinical practice (Table 9.2) and the American College of Cardiology recently issued a clinical report to address the cardiovascular consequences of SARS-CoV-2 infection [40].

Table 9. 2: Overview of COVID-19-associated cardiovascular complications

COVID-19-induced cardiovascular injury	Proposed mechanism of injury
<ul style="list-style-type: none"> • Acute myocarditis 	<ul style="list-style-type: none"> • Direct pathogen invasion • Indirect cytokine storm
<ul style="list-style-type: none"> • Instability of coronary atherosclerotic plaques • Coagulopathy • Acute MI • Hypertension • Left ventricular dilation, hypertrophy and dysfunction • Arrhythmias (long QT-syndrome, torsade de pointes) 	<ul style="list-style-type: none"> • Indirect inflammatory response (Cytokine storm)
<ul style="list-style-type: none"> • Worsening of heart failure 	<ul style="list-style-type: none"> • Indirect inflammatory response (Cytokine storm) • Volume overload due to impaired sodium and water metabolism • Disturbance of endothelial function
<ul style="list-style-type: none"> • Pyroptosis of cardiomyocytes 	<ul style="list-style-type: none"> • Hypoxemia • Activation of the NLRP3 inflammasome
<ul style="list-style-type: none"> • Severe tachycardia, increased peripheral resistance, hypertension, increased myocardial oxygen requirements and ischemia 	<ul style="list-style-type: none"> • Pneumonia-induced increase in sympathetic activity

9.3 Potential mechanisms of cardiovascular complications in COVID-19 patients

To date, there have been few reports about the pathologic features of COVID-19 and consequently the exact pathophysiological mechanisms of myocardial injury secondary to COVID-19 remain elusive. However, direct damage by the virus, exaggerated uncontrolled inflammatory responses, instability of coronary plaques, thrombosis and hypoxia have been proposed as possible mechanisms [32, 33, 35]. Importantly, the severity of infection, patient characteristics and host reaction all participate in the development of cardiac complications. The main proposed mechanisms for cardiovascular deterioration in patients with COVID-19 can be summarized as follows (Figure 9.1).

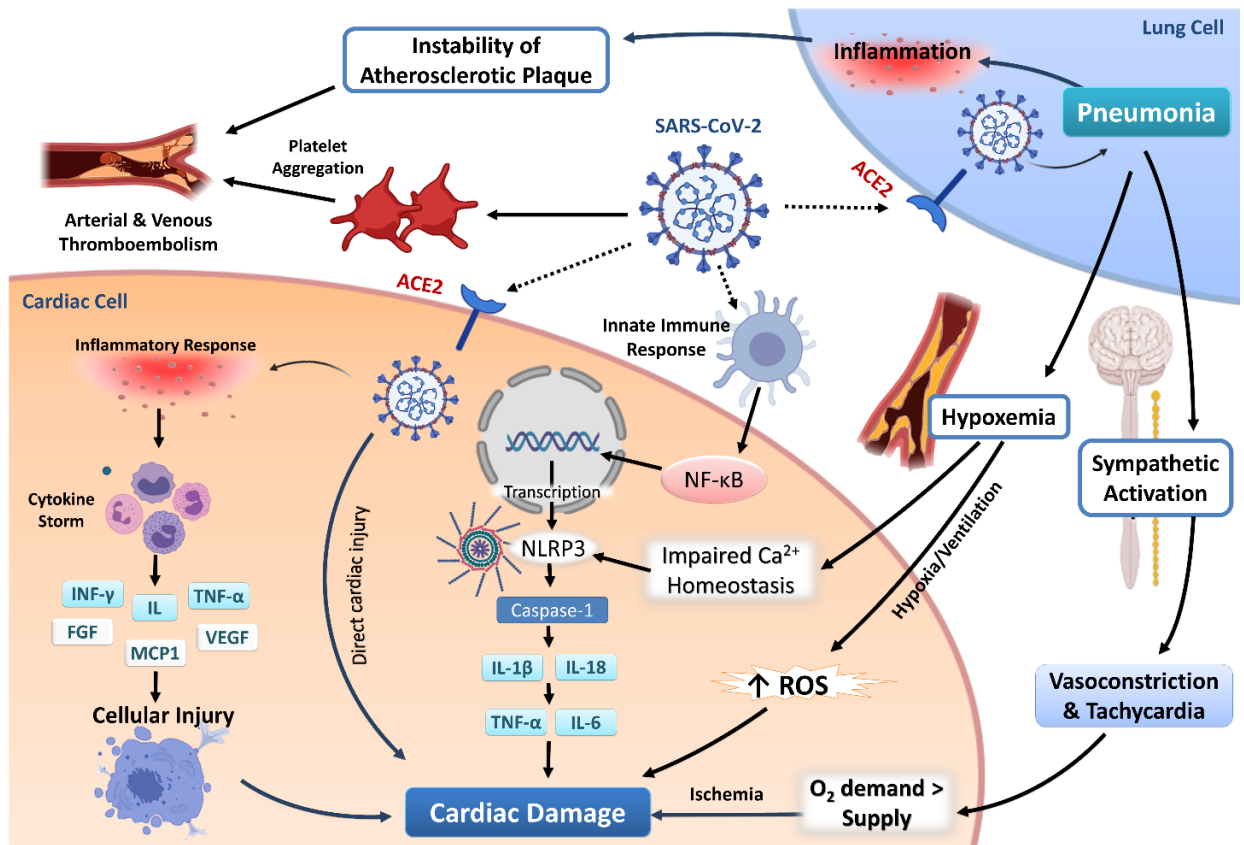


Figure 9. 1: Potential mechanisms of SARS-CoV-2-induced cardiovascular complications.

SARS-Cov-2 may be taken up by cardiac cells using different routes, such as via ACE2 receptors expressed on the cell surface. Following entry, SARS-CoV-2 may exert cardiac injury by direct action and/or induction of immune responses resulting in release of pro-inflammatory cytokines ('Cytokine storm') such as IL, TNF- α , INF- γ , FGF, MCP1 and VEGF. SARS-CoV-2 can trigger the innate immune response involving NLRP3 inflammasomes which lead to activation of pro-inflammatory cytokines, IL-1 β and IL-18 and the inflammatory cascade (IL-6 and TNF- α) resulting in tissue damage and fibrosis. SARS-CoV-2-induced pneumonia results in the development of hypoxemia which can impair Ca²⁺ homeostasis, increase ROS production and activate NLRP3 inflammasomes leading to cardiac damage. Activation of the sympathetic nervous system response to pneumonia leads to vasoconstriction and tachycardia compromising coronary perfusion. This results in a mismatch of myocardial O₂ demand and supply precipitating ischemia. SARS-CoV-2 can destabilize coronary atherosclerotic plaques and mediate platelet aggregation resulting in arterial and venous thrombosis. Altogether, these SARS-CoV-2 mediated effects may be contributing to the observed cardiovascular injury. ACE2, Angiotensin-converting enzyme-2; Ca²⁺, Calcium; FGF, Fibroblast growth factor; IL, Interleukin; INF, Interferon; MCP-1, Monocyte chemoattractant protein-1; NF κ B, Nuclear factor kappa-light-chain enhancer activated B-cells; NLRP3, NACHT, LRR and PYD domains-containing protein 3; O₂, Oxygen; ROS, Reactive oxygen species; SARS-CoV-2, Severe and acute respiratory syndrome coronavirus; TNF- α , Tumor necrosis factor- α ; VEGF, Vascular endothelial growth factor.

9.3.1 Direct pathogen invasion

Direct invasion of pathogens to the cardiac tissue has been confirmed in patients with severe pneumonia. For example, *Streptococcus pneumoniae* was identified in the myocardium of patients with severe pneumococcal disease, leading to local inflammatory reactions and consequently cardiac injury [39]. Oudit et al. reported SARS-CoV RNA was detected in 35% (7/20) of autopsied human heart samples obtained from SARS patients during the Toronto SARS outbreak, suggesting the likelihood of direct damage to cardiomyocytes by the virus [41]. In the same report, a study in mice infected with the human strain of the SARS-CoV demonstrated that pulmonary infection with SARS-CoV also precipitated myocardial infection [41]. As SARS-CoV-2 is genetically related to SARS-CoV, there is a high potential that it shares a similar mechanism and the same functional host-cell receptor, angiotensin-converting enzyme 2 (ACE2) for cell entry [42]. Importantly, ACE2 is highly expressed in both the heart and the lung [43] and evidence indicates the affinity of SARS-CoV-2 to ACE2 is approximately 10- to 20-fold higher than that for SARS-CoV which may account for both the greater pathogenicity of SARS-CoV-2 and the rapid spread [42, 44]. Altogether, SARS-CoV-2 might directly infect the myocardial tissue leading to severe cardiac injury [45]. However, large-scale biopsy studies are still warranted to further confirm the direct myocardial infection by SARS-CoV-2.

9.3.2 Indirect inflammatory response - Cytokine storm

Inflammation plays an important role in the development of cardiovascular impairment in the setting of COVID-19. Similar to SARS-CoV and MERS-CoV infection, SARS-CoV-2 infection can also trigger excessive host immune responses, leading to extensive and uncontrolled release of proinflammatory cytokines termed as cytokine storm [46, 47]. Cytokines play a pivotal role in the immune response to defend against different bacterial and viral infections. However, it has also been established that dysregulated, amplified and uncontrolled immune responses may cause immunopathology leading to systematic self-attack contributing to multiple organ damage and cardiovascular injury secondary to SARS-CoV-2 infection [48]. A plethora of studies have shown increased amounts of cytokines, such as interleukin-6 (IL-6), IL-7, IL-8, IL-9, IL-10, IL-1 β , IL-1RA, tumor necrosis factor-alpha (TNF- α), granulocyte-macrophage colony-stimulating factor, fibroblast growth factor, macrophage inflammatory protein 1 alpha, platelet-derived growth factor, monocyte chemoattractant protein and vascular endothelial growth factor in the serum of COVID-19 patients, especially in ICU patients [6, 10, 11, 48, 49]. Importantly, there is a strong correlation between serum cytokine levels and mortality rates in patients with COVID-19. The amplified and uncontrolled inflammatory response induces cellular apoptosis or necrosis of the affected cells. This is followed by increased permeability of blood vessels leading to the accumulation of inflammatory monocytes, macrophages and neutrophils in different body organs fueling the inflammatory cascade [50]. The vicious circle intensifies the situation as the cytokine storm is further stimulated and the regulation of immune response is lost resulting in severe consequences. Collectively, this indicates the uncontrolled inflammatory response is a major factor in the adverse response observed in COVID-19 patients. In that sense, it would seem reasonable

that ameliorating the exaggerated immune response would improve the clinical outcomes in patients with COVID-19 (Table 9.3).

Table 9. 3: Overview of the pharmacological approaches under investigation for ameliorating cytokine storm, hyperinflammatory state, and the associated secondary organ complications in COVID-19 patients.

Pharmacological intervention	Sample size and criteria	Treatment protocol	Key findings	Conclusion	Reference
<ul style="list-style-type: none"> • Tocilizumab for IL-6 cytokine release syndrome 	<ul style="list-style-type: none"> • Multicenter Randomized controlled trial (RCT) • Severe COVID-19 infections • 18-85 years of age • Elevated serum IL-6 • N = 94 standard therapy + tocilizumab • N = 94 standard therapy 	<ul style="list-style-type: none"> • 4-8 mg/kg tocilizumab i.v. once • Additional dose if fever persists in 24hrs after first dose 	<ul style="list-style-type: none"> • First phase showed normalization of fever within 24hrs of tocilizumab • Improved respiratory function, oxygenation, and pulmonary lesions 	<ul style="list-style-type: none"> • Phase 4 study completed in May 2020. • Results pending • Tocilizumab may be a promising investigative therapy to reduce cytokine release syndrome and associated multi-organ damage 	[51]
<ul style="list-style-type: none"> • Tocilizumab to mitigate cytokine storm and associated complications 	<ul style="list-style-type: none"> • Retrospective cohort study • >18 years of age • Intensive care unit (ICU) COVID-19 hospitalization • Primary endpoint of hospital-related mortality • N = 210 standard care + tocilizumab • N = 420 standard care 	<ul style="list-style-type: none"> • 400 mg single dose or 8 mg/kg tocilizumab • 88% required 1 infusion, 12% received a second infusion 	<ul style="list-style-type: none"> • Hazard ratio (HR) 0.71 for hospital related mortality (95% confidence interval (CI) 0.56 – 0.89). • Treatment was more effective in patients with C-reactive protein (CRP) >15mg/dL • HR 0.48 (95% CI 0.30 – 0.77) than those with CRP <15 mg/dL HR 0.92 (95% CI 0.57 – 1.48) 	<ul style="list-style-type: none"> • Tocilizumab treatment is associated with a lower rate of mortality, particularly in those with enhanced inflammatory state • Double blind RCT recently completed with results pending NCT04320615 	[52]

<ul style="list-style-type: none"> • Tocilizumab to mitigate cytokine storm 	<ul style="list-style-type: none"> • Prospective observational study • Severe or critical COVID-19 infection • 25 to 88 years of age • N = 21 tocilizumab + standard therapy • 42.9% had CVD 	<ul style="list-style-type: none"> • 4-8 mg/kg or 400 mg tocilizumab i.v. once • 85.7% received single dose of tocilizumab, 14.3% required second dose within 12hrs of first dose 	<ul style="list-style-type: none"> • Fever normalized within 24hrs • Reduced O₂ therapy requirements • Minimal improvement in IL-6 levels • CT lung lesion improvement • All patients discharged 	<ul style="list-style-type: none"> • Limited sample size and no control group • Tocilizumab treatment in severe COVID-19 cases may improve clinical symptoms in hyperinflammatory state 	<p>[53]</p>
<ul style="list-style-type: none"> • Intensive methylprednisolone regimen +/- tocilizumab for management of cytokine storm 	<ul style="list-style-type: none"> • Prospective observational study • O₂ sat ≤ 94% OR tachypnea, elevated CRP, high D-dimer • Primary outcome of hospital discharge or clinical improvement • N = 86 methylprednisolone +/- tocilizumab • N = 86 standard care 	<ul style="list-style-type: none"> • Stage 1: Immediate methylprednisolone 250 mg i.v. on day 1, then 80 mg on days 2-5 • Stage 2 (lack of clinical improvement or worsening respiratory status): Add tocilizumab 8 mg/kg i.v. once between days 2-5 	<ul style="list-style-type: none"> • Improvement in respiratory status HR 1.79 (95% CI 1.20 – 2.67). • Improvement reached in a shorter time vs. control • Reduced hospital mortality and need for mechanical ventilation 	<ul style="list-style-type: none"> • Short duration of intensive immunosuppressive therapy is associated with improved clinical outcomes in patients with hyperinflammatory state 	<p>[54]</p>
<ul style="list-style-type: none"> • Ruxolitinib treatment for elevated cytokine levels and inflammatory response 	<ul style="list-style-type: none"> • Prospective RCT • 18 to 75 years of age with severe infection • Primary outcome of time to clinical improvement • N = 20 ruxolitinib + standard care 	<ul style="list-style-type: none"> • Ruxolitinib 5 mg twice daily • Placebo vitamin C 100 mg twice daily 	<ul style="list-style-type: none"> • No difference in primary endpoint HR 1.669 (95% CI 0.836 – 3.335). • Improvement in lung computerized tomography (CT) scans • Significantly reduced cytokine 	<ul style="list-style-type: none"> • Ruxolitinib may hasten time of chest CT scan improvement and mitigate systemic inflammation 	<p>[55]</p>

	<ul style="list-style-type: none"> • N = 21 placebo + standard care 		<p>levels and CRP by day 3</p>		
<ul style="list-style-type: none"> • Anakinra for targeting the cytokine inflammatory cascade through IL-1 blockade 	<ul style="list-style-type: none"> • Open label case series • Elevated CRP N = 9 • 6/9 with CVD risk factors (diabetes, obesity) • 3/9 with hypertension 	<ul style="list-style-type: none"> • Anakinra 100 mg every 12hr s.c. on days 1-3 • Anakinra 100 mg once daily s.c. on days 4-10 	<ul style="list-style-type: none"> • Fever subsided by day 3 • CRP normalized in 5 patients by day 11 • Halted progression of CT lung lesions • 100% survival 	<ul style="list-style-type: none"> • Small case series, potential for confounding factors • Potential therapy to target inflammatory cascade • Positive results in patients with hypertension and other CVD risk factors 	[56]
<ul style="list-style-type: none"> • Ana-COVID study • Anakinra for COVID-19 hyperinflammatory state 	<ul style="list-style-type: none"> • Prospective/retrospective cohort study • Hospitalized adults with critical lung function • Cohort with CVD (hypertension, stroke, cardiopathy) • Primary outcome of ICU admission with mechanical ventilation or death • N = 52 anakinra + standard care • N = 44 standard care 	<ul style="list-style-type: none"> • Anakinra 100 mg s.c. twice daily for 3 days • Then anakinra 100 mg s.c. once daily for 7 days 	<ul style="list-style-type: none"> • Significantly reduced need for mechanical ventilation or death HR 0.22 (0.11 – 0.41) 	<ul style="list-style-type: none"> • Anakinra may be associated with improved outcomes in patients with severe COVID-19 infection, including those with CVD and history of cardiovascular events • May be due to mitigation of inflammatory cascade 	[57]

The innate immune system detects viral infections by using pattern recognition receptors, particularly Toll-like receptors (TLR), to recognize pathogen-associated molecular patterns of the virus including lipids, lipoproteins, proteins and nucleic acids [58]. Activation of the TLR increases the expression of the transcription factors nuclear factor kappa-light-chain-enhancer of activated B cells (NF- κ B), interferon (IFN) regulatory factor 3 and mitogen-activated protein kinases, which subsequently induce the expression of a myriad of inflammatory factors [59]. For example, the binding of SARS-CoV-2 to TLR activates the NF- κ B inflammatory pathway triggering the transcription of the different components of the NLRP3 (NOD-, LRR-, and pyrin domain-containing 3) inflammasome [60, 61]. The NLRP3 inflammasome is a large multiple protein platform consisting of main 3 components, the NLRP3 scaffold, the adapter component apoptosis-associated speck-like protein carrying a caspase activation and recruitment domain and the inactive zymogen procaspase-1 [62, 63]. Upon activation of the NLRP3 inflammasome and once assembled, procaspase-1 is converted into the active effector protease caspase-1, which then causes cleavage and maturation of proinflammatory cytokines pro-interleukin-1 β (pro-IL-1 β) and pro-IL-18 into their corresponding active forms, inflammatory IL-1 β and IL-18. This, in turn, triggers a cascade of other downstream mediators of inflammation such as TNF- α , IL-6, prostaglandins and leukotrienes which induces more tissue damage, fever, and fibrosis [49, 64]. Based on the robust inflammatory response triggered by the NLRP3 inflammasome cascade, targeting the pathway has potential therapeutic value, which can reduce the detrimental consequences of uncontrolled inflammation from SARS-CoVs infections.

Inflammation is well known to participate in various CVDs, such as atherosclerosis, coagulopathy, coronary artery disease and HF [65]. In the majority of severe cases of COVID-19, the cytokine storm has been coupled with elevated levels of erythematosis sedimentation rate and

C-reactive protein (CRP). Subsequently, hypercoagulation and disseminated intravascular coagulation would present as thrombosis, thrombocytopenia and gangrene of the limbs [48, 66]. The identification of key cytokines such as TNF α in patients with HF demonstrated a strong positive correlation between cytokines and the severity of left ventricular dilation/hypertrophy and left ventricular dysfunction [67, 68]. Other evidence indicates increased IL-1 β and IL-6 levels detected in patients with acute myocarditis and acute MI [39]. Increased IL-6 levels have been associated with long QT-syndrome in patients with systemic inflammation, leading to higher risks for arrhythmias such as torsade de pointes [69]. As well, the level of IL-6 can be used as a predictor of adverse cardiovascular events after acute coronary syndrome and chronic HF [70, 71]. The serum levels of IL-8 are increased in patients with acute MI and is associated with higher mortality rates [72]. Collectively, we can conclude there is a strong correlation between elevated inflammatory markers and the adverse cardiovascular outcomes observed in patients with COVID-19 suggesting the potential role of an inflammatory storm in the development and progression of cardiac injury.

Importantly, it has been reported that populations at high risk to develop the more severe forms of cardiac complications secondary to COVID-19 are patients with advanced age, obesity, metabolic syndrome, hypertension and diabetes. These conditions share a common feature where immune changes favour a hyperinflammatory state and compromised inflammatory resolution [73-76]. Therefore, traditional cardiovascular treatment plus anti-inflammatory therapy targeting key steps and components of the cytokine storm could be hypothesized as a therapeutic strategy and management of cardiovascular impairment in severe cases of COVID-19. As the inflammatory response in different organs share common pathways, ameliorating the systematic inflammatory response will benefit the cardiovascular system and have potential advantages for other organs.

9.3.3 Miscellaneous mechanisms

Other proposed mechanisms of COVID-19–associated cardiovascular impairment include instability of coronary atherosclerotic plaques [77] and increased platelet-aggregating activity [78] leading to excessive and uncontrolled coagulation and thrombosis [79]. The systemic inflammatory response to pneumonia induces endothelial dysfunction, increases the procoagulant activity of the blood and consequently triggers inflammatory reactions within coronary atherosclerotic plaques, making them unstable and susceptible to rupture. Together, this contributes to the formation of an occlusive thrombus over a ruptured coronary plaque. It is documented that COVID-19 patients are prone to arterial and venous thromboembolisms due to hypoxia, excessive inflammation and diffuse intravascular coagulation. In a Dutch study of 184 ICU patients with proven COVID-19 pneumonia, one-third of patients exhibited blood clots and thrombotic complications. These findings, consequently, reinforced the recommendation to use antiplatelets and other pharmacological thrombosis prophylaxis drugs in all COVID-19 patients [80] (Table 9.4).

Table 9. 4: Overview of the pharmacological interventions under investigation targeting hypercoagulability and platelet activation in COVID-19 patients.

Pharmacological intervention	Sample size and criteria	Treatment protocol	Key findings	Conclusion	Reference
<ul style="list-style-type: none"> Heparin anticoagulant treatment in sepsis-induced coagulopathy 	<ul style="list-style-type: none"> Retrospective cohort study ≥ 18 years of age Severe COVID-19 infection Evaluation of 28-day mortality in heparin and non-heparin users 48.5% comorbid hypertension and/or heart disease N = 99 heparin N = 350 no heparin 	<ul style="list-style-type: none"> Unfractionated (10, 000 – 15, 000 U/day) or low molecular weight heparin (40-60 mg enoxaparin/day) for 7 days or longer 	<ul style="list-style-type: none"> No difference in 28-day mortality endpoint between heparin and non-heparin users. Lower 28-day mortality in patients with sepsis-induced coagulopathy (SIC) score of ≥ 4 in stratified analysis Odd Ratio (OR) 0.372 (95% CI 0.154 – 0.901) 	<ul style="list-style-type: none"> Heparin may be associated with a lower 28-day mortality rate only in patients with enhanced coagulopathy risk such as SIC score of 4 or greater 	[81]
<ul style="list-style-type: none"> Antiplatelet and anticoagulant combination therapy for hypoxemia, respiratory failure, and cardiac adverse events 	<ul style="list-style-type: none"> Case control, proof-of-concept study Adult patients with hypoxemic respiratory failure N = 5 ASA + clopidogrel + tirofiban + fondaparinux + standard care N = 5 matched controls given low molecular weight heparin Secondary outcome included major and minor cardiac adverse events 	<ol style="list-style-type: none"> Single dose of acetylsalicylic acid (ASA) 250 mg i.v. and single loading dose of oral clopidogrel 300 mg ASA and clopidogrel continued at 75 mg orally for 30 days Tirofiban 25 µg/kg as bolus i.v. injection, then 0.15 ug/kg/minute continuous i.v. infusion for 48 hours Fondaparinux 2.5 mg/day s.c. for the duration of the hospital stay 	<ul style="list-style-type: none"> Significant improvement in alveolar-arterial oxygen gradient Significant improvement in CRP and lymphocyte count Patients in treatment group did not experience any cardiac adverse events 	<ul style="list-style-type: none"> Small study and not a randomized controlled trial (RCT) Intensive antithrombotic therapy may be useful in patients with severe respiratory distress with prothrombotic state at risk for acute cardiac events 	[82]

A 12-year follow-up study conducted by Wu et al. of 25 patients who recovered from SARS-CoV infection demonstrated patients were affected by various metabolic disturbances altering lipid metabolism and the cardiovascular system. These patients suffered from hyperlipidemia, increased serum concentrations of free fatty acids, abnormal glucose metabolism and other cardiovascular abnormalities [83]. Considering the genetic similarities between SARS-CoV and SARS-CoV-2, Zhang et al. recently proposed the use of the lipid-lowering statins, which also possess anti-inflammatory properties, as a therapeutic option for patients with COVID-19. This study reported that amongst 13,981 cases of COVID-19, in-hospital use of statins was associated with a lower risk of death and a significantly lower inflammatory response during the entire hospitalization period [84]. Thus, suggesting the use of lipid-lowering drugs with anti-inflammatory properties can improve the cardiovascular outcomes in patients with COVID-19.

COVID-19 patients are susceptible to hypoxemia due to reduced lungs performance, impaired gas exchange across the inflamed alveoli and abnormal ventilation/perfusion. This will lead to decreased myocardial oxygen supply, myocardial ischemia and impaired calcium homeostasis. This disturbance in calcium balance will trigger the activation of the NLRP3 inflammasome and different inflammatory components which consequently lead to the death of cardiomyocytes [32, 85]. Additionally, the systemic response to pneumonia includes an increase in sympathetic activity causing severe tachycardia and increased peripheral resistance. Subsequently, a rapid heart rate together with vasoconstriction may result in elevated myocardial oxygen requirements and a shortened diastolic interval, the period during which coronary perfusion occurs. The mismatch between myocardial oxygen demand and supply can lead to cardiac ischemia and infarction, especially in the presence of pre-existing coronary artery disease [86]. Volume overload due to impaired sodium and water metabolism [87], transient disturbance

of endothelial function and vascular tone [88, 89] and cardiac arrhythmias [24] may also contribute to decreased left ventricular function or worsening of HF in patients with COVID-19.

Collectively, these effects can all result in the aggravation of existing CVDs and trigger severe events, such as acute coronary syndromes, thrombosis, myocardial ischemia or exacerbation of HF. Indeed, cardiovascular protective strategies are needed for the prevention and management of severe adverse cardiovascular events to improve the prognosis of COVID-19 patients (Table 9.5 and 9.6).

Table 9. 5: Overview of some proposed pharmacological approaches to attenuate COVID-19 associated cardiovascular injury

Pharmacologic intervention	Sample size and criteria	Treatment protocol	Key findings	Conclusion	Reference
<ul style="list-style-type: none"> Colchicine for the improvement of cardiac biomarkers, inflammation, and clinical outcomes 	<ul style="list-style-type: none"> Prospective, open-label randomized controlled trial (RCT) N = 55 colchicine + standard care N = 50 standard care Primary endpoints included maximum cardiac troponin level, time for C-reactive protein (CRP) to reach 3x upper limit normal, time to deterioration by at least 2 points on clinical status scale 	<ul style="list-style-type: none"> Colchicine 1.5 mg loading dose, 0.5 mg after 60 minutes, and then 0.5 mg twice daily + standard care for up to 3 weeks 	<ul style="list-style-type: none"> No difference in cardiac troponin or CRP levels Clinical deterioration less common with colchicine treatment odd ratio (OR) 0.11 (95% CI 0.01 – 0.96) Abdominal pain and diarrhea significantly more common with colchicine treatment 	<ul style="list-style-type: none"> Colchicine may not have a significant effect on cardiac or inflammatory biomarkers, however it may be useful in stabilizing patients with severe COVID-19 infection and preventing clinical deterioration 	[90]
<ul style="list-style-type: none"> Statin therapy and impact on inflammation and patient prognosis 	<ul style="list-style-type: none"> Retrospective cohort study Primary endpoint of 28-day all-cause mortality Secondary endpoint included acute cardiac injury N = 1,219 statin use N = 12, 762 no statin 	<ul style="list-style-type: none"> In-hospital statin use Atorvastatin 83.2%, Rosuvastatin 15.6% Dose differences between statins were converted to a daily equivalent dose of atorvastatin ranging from 18.9 – 20.0 mg/day 	<ul style="list-style-type: none"> Reduced all-cause mortality with statin use hazard ratio (HR) 0.63 (95% CI 0.48 – 0.84) Patients on ACEi/ARB therapy in addition to statin did not have increased mortality compared to statin alone Statin therapy not associated with acute cardiac injury 	<ul style="list-style-type: none"> Reduced mortality and improved prognosis associated with in-hospital statin use may be due to the anti-inflammatory and immunomodulatory effects of statins 	[84]

			<ul style="list-style-type: none"> • Inflammatory markers CRP, IL-6 were lower in statin treated patients while in hospital 		
<ul style="list-style-type: none"> • ACEi/ARB impact on mortality in COVID-19 patients with concomitant hypertension 	<ul style="list-style-type: none"> • Retrospective, multi-centre cohort study • Patients with comorbid hypertension hospitalized with COVID-19 • Age 18 to 74 years • Primary endpoint of 28-day all-cause mortality • N = 188 ACEi/ARB therapy • N = 940 no ACEi/ARB 	<ul style="list-style-type: none"> • ACEi/ARB for treatment of hypertension • individual patient dosing regimens not specified 	<ul style="list-style-type: none"> • Risk of all-cause mortality lower in ACEi/ARB treated group HR 0.42 (95% CI 0.19 – 0.92). • Use of ACEi/ARB in comparison to other anti-hypertension therapies was associated with lower mortality HR 0.30 (95% CI 0.12 – 0.70). • No difference in acute cardiac injury outcome between groups 	<ul style="list-style-type: none"> • Chronic ACEi/ARB therapy may not increase mortality of COVID-19 patients • May not have much benefit in acute heart injury due to COVID-19 inflammation 	[91]
<ul style="list-style-type: none"> • Statin use impact on acute myocardial injury patient outcomes 	<ul style="list-style-type: none"> • Retrospective observational cohort study • Patients with elevated troponin • History of CVD in 24% of patients • N = 3069 • Objective to characterize myocardial injury and associated outcomes 	<ul style="list-style-type: none"> • 36% of patients using statins • Doses and regimens not specified 	<ul style="list-style-type: none"> • Statin use amongst patients with acute myocardial injury was associated with improved survival HR 0.57 (95% CI 0.47 – 0.69) 	<ul style="list-style-type: none"> • Statin treatment may be associated with a survival benefit in patients with CVD and elevated troponin levels • Exact beneficial mechanism(s) associated with statins in COVID-19 remain to be studied 	[92]

Table 9. 6: Summary of the ongoing trials investigating pharmacological agents targeting cytokine storm and acute cardiac injury secondary to SARS-CoV-2 infection.

Pharmacological intervention	Sample size and criteria	Treatment protocol	Reference
<ul style="list-style-type: none"> • TACTIC-E Trial • Immunomodulatory agents 	<ul style="list-style-type: none"> • Multi-arm randomized trial • Pre-intensive care unit (ICU) COVID-19 patients • Immunomodulatory drug EDP1815 vs. dapagliflozin + ambrisentan vs. standard care • Primary outcome includes need for cardiovascular organ support 	<ul style="list-style-type: none"> • EDP1815 as 2 capsules twice daily (1.6 x 10¹¹ cells) for up to 7 days • Dapagliflozin 10mg + ambrisentan 5mg once daily 	[93]
<ul style="list-style-type: none"> • High dose IV Vitamin C to ameliorate cytokine storm and associated organ dysfunction 	<ul style="list-style-type: none"> • Prospective placebo controlled randomized controlled trial (RCT) • N = 308 • High dose i.v. vitamin C (HIVC) vs. placebo • Primary outcome of ventilator-free days 	<ul style="list-style-type: none"> • 12g/50ml vitamin C infusion 12ml/h twice daily for 7 days vs. 50 ml sterile water for injection infused at 12ml/h 	[94]
<ul style="list-style-type: none"> • TOC-COVID Trial 	<ul style="list-style-type: none"> • Prospective placebo controlled RCT • N = 100 tocilizumab + standard treatment • N = 100 placebo + standard treatment • Primary outcome of ventilation-free days 	<ul style="list-style-type: none"> • Tocilizumab 8 mg/kg single i.v. dose 	[95]
<ul style="list-style-type: none"> • TACTIC-R Trial • Immunomodulatory agents 	<ul style="list-style-type: none"> • Randomized parallel 3-arm open label trial • N = 125 Baricitinib • N = 125 Ravulizumab • N = 125 standard of care • Primary outcome includes need for cardiovascular organ support 	<ul style="list-style-type: none"> • Baricitinib 4 mg orally once daily on days 1-14 • Ravulizumab single i.v. weight-based dose regimen 	[96]
<ul style="list-style-type: none"> • CytoResc Trial • Cytokine storm in hyperinflammation and shock 	<ul style="list-style-type: none"> • Prospective, open-label, pilot study • ‘CytoSorb’ polystyrene-based hemoadsorber to adsorb circulating cytokines • N = 40-50 ‘CytoSorb’ • N = 40-50 standard care • Primary outcome is time to resolution of vasoplegic shock 	<ul style="list-style-type: none"> • ‘CytoSorb’ therapy administered via a shaldon catheter for 3-7 days 	[97]

<ul style="list-style-type: none"> • MelCOVID Trial 	<ul style="list-style-type: none"> • Double blind placebo controlled RCT • ICU COVID-19 patients • N= 12 melatonin + standard of care • N = 6 placebo control + standard care • Secondary outcome includes CRP, IL-6 levels 	<ul style="list-style-type: none"> • Melatonin 5mg/kg/day i.v. divided every 6 hours for 7 days • Placebo dose of 5mg/kg/day i.v. divided every 6 hours for 7 days 	<p>[98]</p>
<ul style="list-style-type: none"> • Siltuximab for patients diagnosed with severe respiratory complications due to COVID-19 • Anti-IL-6 mitigation of cytokine storm 	<ul style="list-style-type: none"> • Observational retrospective cohort study • Cohort A: continuous positive airway pressure followed by siltuximab • Cohort B: intubation followed by siltuximab • Control group receiving continuous positive airway pressure or intubation only • N = 220 • Primary outcome of mortality over 30 days 	<ul style="list-style-type: none"> • Detailed siltuximab dosing regimen not specified. • Treatment procedure was based on clinicians judgement • Study completed May 8, 2020. Results pending 	<p>[99]</p>
<ul style="list-style-type: none"> • COV-AID Trial • Use of anti-interleukin agents for cytokine storm 	<ul style="list-style-type: none"> • Phase 3 prospective RCT • Patients with signs of cytokine storm • N=38 Anakinra alone (anti-IL-1 receptor) • N=76 Siltuximab alone (anti-IL-6) • N=38 Anakinra + siltuximab • N= 76 Tocilizumab alone (anti-IL-6 receptor) • N=38 Anakinra + tocilizumab • N= 76 standard care alone • Primary outcome as time to clinical improvement 	<ul style="list-style-type: none"> • Anakinra 100mg s.c. daily for 28 days • Siltuximab single i.v. infusion 11 mg/kg • Tocilizumab single i.v. infusion 8 mg/kg max 800mg 	<p>[100]</p>
<ul style="list-style-type: none"> • Sarilumab for hospitalized COVID-19 infections • Cytokine storm syndrome 	<ul style="list-style-type: none"> • Phase 2/3 RCT • Phase 2: Sarilumab in hospitalized patients regardless of disease severity vs. placebo • Primary outcome of % change in CRP in patients with serum IL-6 > upper limit normal • Phase 3 Cohort 1: Sarilumab in hospitalized critical infection receiving 	<ul style="list-style-type: none"> • Phase 2: Low dose sarilumab i.v. • Phase 2: Mid-dose sarilumab i.v. • Phase 3 Cohort 1: Low dose sarilumab i.v. • Phase 3 Cohort 1: Mid-dose sarilumab i.v. • Phase 3 Cohort 2: High dose sarilumab i.v. • Placebo given to match sarilumab administration 	<p>[101]</p>

	<ul style="list-style-type: none"> mechanical ventilation vs. placebo Cohort 2: Sarilumab in hospitalized infection receiving mechanical ventilation vs. placebo N = 1912 Primary outcome of at least 1 point improvement on 7 point clinical scale 		
<ul style="list-style-type: none"> CORIMUNO-SARI Trial Sarilumab to mitigate enhanced IL-6 signalling 	<ul style="list-style-type: none"> RCT Moderate, severe, or critical COVID-19 pneumonia Sarilumab vs. standard of care N = 239 	<ul style="list-style-type: none"> Sarilumab 400 mg single i.v. infusion over 1 hour on day 1 	[102]
<ul style="list-style-type: none"> Baricitinib for hospitalized COVID-19 patients 	<ul style="list-style-type: none"> Non-randomized clinical trial Any adult patient hospitalized with moderate/severe COVID-19 Baricitinib + standard care vs. standard care alone Primary outcome of clinical status after 15 days 	<ul style="list-style-type: none"> Baricitinib 2 mg orally daily for 10 days 	[103]
<ul style="list-style-type: none"> RUXCOVID Trial 	<ul style="list-style-type: none"> Phase 3 placebo-controlled RCT Patients age ≥ 12 with cytokine storm Ruxolitinib + standard care vs. placebo + standard care N = 402 randomized in 2:1 ratio treatment: placebo 	<ul style="list-style-type: none"> Ruxolitinib 5 mg orally twice daily for 14 days May extend treatment to 28 days 	[104]
<ul style="list-style-type: none"> Losartan (ARB) in patients hospitalized for COVID-19 	<ul style="list-style-type: none"> Phase 2 RCT Losartan vs. placebo + standard care N = 200 Secondary outcome includes cardiovascular organ failure/dysfunction 	<ul style="list-style-type: none"> Losartan 50 mg orally once daily 	[105]
<ul style="list-style-type: none"> Losartan (ARB) in patients not requiring hospitalization for COVID-19 	<ul style="list-style-type: none"> Phase 2 RCT Losartan vs. placebo + standard care N = 500 Primary outcome of patients admitted to hospital within 15 days of randomization 	<ul style="list-style-type: none"> Losartan 25mg orally once daily 	[106]
<ul style="list-style-type: none"> Eicosapentaenoic acid (EPA) free 	<ul style="list-style-type: none"> Phase 3 interventional trial 	<ul style="list-style-type: none"> Eicosapentaenoic acid free fatty acid (EPA-FFA) 1 g gastro- 	[107]

<p>fatty acid for hospitalized COVID-19 patients</p>	<ul style="list-style-type: none"> • Treatment with EPA gastro-resistant capsules vs. standard care • 28-day treatment period • Primary outcome of time to treatment failure i.e. need for additional therapy, intubation, transfer to ICU, or death • Secondary outcome includes reduction of IL-6 levels 	<p>resistant capsules twice daily (2 g total)</p>	
<ul style="list-style-type: none"> • COLCORONA Trial • Colchicine and inflammatory cytokine storm 	<ul style="list-style-type: none"> • Phase 3 multi-centre placebo-controlled randomized controlled trial (RCT) • Age 40 years or older • Patients must have at least one high-risk factor i.e. uncontrolled hypertension, HF, coronary artery disease (CAD), diabetes, obesity, etc. • Colchicine vs. placebo • 30-day treatment • N = 6000 • Primary composite endpoint of need for hospitalization or death 	<ul style="list-style-type: none"> • Colchicine 0.5 mg orally twice daily for 3 days, then 0.5 mg once daily for 27 days • Placebo will match colchicine administration 	<p>[108]</p>

9.4 Adverse cardiovascular effects of the proposed empirical/supportive treatments

Currently, there is no approved vaccination or effective drug for protecting against or treating COVID-19; only symptomatic therapy and empirical/supportive treatments are available. Many of the mortalities related to COVID-19 have been primarily attributed to original patient comorbidities instead of pneumonia [109]. This highlights the importance of focusing on pre-existing comorbidities of COVID-19 patients, particularly those of the cardiovascular system. Attention to therapies with cardiovascular side effects being proposed and applied to patients with COVID-19, especially those with underlying CVD is important. Notably, many of the therapies proposed to ameliorate the poor prognosis of COVID-19 patients are associated with cardiovascular adverse effects. For example, treatment of patients with COVID-19 with non-steroidal anti-inflammatory drugs, glucocorticoids and anti-viral agents, such as ribavirin, lopinavir/ritonavir, INF- α and the antibiotic azithromycin, could further increase the cardiovascular risk of COVID-19 patients.

Excessive use of non-steroidal anti-inflammatory drugs and glucocorticoids is associated with deleterious effects on the cardiovascular system increasing the risk of events including, ischemia, MI, arrhythmias and HF [110, 111]. Although corticosteroids are sometimes prescribed for the treatment of patients with severe SARS-CoV infection for the possible relief of inflammation [112], recent evidence suggests corticosteroids may exacerbate lung injury associated with SARS-CoV-2 due to delayed viral clearance [113, 114]. The antiviral agents lopinavir and ritonavir have been tested in a randomized controlled, open-label trial in hospitalized adult patients with COVID-19 and concluded that no benefit was observed with lopinavir–ritonavir treatment beyond standard care. Moreover, about 14% of lopinavir–ritonavir recipients were unable to complete the full 14-day course of administration due primarily to the adverse events

including the risks of QT prolongation [115]. It is important to highlight that the adverse effects of these antivirals involve altering the cardiac electrical conduction system causing QTc and/or PR interval prolongation, which can lead to atrioventricular block and torsade de pointes arrhythmias increasing the risk of MI [116]. Further, the use of these protease inhibitors can lead to metabolic disturbances such as hyperglycemia, hyperlipidemia, and lipodystrophy which may also contribute to adverse cardiovascular outcomes [117, 118]. Recently, IFN- α 2b was used in an uncontrolled exploratory study including 77 hospitalized adults with confirmed COVID-19 in Wuhan, China [119]. The trial showed that treatment with IFN- α 2b markedly decreased the duration of detectable virus in the upper respiratory tract and also reduced the interval of the elevated inflammatory markers IL-6 and CRP in the blood. However, treatment with IFN- α has been associated with hypertension, hypertriglyceridemia and direct cardiotoxicities, including arrhythmias, MI and cardiomyopathy, which could exacerbate underlying cardiac dysfunction [120]. An open-label randomized trial has been conducted to test the efficacy of IFN beta-1b, lopinavir–ritonavir and ribavirin for treating patients admitted to hospital with COVID-19 and concluded early triple antiviral therapy was effective in alleviating symptoms and shortening the duration of hospital stay in patients with mild to moderate infections [121]. However, it is worth noting ribavirin has a US boxed warning issued for hemolytic anemia associated with use that may worsen underlying cardiac disease and lead to fatal and non-fatal MI [122]. Numerous recent studies proposed the use of hydroxychloroquine and azithromycin as a treatment of COVID-19 in open-label non-randomized clinical trials, however, no positive results were produced [123-126]. Well known adverse effects associated with azithromycin or hydroxychloroquine include development of severe QT prolongation [127], which worsened when azithromycin is combined with hydroxychloroquine to treat COVID-19 patients [128, 129].

Currently, there are multiple *in vitro* experiments and preclinical studies being performed around the world to test novel COVID-19 therapies, which are quickly moving into clinical trials. Importantly, the early efficacy results have been limited to small-scale clinical studies in which the safety profiles have not been well-identified. The safety profiles will be critical for COVID-19 patients with underlying comorbidities such as cardiovascular dysfunction. Therefore, as there is a need for rapid clinical translation and a wide use of novel therapies for COVID-19, continued attention to safety profiles is important. The rapid spread of COVID-19 globally continues to impact susceptible populations, like elderly patients and individuals with underlying comorbidities. While underlying cardiovascular issues are impacted by COVID-19 infection, many existing and novel therapeutic strategies have direct adverse cardiovascular effects, highlighting the importance for consideration in new drug research and development.

9.5 Overview of the n-3 polyunsaturated fatty acids

The long-chain n-3 polyunsaturated fatty acids (n-3 PUFAs) are essential fatty acids obtained from both dietary and non-dietary sources. The simplest n-3 PUFA is α -linolenic acid (ALA, 18:3 n-3). Once inside the body, ALA can be converted through a series of elongation and desaturation reactions into other n-3 PUFAs. For instance, ALA is metabolized into eicosapentaenoic acid (EPA, C20:5n-3) which can be further metabolized into docosahexaenoic acid (DHA, C22:6n-3), the two most abundant n-3 PUFAs in mammalian tissues [130]. Mammals lack the necessary enzymes (delta-12 and delta-15 desaturase) required to synthesize ALA *de novo*. As such, these fatty acids are described as “essential” and must be obtained from the diet such as fish, other marine sources, and supplements [131, 132]. Conversely, linoleic acid (LA, 18:2 n-6) is considered the primary source of the essential n-6 PUFAs. LA can be further metabolized into arachidonic acid (AA, 20:4n-6) by the same series of elongase and delta-4,-5,-6

desaturase enzymes. As n-3 PUFAs can compete for the same metabolic pathways with n-6 PUFAs, n-3 PUFAs supplementation may reduce the synthesis of n-6 PUFA-derived metabolites, thus, altering the metabolite profile and impacting numerous signaling pathways within the body, including the immune system, leading to disparate effects [133].

9.5.1 Role of n-3 polyunsaturated fatty acids in patients with respiratory infections and/or sepsis

A plethora of human and animal studies have investigated the beneficial effects of EPA and DHA in patients with ALI and ARDS which are common characteristics observed in severe SARS-CoV-2 patients [134-137]. Mancuso et al. demonstrated Long-Evans rats fed enteral diets containing fish oil as a source of n-3 PUFAs for 21 days were subjected to acute inflammation caused by an intravenous injection of Salmonella endotoxin. N-3 PUFA fed rats had a lower severity of pulmonary microvascular protein permeability and decreased pulmonary neutrophil accumulation compared to rats fed the n-6 PUFA enriched diet [138, 139]. Furthermore, stimulated alveolar macrophages had lower concentrations of AA-derived metabolites, such as thromboxane B2 (TXB2) and prostaglandin E2 (PGE2) suggesting a beneficial effect of n-3 PUFAs over n-6 PUFAs in attenuation of ALI [138, 139]. Saedisomeolia et al. demonstrated in Calu-3 epithelial cells infected with Rhinovirus RV-43 and RV-1B that pre-incubating with DHA significantly reduced the release of IL-6 and IFN- γ -inducible protein, suppressing RV-induced inflammation [140]. Collectively, these studies demonstrate that the anti-inflammatory properties of n-3 PUFAs play a pivotal role in attenuating the uncontrolled immune response in the lungs secondary to bacterial or viral infections which could be helpful in the setting of COVID-19.

Clinical evidence from trials assessing the role of n-3 PUFAs in ameliorating ALI, ARDS and sepsis has been limited. Pontes-Arruda et al. investigated the effect of a diet enriched with

EPA, γ -linolenic acid and antioxidants in patients with severe sepsis or septic shock who required mechanical ventilation [141]. The data suggested the diet contributed to improved ICU and hospital clinical outcomes and was associated with lower mortality rates when compared to the control groups. Meta-analysis reported a significant reduction in ventilator-free days, organ failures, length of stay in ICU, mortality rates as well as relevant improvements in oxygenation and clinical outcomes of ventilated patients with ALI/ARDS given EPA and γ -linolenic acid [142]. The efficacy and safety of a diet supplemented with a high-dose EPA and DHA (9 g/d added of 1g/d ascorbic acid, 400UI/12h α -tocopherol and 100 μ g/d selenium) was assessed in patients with early-stage sepsis for 7 days. The investigators found patients had lower levels of CRP, IL-6 and procalcitonin, as well as less need for mechanical ventilation and reduced development of severe sepsis [143]. Evidence for beneficial effects of n-3 PUFA-containing diets in patients with severe ARDS demonstrated similar outcomes such as reduced duration of mechanical ventilation, shorter ICU length and improved oxygenation [144]. These effects are highlighted in a recent systematic review with a meta-analysis demonstrated critically ill patients receiving parenteral nutrition therapy enriched with fish oil lipid emulsion had reduced risk for infection and sepsis (40% and 56%, respectively) as well a reduction of hospital and ICU stay by about two days [145]. Together, these studies demonstrate n-3 PUFA supplementation has favorable results in terms of multiple inflammatory, respiratory and clinical outcomes.

Recently, Bristrian proposed the use of parenteral supplementation of fish-oil emulsions, containing substantial amounts of EPA and DHA (4–6 g/d), to treat patients with severe SARS-CoV-2, in order to inhibit cytokine secretion and mitigate the inflammatory response [146]. In agreement with this idea, Torrinhas et al. agreed the immune modulatory properties of n-3 PUFAs will provide important and beneficial effects to improve clinical outcomes of COVID-19

particularly in hospitalized high-risk populations with severe underlying conditions including the elderly, obese, hypertensive, oncologic and diabetic patients [147]. Furthermore, they suggested n-3 PUFAs could provide additional benefits by attenuating the aggravated inflammatory state observed with pre-existing health conditions which might have a role in triggering detrimental outcomes associated with severe COVID-19 phenotypes.

Currently, there is an open-label, randomized control study to investigate the effect of n-3 PUFAs in hospitalized subjects with confirmed SARS-CoV-2 (NCT04335032) [107]. The study comprises 240 participants, with one group receiving standard care, the other additionally being provided 2 g daily of EPA capsules. Interventions will be carried out between 28 and 90 days and the efficacy of EPA in the treatment of the disease, oxygen saturation, levels of pro-inflammatory IL-6, mortality rate, ICU stays, hospitalization days and need for mechanical ventilation will be determined. While the results from this study are not available, the evidence suggests oral or intravenous administration of bioactive lipids could potentially reduce the severity and/or enhance the recovery of those infected with COVID-19 [148]. However, further research is undoubtedly required.

9.5.2 Cardiovascular benefits of n-3 polyunsaturated fatty acids

N-3 PUFAs and many of their endogenously generated metabolites act as bioactive lipid molecules with a wide array of properties against numerous disorders including CVD [149-151]. Numerous studies have suggested higher consumption of n-3 PUFAs lowers the number of mortalities related to CVD [152-155]. For instance, Mozaffarian et al. demonstrated higher plasma levels of n-3 PUFA biomarkers in a U.S. adults cohort study was associated with lower total mortality attributable with fewer cardiovascular compared to non-cardiovascular deaths [156].

Currently, the intake of n-3 PUFAs is still recommended by the American Heart Association to prevent clinical CVD episodes in individuals with predominant coronary heart disease, such as a recent MI, to reduce death rates as well as individuals with prevalent HF to reduce hospitalizations and number of mortalities [157, 158].

The cardiovascular benefits of n-3 PUFAs could be attributed to their pleiotropic effects on the different elements of the cardiovascular system. Evidence suggests a higher intake of n-3 PUFAs has a beneficial effect on lipid profiles by replacing saturated fatty acids and lowering triglyceride levels, thereby stabilizing atherosclerotic plaques and reducing the incidence of thrombus formation [159, 160]. Furthermore, n-3 PUFAs can enrich cell membranes and alter the lipid raft structure and function leading to improved organelle and cellular function [161], autonomic tone [162, 163], elevated arrhythmic thresholds [164] and ameliorating hypertension [163, 165]. Importantly, several experimental, clinical and epidemiological studies hypothesize that the cardioprotective effects of n-3 PUFAs and their metabolites are attributed mainly to their immunomodulatory properties. Notably, emerging evidence demonstrates the ability of n-3 PUFAs to reduce circulating levels of inflammatory chemokines, cytokines, and the pro-inflammatory metabolites derived from n-6 PUFAs [166, 167].

9.5.3 Potential cardioprotective mechanisms of n-3 PUFAs in the setting of COVID-19

Based on several clinical reports, COVID-19 patients with severe ALI/ARDS may also suffer from increased risk of sepsis and cardiac arrest [10]. Accumulating reports have indicated that n-3 PUFAs could improve resolution of inflammation, sepsis survival and precondition the heart against septic cardiomyopathy [168, 169]. In this review, we propose that n-3 PUFAs can protect against and ameliorate cardiovascular complications associated with COVID-19 mainly

due to their immunomodulatory features, antioxidant potential as well as their ability to maintain tissue hemostasis. This section will highlight the cardioprotective mechanisms of n-3 PUFAs and their metabolites implicating that n-3 PUFAs might have a supportive adjuvant utility in treating and protecting against cardiac complications associated with COVID-19 (Figure 9.2).

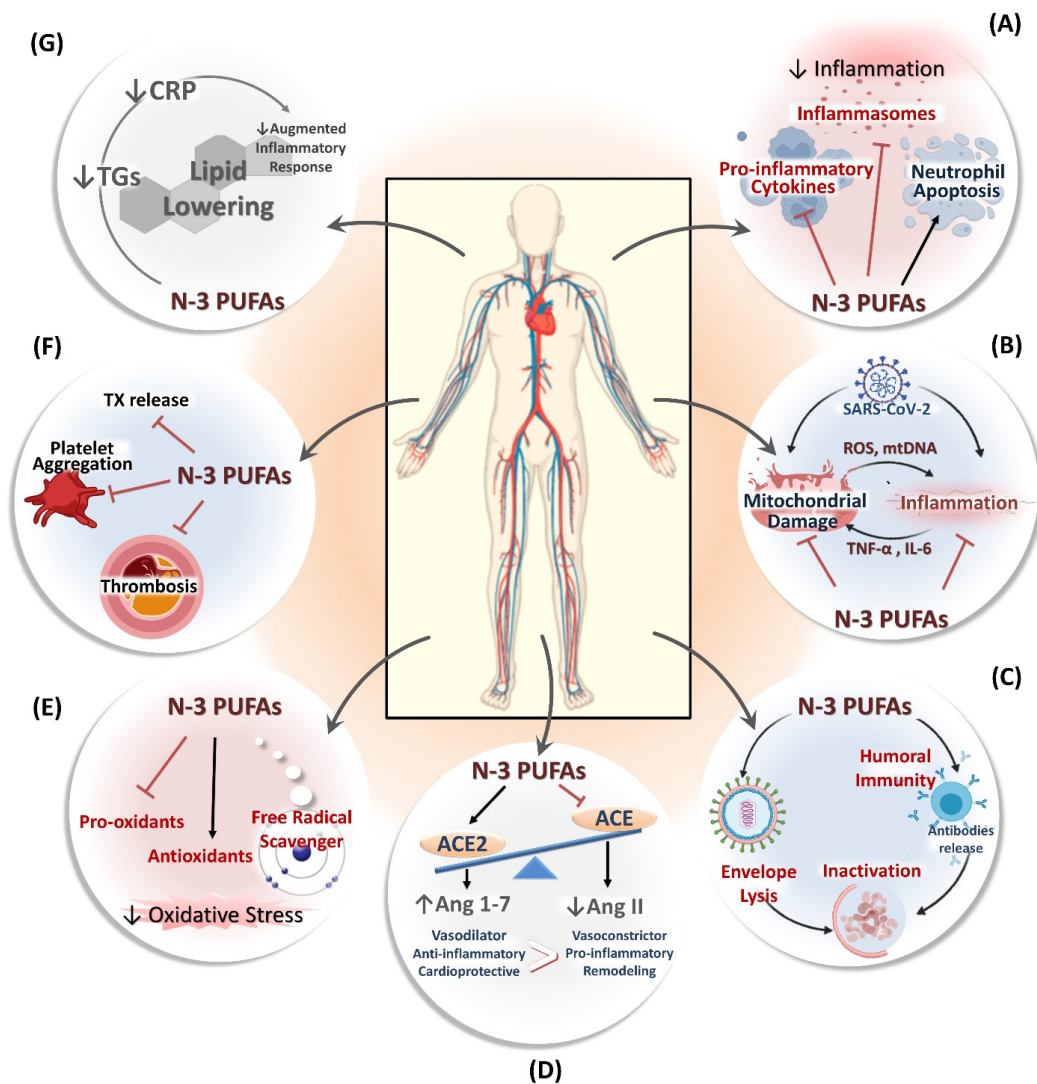


Figure 9. 2: Potential cardioprotective mechanisms of n-3 PUFAs in the setting of COVID-19. (A) N-3 PUFAs ameliorate uncontrolled immune responses and exert anti-inflammatory effects via several mechanisms. (B) N-3 PUFAs attenuate the vicious cycle/interaction of mitochondrial dysfunction and aggravated immune response. (C) N-3 PUFAs have the capability to attenuate viral infections via both direct effects on membrane integrity and indirect mechanisms through activating the humoral response to decrease overall viral load. (D) N-3 PUFAs have the ability to regulate the RAAS system in the favor of the vasodilatory, the anti-inflammatory and the cardioprotective ACE2/Ang (1-7) effectors. (E) N-3 PUFAs enhance antioxidant capacity and attenuate oxidative stress in the tissue. (F) N-3 PUFAs ameliorate coagulopathy by exerting anti-thrombotic effects. (G) The triglyceride-lowering effect of n-3 PUFAs may play a key role in blunting the exaggerated inflammation observed in patients with COVID-19. ACE, Angiotensin-converting enzyme; Ang, Angiotensin; CRP, C-reactive protein; IL, Interleukin; mtDNA, Mitochondrial DNA; PUFA, Poly unsaturated fatty acid; ROS, Reactive oxygen species; TGs, Triglycerides; TNF- α , Tumor necrosis factor alpha; TX, Thromboxane.

9.5.3.1 The anti-inflammatory properties of n-3 PUFAs

As mentioned earlier, an exacerbated immune system response and uncontrolled inflammation are fundamental mechanisms in the development of cardiovascular impairment in patients with COVID-19. Accordingly, a plethora of experimental studies and clinical trials demonstrate that targeting different inflammatory components may be considered promising strategies to control cardiovascular impairment during the acute and remission phases of COVID-19 (Figure 9.3).

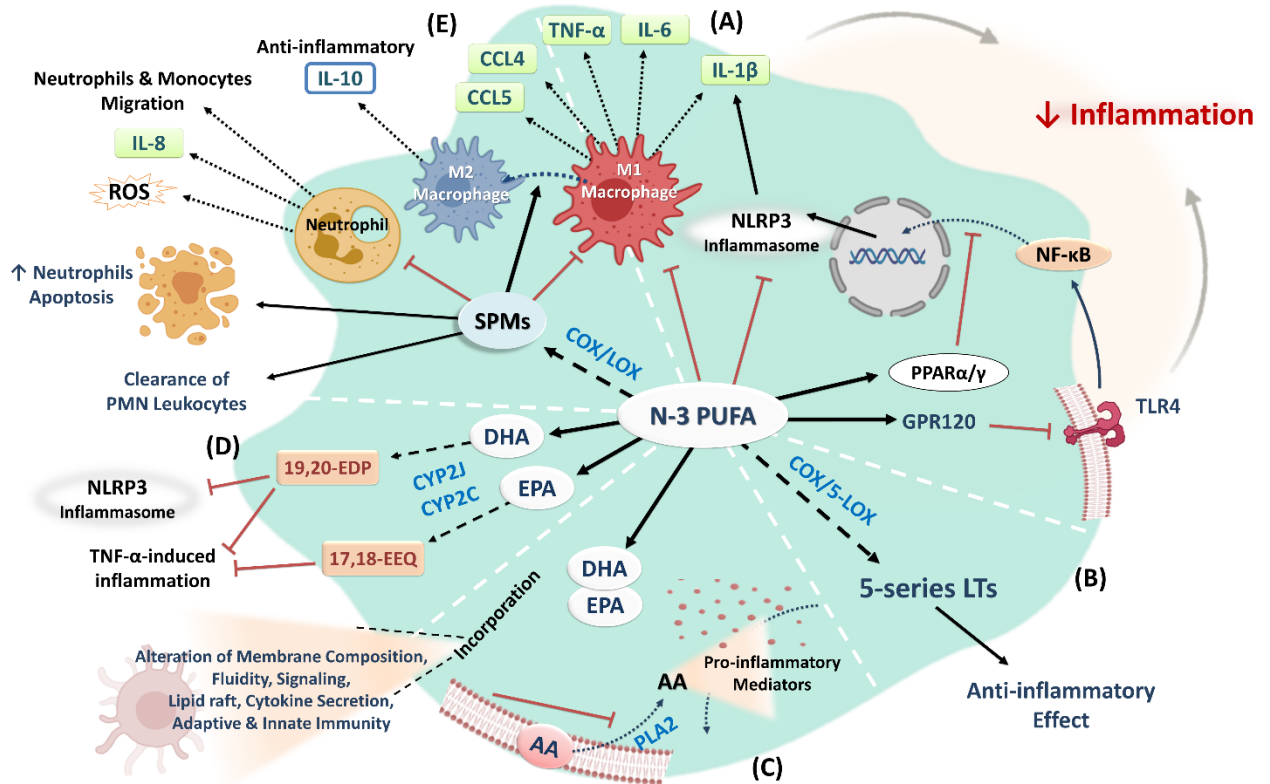


Figure 9. 3: A summary of the anti-inflammatory mechanisms of n-3 PUFAs. (A) N-3 PUFAs can regulate expression of inflammatory cytokines, chemokines and adhesion molecules, inhibit NLRP3 inflammasomes, activate anti-inflammatory transcription factors (PPAR α/γ) and activate GPR120 receptors which inhibit TLR4-mediated activation of NF- κ B. (B) N-3 PUFAs are metabolized by COX/5-LOX into 5-series LTs which exert anti-inflammatory effects. (C) N-3 PUFAs can replace n-6 PUFAs, such as AA, altering the inflammatory response. N-3 PUFA will alter cell membrane composition, fluidity and mediated signaling. (D) N-3 PUFAs, DHA and EPA, are metabolized by CYP epoxygenases into bioactive epoxy lipids with anti-inflammatory properties. (E) N-3 PUFAs are metabolized by COX/LOX into SPMs which act as potent anti-inflammatory modulators. AA, Arachidonic acid; CCL, Chemokine ligand; COX, Cyclooxygenase; CYP, Cytochrome P450; DHA, Docosahexaenoic acid; EDP, Epoxydocosapentaenoic acid; EEQ, Epoxyeicosatetraenoic acid; EPA, Eicosapentaenoic acid; GRP, G-protein coupled receptor; IL, Interleukin; LOX, Lipoxygenase; LT, Leukotriene; PUFA, Poly unsaturated fatty acid; NF κ B, Nuclear factor kappa-light-chain enhancer activated B-cells; NLRP3, NACHT, LRR and PYD domains-containing protein 3; PLA2, Phospholipase A2; PMN, Polymorphonuclear neutrophils; PPAR, Peroxisome proliferator-activated receptor; ROS, Reactive oxygen species; SPMs, Specialized pro-resolving mediators; TLR, Toll like receptor; TNF- α , Tumor necrosis factor- α .

9.5.3.1.1 N-3 PUFAs regulate the expression of several proinflammatory innate immune components and modulate macrophage response

A ‘cytokine storm’ and activation of the central innate immune pathway linking the NLRP3 inflammasome, IL-1 β , TNF- α and IL-6 response is a primary cause of excessive inflammation reported in COVID-19 that negatively impacts cardiovascular system. Therefore, targeting the different components is a promising approach to ameliorate cardiac complications secondary to COVID-19 [10]. While there is no direct clinical evidence related to the use of n-3 PUFAs in COVID-19 patients, the application of n-3 PUFAs in several inflammatory settings, including cardiovascular disorders, has been demonstrated to ameliorate detrimental immune reactions by several mechanisms [170]. The anti-inflammatory effect of n-3 PUFAs seems to be consistent across several previous clinical findings [171-174]. Intriguingly, Tan et al. recently demonstrated in a randomized controlled study that high-dose n-3 PUFA supplementation (1.5 g/day EPA and 1.0 g/day DHA) markedly reduces plasma levels of IL-6, IL-1 β and TNF- α after 4 weeks of therapy in middle or late-aged patients with chronic venous leg ulcers suggesting n-3 PUFAs as an effective low-risk dietary intervention to modulate inflammation [175]. This study indicates that n-3 PUFAs could have direct modulatory effects on the main components of the cytokine storm IL-6, IL-1 β and TNF- α .

N-3 PUFAs can modulate the transcription and expression of inflammatory genes including cytokines, chemokines and adhesion molecules in cardiomyocytes, fibroblasts, endothelial cells, monocytes and macrophages [176-180]. This is primarily achieved through the regulation of key transcription factors, such as inhibiting NF- κ B [181-184] or activating peroxisome proliferator-activated receptors- α/γ (PPAR α/γ) [185, 186]. Activation of PPAR α/γ can directly interfere with the activation of NF- κ B and prevent its shuttling to the nucleus reducing

the inflammatory burst [187-191]. Interestingly, direct activation of PPAR, using PPAR agonists, was proposed as a therapeutic target for blunting and regulating cytokine storm in COVID-19 patients suggesting n-3 PUFAs could have a promising effect [192]. Another important immunomodulatory mechanism induced by n-3 PUFAs involves activation of G protein-coupled receptor 120 (GPR120), which mediates strong and wide-ranging anti-inflammatory effects. Research from Oh et al. indicates n-3 PUFAs stimulate GPR120 in both monocytic RAW 264.7 cells and primary intraperitoneal macrophages inhibiting TLR4-mediated inflammatory responses. Knockdown of GPR120 attenuates the protective effects attributed to n-3 PUFA consumption [193]. These studies together provide evidence that n-3 PUFAs mediate anti-inflammatory effects through different mechanistic pathways.

Cardiac macrophages are primarily derived and replenished from inflammatory monocytes in response to an infection with resident macrophages also having a role. Briefly, macrophages will differentiate into classical M1 inflammatory cells to clean cellular and matrix debris [194]. Subsequently, M1 macrophages may undergo polarization and transformation to the alternatively activated or reparatory M2 stage which secrete IL-10 to promote resolution and contribute to wound healing and tissue repair [195]. Controlling the migration and the polarization of macrophages to the myocardium in the context of COVID-19 is a tentative approach to limit cardiac injury [196-199]. In COVID-19, an excessive cardiac recruitment and accumulation of pro-inflammatory M1 macrophages potentially aggravates cardiovascular injury. Notably, as M1 macrophages secrete a large variety of chemokines and cytokines such as TNF- α and IL-1 β to recruit and activate other immune cells from both the innate and the adaptive immune system. The effect will impede the reparative phase mediated by M2 macrophages and thus aggravates adverse cardiac remodeling [200-203].

Interestingly, evidence demonstrates n-3 PUFAs and/or their biologically active metabolites have the ability to blunt the expression, production and release of IL-1 β , TNF- α , and IL-6 by M1 macrophages [204-206]. Schoeniger et al., showed n-3 PUFAs have the ability to down-regulate inflammatory processes and reduce the production and secretion of pro-inflammatory cytokines from RAW 264.7 macrophages infected with microorganisms, *R. equi* and *P. aeruginosa* [207]. Moreover, the inhibitory effects of EPA and DHA on the pro-inflammatory NLRP3 inflammasome pathway has also been well-documented in macrophage cell lines as well as in primary human and mouse macrophages [208, 209]. Kumar et al., investigated the effects of 15-lipoxygenase (LOX) metabolites of ALA on lipopolysaccharide (LPS) -induced inflammation in RAW 264.7 cells and peritoneal macrophages. The findings revealed the anti-inflammatory effects of these metabolites involve inactivation of the NLRP3 inflammasome complex through the PPAR- γ pathway [208]. N-3 PUFAs can increase the phagocytic capacity of macrophages, which has been shown through the engulfment of zymosan particles [210], *Pseudomonas aeruginosa*, *Rhodococcus equi* [211], *E.coli* [212] and apoptotic cells [210]. It has been suggested the increase in phagocytic capacity of macrophages upon n-3 PUFA treatment could be attributed to changes in the cellular membrane composition and structure caused by the incorporation of the n-3 PUFAs [213, 214]. Importantly, n-3 PUFAs have been found to promote M2 polarization in macrophage cell lines and primary mouse macrophages enhancing resolution of inflammation and tissue repair after infection [210, 215]. Collectively, the modulatory properties of n-3 PUFAs on the immune system could impart a promising beneficial effect on the cardiovascular system in the context of COVID-19, an effect which needs further exploration and confirmation in larger clinical trials.

9.5.3.1.2 Shifting to the anti-inflammatory COX- and LOX-derived metabolites of n-3 PUFAs

Accumulating literature demonstrates potent immunomodulatory properties of metabolites generated from n-3 PUFAs and consequently their impact on cardiovascular health [216, 217]. The metabolism of n-3 and n-6 PUFAs is closely interconnected as parent compounds compete for the same metabolic enzymes but result in the production of a wide array of either pro- or anti-inflammatory metabolites. For example, cyclooxygenase (COX) converts the n-6 PUFA arachidonic acid (AA) to the 2-series of prostaglandins (PGs) and the 2-series of thromboxanes (TX), while lipoxygenase (LOX) enzymes metabolize AA to the 4-series leukotrienes (LTs) and the hydroxyicosatetraenoic acids. These lipid mediators are considered pro-inflammatory and are involved in various pathological processes including cardiovascular disorders [218-220]. The synthesis and production of PGE₂ occurs in several cells, including dendritic cells, macrophages, fibroblasts and endothelial cells. PGE₂ not only mediates vasodilation, endothelial permeability and increase of pain [221] but also contributes to the tissue influx of neutrophils, mast cells and macrophages and can affect the differentiation of these cells [218].

N-3 PUFAs can also act as a substrate for COX and 5-LOX enzymes resulting in production of the 3-series of PGs and TXAs as well as 5-series LTs, which are a set of less inflammatory or even anti-inflammatory metabolites in comparison to the metabolite family derived from AA [222-224]. These eicosanoids are responsible for producing several physiological responses related to inflammation, and their imbalance has been observed in several diseases [225, 226]. For example, the production of PGE₂ and LTB₄ by human inflammatory cells was significantly decreased in a diet rich in fish oil [227-230]. Therefore, the metabolism of n-3 PUFAs by COX and LOX enzymes not only reduce the AA-derived pro-inflammatory

metabolites but also alter the metabolic profile towards more biologically active anti-inflammatory mediators [223, 231, 232]. This may represent one of the central anti-inflammatory and consequently cardioprotective mechanisms of n-3 PUFAs against cardiac complications associated with COVID-19.

9.5.3.1.3 Anti-inflammatory features of the n-3 PUFAs-derived specialized pro-resolving mediators (SPMs)

Metabolism of n-3 PUFAs also generates another group of highly specialized pro-resolving mediators (SPMs) which include resolvins ‘resolution phase interaction products’ produced from both EPA (E-series, RvE1-2) and DHA (D-series, RvD1-6) as well as protectins and maresins produced from DHA [233, 234]. Both the COX and LOX pathways are involved in the synthesis of these metabolites with distinct epimers being produced in the presence and absence of aspirin [235].

SPMs possess potent anti-inflammatory and inflammation resolving properties which is essential to terminate ongoing inflammatory processes, accelerate the cleaning process and aid in tissue regeneration and wound healing allowing tissue homeostasis to return [233, 236-238]. Several mechanistic pathways contribute to the anti-inflammatory effects of resolvins, protectins and maresins. This includes preventing the migration of neutrophils and monocytes across epithelial cells and promoting clearance of polymorphonuclear (PMNs) leukocytes, apoptotic cells and debris from the site of inflammation [233, 239]. Krishnamoorthy et al. showed resolvins inhibit tissue migration of neutrophils by lowering the expression of surface adhesion receptors on neutrophils, such as CD11b or CD18, and reducing the production of the chemokine IL-8 [240]. Additionally, the partial agonist/antagonist activity of RvE1 toward LTB₄ receptors on PMNs will inhibit NF- κ B activation, abolish pro-inflammatory cytokine production and reduce PMN

leukocyte infiltration [233, 234, 241]. Resolvins can blunt reactive oxygen species (ROS) production from neutrophils, induce neutrophil apoptosis and clearance by macrophages, as well contribute to inhibiting chemokine signaling [242-244]. Furthermore, Morin et al. demonstrated a diet enriched with DHA and monoglycerides can significantly increase the levels of RvD2 and RvD3, which correlate with reduced levels of proinflammatory mediators CRP, IL-6, TNF- α , and IL-1 β in a rat model of hypertension [245]. Additionally, there is growing evidence for a role of SPMs in regulating the humoral immune response. A study conducted by Ramon et al., showed 17-hydroxydocosahexaenoic acid (17-HDHA), the precursor of the D-series SPMs (RvD1, 17R-RvD1, RvD2), can reduce IL-6 secretion in human B cells, increase B cell antibody production and promote B cell differentiation to an antibody secreting cell [246]. These new findings highlight the potential applications of SPMs as non-toxic, supportive adjuvants and as anti-inflammatory therapeutic molecules particularly during infection as in the case of COVID-19.

Resolvins, protectins and maresins play a pivotal role regulating the function of macrophages. Sulciner et al. demonstrates RvD1, RvD2 or RvE1 can inhibit debris-stimulated cancer progression by enhancing clearance of debris via macrophage phagocytosis in multiple tumors. These resolvins suppressed the release of the proinflammatory cytokines/chemokines, including TNF α , IL-6, IL-8, chemokine ligand 4, and chemokine ligand 5, by human macrophages cocultured with tumor cell debris [247]. Maresins are conjugates of sulfides synthesized by macrophages, which are also participants in acute inflammation resolution and seem to promote tissue regeneration [248]. Maresin 1 biosynthesis involves an active intermediate (13S,14S-epoxi-DHA) that stimulates macrophage conversion from M1 (pro-inflammatory) to M2 (anti-inflammatory) phenotype [249]. It is noteworthy that M2 macrophages secrete resolvins, protectins and maresins to dampen inflammation and restore homeostasis [250, 251] and at the

same time augment phagocytic capacity of macrophages and other cells to remove debris from the site(s) of infection and injury and enhance microbial clearance [252-254].

The role of resolvins in the resolution of inflammation has been demonstrated in several animal models of ALI and ARDS [255-258]. These studies carried out using rat and mouse models infected with the E.coli endotoxin, LPS, suggested the pro-resolving effects of these molecules could be attributed, for example, to the suppression of neutrophil infiltration due to reduced expression and release of pro-inflammatory cytokines from alveolar macrophages [255, 256]. Further, it has been demonstrated protectins may reduce the replication of influenza [259] and potentially affect the inflammatory manifestations of respiratory viral diseases [260].

Importantly, pro-inflammatory cytokines, TNF- α and IL-6, will inhibit the activities of desaturases, which are essential for the generation of AA, EPA and DHA from their precursors LA and ALA [261]. Hence, in instances where there is a substantial degree of inflammation due to high levels of IL-6 and TNF- α , such as following COVID-19 infection, a deficiency of EPA and DHA and subsequent decreased generation of resolvins, protectins and maresins can occur [262]. Thus, administration of PUFAs and/or their metabolites, resolvins, protectins and maresins can suppress inappropriate production of IL-6 and TNF- α to resolve inflammation, enhance recovery and limit cytokine storm [263] in COVID-19. Together, the studies imply administration of n-3 PUFA may enhance recovery from infections and further, if present in adequate amounts, may modulate the response to infections.

9.5.3.1.4 Role of CYP-mediated metabolites in ameliorating inflammation

CYP2J and CYP2C isoforms, the constitutively expressed cytochrome P450 (CYP) epoxygenases found in the cardiovascular system, metabolize EPA into 5 regioisomeric

epoxyeicosatetraenoic acids (5,6-, 8,9-, 11,12-, 14,15-, 17,18-EEQ) and DHA into 6 regioisomeric epoxydocosapentaenoic acids (4,5-, 7,8-, 10,11-, 13,14-, 16,17-, 19,20-EDP) [264-266]. Recent evidence suggests that 17,18-EEQ and 19,20-EDP mediate several anti-inflammatory effects of n-3 PUFAs in various models of tissue injury [266-268]. For example, Fang et al. demonstrated a n-3 PUFA-rich diet attenuates MI injury in mice by producing a protective eicosanoid pattern, which results in shifting the metabolite profile to a more anti-inflammatory state by increasing the levels of the 19,20-EDP and 17,18-EEQ and decreasing the pro-inflammatory PGE₂ [269]. The cardioprotective effects of n-3 PUFAs are also attributed to their ability to attenuate the NLRP3 inflammasome complex cascade [270]. Importantly, the anti-inflammatory features of CYP-derived epoxy metabolites have been reported in numerous models. For example, in TNF α -induced retinal vascular inflammation, Capozzi et al. demonstrated 19,20-EDP can ameliorate vascular adhesion molecule and intracellular adhesion molecule expression and reduce leukocyte adherence to human retinal microvascular endothelial cell monolayers [271]. Additionally, evidence demonstrates intraperitoneal infusions of 17,18-EEQ and 19,20-EDP protect against allergic intestinal inflammation and kidney fibrosis in corresponding mouse models [272, 273]. 17,18-EEQ was able to inhibit TNF α -induced inflammation in human lung tissue obtained from patients undergoing surgery for lung carcinoma via inhibition of NF- κ B and activation of the transcription factor PPAR- γ [274]. The anti-inflammatory properties of DHA epoxides were also well demonstrated using animal models of inflammatory pain. For example, Morisseau et al. demonstrated that direct injection of the DHA epoxides, EDPs, together with the pro-inflammatory carrageenan into the paw or spinal cord of male Sprague-Dawley rats resulted in significant antihyperalgesic activity. Surprisingly, both the parent free fatty acid DHA and the corresponding diols were inactive, supporting the hypothesis that the epoxy lipids mediate many of the beneficial

effects of the parent compounds [275]. The bacterial endotoxin, LPS, has a marked role in triggering inflammatory injury which can result in several cardiovascular complications. In a study using HL-1 cardiac cells, 19,20-EDP protected against LPS-stimulated inflammatory injury by activating the histone deacetylase Sirtuin-1 inhibiting the activation the pro-inflammatory transcription factor NF- κ B [276]. The accumulating evidence suggests the anti-inflammatory properties of CYP-epoxygenase metabolites of n-3 PUFAs have a substantial role in activating protective responses in models of cardiovascular injury. However, further investigation is required to elucidate whether the protective properties limit cardiovascular injury secondary to COVID-19 infection.

9.5.3.1.5 N-3 PUFAs alter cell membrane structure and function - modulation of the lipid raft

Within a cell, n-3 PUFAs can be found incorporated into phospholipid membranes where elevating levels will replace existing n-6 PUFAs thereby altering the composition and properties of lipid rafts [149, 150]. The increased incorporation of n-3 PUFAs into membrane bilayers can have a role in mediating immunomodulatory effects by altering membrane composition, fluidity and function. These changes will impact membrane-mediated signaling, protein trafficking, generation of bioactive lipids, cytokine secretion and gene activation in both innate and adaptive immune responses. For example, a change in fluidity can interfere with the dimerization and expression of the TLR4 subunits, blocking the downstream inflammatory reaction [277, 278]. Evidence of these effects by n-3 PUFAs have been demonstrated to impact the maturation of dendritic cells, macrophage function and T and B cell polarization/activation [279-284]. Interestingly, DHA appears to be better than EPA in replacing n-6 PUFAs and cholesterol in

plasma membranes of aortic endothelial cells enhancing the fluidity of the phospholipid membrane [285].

In most cell types, AA is the predominant n-6 PUFA in membrane phospholipids [286]. Inflammatory immune cells such as monocytes, neutrophils, macrophages and lymphocytes often contain a large amount of AA in their membrane. The high membrane AA composition is important during normal inflammatory responses. Under stress conditions activation of phospholipase A2 liberates AA from the cell membrane leading to metabolism and production of many pro-inflammatory metabolites [287-290]. Supplementation with n-3 PUFAs leads to the substitution of AA with EPA and DHA in the cell membrane which can alter immune cell reaction in response to stress stimuli by shifting the metabolic profile to less proinflammatory or even anti-inflammatory metabolite predominance [291-294]. Therefore, increasing n-3 PUFAs, such as EPA and DHA, in the phospholipids has a potential benefit of ameliorating detrimental effects during uncontrolled inflammatory responses [149].

9.5.3.2 N-3 PUFAs have the potential to ameliorate mitochondrial dysfunction in the pathogenesis of COVID-19

Under normal physiological conditions, it is essential for all body organs and physiological systems, particularly the cardiovascular system, to maintain a large number of functional mitochondria to provide energy, as well as preserve and regulate different cellular functions [295]. Maintaining a healthy pool of mitochondria depends upon a delicate balance between the formation of newly generated mitochondria termed as “mitochondrial biogenesis”, to meet the increased energy demand, and the efficient elimination of irreversibly damaged mitochondria through mitophagy [296, 297]. Mitochondrial damage, decreased biogenesis and impaired mitophagy has been implicated in several pathologies including diabetes, CVDs, aging, as well as

viral and bacterial infections [298-302]. While the intrinsic mechanism(s) involved in the pathogenesis of cardiovascular insult secondary to COVID-19 are not fully understood, altered mitochondrial homeostasis could be a major contributing factor [295, 303-305]. Notably, symptoms such as sleep and appetite disturbance, loss of energy, fatigue and muscle weakness, observed in COVID-19 patients, are cardinal signs of mitochondrial distress [306].

Recent studies identified a level of interaction or interplay between mitochondria and innate immune inflammatory responses. Mitochondrial dysfunction is considered both a trigger and target of uncontrolled inflammatory responses [307-309]. As such, this implicates the potential role of impaired mitochondrial homeostasis in the aggravation of cardiovascular injury secondary to COVID-19 [270, 310-312]. Inflammatory mediators are well documented to trigger several intracellular cascades that alter mitochondrial metabolism and function. For example, the pro-inflammatory cytokines TNF- α , IL-1 β and IL-6, found in the serum from COVID-19 patients, can impede mitochondrial oxidative phosphorylation, inhibit ATP production and mitochondrial ROS production exacerbating injury [313, 314]. Furthermore, IFN- γ and IL-6 can increase mitochondrial ROS production and directly affect the activity of the electron transport chain, which may cause mitochondrial membrane permeabilization, altered mitochondrial dynamics and cell death [315].

Conversely, direct mitochondrial damage was found to aggravate the production of proinflammatory cytokines and worsen disease prognosis. Briefly, the pathological changes observed in patients infected with SARS-CoV-2 such as pneumonia, hypoxia and impaired calcium homeostasis can indirectly induce mitochondrial dysfunction. Moreover, a very recent study conducted by Singh et al. interestingly showed both RNA and RNA transcripts of SARS-CoV-2 can directly target and localize to mitochondria hijacking the host cell's mitochondrial

function to viral advantage [316]. Subsequently, SARS-CoV-2 will manipulate the host cell's mitochondrial function to evade removal and facilitate virus replication and progression. These effects lead to the release of mitochondrial DNA and ROS in the cytosol [317-322], which drives the activation and release of central pro-inflammatory cytokines such as NLRP3 inflammasomes, IL-1 β and IL-6 [313, 314, 321, 323], the hallmark cytokines of the COVID-19 severity. Thus, highlighting a vicious cycle of mitochondrial damage and inflammation that has a critical role in aggravating cardiovascular injury. Accordingly, mitochondria are considered a strategic therapeutic target to improve the outcomes in the context of COVID-19.

Numerous studies have demonstrated cardioprotective properties of n-3 PUFA, and their epoxy lipid metabolites, involve an ability to preserve a healthy mitochondrial pool and attenuate exaggerated inflammatory responses under stress conditions. For example, n-3 PUFAs could impart a cardioprotective effect via enriching mitochondrial membrane phospholipid composition, which enhances mitochondrial function promoting efficient ATP generation [324, 325]. In a mouse model of ischemia reperfusion injury, both DHA and its epoxy metabolite, 19,20-EDP, were able to improve postischemic functional recovery by preserving mitochondrial function and attenuating NLRP3 inflammasome response [270]. Moreover, recent data indicates a synthetic EDP analogue imparts cardioprotective effects against ischemia reperfusion injury via preservation of mitochondrial homeostasis and anti-oxidant defenses, which blunted a detrimental innate NLRP3 inflammasome response [326]. Earlier data demonstrated 19,20-EDP protected HL-1 cardiac cells from the bacterial endotoxin, LPS, cell injury by preserving mitochondrial biogenesis and integrity [276]. These data suggest n-3 PUFAs and their metabolites provide beneficial protective responses in models of cardiovascular injury via maintaining mitochondrial

quality and ameliorating detrimental immune responses. However, further research is required to investigate the proposed hypothesis in the context of COVID-19.

9.5.3.3 Direct and indirect effects of n-3 PUFAs on the viral load

Although EPA and DHA have been widely used to ameliorate chronic inflammatory diseases their effect on viral infections remains limited [262, 327-330]. Some evidence indicates EPA, DHA and other dietary unsaturated fatty acids can inactivate viruses by directly causing leakage or lysis of the viral envelopes, which will disrupt the membrane integrity or activate the humoral immune system to produce antibodies against these pathogens [148, 262, 331, 332]. Morita et al. demonstrated n-3 PUFA-derived lipid mediator, protectin D1, exhibits antiviral activity, markedly attenuates influenza A virus replication and improves survival in severe influenza infection in male C57Bl/6J mice. This study highlighted the importance of the endogenous protectin D1 as an innate suppressor of influenza virus replication attenuating lethal infection [259]. In another study, Ramon et al evaluated the ability of 17-HDHA, a SPM derived from DHA, for improving the immune response to H1N1 influenza virus. The results showed 17-HDHA was able to enhance the humoral immunity against viruses by increasing the number of antibody-secreting cells and the levels of H1N1 antibodies, which resulted in greater protection against live H1N1 influenza infection in mice [333]. More recently, Braz-De-Melo highlighted the beneficial effects of n-3 PUFAs against viral infections by showing that DHA pre-treatment to neuroblastoma SH-SY5Y cells infected with Zika virus increased their viability and proliferation, restored mitochondrial function, reduced viral load and triggered an anti-inflammatory response identifying n-3 PUFAs as useful therapeutic tools in combating viruses [334]. Additionally, Yan et al. has shown that EPA and DHA can inhibit the replication of both enterovirus A71 and coxsackievirus A16 the most common causes of hand, foot, and mouth disease [335]. Collectively,

we can conclude that n-3 PUFAs have the capability to attenuate viral infections via both direct effects on membrane integrity and indirect mechanisms activating the humoral response to decrease overall viral load.

In contrast, the immunosuppressive effects of EPA and DHA supplementation can decrease the immune response against viral infections and thus compromising removal from the body. C57BL/6J mice supplemented with fish oil and infected with H1N1 influenza virus showed a 40% higher mortality rate and 70% higher viral load compared to the corresponding control. Moreover, the treated mice had markedly reduced numbers of CD8⁺ T lymphocytes and reduced mRNA expression of inflammatory mediators IL-6 and TNF- α [336]. Similarly, BALB/c mice fed a high-fat diet rich in EPA and DHA had reduced levels of IFN- γ , serum immunoglobulin G and lung immunoglobulin A-specific antibodies following infection with the influenza virus, indicating a virus-specific lung T cell cytotoxicity. These results suggested supplementation with a diet rich in EPA and DHA could impair immune response by delaying virus clearance. However, differences noticed during the course of infection did not affect the ultimate outcome as n-3 PUFA-fed mice were finally able to clear the virus and returned to pre-infection food consumption and body weight similar to the control group [337, 338]. Importantly, other factors contribute to these opposite results, for example, an initial weight loss is typically observed when mice are supplemented with fish oil [337]. In addition, thoroughly controlled animal studies have not been conducted with the SARS-CoV-2 virus and significant variations between viruses should be considered. Therefore, further research is needed to understand the role of EPA and DHA in the immune response related specifically to SARS-CoV-2 viral infections.

9.5.3.4 Role of n-3 PUFAs in modulating the renin-angiotensin aldosterone system in the setting of COVID-19

The renin-angiotensin aldosterone system (RAAS) is a key regulator of vascular function modulating natriuresis, blood volume and blood pressure. Briefly, angiotensin I (Ang I) is metabolized by angiotensin-converting enzyme (ACE) to form the vasoconstrictor angiotensin II (Ang II). Accumulation, prolonged and excessive binding of Ang II to the angiotensin 1 receptor in the heart and blood vessels mediates several effects which include vasoconstriction, hypertension, cardiac hypertrophy, increased ROS production and adverse fibrosis [339, 340]. Accumulating literature demonstrates Ang II may act as a proinflammatory cytokine potentially having a significant role in cardiac remodeling [341, 342]. Conversely, the master regulator ACE2, a type 1 integral membrane glycoprotein expressed in most tissues including the lungs, kidneys, heart and vascular endothelium layers, can metabolize Ang II to produce the vasodilator angiotensin (Ang 1–7) which protects the cardiovascular system against the actions of Ang II [262, 343, 344]. Beside its vasodilatory properties, Ang-(1–7) promotes resolution of inflammation by decreasing TNF- α , IL-6, vascular adhesion molecule, monocyte chemoattractant protein-1 and macrophage infiltration enhancing the survival of cardiomyocytes and endothelial cells during severe immune responses [345, 346]. Accordingly, several clinical and experimental studies reported dysregulation of RAAS due to increased Ang II and decreased ACE2 can lead to detrimental inflammatory responses and worsening of cardiovascular disorders. Therefore, maintaining the activity of ACE2 is essential in preserving the balance of the RAAS and effects on vasoconstriction, sodium retention and fibrosis and may elicit protective effects against hypertension, HF, MI and other CVDs [43, 347, 348].

Recent evidence has demonstrated SARS-CoV-2 uses ACE2 as an internalization receptor to enter the target cells. The spike (S) glycoprotein of SARS-CoV-2 recognizes and interacts with its target ACE2 receptor on the host cell surface, mediating viral entry during the infection cycle [343, 349]. Excessive binding of spike protein to ACE2 leads to downregulation of the ACE2 receptor [350]. This finding is consistent with reports in the animal models infected with SARS-CoV [348, 351, 352]. The reduction in ACE2 levels leads to excessive pro-inflammatory responses adversely affecting both lung and cardiovascular systems [348, 351, 352]. These detrimental effects can be explained as the partial decrease in ACE2 function leads to dominant angiotensin II effects, including augmented cytokine storm, inflammation, vasoconstriction and susceptibility for thrombosis. These effects further increase the cardiovascular burden by worsening hypertension, HF and other cardiovascular disorders in predisposed patients [41, 353]. Importantly, the accumulation of Ang II was positively associated to viral load and lung injury [354]. Moreover, reduction in the activity and/or number of ACE2 leads to deficiency of Ang-(1–7) production and consequently loss of its anti-inflammatory, vasodilatory, and cardiovascular protective effects [43, 355]. Therefore, it is hypothesized that inhibition of RAAS may be helpful to attenuate the inflammatory storm and ameliorate end-organ damage. Interestingly, recent data indicates individuals with COVID-19 who are being treated with ACE inhibitors or ARBs, for pre-existing conditions, are at lower risk of 28-day all-cause mortality than those not treated with ACE inhibitors or ARBs [91, 356]. Although ARBs and ACE inhibitors do not directly impact ACE2, they indirectly elevate ACE2 activity and the beneficial Ang-(1–7) production and counter the excessive production of the harmful Ang II [357]. Therefore, it was proposed that maintaining the levels of ACE2 and its downstream effector Ang-(1–7) may limit cardiovascular damage secondary to COVID-19 [356].

Interestingly, several reports showed that n-3 PUFAs can regulate the RAAS system by modulating both Ang II and ACE2 levels. For instance, emerging literature indicates n-3 PUFAs and their endogenously generated metabolites can directly reduce the expression and activity of ACE, thereby reducing angiotensin II formation and cardiovascular burden [344]. Moreover, it has been demonstrated that supplementation of mice with an n-3 PUFA rich diet for three weeks resulted in attenuated Ang-II-induced blood pressure via up-regulation of ACE2 [358]. Alternatively, as previously discussed, incorporation of n-3 PUFAs into the cell membranes will alter key properties, which can consequently affect protein number and affinity of SARS-CoV-2 to ACE2 [359-362]. Together, these studies suggest a novel role for n-3 PUFAs in regulating SARS-CoV-2 infection where the potential benefit as an adjuvant therapy involves increasing the production of Ang-(1–7) and reducing the levels of Ang II, thereby limiting COVID-19-triggered cardiovascular complications.

Importantly, upregulation of ACE2 expression and enhanced activity suggested it will facilitate the infectivity of SARS-CoV-2 [363]. Accordingly, some researchers proposed that ACE inhibitors and ARBs should be discontinued in COVID-19 patients [364, 365]. However, in addition to the direct effects on cardiac ACE2 other mechanisms such as triggering a cytokine storm will markedly contribute SARS-CoV-2-induced injury [366]. A recent study conducted by Yanget al., demonstrated COVID-19 patients with hypertension using ACE inhibitors/ARBs had lower mortality rates than hypertensive COVID-19 patients that were not on ACE inhibitors/ARBs [367]. Moreover, Mancia et al. examined 6272 patients and found no association between RAAS inhibitor use and susceptibility or development of COVID-19 [368]. In that sense, a published statement by American Heart Association (AHA), the American College of Cardiology (ACC) and the Heart Failure Society of America strongly recommended continuation of ACE inhibitor/ARBs

[91]. Together, these data suggest therapies targeting ACE and Ang II do not appear to increase the likelihood of SARS-CoV-2 infection, but may have a role in abrogating the inflammatory response and vasoconstriction that contributes to the clinical deterioration in COVID-19 patients.

In summary, evidence has demonstrated infection with SARS-CoV-2 induces internalization and downregulation of ACE2, which may aggravate a patient's condition by limiting the degradation of Ang II. Elevated Ang II levels induce several detrimental effects on the cardiovascular system including elevated blood pressure, excessive recruitment and infiltration of inflammatory immune cells to the heart as well as increased secretion of pro-inflammatory cytokines. Reduced ACE2 levels are associated with decreased formation of Ang-(1–7) and thus loss of its vasodilatory, anti-inflammatory and CVD-protective effects. Therefore, intervention with treatments to correct an imbalance in the RAAS system, such as ACE inhibitors, ARBs and n-3 PUFAs, can possibly improve the outcomes.

9.5.3.5 N-3 PUFAs possess anti-oxidant properties

The pneumonia-induced hypoxemia caused by RNA virus infections reduces the energy production from cell metabolism, increases the anaerobic fermentation, intracellular acidosis and the generation of ROS [369]. The subsequent increased ROS production causes damage to different cellular components including the DNA, lipids and proteins. The increased ROS levels will deplete the antioxidant defense system resulting in severe oxidative stress and chronic activation of immune responses, aggravating tissue injury and damage [370, 371].

Several studies reveal n-3 PUFAs possess anti-oxidant properties attributable to their ability to up-regulate anti-oxidant enzymes (e.g. superoxide dismutase), down-regulate pro-oxidant enzymes (e.g. nitric oxide synthase) and potential to interact directly with free radicals.

Antioxidant effects of n-3 PUFAs have been demonstrated in different organs including lungs, kidneys and the cardiovascular system [270, 310, 326, 372, 373]. Anderson et al. reported patients were administered a moderately high dose of n-3 PUFAs (3.4 g/day EPA and DHA ethyl-esters) for a period of 2–3 weeks before having elective cardiac surgery and then myocardial tissue was dissected from the right atrium during surgery. Intriguingly, myocardial tissues obtained from patients displayed improved antioxidant capacity attributed to increased expression and activity of key antioxidants such as glutathione peroxidase-1, glutathione peroxidase-4, NADPH-quinone oxidoreductase-1, thioredoxin reductase-2 and total glutathione compared to the control patients. Moreover, the mitochondrial outer membrane-bound enzyme monoamine oxidase, a substantial generator of ROS, was also determined to have significantly lower activity in myocardial tissue obtained from n-3 PUFA-treated patients [374]. Interestingly, isolated mouse hearts perfused with DHA derived epoxy lipids had improved postischemic recovery which correlated with better activities of the antioxidants thioredoxin -1 and thioredoxin-2 [270]. Importantly, with COVID-19, especially in advanced stages and in ICU, severe inflammation, hypoxemia and mechanical ventilation with high oxygen concentrations will inevitably increase ROS generation locally and systemically notably within the lungs and the heart. Thus, it can be hypothesized that increased n-3 PUFAs and their corresponding metabolites would provide beneficial control of exaggerated inflammation and ROS production.

9.5.3.6 N-3 PUFAs have the potential to ameliorate coagulopathy

Laboratory examinations from COVID-19 patients indicate serious coagulopathy has occurred in some individuals. This is reflected by widespread microvascular thrombosis and consumption of coagulation factors as evidenced by markers such as thrombocytopenia, prolongation of the prothrombin, elevation of D-dimer, increased fibrin degradation product levels

and decreased fibrinogen levels [81]. In a study with 184 Dutch ICU COVID-19 patients, 38% were reported to have abnormal blood clotting and 33% with identified clots [80]. Importantly, blood clots may cause lung emboli, cardiovascular complications or stroke. In addition, long-term bed rest has been linked to increased risk of venous thromboembolism in severe SARS-CoV-2 infected patients [375, 376]. Accordingly, the active application of anticoagulants (such as heparin) for patients with severe SARS-CoV-2 infection has been recommended and appears to be associated with better prognosis [81]. Tang et al. recently published a study indicating anticoagulant therapy, mainly with low molecular weight heparin, is associated with better prognosis in severe SARS-CoV-2 infected patients [81].

N-3 PUFAs contain polar lipids that exhibit potent antithrombotic effects against platelet-activating factor and other prothrombotic pathways, including thrombin, collagen, and adenosine diphosphate [149, 377, 378]. Increased levels of n-3 PUFAs may alter platelet phospholipid membrane composition and affect platelet function, which can be predicted to alter the progression and thrombotic complications of CVD. Adili et al. outlined that EPA and DHA act on the platelet membrane to reduce platelet aggregation and TX release via COX-1 and 12-LOX, which metabolize fatty acids into a group of beneficial oxylipins in platelets that contribute significantly to the regulation of platelet function in hemostasis and thrombosis. [379]. This is supported by Park and Harris who demonstrated healthy subjects supplemented with EPA for 4 weeks had reduced platelet activation, an early step in platelet aggregation [380]. While the evidence is limited, it appears EPA is more active than DHA in altering platelet function because it is a COX substrate. However, DHA appears to decrease TXA₂ and PGH₂ receptor affinity [380]. Although dietary supplementation of EPA and DHA has been shown to reduce platelet activation and aggregation in healthy subjects, a higher recommended dose of n-3 PUFAs may be needed in

platelet hyperactivity prothrombotic conditions such as in CVD [379]. These anticoagulant properties of n-3 PUFAs suggest potential effects on the platelet aggregation in severe cases of SARS-CoV-2 infected subjects. Our current level of knowledge only permits speculation on whether n-3 PUFAs can mitigate the coagulopathy associated with severe COVID-19.

9.5.3.7 Lipid-lowering properties of n-3 PUFAs in the context of COVID-19

Patients with comorbidities such as diabetes, dyslipidemia, aberrations in plasma cholesterol and triglycerides and coronary heart disease are more susceptible to severe COVID-19 outcomes such as cardiac complications, sepsis, ARDS and death [6, 33, 34, 381, 382]. The acute inflammatory syndrome associated with COVID-19 has the capacity to destabilize plaques, which can lead to ischemic events [77]. Recent studies indicated serum triglyceride concentrations were significantly higher in individuals who died as a result of COVID-19 likely due to augmented inflammatory TNF- α levels causing reduced lipoprotein lipase activity [382, 383]. Triglyceride-glucose index, a product of fasting triglyceride and fasting plasma glucose levels, is used as a surrogate marker for insulin resistance [384]. COVID-19 patients with a higher triglyceride-glucose index have been shown to experience more severe COVID-19 infection and death. Furthermore, levels of high density lipoprotein cholesterol (HDL-c) are also reduced in COVID-19 patients with the magnitude of reduction correlating with disease severity [385]. Generally, HDL-c is considered to be anti-inflammatory and antithrombotic [386, 387]. So, the robust, maladaptive inflammatory and hypercoagulability responses observed in more severe COVID-19 cases could possibly be attributed— in part – to reduced levels of HLD-c and a dysregulated lipid profile. Given the potential for COVID-19 infection to alter the lipid profile acutely and the association of dyslipidemia with conditions such as diabetes, coronary artery disease, and obesity

raises the question whether normalization of plasma lipid profiles in COVID-19 patients can offer clinical benefit.

Use of statins and other lipid-modulating therapies can reduce the risk of primary or secondary cardiovascular events in at-risk individuals, including those with diabetes, metabolic syndrome, and coronary artery disease – conditions that are risk factors for severe COVID-19 outcomes [388]. A large retrospective study of over 13,000 COVID-19 patients has shown the in-hospital use of statin therapy, potent lipid-lowering agents with anti-inflammatory properties, was associated with a reduced rate of mortality compared to non-statin users [84]. This important study disrupts the previous dogma that statins may enhance the COVID-19 virus pathology via ACE2 expression and may in fact be overwhelmingly beneficial in the treatment of COVID-19. However, despite statin monotherapy, many patients with dyslipidemia still suffer from persistently elevated triglyceride levels which may continue to be a risk factor for coronary artery disease, cardiac events and more severe COVID-19 infection outcomes [389, 390]. The triglyceride-lowering effect of n-3 PUFA supplementation has been demonstrated in a plethora of clinical trials [390-395]. Lower levels of triglycerides present a lower risk of developing a cytokine storm based on the score from the available secondary haemophagocytic lymphohistiocytosis score system [113]. Additionally, n-3 PUFAs have been shown to significantly lower CRP in patients with hypertriglyceridemia [390]. Thus, the rationale for the use of n-3 PUFAs in COVID-19 patients not only focuses on the attenuation of the infection-induced respiratory disorders but also on an overall improvement of patients' wellbeing and prevention of potential complications due to comorbidities.

9.5.4 When and how to intervene with n-3 PUFAs in the context of COVID-19

An important aspect in considering n-3 PUFAs as adjunctive therapy in critically or severe ill patients is the time of intervention, duration of treatment, dose, composition of the preparation and route of administration. The type and intensity of supportive treatment required by a patient is dependent upon the severity of disease and the possible need for hospitalization. Existing literature demonstrates it may take weeks or months for standard doses of n-3 PUFAs to exert a biological effect due to a gradual replacement of membrane AA. It has been hypothesized the acute supplementation with n-3 PUFAs may influence the inflammatory response in critically ill patients, particularly those with ALI [396]. For example, a randomized clinical trial showed daily enteral feeding of critically ill ALI patients with elevated levels EPA, DHA and gamma-linolenic acid significantly reduced lung inflammation and improved oxygenation by 4 days. This was associated with a decreased duration of mechanical ventilation, ICU length of stay and mortality [134, 397]. In a trial conducted by Pontes-Arruda et al. who studied patients with sepsis requiring mechanical ventilation, a diet enriched with EPA, gamma-linolenic acid and antioxidants delivered at a constant rate during a minimum of 4 days contributed to better ICU and hospital outcomes, oxygenation status, ventilator-free days and was associated with lower mortality at 28-day interval [141].

There are many studies suggesting the beneficial effects of parenteral fish oil emulsions in critically ill patients. For example, parenteral supplementation of severe ill patients with lipid emulsions containing fish oil was associated with reduced inflammation, improved gas exchange and shorter length of ICU and hospital stay [398]. In a study by Mayer et al., patients with sepsis were randomized in an open-label trial to receive an omega-3 FA rich lipid emulsion or a standard omega-6 rich lipid emulsion for 5 days. Within 2 days of fish oil infusion, free n-3 fatty acids

increased and the n-3/n-6 ratio was reversed favoring EPA and DHA over AA, with rapid incorporation of n-3 fatty acids into mononuclear leukocyte membranes and reaching maximum effect in 3 days [399]. Furthermore, a parenteral lipid emulsion enriched in n-3 PUFA for 7 days was found to reduce acetic acid-induced colitis in rats [400]. In a randomized controlled trial conducted by Wang et al., patients with severe acute pancreatitis were randomly assigned to receive parenteral nutrition for 5 days containing similar amounts of amino acids, glucose and fat but different lipid compositions: the control group received a soybean oil-based fat solution and the omega-3 group received fish oil. Interestingly, patients treated with the fish oil or n-3 PUFAs had a markedly lower inflammatory marker CRP and better oxygenation index after 5 days of parenteral nutrition [401].

Together, these studies demonstrated that acute enteral or parenteral administration of n-3 PUFAs in the setting of severe illness could significantly improve the clinical outcomes. Notably, it has been shown that fish oil emulsions containing substantial amounts of EPA and DHA have an excellent safety record in both critically ill adults and children [402-404] making them a suitable candidate for use in severe stress conditions as in COVID-19 patients. However, with the research that has been completed to date, it is not possible to definitively determine the dose, route of administration and the best timing to intervene with n-3 PUFAs in the setting of COVID-19. More research is undoubtedly needed before definitive recommendations about the routine use of n-3 PUFAs in the context of COVID-19 can be made particularly that dosing data and pharmacokinetics studies of both enteral and parenteral n-3 PUFAs in critically ill patients are highly variable and incomplete.

9.6 Summary and conclusion

To summarize, COVID-19 is rapidly spreading around the globe and our understanding of the virus is limited. To date, there is no effective, approved therapy or vaccination to treat the disease or protect against its complications. Although the lungs are considered the main target organ of SARS-CoV-2, the virus can affect many other organs, leading to multiple organ damage. Cardiovascular injury has been noted as a protruding clinical feature in COVID-19 patients. The dysregulation of RAAS can lead to a harmful inflammatory response and worsening of cardiovascular consequences in patients with COVID-19. Therefore, intervention with drugs that counteract Ang II may have a potential role in preventing the deleterious cardiovascular outcomes. Although increased ACE2 levels may raise the concern of increased SARS-CoV-2 infectivity, we propose here that n-3 PUFAs may be beneficial rather than harmful for cardiovascular outcomes in COVID-19 patients by limiting Ang II-induced detrimental signaling and enhancing Ang (1-7) cardioprotective effects.

In this review we highlight the different mechanisms of cardiovascular complications secondary to COVID-19 and draw attention toward the potential roles n-3 PUFAs in mitigating these cardiovascular complications. Currently, there is no direct evidence of any beneficial or deleterious effect of n-3 PUFAs in COVID-19 patients. However, it is evident from the preceding discussion the dietary or non-dietary intake of n-3 PUFAs and/or their biologically active metabolites have many beneficial actions leading to prevention and management of cardiovascular complications. N-3 PUFAs and/or their biologically active metabolites have the potential to modulate many of the adverse effects of an exaggerated immune response, inactivate enveloped viruses, enhance macrophage phagocytic capacity, ameliorate coagulopathy, modify cell signaling and gene expression, shift the pattern of the lipid metabolites produced under stress conditions to

a more anti-inflammatory metabolite profile and enhance the anti-oxidative capacity of the heart. Despite these promising effects of n-3 PUFAs, more experimental, randomized control trials and epidemiological research is warranted to test and translate these proposed effects in the setting of SARS-CoV-2 infection.

References

1. Zaki, A.M., et al., *Isolation of a novel coronavirus from a man with pneumonia in Saudi Arabia*. N Engl J Med, 2012. **367**(19): p. 1814-20.
2. de Wit, E., et al., *SARS and MERS: recent insights into emerging coronaviruses*. Nat Rev Microbiol, 2016. **14**(8): p. 523-34.
3. Ren, L.L., et al., *Identification of a novel coronavirus causing severe pneumonia in human: a descriptive study*. Chin Med J (Engl), 2020. **133**(9): p. 1015-1024.
4. Coronaviridae Study Group of the International Committee on Taxonomy of, V., *The species Severe acute respiratory syndrome-related coronavirus: classifying 2019-nCoV and naming it SARS-CoV-2*. Nat Microbiol, 2020. **5**(4): p. 536-544.
5. Zhou, P., et al., *A pneumonia outbreak associated with a new coronavirus of probable bat origin*. Nature, 2020. **579**(7798): p. 270-273.
6. Wang, D., et al., *Clinical Characteristics of 138 Hospitalized Patients With 2019 Novel Coronavirus-Infected Pneumonia in Wuhan, China*. JAMA, 2020.
7. <https://coronavirus.jhu.edu/map.html>, J.H.U., *COVID-19 dashboard by the Center for Systems Science and Engineering (CSSE) at Johns Hopkins*. August 12th, 2020.
8. Cui, J., F. Li, and Z.L. Shi, *Origin and evolution of pathogenic coronaviruses*. Nat Rev Microbiol, 2019. **17**(3): p. 181-192.
9. Wadman, M., et al., *A rampage through the body*. Science, 2020. **368**(6489): p. 356-360.
10. Huang, C., et al., *Clinical features of patients infected with 2019 novel coronavirus in Wuhan, China*. Lancet, 2020. **395**(10223): p. 497-506.
11. Chen, N., et al., *Epidemiological and clinical characteristics of 99 cases of 2019 novel coronavirus pneumonia in Wuhan, China: a descriptive study*. Lancet, 2020. **395**(10223): p. 507-513.
12. Wu, Z. and J.M. McGoogan, *Characteristics of and Important Lessons From the Coronavirus Disease 2019 (COVID-19) Outbreak in China: Summary of a Report of 72314 Cases From the Chinese Center for Disease Control and Prevention*. JAMA, 2020.
13. Wang, J.Z., R.Y. Zhang, and J. Bai, *An anti-oxidative therapy for ameliorating cardiac injuries of critically ill COVID-19-infected patients*. Int J Cardiol, 2020. **312**: p. 137-138.

14. Zhang, R., et al., *COVID-19: Melatonin as a potential adjuvant treatment*. Life Sci, 2020. **250**: p. 117583.
15. Rizk, J.G., et al., *Pharmaco-Immunomodulatory Therapy in COVID-19*. Drugs, 2020. **80**(13): p. 1267-1292.
16. Akhmerov, A. and E. Marban, *COVID-19 and the Heart*. Circ Res, 2020. **126**(10): p. 1443-1455.
17. Hendren, N.S., et al., *Description and Proposed Management of the Acute COVID-19 Cardiovascular Syndrome*. Circulation, 2020. **141**(23): p. 1903-1914.
18. Convertino, I., et al., *Exploring pharmacological approaches for managing cytokine storm associated with pneumonia and acute respiratory distress syndrome in COVID-19 patients*. Crit Care, 2020. **24**(1): p. 331.
19. Richardson, P., et al., *Baricitinib as potential treatment for 2019-nCoV acute respiratory disease*. Lancet, 2020. **395**(10223): p. e30-e31.
20. Alijotas-Reig, J., et al., *Immunomodulatory therapy for the management of severe COVID-19. Beyond the anti-viral therapy: A comprehensive review*. Autoimmun Rev, 2020. **19**(7): p. 102569.
21. Guglielmetti, G., et al., *"War to the knife" against thromboinflammation to protect endothelial function of COVID-19 patients*. Crit Care, 2020. **24**(1): p. 365.
22. De Flora, S., R. Balansky, and S. La Maestra, *Rationale for the use of N-acetylcysteine in both prevention and adjuvant therapy of COVID-19*. FASEB J, 2020.
23. Hammock, B.D., et al., *Eicosanoids: The Overlooked Storm in Coronavirus Disease 2019 (COVID-19)?* Am J Pathol, 2020. **190**(9): p. 1782-1788.
24. Cilli, A., et al., *Acute cardiac events in severe community-acquired pneumonia: A multicenter study*. Clin Respir J, 2018. **12**(7): p. 2212-2219.
25. Corrales-Medina, V.F., et al., *Cardiac complications in patients with community-acquired pneumonia: a systematic review and meta-analysis of observational studies*. PLoS Med, 2011. **8**(6): p. e1001048.
26. Corrales-Medina, V.F., et al., *Association between hospitalization for pneumonia and subsequent risk of cardiovascular disease*. JAMA, 2015. **313**(3): p. 264-74.

27. Corrales-Medina, V.F., et al., *Cardiac complications in patients with community-acquired pneumonia: incidence, timing, risk factors, and association with short-term mortality*. *Circulation*, 2012. **125**(6): p. 773-81.
28. Viasus, D., et al., *Risk stratification and prognosis of acute cardiac events in hospitalized adults with community-acquired pneumonia*. *J Infect*, 2013. **66**(1): p. 27-33.
29. Yu, C.M., et al., *Cardiovascular complications of severe acute respiratory syndrome*. *Postgrad Med J*, 2006. **82**(964): p. 140-4.
30. Li, S.S., et al., *Left ventricular performance in patients with severe acute respiratory syndrome: a 30-day echocardiographic follow-up study*. *Circulation*, 2003. **108**(15): p. 1798-803.
31. Alhogbani, T., *Acute myocarditis associated with novel Middle east respiratory syndrome coronavirus*. *Ann Saudi Med*, 2016. **36**(1): p. 78-80.
32. Zheng, Y.Y., et al., *COVID-19 and the cardiovascular system*. *Nat Rev Cardiol*, 2020. **17**(5): p. 259-260.
33. Zhou, F., et al., *Clinical course and risk factors for mortality of adult inpatients with COVID-19 in Wuhan, China: a retrospective cohort study*. *Lancet*, 2020. **395**(10229): p. 1054-1062.
34. Shi, S., et al., *Association of Cardiac Injury With Mortality in Hospitalized Patients With COVID-19 in Wuhan, China*. *JAMA Cardiol*, 2020.
35. Guo, T., et al., *Cardiovascular Implications of Fatal Outcomes of Patients With Coronavirus Disease 2019 (COVID-19)*. *JAMA Cardiol*, 2020.
36. Epidemiology Working Group for Ncip Epidemic Response, C.C.f.D.C. and Prevention, *[The epidemiological characteristics of an outbreak of 2019 novel coronavirus diseases (COVID-19) in China]*. *Zhonghua Liu Xing Bing Xue Za Zhi*, 2020. **41**(2): p. 145-151.
37. Inciardi, R.M., et al., *Cardiac Involvement in a Patient With Coronavirus Disease 2019 (COVID-19)*. *JAMA Cardiol*, 2020.
38. Guan, W.J., et al., *Clinical Characteristics of Coronavirus Disease 2019 in China*. *N Engl J Med*, 2020. **382**(18): p. 1708-1720.
39. Xu, Z., et al., *Pathological findings of COVID-19 associated with acute respiratory distress syndrome*. *Lancet Respir Med*, 2020. **8**(4): p. 420-422.

40. Mohammad Madjid, S.D.S., Orly Vardeny, Thomas M. Maddox, Eric C. Stecker, Biykem Bozkurt, Nathalie DeMichelis, John U. Doherty, Andrew Freeman, Ty Gluckman, Dipti Itchhaporia, Andrew P. Miller, Andrea L. Price, Lonny Reisman, Prem Soman, *Acc Clinical Bulletin: Cardiac Implications of Novel Wuhan Coronavirus (2019-ncov)*. American College of Cardiology, 2020.
41. Oudit, G.Y., et al., *SARS-coronavirus modulation of myocardial ACE2 expression and inflammation in patients with SARS*. *Eur J Clin Invest*, 2009. **39**(7): p. 618-25.
42. Gheblawi, M., et al., *Angiotensin-Converting Enzyme 2: SARS-CoV-2 Receptor and Regulator of the Renin-Angiotensin System: Celebrating the 20th Anniversary of the Discovery of ACE2*. *Circ Res*, 2020. **126**(10): p. 1456-1474.
43. Patel, V.B., et al., *Role of the ACE2/Angiotensin 1-7 Axis of the Renin-Angiotensin System in Heart Failure*. *Circ Res*, 2016. **118**(8): p. 1313-26.
44. Hoffmann, M., et al., *SARS-CoV-2 Cell Entry Depends on ACE2 and TMPRSS2 and Is Blocked by a Clinically Proven Protease Inhibitor*. *Cell*, 2020. **181**(2): p. 271-280 e8.
45. Wu, F., et al., *A new coronavirus associated with human respiratory disease in China*. *Nature*, 2020. **579**(7798): p. 265-269.
46. Restrepo, M.I. and L.F. Reyes, *Pneumonia as a cardiovascular disease*. *Respirology*, 2018. **23**(3): p. 250-259.
47. Zumla, A., et al., *Reducing mortality from 2019-nCoV: host-directed therapies should be an option*. *Lancet*, 2020. **395**(10224): p. e35-e36.
48. Zhang, W., et al., *The use of anti-inflammatory drugs in the treatment of people with severe coronavirus disease 2019 (COVID-19): The Perspectives of clinical immunologists from China*. *Clin Immunol*, 2020. **214**: p. 108393.
49. Conti, P., et al., *Induction of pro-inflammatory cytokines (IL-1 and IL-6) and lung inflammation by Coronavirus-19 (COVI-19 or SARS-CoV-2): anti-inflammatory strategies*. *J Biol Regul Homeost Agents*, 2020. **34**(2).
50. Channappanavar, R., et al., *Dysregulated Type I Interferon and Inflammatory Monocyte-Macrophage Responses Cause Lethal Pneumonia in SARS-CoV-Infected Mice*. *Cell Host Microbe*, 2016. **19**(2): p. 181-93.
51. ChiCTR2000029765, *A multicenter, randomized controlled trial for the efficacy and safety of tocilizumab in the treatment of new coronavirus pneumonia (COVID-19)*. <http://www.chictr.org.cn/showprojen.aspx?proj=49409>, 2020.

52. Biran, N., et al., *Tocilizumab among patients with COVID-19 in the intensive care unit: a multicentre observational study*. *Lancet Rheumatol*, 2020.
53. Xu, X., et al., *Effective treatment of severe COVID-19 patients with tocilizumab*. *Proc Natl Acad Sci U S A*, 2020. **117**(20): p. 10970-10975.
54. Ramiro, S., et al., *Historically controlled comparison of glucocorticoids with or without tocilizumab versus supportive care only in patients with COVID-19-associated cytokine storm syndrome: results of the CHIC study*. *Annals of the Rheumatic Diseases* 2020(79): p. 1143-1151.
55. Cao, Y., et al., *Ruxolitinib in treatment of severe coronavirus disease 2019 (COVID-19): A multicenter, single-blind, randomized controlled trial*. *J Allergy Clin Immunol*, 2020. **146**(1): p. 137-146 e3.
56. Aouba, A., et al., *Targeting the inflammatory cascade with anakinra in moderate to severe COVID-19 pneumonia: case series*. *Ann Rheum Dis*, 2020. **79**(10): p. 1381-1382.
57. Huet, T., et al., *Anakinra for severe forms of COVID-19: a cohort study*. *Lancet Rheumatol*, 2020. **2**(7): p. e393-e400.
58. Li, G., et al., *Coronavirus infections and immune responses*. *J Med Virol*, 2020. **92**(4): p. 424-432.
59. Akira, S., *Pathogen recognition by innate immunity and its signaling*. *Proc Jpn Acad Ser B Phys Biol Sci*, 2009. **85**(4): p. 143-56.
60. Siu, K.L., et al., *Severe acute respiratory syndrome coronavirus ORF3a protein activates the NLRP3 inflammasome by promoting TRAF3-dependent ubiquitination of ASC*. *FASEB J*, 2019. **33**(8): p. 8865-8877.
61. Chen, I.Y., et al., *Severe Acute Respiratory Syndrome Coronavirus Viroporin 3a Activates the NLRP3 Inflammasome*. *Front Microbiol*, 2019. **10**: p. 50.
62. Elliott, E.I. and F.S. Sutterwala, *Initiation and perpetuation of NLRP3 inflammasome activation and assembly*. *Immunol Rev*, 2015. **265**(1): p. 35-52.
63. Latz, E., T.S. Xiao, and A. Stutz, *Activation and regulation of the inflammasomes*. *Nat Rev Immunol*, 2013. **13**(6): p. 397-411.
64. Yue, Y., et al., *SARS-Coronavirus Open Reading Frame-3a drives multimodal necrotic cell death*. *Cell Death Dis*, 2018. **9**(9): p. 904.

65. Libby, P., P.M. Ridker, and A. Maseri, *Inflammation and atherosclerosis*. *Circulation*, 2002. **105**(9): p. 1135-43.
66. Siddiqi, H.K. and M.R. Mehra, *COVID-19 illness in native and immunosuppressed states: A clinical-therapeutic staging proposal*. *J Heart Lung Transplant*, 2020. **39**(5): p. 405-407.
67. Janczewski, A.M., et al., *Morphological and functional changes in cardiac myocytes isolated from mice overexpressing TNF-alpha*. *Am J Physiol Heart Circ Physiol*, 2003. **284**(3): p. H960-9.
68. Dibbs, Z.I., et al., *Targeted overexpression of transmembrane tumor necrosis factor provokes a concentric cardiac hypertrophic phenotype*. *Circulation*, 2003. **108**(8): p. 1002-8.
69. Aromolaran, A.S., et al., *Interleukin-6 inhibition of hERG underlies risk for acquired long QT in cardiac and systemic inflammation*. *PLoS One*, 2018. **13**(12): p. e0208321.
70. Fanola, C.L., et al., *Interleukin-6 and the Risk of Adverse Outcomes in Patients After an Acute Coronary Syndrome: Observations From the SOLID-TIMI 52 (Stabilization of Plaque Using Darapladib-Thrombolysis in Myocardial Infarction 52) Trial*. *J Am Heart Assoc*, 2017. **6**(10).
71. Held, C., et al., *Inflammatory Biomarkers Interleukin-6 and C-Reactive Protein and Outcomes in Stable Coronary Heart Disease: Experiences From the STABILITY (Stabilization of Atherosclerotic Plaque by Initiation of Darapladib Therapy) Trial*. *J Am Heart Assoc*, 2017. **6**(10).
72. Cavusoglu, E., et al., *Elevated baseline plasma IL-8 levels are an independent predictor of long-term all-cause mortality in patients with acute coronary syndrome*. *Atherosclerosis*, 2015. **242**(2): p. 589-94.
73. Goldstein, D.R., *Aging, imbalanced inflammation and viral infection*. *Virulence*, 2010. **1**(4): p. 295-8.
74. Lawrence, T. and D.W. Gilroy, *Chronic inflammation: a failure of resolution?* *Int J Exp Pathol*, 2007. **88**(2): p. 85-94.
75. Bruunsgaard, H. and B.K. Pedersen, *Age-related inflammatory cytokines and disease*. *Immunol Allergy Clin North Am*, 2003. **23**(1): p. 15-39.
76. Rius, B., et al., *Resolution of inflammation in obesity-induced liver disease*. *Front Immunol*, 2012. **3**: p. 257.

77. Madjid, M., et al., *Systemic infections cause exaggerated local inflammation in atherosclerotic coronary arteries: clues to the triggering effect of acute infections on acute coronary syndromes*. *Tex Heart Inst J*, 2007. **34**(1): p. 11-8.
78. Modica, A., F. Karlsson, and T. Mooe, *Platelet aggregation and aspirin non-responsiveness increase when an acute coronary syndrome is complicated by an infection*. *J Thromb Haemost*, 2007. **5**(3): p. 507-11.
79. Milbrandt, E.B., et al., *Prevalence and significance of coagulation abnormalities in community-acquired pneumonia*. *Mol Med*, 2009. **15**(11-12): p. 438-45.
80. Klok, F.A., et al., *Incidence of thrombotic complications in critically ill ICU patients with COVID-19*. *Thromb Res*, 2020. **191**: p. 145-147.
81. Tang, N., et al., *Anticoagulant treatment is associated with decreased mortality in severe coronavirus disease 2019 patients with coagulopathy*. *J Thromb Haemost*, 2020. **18**(5): p. 1094-1099.
82. Viecca, M., et al., *Enhanced platelet inhibition treatment improves hypoxemia in patients with severe Covid-19 and hypercoagulability. A case control, proof of concept study*. *Pharmacol Res*, 2020. **158**: p. 104950.
83. Wu, Q., et al., *Altered Lipid Metabolism in Recovered SARS Patients Twelve Years after Infection*. *Sci Rep*, 2017. **7**(1): p. 9110.
84. Zhang, X.J., et al., *In-Hospital Use of Statins Is Associated with a Reduced Risk of Mortality among Individuals with COVID-19*. *Cell Metab*, 2020.
85. Moccia, F., et al., *COVID-19-associated cardiovascular morbidity in older adults: a position paper from the Italian Society of Cardiovascular Researches*. *Geroscience*, 2020.
86. Corrales-Medina, V.F., et al., *Acute pneumonia and the cardiovascular system*. *Lancet*, 2013. **381**(9865): p. 496-505.
87. Dreyfuss, D., et al., *Acute infectious pneumonia is accompanied by a latent vasopressin-dependent impairment of renal water excretion*. *Am Rev Respir Dis*, 1988. **138**(3): p. 583-9.
88. Benson, H., et al., *Hemodynamic effects of pneumonia. I. Normal and hypodynamic responses*. *J Clin Invest*, 1970. **49**(4): p. 791-8.
89. Kumar, R., et al., *Hemodynamic effects of pneumonia. II. Expansion of plasma volume*. *J Clin Invest*, 1970. **49**(4): p. 799-805.

90. Deftereos, S.G., et al., *Effect of Colchicine vs Standard Care on Cardiac and Inflammatory Biomarkers and Clinical Outcomes in Patients Hospitalized With Coronavirus Disease 2019: The GRECCO-19 Randomized Clinical Trial*. JAMA Netw Open, 2020. **3**(6): p. e2013136.
91. Zhang, P., et al., *Association of Inpatient Use of Angiotensin-Converting Enzyme Inhibitors and Angiotensin II Receptor Blockers With Mortality Among Patients With Hypertension Hospitalized With COVID-19*. Circ Res, 2020. **126**(12): p. 1671-1681.
92. Lala, A., et al., *Prevalence and Impact of Myocardial Injury in Patients Hospitalized With COVID-19 Infection*. J Am Coll Cardiol, 2020. **76**(5): p. 533-546.
93. NCT04393246, *mulTi-Arm Therapeutic Study in Pre-ICu Patients Admitted With Covid-19 - Experimental Drugs and Mechanisms*. <https://clinicaltrials.gov/ct2/show/NCT04393246>, 2020.
94. Liu, F., et al., *Intravenous high-dose vitamin C for the treatment of severe COVID-19: study protocol for a multicentre randomised controlled trial*. BMJ Open, 2020. **10**(7): p. e039519.
95. Rilinger, J., et al., *A prospective, randomised, double blind placebo-controlled trial to evaluate the efficacy and safety of tocilizumab in patients with severe COVID-19 pneumonia (TOC-COVID): A structured summary of a study protocol for a randomised controlled trial*. Trials, 2020. **21**(1): p. 470.
96. Kulkarni, S., et al., *Repurposed immunomodulatory drugs for Covid-19 in pre-ICu patients - mulTi-Arm Therapeutic study in pre-ICu patients admitted with Covid-19 - Repurposed Drugs (TACTIC-R): A structured summary of a study protocol for a randomised controlled trial*. Trials, 2020. **21**(1): p. 626.
97. Stockmann, H., et al., *CytoResc - "CytoSorb" Rescue for critically ill patients undergoing the COVID-19 Cytokine Storm: A structured summary of a study protocol for a randomized controlled trial*. Trials, 2020. **21**(1): p. 577.
98. Rodriguez-Rubio, M., et al., *A phase II, single-center, double-blind, randomized placebo-controlled trial to explore the efficacy and safety of intravenous melatonin in patients with COVID-19 admitted to the intensive care unit (MelCOVID study): a structured summary of a study protocol for a randomized controlled trial*. Trials, 2020. **21**(1): p. 699.
99. NCT04322188, *An Observational Study of the Use of Siltuximab (SYLVANT) in Patients Diagnosed With COVID-19 Infection Who Have Developed Serious Respiratory Complications (SISCO)*. <https://www.clinicaltrials.gov/ct2/show/study/NCT04322188>, 2020.

100. Maes, B., et al., *Treatment of severely ill COVID-19 patients with anti-interleukin drugs (COV-AID): A structured summary of a study protocol for a randomised controlled trial*. *Trials*, 2020. **21**(1): p. 468.
101. NCT04315298, *Evaluation of the Efficacy and Safety of Sarilumab in Hospitalized Patients With COVID-19*. <https://clinicaltrials.gov/ct2/show/NCT04315298>, 2020.
102. NCT04324073, *Cohort Multiple Randomized Controlled Trials Open-label of Immune Modulatory Drugs and Other Treatments in COVID-19 Patients - Sarilumab Trial - CORIMUNO-19 - SARI (CORIMUNO-SARI)*. <https://clinicaltrials.gov/ct2/show/NCT04324073>, 2020.
103. NCT04321993, *Treatment of Moderate to Severe Coronavirus Disease (COVID-19) in Hospitalized Patients*. <https://clinicaltrials.gov/ct2/show/NCT04321993>, 2020.
104. NCT04362137, *Phase 3 Randomized, Double-blind, Placebo-controlled Multi-center Study to Assess the Efficacy and Safety of Ruxolitinib in Patients With COVID-19 Associated Cytokine Storm (RUXCOVID) (RUXCOVID)*. <https://clinicaltrials.gov/ct2/show/NCT04362137>, 2020.
105. NCT04312009, *Losartan for Patients With COVID-19 Requiring Hospitalization*. <https://clinicaltrials.gov/ct2/show/NCT04312009>, 2020.
106. NCT04311177, *Losartan for Patients With COVID-19 Not Requiring Hospitalization*. <https://clinicaltrials.gov/ct2/show/NCT04311177>, 2020.
107. NCT04335032, *A randomized controlled study of eicosapentaenoic acid (EPA-FFA) gastro-resistant capsules to treat hospitalized subjects with confirmed SARS-CoV-2*. <https://clinicaltrials.gov/ct2/show/NCT04335032>, 2020.
108. NCT04322682, *Colchicine Coronavirus SARS-CoV2 Trial (COLCORONA) (COVID-19)*. <https://clinicaltrials.gov/ct2/show/NCT04322682>, 2020.
109. Wang, T., et al., *Comorbidities and multi-organ injuries in the treatment of COVID-19*. *Lancet*, 2020. **395**(10228): p. e52.
110. England, B.R., et al., *Increased cardiovascular risk in rheumatoid arthritis: mechanisms and implications*. *BMJ*, 2018. **361**: p. k1036.
111. Roubille, C., et al., *The effects of tumour necrosis factor inhibitors, methotrexate, non-steroidal anti-inflammatory drugs and corticosteroids on cardiovascular events in rheumatoid arthritis, psoriasis and psoriatic arthritis: a systematic review and meta-analysis*. *Ann Rheum Dis*, 2015. **74**(3): p. 480-9.

112. Wong, C.K., et al., *Plasma inflammatory cytokines and chemokines in severe acute respiratory syndrome*. Clin Exp Immunol, 2004. **136**(1): p. 95-103.
113. Mehta, P., et al., *COVID-19: consider cytokine storm syndromes and immunosuppression*. Lancet, 2020. **395**(10229): p. 1033-1034.
114. Russell, C.D., J.E. Millar, and J.K. Baillie, *Clinical evidence does not support corticosteroid treatment for 2019-nCoV lung injury*. Lancet, 2020. **395**(10223): p. 473-475.
115. Cao, B., et al., *A Trial of Lopinavir-Ritonavir in Adults Hospitalized with Severe Covid-19*. N Engl J Med, 2020. **382**(19): p. 1787-1799.
116. Worm, S.W., et al., *Risk of myocardial infarction in patients with HIV infection exposed to specific individual antiretroviral drugs from the 3 major drug classes: the data collection on adverse events of anti-HIV drugs (D:A:D) study*. J Infect Dis, 2010. **201**(3): p. 318-30.
117. Tsiodras, S., et al., *Effects of protease inhibitors on hyperglycemia, hyperlipidemia, and lipodystrophy: a 5-year cohort study*. Arch Intern Med, 2000. **160**(13): p. 2050-6.
118. Hill, A., W. Sawyer, and B. Gazzard, *Effects of first-line use of nucleoside analogues, efavirenz, and ritonavir-boosted protease inhibitors on lipid levels*. HIV Clin Trials, 2009. **10**(1): p. 1-12.
119. Zhou, Q., et al., *Interferon-alpha2b Treatment for COVID-19*. Front Immunol, 2020. **11**: p. 1061.
120. Page, R.L., 2nd, et al., *Drugs That May Cause or Exacerbate Heart Failure: A Scientific Statement From the American Heart Association*. Circulation, 2016. **134**(6): p. e32-69.
121. Hung, I.F., et al., *Triple combination of interferon beta-1b, lopinavir-ritonavir, and ribavirin in the treatment of patients admitted to hospital with COVID-19: an open-label, randomised, phase 2 trial*. Lancet, 2020. **395**(10238): p. 1695-1704.
122. Durante-Mangoni, E., et al., *Safety and efficacy of peginterferon alpha plus ribavirin in patients with chronic hepatitis C and coexisting heart disease*. Dig Liver Dis, 2011. **43**(5): p. 411-5.
123. Gautret, P., et al., *Hydroxychloroquine and azithromycin as a treatment of COVID-19: results of an open-label non-randomized clinical trial*. Int J Antimicrob Agents, 2020: p. 105949.

124. Cavalcanti, A.B., et al., *Hydroxychloroquine with or without Azithromycin in Mild-to-Moderate Covid-19*. N Engl J Med, 2020.
125. Arshad, S., et al., *Treatment with hydroxychloroquine, azithromycin, and combination in patients hospitalized with COVID-19*. Int J Infect Dis, 2020. **97**: p. 396-403.
126. Tang, W., et al., *Hydroxychloroquine in patients with mainly mild to moderate coronavirus disease 2019: open label, randomised controlled trial*. BMJ, 2020. **369**: p. m1849.
127. Gibson, P.G., et al., *Effect of azithromycin on asthma exacerbations and quality of life in adults with persistent uncontrolled asthma (AMAZES): a randomised, double-blind, placebo-controlled trial*. Lancet, 2017. **390**(10095): p. 659-668.
128. Choi, Y., et al., *Risk Evaluation of Azithromycin-Induced QT Prolongation in Real-World Practice*. Biomed Res Int, 2018. **2018**: p. 1574806.
129. Mercurio, N.J., et al., *Risk of QT Interval Prolongation Associated With Use of Hydroxychloroquine With or Without Concomitant Azithromycin Among Hospitalized Patients Testing Positive for Coronavirus Disease 2019 (COVID-19)*. JAMA Cardiol, 2020.
130. Wiktorowska-Owczarek, A., M. Berezinska, and J.Z. Nowak, *PUFAs: Structures, Metabolism and Functions*. Adv Clin Exp Med, 2015. **24**(6): p. 931-41.
131. Sprecher, H., *Biochemistry of essential fatty acids*. Prog Lipid Res, 1981. **20**: p. 13-22.
132. Burdge, G.C. and P.C. Calder, *Introduction to fatty acids and lipids*. World Rev Nutr Diet, 2015. **112**: p. 1-16.
133. Arterburn, L.M., E.B. Hall, and H. Oken, *Distribution, interconversion, and dose response of n-3 fatty acids in humans*. Am J Clin Nutr, 2006. **83**(6 Suppl): p. 1467S-1476S.
134. Singer, P., et al., *Benefit of an enteral diet enriched with eicosapentaenoic acid and gamma-linolenic acid in ventilated patients with acute lung injury*. Crit Care Med, 2006. **34**(4): p. 1033-8.
135. Shirai, K., et al., *Effect of enteral diet enriched with eicosapentaenoic acid, gamma-linolenic acid, and antioxidants in patients with sepsis-induced acute respiratory distress syndrome*. J Intensive Care, 2015. **3**(1): p. 24.
136. Nelson, J.L., et al., *Effect of enteral feeding with eicosapentaenoic acid, gamma-linolenic acid, and antioxidants on antioxidant status in patients with acute respiratory distress syndrome*. JPEN J Parenter Enteral Nutr, 2003. **27**(2): p. 98-104.

137. Messina, G., et al., *Functional Role of Dietary Intervention to Improve the Outcome of COVID-19: A Hypothesis of Work*. Int J Mol Sci, 2020. **21**(9).
138. Mancuso, P., et al., *Effects of eicosapentaenoic and gamma-linolenic acid on lung permeability and alveolar macrophage eicosanoid synthesis in endotoxic rats*. Crit Care Med, 1997. **25**(3): p. 523-32.
139. Mancuso, P., et al., *Dietary fish oil and fish and borage oil suppress intrapulmonary proinflammatory eicosanoid biosynthesis and attenuate pulmonary neutrophil accumulation in endotoxic rats*. Crit Care Med, 1997. **25**(7): p. 1198-206.
140. Saedisomeolia, A., et al., *Anti-inflammatory effects of long-chain n-3 PUFA in rhinovirus-infected cultured airway epithelial cells*. Br J Nutr, 2009. **101**(4): p. 533-40.
141. Pontes-Arruda, A., A.M. Aragao, and J.D. Albuquerque, *Effects of enteral feeding with eicosapentaenoic acid, gamma-linolenic acid, and antioxidants in mechanically ventilated patients with severe sepsis and septic shock*. Crit Care Med, 2006. **34**(9): p. 2325-33.
142. Pontes-Arruda, A., et al., *The use of an inflammation-modulating diet in patients with acute lung injury or acute respiratory distress syndrome: a meta-analysis of outcome data*. JPEN J Parenter Enteral Nutr, 2008. **32**(6): p. 596-605.
143. Hosny, M., et al., *Impact of oral omega-3 fatty acids supplementation in early sepsis on clinical outcome and immunomodulation*. J. Crit. Care Med. , 2013: p. 119–126.
144. Langlois, P.L., et al., *Omega-3 polyunsaturated fatty acids in critically ill patients with acute respiratory distress syndrome: A systematic review and meta-analysis*. Nutrition, 2019. **61**: p. 84-92.
145. Pradelli, L., et al., *omega-3 Fatty-Acid Enriched Parenteral Nutrition in Hospitalized Patients: Systematic Review With Meta-Analysis and Trial Sequential Analysis*. JPEN J Parenter Enteral Nutr, 2020. **44**(1): p. 44-57.
146. Bistrrian, B.R., *Parenteral Fish-Oil Emulsions in Critically Ill COVID-19 Emulsions*. JPEN J Parenter Enteral Nutr, 2020.
147. Torrinhas, R.S., P.C. Calder, and D.L. Waitzberg, *Response to Bistrrian BR. Parenteral Fish-Oil Emulsions in Critically Ill COVID-19 Emulsions*. JPEN J Parenter Enteral Nutr, 2020.
148. Das, U.N., *Can Bioactive Lipids Inactivate Coronavirus (COVID-19)?* Arch Med Res, 2020. **51**(3): p. 282-286.

149. Lordan, R., et al., *Inflammation and cardiovascular disease: are marine phospholipids the answer?* Food Funct, 2020. **11**(4): p. 2861-2885.
150. Lordan, R., A. Tsoupras, and I. Zabetakis, *Phospholipids of Animal and Marine Origin: Structure, Function, and Anti-Inflammatory Properties*. Molecules, 2017. **22**(11).
151. Moro, K., et al., *Resolvins and omega three polyunsaturated fatty acids: Clinical implications in inflammatory diseases and cancer*. World J Clin Cases, 2016. **4**(7): p. 155-64.
152. Kris-Etherton, P.M., et al., *Fish consumption, fish oil, omega-3 fatty acids, and cardiovascular disease*. Arterioscler Thromb Vasc Biol, 2003. **23**(2): p. e20-30.
153. Mozaffarian, D., *JELIS, fish oil, and cardiac events*. Lancet, 2007. **369**(9567): p. 1062-3.
154. Lee, J.H., et al., *Omega-3 fatty acids: cardiovascular benefits, sources and sustainability*. Nature Reviews Cardiology, 2009. **6**: p. 753.
155. Darwesh, A.M., et al., *Insights into the cardioprotective properties of n-3 PUFAs against ischemic heart disease via modulation of the innate immune system*. Chem Biol Interact, 2019. **308**: p. 20-44.
156. Mozaffarian, D., et al., *Plasma phospholipid long-chain omega-3 fatty acids and total and cause-specific mortality in older adults: a cohort study*. Ann Intern Med, 2013. **158**(7): p. 515-25.
157. Siscovick, D.S., et al., *Omega-3 Polyunsaturated Fatty Acid (Fish Oil) Supplementation and the Prevention of Clinical Cardiovascular Disease: A Science Advisory From the American Heart Association*. Circulation, 2017. **135**(15): p. e867-e884.
158. Sacks, F.M., et al., *Dietary Fats and Cardiovascular Disease: A Presidential Advisory From the American Heart Association*. Circulation, 2017. **136**(3): p. e1-e23.
159. Thies, F., et al., *Association of n-3 polyunsaturated fatty acids with stability of atherosclerotic plaques: a randomised controlled trial*. Lancet, 2003. **361**(9356): p. 477-85.
160. Plutzky, J., *Atherosclerotic plaque rupture: emerging insights and opportunities*. Am J Cardiol, 1999. **84**(1A): p. 15J-20J.
161. Din, J.N., et al., *Dietary intervention with oil rich fish reduces platelet-monocyte aggregation in man*. Atherosclerosis, 2008. **197**(1): p. 290-6.

162. Abuisse, H., et al., *Autonomic function, omega-3, and cardiovascular risk*. Chest, 2005. **127**(4): p. 1088-91.
163. O'Keefe, J.H., Jr., et al., *Effects of omega-3 fatty acids on resting heart rate, heart rate recovery after exercise, and heart rate variability in men with healed myocardial infarctions and depressed ejection fractions*. Am J Cardiol, 2006. **97**(8): p. 1127-30.
164. Anand, R.G., et al., *The role of fish oil in arrhythmia prevention*. J Cardiopulm Rehabil Prev, 2008. **28**(2): p. 92-8.
165. Geleijnse, J.M., et al., *Blood pressure response to fish oil supplementation: meta-regression analysis of randomized trials*. J Hypertens, 2002. **20**(8): p. 1493-9.
166. Calder, P.C., *Omega-3 fatty acids and inflammatory processes: from molecules to man*. Biochem Soc Trans, 2017. **45**(5): p. 1105-1115.
167. Calder, P.C., *Omega-3 polyunsaturated fatty acids and inflammatory processes: nutrition or pharmacology?* Br J Clin Pharmacol, 2013. **75**(3): p. 645-62.
168. Korner, A., et al., *Resolution of inflammation and sepsis survival are improved by dietary Omega-3 fatty acids*. Cell Death Differ, 2018. **25**(2): p. 421-431.
169. Leger, T., et al., *Antioxidant and Cardioprotective Effects of EPA on Early Low-Severity Sepsis through UCP3 and SIRT3 Upholding of the Mitochondrial Redox Potential*. Oxid Med Cell Longev, 2019. **2019**: p. 9710352.
170. Rogero, M.M., et al., *Potential benefits and risks of omega-3 fatty acids supplementation to patients with COVID-19*. Free Radic Biol Med, 2020. **156**: p. 190-199.
171. Fritsche, K., *Fatty acids as modulators of the immune response*. Annu Rev Nutr, 2006. **26**: p. 45-73.
172. Vedin, I., et al., *Effects of docosahexaenoic acid-rich n-3 fatty acid supplementation on cytokine release from blood mononuclear leukocytes: the OmegAD study*. Am J Clin Nutr, 2008. **87**(6): p. 1616-22.
173. Kiecolt-Glaser, J.K., et al., *Omega-3 supplementation lowers inflammation in healthy middle-aged and older adults: a randomized controlled trial*. Brain Behav Immun, 2012. **26**(6): p. 988-95.
174. Calder, P.C., et al., *Optimal Nutritional Status for a Well-Functioning Immune System Is an Important Factor to Protect against Viral Infections*. Nutrients, 2020. **12**(4).

175. Tan, A., et al., *Supplementation with eicosapentaenoic acid and docosahexaenoic acid reduces high levels of circulating proinflammatory cytokines in aging adults: A randomized, controlled study*. Prostaglandins Leukot Essent Fatty Acids, 2018. **132**: p. 23-29.
176. Hughes, D.A., S. Southon, and A.C. Pinder, *(n-3) Polyunsaturated fatty acids modulate the expression of functionally associated molecules on human monocytes in vitro*. J Nutr, 1996. **126**(3): p. 603-10.
177. De Caterina, R., et al., *The omega-3 fatty acid docosahexaenoate reduces cytokine-induced expression of proatherogenic and proinflammatory proteins in human endothelial cells*. Arterioscler Thromb, 1994. **14**(11): p. 1829-36.
178. Collie-Duguid, E.S. and K.W. Wahle, *Inhibitory effect of fish oil N-3 polyunsaturated fatty acids on the expression of endothelial cell adhesion molecules*. Biochem Biophys Res Commun, 1996. **220**(3): p. 969-74.
179. Miles, E.A., F.A. Wallace, and P.C. Calder, *Dietary fish oil reduces intercellular adhesion molecule 1 and scavenger receptor expression on murine macrophages*. Atherosclerosis, 2000. **152**(1): p. 43-50.
180. Sanderson, P. and P.C. Calder, *Dietary fish oil diminishes lymphocyte adhesion to macrophage and endothelial cell monolayers*. Immunology, 1998. **94**(1): p. 79-87.
181. Lo, C.J., et al., *Fish oil decreases macrophage tumor necrosis factor gene transcription by altering the NF kappa B activity*. J Surg Res, 1999. **82**(2): p. 216-21.
182. Novak, T.E., et al., *NF-kappa B inhibition by omega -3 fatty acids modulates LPS-stimulated macrophage TNF-alpha transcription*. Am J Physiol Lung Cell Mol Physiol, 2003. **284**(1): p. L84-9.
183. Zhao, Y., et al., *Eicosapentaenoic acid prevents LPS-induced TNF-alpha expression by preventing NF-kappaB activation*. J Am Coll Nutr, 2004. **23**(1): p. 71-8.
184. Kumar, A., et al., *Nuclear factor-kappaB: its role in health and disease*. J Mol Med (Berl), 2004. **82**(7): p. 434-48.
185. Gani, O.A. and I. Sylte, *Molecular recognition of docosahexaenoic acid by peroxisome proliferator-activated receptors and retinoid-X receptor alpha*. J Mol Graph Model, 2008. **27**(2): p. 217-24.
186. Zapata-Gonzalez, F., et al., *Human dendritic cell activities are modulated by the omega-3 fatty acid, docosahexaenoic acid, mainly through PPAR(gamma):RXR heterodimers*:

- comparison with other polyunsaturated fatty acids*. J Leukoc Biol, 2008. **84**(4): p. 1172-82.
187. Poynter, M.E. and R.A. Daynes, *Peroxisome proliferator-activated receptor alpha activation modulates cellular redox status, represses nuclear factor-kappaB signaling, and reduces inflammatory cytokine production in aging*. J Biol Chem, 1998. **273**(49): p. 32833-41.
188. Ricote, M., et al., *The peroxisome proliferator-activated receptor(PPARgamma) as a regulator of monocyte/macrophage function*. J Leukoc Biol, 1999. **66**(5): p. 733-9.
189. Vanden Berghe, W., et al., *A paradigm for gene regulation: inflammation, NF-kappaB and PPAR*. Adv Exp Med Biol, 2003. **544**: p. 181-96.
190. Mishra, A., A. Chaudhary, and S. Sethi, *Oxidized omega-3 fatty acids inhibit NF-kappaB activation via a PPARalpha-dependent pathway*. Arterioscler Thromb Vasc Biol, 2004. **24**(9): p. 1621-7.
191. Matsumoto, M., et al., *Orally administered eicosapentaenoic acid reduces and stabilizes atherosclerotic lesions in ApoE-deficient mice*. Atherosclerosis, 2008. **197**(2): p. 524-33.
192. Ciavarella, C., et al., *Pharmacological (or Synthetic) and Nutritional Agonists of PPAR-gamma as Candidates for Cytokine Storm Modulation in COVID-19 Disease*. Molecules, 2020. **25**(9).
193. Oh, D.Y., et al., *GPR120 is an omega-3 fatty acid receptor mediating potent anti-inflammatory and insulin-sensitizing effects*. Cell, 2010. **142**(5): p. 687-98.
194. Epelman, S., et al., *Embryonic and adult-derived resident cardiac macrophages are maintained through distinct mechanisms at steady state and during inflammation*. Immunity, 2014. **40**(1): p. 91-104.
195. Murray, P.J., *Macrophage Polarization*. Annu Rev Physiol, 2017. **79**: p. 541-566.
196. van Amerongen, M.J., et al., *Macrophage depletion impairs wound healing and increases left ventricular remodeling after myocardial injury in mice*. Am J Pathol, 2007. **170**(3): p. 818-29.
197. Leblond, A.L., et al., *Systemic and Cardiac Depletion of M2 Macrophage through CSF-1R Signaling Inhibition Alters Cardiac Function Post Myocardial Infarction*. PLoS One, 2015. **10**(9): p. e0137515.

198. Frantz, S. and M. Nahrendorf, *Cardiac macrophages and their role in ischaemic heart disease*. Cardiovasc Res, 2014. **102**(2): p. 240-8.
199. Fujiu, K., J. Wang, and R. Nagai, *Cardioprotective function of cardiac macrophages*. Cardiovasc Res, 2014. **102**(2): p. 232-9.
200. ter Horst, E.N., et al., *Modulators of Macrophage Polarization Influence Healing of the Infarcted Myocardium*. Int J Mol Sci, 2015. **16**(12): p. 29583-91.
201. Dewald, O., et al., *CCL2/Monocyte Chemoattractant Protein-1 regulates inflammatory responses critical to healing myocardial infarcts*. Circ Res, 2005. **96**(8): p. 881-9.
202. Murray, P.J. and T.A. Wynn, *Protective and pathogenic functions of macrophage subsets*. Nat Rev Immunol, 2011. **11**(11): p. 723-37.
203. Gordon, S., A. Pluddemann, and F. Martinez Estrada, *Macrophage heterogeneity in tissues: phenotypic diversity and functions*. Immunol Rev, 2014. **262**(1): p. 36-55.
204. Mildenerger, J., et al., *N-3 PUFAs induce inflammatory tolerance by formation of KEAP1-containing SQSTM1/p62-bodies and activation of NFE2L2*. Autophagy, 2017. **13**(10): p. 1664-1678.
205. Allam-Ndoul, B., et al., *A Study of the Differential Effects of Eicosapentaenoic Acid (EPA) and Docosahexaenoic Acid (DHA) on Gene Expression Profiles of Stimulated Thp-1 Macrophages*. Nutrients, 2017. **9**(5).
206. Liu, Y., et al., *The fish oil ingredient, docosahexaenoic acid, activates cytosolic phospholipase A(2) via GPR120 receptor to produce prostaglandin E(2) and plays an anti-inflammatory role in macrophages*. Immunology, 2014. **143**(1): p. 81-95.
207. Schoeniger, A., et al., *The impact of membrane lipid composition on macrophage activation in the immune defense against Rhodococcus equi and Pseudomonas aeruginosa*. Int J Mol Sci, 2011. **12**(11): p. 7510-28.
208. Kumar, N., et al., *15-Lipoxygenase metabolites of alpha-linolenic acid, [13-(S)-HPOTrE and 13-(S)-HOTrE], mediate anti-inflammatory effects by inactivating NLRP3 inflammasome*. Sci Rep, 2016. **6**: p. 31649.
209. Iverson, C., et al., *Omega-3-carboxylic acids provide efficacious anti-inflammatory activity in models of crystal-mediated inflammation*. Sci Rep, 2018. **8**(1): p. 1217.

210. Chang, H.Y., et al., *Docosahexaenoic acid induces M2 macrophage polarization through peroxisome proliferator-activated receptor gamma activation*. Life Sci, 2015. **120**: p. 39-47.
211. Adolph, S., H. Fuhrmann, and J. Schumann, *Unsaturated fatty acids promote the phagocytosis of P. aeruginosa and R. equi by RAW264.7 macrophages*. Curr Microbiol, 2012. **65**(6): p. 649-55.
212. Davidson, J., et al., *Prostaglandin and fatty acid modulation of Escherichia coli O157 phagocytosis by human monocytic cells*. Immunology, 1998. **94**(2): p. 228-34.
213. Schoeniger, A., H. Fuhrmann, and J. Schumann, *LPS- or Pseudomonas aeruginosa-mediated activation of the macrophage TLR4 signaling cascade depends on membrane lipid composition*. PeerJ, 2016. **4**: p. e1663.
214. Hellwing, C., et al., *Lipid composition of membrane microdomains isolated detergent-free from PUFA supplemented RAW264.7 macrophages*. J Cell Physiol, 2018. **233**(3): p. 2602-2612.
215. Ohue-Kitano, R., et al., *alpha-Linolenic acid-derived metabolites from gut lactic acid bacteria induce differentiation of anti-inflammatory M2 macrophages through G protein-coupled receptor 40*. FASEB J, 2018. **32**(1): p. 304-318.
216. Schunck, W.H., et al., *Therapeutic potential of omega-3 fatty acid-derived epoxyeicosanoids in cardiovascular and inflammatory diseases*. Pharmacol Ther, 2018. **183**: p. 177-204.
217. Jamieson, K.L., et al., *Cytochrome P450-derived eicosanoids and heart function*. Pharmacol Ther, 2017. **179**: p. 47-83.
218. Kalinski, P., *Regulation of immune responses by prostaglandin E2*. J Immunol, 2012. **188**(1): p. 21-8.
219. Lewis, R.A., K.F. Austen, and R.J. Soberman, *Leukotrienes and other products of the 5-lipoxygenase pathway. Biochemistry and relation to pathobiology in human diseases*. N Engl J Med, 1990. **323**(10): p. 645-55.
220. Innes, J.K. and P.C. Calder, *Omega-6 fatty acids and inflammation*. Prostaglandins Leukot Essent Fatty Acids, 2018. **132**: p. 41-48.
221. Ricciotti, E. and G.A. FitzGerald, *Prostaglandins and inflammation*. Arterioscler Thromb Vasc Biol, 2011. **31**(5): p. 986-1000.

222. Corey, E.J., C. Shih, and J.R. Cashman, *Docosahexaenoic acid is a strong inhibitor of prostaglandin but not leukotriene biosynthesis*. Proc Natl Acad Sci U S A, 1983. **80**(12): p. 3581-4.
223. Lee, T.H., et al., *Effects of exogenous arachidonic, eicosapentaenoic, and docosahexaenoic acids on the generation of 5-lipoxygenase pathway products by ionophore-activated human neutrophils*. J Clin Invest, 1984. **74**(6): p. 1922-33.
224. Surette, M.E., *The science behind dietary omega-3 fatty acids*. CMAJ, 2008. **178**(2): p. 177-80.
225. Calder, P.C., *n-3 polyunsaturated fatty acids, inflammation, and inflammatory diseases*. Am J Clin Nutr, 2006. **83**(6 Suppl): p. 1505S-1519S.
226. Falck, J.R., et al., *17(R),18(S)-epoxyeicosatetraenoic acid, a potent eicosapentaenoic acid (EPA) derived regulator of cardiomyocyte contraction: structure-activity relationships and stable analogues*. J Med Chem, 2011. **54**(12): p. 4109-18.
227. Lee, T.H., et al., *Effect of dietary enrichment with eicosapentaenoic and docosahexaenoic acids on in vitro neutrophil and monocyte leukotriene generation and neutrophil function*. N Engl J Med, 1985. **312**(19): p. 1217-24.
228. Caughey, G.E., et al., *The effect on human tumor necrosis factor alpha and interleukin 1 beta production of diets enriched in n-3 fatty acids from vegetable oil or fish oil*. Am J Clin Nutr, 1996. **63**(1): p. 116-22.
229. von Schacky, C., et al., *n-3 fatty acids and cysteinyl-leukotriene formation in humans in vitro, ex vivo, and in vivo*. J Lab Clin Med, 1993. **121**(2): p. 302-9.
230. Prescott, S.M., *The effect of eicosapentaenoic acid on leukotriene B production by human neutrophils*. J Biol Chem, 1984. **259**(12): p. 7615-21.
231. Goldman, D.W., W.C. Pickett, and E.J. Goetzl, *Human neutrophil chemotactic and degranulating activities of leukotriene B5 (LTB5) derived from eicosapentaenoic acid*. Biochem Biophys Res Commun, 1983. **117**(1): p. 282-8.
232. Lee, T.H., et al., *Characterization and biologic properties of 5,12-dihydroxy derivatives of eicosapentaenoic acid, including leukotriene B5 and the double lipoxygenase product*. J Biol Chem, 1984. **259**(4): p. 2383-9.
233. Serhan, C.N., et al., *Resolvins: a family of bioactive products of omega-3 fatty acid transformation circuits initiated by aspirin treatment that counter proinflammation signals*. J Exp Med, 2002. **196**(8): p. 1025-37.

234. Serhan, C.N., N. Chiang, and T.E. Van Dyke, *Resolving inflammation: dual anti-inflammatory and pro-resolution lipid mediators*. Nat Rev Immunol, 2008. **8**(5): p. 349-61.
235. Mas, E., et al., *Resolvins D1, D2, and other mediators of self-limited resolution of inflammation in human blood following n-3 fatty acid supplementation*. Clin Chem, 2012. **58**(10): p. 1476-84.
236. Serhan, C.N., et al., *Novel functional sets of lipid-derived mediators with antiinflammatory actions generated from omega-3 fatty acids via cyclooxygenase 2-nonsteroidal antiinflammatory drugs and transcellular processing*. J Exp Med, 2000. **192**(8): p. 1197-204.
237. Spite, M., et al., *Resolvin D2 is a potent regulator of leukocytes and controls microbial sepsis*. Nature, 2009. **461**(7268): p. 1287-91.
238. Titos, E., et al., *Resolvin D1 and its precursor docosahexaenoic acid promote resolution of adipose tissue inflammation by eliciting macrophage polarization toward an M2-like phenotype*. J Immunol, 2011. **187**(10): p. 5408-18.
239. Campbell, E.L., et al., *Resolvin E1 promotes mucosal surface clearance of neutrophils: a new paradigm for inflammatory resolution*. FASEB J, 2007. **21**(12): p. 3162-70.
240. Krishnamoorthy, S., et al., *Resolvin D1 binds human phagocytes with evidence for proresolving receptors*. Proc Natl Acad Sci U S A, 2010. **107**(4): p. 1660-5.
241. Arita, M., et al., *Resolvin E1 selectively interacts with leukotriene B4 receptor BLT1 and ChemR23 to regulate inflammation*. J Immunol, 2007. **178**(6): p. 3912-7.
242. Ariel, A., et al., *Apoptotic neutrophils and T cells sequester chemokines during immune response resolution through modulation of CCR5 expression*. Nat Immunol, 2006. **7**(11): p. 1209-16.
243. Schwab, J.M., et al., *Resolvin E1 and protectin D1 activate inflammation-resolution programmes*. Nature, 2007. **447**(7146): p. 869-74.
244. Serhan, C.N. and N. Chiang, *Novel endogenous small molecules as the checkpoint controllers in inflammation and resolution: entree for resolomics*. Rheum Dis Clin North Am, 2004. **30**(1): p. 69-95.
245. Morin, C., et al., *Effect of docosahexaenoic acid monoacylglyceride on systemic hypertension and cardiovascular dysfunction*. Am J Physiol Heart Circ Physiol, 2015. **309**(1): p. H93-H102.

246. Ramon, S., et al., *Specialized proresolving mediators enhance human B cell differentiation to antibody-secreting cells*. J Immunol, 2012. **189**(2): p. 1036-42.
247. Sulciner, M.L., et al., *Resolvins suppress tumor growth and enhance cancer therapy*. J Exp Med, 2018. **215**(1): p. 115-140.
248. Serhan, C.N., et al., *Maresins: novel macrophage mediators with potent antiinflammatory and proresolving actions*. J Exp Med, 2009. **206**(1): p. 15-23.
249. Dalli, J., et al., *Novel proresolving and tissue-regenerative resolvin and protectin sulfido-conjugated pathways*. FASEB J, 2015. **29**(5): p. 2120-36.
250. Bouchery, T. and N.L. Harris, *Specific repair by discerning macrophages*. Science, 2017. **356**(6342): p. 1014.
251. Ramon, S., et al., *The Protectin PCTRI Is Produced by Human M2 Macrophages and Enhances Resolution of Infectious Inflammation*. Am J Pathol, 2016. **186**(4): p. 962-73.
252. Norris, P.C., et al., *Resolvin D3 multi-level proresolving actions are host protective during infection*. Prostaglandins Leukot Essent Fatty Acids, 2018. **138**: p. 81-89.
253. Dalli, J., et al., *Resolvin D3 and aspirin-triggered resolvin D3 are potent immunoresolvents*. Chem Biol, 2013. **20**(2): p. 188-201.
254. Poorani, R., et al., *COX-2, aspirin and metabolism of arachidonic, eicosapentaenoic and docosahexaenoic acids and their physiological and clinical significance*. Eur J Pharmacol, 2016. **785**: p. 116-132.
255. Uddin, M. and B.D. Levy, *Resolvins: natural agonists for resolution of pulmonary inflammation*. Prog Lipid Res, 2011. **50**(1): p. 75-88.
256. Zhang, H.W., et al., *RvD1 ameliorates LPS-induced acute lung injury via the suppression of neutrophil infiltration by reducing CXCL2 expression and release from resident alveolar macrophages*. Int Immunopharmacol, 2019. **76**: p. 105877.
257. Gao, Y., et al., *Resolvin D1 Improves the Resolution of Inflammation via Activating NF-kappaB p50/p50-Mediated Cyclooxygenase-2 Expression in Acute Respiratory Distress Syndrome*. J Immunol, 2017.
258. Wang, Q., et al., *Specialized Pro-resolving Mediators Regulate Alveolar Fluid Clearance during Acute Respiratory Distress Syndrome*. Chin Med J (Engl), 2018. **131**(8): p. 982-989.

259. Morita, M., et al., *The lipid mediator protectin D1 inhibits influenza virus replication and improves severe influenza*. Cell, 2013. **153**(1): p. 112-25.
260. Russell, C.D. and J. Schwarze, *The role of pro-resolution lipid mediators in infectious disease*. Immunology, 2014. **141**(2): p. 166-73.
261. Das, U.N., *Is sepsis a pro-resolution deficiency disorder?* Med Hypotheses, 2013. **80**(3): p. 297-9.
262. Das, U.N., *Arachidonic acid and other unsaturated fatty acids and some of their metabolites function as endogenous antimicrobial molecules: A review*. J Adv Res, 2018. **11**: p. 57-66.
263. Das, U.N., *Can Bioactive Lipids Augment Anti-cancer Action of Immunotherapy and Prevent Cytokine Storm?* Arch Med Res, 2019. **50**(6): p. 342-349.
264. Konkel, A. and W.H. Schunck, *Role of cytochrome P450 enzymes in the bioactivation of polyunsaturated fatty acids*. Biochim Biophys Acta, 2011. **1814**(1): p. 210-22.
265. Westphal, C., A. Konkel, and W.H. Schunck, *Cytochrome p450 enzymes in the bioactivation of polyunsaturated Fatty acids and their role in cardiovascular disease*. Adv Exp Med Biol, 2015. **851**: p. 151-87.
266. Arnold, C., et al., *Arachidonic acid-metabolizing cytochrome P450 enzymes are targets of {omega}-3 fatty acids*. J Biol Chem, 2010. **285**(43): p. 32720-33.
267. Wang, R.X., et al., *Activation of vascular BK channels by docosahexaenoic acid is dependent on cytochrome P450 epoxygenase activity*. Cardiovasc Res, 2011. **90**(2): p. 344-52.
268. Ulu, A., et al., *An Omega-3 Epoxide of Docosahexaenoic Acid Lowers Blood Pressure in Angiotensin-II-Dependent Hypertension*. J Cardiovasc Pharmacol, 2014. **64**(1): p. 87-99.
269. Fang, X., et al., *Omega-3 PUFA attenuate mice myocardial infarction injury by emerging a protective eicosanoid pattern*. Prostaglandins Other Lipid Mediat, 2018. **139**: p. 1-9.
270. Darwesh, A.M., et al., *Cardioprotective effects of CYP-derived epoxy metabolites of docosahexaenoic acid involve limiting NLRP3 inflammasome activation*. Can J Physiol Pharmacol, 2019. **97**(6): p. 544-556.
271. Capozzi, M.E., et al., *Epoxygenated Fatty Acids Inhibit Retinal Vascular Inflammation*. Sci Rep, 2016. **6**: p. 39211.

272. Kunisawa, J., et al., *Dietary omega3 fatty acid exerts anti-allergic effect through the conversion to 17,18-epoxyeicosatetraenoic acid in the gut*. Sci Rep, 2015. **5**: p. 9750.
273. Sharma, A., et al., *Novel Omega-3 Fatty Acid Epoxygenase Metabolite Reduces Kidney Fibrosis*. Int J Mol Sci, 2016. **17**(5).
274. Morin, C., et al., *17,18-epoxyeicosatetraenoic acid targets PPARgamma and p38 mitogen-activated protein kinase to mediate its anti-inflammatory effects in the lung: role of soluble epoxide hydrolase*. Am J Respir Cell Mol Biol, 2010. **43**(5): p. 564-75.
275. Morisseau, C., et al., *Naturally occurring monoepoxides of eicosapentaenoic acid and docosahexaenoic acid are bioactive antihyperalgesic lipids*. J Lipid Res, 2010. **51**(12): p. 3481-90.
276. Samokhvalov, V., et al., *CYP-epoxygenase metabolites of docosahexaenoic acid protect HL-1 cardiac cells against LPS-induced cytotoxicity Through SIRT1*. Cell Death Discov, 2015. **1**.
277. Takashima, A., et al., *Combination of n-3 polyunsaturated fatty acids reduces atherogenesis in apolipoprotein E-deficient mice by inhibiting macrophage activation*. Atherosclerosis, 2016. **254**: p. 142-150.
278. Ciesielska, A. and K. Kwiatkowska, *Modification of pro-inflammatory signaling by dietary components: The plasma membrane as a target*. Bioessays, 2015. **37**(7): p. 789-801.
279. Katagiri, Y.U., N. Kiyokawa, and J. Fujimoto, *A role for lipid rafts in immune cell signaling*. Microbiol Immunol, 2001. **45**(1): p. 1-8.
280. McMurray, D.N., D.L. Bonilla, and R.S. Chapkin, *n-3 Fatty acids uniquely affect anti-microbial resistance and immune cell plasma membrane organization*. Chem Phys Lipids, 2011. **164**(7): p. 626-35.
281. Shaikh, S.R. and M. Edidin, *Polyunsaturated fatty acids, membrane organization, T cells, and antigen presentation*. Am J Clin Nutr, 2006. **84**(6): p. 1277-89.
282. Kim, W., et al., *Regulatory activity of polyunsaturated fatty acids in T-cell signaling*. Prog Lipid Res, 2010. **49**(3): p. 250-61.
283. Rockett, B.D., et al., *n-3 PUFA improves fatty acid composition, prevents palmitate-induced apoptosis, and differentially modifies B cell cytokine secretion in vitro and ex vivo*. J Lipid Res, 2010. **51**(6): p. 1284-97.

284. Shaikh, S.R. and M. Edidin, *Polyunsaturated fatty acids and membrane organization: elucidating mechanisms to balance immunotherapy and susceptibility to infection*. Chem Phys Lipids, 2008. **153**(1): p. 24-33.
285. Hashimoto, M., et al., *Effects of eicosapentaenoic acid and docosahexaenoic acid on plasma membrane fluidity of aortic endothelial cells*. Lipids, 1999. **34**(12): p. 1297-304.
286. Yaqoob, P., et al., *Encapsulated fish oil enriched in alpha-tocopherol alters plasma phospholipid and mononuclear cell fatty acid compositions but not mononuclear cell functions*. Eur J Clin Invest, 2000. **30**(3): p. 260-74.
287. Hazen, S.L., D.A. Ford, and R.W. Gross, *Activation of a membrane-associated phospholipase A2 during rabbit myocardial ischemia which is highly selective for plasmalogen substrate*. J Biol Chem, 1991. **266**(9): p. 5629-33.
288. Ford, D.A., et al., *The rapid and reversible activation of a calcium-independent plasmalogen-selective phospholipase A2 during myocardial ischemia*. J Clin Invest, 1991. **88**(1): p. 331-5.
289. Mancuso, D.J., et al., *Cardiac ischemia activates calcium-independent phospholipase A2beta, precipitating ventricular tachyarrhythmias in transgenic mice: rescue of the lethal electrophysiologic phenotype by mechanism-based inhibition*. J Biol Chem, 2003. **278**(25): p. 22231-6.
290. Leslie, C.C., *Cytosolic phospholipase A(2): physiological function and role in disease*. J Lipid Res, 2015. **56**(8): p. 1386-402.
291. Brouard, C. and M. Pascaud, *Effects of moderate dietary supplementations with n-3 fatty acids on macrophage and lymphocyte phospholipids and macrophage eicosanoid synthesis in the rat*. Biochim Biophys Acta, 1990. **1047**(1): p. 19-28.
292. Faber, J., et al., *Supplementation with a fish oil-enriched, high-protein medical food leads to rapid incorporation of EPA into white blood cells and modulates immune responses within one week in healthy men and women*. J Nutr, 2011. **141**(5): p. 964-70.
293. Gibney, M.J. and B. Hunter, *The effects of short- and long-term supplementation with fish oil on the incorporation of n-3 polyunsaturated fatty acids into cells of the immune system in healthy volunteers*. Eur J Clin Nutr, 1993. **47**(4): p. 255-9.
294. Grando, F.C., et al., *Modulation of peritoneal macrophage activity by the saturation state of the fatty acid moiety of phosphatidylcholine*. Braz J Med Biol Res, 2009. **42**(7): p. 599-605.

295. Murphy, E., et al., *Mitochondrial Function, Biology, and Role in Disease: A Scientific Statement From the American Heart Association*. *Circ Res*, 2016. **118**(12): p. 1960-91.
296. Meyers, D.E., H.I. Basha, and M.K. Koenig, *Mitochondrial cardiomyopathy: pathophysiology, diagnosis, and management*. *Tex Heart Inst J*, 2013. **40**(4): p. 385-94.
297. Bayeva, M., M. Gheorghiadu, and H. Ardehali, *Mitochondria as a therapeutic target in heart failure*. *J Am Coll Cardiol*, 2013. **61**(6): p. 599-610.
298. Srivastava, S., *The Mitochondrial Basis of Aging and Age-Related Disorders*. *Genes (Basel)*, 2017. **8**(12).
299. Wu, N.N., Y. Zhang, and J. Ren, *Mitophagy, Mitochondrial Dynamics, and Homeostasis in Cardiovascular Aging*. *Oxid Med Cell Longev*, 2019. **2019**: p. 9825061.
300. Rovira-Llopis, S., et al., *Mitochondrial dynamics in type 2 diabetes: Pathophysiological implications*. *Redox Biol*, 2017. **11**: p. 637-645.
301. Cho, D.H., J.K. Kim, and E.K. Jo, *Mitophagy and Innate Immunity in Infection*. *Mol Cells*, 2020. **43**(1): p. 10-22.
302. Kim, S.J., et al., *The essential role of mitochondrial dynamics in antiviral immunity*. *Mitochondrion*, 2018. **41**: p. 21-27.
303. Saleh, J., et al., *Mitochondria and microbiota dysfunction in COVID-19 pathogenesis*. *Mitochondrion*, 2020. **54**: p. 1-7.
304. Grivennikova, V.G., A.V. Kareyeva, and A.D. Vinogradov, *What are the sources of hydrogen peroxide production by heart mitochondria?* *Biochim Biophys Acta*, 2010. **1797**(6-7): p. 939-44.
305. Melser, S., J. Lavie, and G. Benard, *Mitochondrial degradation and energy metabolism*. *Biochim Biophys Acta*, 2015. **1853**(10 Pt B): p. 2812-21.
306. Filler, K., et al., *Association of Mitochondrial Dysfunction and Fatigue: A Review of the Literature*. *BBA Clin*, 2014. **1**: p. 12-23.
307. Yu, J., et al., *Inflammasome activation leads to Caspase-1-dependent mitochondrial damage and block of mitophagy*. *Proc Natl Acad Sci U S A*, 2014. **111**(43): p. 15514-9.
308. Gurung, P., J.R. Lukens, and T.D. Kanneganti, *Mitochondria: diversity in the regulation of the NLRP3 inflammasome*. *Trends Mol Med*, 2015. **21**(3): p. 193-201.

309. Mohanty, A., R. Tiwari-Pandey, and N.R. Pandey, *Mitochondria: the indispensable players in innate immunity and guardians of the inflammatory response*. J Cell Commun Signal, 2019. **13**(3): p. 303-318.
310. Darwesh, A.M., et al., *Genetic Deletion or Pharmacological Inhibition of Soluble Epoxide Hydrolase Ameliorates Cardiac Ischemia/Reperfusion Injury by Attenuating NLRP3 Inflammasome Activation*. Int J Mol Sci, 2019. **20**(14).
311. Keshavarz-Bahaghighat, H., et al., *Mitochondrial Dysfunction and Inflammation in Heart Failure: Novel Roles of CYP-Derived Epoxy lipids*. Cells, 2020. **9**(7).
312. Samokhvalov, V., et al., *Deficiency of Soluble Epoxide Hydrolase Protects Cardiac Function Impaired by LPS-Induced Acute Inflammation*. Front Pharmacol, 2018. **9**: p. 1572.
313. Jo, E.K., et al., *Molecular mechanisms regulating NLRP3 inflammasome activation*. Cell Mol Immunol, 2016. **13**(2): p. 148-59.
314. Naik, E. and V.M. Dixit, *Mitochondrial reactive oxygen species drive proinflammatory cytokine production*. J Exp Med, 2011. **208**(3): p. 417-20.
315. Li, X., et al., *Targeting mitochondrial reactive oxygen species as novel therapy for inflammatory diseases and cancers*. J Hematol Oncol, 2013. **6**: p. 19.
316. Singh, K.K., et al., *Decoding SARS-CoV-2 hijacking of host mitochondria in COVID-19 pathogenesis*. Am J Physiol Cell Physiol, 2020. **319**(2): p. C258-C267.
317. Starkov, A.A., *The role of mitochondria in reactive oxygen species metabolism and signaling*. Ann N Y Acad Sci, 2008. **1147**: p. 37-52.
318. Herst, P.M., et al., *Functional Mitochondria in Health and Disease*. Front Endocrinol (Lausanne), 2017. **8**: p. 296.
319. Twig, G. and O.S. Shirihai, *The interplay between mitochondrial dynamics and mitophagy*. Antioxid Redox Signal, 2011. **14**(10): p. 1939-51.
320. Mittal, M., et al., *Reactive oxygen species in inflammation and tissue injury*. Antioxid Redox Signal, 2014. **20**(7): p. 1126-67.
321. West, A.P., et al., *Mitochondrial DNA stress primes the antiviral innate immune response*. Nature, 2015. **520**(7548): p. 553-7.

322. Kozlov, A.V., et al., *Mitochondria-mediated pathways of organ failure upon inflammation*. Redox Biol, 2017. **13**: p. 170-181.
323. Nakahira, K., et al., *Autophagy proteins regulate innate immune responses by inhibiting the release of mitochondrial DNA mediated by the NALP3 inflammasome*. Nat Immunol, 2011. **12**(3): p. 222-30.
324. Duda, M.K., K.M. O'Shea, and W.C. Stanley, *omega-3 polyunsaturated fatty acid supplementation for the treatment of heart failure: mechanisms and clinical potential*. Cardiovasc Res, 2009. **84**(1): p. 33-41.
325. Samokhvalov, V., et al., *SIRT Is Required for EDP-Mediated Protective Responses toward Hypoxia-Reoxygenation Injury in Cardiac Cells*. Front Pharmacol, 2016. **7**: p. 124.
326. Darwesh, A.M., et al., *A Synthetic Epoxydocosapentaenoic Acid Analogue Ameliorates Cardiac Ischemia/Reperfusion Injury: The Involvement of the Sirtuin 3-NLRP3 Pathway*. Int J Mol Sci, 2020. **21**(15).
327. Husson, M.O., et al., *Modulation of host defence against bacterial and viral infections by omega-3 polyunsaturated fatty acids*. J Infect, 2016. **73**(6): p. 523-535.
328. Ingram, L.O., et al., *Unsaturated fatty acid requirement in Escherichia coli: mechanism of palmitate-induced inhibition of growth of strain WNI*. J Membr Biol, 1982. **65**(1-2): p. 31-40.
329. Territo, M.C. and D.W. Golde, *The function of human alveolar macrophages*. J Reticuloendothel Soc, 1979. **25**(1): p. 111-20.
330. Juers, J.A., et al., *Enhancement of bactericidal capacity of alveolar macrophages by human alveolar lining material*. J Clin Invest, 1976. **58**(2): p. 271-5.
331. Kohn, A., J. Gitelman, and M. Inbar, *Unsaturated free fatty acids inactivate animal enveloped viruses*. Arch Virol, 1980. **66**(4): p. 301-7.
332. Hilmarsson, H., L.V. Larusson, and H. Thormar, *Virucidal effect of lipids on visna virus, a lentivirus related to HIV*. Arch Virol, 2006. **151**(6): p. 1217-24.
333. Ramon, S., et al., *The specialized proresolving mediator 17-HDHA enhances the antibody-mediated immune response against influenza virus: a new class of adjuvant?* J Immunol, 2014. **193**(12): p. 6031-40.

334. Braz-De-Melo, H.A., et al., *Potential neuroprotective and anti-inflammatory effects provided by omega-3 (DHA) against Zika virus infection in human SH-SY5Y cells*. Sci Rep, 2019. **9**(1): p. 20119.
335. Yan, B., et al., *Lipidomic Profiling Reveals Significant Perturbations of Intracellular Lipid Homeostasis in Enterovirus-Infected Cells*. Int J Mol Sci, 2019. **20**(23).
336. Schwerbrock, N.M., et al., *Fish oil-fed mice have impaired resistance to influenza infection*. J Nutr, 2009. **139**(8): p. 1588-94.
337. Byleveld, P.M., et al., *Fish oil feeding delays influenza virus clearance and impairs production of interferon-gamma and virus-specific immunoglobulin A in the lungs of mice*. J Nutr, 1999. **129**(2): p. 328-35.
338. Byleveld, M., et al., *Fish oil feeding enhances lymphocyte proliferation but impairs virus-specific T lymphocyte cytotoxicity in mice following challenge with influenza virus*. Clin Exp Immunol, 2000. **119**(2): p. 287-92.
339. Fyhrquist, F., K. Metsarinne, and I. Tikkanen, *Role of angiotensin II in blood pressure regulation and in the pathophysiology of cardiovascular disorders*. J Hum Hypertens, 1995. **9 Suppl 5**: p. S19-24.
340. Perazella, M.A. and J.F. Setaro, *Renin-angiotensin-aldosterone system: fundamental aspects and clinical implications in renal and cardiovascular disorders*. J Nucl Cardiol, 2003. **10**(2): p. 184-96.
341. Gibbons, G.H., R.E. Pratt, and V.J. Dzau, *Vascular smooth muscle cell hypertrophy vs. hyperplasia. Autocrine transforming growth factor-beta 1 expression determines growth response to angiotensin II*. J Clin Invest, 1992. **90**(2): p. 456-61.
342. Griendling, K.K., et al., *Angiotensin II stimulates NADH and NADPH oxidase activity in cultured vascular smooth muscle cells*. Circ Res, 1994. **74**(6): p. 1141-8.
343. Yan, R., et al., *Structural basis for the recognition of SARS-CoV-2 by full-length human ACE2*. Science, 2020. **367**(6485): p. 1444-1448.
344. Kumar, K.V. and U.N. Das, *Effect of cis-unsaturated fatty acids, prostaglandins, and free radicals on angiotensin-converting enzyme activity in vitro*. Proc Soc Exp Biol Med, 1997. **214**(4): p. 374-9.
345. Simoes e Silva, A.C., et al., *ACE2, angiotensin-(1-7) and Mas receptor axis in inflammation and fibrosis*. Br J Pharmacol, 2013. **169**(3): p. 477-92.

346. Zhang, Y.H., et al., *ACE2 and Ang-(1-7) protect endothelial cell function and prevent early atherosclerosis by inhibiting inflammatory response*. *Inflamm Res*, 2015. **64**(3-4): p. 253-60.
347. Wang, K., M. Gheblawi, and G.Y. Oudit, *Angiotensin Converting Enzyme 2: A Double-Edged Sword*. *Circulation*, 2020.
348. Crackower, M.A., et al., *Angiotensin-converting enzyme 2 is an essential regulator of heart function*. *Nature*, 2002. **417**(6891): p. 822-8.
349. Letko, M., A. Marzi, and V. Munster, *Functional assessment of cell entry and receptor usage for SARS-CoV-2 and other lineage B betacoronaviruses*. *Nat Microbiol*, 2020. **5**(4): p. 562-569.
350. Jung, S.Y., et al., *Association of renin-angiotensin-aldosterone system inhibitors with COVID-19-related outcomes in Korea: a nationwide population-based cohort study*. *Clin Infect Dis*, 2020.
351. Imai, Y., et al., *Angiotensin-converting enzyme 2 protects from severe acute lung failure*. *Nature*, 2005. **436**(7047): p. 112-6.
352. Kuba, K., et al., *A crucial role of angiotensin converting enzyme 2 (ACE2) in SARS coronavirus-induced lung injury*. *Nat Med*, 2005. **11**(8): p. 875-9.
353. Liu, P.P., et al., *The Science Underlying COVID-19: Implications for the Cardiovascular System*. *Circulation*, 2020. **142**(1): p. 68-78.
354. Liu, Y., et al., *Clinical and biochemical indexes from 2019-nCoV infected patients linked to viral loads and lung injury*. *Sci China Life Sci*, 2020. **63**(3): p. 364-374.
355. Lelis, D.F., et al., *Angiotensin-(1-7), Adipokines and Inflammation*. *Metabolism*, 2019. **95**: p. 36-45.
356. Wang, J.J., et al., *Good or bad: Application of RAAS inhibitors in COVID-19 patients with cardiovascular comorbidities*. *Pharmacol Ther*, 2020: p. 107628.
357. Hanff, T.C., et al., *Is There an Association Between COVID-19 Mortality and the Renin-Angiotensin System? A Call for Epidemiologic Investigations*. *Clin Infect Dis*, 2020. **71**(15): p. 870-874.
358. Ulu, A., et al., *Anti-inflammatory effects of omega-3 polyunsaturated fatty acids and soluble epoxide hydrolase inhibitors in angiotensin-II-dependent hypertension*. *J Cardiovasc Pharmacol*, 2013. **62**(3): p. 285-97.

359. Glende, J., et al., *Importance of cholesterol-rich membrane microdomains in the interaction of the S protein of SARS-coronavirus with the cellular receptor angiotensin-converting enzyme 2*. *Virology*, 2008. **381**(2): p. 215-21.
360. Das, U.N., *GLUT-4, tumor necrosis factor, essential fatty acids and daf-genes and their role in insulin resistance and non-insulin dependent diabetes mellitus*. *Prostaglandins Leukot Essent Fatty Acids*, 1999. **60**(1): p. 13-20.
361. Candelario, J. and M. Chachisvilis, *Activity of Bradykinin B2 Receptor Is Regulated by Long-Chain Polyunsaturated Fatty Acids*. *PLoS One*, 2013. **8**(6): p. e68151.
362. Das, U.N., *Reply to: Bioactive Lipids and Coronavirus (COVID-19)-further Discussion*. *Arch Med Res*, 2020.
363. South, A.M., D.I. Diz, and M.C. Chappell, *COVID-19, ACE2, and the cardiovascular consequences*. *Am J Physiol Heart Circ Physiol*, 2020. **318**(5): p. H1084-H1090.
364. Diaz, J.H., *Hypothesis: angiotensin-converting enzyme inhibitors and angiotensin receptor blockers may increase the risk of severe COVID-19*. *J Travel Med*, 2020. **27**(3).
365. Esler, M. and D. Esler, *Can angiotensin receptor-blocking drugs perhaps be harmful in the COVID-19 pandemic?* *J Hypertens*, 2020. **38**(5): p. 781-782.
366. Chen, L., et al., *The ACE2 expression in human heart indicates new potential mechanism of heart injury among patients infected with SARS-CoV-2*. *Cardiovasc Res*, 2020. **116**(6): p. 1097-1100.
367. Yang, G., et al., *Effects of Angiotensin II Receptor Blockers and ACE (Angiotensin-Converting Enzyme) Inhibitors on Virus Infection, Inflammatory Status, and Clinical Outcomes in Patients With COVID-19 and Hypertension: A Single-Center Retrospective Study*. *Hypertension*, 2020. **76**(1): p. 51-58.
368. Mancia, G., et al., *Renin-Angiotensin-Aldosterone System Blockers and the Risk of Covid-19*. *N Engl J Med*, 2020. **382**(25): p. 2431-2440.
369. Li, B., et al., *Prevalence and impact of cardiovascular metabolic diseases on COVID-19 in China*. *Clin Res Cardiol*, 2020. **109**(5): p. 531-538.
370. Khomich, O.A., et al., *Redox Biology of Respiratory Viral Infections*. *Viruses*, 2018. **10**(8).
371. Reshi, M.L., Y.C. Su, and J.R. Hong, *RNA Viruses: ROS-Mediated Cell Death*. *Int J Cell Biol*, 2014. **2014**: p. 467452.

372. De Caterina, R., *n-3 fatty acids in cardiovascular disease*. N Engl J Med, 2011. **364**(25): p. 2439-50.
373. Mozaffarian, D. and J.H. Wu, *Omega-3 fatty acids and cardiovascular disease: effects on risk factors, molecular pathways, and clinical events*. J Am Coll Cardiol, 2011. **58**(20): p. 2047-67.
374. Anderson, E.J., et al., *Do fish oil omega-3 fatty acids enhance antioxidant capacity and mitochondrial fatty acid oxidation in human atrial myocardium via PPARgamma activation?* Antioxid Redox Signal, 2014. **21**(8): p. 1156-63.
375. Iba, T., et al., *Diagnosis and management of sepsis-induced coagulopathy and disseminated intravascular coagulation*. J Thromb Haemost, 2019. **17**(11): p. 1989-1994.
376. Zhang, M.Q., et al., *[Clinical features of 2019 novel coronavirus pneumonia in the early stage from a fever clinic in Beijing]*. Zhonghua Jie He He Hu Xi Za Zhi, 2020. **43**(3): p. 215-218.
377. Tsoupras, A., et al., *Bioprospecting for Antithrombotic Polar Lipids from Salmon, Herring, and Boarfish By-Products*. Foods, 2019. **8**(9).
378. Tsoupras, A., et al., *In Vitro Antithrombotic Properties of Salmon (Salmo salar) Phospholipids in a Novel Food-Grade Extract*. Mar Drugs, 2019. **17**(1).
379. Adili, R., M. Hawley, and M. Holinstat, *Regulation of platelet function and thrombosis by omega-3 and omega-6 polyunsaturated fatty acids*. Prostaglandins Other Lipid Mediat, 2018. **139**: p. 10-18.
380. Park, Y. and W. Harris, *EPA, but not DHA, decreases mean platelet volume in normal subjects*. Lipids, 2002. **37**(10): p. 941-6.
381. Petersen, A., et al., *The role of visceral adiposity in the severity of COVID-19: Highlights from a unicenter cross-sectional pilot study in Germany*. Metabolism, 2020. **110**: p. 154317.
382. Chen, T., et al., *Clinical characteristics of 113 deceased patients with coronavirus disease 2019: retrospective study*. BMJ, 2020. **368**: p. m1091.
383. Skevaki, C., et al., *Laboratory characteristics of patients infected with the novel SARS-CoV-2 virus*. J Infect, 2020. **81**(2): p. 205-212.
384. Ren, H., et al., *Association of the insulin resistance marker TyG index with the severity and mortality of COVID-19*. Cardiovasc Diabetol, 2020. **19**(1): p. 58.

385. Hu, X., et al., *Declined serum high density lipoprotein cholesterol is associated with the severity of COVID-19 infection*. Clin Chim Acta, 2020. **510**: p. 105-110.
386. Suzuki, M., et al., *High-density lipoprotein suppresses the type I interferon response, a family of potent antiviral immunoregulators, in macrophages challenged with lipopolysaccharide*. Circulation, 2010. **122**(19): p. 1919-27.
387. van der Stoep, M., S.J. Korporaal, and M. Van Eck, *High-density lipoprotein as a modulator of platelet and coagulation responses*. Cardiovasc Res, 2014. **103**(3): p. 362-71.
388. Stone, N.J., et al., *2013 ACC/AHA guideline on the treatment of blood cholesterol to reduce atherosclerotic cardiovascular risk in adults: a report of the American College of Cardiology/American Heart Association Task Force on Practice Guidelines*. J Am Coll Cardiol, 2014. **63**(25 Pt B): p. 2889-934.
389. Davidson, M.H., et al., *Efficacy and tolerability of adding prescription omega-3 fatty acids 4 g/d to simvastatin 40 mg/d in hypertriglyceridemic patients: an 8-week, randomized, double-blind, placebo-controlled study*. Clin Ther, 2007. **29**(7): p. 1354-67.
390. Ballantyne, C.M., et al., *Efficacy and safety of eicosapentaenoic acid ethyl ester (AMR101) therapy in statin-treated patients with persistent high triglycerides (from the ANCHOR study)*. Am J Cardiol, 2012. **110**(7): p. 984-92.
391. Zhou, Q., et al., *EPA+DHA, but not ALA, Improved Lipids and Inflammation Status in Hypercholesterolemic Adults: A Randomized, Double-Blind, Placebo-Controlled Trial*. Mol Nutr Food Res, 2019. **63**(10): p. e1801157.
392. Yanai, H., et al., *An Improvement of Cardiovascular Risk Factors by Omega-3 Polyunsaturated Fatty Acids*. J Clin Med Res, 2018. **10**(4): p. 281-289.
393. Abdelhamid, A.S., et al., *Omega-3 fatty acids for the primary and secondary prevention of cardiovascular disease*. Cochrane Database Syst Rev, 2020. **3**: p. CD003177.
394. Maki, K.C., et al., *A highly bioavailable omega-3 free fatty acid formulation improves the cardiovascular risk profile in high-risk, statin-treated patients with residual hypertriglyceridemia (the ESPRIT trial)*. Clin Ther, 2013. **35**(9): p. 1400-11 e1-3.
395. Chan, D.C., et al., *Randomized controlled trial of the effect of n-3 fatty acid supplementation on the metabolism of apolipoprotein B-100 and chylomicron remnants in men with visceral obesity*. Am J Clin Nutr, 2003. **77**(2): p. 300-7.

396. Martin, J.M. and R.D. Stapleton, *Omega-3 fatty acids in critical illness*. Nutr Rev, 2010. **68**(9): p. 531-41.
397. Gadek, J.E., et al., *Effect of enteral feeding with eicosapentaenoic acid, gamma-linolenic acid, and antioxidants in patients with acute respiratory distress syndrome. Enteral Nutrition in ARDS Study Group*. Crit Care Med, 1999. **27**(8): p. 1409-20.
398. Zhao, Y. and C. Wang, *Effect of omega-3 polyunsaturated fatty acid-supplemented parenteral nutrition on inflammatory and immune function in postoperative patients with gastrointestinal malignancy: A meta-analysis of randomized control trials in China*. Medicine (Baltimore), 2018. **97**(16): p. e0472.
399. Mayer, K., et al., *Parenteral nutrition with fish oil modulates cytokine response in patients with sepsis*. Am J Respir Crit Care Med, 2003. **167**(10): p. 1321-8.
400. Campos, F.G., et al., *Impact of parenteral n-3 fatty acids on experimental acute colitis*. Br J Nutr, 2002. **87 Suppl 1**: p. S83-8.
401. Wang, X., et al., *Omega-3 fatty acids-supplemented parenteral nutrition decreases hyperinflammatory response and attenuates systemic disease sequelae in severe acute pancreatitis: a randomized and controlled study*. JPEN J Parenter Enteral Nutr, 2008. **32**(3): p. 236-41.
402. Calder, P.C., *Intravenous Lipid Emulsions to Deliver Bioactive Omega-3 Fatty Acids for Improved Patient Outcomes*. Mar Drugs, 2019. **17**(5).
403. Calder, P.C., *Hot topics in parenteral nutrition. Rationale for using new lipid emulsions in parenteral nutrition and a review of the trials performed in adults*. Proc Nutr Soc, 2009. **68**(3): p. 252-60.
404. Nandivada, P., et al., *Lipid emulsions in the treatment and prevention of parenteral nutrition-associated liver disease in infants and children*. Am J Clin Nutr, 2016. **103**(2): p. 629S-34S.